



Durham E-Theses

Water and Territorial Empires

RAYNE, LOUISE,ELIZABETH

How to cite:

RAYNE, LOUISE,ELIZABETH (2014) *Water and Territorial Empires*, Durham theses, Durham University. Available at Durham E-Theses Online: <http://etheses.dur.ac.uk/10921/>

Use policy

The full-text may be used and/or reproduced, and given to third parties in any format or medium, without prior permission or charge, for personal research or study, educational, or not-for-profit purposes provided that:

- a full bibliographic reference is made to the original source
- a [link](#) is made to the metadata record in Durham E-Theses
- the full-text is not changed in any way

The full-text must not be sold in any format or medium without the formal permission of the copyright holders.

Please consult the [full Durham E-Theses policy](#) for further details.

Water and Territorial Empires

The application of remote sensing techniques to ancient imperial water management in northern Mesopotamia

Louise Elizabeth Rayne

PhD Thesis

Departments of Archaeology and Geography, Durham University

2014

Abstract

The ability of the ancient territorial empires to control water management strategies has been proposed but not yet fully explored. Given that most of the evidence is derived from historical information, or from isolated, specific archaeological studies, a detailed map of ancient irrigation in northern Mesopotamia was needed. The present interdisciplinary study used techniques of remote sensing and GIS to generate this map.

CORONA images (1960-1972) were used to identify and record known and new water management features, showing the landscape before recent agricultural and urban intensification removed archaeological remains. The results of the image interpretation were validated through DEM analysis; low resolution SRTM and ASTER DEMs were used, as well as a high resolution CORONA DEM, generated through applying photogrammetry techniques to CORONA stereopairs. A sample of the results was also investigated in the field in July 2010.

Using multiple techniques to locate and validate data, the large area of northern Mesopotamia could be mapped relatively quickly and inexpensively. The results of the remote sensing analysis showed that water management developed throughout northern Mesopotamia from the Neo-Assyrian to the Early Islamic period. Detailed information about the scale and distribution of whole irrigation systems was obtained. The present study concluded that the Neo-Assyrian Empire had established changes in the landscape that promoted the development of large-scale water management; a significant peak later occurred during the time of the Early Islamic Empire. Conversely, interruptions to water management occurred at times of political instability, (with modern parallels). The powerful later territorial empires were able to impose and encourage the development of water management throughout the formerly marginal rain-fed zone.

Contents

Abstract	2
Contents	3
List of Figures	6
List of Tables	18
Statement of copyright	20
Acknowledgements	21
Chapter 1 Introduction	23
1.1 Introduction	23
1.2 Aims and research questions	26
1.3 Theoretical context and research trajectory	28
1.4 Environmental context	36
1.5 Thesis outline	48
Chapter 2: Spatial Literature review	50
2.1 Introduction	50
2.2 Jerablus	53
2.3 Membij Qanats	57
2.4 Dibsi Faraj	57
2.5 Canal between Tell Frey to Qa'lat Ja'bar	59
2.6 Resafa	60
2.7 Heraqlah	64
2.8 The Balikh	65
2.9 The Habur	72
2.10 Balikh-Mari	80
2.11 Assyrian water management in Northern Iraq	84
2.12 Qanats in Northern Iraq	92
2.13 Summary	93
Chapter 3: Methods	97
3.1 Methodology	97

3.2 Image interpretation	102
3.3 Fieldwork	117
3.4 SRTM and ASTER	121
3.5 CORONA Photogrammetry	132
3.6 Precipitation isohyets and inter-annual variability	151
3.7 Summary	162
Chapter 4: Irrigation and drainage	163
4.1 Introduction	163
4.2 Local conditions and water resources	164
4.3 Water management methods	166
4.4 Components of systems	169
4.5 Qanats	177
4.6 Efficiency and environmental limitations	178
4.7 Case study: Hohokam water management	181
4.8: Case study: Irrigation of the Wadi Zerqa, Jordan	186
4.9 Scales of control of water management strategies	187
4.10 Summary	189
Chapter 5: Water management in northern Mesopotamia	190
5.1 Introduction	190
5.2 Jerablus	193
5.3 Euphrates-Balikh	198
5.4 Membij-Dibsi Faraj	200
5.5 Dibsi Faraj	201
5.6 Tell Fray-Qa'lat Ja'bar	206
5.7 Resafa	207
5.8 Balikh-Habur	210
5.9 The Habur	214
5.10 Habur-Iraq border	225
5.11 Qanats on the Tell Afar/Sinjar Plain	230
5.12 North Jazira	238

5.13 The Tigris and Northern Iraq	238
5.14 Summary	239
Chapter 6: Water management in the Balikh Valley	241
6.1 Geomorphology and land use	241
6.2 Sahlan and Hammam canals	253
6.3 Nahr al Abbara	257
6.4 Central Balikh	284
6.5 Qara Mokh/West System	292
6.6 Raqqa	304
6.7 Summary	316
Chapter 7: Discussion	319
7.1 Introduction	319
7.2 Theoretical framework	319
7.3 Chronology	323
7.4 Advances in methods	328
7.5 Data validation	330
7.6 Types of channels: form and function	336
7.7 Scale and distribution of water systems	346
7.8 Scales of Imperial control	358
7.9 Justification	373
7.10 Summary	375
Chapter 8: Conclusion	376
8.1 Aims and results	376
8.2 Development of water management at the time of the later territorial empires	378
8.3 Evaluation	381
8.4 Future research	382
Data references	384
References	386
Appendix	424

List of figures

Figure 1.1: <i>Project study area with main drainages.</i>	24
Figure 1.2: <i>Approximate chronology of the later territorial empires.</i>	25
Figure 1.3: <i>Average precipitation in northern Mesopotamia.</i>	37
Figure 1.4: <i>Mean relative interannual rainfall variability in northern Mesopotamia.</i>	39
Figure 1.5: <i>CORONA image of truncated canal along Euphrates.</i>	41
Figure 1.6: <i>Gilgai in the Balikh Valley.</i>	43
Figure 2.1: <i>Known ancient irrigation systems in northern Mesopotamia</i>	
Figure 2.2: <i>Ancient water features in the Jerablus region.</i>	55
Figure 2.3: <i>Features around Membij.</i>	57
Figure 2.4: <i>Water management features now inundated by the Tabqa Dam.</i>	59
Figure 2.5: <i>Location of Resafa on the Wadi es Sele.</i>	61
Figure 2.6: <i>Cistern at Resafa (from Brinker, 1991, p123).</i>	63
Figure 2.7: <i>Water management at Resafa (from Brinker, 1991, p125).</i>	64
Figure 2.8: <i>Canals at Heraqlah and Raqqa discussed in the existing literature.</i>	65
Figure 2.9: <i>Known water management features in the Balikh Valley, recorded by Wilkinson (1998), and Heidemann (2006).</i>	68
Figure 2.10: <i>Canals recorded by Wilkinson (1998).</i>	72
Figure 2.11: <i>Water management features in the Habur region. The features around Hamoukar were mapped by Jason Ur (shapefiles provided by Ur, pers. comm; also see Ur, 2010a).</i>	74
Figure 2.12: <i>Water management features alongside the Habur recorded by Ergenzinger et al (1988). The canals alongside the Euphrates were recorded by Geyer and Monchambert (2003).</i>	75
Figure 2.13: <i>Mapped location of Habur canals, from Ergenzinger et al (1988, p119).</i>	79
Figure 2.14: <i>Canals and Bronze Age sites mapped by Geyer and Monchambert (2003, p247).</i>	83

Figure 2.15: <i>From Margueron (2004, p50, Pl. 17).</i>	84
Figure 2.16: <i>map of known canals in Northern Iraq. These were located by Ur (2005), Ur et al (2013) and Altaweel (2008).</i>	86
Figure 2.17: <i>Canals in northern Iraq mapped by Ur (2005, p320; pers comm).</i>	87
Figure 2.18: <i>CORONA image of Bandwai canal, Ur, 2005 (pers. comm).</i>	88
Figure 3.1: <i>Areas surveyed by the Fragile Crescent Project.</i>	103
Figure 3.2: <i>Process of image interpretation used by the present study.</i>	105
Figure 3.3: <i>Outlines of areas investigated using imagery.</i>	106
Figure 3.4: <i>CORONA image divided into three transects, viewable at a scale of 1:30,000.</i>	107
Figure 3.5: <i>Examples of channel types in Syria identifiable in 1960s CORONA images.</i>	109
Figure 3.6 <i>The panchromatic CORONA images can be enhanced. For example, the left image uses a standard deviation stretch, while the right image uses a histogram equalise stretch.</i>	110
Figure 3.7: <i>Schematic diagram of a typical irrigation system.</i>	111
Figure 3.8: <i>Masonry block with mason's mark from a rock-cut channel in the Jerablus region of north Syria.</i>	112
Figure 3.9: <i>Modern concrete-lined canal in the Balikh in 2010.</i>	113
Figure 3.10: <i>Eroded canal. The upcast banks of the Hammam channel (foreground) were still visible in the 1990s (photograph from Tony Wilkinson, pers.comm).</i>	113
Figure 3.11: <i>Linear features around the Early Islamic site of Medinat al Farr.</i>	115
Figure 3.12: <i>This example of a hollow way runs across the natural gradient of the landscape, disregarding it.</i>	116
Figure 3.13: <i>This example of a canal longitudinal profile shows that it is constrained by the need for gravity flow, therefore following the natural contours of the landscape.</i>	116
Figure 3.14: <i>ASTER has a pixel size of 30m and SRTM of 90m; both are</i>	122

generally too coarse to show relict canals.

Figure 3.15: The process of creating a stream network using the ArcGIS hydrology tools is straightforward.	125
Figure 3.16: The difference between the lowest pixel and the lowest surrounding pixel forms the 'z limit'.	126
Figure 3.17: The pink dots represent sinks in the SRTM throughout the project area.	126
Figure 3.18: Flow direction coding.	127
Figure 3.19: Flow direction can be modelled using an elevation model such as SRTM.	128
Figure 3.20: The raster output of the Flow Accumulation tool identifies the locations where flow is most concentrated.	129
Figure 3.21: Drainage network as established using digital elevation models (SRTM and ASTER).	131
Figure 3.22: CORONA image capture.	132
Figure 3.23: The J3 camera system used by CORONA mission KH4B.	134
Figure 3.24: CORONA camera systems.	134
Figure 3.25: Illustration of relief displacement.	136
Figure 3.26: Areas of CORONA stereo-pair subsets. 4 November 1968.	139
Figure 3.27: Features such as road intersections can make good control points.	143
Figure 3.28: Tie-point generation using LPS.	144
Figure 3.29: Blockfile setup using ERDAS LPS.	146
Figure 3.30: Image matching strategy selection using lps eATE.	148
Figure 3.31: Rainfall at GPCC grid point 25 km from Carchemish.	152
Figure 3.32: Rainfall at GPCC grid point 34 km south-west of Raqqa.	153
Figure 3.33: Boxplot showing statistics for grid points near Carchemish and Raqqa.	153
Figure 3.34: Isohyets (31 year average).	155
Figure 3.35: Interannual variability.	166
Figure 3.36: The distribution of rain gauges in Syria and Turkey is sparse.	159
Figure 3.37: Comparison of interpolation methods showing a positive	160

correlation.

Figure 4.1: Water diversion from a wadi onto the fields using small weirs.	167
Figure 4.2: Conveyance systems comprise a series of channels enabling abstraction, transport of water, and drainage. Storage of water can also be incorporated into these systems.	169
Figure 4.3: Sequence of irrigation channels.	170
Figure 4.4: An outlet in a wadi floods a series of basins bounded by earth dikes.	171
Figure 4.5: Furrow irrigation at Jerablus Tahtani, Syria, July 2010.	175
Figure 4.6: Illustration of furrow irrigation.	175
Figure 4.7: Subterranean qanat tunnels extract groundwater and transport it, by gravity flow, to the surface.	178
Figure 4.8: Waterlogging and canal seepage can lead to a rise in the water table, drawing salts into the root zone. Salts can also be left behind when surface water evaporates.	180
Figure 4.9: Drainage basins of Phoenix, Arizona (from Waters, 2008, p334).	182
Figure 4.10: Position of irrigation laterals relative to the main/sub-mains.	184
Figure 5.1: Schematic diagram showing the morphological difference between active and disused canals.	192
Figure 5.2: Canal at Carchemish with vegetation.	193
Figure 5.3: Exposed section in the Wadi Armane showing different layers of sediments.	194
Figure 5.4: Map of Jerablus channels	194
Figure 5.5: Rock-cut tunnel in the Wadi Armana.	196
Figure 5.6: Map of locations of rock-cut channels and CORONA image. Image 22 January 1967.	196
Figure 5.7: Block inscribed with a mason's mark.	197

Figure 5.8: Water features in the steppe between the Euphrates and the Balikh.	198
Figure 5.9: Large site and trace of a qanat (marked by arrows) identified by present project and also recorded by Dan Lawrence and Niko Galiatsatos. Image 22 January 1967.	199
Figure 5.10: See inset within Figure 5.8. Features including a qanat in the steppe between the Euphrates and the Balikh. Image 22 January 1967.	200
Figure 5.11: Qanats between Membij and Dibsi Faraj. Mapped by Dan Lawrence, Niko Galiatsatos and present study.	201
Figure 5.12: A truncated canal on the edge of the Euphrates floodplain.	202
Figure 5.13: Features alongside the Euphrates between Dibsi Faraj and Qa'lat Ja'bar.	203
Figure 5.14: The Nahr Maslama and Dibsi Faraj. CORONA Image 22 January 1967.	204
Figure 5.15: Section of the Nahr Maslama (from Harper and Wilkinson, 1975, Fig.2).	204
Figure 5.16: Water features at Dibsi Faraj (from Wilkinson and Rayne, 2010, p127).	205
Figure 5.17: The qanat is visible as a line of white dots, representing upcast mounds. It is difficult to see at this scale of 1:24000. CORONA image 22 January 1967.	205
Figure 5.18: The scale at which this features is clearly visible (1:10000) shows the care needed when undertaking an image interpretation study.	206
Figure 5.19: CORONA image of the Fray-Ja'bar canal. CORONA image 22 January 1967.	207
Figure 5.20: Location of Resafa .	208
Figure 5.21: The CORONA image (22 January 1967) shows water features around Resafa.	208
Figure 5.22: Canal traces in the basin of the Wadi es Sele, 3km north of Resafa. CORONA image 22 January 1967.	209
Figure 5.23: A similar feature to the dam at Resafa was identified 28 km to the south west. CORONA image 22 January 1967.	210
Figure 5.24: Canal on north bank of Euphrates. See Figure 5.26 for	211

location. CORONA Image 5 November 1968.

- Figure 5.25:** *Traces of the Nahr Semiramis are visible on the CORONA imagery.* 212
- Figure 5.26:** *Relict water features alongside the Euphrates located using CORONA images.* 213
- Figure 5.27:** *Segments of canals visible using CORONA and locations of profiles and CORONA screenshots.* 215
- Figure 5.28** *CORONA image 11 December 1967.* 216
- Figure 5.29:** *CORONA image 11 December 1967.* 217
- Figure 5.30:** *In some places segments of canals along the Habur cross wadis.* 218
- Figure 5.31:** *Longitudinal profile.* 218
- Figure 5.32:** *CORONA image 11 December 1967* 219
- Figure 5.33:** *A canal and offtakes are visible in the CORONA image (11 December 1967).* 220
- Figure 5.34:** *Canals and possible offtakes. CORONA image 11 December 1967.* 221
- Figure 5.35:** *The canal is only identifiable in the CORONA images as short fragments after Tell Sheikh Hamad. A short stretch of canal is visible close to the Habur's confluence with the Euphrates.* 222
- Figure 5.36:** *Traces of a canal are apparent on the right bank of the Habur. CORONA image 11 December 1967.* 223
- Figure 5.37:** *Segment of canal with upcast banks. CORONA image 11 December 1967.* 223
- Figure 5.38:** *Longitudinal profile of a canal segment.* 224
- Figure 5.39:** *Further downstream the canal is represented by a dark line lacking upcast banks, with associated offtakes. CORONA image 5 November 1968.* 225
- Figure 5.40:** *Canals traces between the Habur and the Iraq border.* 227
- Figure 5.41:** *Two parallel segments of canal flow close to the floodplain.* 228
- Figure 5.42:** *Longitudinal profile of a segment of the Nahr Dawrin.* 228
- Figure 5.43:** *A segment of the Nahr Dawrin is also visible closer to the Iraqi border. CORONA image 5 November 1968.* 229

Figure 5.44: Qanats clustering south of Sinjar.	231
Figure 5.45: A dense cluster of qanats/tunnels as well as sites and follow ways south of Sinjar is identifiable using CORONA. Image 11 December 1967.	231
Figure 5.46: 'Cut and cover' channel and resulting open channel south of Sinjar. CORONA image 11 December 1967	232
Figure 5.47: More 'traditional' conduits; shafts are more widely separated. CORONA image 11 December 1967	233
Figure 5.48: Qanats and sites. CORONA image 11 December 1967.	233
Figure 5.49: Walled site and qanat. CORONA image 11 December 1967.	234
Figure 5.50: Former settlement and qanat. CORONA image 11 December 1967.	234
Figure 5.51: The major 3rd millennium BC site of Tell Khoshi cut by a qanat.	235
Figure 5.52: Complex qanat systems. CORONA image 11 December 1967.	235
Figure 5.53: Small sample of the irrigation systems and qanats south of Sinjar.	237
Figure 5.54: Canal on south bank of Lower Zab. CORONA image 9 August 1968.	239
Figure 6.1: Gilgai are visible on this CORONA image. 22 January 1967.	243
Figure 6.2: ASTER-generated stream network and palaeochannels.	244
Figure 6.3: Cross section.	245
Figure 6.4: Cross section.	245
Figure 6.5: Cross section.	247
Figure 6.6: Cross section.	247
Figure 6.7: This sequence of Landsat images, all taken at a similar time of year, shows the expansion of modern irrigation in the Balikh.	249
Figure 6.8: The Balikh Valley is crowded with artificial canals.	251
Figure 6.9: Locations of longitudinal canal profiles 1-6.	252
Figure 6.10: The Sahlan canal is very apparent by the dark trace of the	253

infilled channel and the pale-coloured upcast mounds on this CORONA image.

Figure 6.11: Sahlan-Hammam canals and a relict canal of unknown date	254
Figure 6.12: The gradient of the Sahlan channel estimated from SRTM.	255
Figure 6.13: Section through Sahlan canal, from Wilkinson, 1998: fig. 5.	255
Figure 6.14: Sites occupied in each period period alongside palaeochannel.	256
Figure 6.15: Sites occupied in each period period alongside Sahlan canal	256
Figure 6.16: Archaeological sites alongside the Balikh palaeochannel and the Sahlan-Hammam canal.	258
Figure 6.17: The Sahlan canal truncates the Bronze age site 242 (arrowed). Image 22 January 1967.	259
Figure 6.18: Lower end of Hamman channel, near Tell Hamman et Turkman. Image 22 January 1967.	260
Figure: 6.19: The upcast banks of the Hammam channel (foreground) were still visible in the 1990s (Photograph from Tony Wilkinson, who also provides scale).	261
Figure 6.20: Canal profile 2.	261
Figure 6.21: The canal is visible as a broad brown line in the CORONA DEM of c.10m resolution.	262
Figure 6.22: Filtered 3D surface of the Hammam canal created using the CORONA DEM.	262
Figure 6.23: Cross section of the canal taken using SRTM.	263
Figure 6.24: The canal is discernible using the CORONA DEM.	263
Figure 6.25: The locations of later sites in the vicinity of the Sahlan-Hammam canals and the hypothetical route of the missing segment.	265
Figure 6.26: While a DEM can reveal the surface morphology of a canal, excavation is needed to get a more accurate value for depth.	267
Figure 6.27: Sketch indicating the varying estimates of flow depending upon different parameters.	267
Figure 6.28: The Nahr al Abbara water management system.	270
Figure 6.29: Early Islamic features are visible on the 1960s CORONA images. Image 22 January 1967.	271

Figure 6.30: Early Islamic sites as recorded from survey in the vicinity of the Nahr al Abbara.	272
Figure 6.31: Nahr al Abbara main conveyor longitudinal profile	273
Figure 6.32: The ASTERDEM (spatial resolution 30m) shows that the Nahr al Abbara main canal flows along a slight ridge.	274
Figure 6.33: Canal profile 4.	275
Figure 6.34: CORONA DEM showing the gradient of the distributary channels of the Nahr al Abbara.	275
Figure 6.35: Nahr al Abbara with laterals and location of Nahr al Abbara lateral longitudinal profile.	276
Figure 6.36: Canal profile 5. Nahr al Abbara lateral longitudinal profile (SRTM).	276
Figure 6.37: Bronze Age sites in relation to the Nahr al Abbara main conveyor.	278
Figure 6.38: Traces of two main canals along the route of the Nahr al Abbara can be seen in the CORONA image.	279
Figure 6.39: Flow network calculated using the ASTER DEM.	281
Figure 6.40: Nahr al Abbara drainage zone.	282
Figure 6.41: Canal profile 6.	282
Figure 6.42: Canals in the central Balikh, near the Qara Mokh.	285
Figure 6.43: Locations of longitudinal longitudinal profiles, based on the SRTM DEM.	286
Figure 6.44: The upper main canal within the central Balikh system.	287
Figure 6.45: The irrigated zone of the Hellenistic system is south of the main canal. CORONA image 22 January 1967.	288
Figure 6.46: Canal long profile 1.	289
Figure 6.47: Canal long profile 2.	289
Figure 6.48: Canal profile 3.	290
Figure 6.49: Settlement in the area achieved a peak during the Hellenistic period and sites of this date are closely aligned to the canal system.	291
Figure 6.50: Flow network and wadis and canals digitised from CORONA imagery in the west Balikh horseshoe.	294
Figure 6.51: 2010 Google Earth image shows how modern irrigation	295

schemes have transformed the landscape and removed and obscured the relict channels.

Figure 6.52: *A newly constructed grid of canals is being built, overlaying the channel pattern visible in the earlier CORONA image. Image 16 May 1972.* 296

Figure 6.53: *A newly constructed grid of (dry) canals is being built, overlaying the channel pattern visible in the earlier CORONA image. Image 16 May 1972.* 297

Figure 6.54: *1967 CORONA image showing the same area before the new irrigation scheme was constructed.* 298

Figure 6.55: *A main canal abstracting from the Qara Mokh is visible along with laterals draining eastwards towards the Balikh.* 300

Figure 6.56: *Longitudinal profile of the main canal of the Qara Mokh/West Balikh system.* 301

Figure 6.57: *CORONA image showing multiple conveyors along a hill slope. Image 22 January 1967.* 301

Figure 6.58: *Cross section across multiple conveyors of Qara Mokh system.* 302

Figure 6.59: *Tunnels and qanats around Raqqa.* 304

Figure 6.60: *Eroded and overgrown post-Abbasid canal viewed from the north in 2010.* 305

Figure 6.61: *Sketch profile of post-Abbasid canal.* 306

Figure 6.62: *The east-west canal which clearly truncated Heraqlah. 1967 CORONA image.* 306

Figure 6.63: *A qanat north of Raqqa terminates in an open channel. CORONA image 22 January 1967.* 307

Figure 6.64: *General location of canals derived from a qanat which supplied Raqqa. CORONA image 22 January 1967.* 308

Figure 6.65: *Canals, the depression of a former cistern, and part of a qanat identified on the 1967 CORONA.* 309

Figure 6.66: *A qanat originates in an area of elevated ground north of Raqqa.* 310

Figure 6.67: *Tunnel shafts indicated by pale coloured upcast mounds.* 311

Figure 6.68: <i>This example of a Neo-Assyrian tunnel in Iraq can be used to gain an idea of what the Raqqa tunnel might have looked like (personal communication, Stephanie Dalley).</i>	312
Figure 6.69: <i>The surface of the Raqqa tunnel compared with its projected route.</i>	313
Figure 6.70: <i>Schematic view of suggested tunnel.</i>	313
Figure 6.71: <i>Abbasid palace with a possible race course and an outlet channel with cisterns.</i>	314
Figure 6.72: <i>Early Islamic canals, sites and other water features around Raqqa and Heraqlah.</i>	315
Figure 6.73: <i>Several separate water management systems in the Balikh valley could be unpicked from the layers of channels and investigated using DEMs and archaeological data.</i>	316
Figure 7.1: <i>Limestone block with mason's mark, recorded in the Wadi Amarna during fieldwork in July 2010.</i>	326
Figure 7.2: <i>Linear features around Medinat Al Farr. CORONA image dating to 22 January 1967.</i>	331
Figure 7.3: <i>A sequence of channels around the Abbasid site of Heraqlah.</i>	334
Figure 7.4: <i>Possible check dams in the steppe, 68 km to the east of the Balikh. CORONA image dating to 22 January 1967.</i>	338
Figure 7.5: <i>Canal between Carchemish and Jerablus Tahtani.</i>	340
Figure 7.6: <i>The results of the present research and other published CORONA studies show ancient water management systems throughout northern Mesopotamia.</i>	346
Figure 7.7: <i>Nahr al Abbara dual channels. CORONA image from 22 January 1967.</i>	351
Figure 7.8: <i>Earthwork of a possible canal segment between the Balikh and the Habur. CORONA image from 5 November 1968.</i>	353
Figure 7.9: <i>Segments of an eroded canal on the edge of the Euphrates floodplain between Dibsi Faraj and Sura. CORONA image 22 January 1967.</i>	354

List of Tables

Table 2.1: Conduits and canals in the Jerablus region. See Chapter 5 for images of specific features and Figure 2.2 for a map.	54
Table 2.2: Suggested dates for canals between Deir ez Zor and Mari, from Geyer and Monchambert 2003 (p175-231).	81
Table 2.3: Dating of features from existing literature.	94
Table 3.1 Remote sensing data used to record ancient irrigation systems	97
Table 3.2: Survey, excavation and historical data.	98
Table 3.3: Water management features around Jerablus visited during fieldwork in 2010. See Chapter 2 Table 2.1 and Figure 2.2 and Chapter 5.2 .	119
Table 3.4: State of preservation of canals in the Balikh in 2010.	119
Table 3.5: Conditional threshold applied to flow accumulation rasters; shown in Figure 3.21	130
Table 3.6: CORONA mission parameters.	133
Table 3.7: CORONA frame subset sizes	139
Table 3.8: Interior orientation and camera parameters	140
Table 3.9: Exterior orientation parameters	141
Table 3.10: Estimated exterior orientation parameters calculated by LPS for a CORONA DEM of the Sahlan-Hamman canal.	141
Table 3.11: Control points and automatically generated tie points.	142
Table 3.12: Triangulation results	145
Table 3.13: Strategy parameters	149
Table 4.1: Recommended gradients for parts of irrigations systems (After Zimmerman, 1966; Kruse et al, 1983)	173
Table 5.1: Parameters of the Nahr Maslama and discharge calculated using Manning's formula. The gradient value is based on assuming a slightly shallower gradient than the Euphrates, which was measured using the SRTM DEM between the Tabqa Dam and Raqqa.	202
Table 5.2: Canal gradients in northern Mesopotamia.	240

Table 6.1: *Discharge estimates. Small changes in the input parameters (based on the CORONA DEM), as these two examples show, have significant impact on the results.*

268

Table 6.2: *Comparison between gradients of channels within Nahr al Abbara system and gradients suggested as ideal by the water management literature (in this example these are from Zimmerman, 1966).*

277

Table 6.3: *Summary of key results*

317

Table 7.1: *Chronology of features with dating evidence*

324

Table 7.2: *Dimensions of selected ancient canals*

347

Table 7.3: *Potential areas irrigated by selected ancient canals, assuming that about 1 litre/second irrigates 1 ha (see Wilkinson, 1998, p81).*

348

Statement of copyright

The copyright of this thesis rests with the author. No quotation from it should be published without the author's prior written consent and information derived from it should be acknowledged.

Acknowledgements

I would like to thank my supervisors, Tony Wilkinson and Danny Donoghue, for their advice throughout this research and during the production of this thesis. I am also grateful to individuals who lent me data, shapefiles and images (Tony Wilkinson, Eleanor Wilkinson, Dan Lawrence, Niko Galiatsatos, Carrie Hritz, Jason Ur, Sebastien Rey and Stephanie Dalley) and also to the participants of the Fragile Crescent Project, Durham University. I am grateful to the Faculty of Social Sciences and Health for funding my research.

I would also especially like to thank the inhabitants of the GIS room and my friends and family for their support and encouragement.

Chapter 1: Introduction

1.1 Introduction

This thesis has taken an interdisciplinary approach to the subject of ancient water management in northern Mesopotamia under the later territorial empires (from c.1200 BC-1200 AD), applying methods and concepts from archaeology, geography and history. Data were derived from remote sensing analyses, fieldwork, and existing surveys and were compiled into a detailed database.

Water resource management strategies are driven by natural conditions such as climate and geology, but also by social and political structures. Modern water management in Syria is affected by problems of over-exploitation (Varela-Ortega and Sargardoy, 2003) and most recently by the current conflict (e.g. see FAO, 2012, p2). Recent intensification of irrigated agriculture in the Near East, and the political and environmental conflicts that arise from it, have the potential to be a source of future problems. Projects in northern Mesopotamia initiated from the mid 20th century to the present day re-shaped a landscape where rain-fed cultivation was often the norm (e.g. see Beaumont, 1996, p137) and where large-scale water abstraction was rare.

The current intensification of water management and control of the landscape using large-scale irrigation systems is not unprecedented, however. Archaeologists, geographers, historians and early travellers have recorded traces of relict irrigation in northern Mesopotamia, much of which is associated with the later territorial empires. These are features which are rapidly disappearing due to modern agriculture and urbanisation, and which are currently inaccessible because of the political issues in Syria and Iraq.

However, remote sensing technologies are increasingly revolutionising our ability to quickly identify ancient water features which are often difficult to locate and record on the ground. The present study's remote sensing approach included the use of declassified spy satellite data from the 1960s and 1970s as well as modern satellite data and elevation models to identify and record these features, generating an innovative region-wide map and locating previously unknown features despite their inaccessibility. Because the existing studies had tended to

be focused on specific areas or channels, this regional map of known and new water management systems was needed.

A large region (about 100,000 km²) was selected in order to facilitate a more detailed and comparative dataset than earlier field-based studies could provide. The study area, represented in **Figure 1.1**, comprised the region of northern Mesopotamia, the lands between the Euphrates in northern Syria and the Tigris in northern Iraq. The Jazira, the area between the Euphrates and the Turkish border, and the lands adjacent to the Euphrates and Tigris were examined. This area was selected because it comprised a zone where multiple later territorial empires were active, and also because it fits into the 'zone of uncertainty'. This definition refers to the area of northern Mesopotamia where rainfall is at the minimum levels required for agriculture (see Wilkinson, 1994, p484). Relying only on rain-fed cultivation was possible, but risky, given high variability of precipitation. Irrigation was not necessarily essential in this zone, but it represented a way of mitigating against the risk. Water systems throughout the zone of variability were recorded and analysed using GIS and remote sensing.

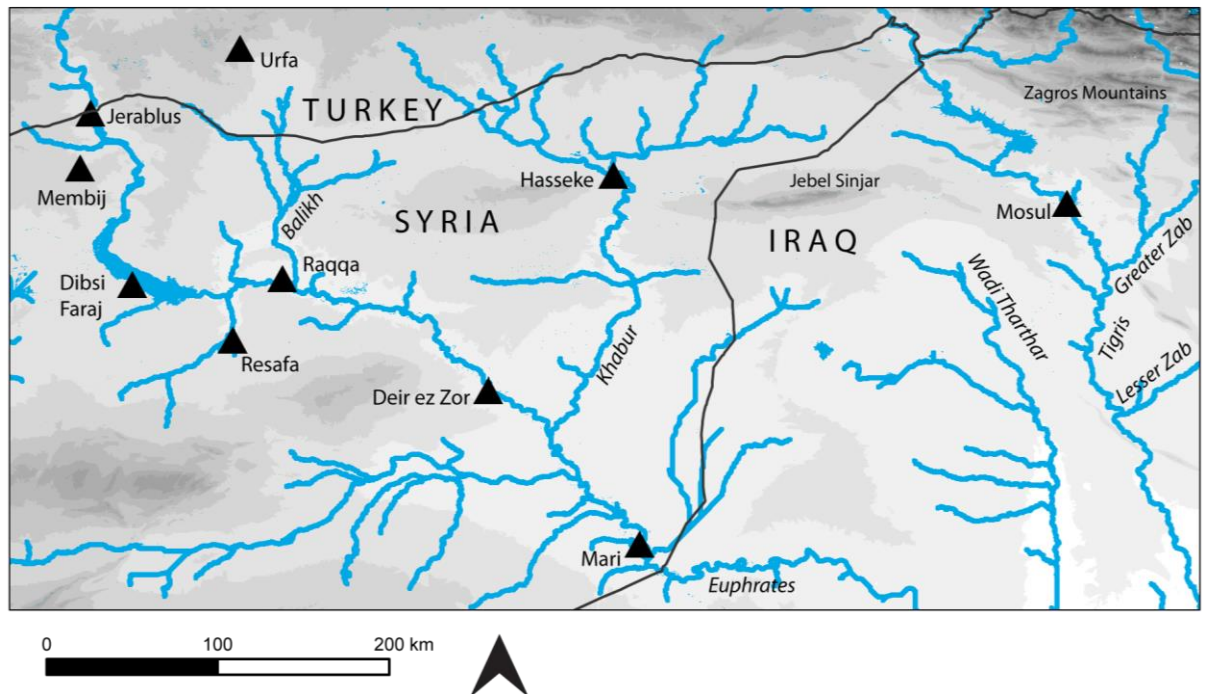


Figure 1.1: Project study area with main drainages (derived from a SRTM DEM using the ArcGIS hydrology tools; the background is also SRTM).

These technologies are ideal for recording large, complex irrigation systems. Techniques that incorporate the use of 'historical' imagery with more recent satellite image and elevation data, and with some fieldwork, have enabled features to be recorded, including those that have recently been destroyed and obscured. Image interpretation using CORONA imagery (1960-1972) facilitated this. 21st century high resolution imagery (e.g. IKONOS, GeoEye-1, at resolutions of 0.5-1 m) has aided image interpretation and in some cases was used as a way of obtaining control points for rectification of other data. Detailed hydrological and topographical analysis has been facilitated by the generation of DEMs (Digital Elevation Models). These have been derived from the 90 m resolution SRTM (Shuttle Radar Topography Mission), 30 m ASTER (Advanced Spaceborne Thermal Emission and Reflection Radiometer) and for selected features using CORONA stereo pair DEMs (c.10m).

The results of the study were examined in a wider historical context of the later territorial empires. Relict water management features in northern Mesopotamia are linked to the organising ability of the later territorial empires, from the Neo-Assyrians (c.1200-600 BC) in the Iron Age to the Early Islamic states (c.700-1200 AD). While this study discusses the relation between the scale and distribution of water management and the economic and political power of these later territorial empires, it does so with an understanding of earlier water features that these systems succeeded and the later ones that can obscure them (see **Figure 1.2**).

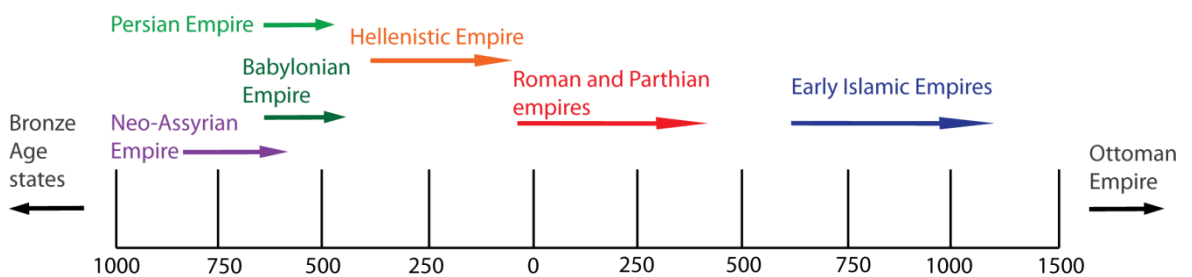


Figure 1.2: Approximate chronology of the later territorial empires (after Wilkinson, 2003).

Some of the earliest evidence for water management is Bronze Age in date, such as, for example, historical accounts from Mari and Tell Fray, both on the Euphrates. However, archaeological evidence for large-scale canal irrigation is first clearly identifiable for the Iron Age (e.g. see Ur, 2005). The centre of the Neo-Assyrian empire, the region around Nineveh, Assur and Nimrud, was well-watered by large-scale canal systems (e.g. see Jacobsen and Lloyd, 1955; Bagg, 2000b; Ur, 2005; Altaweel, 2008). Much of the rest of northern Mesopotamia was also under the administration of the Assyrians, in territories stretching to the west of the well-known Northern Iraq systems. After the fall of the empire in the late 7th century BC, the region was contested by the Babylonians and Achaemenid Persians (e.g. see Akkermans and Schwartz, 2003, p389), and subsequently controlled and contested by the Hellenistic, Parthian, Sasanian, Roman and Byzantine empires, states which were interested in ensuring a reliable water supply and in underpinning an agricultural economy in their frontier zones. This water management activity declined in the 5th and 6th centuries AD, possibly as a result of conflict and plague (Kennedy, 2007, p92-95; Morony, 2007), but irrigation and cultivation appears to have revived and expanded during the Early Islamic period (e.g. see Kennedy, 2011). After the Mongol invasion in the 13th century, irrigation up until the mid 20th century is mainly known from sources such as traveller's accounts (e.g. see Bell, 1924); on the whole, sedentism seems to have declined (e.g. see Imber, 2002, p2) presumably along with large-scale irrigation. The landscape remained less intensively cultivated, and less intensively irrigated, until the later 20th century.

1.2 Aims and research questions

The aim of this thesis is to map ancient water management in northern Mesopotamia at the time of the later empires, taking an innovative and interdisciplinary approach which uses remote sensing, GIS and archaeological survey.

Before the objectives which arise from this aim can be discussed, three initial problems need to be outlined:

1. Although research into past irrigation exists, most of it tends to be focused on specific, contained geographical regions rather than the entirety of northern Mesopotamia, or on specific states (although Wilkinson and Rayne, 2010 provides an initial discussion). This makes it difficult to draw wider conclusions about the scale and distribution of ancient water management.
2. In terms of the literature on water management and Mesopotamia, there has been a general focus on the connection between water and power (e.g. Scarborough, 2003). However, due the problem described above, any conclusions that have been drawn are incomplete.
3. For a wider-reaching study that considers the relationships between water and power, methods that enable a very large area to be examined in detail relatively quickly and cheaply are required. The current political situation in Syria and Iraq prevents fieldwork, and the damage to archaeological remains due to recent agricultural intensification and urbanisation have limited the use of some recently gathered remote sensing data (e.g. Cunliffe, 2013).

The present research t needed to mitigate against all three of the above issues. Remote sensing and GIS facilitate relatively fast and inexpensive mapping of water management features, addressing the problems with undertaking survey in Syria. Combining a range of data, both newly identified by this project and from existing sources, for example GIS and survey datasets, allowed a detailed map of irrigation across a large area to be generated. This enables a new and more regional perspective. Given these mitigation strategies, the key research questions which this study addresses can be stated:

1. Is there archaeological evidence for extensive water management systems in northern Mesopotamia, and if so, can this evidence be mapped from satellite imagery and validated using DEMs (Digital Elevation Models)?
2. Can declassified 'historic' spy satellite data be used to interpret the function, development, scale and distribution of ancient water features?
3. How can we make interpretations from these data to investigate how the later territorial empires might have imposed, incentivised and encouraged the use of water management technology?

The present research compiled the archaeological evidence for water management in a detailed database. Rather than focusing on any one piece of evidence, multiple sources were drawn upon. The whole study area was examined using CORONA images (from the Fragile Crescent Project server, originally from <http://earthexplorer.usgs.gov/> and the CORONA Atlas of the Middle East, <http://corona.cast.uark.edu/index.html>). Features recognizable as relict artificial channels were digitised; they were assigned context and chronology where possible, using existing survey and excavation reports. Several of the identified features were visited in the field in July 2010. This process enabled the identifiable features to be plotted on a map, allowing a detailed and regional-scale picture of irrigation at the time of the later empires to be developed. Further key information, including validation of function and dating, was provided by DEMs (for example, SRTM and ASTER) and survey evidence.

Once the GIS database had been generated, the mapped water management features were analysed in terms of their historical context and scale and distribution. Existing archaeological literature suggests that water management systems increase in size and complexity over time (see **Chapter 1.3**). The data collected by this study allow the development in terms of scale and distribution of water management at the time of the later territorial empires to be mapped, and the implications this had for the organising abilities and structures of these empires. In the context of this research, scale can be defined as both the size of a canal, and the overall size of the system. For example, a canal system with a main canal of over 1 km in length can be defined as large scale, while water collection using cisterns or check dams can be described as small scale.

1.3 Theoretical context and research trajectory

This thesis will discuss how the powerful later territorial empires used and developed water management technologies which already existed, expanding these into previously marginal areas and into the rain-fed zone of northern Mesopotamia, where cultivation relying on rainfall was possible, but risky. Conversely, water management in the Near East has often been discussed in terms of its ability to drive the development of states, rather than as a tool. In these

terms, the earlier states developed in areas such as southern Mesopotamia where cultivation was not possible without irrigation.

The connections between the power of states and how they managed water have been discussed by many researchers (e.g. Wilkinson, 2010, p85; Scarborough, 2003). Given that this project has examined the water management strategies of the later territorial empires, and how these developed, the theoretical context needs to be recognised.

In terms of the present study, two important concepts need to be addressed. Wittfogel's 'hydraulic hypothesis' (1957) initiated much of the interest in the connection between water and power in the ancient Near East, and so will be discussed with reference to more recent ideas. Secondly, the idea of the organising power of empires, and the differences between their centres and frontiers, will be examined.

Wittfogel

While current archaeological ideas of water management have made efforts to distance the sub-discipline from the details of Wittfogel's 'hydraulic hypothesis' (e.g. see Price, 1994 and Butzer, 1996 for arguments against the hypothesis), an understanding of how the research trajectory developed is not possible without an understanding of Wittfogel's Marxist ecological theory and how it influenced later work. The hydraulic hypothesis (Wittfogel, 1957) suggested a link between the development of irrigation and the development of powerful, and ultimately 'despotic' states.

Wittfogel translated the ideas of Marx and Engels into a more environmental theory (Worster, 1993, p32) in which the relationship between nature and humankind is significant (e.g. Foster, 2009, p9; Ulmen, 1978, p43). To Wittfogel, water was more than the

... object of utility... to be manipulated and used... tame[d] and harness[ed] (as water)... (Parsons, 1977, p64).

Wittfogel believed that water management could exert strong influence on the structure of society (for example increasing levels of bureaucracy, see Wittfogel, 1957, p39) when specific criteria were present:

It is only above the level of an extractive subsistence economy, beyond the influence of strong centres of rainfall agriculture, and below the level of a property-based industrial civilisation that man, reacting specifically to the water deficient landscape, moves toward a specific hydraulic order of life.'(Wittfogel,1957, p12).

Subsequently, research has attempted to test and question the model (e.g. for a summary of early 'testing', see Mitchell, 1973). Unfortunately, Wittfogel used very little empirical evidence to support his theories. Whether Wittfogel was right to attribute large-scale irrigation to large-scale states is a recurring theme in the literature. While some fear that Wittfogel did not do enough to define the issue of 'scale', (e.g. see Perry, 1988, p79), nevertheless, the terms 'large-scale' and 'small-scale' occur frequently as the basis for both affirmation of the hypothesis and for criticism. Specific evidence against it has frequently been cited. Robert Adams argues that Mesopotamia, an area to which significant ancient irrigation is often attributed, only adopted large-scale irrigation during later periods, at a time when states were already in existence (Adams, 1974, p4; Mabry, 2000, p287; also see Mitchell, 1973, p534). Others have also indicated that large-scale water management was a technology applied by ancient states rather than one which facilitated them in the first place (e.g. Wilkinson, 2010, p86; Lees, 1994).

It does seem to be the case that many of the later Empires and states (for example, the Assyrian Empire) intensified their agricultural basis with extensive, highly managed irrigation systems. However, especially in the early days of Wittfogel's theory some suggested that centralized organisation of water management was a necessity (for example, Steward and Murphy, 1977) that led to 'bureaucratic abuse' (Lees, 1994, p362), and indeed a kind of dependence on this organisation (Hole, 1974, p271). This school of thought focuses on the complexity of managing water; on the problems of maintenance and conflict especially. These problems could not be mitigated against without some form of 'water authority'; however it has also been argued that many issues of conflict over water rights

could be dealt with by the community, often not requiring recourse to a higher authority (e.g. Hunt, 1994, p208).

More energy has increasingly been devoted to generating case studies that question the details of Wittfogel's theory. Some of these studies demonstrate examples where smaller communities appear have organised water management themselves (e.g. Butzer, 1996, p202; Hunt and Hunt, 1974, p153; Stride et al, 2009, p73). The inefficiency of a large system has also been discussed (e.g. Hunt and Hunt, 1974, p152): the maintenance and management of extensive and large-scale irrigation may have set up such systems for failure, or inhibited their wider adoption. Indeed, it does seem to have been the case that the later Middle Eastern systems were plagued by the issues of salinisation and siltation (e.g. Christensen, 1993; Adams, 1974, p5). Smaller systems could be more sustainable, avoiding the aforementioned problems, and in addition, could be more easily managed at a local level, generally requiring less organizational investment (Lees, 1994, p371). Qanats are an interesting example of systems which can be managed by local communities or landowners rather than administered by a state. For example, recent observations of Iranian qanats indicate that some examples could have been administered by local landlords or farmers (Yazdi and Khaneiki, 2010).

As the evidence from northern Mesopotamia indicates, irrigation sometimes

seems to have been the result rather than the cause of the growth of states (Steward and Murphy 1977, p88).

In some cases powerful states, for example the Assyrian Empire, may have deliberately modified the landscape in order to intensify agricultural production (e.g. see Morandi Bonacossi 2000, p360). Wittfogel himself recognised that

...water-regulation must be carried out socially, either through a state already established through some other means... (Wittfogel 1968, p187).

The later empires operating in northern Mesopotamia support this argument; they used existing technology and methods to develop water management throughout their territories (e.g. see Wilkinson and Rayne, 2010, p3).

It is possible that different kinds of systems, managed in different ways, existed within the political sphere of the same 'state' or Empire; this might vary with reference to the differences between the 'core' and the 'periphery'. However, as it is important to recognise that inscriptions on Assyrian canal works (Bagg, 2000a, p305), for example, might give an impression of a highly state managed system, there can always be an element of propaganda present in such evidence.

The Wittfogel idea has raised more questions than it has answered; many of these being interesting and significant sources of potential research. Some believe that

Wittfogel hysterically saw hydraulic states everywhere he looked...

(Price, 1994, p192).

Others suggest that the rejection and perhaps even misuse of the theory has led to 'a misconceived view of the role of irrigation in early complex societies' (Davies, 2009, p17).

Despite this, water management does seem to have been a technology employed by powerful states in northern Mesopotamia. This is almost the inverse of the Wittfogel model; in the north powerful states imposed existing water management technologies in an area of rain-fed cultivation, rather than developing themselves as a response to water management. How empires themselves are understood must now be examined before studying how and why they might have managed water resources. This thesis is moving away from the attempts to 'test' Wittfogel's hydraulic hypothesis; rather, it aims to apply methods of remote sensing to generating a more detailed and empirical understanding of whole irrigation systems, grounded in real evidence.

Empires

This research has investigated water management at the time of the later empires. By incorporating some historical information with the GIS database and survey evidence, it is possible to discuss the distribution and patterns in how empires managed water. While it was not within the remit of this study to focus on text-based research, several sources (e.g. Bounni, 1979) contextualised and provided

dating information for some canals also identifiable using CORONA (see **Chapters 2, 5 and 6**). Le Strange (1930) was the principle source used for the Early Islamic data.

Although the Mesopotamian languages lacked a word for empire (Larsen, 1979, p91), empires can be defined very simply as 'political mechanisms for capital accumulation' (Sinopoli, 1994, p161). The degree of control exercised and autonomy experienced across an empire is also part of their definition; while some earlier research insisted perhaps too rigidly that no regions within an empire could be 'sovereign' (Taagepera, 1978a, p113), more recently empires have been described as very varied structures, mixtures of centrally controlled and semi-autonomous provinces and client kingdoms (e.g. see Sinopoli, 1994, P160). The Neo-Assyrian empire conforms to this model, comprising intermixed provinces and client states (Bedford, 2009, p42). It may be the first true 'territorial' empire.

The differences between how the centres and frontiers of empires were managed need to be recognised. While it is indeed not simple to define (Larsen, 1979, p93), the 'core and periphery' concept may need some clarification. Typically, the centre of the empire is seen as being a tightly managed core of the central bureaucracy. The capital city, the core, would usually be the political, economic and religious focus of the state (Matthews, 2003b p134). With greater distance, this control weakens or changes, with the most peripheral parts of the empire being semi-autonomous. The restructuring of relations between the differently controlled parts of an empire can be complex and deliberate (Eisenstadt, 1979, p22).

The degrees of control empires exercised over their territories has implications for the understanding of how they managed water resources. There is evidence in some cases of empires investing significantly in irrigation in the centre of their states; the Neo-Assyrian canals in Northern Iraq are an example . Interestingly, evidence for similarly intensive canal construction elsewhere in the Neo-Assyrian lands is less well known, despite evidence for Assyrian canals in the Habur (e.g. see Kuhne, 1991; Ergenzinger et al, 1988). Other empires also invested in water management at their centres, including the Roman and Early Islamic empires; evidence of irrigation outside the core imperial areas exists in these cases, however.

Some research has specifically related the presence or absence of water management remains to the frontiers of empires. For example, Decker suggested that a lack of investment in irrigation in the 6th and 7th centuries was related to instability in the Byzantine/Islamic frontier zone (Decker, 2007, p251). Other research identified integration of water management and defence, which can be illustrated here by the canals and cisterns at Resafa (e.g. see Brinker, 1991), and also further afield at the Gorgan Wall in Iran (see Wilkinson et al, 2013). Scholars agree that expansion is a crucial, and indeed defining, activity for all empires: expansion obviously provides more power for rulers (Burbank and Cooper, 2010, p9-10), and regular revenue (Larsen, 1979, P42). Expanding cultivation into formerly marginal and uncultivated, unirrigated, lands would have been one facet of this. For example, the activities of the Early Islamic state brought these kinds of lands into cultivation, often using irrigation, providing tax incentives to wealthy individuals who undertook this work (Kennedy, 2011, p181-182).

Research trajectory

The theoretical debates outlined above have formed a backdrop to research into ancient water management in the Near East. However, water management may well be more complex than the previous theories indicated (Scarborough, 2003, p19). Certainly, the Wittfogel theory is not evidence based, and lacks any empirical data. In order to understand how the later empires managed their water resources, a more detailed dataset is needed, along with a focus on later periods (e.g. Taagepera, 1978a, p123) and with more interdisciplinary outlooks and skills (Matthews, 2003b, p153; Sinopoli, 1994, p173).

Given this, this project has applied an interdisciplinary approach with an emphasis on remote sensing to generate an evidence-informed approach to understanding how water may have been managed by the later empires, within wider hydrological, geomorphological and environmental contexts.

In order to understand how the later systems might have developed, the evidence for earlier ones can be summarised here. While there is evidence that water management systems existed prior to the Iron Age, in most cases this is nto

comparable to the data for large-scale irrigation at the time of the later empires (see chapters 5 and 6). Some of the earlier data is Bronze Age and derived from botanical evidence. Evidence from research into phytoliths suggests that they can be an indicator of whether or not crops received additional water (Rosen and Weiner, 1994; Jenkins et al, 2011, p347).

Data about Bronze Age irrigation is also contained in some historical texts, for example referring to water abstraction in the Balikh and a canal at the site of Tell Fray (e.g. see Villard 1987; Bounni 1988). Canals in the Habur may also have initially been used in the Middle Assyrian period (see Ergenzinger and Kuhne 1991; Ergenzinger et al 1988).

It is important to note, however, that there is little evidence that many of these systems were larger-scale, reticulated canal networks. Pre-Iron Age irrigation may have consisted mainly of smaller scale offtakes and water harvesting.

The existing research has approached the subject from a number of disciplines. In some areas, research initially focused on monumental canals associated with high-status sites (e.g. Dalley, 1994), using historical sources and inscriptions as a main source of evidence. Archaeological work has produced surveys and excavations of canals, offering a more detailed impression of their morphology and enabling an understanding of potential irrigable areas (e.g. see Harper and Wilkinson, 1975; Wilkinson, 1998).

Aerial survey and remote sensing techniques have also been used to map relict irrigation. This way of gaining a wider perspective of a landscape has been used in archaeology in the Near East since the early days of the technology (e.g. see Poidebard, 1934); some of the earliest aerial analysis to record ancient water management identified canals around Samarra (Beazley, 1919, 1920). A somewhat later example includes the uses of aerial photographs to map extensive canals in the Habur (Van Liere and Lauffray, 1954-55). More recently, Ur (2005) and Altaweel (2008) used CORONA images to map irrigation in specific areas of northern Iraq.

This thesis also uses remote sensing, but applies it over a much wider scale, across the zone of northern Mesopotamia. Techniques such as image

interpretation and hydrological analysis are combined with archaeological survey data and historical information. This interdisciplinary approach facilitated the recording of many known features using CORONA satellite imagery for the first time, and also identified and mapped previously unknown features (see **Chapters 5 and 6**). By analysing the data over such a large region, an evidence-based understanding of the scale and distribution of ancient water management can be gained.

1.4 Environmental context

The distribution of ancient water management features is affected by the availability and type of water resources. The project area lies within the so-called 'zone of uncertainty' (e.g. Jas, 2000). In this region of northern Mesopotamia, rainfall is often low and highly variable (e.g. Dennett et al, 1984); making reliance on precipitation alone risky. However, resources are available for irrigation in the form of permanent natural channels, ephemeral wadis, occasional runoff and as ground water.

Any study of water management in the area of northern Mesopotamia needs to consider the climatic, hydrological and geomorphological contexts in which ancient agriculture operated. The contextual information will be outlined here. The modern climate and its drivers will firstly be summarized, with a description of current hydrological regimes and precipitation trends. Secondly, land use in terms of agriculture and water management will also be indicated, with a discussion of current research into past climates through the use of proxies.

The Jazira is located in the sub-tropical high pressure belt; precipitation occurs in the winter, and, due to subsiding air, dry conditions prevail in the summer (Wilkinson, 2003, p17), with maximum rainfall in January (Fisher, 1978, p64). To the north of the Jazira, the presence of high uplands forces currents of air to rise, which influences the pattern of rainfall for much of the fertile crescent (ibid, p66). **Figure 1.3** shows that the locations of isohyetal lines of average rainfall are shaped, to a general degree, by the region's topography (in some parts of the area shown in **Figure 1.3** the locations of mountain ranges have influenced the

locations of the isohyets); the rainfall data can be compared with the SRTM elevation data.

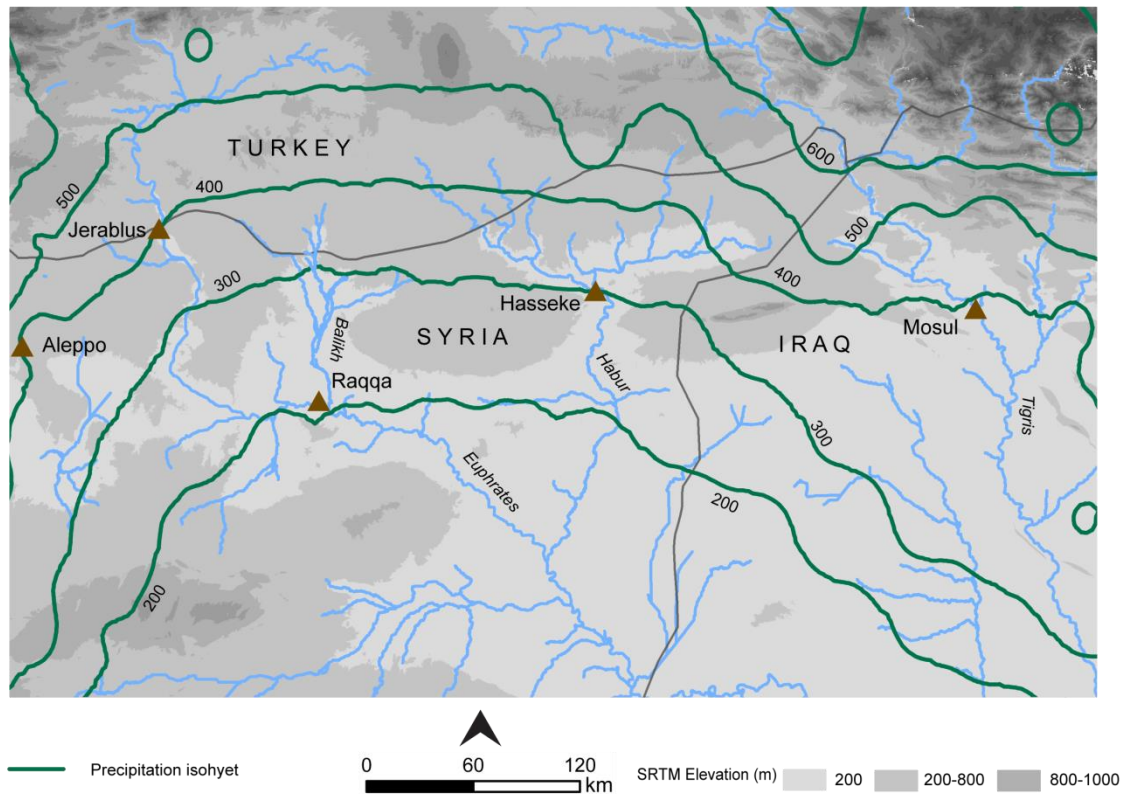


Figure 1.3: Average precipitation in northern Mesopotamia, based on the GPCC Full Data Product Version 6 between 1980-2010. Background: SRTM.

Around 200-250 mm per annum is often defined as the amount of rainfall needed when it is used as the main water source for agriculture (e.g. see Wilkinson, 1994, p484; FAO and UNESCO, 1962); when less than this is generally the norm, irrigation becomes a necessity. However, many archaeological sites are found in this marginal zone, right at the edge of rain-fed cultivation: this is inevitably a region where agricultural practice is linked to water availability, both in terms of rainfall and in terms of rivers and streams (see Riehl, 2009, p94).

While rain-fed agriculture has often predominated, including in the recent past (Beaumont, 1996, p137), in the marginal zone of northern Mesopotamia precipitation is also highly variable. It is all too easy to view averages of yearly rainfall data in the form of isohyets as boundaries similar to contour lines, however, the averages, while informative, mask a considerable degree of

variability. If a high proportion of years are dry the agricultural economy will be disrupted; while conditions in the past may have been wetter or drier, the potential for variability was presumably the same. Some studies have attempted to calculate the probability of rainfall in the Near East (Dennett et al, 1984; Weiss, 1982); for example, the model of Dennett et al used daily rainfall data and suggested a high probability of dry spells in March and April at Aleppo (1984, p326). Rain gauge data were used by this thesis to model the variability of rainfall data from the years 1981-2010 (see **Chapter 3**). In general, existing studies of rainfall patterns were constrained to shorter datasets without the use of the interpolated grid used here (e.g. Dennett et al, 1984). The present analysis uses a longer, gridded dataset and reveals that much of the study area lies within a zone where only 10-15 out of 31 recent years received enough rainfall to cultivate without irrigation.

Wallen's method (1967) was applied to the GPCC (Global Precipitation Climatology Centre) rain gauge dataset in this case. This method calculated values of interannual variability relative to the mean values, summing the differences between each year; this value was then divided by the mean rainfall (see **Chapter 3**). The present analysis uses a longer dataset, in this case for the period 1980-2010 (GPCC Full Data Product Version 6). The use of computer statistical packages and GIS made it possible to extrapolate and display these estimates for a large geographical area.

The differences in amounts of rainfall from year to year were compared against the mean, generating an index of mean relative interannual variability (shown in **Figure 1.4**). The validity of these data for making assumptions about rainfall should be assessed. The IPCC indicate the need to qualify uncertainty carefully (Matschoss et al, 2010, p3). The GPCC describe the Full Data Reanalysis product as of 'higher accuracy' than some of their other datasets (see Schneider et al, 2011, p3). However, factors such as relatively sparse rain gauge data and the possibility of measurement error could be limitations; these are discussed in detail in **Chapter 3**.

It can be problematic to attempt to apply modern data to the past. However, while the period preceding the Iron Age may have been wetter than conditions are today

(e.g. see Wick et al, 2003, p673), aridity may have been more comparable to the modern situation in the subsequent period of the Later Empires (Iron Age onwards). Although the available proxy data are limited, they appear to indicate a trend towards increasing aridity (see Wick et al, 2003, p673; Bar-Matthews et al, 1997, p166).

Much of the study area falls within zones where variability can be as high as 30-50%. It is therefore not surprising that when states want to ensure more reliable yields, above subsistence level and often for purposes of taxation, water management strategies are adopted; such decisions were made by powerful past empires as well as by modern states.

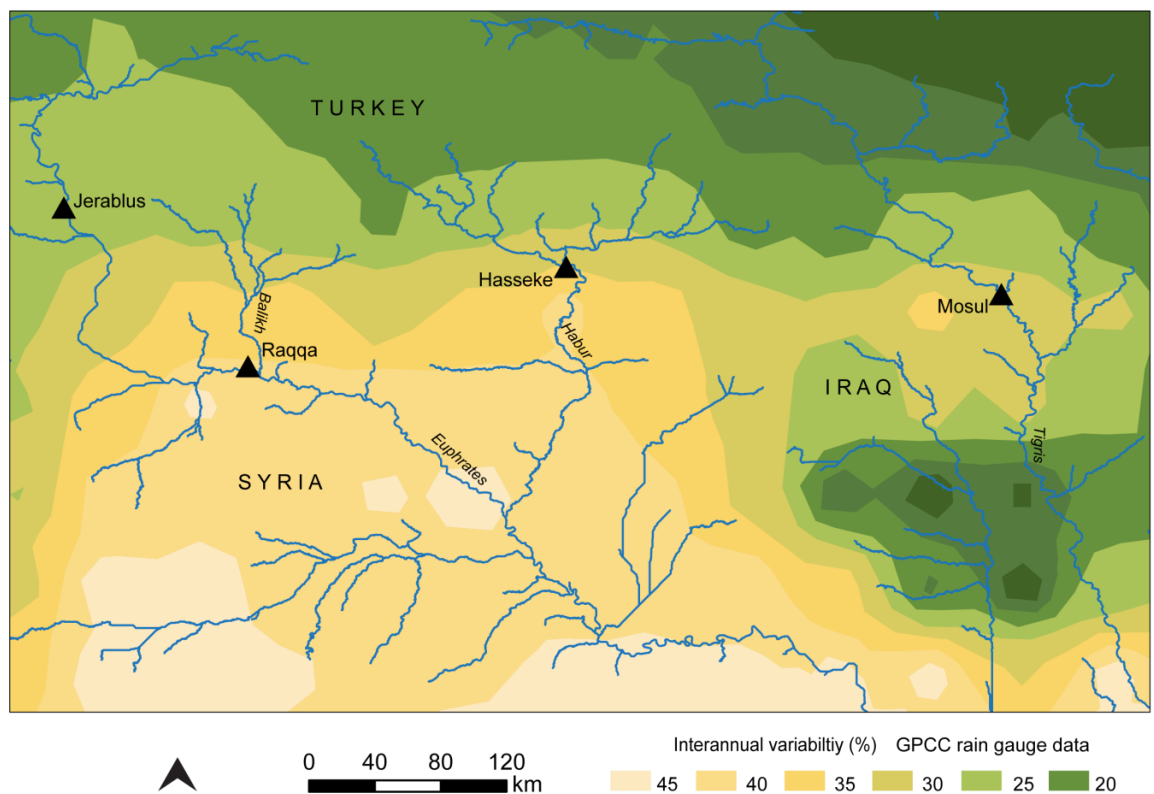


Figure 1.4: Mean relative interannual rainfall variability in Northern Mesopotamia. Based on the GPCC Full Data Product Version 6 between 1980-2010.

Irrigation offers a way of ensuring more reliable yields by mitigating against temporal and spatial unevenness; it allows for the storage of water at times when it is abundant so that it can be used when it is scarcer, for example in cisterns or using dams. It also includes transporting water resources to the areas in which cultivation occurs, by using canals to channel water to fields away from a river or

stream. Diverting water in a canal from an upstream location, for example on the Euphrates, allows a downstream area to be irrigated which is elevated above the river level.

The drainage basins of the northern Syrian and Iraqi parts of the Euphrates and Tigris form the project area. These rivers and their tributaries (notably the Balikh and Habur) provide water for irrigation, obtaining much of their water from catchments in Turkey (Kolars and Mitchell, 1991, p81), and also to a lesser degree from Syria. The Tigris floods annually in April; the Euphrates floods in May (Fisher, 1978, p366). However, like rainfall in the region, the annual floods are variable (Kliot, 1994, p111), necessitating careful water management both currently and in the past.

Occasional events of high runoff can occur throughout Northern Mesopotamia, with water sometimes channeled by seasonal wadis which are otherwise dry. While there is evidence that in the past temporary sources of water such as runoff and flood water were utilized in the Near East (e.g. Lavee et al, 1997; Berking et al, 2010; Beckers et al, 2013) uncontrolled, high-volume flow can conversely be catastrophic to cultivation, damaging canals and crops.

The above hydrologic characteristics of northern Mesopotamia have generated a complex geomorphological history. Traces of this have been mapped, including relict terraces and meanders of the Euphrates (e.g. Demir et al, 2007; Sanlaville and Besancon, 1981). The CORONA images reveal the patterns of past meanders. The relationship between the dynamism of the Euphrates and archaeology is significant; the river often removes archaeological remains. This includes irrigation features dating to the time of the later empires. For example, **Figure 1.5** shows the truncation of a canal near Tell Fray, between Dibsi Faraj and Raqqa. Irrigation in the floodplain of the Euphrates itself therefore probably post-dates the medieval period.

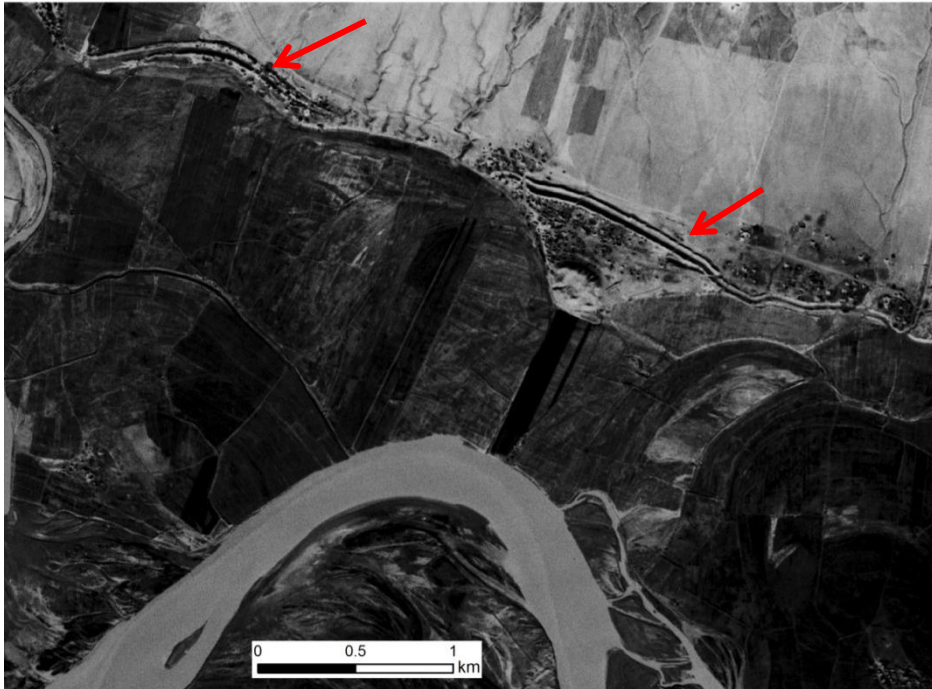


Figure 1.5: CORONA image of truncated canal along Euphrates. Mission KH-4A, 22 January 1967.

The tributaries of the Euphrates are also dynamic. The Balikh Valley is an example where there are clear traces of a paleochannel in the north, left dry after the river avulsed, and a relict valley created by a former course of the Balikh in the south (Hritz, 2013a, p1978). Another example is the Wadi Amarna near Jerablus, which is now dry, but evidence of past high episodic flows is indicated in exposed sections through its alluvial fills (see **Chapter 5**). Many other dry channels can be traced in the landscape, some revealing relict drainage patterns dating to the Pleistocene (Berking et al, 2010, p819) and some which flowed more recently.

The hydrology and geomorphology of specific channels will be discussed in more detail in the results chapters; the hydrologic regimes and development of specific channels have a direct impact on the presence and survival of past irrigation features.

Land use

An understanding of the modern agricultural situation in the Near East allows it to be compared with the archaeological and historical data and secondly also makes it possible to recognize how modern land use impacts on the survival of archaeological remains and affects any interpretations of the landscape. Given that canals are constructed in the specific locations suitable for irrigation, they are often erased and replaced with new systems. The factors which govern land use in the Near East will be summarized below: the types of crops grown, current irrigation strategies and soil management issues will be outlined.

Barley and wheat are the most commonly grown crops (Anderson, 2000, p177) in northern Syria and Iraq. Wheat is planted on around 60% of cultivated land, much of which is irrigated (Yigezu et al, 2013, p15). However, in drier areas, where rainfall is less than 300 mm per annum, barley predominates. Cotton (Anderson, 2000, p177) and sorghum are also grown. The latter is fairly drought resistant and can also tolerate some waterlogging, calcareous soils and moderate salinity (Young, 1976, p311), making it a good choice of cultivar in more marginal lands in the Near East.

Agriculture in semi-arid environments is constrained by the distribution and timing of water resources. In order to take advantage of winter precipitation, crops are generally sown in the autumn and harvested in May-June (Charles et al, 2010, p186). The crops are most dependent on watering during the stages of reproduction and grain filling (Karrou and Oweis, 2012, p95). Water must therefore be supplied at this time either through precipitation or irrigation; if the availability of water in sufficient quantities does not coincide with these crucial growth stages, it will need to be stored, and/or transported from further afield using irrigation.

Ancient and modern agriculture has also been constrained by soil quality, and at the same time has had an effect on it. While there are some extensive areas of good soil in the Jazira (Charles et al, 2010, p186) there has been long-term soil removal and loss of vegetation due to human activity (Fisher, 1978, p75). Dryland soils tend to contain products of weathering such as calcium carbonates and salts (Jewitt, 1966, p105), making them more suitable for grazing than for cultivation. In contrast, the alluvial river valleys are more conducive to agriculture because the

soils are capable of holding more moisture (Jewitt, 1966, p109); such areas therefore become the foci of cultivation.

Shown in **Figure 1.6**, gilgai are soil features found in the study area, especially in the Balikh Valley. These consist of depressions accompanied by low mounds, formed by the expansion of soil after wetting (Young, 1976, p189). Significantly, they often arise in areas of former irrigation, indicating that they may sometimes also be the result of human activity. This topic will be explored in later chapters.



Figure 1.6: *Gilgai in the Balikh Valley. CORONA image 22 January 1967.*

In order to ensure longer-term yields some degree of soil management is necessary. For example, the method of fallowing was practiced in the past; this increases soil nitrogen and water storage. Manuring was also employed, represented by scatters of material on the ground surface, which were contained within deposited refuse, and are evidence for the longevity of this practice (Wilkinson, 1982; Whyte, 1966, p349). Different tillage methods can also conserve soil (e.g. see Morell et al, 2011; Sommer et al, 2012).

Salinization is a significant problem that affects soils in the arid and semi-arid zones, due to high evapotranspiration caused by high temperatures: In Iraq, 80% of the soil area was classed as saline in the '70s (Fisher, 1978, p85). Most simply, the problem is caused by drying of the soil surface, which leads to the capillary rise of salts. Waterlogging can lead to a rise in the water table and exacerbate this problem, sometimes caused by over-irrigation. However, mitigation can be employed through leaching and draining of the affected soils; in **Chapter 4** these issues and processes will be discussed in more detail.

Recently, agriculture has become more intensive, necessitating the construction of large-scale irrigation projects. As well as agricultural usage, urban, domestic and industrial demands have also grown (Fisher, 1978, p37), putting even more pressure on water resources. While traditional surface canal irrigation is the predominant method used for agriculture (Yigezu et al, 2013, p14), pumps and sprinklers are also common.

Since the early 20th century, major irrigation schemes have been proposed and implemented for Mesopotamia (Willcocks, 1917, p2). Interestingly, one proposal suggested copying constructions used in antiquity (Willcocks, 1917, p4). More recently however Turkey's GAP scheme (Southeastern Anatolia Project) is impacting on the water resources of its co-riparians Syria and Iraq, with potentially serious results. This project involves irrigation and hydro-electric power programmes (Anderson, 2000, p176), with a proposal to irrigate 5.9 million ha of land (Kolars and Mitchell, 1991, p1). As a result of this scheme, Iraq is likely to face water shortages in the immediate future, with Syria following (Kliot, 1994, p148); as much as 98% of the flow of the Euphrates comes from Turkey (Kolars and Mitchell, 1991, p222). Much of this will be wasted: a significant proportion of the resources are likely to be lost through the problems of leakage that are well attested in arid regions (Cantor, 1967, p50). There will also be a loss of water in the Euphrates-Tigris system due to evaporation and infiltration (Jones et al, 2008, p71). In addition, the use of motor-driven pumps and sprinklers has increased; sprinklers waste up to 50% of the water used due to evaporation (Fisher, 1978, p37).

While returns must be seen as worthwhile in the short term, this kind of water management is not sustainable in the long term. Methods such as pumping can lead to additional problems when overused: for example, groundwater levels in Syria have dropped rapidly since the 1980s (Yigezu et al, 2013, p14). Conversely, poor drainage can lead to problems of waterlogging.

Finally it must be recognized that the problem is not just one of quantity, but also one of quality. Poor-quality, saline water draining from irrigation works in Turkey would re-enter the system (Kolars and Mitchell, 1991, p255) in Syria. In the 1990s, the Balikh had run dry due to abstraction for irrigation. However, from the mid 1990s, it began to flow again as a result of outflow of waste water from the Harran Plain to the north. Much of the project area is now watered mainly by big irrigation schemes such as the Tabqa dam, with water carried over large distances in open canals. Huge irrigation schemes continue to replace earlier, long-term systems, potentially with problematic results (e.g. see Beaumont, 1996).

The proxy evidence for palaeoclimate

The modern situation in terms of climate and land use has been summarised above. In order to relate this to water management at the time of the later empires, however, the nature of past climate needs to be addressed. While there can be uncertainties when dealing with proxy data, evidence would seem to suggest that the climate at the time of the later territorial empires, beginning in around 2000 BC, was comparable to the present time, although there have been minor fluctuations (Bar Matthews et al, 1997, p166); this would make a general comparison with the modern rainfall patterns and data worthwhile. The evidence for past climate will now be summarised.

Proxy data from sources such as lake cores, cave sediments and ocean cores can give an indication of how climate has changed (e.g. see the research discussed by Staubwasser and Weiss, 2006; Wick et al, 2003). Material such as pollen and charcoal can be obtained within lake cores (Charles et al, 2010, p189). These can be subjected to isotope and chemical analysis; techniques that also can be applied to sediments from caves (speleothems).

The pollen evidence from the Middle East indicates a drying of the climate from around 4200 BP (e.g. see Wick et al, 2003, p673), although it is important to note that it can also reflect changes in land use, often initiated by humans. Pollen remains, when they can be dated, indicate which tree species were most prevalent at which time and in what quantities; this can both reveal information about the climate, and about the effects of human activity on the landscape. One of the nearest pollen cores to the study area was obtained from Lake Van in Turkey: In general, the evidence from this core indicated that tree species declined between around 4200-3500 BP. This might indicate increasing aridity (Wick et al, 2003, p673). Conversely it could represent tree clearance by humans (Wilkinson, 2003, p27). It is important to note therefore that in some cases the pollen evidence might indicate human activity rather than climate change. Information about crop species grown at this period is complementary: the predominance of more drought resistant crops in the Middle Bronze Age (Riehl, 2012, p115; Riehl, 2009, p158) also suggests aridity and changes in land use. Similarly, pollen data from the Dead Sea indicates drier and warmer conditions from around 3200 BP (Litt et al, 2012).

The isotope evidence gives similar results. A well-known source of data comes from Soreq Cave in Israel: differences in the equilibrium of isotopes within growth layers of stalagmites were analysed (see Bar-Matthews et al, 1997). These sediments are affected by water and temperature, and as such can give a record of climate. While the resolutions of the datasets are different, the Soreq Cave evidence suggests that rainfall amounts for the period of 7000-1000 BP are similar to those of today (ibid, p166). Kalayci (2013) used the link between modern average rainfall patterns and the isotope values derived from Soreq cave to extrapolate Bronze Age rainfall (e.g. see ibid. p103-105); using these data, he estimated that precipitation reached low values by 2800-2000 BC (ibid. p105), reinforcing the trends suggested by the other records. Similarly, the isotopic composition of carbon and oxygen in carbonate coatings on stones at Gobekli Tepe in Turkey also showed a trend towards higher temperatures and higher aridity through the Holocene (Pustovoytov et al, 2007).

Isotopic balances in plant remains can also be revealing. For example, this evidence indicates increasing aridity from around 2000-1600 BC in North East Syria (Riehl et al, 2008, p1011). Similarly, juniper charcoals from Arslantepe in

Turkey indicated an arid summer climate in around 2200 BC (Masi et al, 2013, p70).

The limitations of the proxy evidence should also be noted. There is some degree of uncertainty about past climate conditions. First, it is important to take care when extrapolating from one climate zone to the next. In addition, to an extent, the fine details of this information are lost due to what is often relatively coarse resolution. Evidence is restricted to proxy information which has been preserved, even if it is far enough away from a study site that local variations will be lost. Evidence is also restricted temporally; there is often a lack of chronological control (see Riehl, 2007, p99). For example, stone remains at Gobekli Tepe did not yield isotopic information after around 4000 BP (Pustovoytov et al, 2007). However, the palaeoclimate research does enable the general climatic context for this project to be summarised. Analysis of plant remains and isotopes indicates that after around 4000 BP aridity in Northern Mesopotamia and the Levant increased (e.g. see Riehl, 2012, p115; Wick et al, 2003). This can also be corroborated by data from a marine core from the Gulf of Oman; an increase of aeolian dust was suggested to be representative of an increase in aridity (see Cullen et al, 2000; Roberts et al, 2011, p150). A drying, but also fluctuating, climate at the time of the later territorial empires can be suggested.

Summary and climatic implications

It was in the above climatic context that the large-scale irrigation systems of late antiquity developed. In general the climate was more arid than it had been in earlier periods, when rain-fed agriculture seems to have predominated. The change from a wetter climate earlier on in the Holocene to the present day aridity has been interpreted as a causal factor in social and political events in the Bronze Age (e.g. see Staubwasser and Weiss, 2006, p372; Weiss, 1982).

The change to aridity would have necessitated different production strategies. Rainfall quantity may have been a limiting factor for settlement prior to the period of the later territorial empires (e.g. Wilkinson, 1994), and as both the present study and Kalayci's study (2013) indicates, rainfall variation may also be significant.

Changes to more water-intensive crops in the Iron Age have been proposed, based on archaeobotanical evidence (Riehl, 2007, p112); possibly this was because irrigation was replacing riskier rain-fed methods in Northern Mesopotamia.

Despite the 'push' of aridity, irrigation is not a simple phenomenon. It requires some form of management whether at a local or state scale. Empires had the political and economic resources to irrigate, and also the incentive of needing to maximize yields in the face of variable precipitation. Water management is tied to water politics. Historical records suggest that this was the case as early as the Bronze Age (e.g. see Villard, 1987, for evidence of water conflict in the Balikh). This is an issue that has not changed; today, management of the Tigris/Euphrates system by Turkey, Syria and Iraq has the potential to have massive environmental impacts and to stimulate conflict. Turkey is in a position of water-power, having the upper riparian position, and a lack of coordinated planning between the co-riparians has been a source of complaint (Kliot, 1994, p116).

The issues faced by modern land use described in this chapter will also have applied to the ancient systems; natural conditions such as water availability and geomorphological constraints affect the design of irrigation. Similarly, competition over water resources and political drivers such as tax incentives or instability are not new phenomena and will also have been factors in the distribution and longevity of past water features.

1.5 Thesis outline

With the theoretical and environment context of the present study recognised, its structure can now be outlined. First, the project will move on to review the existing studies that have recorded water management in northern Mesopotamia. **Chapter 2** describes these geographically, generating a detailed map which in itself is a significant original contribution.

Chapter 3 outlines the methods used to map known water management features and locate and map previously unknown features. The image interpretation used for the initial digitisation is described, followed by explanations of the DEM processing and interpretation used to confirm the results and understand the

hydrological context of features. The typical forms and functions of these features and systems are explained in **Chapter 4** with reference to the literature of irrigation design and construction.

Chapters 5 and **6** present the results of the remote sensing study. In **5**, which is organised spatially, a description is given of the results of locating known features using CORONA, and of identifying newly discovered features. The results for the Balikh Valley are discussed in a separate chapter (**6**) because water management in the Balikh is particularly complex when compared with data from the rest of the study area.

Finally, the implications of the results are discussed in **Chapter 7**. These will be considered in terms of assessing the original contribution of the present study, of how its findings can be validated, and of the theoretical framework in which they were analysed. The implications of the results in terms of chronological and distributary patterns are investigated. **Chapter 8** concludes the study and examines the potential for future research.

Chapter 2: Spatial Literature review

2.1 Introduction

Given the interdisciplinary nature of this study, it is not within its remit to outline all the research into ancient occupation of northern Mesopotamia, nor is it possible to discuss in detail the many irrigation systems of southern Iraq, which have already been researched by several scholars (e.g. Pournelle, 2013; Hritz and Wilkinson, 2006; Adams, 1981, 1974; Gibson, 1972; Jacobsen, 1960). Before a summary of the northern irrigation systems is given, however, the key differences between southern and northern Mesopotamia can be outlined here in order to contextualise the differences between the present study and Wittfogel's (1957) hypothesis.

While irrigation in southern Mesopotamia has been linked explicitly to the development of the totalitarian power of early states in the region (Wittfogel, 1957), water management in northern Mesopotamia may have taken a different trajectory. Geomorphologically and climatically the south is also different from the north, with rivers forming raised levees, and much lower rainfall. Wilkinson has suggested that early irrigation may have been more concerned with modifying and maintaining the natural channels than with constructing new systems (Wilkinson, 2003, p85). More comparably with northern Mesopotamia, large-scale canals are known for later periods, from at least as early as the Neo-Babylonian era and into the Early Islamic (Wilkinson, 2003, p92-95).

The aim of this thesis is to use remote sensing to investigate water management in northern Mesopotamia. Large-scale irrigation may have been adopted in the north later than it was in the south, and was used to make agriculture more reliable, rather than simply to make it possible (see Wilkinson and Rayne, 2010, p2-3).

The water management features summarised in this chapter have been presented in the existing literature. It is important to note here that the published work originates from multiple different perspectives and disciplines, including traditional archaeology, landscape archaeology, geomorphology and ancient history. A few

specific studies have used remote sensing. However, because CORONA images were not declassified until relatively recently, this task had not yet been undertaken for many sites.

This chapter presents a detailed overview of the existing research and establishes the need for the detailed mapping undertaken in the two results chapters (**5** and **6**). One of the original contributions of this study is the map (**Figure 2.1**), which shows the features mentioned in the literature which could be located and digitised. The results generated by this project will be added to the map, demonstrating how a more detailed perspective can be gained through the use of remote sensing. The irrigation features indicated by the existing research were examined using satellite imagery, and previously unknown features located and digitised.

Installations such as dams and reservoirs, as well as damage through agriculture and urbanism, have destroyed and obscured many sites. This makes it especially important to present a discussion of existing knowledge, because recent changes now prevent further research from being undertaken in some areas (for example, many sites are now lost underneath the lake Tabqa in Syria). It is also important to note here that traditional survey and excavation has been suspended in Syria due to the current political turmoil; several on-going projects have turned more to the use of remote sensing in the meantime (e.g. see the current project, Wilkinson and Rayne, 2010, and Hritz, 2013a, 2013b in the Balikh).

There are numerous studies that deal with particular water management systems or individual features throughout Northern Mesopotamia; these are summarised in this chapter. A detailed comprehensive study does not yet exist, although an overview of some areas and some results from this study has already been presented (Wilkinson and Rayne, 2010). There are a few volumes which compiled several specific studies, generally of disparate geographical, temporal and functional nature, including some papers relating to the Near East; for example, Bienert and Haser (2004) comprised a range of different studies, including McQuilty's study of watermills in Jordan (2004) and Bagg's analysis of Assyrian tunnelling (2004). Wikander (2000) similarly edited a volume of different specific

studies and general studies on water management, Ortloff (2009) reviewed several key examples of irrigation, Hodge (1991) compiled papers relating to features such as aqueducts and mills, and Lightfoot (2009; 1996) presented two reports on qanats throughout Syria and Iraq of the Middle East. While the locations of qanats were recorded, and the influence of the early territorial empires discussed, a detailed record of each mapped feature was generally not provided (Lightfoot, 2009; 1996). Beaumont et al also presented studies on qanats (Beaumont et al, 1989). In some cases reports from these compilations have informed this project; these will be outlined as part of the spatial literature review below.

Currently, the separate nature of the literature makes it difficult to understand wider regional issues; a detailed understanding of the chronology and distribution of water systems development across Northern Mesopotamia is unclear. However, this project has integrated the available data in the literature into a GIS database alongside new data described in the results (**Chapter 5**). Canal systems which could be clearly and unambiguously identified using CORONA/maps provided by the literature were digitised. This process involved rigorous decisions not to include features for which the location was not clearly identifiable. Mapping was done systematically for the whole study area, making it possible to address wider questions of the scale and distribution of irrigation. An overview of the known water systems in Northern Mesopotamia is presented below.

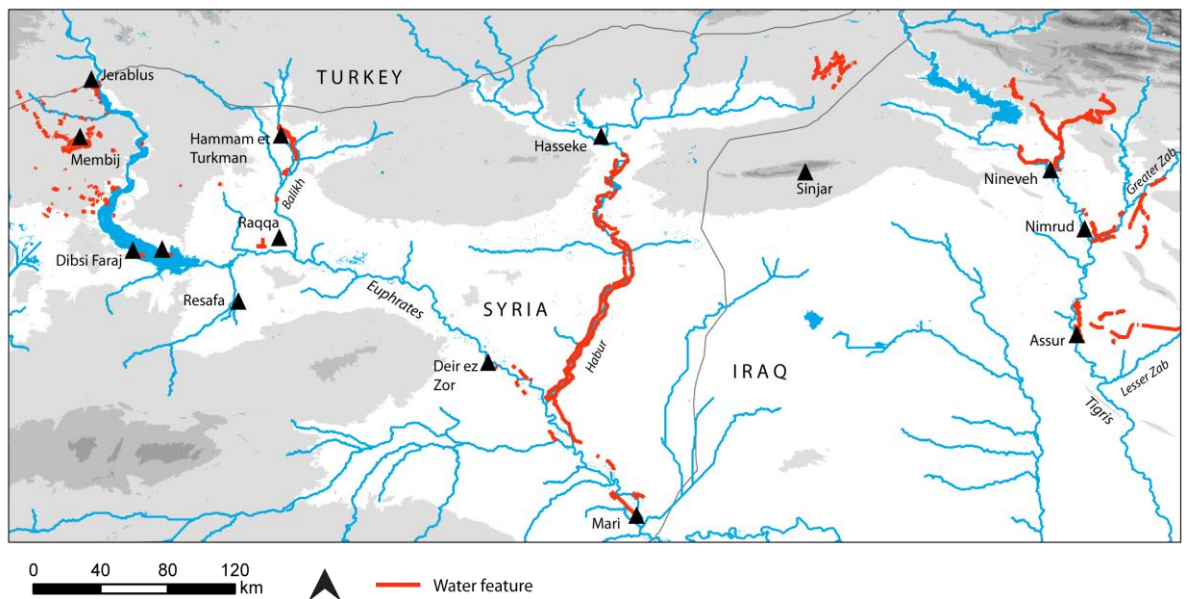


Figure: 2.1: Known ancient irrigation systems in northern Mesopotamia (see below for more detailed maps and information on each region).

Known water systems in northern Mesopotamia

2.2 Jerablus

The region close to the Syrian-Turkish border is the starting point for this study. The floodplain terraces adjacent to the Euphrates, the valleys of several tributaries and the limestone uplands to the west contain the remains of water management features. As in the rest of the study area, cultivation that relies on rainfall holds some degree of risk. Precipitation in the Jerablus region is around 400mm per year, but with an interannual variability of about 25-30% (see **Chapter 3.6**, GPCC data). The geomorphological and climatic conditions of the region have been outlined by Besancon and Sanlaville (1985) and Wilkinson et al (2007).

Research into settlement remains and other landscape features has been undertaken in the region by several projects. Early archaeological research focused on the monumental site of Carchemish (Woolley, 1921). Surveys were later undertaken in the Upper Euphrates region (e.g. see Copeland and Moore, 1985; McClellan, 1999). Recent research has adopted a landscape approach and recorded 80 archaeological sites as well as off-site features such as canals and

routeways, as part of the Land of Carchemish Project (see **Table 2.1**, also Wilkinson et al, 2007; Wilkinson et al, 2011; Wilkinson et al forthcoming).

Table 2.1: *Conduits and canals in the Jerablus region. See **Chapter 5** for images of specific features and **Figure 2.2** for a map.*

Name of canal (no. in (--) see Fig. 2.2)	Estimated date	Approximate size (W x D)	Type	Comments or reference
Jemal Canal (1)	Late Antique- Early Islamic	9-14 m wide (surface)	Euphrates canal.	Wilkinson et al 2007
Jerablus Tahtani canal (2)	Iron Age		Euphrates canal.	
Hajaliyyeh (3)	Late Antique?		Rock-cut qanat.	
Wadi Sha'ir (4)	Late Antique?	50 cm wide	Open channel.	Wilkinson et al 2007
al-Gini' at (5)	Late Antique?		Rock-cut qanat.	Wilkinson et al 2007
Nahr al-Amarna- 1 (6)	Hellen.- Late Antique?	1: 3-4 m x 2.3m 0.80m x 1.3m	Earthen canal followed by stone & rock conduit (N bank).	Wilkinson et al 2007
Nahr al-Amarna- 2 (7)	Late Antique		Rock-cut conduit (on S bank).	
LCP 18 (8)	Hellen.-Roman		Rock-cut conduit.	
Wadi Seraisat (9)	Late Antique		Rock-cut conduit.	
Kirk Maghara (10)	Late Antique		Rock-cut conduit.	Wilkinson, pers.comm
Sajur (11)	Late Antique & later			2008 season (LCP)

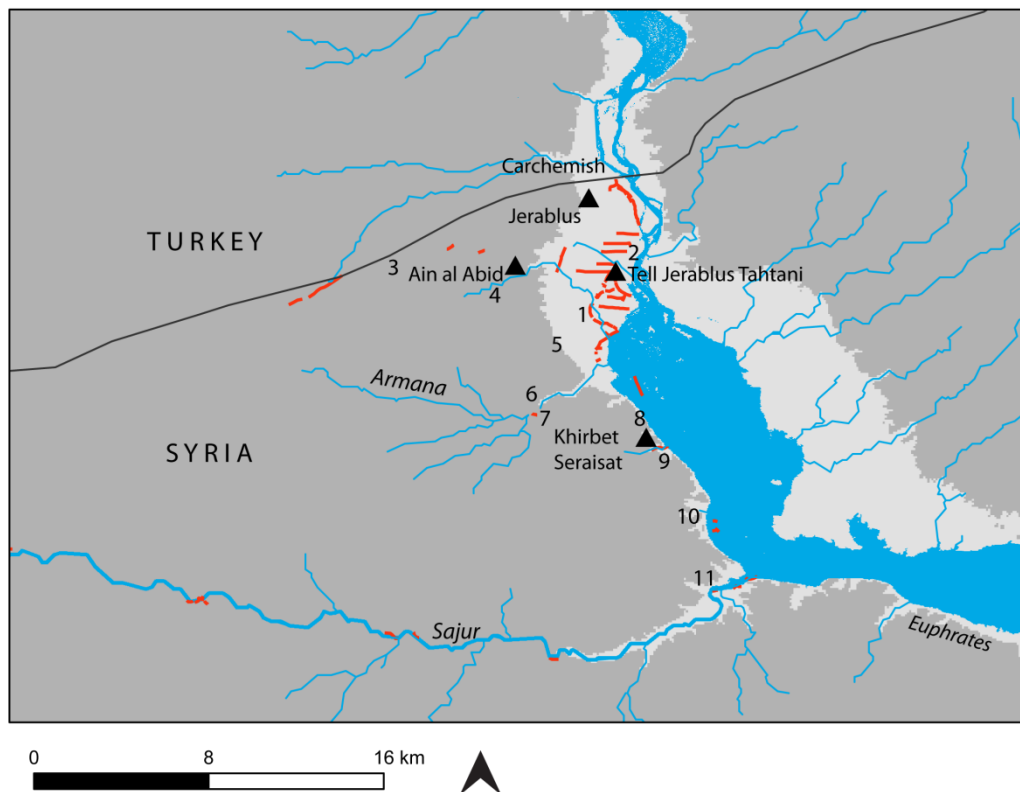


Figure: 2.2: Ancient water features in the Jerablus region (mapped by the Land of Carchemish Project, Durham University. See **Table 2.1** for numbered features).

Archaeological remains have been recorded throughout this landscape which represent the period of the later empires. Carchemish was an administrative centre of first a Neo-Hittite state and then the Neo-Assyrian empire, having already attained political significance in the Bronze Age (Wilkinson et al, 2011). Copeland and Moore (1985) recorded mainly tell sites, including evidence of occupation during the period of the later empires. The Land of Carchemish Project located tells as well as smaller sites dispersed throughout the surrounding area and dated by remains recovered from field surfaces, with occupation identified for the Hellenistic, Roman, Byzantine and Early Islamic periods (Wilkinson et al, 2007). By the Hellenistic and Roman periods, sites became less tell-based, smaller, and more dispersed (Wilkinson et al, 2007, p235), with a similar pattern persisting in the Byzantine and Early Islamic periods (Wilkinson et al, 2007, p235). For example, a notable Early Islamic site was recorded at Khirbet Seraisat (Wilkinson et al, 2007).

While earlier surveys mention water management features (e.g. see Copeland and Moore, 1985), these were not comprehensively surveyed until recently by the Land of Carchemish Project. Woolley (1921) and more recently Wilkinson et al (2007) investigated a canal at Jerablus Tahtani. This 9-14 m wide feature flowed between the village of Jemal and Tell Jerablus Tahtani. Wilkinson et al (2007) suggest, based on associated sites and pottery, that the feature was in use during the Byzantine – Early Islamic periods (p236). This survey also indicates that it abstracted water from the Euphrates, although its termination is not clear (Wilkinson et al, 2007, p236).

The Land of Carchemish Project also recorded water management features along the nearby wadis which drain into the Euphrates, including the Amarna and Sajur, both of which formerly flowed year-round. A rock-cut channel was found to have abstracted from 'Ain Abid which may have been in use from the late Roman/Byzantine periods up until some time in the 20th century (Wilkinson et al, 2007, p236). In addition, the shafts of a rock-cut tunnel were recorded along Wadi al Gini'at, to the north of Tell Amarna, although the feature could not be dated (Wilkinson et al, 2007, p236).

Another rock-cut channel was found along the dry Nahr al-Armana and was lined with dressed ashlar blocks. This channel may have cut into an earlier feature; the later channel may be Hellenistic to Late Antique (Wilkinson et al, 2007, p236), dated by the typical Late Antique claw-tooth chisel marks (Wilkinson et al, 2010, p16; Wilkinson and Rayne, 2010, p14).

At the large Roman, Byzantine and Early Islamic site of Khirbet Seraisat rock-cut water channels (see **Table 2.1**; **Figure 2.2**) were also recorded, possibly with final phases in the Ottoman period. Wilkinson et al (2007) suggest that this series of channels may have supplied settlements and agriculture on the floodplain and lower terraces. The canals consisted of several channels and a former aqueduct taking water into a canyon at the edge of the flood plain, possibly with an associated mill (Wilkinson et al, 2007, p236-239). During fieldwork in 2010 this study recorded further water management features throughout the Jerablus region, which will be outlined in **Chapter 5**.

2.3 Membij Qanats

To the south of the Sajur numerous water supply features have been recorded by Dan Lawrence and Niko Galiatsatos (pers. comm.) in the vicinity of the town of Membij (ancient Hierapolis and Bambyce). These include several qanats (mentioned briefly by Lightfoot, 1996, p333), also noted by Kamash (2009, vol.3, p9-10). While so far evidence for the chronology and significance of these is limited, historical sources suggest that there may be a religious association with the use of water in Membij. Specifically, Lucian of Samosata, writing in the Hellenistic period, recorded water features associated with a temple in the city (see Lightfoot, 2003), which may have had a ritual function (Kamash, 2010, p170). These qanats appear to have been associated with Hellenistic and Roman settlement in the vicinity of Membij (pers comm. Dan Lawrence/Niko Galiatsatos).

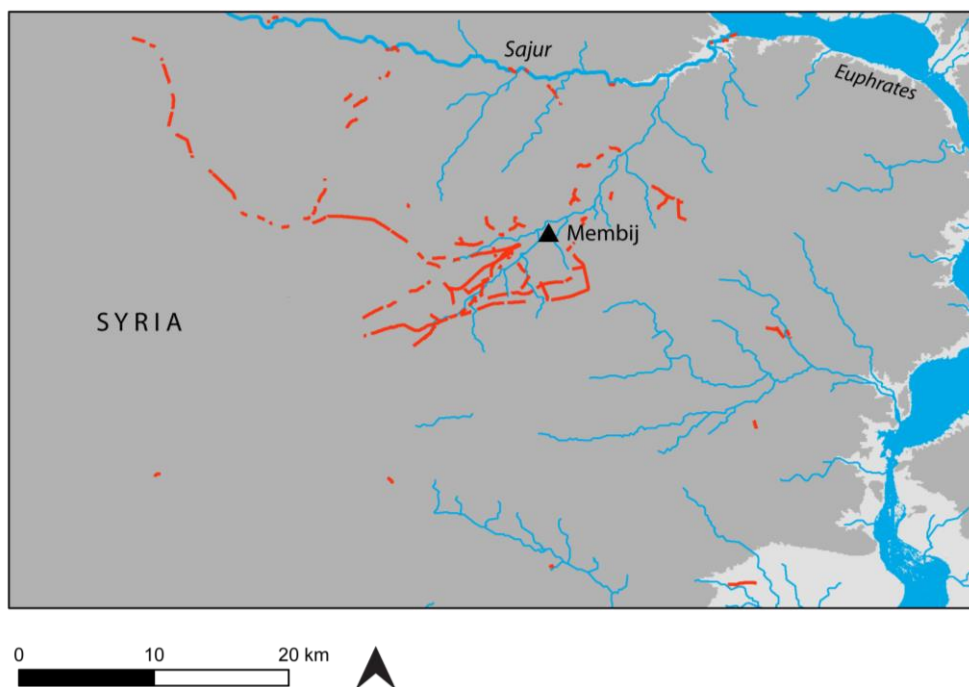


Figure 2.3: Features around Membij. Mapped by Dan Lawrence and Niko Galiatsatos (pers. comm).

2.4 Dibsi Faraj

The fortified Late Roman-Early Islamic site of Dibsi Faraj was also associated with water management features. Although they are now lost under the waters of the Tabqa Dam, excavation and survey was undertaken in the 1970s (see Harper and

Wilkinson, 1975); this project also interpreted historical sources relating to the site. Significantly in terms of its location, the Peutinger Table suggests that Dibsi Faraj was close to the route to Resafa (Harper and Wilkinson, 1975, p321). The historical sources also indicate that a canal flowing close to the site, the Nahr Maslama, was a channel built by the Ummayyad general Maslama ibn Abdalmalik in the 8th century AD (Harper and Wilkinson, 1975, p324). Dibsi Faraj itself consisted of a citadel and an outer town on the edge of the limestone steppe, overlooking the floodplain (Harper and Wilkinson, 1975, p334). Much of the site was built in the 3rd century AD with construction continuing into the 4th and 5th centuries (Harper and Wilkinson, 1975, p322). The site seems eventually have been destroyed by an earthquake in AD 859, after which occupation was limited; finally, the site was deserted from the 12th Century until modern times (Harper and Wilkinson, 1975, p324).

During excavation of the Nahr Maslama, a plaster lined conduit at a depth of 7 m was identified (Harper and Wilkinson, 1975, p337). Wilkinson estimates that the canal must have flowed at least 8 km upstream in order to have joined with the river level (Harper and Wilkinson, 1975, p337). In the 1970s, most of the channel had been eroded by the Euphrates (Harper and Wilkinson, 1975, p337), although short stretches were still present to the east of the citadel. Within the site itself, close to the north wall, two shafts were found which were interpreted as possible well shafts, connected by a tunnel (Harper and Wilkinson, 1975, p337).

The canal may be part of the same system as a canal recorded at Barbalissos, upstream of Dibsi Faraj (see Decker, 2009a, p179; Kamash, 2009, vol3 p3), although no traces of it upstream of Dibsi Faraj could be detected using the CORONA images. Historical research suggests that there was also an irrigation channel downstream at the Late Roman site of Sura (see Kamash, 2009, vol3, p3). In **Chapter 5**, CORONA images of Dibsi Faraj and its environs are presented (these were not available at the time of the original investigations) which enabled further water management features to be identified.

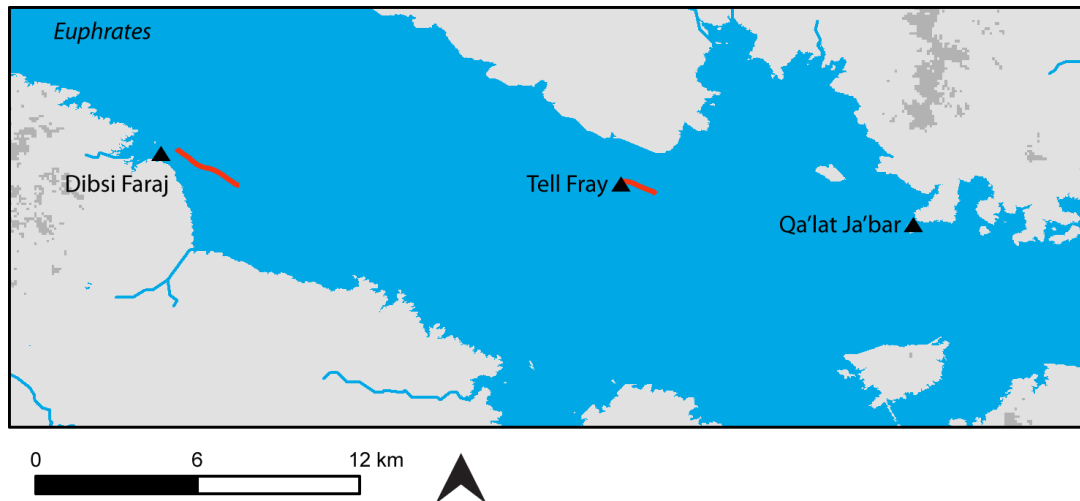


Figure 2.4: Water management features now inundated by the Tabqa Dam. The canal at Dibsī Faraj was recorded by Harper and Wilkinson (1975). The canal at Tell Fray was discussed by Bounni (1988; 1979).

2.5 Canal between Tell Fray to Qa'lat Ja'bar

Until the construction of the Tabqa Dam, the partially eroded remains of a prominent canal could be seen stretching for about 10 km along the left bank of the Euphrates. This was first visible (using CORONA images; see **Chapter 5**) about 1 km upstream of Tell Fray, passing that site, and finally terminating at Qa'lat Ja'bar. While Tell Fray and the canal are now submerged, Qa'lat Ja'bar is currently situated on the edge of the lake.

The site of Tell Fray, located within the frontier zones of the Hittite and Assyrian empires (Akkermans and Schwartz, 2003, p341), was investigated during campaigns in the 1970s. Remains of Hittite, Babylonian and Assyrian occupation up until the 13th Century BC were discovered and the location of the Tell Fray part of the canal was noted, a feature known as 'The little Euphrates' which gave the site its modern name (Bounni, 1988, p368-9). The full extent of the canal was not identified.

The ancient name of the site, Yakharisha, was identified from an examination of textual evidence from the Nuzi tablets and from texts found at Tell Fray itself (Bounni, 1979, p7). Some of the texts also refer to the canal, mentioning that an official present at the site was responsible for maintaining canals (Bounni, 1988,

p369). Bell also identified the canal, mentioning that part of it had silted up (1924, p48-49).

The CORONA images show that the canal terminates at Qa'lat Ja'bar, a fortified citadel which was a major Seljuk, Ayyoubid, and late Abbasid centre (Bounni, 1979, p7), although the existing literature did not record this segment of the feature. Contextual information for this part of the canal can be taken from research into the site. Historical accounts suggest that Qa'lat Ja'bar was abandoned after the Mongol invasions (Tonghini, 1998, p22). Excavation and pottery evidence indicate that the site was re-occupied and then again abandoned at some point in the Mamluk period. A small number of Ottoman finds were recovered (Zaazuq, 1985; Tonghini, 1998).

The site is well attested to historically. Excavations have, however, enabled the creation of pottery sequences (Tonghini, 1998) and investigated water storage devices. Zaazuq (1985) and Tonghini (1998) recorded water towers associated with the mosque, a cistern, and rock-cut channels (Tonghini, 1998, p26). Unfortunately, most of the documents relating to the 1970s and '80s excavations were lost (see Tonghini, 1998, p25). Any possible link with the canal will be explored in later chapters (see **Chapter 5**).

Unfortunately, given that the feature is now submerged, the projects summarised here did not undertake detailed investigations into the canal. Attempts to trace it over a greater distance were not made. **Chapter 5** presents the results of image interpretation undertaken by the present thesis which located a much longer feature.

2.6 Resafa

The Roman- Early Islamic site of Resafa, occupied between the 1st-13th centuries AD (Beckers 2007-9), is located well into the area where interannual rainfall variability is 40-45% (see **Chapter 1** for precipitation averages and variability). Although the average rainfall figure places the site in the 200 mm per annum zone, about 18-20 years out of 31 received less than 200 mm rainfall.

The historical context of Resafa is well known (e.g. see Sack, 2007-9). The site was strategically and politically important in late antiquity and into the Early Islamic period. Historical accounts indicate that it was linked to the Roman road system between Sura and Palmyra (Kennedy and Riley, 1990, p117), which connected to an important route on the Roman frontier, the *Strata Diocletiana* (Stark, 1966, p306). Further evidence from historical sources indicates that water management features at the site were in use in the Islamic period, during caliph Hisham's time (Beckers, 2009, p31; Hof, 2007-9, p33).

Some studies have also used archaeological approaches to record water management features. The cisterns at Resafa are well-known, originally from historical sources and also now from these archaeological investigations (e.g. Sack 2007-9; Brinker 1991).

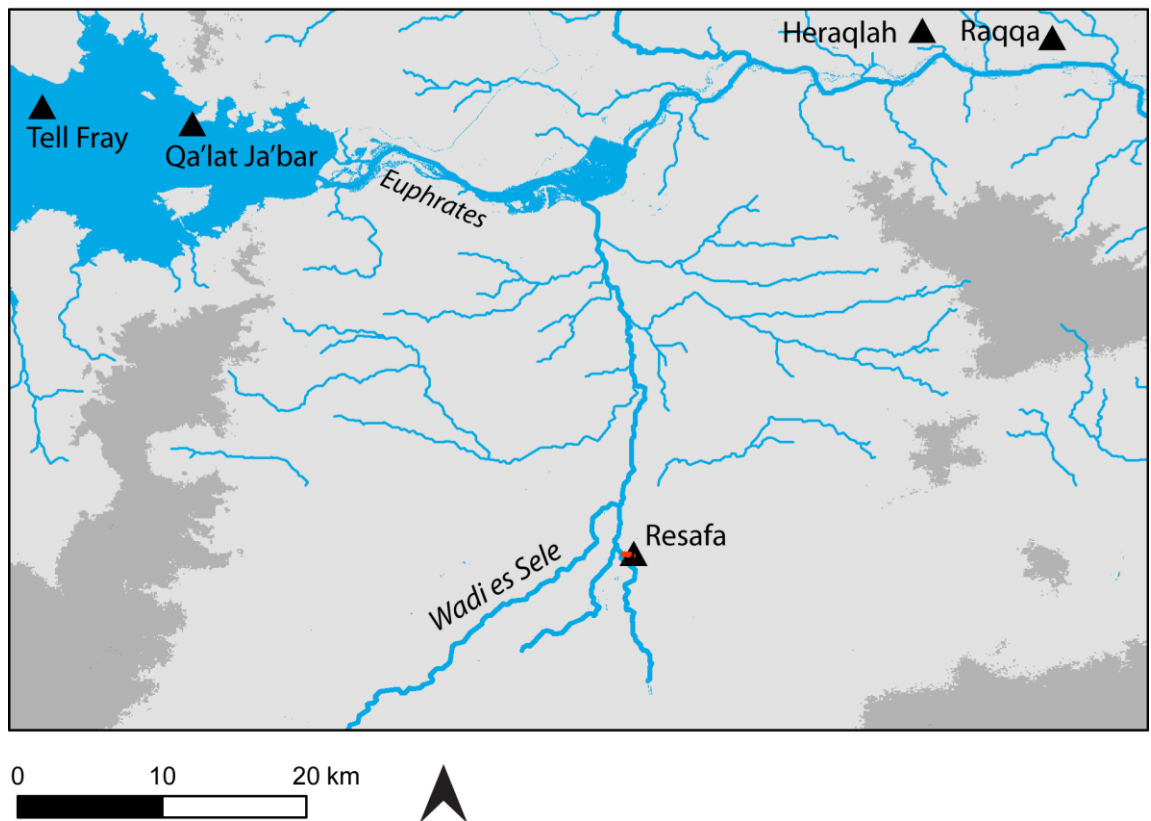


Figure 2.5: Location of Resafa on the Wadi es Sele.

Evidence for different kinds of water storage and collection devices was found. Covered bottle-shaped underground tanks (see **Figure 2.6**) and rooftop cisterns collected and stored rainwater (Brinker, 1991, p123) and functioned as an urban water supply. A 13th century source indicated that these cisterns dried out towards the end of the summer (ibid, p121). Use of groundwater was also problematic, given the brackish nature of the water accessed via wells, as described by a 9th century AD source (ibid, p120).

Far larger cisterns, also within the city walls, were fed by water brought in from outside. One of these could more correctly be termed a reservoir; Kamash's historical study of Roman water management suggests that it is the largest cistern in the Near East, with a capacity of 14600 m³ (Kamash, 2009, p142). As **Figure 2.7** shows, a dam on the Wadi es Sele directed water, via a channel, into the cisterns (Berking et al, 2010). The dam, which was recorded as being about 1.70 m high (Brinker, 1991, p140), had provision against flash floods in the form of a spillway (ibid). The point where the canal crossed through the city walls was also carefully designed; it was divided into six small channels to prevent military incursions (Brinker, 1991, p137; Hof, 2007-09, p33). It seems likely that this feature and the presence of the cisterns within the walls may have been constructed with a fear of siege in mind, as Kamash suggests (Kamash, 2009, p176).

Most recently, a rainfall-runoff model was applied to examine how the cisterns could be filled (Berking et al, 2010). The study indicated that runoff water which periodically flowed down the Wadi es Sele was collected behind the dam (Berking et al, 2010, p817). Modern daily rainfall records suggested that periodic annual rainfall events were capable of filling the cisterns and a rate of 35.9 mm within an hour would be sufficient to fill them (Berking et al, 2010, p827).

The source of Resafa's urban water supply seems clear. The existing research has also investigated how Resafa may have produced food. Berking et al suggest that there may have been small gardens alongside the Wadi es Sele, which would have been capable of producing sufficient crops to support the city (Berking et al, 2010, p819). However, it is also possible that other nearby areas such as the

Balikh, where perennial water is more abundant, could also have formed resource bases.

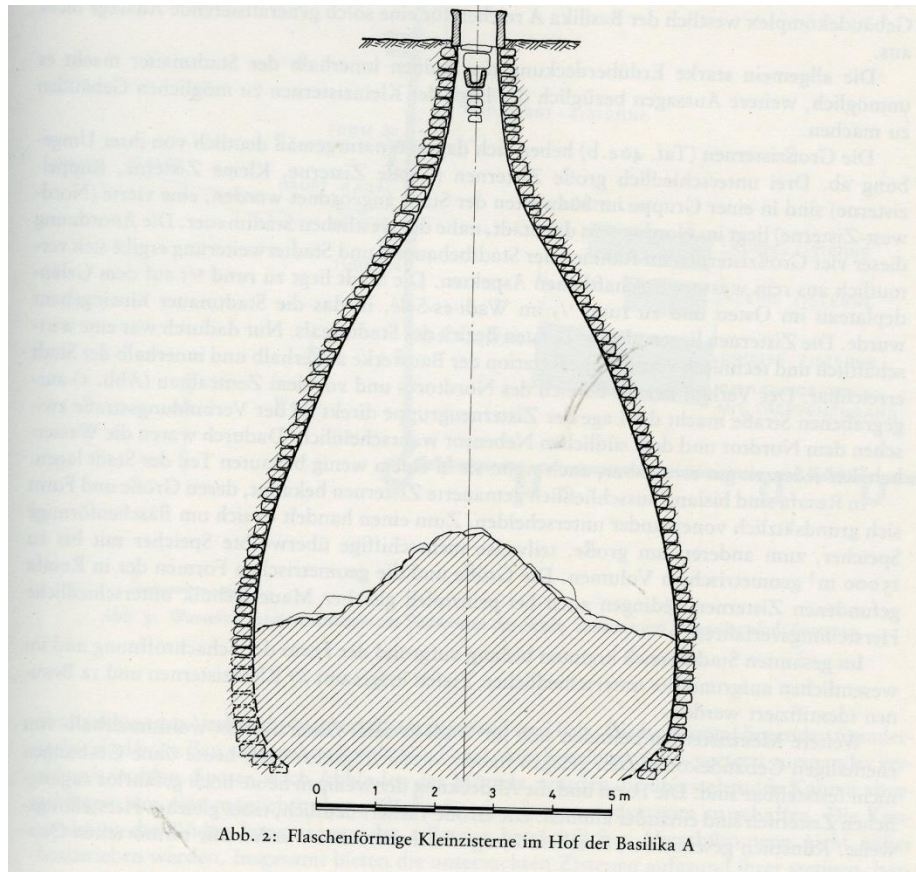


Figure 2.6: Cistern at Resafa (from Brinker, 1991, p123).

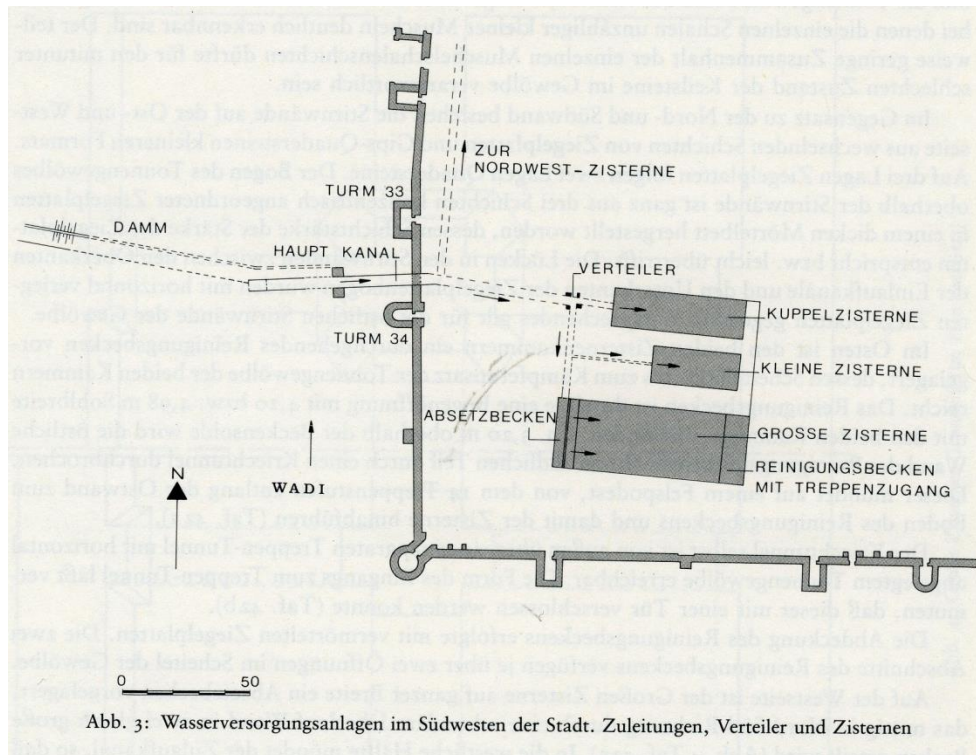


Figure 2.7: Water management at Resafa (from Brinker, 1991, p125).

2.7 Heraqlah

About 12 km west of Raqqa, water management features are apparent close to the small circular walled site of Heraqlah. Several of them have been recorded by existing research (e.g. see Toueir, 1983; Kamash, 2009), although the dating of some of these features is less clear than some reports suggest. Excavations at the site itself indicate that it is Early Islamic (Toueir, 1983).

Gertrude Bell noted the large relict canal which cuts through the walls of Heraqlah, and also another channel and associated dyke to the south at Tell Meraish, interpreting both canals as part of the same, relict, system (Bell, 1924, p54). The Heraqlah canal terminates at Raqqa and has been interpreted by some (e.g. see Touier, 1983, p298; Toueir, 1990, p217; Heidemann, 2006, p36) as Early Islamic. Toueir (1990) linked the canal to historical accounts of a feature known as the Nahr al-Nil, supposedly constructed under the auspices of the Abbasid Caliph Harun al Rashid (Toueir, 1990, p217), although he admitted that the channel was not excavated and its dating was uncertain (ibid. p218). Kamash (2009, vol3 p4) also notes this canal, suggesting that it is cut by an Umayyad qanat and that it

would therefore pre-date it. However, despite these interpretations, the CORONA images show that it cuts through the walls of Heraqlah, and therefore does appear to post-date the site (see **Chapter 6**). The qanat may in fact be earlier than the canal; Kamash's (2009) interpretation of the qanat as Umayyad could be applicable.

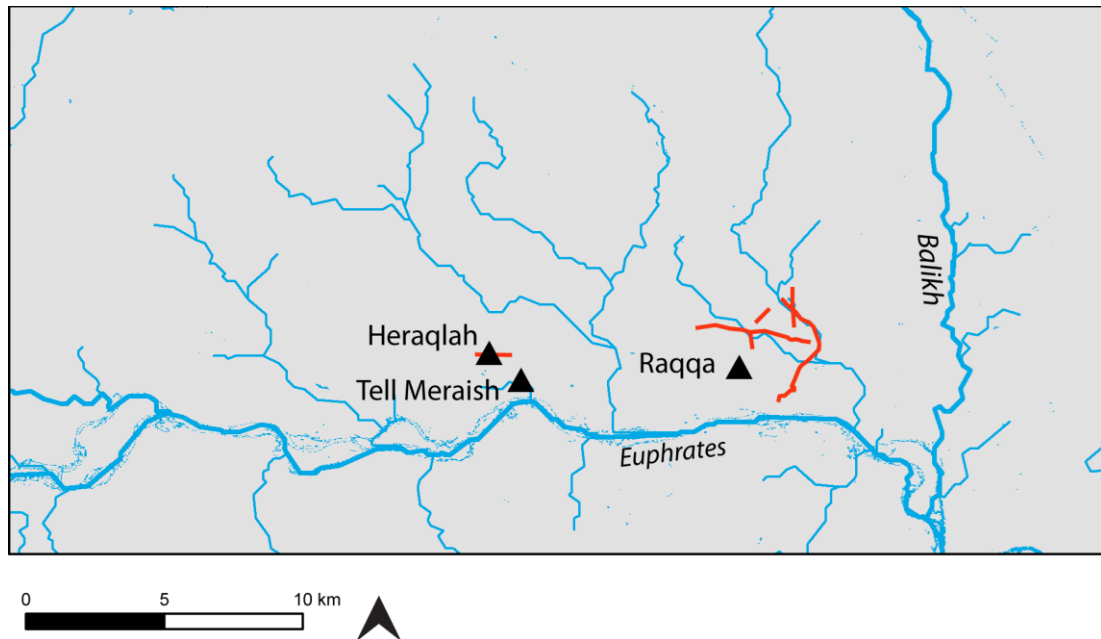


Figure 2.8: Canals at Heraqlah and Raqqa discussed in the existing literature. These were mapped from satellite imagery (Heraqlah) and from Heidemann, (2006) (Raqqa). More detailed mapping using the CORONA images is presented in **Chapter 6**.

2.8 The Balikh

The region with the most complex set of water management remains in Northern Mesopotamia is undoubtedly the Balikh. A brief summary of existing research into these remains is presented here; the results chapter (**Chapter 6**) identifies further features and also attempts to fit them into a chronological and functional framework.

The geomorphological history of the Balikh Valley has created an area of soils conducive to agriculture, surrounded by less cultivable steppe. Rainfall is highly variable and generally low. As such, it is an area with an extremely complex past,

both in terms of settlement and in terms of water management. Early travellers described the valley, noting the presence of ruins (e.g. see Sykes, 1907, p240-; Le Strange, 1930, p101-105). The first archaeological investigations in the Balikh were undertaken by Mallowan (1946, p114), who dismissed the valley as a 'backwater'. However, as was often the case for early surveys, the Roman and later remains were discarded, in favour of earlier remains (ibid). De Jong suggests that study has neglected the Roman and Byzantine periods in the Balikh, while earlier periods and to an extent the Abbasid period are better known (de Jong, 2011, p274).

Despite this issue, there has been recent archaeological interest in many aspects of the Balikh. In terms of excavation, investigations into the widespread prehistoric activity in the Balikh were undertaken by Akkermans, who excavated at Sabi Abyad (Akkermans, 1996). Aspects of the Balikh's small-scale Bronze Age occupation were studied through excavations at several key tell sites including Hammam et Turkman in the centre of the Balikh valley (Van Loon, 1988) and Tell Bi'a in the south (Strommenger, 1981). Other large tell sites include Tell Sahlan in the north of the Valley, close to the Balikh's confluence with the Jullab, and Tell es Seman in the south. Wilkinson (1998) identified a change in settlement patterns in the Balikh from the Iron Age away from a tell-based system to more dispersed farmsteads; there are few large sites dating to this period, but Kirbet Ajlan (BS 386) stands out as a larger site (Wilkinson, 1998, p152). Neo-Assyrian imperial interest in the valley is reflected in a contemporary source, the Harran census (e.g. see Johns, 1901; Fales and Postgate, 1995). Recently, the Hellenistic-Byzantine periods have attracted more attention, with investigations at sites such as Tell Sheikh Hassan (de Jong and Kaneda, 2004-5).

The Early Islamic period is well attested. For example, several projects have excavated at Raqqa, identifying a settlement, industrial area and palace complexes (e.g. see Henderson et al, 2005; al-Khalaf and Kohlmeyer, 1985). At this time, the region attained particular prominence under the caliphs al-Mansur and Harun al-Rashid. Excavation was also undertaken at Medinat al-Far in the north of the Balikh (see Haase, 1996).

Data with a more region-wide focus was gathered by surveys, each with a different focus. For example, Akkermans studied pre 5th Millennium occupation of the valley (Akkermans, 1993), Curvers (1991) focused on the Bronze Age; Bartl (1994) investigated the Early Islamic remains; Gerritsen studied the Hellenistic-Parthian periods (1996). A key study by Wilkinson (1998) recorded sites and landscape features of all periods, including canals as well as sites and field scatters, suggesting that irrigation was more significant in later, post-Bronze Age periods and supported the overall settlement patterns. Wilkinson's study concludes that water availability in the Balikh prevented settlement from expanding beyond a certain size (ibid p84).

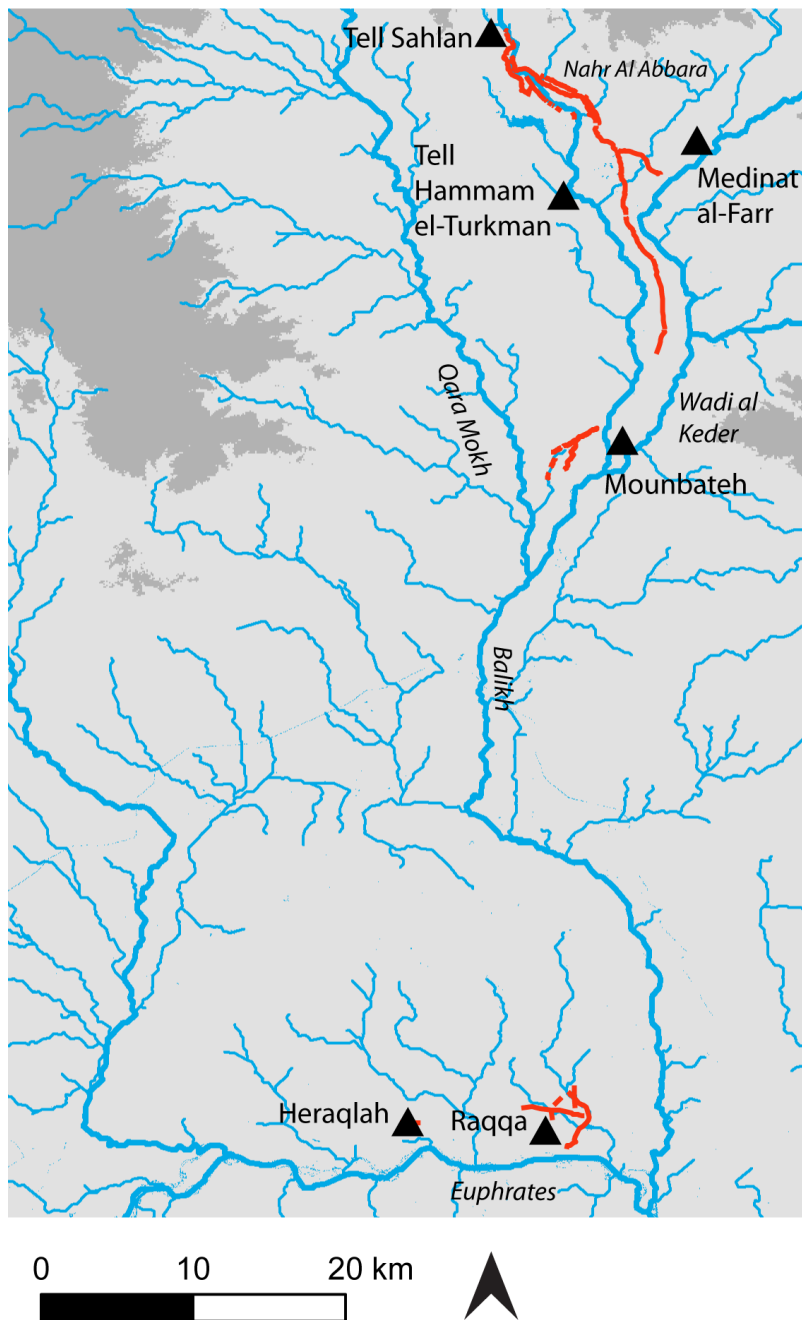


Figure 2.9: Known water management features in the Balikh Valley, recorded by Wilkinson (1998) and Heidemann (2006).

These projects recorded a landscape of tells in the Bronze Age, with a shift to more dispersed, smaller sites from the Iron Age (Wilkinson, 1998) and into the Early Islamic period (Bartl, 1994). Others used the survey data to further investigate the Balikh; incorporating some data provided by Wilkinson and Rayne, (2010), Hritz (2013b) used remotely sense data to examine settlement patterns in the Balikh, defining it as an area which experienced economic stability for long

periods, but which underwent changes from the Iron Age (Hritz, 2013b, p143). De Jong adopted a historical perspective and investigated Roman and Byzantine remains, examining survey, excavated and textual data (2011). She suggests that at this time the Balikh was capable of supporting its large populations, without intensifying production; however, a Roman source indicates that supplies for soldiers at Raqqa were imported into the town (de Jong, 2011, p274-275). De Jong also presented a discussion of Early Islamic settlement in the valley, interpreting the agricultural intensification that occurred at this time as a product of the power of Imperial Raqqa (de Jong, 2012, p523).

Some studies have specifically examined individual water features. Wilkinson's study (1998) was the first that researched specific canals in the Balikh in detail; The Sahlan-Hammam canal was investigated, the Nahr al Abbara, and some potentially Hellenistic canals in the central part of the Balikh were also noted (Wilkinson, 1998). This study also recorded differences in the northern rain-fed zone (north of Tell Zkero) and a drier zone south of this; traces of irrigation are more numerous in the drier zone (ibid p77-78).

Wilkinson excavated a section in the Sahlan part of the Sahlan-Hammam canal, obtaining a date of the 3rd C BC to 6th C AD using ceramic evidence and a radiocarbon date (Wilkinson, 1998, p69; also see **Chapter 6**). He interpreted the two stretches of channels, one close to Tell Sahlan and the other close to Tell Hammam, as part of the same feature, with the middle section removed by erosion (ibid p69). Wilkinson noted that these were well-defined channels with upcast banks, running alongside the Balikh (ibid p67).

This study interpreted the Nahr al Abbara as Early Islamic, based on evidence from ceramic field scatters and by association with nearby sites (ibid p67). The channel was described as a meandering ditch with a straight trace, running along higher ground between the Balikh and wadi al Keder; part of the system had been used as late as the early 20th century, originating in a dam near Tell Sahlan (ibid p67). Other parts of the system were aggraded. Limestone blocks which may have been former sluices were noted (ibid p68).

Parts of other canals were identified. Fragments of a major canal between Tell Hammam and Mounbateh were indicated (ibid p82). Other canals south of Tell Sheikh Hassan were listed (ibid p67). A pattern of Hellenistic sites along one of these canals and away from the river was noted (ibid p82).

More information about these canals, and the locations of some newly identified ones, was presented in Wilkinson and Rayne (2010). Additional channels connected to the Nahr al Abbara system were mapped and channels around Raqqa, including qanats, were also recorded (ibid). The channels described by Wilkinson (1998) and Wilkinson and Rayne (2010) were also discussed by de Jong (2011, 2012) and Hritz (2013b). Hritz also presented a discussion of the geomorphological context of the Raqqa area (Hritz 2013a), interpreting a feature present in the CORONA images as a palaeochannel of the Balikh (ibid p1978). Lightfoot (1996, p326) mapped the presence of a qanat in the vicinity of Raqqa, but it is not clear, however, which of the several different qanats and tunnels identified by the present study was the feature identified by Lightfoot. Heidemann also noted water management features close to Raqqa (Heidemann, 2006, 36).

Past hydrological regimes, current land use and the geomorphological history of the Balikh have also been explored. Mulders (1969) carried out a soil survey for much of the Valley, recording soil types as well as formations such as gilgai, which may be related to waterlogging from past agriculture (on gilgai, see **Chapter 1**). More recently, using remote sensing as well as fieldwork, Alkhaier et al (2012, p1837) suggested that deep water tables in some parts of the Balikh relate to older, better drained cultivation.

Hritz (2013a), Demir et al (2007), and Sanlaville and Besancon (1981) examined the geomorphological conditions of the southern Balikh Valley in the area of Raqqa, alongside the Euphrates. The chronology of Euphrates river terraces was recorded, and in some cases the terraces were dated by association with archaeological remains (Demir et al, 2007, p2848). Hritz (2013a) investigated the western part of the Balikh 'horsehoe', mapping a palaeovalley formed by the Euphrates and Balikh. Further north in the valley, another palaeochannel of the Balikh has been investigated; for example, Akkermans (1993, p170-180) used

coring evidence to suggest that this was a formerly marshy, waterlogged area. Beaumont (1996) and Hole and Zaitchik (2007) investigated the impacts and viability of modern agriculture in the region, discussing available water sources and climatic constraints.

While research has been carried out into water management in the Balikh, it was constrained by several limitations. First, the dynamic nature of the Balikh itself has erased and obscured remains. Recent agricultural intensification has also removed archaeological features. Secondly, the water management situation of the Balikh is highly complex, with layers of use, reuse and abandonment; a bird's eye view is necessary if it is to be untangled. However, fortunately, this project was undertaken with access to a full database of CORONA satellite images (see Wilkinson and Rayne, 2010).

This summary has shown that there is evidence from a range of different studies on the Balikh. The present study incorporated all this evidence into a GIS: the combined data, including information about water management and settlement, could then be compared with the new water management features recorded by the present study so that these could be interpreted within their archaeological context (see **Chapter 6**).

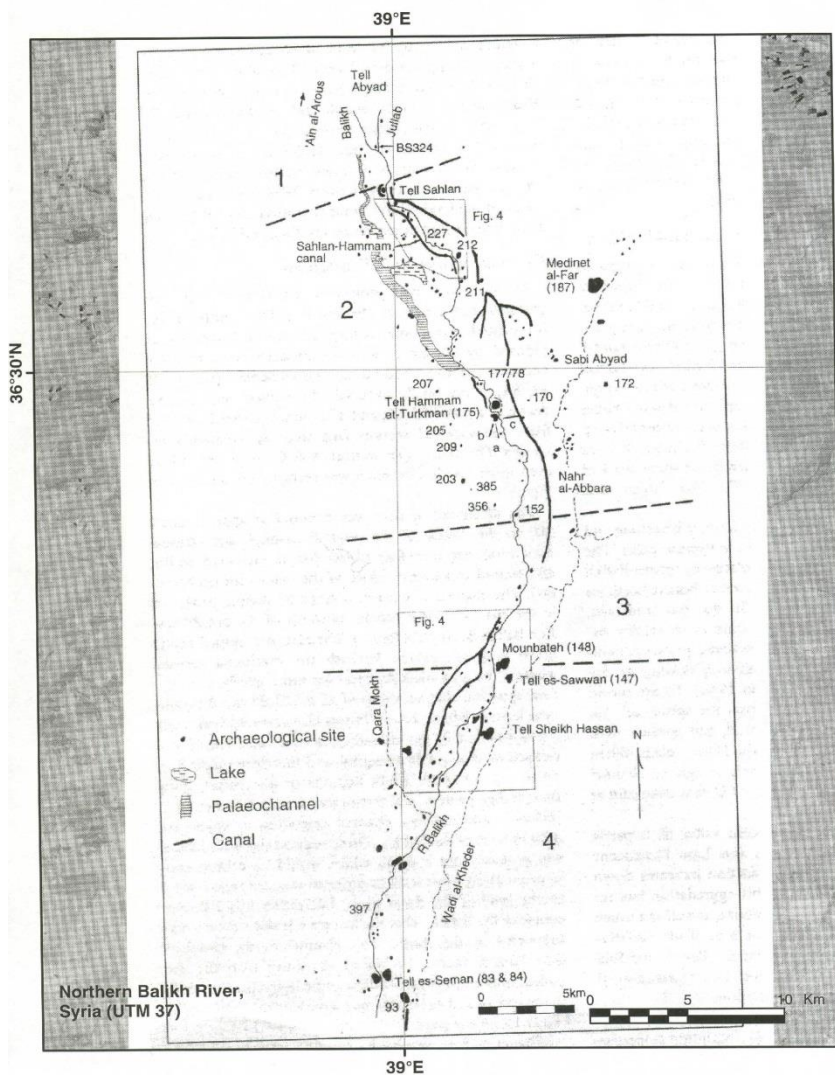


Figure 2.10: Canals recorded by Wilkinson (1998). Map provided by Wilkinson (pers.comm).

2.9 The Habur

Like the Balikh, the Habur is another tributary of the Euphrates where ancient settlement and associated water supply features are known. In general, the Habur region falls into a zone of fairly high uncertain and low rainfall in the south, with more reliable precipitation in the north. Given this, rainfed agriculture has been recorded in the north during the 20th century (Ergenzinger et al, 1988, p110), but the south of the Habur was only used for grazing (ibid.). More recently, new

irrigation schemes have started to transform the landscape (e.g. see Hole and Zaitchik, 2006).

There have been excavations, surveys and analyses undertaken across the Habur region, with some adopting landscape-based/regional approaches; for example, Wilkinson (2000) applied a landscape approach to areas of Northern Mesopotamia, including the Habur; Ur (2010b) also discussed survey in the same area from a regional perspective. Menze and Ur (2012) employed a remote sensing approach to recording archaeological settlements. Much of the existing research in the Habur has focused on the mapping of tell sites, generally of Bronze Age date (e.g. see Meijer, 1986, who proposed a peak in settlement for the Middle Bronze Age) and modelling possible cultivation zones (Deckers and Dreschsler, 2011). A decline in settlement was noted at the end of the Bronze Age (Deckers and Riehl, 2008, p175; Wilkinson and Barbanes, 2000), followed by colonisation and growth involving the Middle and Late Assyrian empires (e.g. see Ur and Wilkinson, 2008). A lack of datable material for the later periods has made it difficult to assess them, although some material representing the Hellenistic-Abbasid periods was collected by Lyonnet (1996).

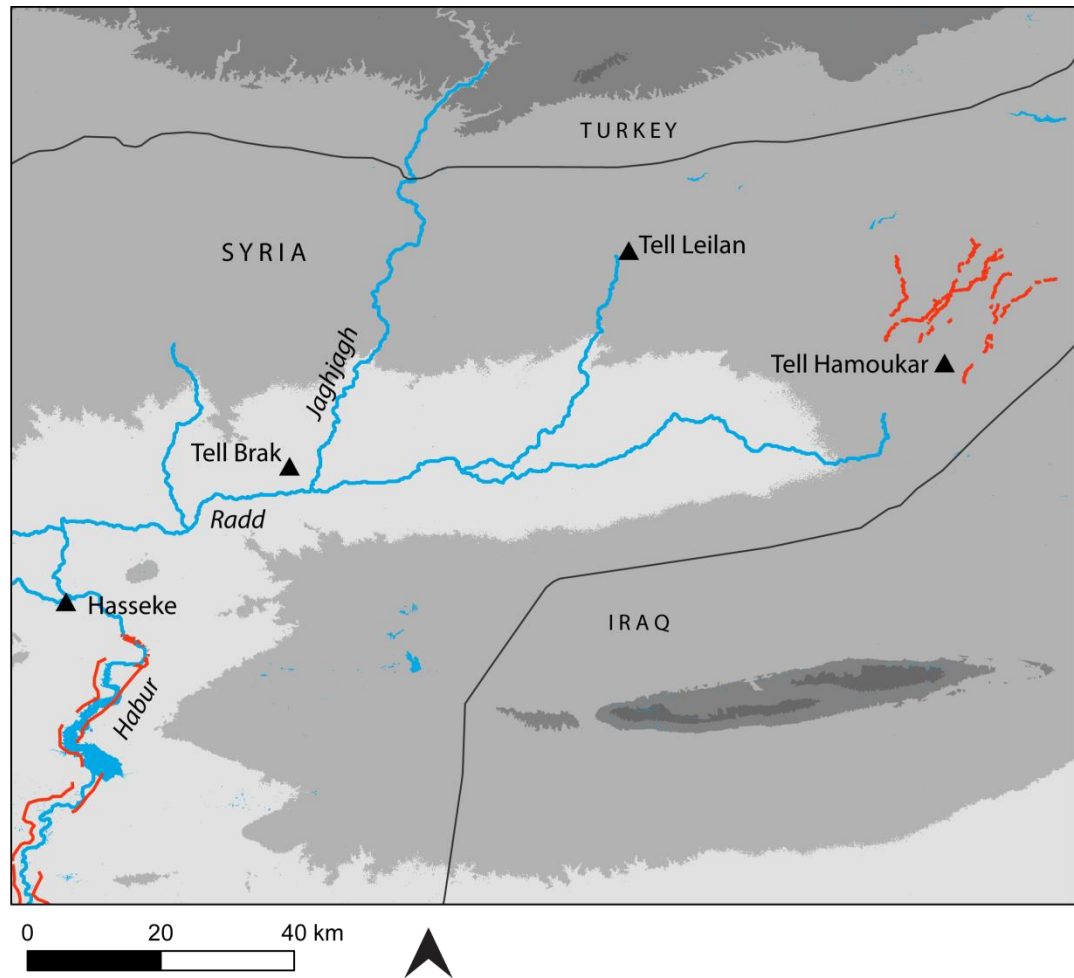


Figure 2.11: Water management features in the Habur region. The features around Hamoukar were mapped by Jason Ur (shapefiles provided by Ur, pers. comm; also see Ur, 2010a).

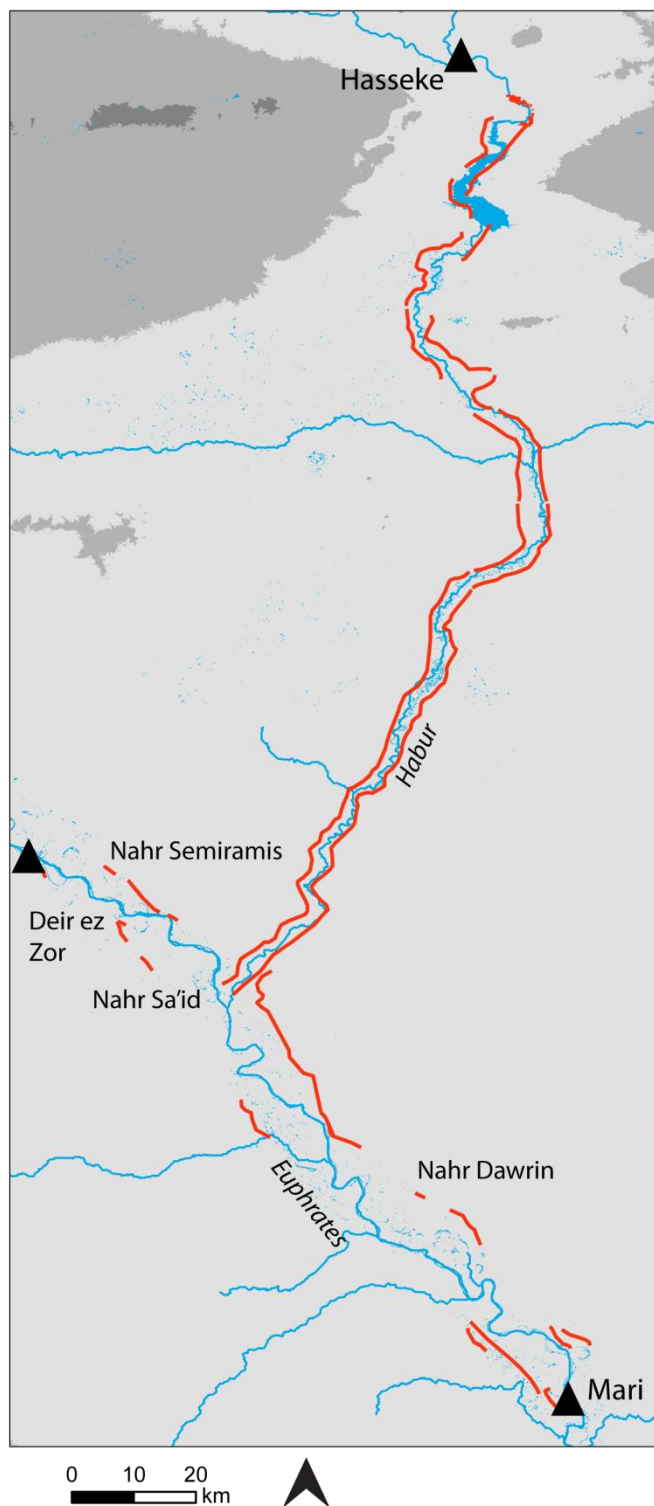


Figure 2.12: Water management features alongside the Habur recorded by Ergenzinger et al (1988). The canals alongside the Euphrates were recorded by Geyer and Monchambert (2003).

Some of the surveys aimed to record off-site features such as hollow ways (e.g. see Ur, 2010), and also water management features. For the northern part of the region, whether the radial lines on the satellite images represent hollow ways or canals has been debated (see Ur and Wilkinson, 2008, p311-12; McClellan et al, 2000, p143-51), although, based on their relationship with the topography, it seems conclusive that these are roads and not water management features. Other studies have also discounted the possibility of significant irrigation in the Upper Habur region (Deckers and Riehl, 2008).

However, some projects have recorded clear evidence for canals further south, along the Habur itself. Relict canals in the Habur region were first photographed by Poidebard (1934). Early investigations into water management as well as into settlement in the region were undertaken by Van Liere and Lauffray (1954-55). In addition to recording radial hollow way routes, they used aerial photographs with a scale of 1:20.000, originally collected for agricultural purposes (*ibid.* p131), to record dark, vegetated lines. They interpreted the lines as canals, based on their tendency to follow the natural contours of the landscape (*ibid.* p146). They recorded traces of canals along the Habur, including some large features south of Hasseke (*ibid.* p147), as well as some branching off-takes and a qanat (*ibid.* p146-147).

The canals alongside both sides of the Habur were investigated by Ergenzinger et al (1988) who surveyed and excavated a canal segment alongside Tell Sheikh Hamad (*ibid.* p113). The excavation gave a chronological range for the feature from the Middle Assyrian to the Early Islamic periods (*ibid.* p117). The canals initially identified by Van Liere and Lauffray (1954-55) were further recorded; according to the published research, they stretched for over 170 km, to the mouth of the Habur (*ibid.* p117). These were found to be up to 6 m wide and with depths of up to 1-2 m (*ibid.* p117). Off-takes were also recorded, notably in a system within a wadi east of Tell Saddada (*ibid.* p117). Significantly, they noted that the proposed modern irrigation systems on the Habur would follow a similar alignment to the ancient canals, which would result in their removal (*ibid.* p126). This means that the existing studies, and any new information which can be extracted from the CORONA images, may now be the only evidence for these canals.

Ergenzinger and Kuhne further investigated these long canal systems (1991), using aerial photographs and recording them on the ground. They recorded several exposed profiles and also undertook excavations. Historical sources and ceramic evidence from the excavations as well as from surface survey were used to date the features (ibid. p178).

Ergenzinger and Kuhne (1991) suggest that the first phase of canal-building was in the Middle Assyrian period on the eastern bank of the Habur. The Neo-Assyrians later modified this system. Although a canal running from the Jaghjagh to Mari has been proposed (Ergenzinger and Kuhne, 1991, p163; p188) it is not clear, from examination of the satellite images, whether there is a single canal on this route. However, canals on both banks of the Habur were in use during the time of the later empires. The left-bank canal was abandoned by the Early Islamic period in favour of a different canal. The right-bank canal went out of use from the time of the Mongol invasion in the 13th century AD (ibid, p163).

At the time of Ergenzinger and Kuhne's survey (1991) traces of the canals were still visible on the ground (p166); they were also identifiable on Poidebard's photographs (1934). They indicate that the canal on the left bank of the Habur may have abstracted from the Habur river and from the Wadi Jaghjagh, and flowed high above the fields, allowing large areas to be irrigated (Ergenzinger and Kuhne, 1991, p171).

Parts of this large canal abstracting from the river were identifiable between Wadi Raml and Tell Sadada. This also flowed high above the fields, at up to 12m above present river level (Ergenzinger and Kuhne, 1991, p172). Based on Van Liere and Lauffray's work (1954-55) off-takes were also noted, for example at Tell Sheikh Hamad (e.g. see Ergenzinger and Kuhne, 1991, p172-173). In some cases the canals needed to cross wadis; dams, weirs and a tunnel were suggested by Ergenzinger and Kuhne (ibid. p170-171).

The same study proposed that the canals and their maintenance would have been the product of considerable labour (Ergenzinger and Kuhne, 1991, p176). A consideration of function was also made, with transport as well as irrigation suggested (ibid. p175). Their flow calculation indicating that up to 10% of the

Habur's flow could have been diverted by the canals (ibid. p174) represents significant water use in the area. Any link between the JaghJagh and the Euphrates, via the Habur canals, however, should be approached cautiously; this was not clear on examination of the CORONA images (see **Chapter 5**).

Ergenzinger and Kuhne (1991) reconstructed the possible routes of the canal (see **Figure 2.13**). Their map gives an impression of a relatively integrated and extant feature on either side of the Habur. Whether or not this is confirmed by the CORONA evidence will also be discussed in **Chapter 5**.

Other studies of water management in the Habur area have also been undertaken. More recently, Ur (2010a) has used remotely sense data to record the landscape further north, around Hamoukar. As well as mapping settlement and hollow way systems, he proposes some further irrigation features. Small-scale possible systems near Hamoukar were recorded (Ur, 2010a, p73). An off-take near Ramadaniya was interpreted as a canal linked to a Sasanian-Early Islamic site (ibid. p89). A comparison between the CORONA images and available DEMs was also used to identify a possible canal system near Tell Mashan (ibid. p89). However, in order to understand these systems more comprehensively, more survey was proposed (ibid. p90).

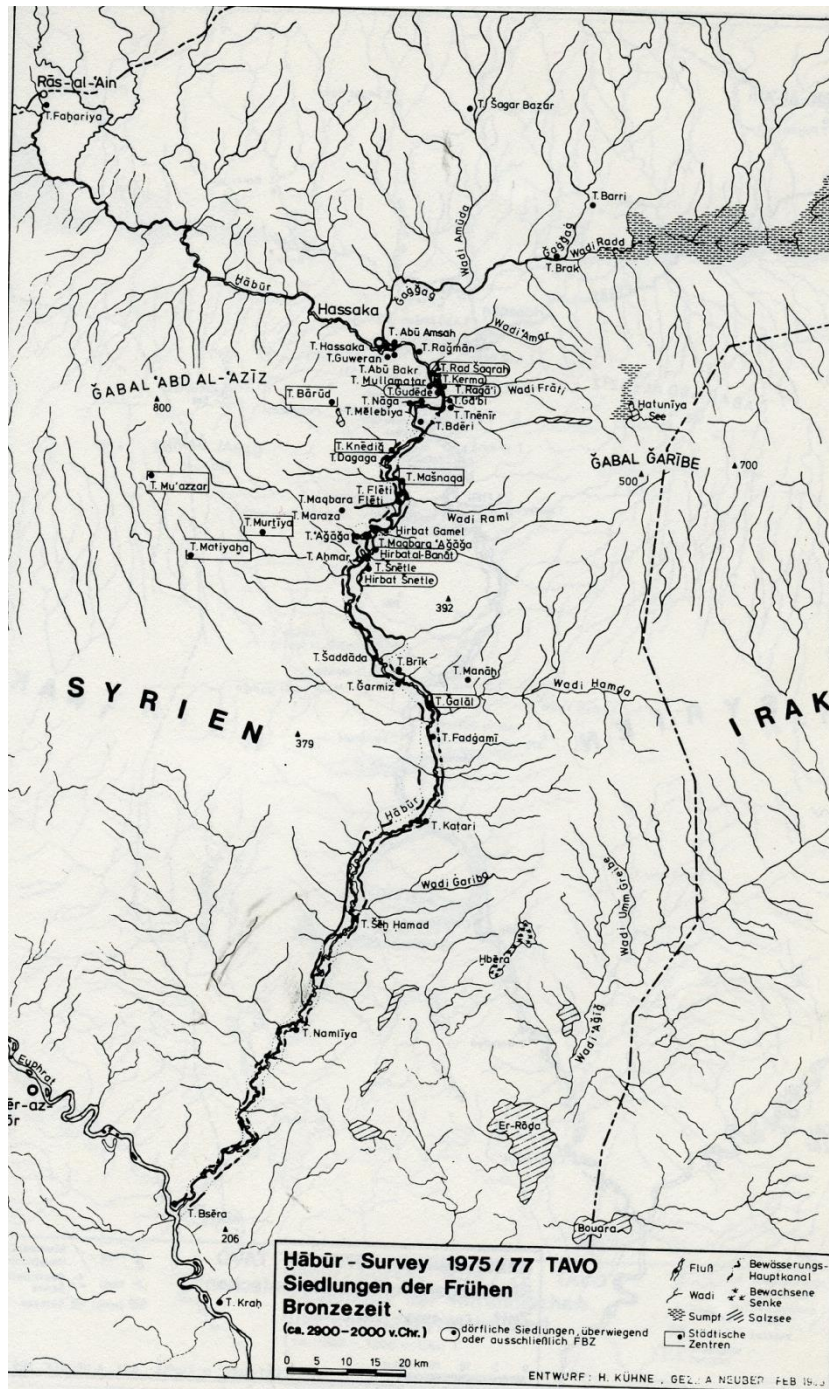


Figure 2.13: Mapped location of Habur canals, from Ergenzinger et al (1988, p119).

2.10 Balikh- Mari

The site of Mari, to the south east of the Habur's confluence with the Euphrates, represents a different situation in terms of water management; the site receives considerably less rainfall than many of the locations discussed in this chapter. Bronze Age water management features of a have been proposed. If this is correct, they would be much earlier in date than the other systems discussed in this chapter, originating before the period of the later empires.

The site itself, located alongside the Euphrates in Syria 20 km from the border with Iraq, has undergone extensive excavations, initially by Parrot (1956) and later by Margueron (2004). The excavations revealed a palace and recovered administrative textual sources dating to the Old Babylonian period (e.g. see Jean, 1952). One of the texts even refers to water management in the Balikh during the Bronze Age (e.g. see Villard, 1987), a rare source of evidence for irrigation and water competition before the time of the later empires.

Traces of canals on both sides of the Euphrates between the Balikh and Mari have been identified (Geyer and Monchambert, 2003; Margueron, 2004; Dalley, 1984), although dating, as ever, proved to be difficult. Margueron recorded and analysed traces of several canals (2004), based on an examination of aerial photographs and survey as well as comparison with texts. Geyer and Monchambert (2003) undertook a detailed archaeological survey of relict canals between Deir ez Zor and Mari (see **Figure 2.12** for a map; also see **Figure 2.14** for an example of their research), based on evidence from surface survey, associated sites and in some cases aerial photographs. They recorded and suggested dates for several significant canals in the region, based on associated field scatters and sites as well as historical texts (see **Table 2.2**). They also noted many shorter segments of unknown canals and possible dams (ibid). Their results are presented in detail in their volume (2003); rather than reproducing them here, this project has examined the evidence for canals visible using CORONA images (**Chapter 5**).

Table 2.2: Suggested dates for canals between Deir ez Zor and Mari, from Geyer and Monchambert 2003 (p175-231).

Canal	Date
Mari canal	Bronze Age
Mohasen canal	Bronze Age-Early Islamic
Nahr Sa'id	Islamic
Canal at El Kita'a	Bronze Age-Early Islamic
Canal near Jebel Mashtala	Late Bronze
Canal of El Jurdi Sharqi	Late Bronze-classical
Nahr Dawrin	Bronze Age-Islamic
Nahr Semiramis	Late Antique

Geyer and Monchambert (2003) and Margueron (2004) interpreted a linear feature close to Mari as a canal associated with the Bronze Age site. Margueron interprets it as a channel which allowed transport from the river to a port (Margueron 2004, p69-70). Another canal, also on the south side of the river, appears to have flowed for a longer distance, and may be associated with a dam on the Wadi es Souab, although dating evidence is unclear (ibid. p71-72). This was a feature raised above the Holocene terrace, so one interpretation could be that it irrigated fields by gravity flow.

Other significant canals have been recorded on the opposite bank of the Euphrates. The Nahr Semiramis originates near Halabiya and flows towards the Habur; a Late Antique date has been suggested based on associated archaeological sites (Geyer and Monchambert, 2003, p217-222). A long canal, the Nahr Dawrin, was traced between the Habur and Abu Kemal with a length of about 120 km (Margueron, 2004, p72-73) and with recorded gradients ranging between 1:1000 – 3:1000 (Geyer and Monchambert, 2003, p200). Bell (1924) also noted the canal, mentioning that a line of qanats aligned NNW-SSE ran along part of its

route (ibid. p78), and recording some active use of the canal (ibid. 82). As discussed above, a connection with the Habur systems has been proposed (e.g. see Geyer and Monchambert, 2003, p199), but, given that this cannot be confirmed, such a long integrated feature seems unlikely (see **Chapter 5**).

Margeuron (2004) emphasises the technological knowledge required to construct the canals, linking this with Mari's power in the 3rd millennium BC, and also raising the possibility of parks and gardens (ibid. p69-82), although the available dating evidence cannot confirm this. However, historical evidence indicates that the Nahr Dawrin canal might have been part of a scheme of agricultural intensification in the area undertaken in the 8th century by the Umayyads (Kennedy, 2011, p194). Early Islamic sites were recorded alongside the Dawrin (e.g. see Berthier and D'Hont, 2005, p265; Kennedy, 2011, p194). The evidence may be suggesting an Early Islamic date for the feature, rather than the earlier, Bronze Age, one proposed by Margeuron (2004).

Another Islamic canal, the Nahr Sa'id, on the opposite bank of the Euphrates, has also been discussed in the literature (Geyer and Monchambert, 2003, p183-187; Kennedy, 2011, p195; Berthier and D'Hont, 2005, p267). Historical accounts from the Umayyad era link it to the 8th century, with possible continuation into the 11th century (Kennedy, 2011). It could not be identified on the CORONA images (see **Chapter 5**). Other canals identified on the ground by Geyer and Monchambert (2003) were also not clearly identifiable using CORONA.

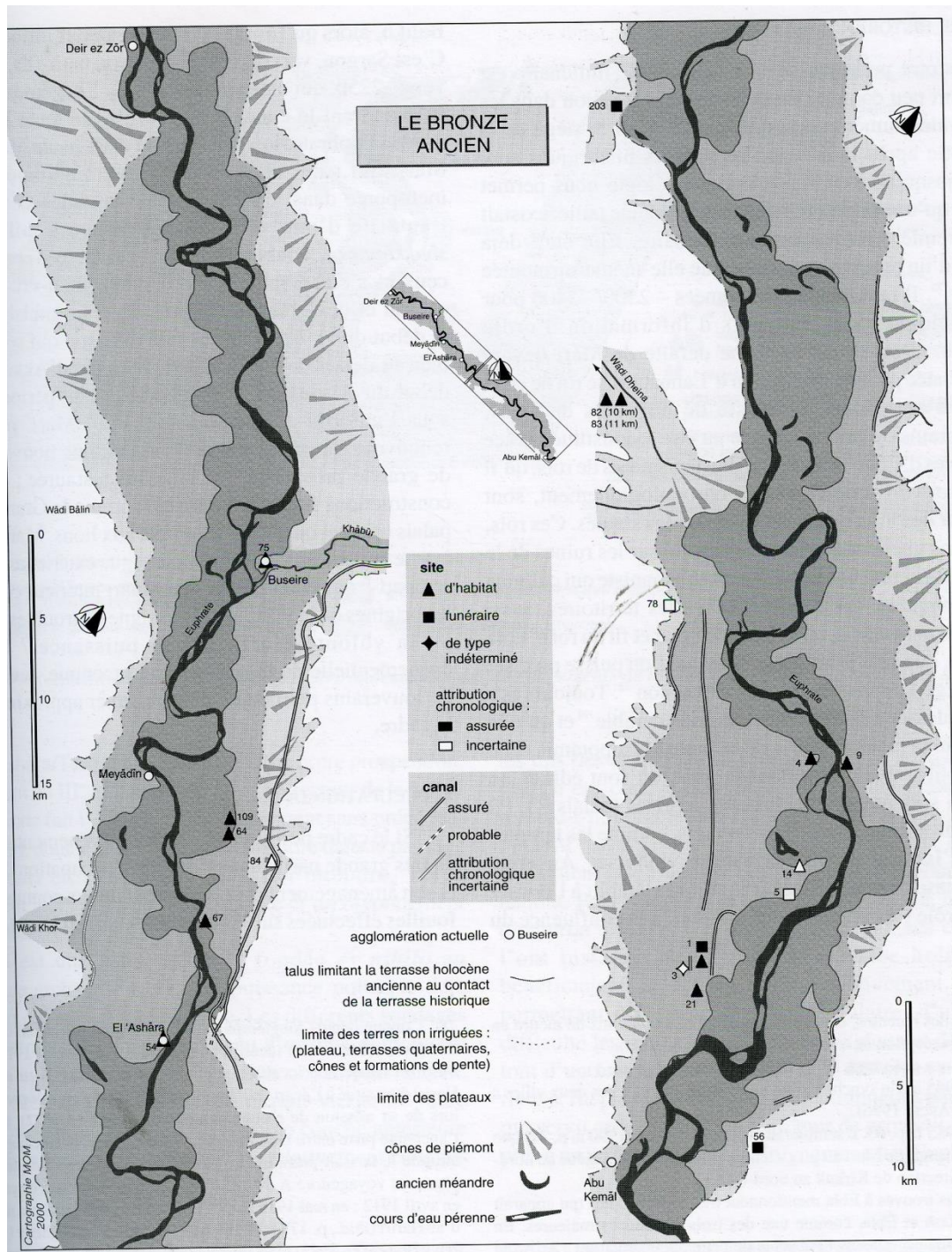


Figure 2.14: Canals and Bronze Age sites mapped by Geyer and Monchambert (2003, p247).

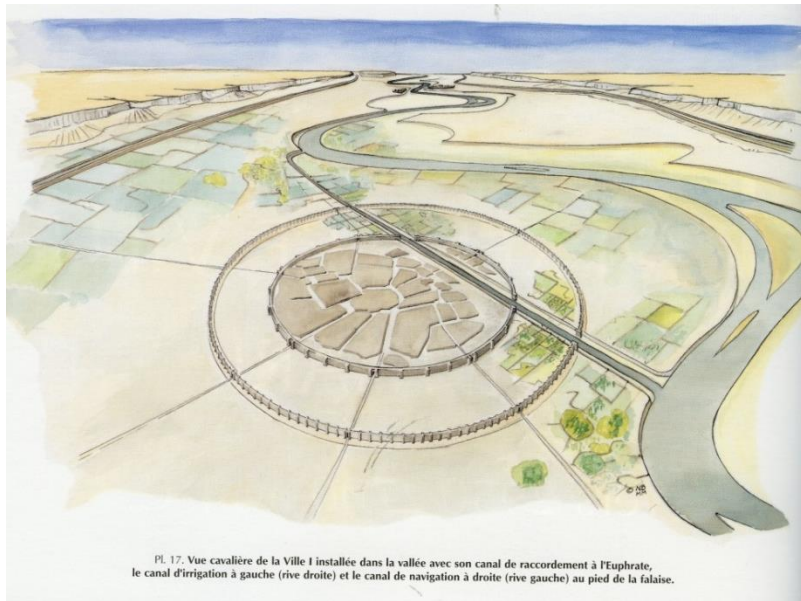


Figure 2.15: Margueron 2004, p50, Pl. 17: Margeuron's (2004) interpretation of water management around Mari is based on a theory that linear features in the vicinity of the site were canals contemporary with Mari. Dating evidence, however, is not clear.

2.11 Assyrian water management in northern Iraq

Also within the broader project area are the large relict canals in northern Iraq. These features are different to the canals already discussed both in terms of the way they have been researched and in terms of their climatic context. They are also somewhat earlier in date than many of the systems discussed thus far in this chapter. Also, in contrast to the other areas already discussed, landscape archaeology research in the northern hinterland of Nineveh, Ashur and Nimrud has focused on water management remains (see Ur, 2005, p3420).

These features are located in a region that generally receives more rainfall and more reliable rainfall than the other regions already discussed in this review. Data collected between 1980-2010 suggests that precipitation in this region was on average at least 400 mm, with around 15-27 % variability (see **Chapter 1** and **Chapter 3.6**).

Text-based research has dated the canals to the period of the Assyrian empire, with many forming part of a programme of construction sponsored by the Neo-

Assyrian King Sennacherib in the 8th century BC (e.g. see Jacobsen and Lloyd, 1955). Given that inscriptions and other ancient sources are available, they have formed the basis of research, with scholars such as Reade (1978a and b) attempting to link the features visible in parts on the ground to those discussed in the ancient sources. Presumably due to the royal nature of the inscriptions and reliefs, there has been significant interest in the ideological nature of Neo-Assyrian irrigation in Northern Iraq (e.g. Dalley, 1994).

Texts and inscriptions have been used extensively to locate canals; in many cases they enable a more complex history of the features to be generated. In some cases these are directly linked to the water management features themselves. The Khinis system is associated with rock-cut inscriptions, including the 'Bavain Inscription', consisting of Sennacherib's boasts of irrigation (Layard, 1853, p212) and an inscription at Jerwan (Jacobsen and Lloyd, 1955).

Bagg (2000b) undertook an extensive discussion of the Middle Assyria and Neo-Assyrian royal inscriptions and other ancient documents relating to water management. In some cases however, the features attested to in texts have not yet been located on the ground (see Ur, 2005, p323).

The preoccupation with luxury parks and gardens has been recognised (see Bagg, 2000a, p303). Dalley has explored the possibility that the idea of 'hanging gardens' can be applied to raised cultivated parks at Nineveh, interpreting an ancient description of a water lifting device as an Archimedes screw (Dalley, 1994, p53). The possibility that water could simply have been delivered to gardens via gravity flow, however, from a canal at a higher elevation than the site, should also be considered.

Archaeological investigations into Assyrian water management north of Nineveh have been undertaken since the 19th century. The interpretation of inscriptions and rock reliefs associated with the canals has long formed part of research in this area (for example, see Jacobsen and Lloyd, 1955). Some segments of the canals themselves were also recorded and discussed by early travellers and scholars (e.g. Jones, 1857, p424- 426).

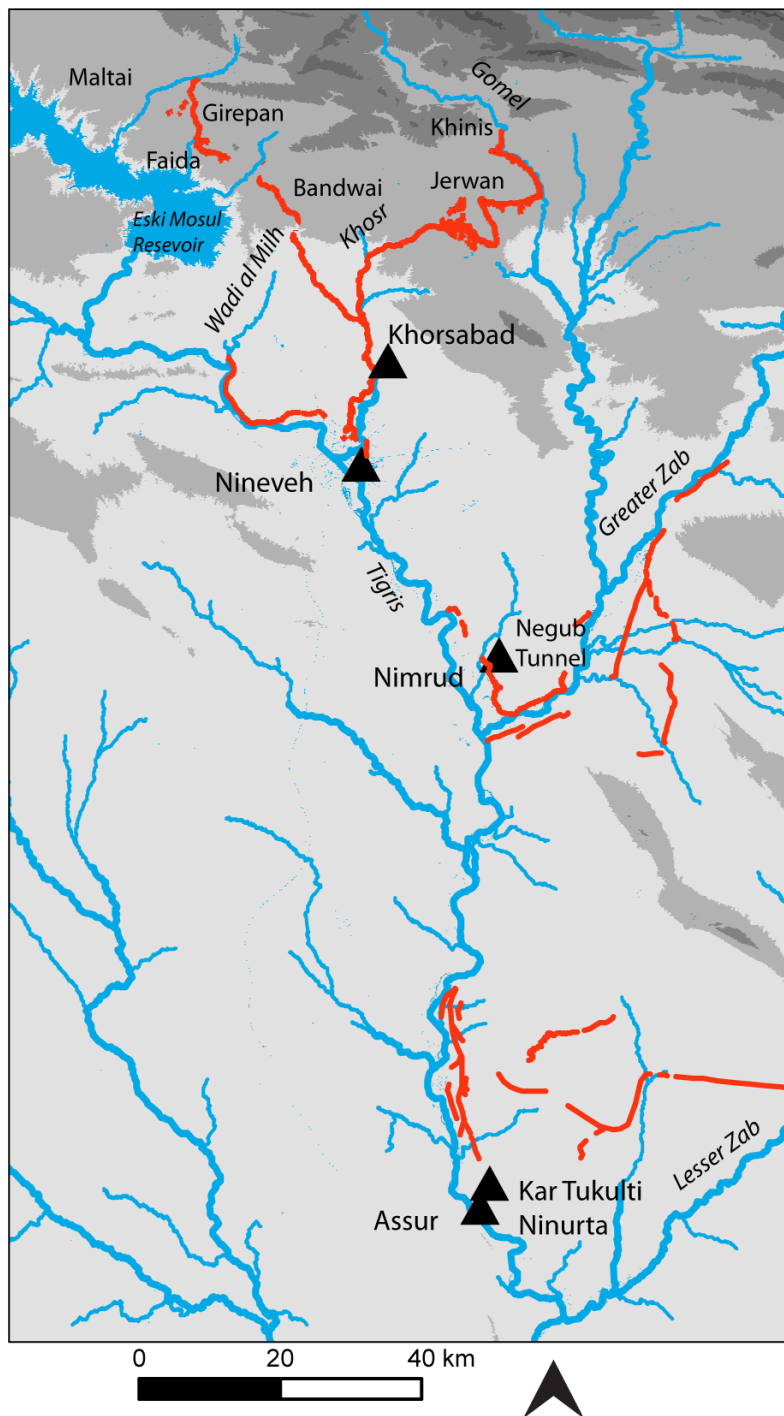


Figure 2.16: map of known canals in northern Iraq. These were located by Ur (2005), Ur et al (2013) and Altaweel (2008).

More detailed archaeological research was undertaken by Oates (1968) and Reade (1978). Both these studies were especially concerned with linking the remains on the ground to the information found in the inscriptions. Most recently, Ur (2005) and Altaweel (2008) mapped the Assyrian canals using remote sensing

techniques, such as CORONA image interpretation and DEM analysis. They found that some channels meandered according to the contours of the landscape, apparently with an intention to maintain gradients of around 1 m per km (1:1000) (Ur, 2005 used SRTM to obtain this figure, p340), but also others which seemed to cut across the natural contours (see Altaweel, 2008, p88). These findings, constituting the most recent and comprehensive archaeological surveys of the Assyrian water management systems in the region, will be summarised here alongside other sources.

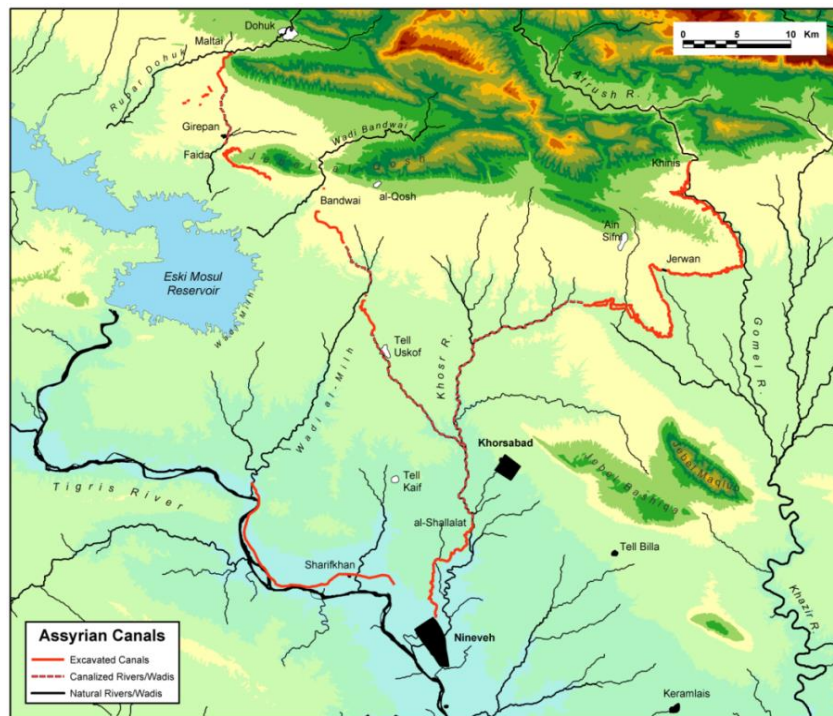


Figure 2.17: Canals in northern Iraq mapped by Ur (2005, p320; pers comm).

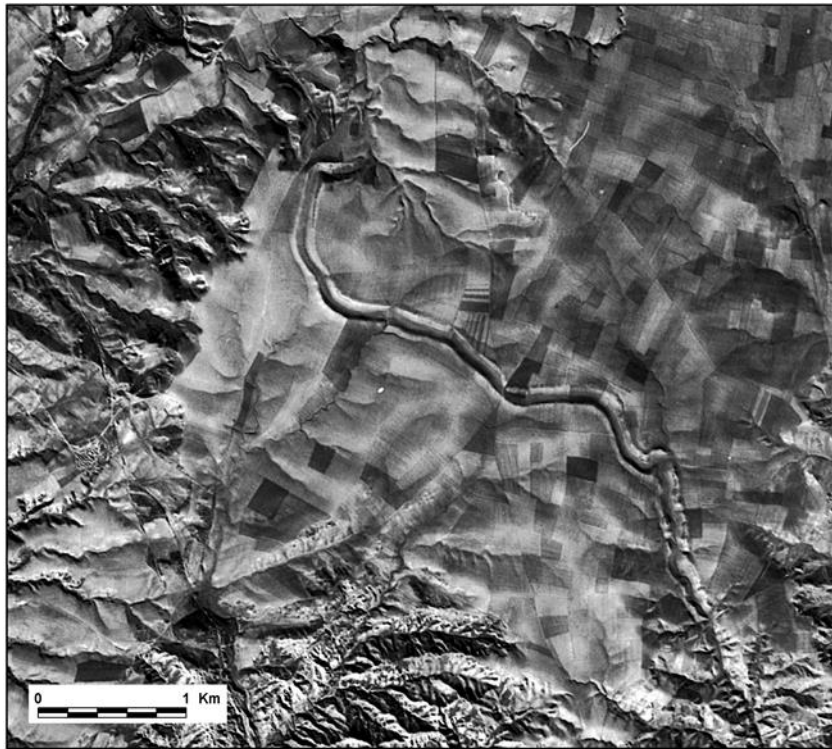


Figure 2.18: CORONA image of Bandwai canal, Ur, 2005, p331 (*pers. comm*).

The first phase of canal construction undertaken by Sennacherib occurred in around 702 BC, and involved a canal which stretched from Kisiri (possibly Tell Inthah or al-Shallalat) to fields north of Nineveh (Ur, 2005, p321-322), a feature which is identifiable in CORONA imagery (see Altaweel, 2008; Ur, 2005). An early account of the system was given in the mid-19th century, recording channels alongside the Khosr and terminating in the Tigris, and interpreting one as a city moat of Nineveh (Jones, 1857, p424). Jones also mentions the remains of sluices and a dam (*ibid*, p426).

Reade later undertook a study of the canal (1978a), suggesting that it originated from a dam at Shallalat (*ibid*. p64). It then ran parallel to the River Khosr, at its right bank, before turning southwards and flowing over a km from the Khosr (Ur, 2005, p322). It eventually separated into two branches, one possibly leading to the site of Nineveh, and the other possibly irrigating fields (Ur, 2005, p322). Reade raises the possibility of a tunnel at the Nineveh end (Reade, 1978a, p66).

Another prominent set of channels is also apparent north of Nineveh, first located by Oates (1968, p51). Attempting to link the texts with features on the ground,

Reade recorded a spring which may have fed part of the system (1978a, p69). Altaweel (2008) and Ur identified channels in this area using CORONA images (Ur, 2005, p323-327): a large earthwork between Maltai and Girepan (the Maltai canal) was compared with the Hellenistic canal in the central Balikh (see Wilkinson, 1998). The canal appears to have terminated in a natural wadi. The CORONA studies also noted traces of other, fragmentary channels in the same area (Ur, 2005, p328).

Irrigation systems originating at Mount Musri are attested to in texts; these may correspond to the modern Jebel Ba'shiqa (see Jacobsen and Lloyd, 1935, p35-36). However, Reade (1978a) recorded carved panels in caverns associated with the Jebel Ba'shiqa springs; he links this with Sennacherib's enlargement of streams in the region, but notes the later, Islamic style of the sculptures (Reade, 1978a, p70).

Originating at the Jebel al-Qosh, the spring-fed Faida canal was excavated through bedrock, flowing to the village of Faida (Ur, 2005, p328-329). The canal was associated with stone reliefs (Reade, 1978b, p162-164). Off-takes could also be recorded, which Ur interpreted as irrigating the hill-slope (Ur, 2005, p330). Altaweel mapped additional channels in this area (2008, fig.50-51).

The Bandwai canal also originates in the Jebel al-Qosh area (Oates, 1968, p51), although its source is unknown (Ur, 2005, p330). Its end point is also debated; while Oates recorded it as draining into the Wadi al-Milh (Oates, 1968, p51), Ur suggests that it joined a northerly tributary of the same wadi (Ur, 2005, p332). In order to lower the canal to a functional depth within its particular landscape, its construction resulted in prominent banks (Ur, 2005, p331). Another canal which Ur identified in the CORONA imagery, the 'Tell Uskof canal', may have been connected to the Bandwai, joining the Kisiri system by linking the Wadi al-Milh with the Khosr (Ur, 2005, p332). Ur indicates that there was a functioning system including these canals, with associated dams, weirs and aqueducts, although these have not yet been identified (Ur, 2005).

Using CORONA, Ur (2005) and Altaweel (2008) traced another canal which may have been connected to the same system, namely the Tarbisu. It originated from

the Wadi al-Milh and terminated at the village of Sharif Khan (Tarbisu), 8 km north of Nineveh (Ur, 2005, p332). The Tarbisu was a straight, linear channel, with 'sharper' upcast banks (Ur, 2005, p332-333), possibly consisting of two main branches (Altaweel, 2008, p73). Ur interpreted it as either a canal which underwent longer use than the others, or as one later in date than the Neo-Assyrian canals described above (Ur, 2005, p332-333). Altaweel (2008, p118) suggests that some of the other canals in Northern Iraq, near the junction between the Tigris and the Upper Zab, may also be of an Early Islamic date.

The Malta, Faida, Bandwai, Uskof and Tarbisu canals have been interpreted as part of an integrated 'Northern System' by Ur who suggests that some parts of it delivered water into the Khosr River, and that other parts were used for local irrigation (Ur, 2005, p333-335). Off-takes were found linked to the Khinis and Faida canals, but others above Kisiri could be post-Assyrian in date (i.e. post 612 BC: Ur, 2005, p341).

A canal flowing between the Khinis and Kisiri systems had already been attested by some early research, including investigations by Layard (see Layard, 1853, p207- 216) and by Lloyd and Jacobsen (1955). The system originated as a weir in the Gomel River (Reade, 1978b, p168), where it was associated with Assyrian rock-carved inscriptions attesting to Sennacherib's efforts to manage the flow of water (Layard, 1853, p207-212). After this, the canal flowed alongside the river, and, at one point, through a tunnel (Ur, 2005, p336). It then crossed a tributary valley via an aqueduct south of this point, at Jerwan (Ur, 2005, p337; Jacobsen and Lloyd, 1955). Using CORONA imagery, Ur recorded some faint off-takes close to this stage (Ur, 2005, p337). The canal eventually turned towards the north and crossed to the Khosr basin (Ur, 2005, p338). Parallel channels of this canal were recorded between Ain Sifni and Kandalah; Ur suggests that a second canal could have been constructed to replace a damaged or poorly-functioning first canal (Ur, 2005, p338-339).

Oates (1968) discussed Assyrian water management efforts around Nimrud, to the south of Nineveh (**Figure. 2.16**). He recorded a canal between the Greater Zab and Nimrud, which was also attested by an Assyrian source linked to

Assurnasirpal (Oates, 1968, p46; Bagg, 2000a, p311). Close to its abstraction point, part of the channel traversed a conglomerate bluff via a tunnel system (Oates, 1968, p46) known as the Negub tunnel (Reade, 1978b, p171). Altaweel more recently also identified further canals in this area visible in the CORONA imagery (2008, p74).

Further south, Assyrian irrigation was identified at Kar-Tukulti-Ninurta (Eickhoff, 1985; Dittman, 1995); Bagg (2000a) compared textual evidence with the existing excavation data, linking inscriptions associated with the king Tukulti-Ninurta in the 13th century BC with a canal system abstracting from the Tigris, passing through the city and draining into the same river (Bagg, 2000a, p307-310). Altaweel identified part of this system, in the form of a wide embanked linear feature in the CORONA images (Altaweel, 2008, p76). Altaweel also used CORONA images to map a significant canal between this area and the Lesser Zab (*ibid.* p76). Bagg associates this canal with the Kar-Tukulti-Ninurta canal, although it lacks dating evidence (Bagg, 2000a, p311).

Most recently, Ur et al (2013) also used CORONA to locate canals south of the Upper Zab. They recorded several long, large-scale features in this area, recording widths of up to 100 m wide from bank-to-bank (Ur et al, 2013, p106). They propose a Neo-Assyrian date for the westernmost canal, based on the location of sites, and a Sasanian-Early Islamic date for the largest canal, which flows parallel to the Upper Zab, based on its straightness and size (*ibid.*).

While research has emphasised a link between the water management features discussed above and luxury royal gardens (e.g. see Reade, 1978b, p174), the significant use of water for irrigation has also been recognised in the literature (Bagg, 2000a, p320). Oates also discussed the economic aspects of Assyrian water management (e.g. see Oates, 1968, p51).

In terms of the implications of the organising power of the Assyrian empire, it appears that the Assyrian irrigators made intelligent use of the natural environment, using canals to link existing wadis and to channel existing streams. As the research summarised above shows, they were capable of integrating large-scale canals, off-takes and associated infrastructure such as aqueducts and dams

to ensure more reliable agricultural yields as well as to supply luxury parks and gardens.

As this study will show, large-scale canal construction in northern Mesopotamia was also a feature of post-Assyrian to Early-Islamic times. For example, in the context of this summary of the research from northern Iraq, Reade (1978b, p170), mentions an Islamic canal on the left bank of the Tigris above Ashur, and Ur recognises that the canal at Tarbisu may also post-date the Neo-Assyrian period (Ur, 2005, p333). Similarly, a canal mapped by Altaweel, the Nahr Qanausa, which flowed alongside the Tigris near Kar-Tukulti-Ninurta, was interpreted as Islamic and included some possible offtakes (Altaweel, 2008, p76). However, in general, there has been less exploration of the possibility of later water management, and of the possibility that earlier canals may have been reused in later times; the preoccupation with the Assyrian texts may have limited interest in irrigation in other periods. An investigation into the dating of the identified features might prove a useful aspect of future research into this region.

2.12 Qanats in northern Iraq

Other water features have been recognized in northern Iraq. There are several sources noting qanats on the Sinjar plains, although they do not discuss them in detail (see Ur, 2013; Lightfoot, 2009; Al-Sawaf, 1977; Fuccaro, 1991; Cressey, 1958; Poidebard, 1934). Al-Sawaf (1977, p48-50), writing from a hydrological/geological perspective, recorded and mapped some of the long-abandoned qanats in the area; Fuccaro's historical thesis (1991) attributes the qanats to the medieval period, suggesting that they went out of use by the Ottoman period (Fuccaro, 1991, p12).

In terms of qanats in Iraq, Lightfoot noted the role of the later empires, from the Achaemenids to the Ottomans, in the construction of qanats (Lightfoot, 2009, p15-16). This is also recognized by Wilkinson and Rayne (2010). The presence of the Roman frontier in the Sinjar area was emphasised by Lightfoot (2009, p16), although any association between this and the qanats cannot be confirmed. Literature dealing with the Sinjar qanats is sparse; it is necessary to rely on CORONA satellite images to verify their existence (see **Chapter 5**).

2.13 Summary

This review attempts to list all the known ancient water management features between the Euphrates in Syria and the Tigris in Iraq: the area known as northern Mesopotamia. This particular region was chosen because;

1. It is easily definable, based on the position of the major rivers, making a comprehensive review of a region possible.
2. It was within a zone where multiple later territorial empires, from the Assyrian to Early Islamic, were active.
3. The implications of the development of irrigation systems in southern Mesopotamia have often been explored. While water management in other areas, such as Jordan and Israel, is often documented, and disparate specific studies exist for northern Mesopotamia, a spatial review of all known features in the area was lacking.
4. Northern Mesopotamia broadly fits into the 'zone of uncertainty', a region where rainfall is highly variable temporally, and generally ranges between 200-500 mm spatially, at the margins of rainfed agriculture.

A summary of the implications identified by the studies reviewed here can now be given. Dating information for canal systems can be difficult to obtain, however, the interpretations given in the literature can give an idea of how irrigation might have developed (summarised in **Table 2.3**). The earliest period for which canal-based irrigation has been proposed is the Bronze Age; canals around Mari were linked to the site (Margueron, 2004), although their date currently cannot be confirmed. Textual evidence also indicates canals in the Balikh during the Middle Bronze Age (e.g. see Villard, 1987). The long canals alongside the Habur have been given a date of origin in the Middle Assyrian period (Late Bronze Age), and most likely they were associated with the site of Dur-Katlimmu (Ergenzinger et al, 1988).

The first real territorial empire, however, was the Neo-Assyrian state (see the chronology presented in **Chapter 1**): this empire has been linked to the extensive, large-scale canal systems in Northern Iraq (e.g. see Oates, 1968; Reade, 1978; Ur, 2005). Hellenistic canal remains have been recorded in the Balikh (Wilkinson, 1998; Wilkinson and Rayne, 2010) and around Membij (pers.comm Dan Lawrence

and Niko Galiatsatos). Roman features are also known throughout the study area (see Kamash's review, 2009), including cisterns, dams and canals associated with the site of Resafa (e.g. see Brinker, 1991). Tunnels around Jerablus may have late Roman-Byzantine links (Wilkinson et al, 2007), and the Sahlan-Hammam canal has also been dated to this era (Wilkinson, 1998).

Although Decker (2009b; 2007) has suggested that the Early Islamic period was not significant terms of water management, large scale canals dated to that period have been located alongside the Euphrates (e.g. see Geyer and Monchambert, 2003), at Dibsi Faraj (Harper and Wilkinson, 1975) and in the Balikh (Wilkinson, 1998; Wilkinson and Rayne, 2010). The long canals alongside the Habur (Ergenzinger et al, 1988) and the Tarbisu canal in Northern Iraq (Ur, 2005) also seem to have continued to function and be maintained in the Early Islamic period.

Table 2.3: *Dating of features from existing literature.*

Period	Sites
Bronze Age	Mari(?), Balikh?
Middle-Assyrian	Habur
Neo-Assyrian	Habur and north Iraq (canals near Kisiri, Maltai, Faida, Bandwai, Tarbisu, Iskof, Khinis-Kisiri, Negub, Nimrud, Kar-Tukulti-Ninurta, Nineveh).
Hellenistic	Balikh? Membij qanats? Habur?
Roman	Resafa, Habur?
Late Roman/Byzantine	Jerablus, Balikh, Habur?
Early Islamic	Dibsi Faraj, Balikh, Habur, Nahr Dawrin, north Iraq

Dating canals is often problematic, partly because absolute dates can generally only be derived from datable material obtained through excavation: the Hammam-Sahlan canal in the Balikh (Wilkinson, 1998) and the Nahr Maslama at Dibsi Faraj (Harper and Wilkinson, 1975) were assigned dates in this way.

Dating is also difficult because water features such as canals and qanats can undergo complex 'lifetimes' of construction, use, modification and reuse. For example, many canals were identified as being still partially in use in the early 20th century; some of these may have very early origins. The Nahr Dawrin on the Euphrates may be at least as old as the Early Islamic period, yet Gertrude Bell, visiting it in the early 20th century, mentioned that parts of the canal were still in use (Bell, 1924, p82). While of course absolute dates should be obtained when possible, rather than thinking of these features only in terms of one period or empire, it is important understand them as multi-period features.

The way these features have been dealt with in the literature should also be noted here; specific ways of interpreting water management do seem to be applied to features of different periods. The Assyrian canals of northern Iraq are part of a tradition of studying water in terms of power, propaganda and luxury. For example, the watering of luxury parks and gardens at Nineveh has been emphasised as a function of some of the large canals (e.g. see Dalley, 1994; Bagg, 2000b). This is generally associated with the power of the king and the empire; the role of propaganda is also often discussed.

In contrast, water management features of other periods have been treated more as practical resources. The Mari canals were interpreted as sources of irrigation water as well as of transport, supporting the port and trading activities of the site (Margeuron, 2004), although dating evidence is still too limited to support this. The Balikh canals (mainly Hellenistic-Early Islamic) have been discussed primarily in terms of irrigation, although the use of water for industrial activity around Raqqa has also been mentioned (Heidemann, 2006).

Applying both modes of thinking to all the known water management features could be attempted. There may be much to be gained from viewing the northern Iraqi canals in terms of economic function, and in applying the ideas of luxury and power to the Early Islamic canals. In order to explain the distribution of these systems, what may be needed is a new framework within which to conceptualise water management:

1. Features should be thought of as multi-period entities which can outlive the state which constructed them, and be adopted by future states. The lifetime of canals and other water features may occur over a different trajectory to the lifetime of other archaeological remains, such as settlement sites and routeways.
2. Features should be regarded in terms of economic use as well as in terms of any ideological associations/consequences.

These issues will be discussed in detail in **Chapter 7**. The spatial literature review presented here has been used to identify the necessary research, and gaps in research, that this project has recorded:

1. There are parts of northern Mesopotamia which still need to be examined for water management features. New features will then be added to the GIS.
2. Many of the existing studies did not have access to remote sensing data such as CORONA when they were conducted; the known features from these studies can be further examined using this data.
3. A detailed overview (presented in the form of GIS maps) can be generated from all the digitised features.

Chapters 5 and **6** present the results of detailed image interpretation using CORONA images and of further validation using DEMs. **Chapter 3** outlines the methods used to produce the results, and **Chapter 4** outlines the different types and scales of water management systems which can be encountered.

Chapter 3: Methods

3.1 Methodology

Given that the aim of this research was to build a detailed database of water management throughout northern Mesopotamia, a set of methods which facilitated relatively fast mapping across a large area were needed. This research employed an interdisciplinary methodology comprising remote sensing techniques alongside fieldwork and the incorporation of existing archaeological surveys, adopting the broad methodological approach of the AHRC-funded Fragile Crescent Project of Durham University (see Galiatsatos et al, 2009). **Tables 3.1** and **3.2** show the wide range of data used. This detailed database of the locations and hydraulic properties of individual systems allowed the distributions of different types of water management systems to be recorded, and therefore the scales of control over water exercised by the later territorial empires (Neo-Assyrian – Early Islamic) to be examined.

Table 3.1 *Remote sensing data used to record ancient irrigation systems.*

Dataset	Sensor	Date	Resolution	Purpose/use
Images	CORONA (Missions KH-4A and KH-4B).	1967, 1968, 1969 1972	2-5 m	To identify water features and to assess land use change from 1960s-2000s.
	GeoEye-1	2010	0.41-1.65 m	Image interpretation and control.
	IKONOS	2010	0.82-3.2 m	Image interpretation and control.
	Landsat TM, ETM	1984, 1990, 2000		Image interpretation, land use.
DEMs	SRTM	2000	90 m	Information about topography of landscape, location of natural drainages and gradients of canals.
	ASTER DEM	1999-2009	30 m	
	CORONA	1968	c.10 m	

Table 3.2: *Survey, excavation and historical data.*

	Data and use	Date	Geographical range	Function
Fieldwork	GPS points New features Survey Validation of features identified using image interpretation	2010	Jerablus region and samples from the Balikh (Heraqlah, Tell es Seman and canals near Tell Hammam et Turkman).	Confirming and surveying the mapped features and identifying new ones.
Existing data	Unpublished survey data (pers. comm. Tony Wilkinson, Dan Lawrence, Niko Galiatsatos and FCP). Published archaeological surveys (see Chapter 2). Historical data (e.g. Kamash, 2009; le Strange, 1930). Travellers accounts (e.g. Bell, 1924; Sykes, 1907).	1990s-2013 20 th and 21 st centuries Bronze Age- Early Islamic 19 th -20 th centuries	Samples from Balikh and Membij qanats. Throughout Near East Throughout Near East. Throughout Near East.	Dating information and archaeological and historical context.

The project aimed to map all the clearly identifiable water management features throughout the study area, a region of about 100,000 km² (see **Chapter 3.2**), recognising that time-intensive traditional fieldwork methods were not practical or feasible for large-area survey. Each mapped feature had to be understood within

its hydrological, geomorphological and historical context, and examined as potentially a part of a more extensive irrigation system.

The mapping was enabled by using the best available images, which could be employed over the large study area. First, an image interpretation survey was undertaken. **Table 3.1** lists the different datasets used. The main resource comprised historical satellite images which were acquired at a time before the modern large-scale landscape changes had taken place. Dating to 1960-1972, and with a resolution of 2-5 m, CORONA images were originally collected and used by the US intelligence agencies. CORONA encompassed several different missions; some of these produced better quality images than others.

Following on from declassification in the 1990s, CORONA images have been used to map archaeological landscapes. For example, one of the first archaeological uses of CORONA, the research of Donoghue et al (2002) in the Orontes Valley of Syria, demonstrated that CORONA provided a high spatial resolution, covering a large area in a single panoramic frame at very low cost (Donoghue et al, 2002, p221). These properties of the imagery made it an ideal dataset for the present study; the majority of images were obtained from the Fragile Crescent Project database and from the CORONA Atlas of the Middle East, and had already been georectified by these projects. A few further images were obtained directly from the United States Geological Survey Earth Explorer service. **Chapter 3.2** describes the process of recording water features using the CORONA images, outlining how features were selected, digitised and validated.

The channels identified using image interpretation (see **Chapter 3.2**) required validation to confirm their function as artificial canals and to recognise their chronology. Fieldwork, the use of Digital Elevation Models (DEMs) and comparison with existing survey data enabled this. Fieldwork (see **Table 3.2**) was undertaken in July 2010 in Syria in the Jerablus and Balikh regions (**Chapter 3.3**): a sample of channels were recorded using GPS, allowing known features to be checked, features identified using image interpretation to be confirmed, and new archaeological data to be added to the database.

Hydraulic validation was provided for most of the features throughout the study area by the use of Digital Elevation Models (DEMs) which model the topography of

the landscape. The Shuttle Radar Topography Mission (SRTM) and Advanced Spaceborne Thermal Emission and Reflection Radiometer (ASTER) DEMs are discussed in **Chapter 3.4** and their properties outlined in **Table 3.1**. These were used to characterise the topography in which each channel flowed, and also to generate networks of natural drainage so that these could be separated from the relict artificial features. For features now under the waters of Lake Tabqa topographic data were not available.

A sample of canals in the north of the Balikh valley (the Sahlan Hammam canal and the Nahr al Abbara) and natural streams (The Balikh and the Wadi al Keder) were also explored using higher resolution DEMs produced using the technique of photogrammetry. CORONA satellite KH-4B was equipped with two panoramic cameras, allowing stereopairs to be produced. **Chapter 3.5** describes how a CORONA stereopair (November 1968) was used to derive a DEM of about 10 m grid cell size, despite technical challenges. The DEM enabled an understanding of the morphology of these individual features which could not be gained through the coarser SRTM and ASTER terrain models.

The issues of rainfall amounts and also variability have been recognised in the field of ancient water management (e.g. Wilkinson, 1994) and of modern cultivation in semi-arid zones (e.g. see Wallen, 1967). The high variability of precipitation experienced in parts of the Near East could have been a factor in decisions to irrigate; it would have allowed the generation of more secure crop yields which could not be guaranteed when relying on rainfall alone. A shift from rain-fed to irrigated agriculture may have occurred at the time of the later territorial empires (Neo-Assyrian-Early Islamic). **Chapter 1** discussed proxies employed for past climate in the study area; **Chapter 3.6**, with these in mind, describes a set of methods used by this project to map modern rainfall variability.

Levels of uncertainty involved with using all of these datasets and methods need to be recognised here (e.g. see definitions by the IPCC, in Matschoss et al, 2010, p3). As Brazier et al suggest, data and model certainty are connected (2014, p266). In some cases errors could arise from the original data sets, for example measurement errors in the rainfall data. Processing errors can also affect the elevation models (SRTM, ASTER, and the CORONA DEM). The CORONA

photogrammetry data is further affected by problems of obtaining all the necessary parameters and because software packages do not always explicitly outline their algorithms. At present, the best way of mitigating against many of these problems is to validate results and interpretations by using a variety of datasets. For example, visual interpretation of a CORONA image might indicate the presence of a canal. Using a DEM might verify that a linear feature has hydraulic properties consistent with canals, and historical accounts might also further validate it with specific descriptions. In order to be explicit about the methods and data sources used, these have been outlined in detail here.

It can be difficult to obtain data for Syria and Iraq, for example ground control and high resolution DEMs. Given this, in general, the data represent the best available evidence for use in this interdisciplinary project. This is why the coarse resolution DEMs and the CORONA DEMs were selected. While TanDEM X data was applied for and granted, it was not delivered within the timescale of this research.

This research needed to mitigate against several potential limitations. Unavoidable technical problems limited the size of the area which could be modelled using CORONA photogrammetry (see **Chapter 3.5**), and the war in Syria prevented further fieldwork beyond the preliminary sampling undertaken in July 2010. Most significantly, the issue of obtaining dates for irrigation systems must be recognised here. This is a well-known problem in the field (e.g. see discussions in Wilkinson and Rayne, 2010) often because canals tend to be reused and modified for long periods of time. However, in many cases relative dates could be assigned to the mapped features through association with dated sites (see **Chapters 5 and 6**); sections of a few of the canals had also been excavated. Given the frequently complex life histories of canals and other artificial channels, this project proposes to view them as potentially multi-period and multi-state features.

Through the application of the techniques discussed in this chapter, a central objective of the thesis could be achieved; a detailed dataset of ancient water management in Northern Mesopotamia was generated. Following on from a description of the methods and irrigation design choices (**Chapter 4**), the results of this dataset will be presented in **Chapters 5 and 6**.

3.2 Image interpretation

3.2.1 Introduction

Image interpretation was the primary technique during this research to record features of ancient water management. The features were digitised from CORONA images and then validated using DEMs and survey data. CORONA images were collected between 1960-1972 and declassified in 1995. They were selected as the main dataset for the image interpretation undertaken by the present study because they represent a time before recent agricultural and urban intensification had removed many archaeological remains from the landscape, and they show the landscape at a relatively good resolution of 2-5 m. Declassified in 1995, they consist of frames scanned from 70 mm X 29.8 inch film at resolutions of 1800-3600 dpi (see USGS, 2012) (for more details see **Chapter 3.5** on Photogrammetry).

The images discussed above were manually examined for traces of water management features. To a lesser extent more modern imagery was also used (GeoEye-1 and IKONOS). Better preservation of remains during the 1960s is captured by the older historical imagery, rendering it the most useful source.

The use of CORONA to locate archaeological remains is by now well established (e.g. see Beck et al, 2007; Wilkinson et al, 2006; Donoghue et al, 2002). The Fragile Crescent Project of Durham University integrated archaeological survey with image interpretation techniques, identifying features of interest using CORONA (Galiatsatos et al, 2009).

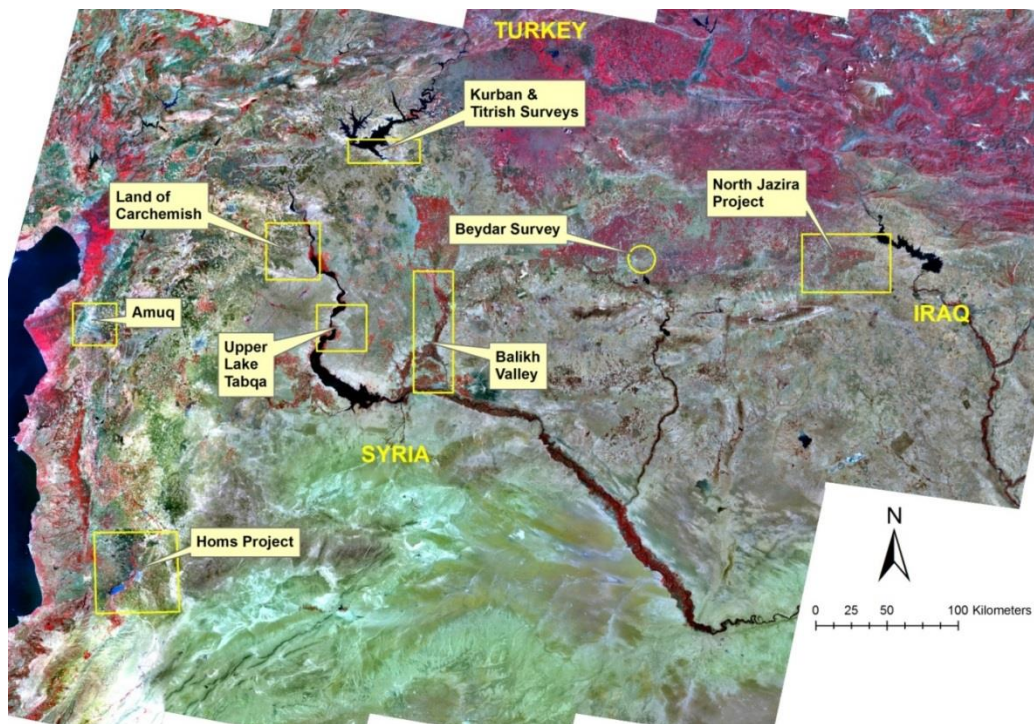


Figure 3.1: Areas surveyed by the Fragile Crescent Project (figure from Niko Galiatsatos).

Within the project area, CORONA has already been applied to several specific areas of water management remains. For example, Wilkinson and Rayne (2010) digitised artificial channels in the Balikh Valley and further east. Altaweel (2008) and Ur (2005) used CORONA to record large-scale canal networks in Northern Iraq, and Ur (2010) also used the imagery to identify possible canal systems near Tell Hamoukar. Galiatsatos and Lawrence (perscomm) used CORONA to map qanats around Membij. These data have been explained in more detail in **Chapter 2**. This project used the same principles but extended the method to encompass the whole of northern Mesopotamia, examining an area of c.100,000 km² using CORONA.

This sampling strategy was chosen for a number of reasons. Firstly, in order to draw wider conclusions about water and imperial power, an area which encompassed more than one immediate zone of any one empire was needed; the selected area comprised the centres and frontier zones of several different empires. Secondly, smaller-scale studies already existed (see **Chapter**). A decision was also made to sample the whole of northern Mesopotamia, unlike the Fragile Crescent Project, which investigated specific survey regions (see **Figure**

3.1 for these regions; also see Galiatsatos et al, 2009, p2). This was because the project aimed to understand patterns of water management throughout the whole region, which would not have been possible if only selected parts of it were sampled.

In some cases the recording of archaeological features using remotely sensed data has been attempted automatically. An example is the study of Menze et al (2006) which used SRTM to classify tell sites. While their model was able to detect sites, false positives also resulted (see Menze et al, 2006, p325). The present project did not use classification to locate water manage features; first, many of these are too small to be identified by the available data, secondly, given the need to examine each result for accuracy when undertaking classification, manual digitisation was more applicable in this case. How this was undertaken and how the results were validated will be outlined below.

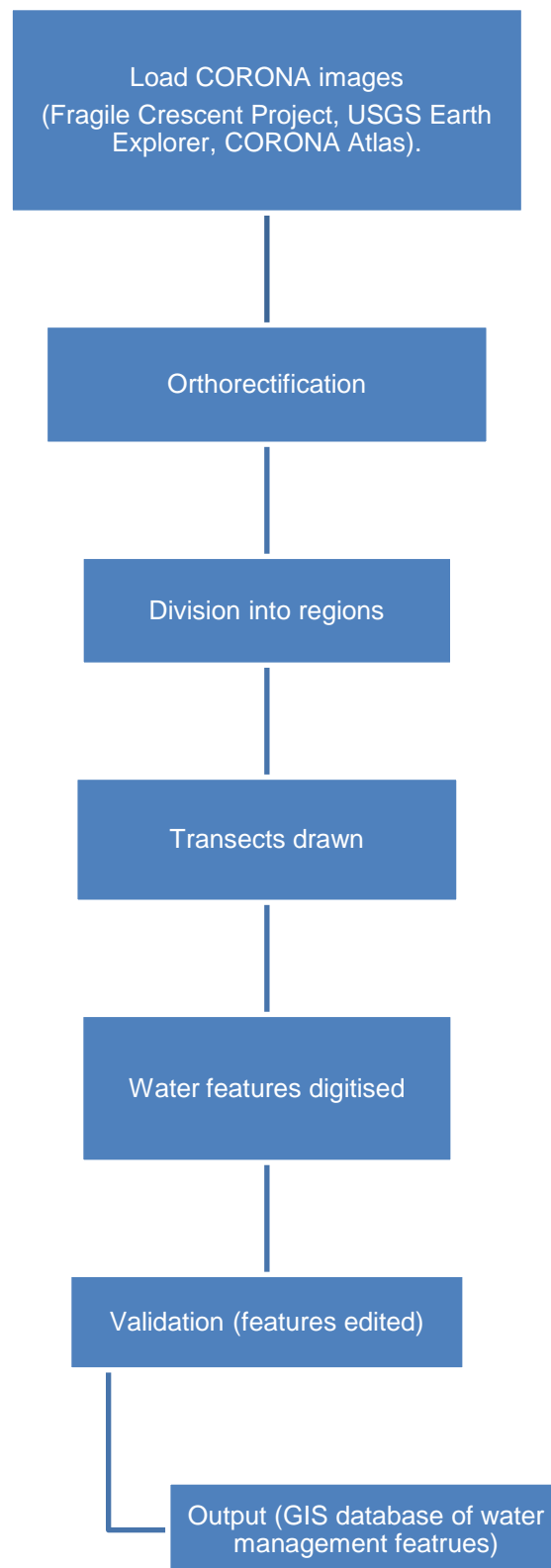


Figure 3.2 *Process of image interpretation used by the present study.*

3.2.2 Processes of Image Interpretation

The image interpretation process used by this study involved several steps, illustrated by **Figure 3.2**. First, images had to be obtained: **Figure 3.3** shows the footprints of the images. Images covering the area between the Euphrates and the steppe to the east of the Balikh in Syria were provided by the Fragile Crescent Project (see Galiatsatos et al, 2009) and had already been orthorectified by the FCP team members. The area between the Habur and the Tigris was mapped using CORONA obtained from the CORONA Atlas of the Near East (Casana et al, 2012). Several additional images were obtained and rectified from the USGS by the present study, in the form of stereo pairs encompassing the Balikh (from November 1968) and a later image of the Western Balikh horseshoe (dating to May 1972). These were rectified with reference to Landsat images and already-rectified CORONA images.

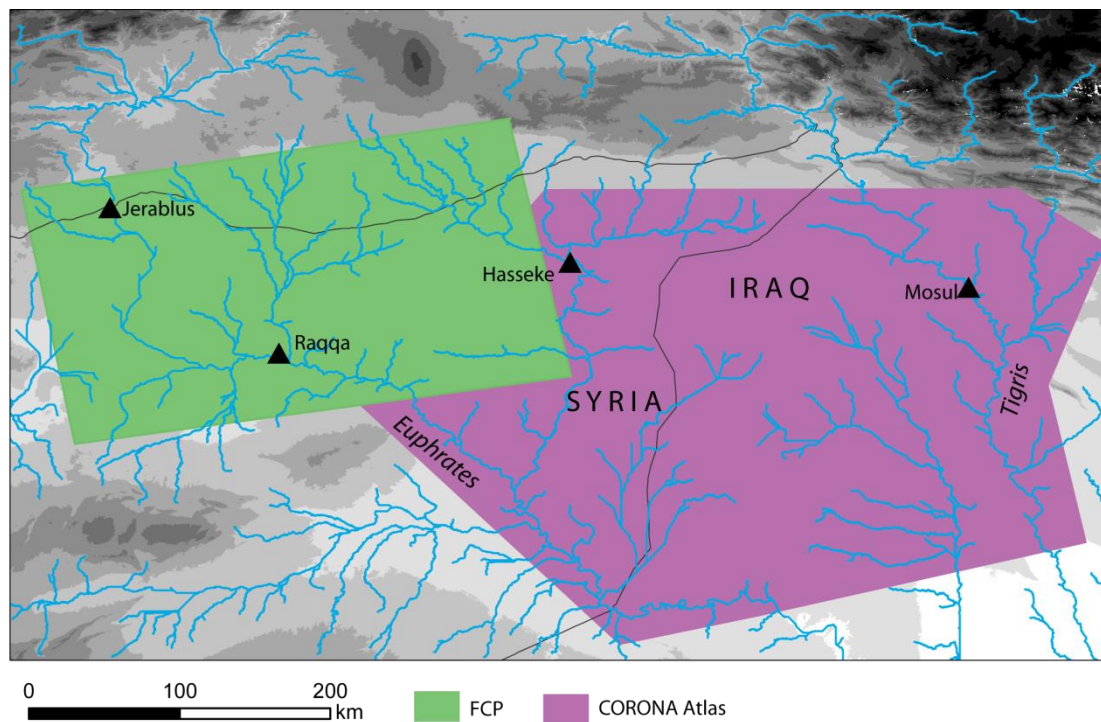


Figure 3.3 Outlines of areas investigated using imagery. Images were obtained from the Fragile Crescent Project and the CORONA Atlas of the Near East (Center for Advanced Spatial Technologies, University of Arkansas/U.S Geological Survey).

In order to speed up computer processing, the CORONA images were loaded into the GIS software (ArcMap in this case) and viewed in regions. Each frame was divided into transects (see **Figure 3.4**) so that it could be examined for features of interest at a scale of 1:30,000. It was found that this scale was sufficient to enable channels to be identified. Water features of interest visible in the imagery were digitised.

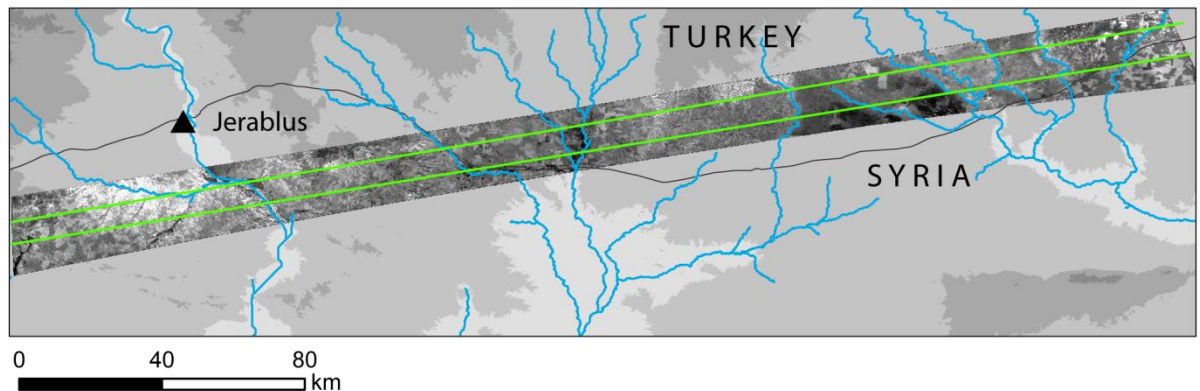


Figure 3.4 CORONA image (22 January 1967) divided into three transects, viewable at a scale of 1:30,000.

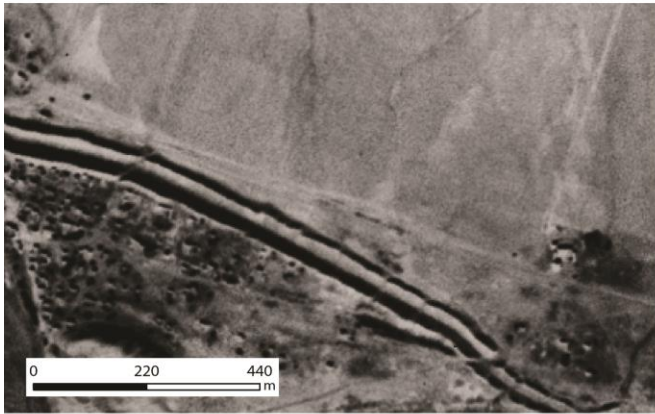
3.2.3 Feature identification and digitisation

While digitising water management features, several principles were adhered to. These involved only digitising and retaining features which could be reliably presumed to be water channels; only retaining those which were clearly artificial rather than natural channels; and only retaining features which were not very modern (20th-21st century). The process of digitisation will be explained in more detail in the validation section below (3.2.4).

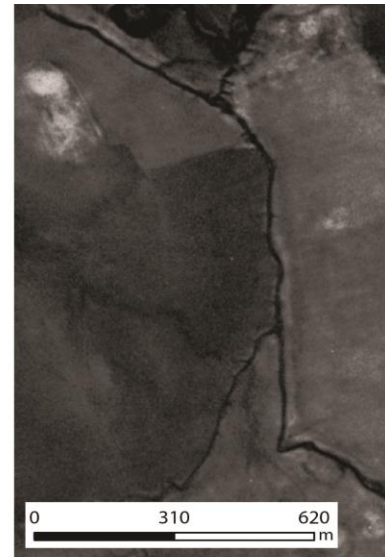
Channels were digitised using the editor toolbar in ArcMap and incorporated into a GIS database. Where possible, different parts of irrigation networks were recorded according to their function (e.g. main canal, lateral. See **Chapter 4** for more information). Once the entire area had been examined and features of interest digitised, the shapefiles were edited. Features which could not be clearly identified as ancient canals were removed.

Different types of canals and other artificial channels could be recognised in the imagery, as **Figure 3.2.5** shows. Given that CORONA imagery is panchromatic, a key tool that can be employed is contrast stretching. As **Figure 3.2.6** shows, different stretches can be employed to enhance the appearance of archaeological features. The histogram equalise stretch makes the fainter channels appear darker than the surrounding soil. Using these tools in ArcGIS revealed that canals consisted of soil-marks or of a channel void depression, and were generally represented by darker pixels either as a result of shadowing from banks or from vegetation. While some canals lack clear embankments, some canals had significant upcast banks (e.g. **Figure 3.2.5**, number 1), sometimes built as part of a need to keep a canal raised above the surrounding fields, and also sometimes the product of the dumping of soil excavated from canals during construction and cleaning.

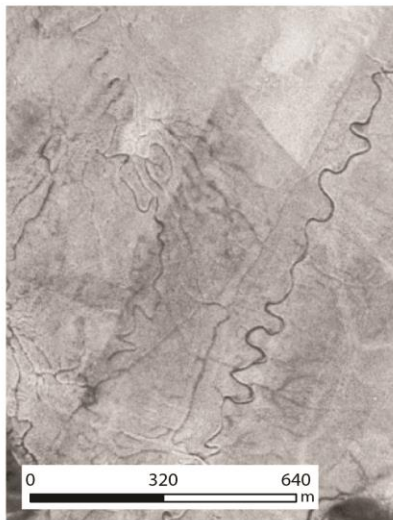
Qanats (see **Chapter 4**) could also be identified. These are underground channels, of which there are several different types. True qanats are groundwater collection devices. Tunnels integrated into existing irrigation systems were also used, generally in order to cut through higher ground. In some cases, subterranean conduits channelled springwater. Generally, they can all be located by the presence of lines of lighter-coloured dots, representing maintenance shafts surrounded by heaps of spoil (**Figure 3.5(4)** is an example).



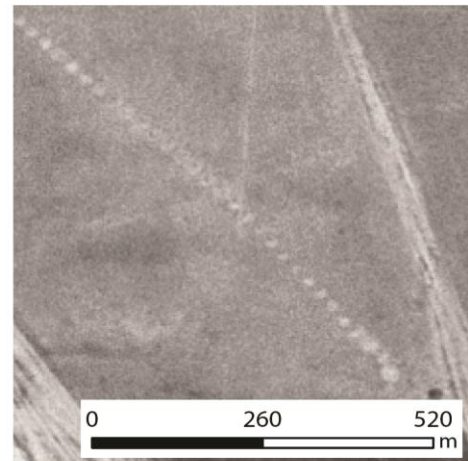
1. Straight trace and form, prominent upcast banks.



2. Straight trace and form, low banks.



3. Straight trace, meandering form.



4. Qanat shafts.

Figure 3.5 Examples of channel types in Syria identifiable in 1960s CORONA images (22 January 1967).

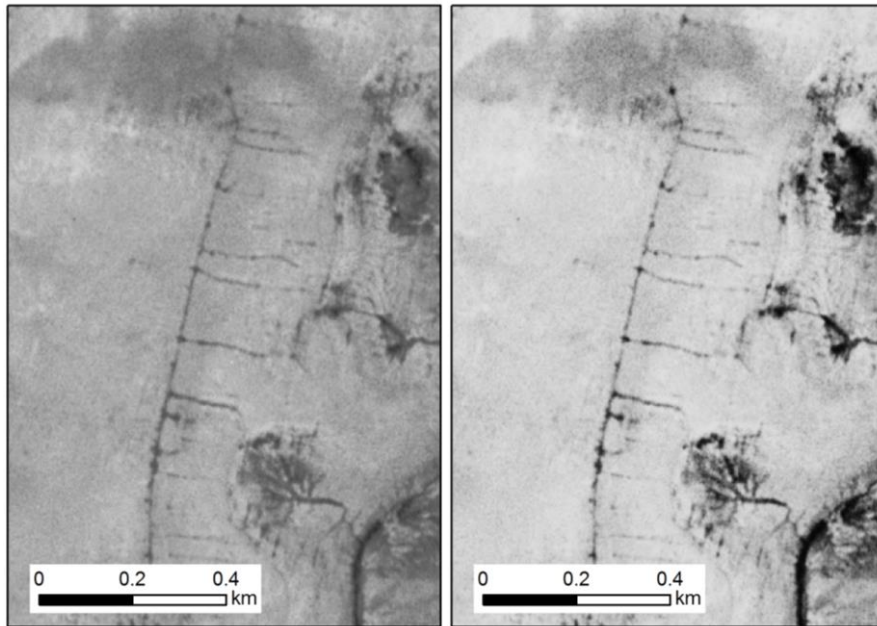


Figure 3.6 *The panchromatic CORONA images can be enhanced. A standard deviation stretch was applied to the left image, and a histogram equalise stretch to the right. CORONA image 22 January 1967.*

The digitised irrigation systems generally form specific parts of a system (depicted in **Figure 3.7** and explained in detail in **Chapter 4**). In some cases they could be identified in the imagery;

1. Abstraction and transportation: an intake system is expected here, from a river or dam, for example in the form of an open canal or a weir. A transportation canal then takes water supplies to the area to be irrigated. The main canals are generally the best preserved parts of relict irrigation systems and therefore are mostly to be identified using image interpretation.
2. Use: Irrigation laterals (offtakes) distribute water to the fields. Being smaller and often erased these are usually not as well preserved as the transportation segments of an irrigation system. In some cases they may be too small to be identified in the CORONA imagery. However, ancient examples of similar layouts are known, for example, the narrow (1-2 m) laterals which were part of the Hohokam systems (Doolittle, 1991, p141).

3. Drainage: At the lower end of an irrigation network excess water is removed from the system, often by being drained back into a natural water course. Occasionally relict examples can be seen in the imagery.

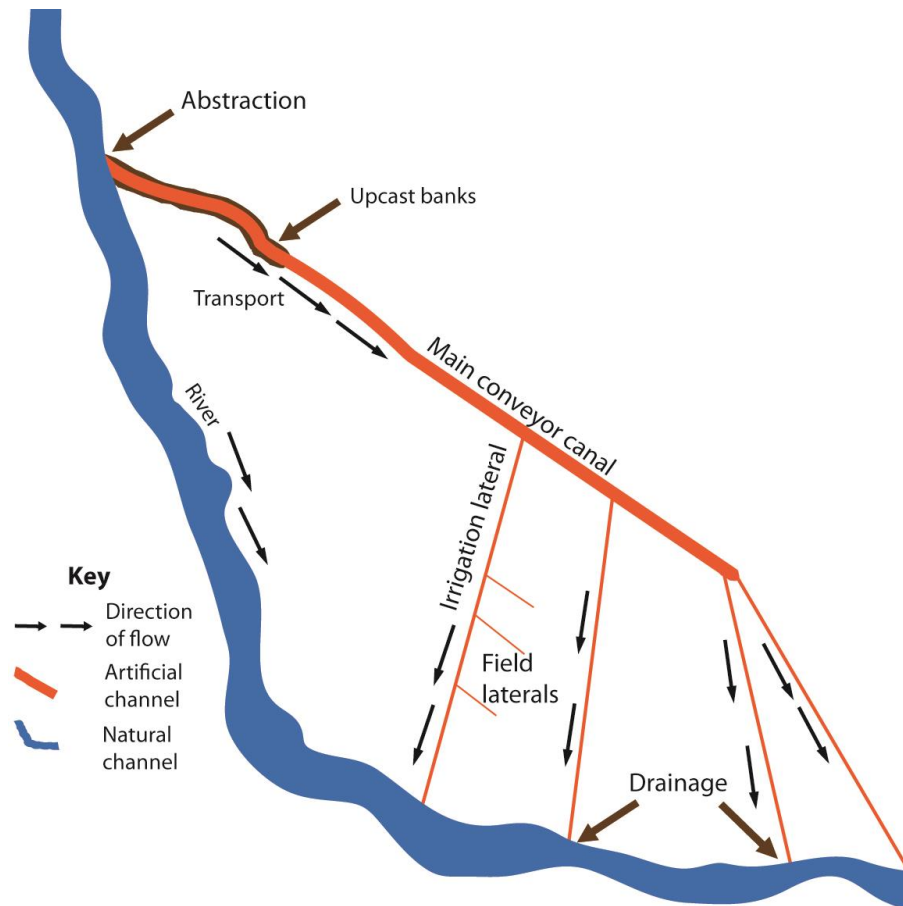


Figure 3.7: Schematic diagram of a typical irrigation system.

Other systems, and parts of systems, for example rock-cut conduits, dams and weirs, are not easily recognisable from space. This was generally because they were small, indistinguishable from natural geology or obscured by other features. These data were therefore derived from fieldwork and existing studies; GPS points were collected for features found in Syria in July 2010. **Figure 3.8** shows a masonry block, discovered in the dry Wadi Armana, indicating the presence of a rock-cut channel that could not be identified in the available imagery. Similarly, stone blocks were known from the Balikh, possibly associated with the offtakes of the Nahr al Abbara system (see Wilkinson, 1998, p68).



Figure 3.8: *Masonry block with mason's mark from a rock-cut channel in the Jerablus region of north Syria. These rock-cut conduits are not visible from space. Photograph: July 2010.*

3.2.4 Validation

While dating of water management features is generally difficult, where possible, the channels were validated by relating them to existing surveys and associated with sites of known date. In some cases it was possible to use multiple types of imagery (e.g. CORONA and IKONOS for the area around Raqqa). Similarly, geomorphological considerations were taken into account. Given that research assigns a post-medieval date to much of the Euphrates floodplain (e.g. Hritz, 2013a, p1878), canals within the floodplain can be regarded as post-medieval.

The appearance of canals can also be used to recognise whether they are pre-20th century AD. First, the overall 'straightness' of canals can be assessed. The straightest and 'sharpest' canals tend to be modern, often constructed from concrete, as **Figure 3.9** shows. Modern engineering and construction methods have facilitated the cutting through of topography. Ancient channels were more likely to follow the natural gradient of the landscape.

In contrast, ancient canals will have been susceptible to erosion and infilling over time, especially after active use ended, causing them to have a less 'sharp' appearance. The Sahlan Hammam canal (see **Figure 3.10**) is a good example. While the channel void and upcast banks are visible in the 1990s photograph, they are much less clearly delineated than in the case of a recently constructed canal.



Figure 3.9: Modern concrete-lined canal in the Balikh in 2010.



Figure 3.10: Eroded and infilled canal. The upcast banks of the Hammam canal (foreground) were still visible in the 1990s (photograph from Tony Wilkinson, pers.comm).

Ancient canals were sometimes subject to siltation, which can affect their form. This can lead to the channels meandering within their original trace, producing a distinctive morphology, as **Figure 3.2.5** shows. Excessive siltation can be a problem in landscapes of low relief and shallow slope (such as the Balikh), necessitating frequent cleaning to maintain channel efficiency.

Areas of ancient irrigation also suffered from problems such as waterlogging and salinization, especially where natural drainage was poor or not constructed as part of the irrigation system. Marshy areas with shallow water tables may in some cases represent the end points of former canal systems (e.g. see Wilkinson and Rayne, 2010, fig.8). Similarly, gilgai (see **Chapter 1** and **Chapter 6**) may also be an indicator of relict irrigation, specifically the former flood basins.

Identification of archaeological features by image interpretation can be further validated, in terms of verifying locations and providing dates of use, through ground-based survey (for example see Wilkinson et al, 2006, p738). As part of this study, a sample of the mapped canals was visited in 2010 during fieldwork. This made it possible to confirm whether the channels were still in use. For example, the canal between Carchemish and Jerablus Tahtani still contained water when it was recorded in the field as well as on satellite images. Known rock cut qanats in the Jerablus region were also visited, and several new features recorded. These were not identifiable on the imagery, indicating the need for both validation and survey using fieldwork. Canals in the Balikh that were visible in the 1960s imagery were found to be further eroded by 2010 and some had disappeared altogether.

In order to validate the linear features visible in the CORONA images, they also had to be identified as canals, as opposed to other linear features such as hollow ways. Discussions of features in the Habur have dealt with these distinctions (Ur and Wilkinson, 2008, p311-12; McClellan et al, 2000, p143-51). Ultimately, however, ancient canals, unlike hollow ways, need to allow for gravity flow, following the natural contours of the landscape.. It should be noted here that while most canals conform to this rule, a few later canals may not. Hollow ways often form distinctive patterns, radiating from archaeological sites and cutting across the contours. SRTM, ASTER and CORONA-derived DEMs were used by this project to test this difference (see **Chapter 3.4** and **3.5**). **Figures 3.11, 3.12** and **3.13**

show the distinction between linear features near Medinat al Farr in the Balikh; the SRTM DEM shows that the hollow way cuts through the landscape with no clear topographic trend, while the canal is closely aligned to it, sloping according to a clear trend.



Figure 3.11: Linear features around the Early Islamic site of Medinat al Farr. CORONA image from 22 January 1967.

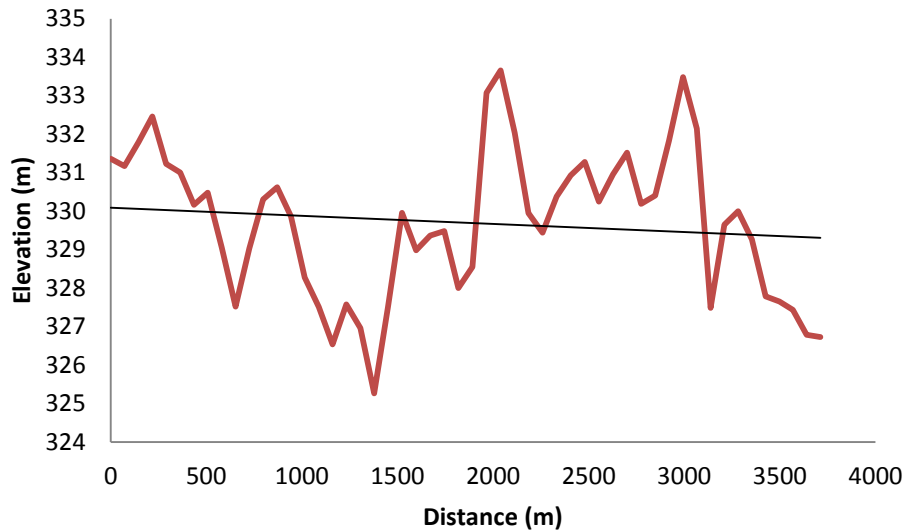


Figure 3.12: This example of a longitudinal profile of a hollow way runs across the natural gradient of the landscape, disregarding it (see **Figure 3.11**).

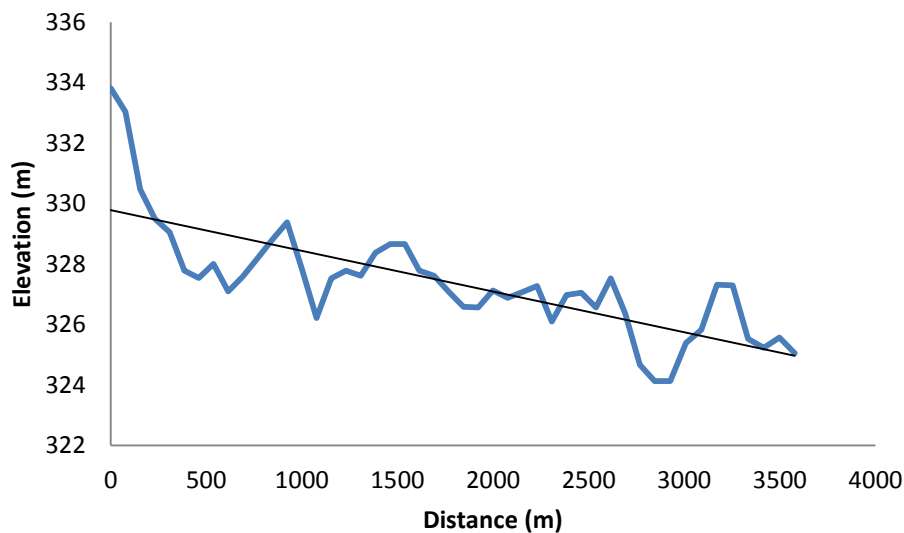


Figure 3.13: This example of a canal longitudinal profile shows that it is constrained by the need for gravity flow, therefore following the natural contours of the landscape (allowing for noise contained in the SRTM DEM) (see **Figure 3.11**).

Whether or not a channel was a natural stream or a canal also needed to be confirmed. To some extent this could be done based on their appearance, because some canals consisted of fairly straight channels and prominent upcast banks. In other cases this was less clear. Again, the DEMs were used for validation. Stream networks were derived from the SRTM and ASTER DEMs (see

Chapter 3.4). These networks represent natural drainage based on locations of flow accumulation. It was found that while the model identified the natural streams, it did not identify canals, allowing the natural and artificial channels to be distinguished. Digitised features which were too similar to the modelled stream network were discarded, although possible modification of natural streams was considered where necessary.

3.2.5 Summary

The validation process described here enabled irrigation systems and individual features and parts of systems to be digitised with a reasonable degree of confidence. The CORONA images allowed features to be located which are no longer present in the modern landscape and are therefore not identifiable using modern imagery. The sampling strategy chosen ensured that a comprehensive region could be mapped in its entirety, allowing for the identification of any spatial trends and patterns. Using this approach also enabled the full extent of preserved segments of canals and offtakes to be recorded, revealing information about the scale of ancient water management systems.

The following sections will describe how DEMs and fieldwork data were used to validate the digitised results. Canals could be distinguished from roads and from natural streams. In many cases, relative dates could also be assigned based on association with known sites.

3.3 Fieldwork

3.3.1 Introduction

An initial season of fieldwork was undertaken in Syria in July 2010, as part of research carried out by the Land of Carchemish project and Fragile Crescent Project of Durham University. Fieldwork enabled several features located using satellite imagery to be visited and surveyed. Unfortunately, further fieldwork was not possible, given the war in Syria since 2011. However, the work that was

undertaken enabled a sample of the remotely sensed evidence to be validated and confirmed.

The Jerablus and Balikh regions were visited. Several relict water features of note had already been identified in the Jerablus region by recent survey (see Wilkinson et al, 2007). In the Balikh, archaeological survey in the 1990s had recorded relict canals (Wilkinson, 1998). On the whole, excavation or fieldwalking were not possible at these locations. However, GPS points were collected in order to locate features of interest.

3.3.2 Jerablus

Most of the fieldwork undertaken for this study was carried out in the vicinity of Carchemish/Jerablus. Several different sites were visited, including previously recorded sites and newly discovered sites. The known sites (already recorded in previous years by the Land of Carchemish Project; see Wilkinson et al, 2007) included a canal between Carchemish and Jerablus Tahtani; features along the Wadis Sajur and Armana; and a rock-cut conduit in the hills south-west of Carchemish near Hajaliyyeh. Several further rock-cut conduits were located in the Wadi Armana. GPS points were logged for these features and measurements noted. They are described in more detail in **Chapter 5**.

It should be mentioned here that fieldwork in the Jerablus region recorded features that were not visible in the remotely sensed datasets, especially the rock-cut conduits in the wadi sides. This raises the likelihood that there are many other similar features throughout Northern Mesopotamia that cannot be identified without fieldwork. The visibility of the sites visited in 2010 is listed in **Table 3.3**

Table 3.3: *Water management features around Jerablus visited during fieldwork in 2010. See Table 2.1, Figure 2.2 and Chapter 5.2.*

Water management features	Visibility
Carchemish- Jerablus Tahtani canal	CORONA and field survey
Nahr al Amarna rock-cut channels	Field survey
Rock cut channel near Hajaliyyeh	Field Survey
Rock-cut conduit at Khirbet Serisat	Field survey

3.3.3 Balikh

In contrast, in the Balikh water management features could be identified using satellite imagery. However, many of the features which were present in the 1960s imagery had since been removed from the landscape due to recent intensification of agriculture (e.g. see Hole and Zaitchik, 2006). As **Table 3.3.2** outlines, three known canals were visited in the Balikh region in 2010. The original survey data (Wilkinson, 1998) and the satellite data could then be compared with the current state of the features.

Table 3.4: *State of preservation of canals in the Balikh in 2010.*

Canals visible in CORONA images	Visibility
Canal at Heraqlah	CORONA and field survey
Sahlan-Hammam channel	CORONA
Nahr al Abbara	CORONA. Removed and replaced by wells on similar alignment

A canal close to Heraqlah was investigated (see **Chapter 5b**). It had already been noted by several researchers (Bell, 1924, p53-54; Heidemann, 2006, p36; Kamash, 2009, vol3 p4) and has been described as Early Islamic (Heidemann, 2006, p36). However, the CORONA imagery suggested that this canal was post-Early-Islamic, based on its truncation of the medieval site of Heraqlah. Fieldwork confirmed this situation, and also found that the canal had further eroded since the time of the CORONA imagery (see **Chapter 6**).

A segment of the Sahlan-Hamman canal, at Tell Hammam et Turkman, was also investigated in the field. Originally surveyed by Wilkinson (1998, p70), it is clearly identifiable using the CORONA imagery and CORONA-derived DEM (see **Chapter 6**). On the east side of the tell, the Early Islamic Nahr al Abbara (also see Wilkinson, 1998, p67) was looked for. Neither canal was present because both had been removed since the 1990s, although a series of what appeared to be modern wells followed the alignment of the Nahr al Abbara, possibly taking advantage of a raised water table within the relict canal. In contrast to the fieldwork undertaken at Jerablus, where fieldwork is especially necessary, this rapid change in the landscape of the Balikh highlights the usefulness of using remote sensing, particularly historical datasets such as CORONA.

3.3.4 Summary

The sample of sites visited in July 2010 enabled those features themselves to be confirmed, and also validated the overall interdisciplinary methodology of the project. A range of evidence was needed to identify the features in the database, because not all features were identifiable in all the datasets. Some sites were identified in the field that were not visible in the imagery, suggesting a need for further fieldwork. The results of the fieldwork undertaken in the Balikh showed that canal remains that can be located using historical imagery are quickly disappearing from the landscape, especially in areas where modern agriculture has been focussed. Many other sites researched by this project have also been removed, including several which are now under the waters of the Tabqa Dam (for example the canals at Dibsi Faraj and Tell Fray discussed in **Chapter 5**). Throughout the whole project area, modern satellite images such as GeoEye-1 and IKONOS were generally devoid of the remains that were present in the CORONA images. CORONA-based remote-sensing techniques, such as the image interpretation and photogrammetry undertaken by this project, are therefore the principal ways in which many of these features can now be further investigated.

The remains only visible on the ground at Jerablus, and the remains only identifiable using CORONA elsewhere, serve to emphasise the need for the kind of multidisciplinary research undertaken by this study.

3.4 SRTM and ASTER

3.4.1 Introduction

Low resolution elevation models were used to recognise the general gradient of the landscape in relation to relict water management systems. Secondly, the models were used to generate stream networks using processes outlined below.

SRTM (NASA) and ASTER (NASA and Japan's METI) DEMs were used in these analyses. Both data sets are referenced to the WGS84 datum. While the data sets are roughly contemporaneous (launched in 1999 for the ASTER and collected in 2000 for the SRTM) it is important to note that they were produced in different ways and have different resolutions, as **Figure 3.14** shows (90m for the SRTM and 30m for the ASTER). The SRTM DEM is radar data generated through interferometry whereas the ASTER GDEM is the output of photogrammetric processing of optical satellite images.

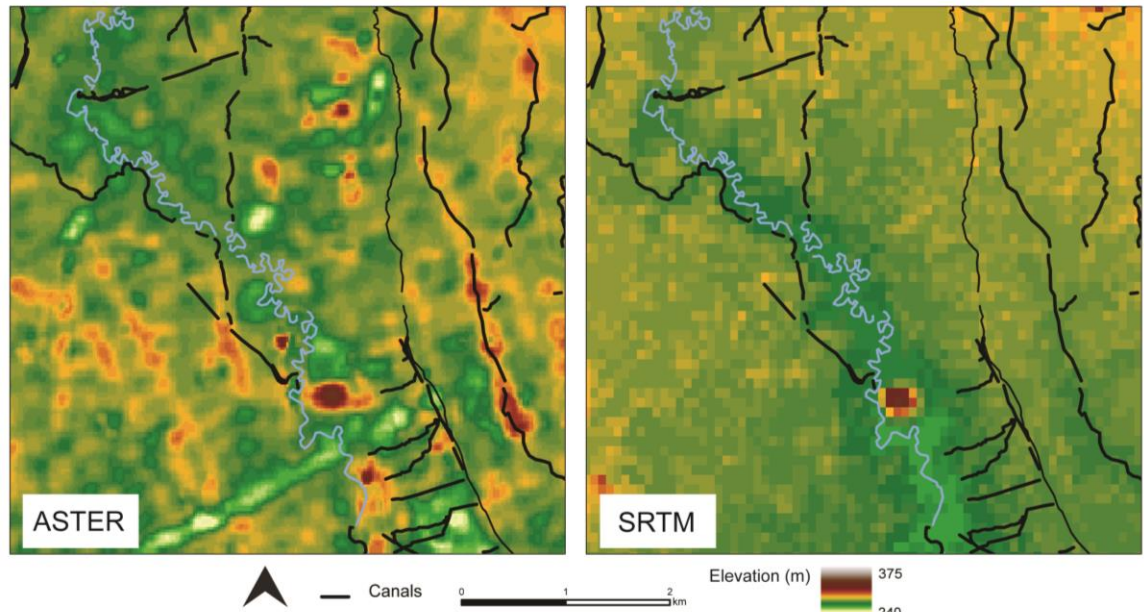


Figure 3.14: ASTER has a pixel size of 30 m and SRTM of 90 m; both are generally too coarse to show relict canals. For this example, contrast stretches were applied that best highlight the difference in resolution between the two datasets. They contain modern features which were not present at the time of the CORONA images used to digitise the canals.

The freely-available Shuttle Radar Topography Mission (SRTM) data is processed to a relatively coarse 90m pixel size (3 arc seconds). However, in general, this has a vertical accuracy of about 9 m (Farr et al, 2007, p19). For this project, Version 2 of the SRTM3 C-band radar data was used; this version has undergone editing before delivery and has been validated using GPS data.

The data were gathered by the NASA space shuttle using dual radar antennas which obtained interferometric radar data: collecting two radar datasets from different but close vantage points enabled the elevation to be measured by triangulating between the position of the antennas and the measured points (Farr et al, 2007, p1-5).

In contrast, the Advanced Spaceborne Thermal Emission and Reflection Radiometer Global Digital Elevation Model (ASTER GDEM) was derived using stereoscopic spaceborne imagery with a spatial resolution of 15 m; the GDEM has a grid cell size of 30 m (1 arc second) (see Abrams et al, 2010). In general,

the vertical accuracy is about 20 m, although this varies (Bulatovic et al, 2012, p5916); sampling indicates that the error is worse for hilly terrain (ibid, p5925).

There are some issues of uncertainty when using SRTM and ASTER data. While for example an analysis of SRTM accuracy indicated that SRTM can over predict gradient in flatter areas (Kinsey-Henderson and Wilkinson, 2013, p129), such as alluvial floodplains (ibid, p133), Vente et al (2009) found that SRTM gave more accurate estimates of slope gradient than ASTER.

Given these problems, one mitigation strategy would be to validate DEMs using GPS, if fieldwork were to again be possible in Syria and Iraq. In the meantime, data should be analysed using more than one DEM, using high-resolution elevation data where possible. CORONA photogrammetry offers the opportunity for this. In the future, GPS and TanDEM X data could be applied.

The different ways the images are obtained can lead to differences in the kinds of errors that are produced. For example, SRTM is affected by random speckles of noise (Rodriguez et al, 2006, p251). Water surfaces were sometimes also measured inaccurately by the C-band radar (Farr et al, 2007, p28), although some editing was undertaken for the Version 2 product. Noise can affect both datasets, especially in low-lying areas in the SRTM (Sanders, 2007). ASTER is affected by cloud cover; some anomalies and missing data values were the result of this (e.g. see an assessment by Hirano et al, 2003, p366).

The focus of this discussion will be the data produced, rather than the undertaking of an exercise of comparison. Comparisons between the two datasets have already been made: for example, Hayakawa et al (2008, p3-4) suggest that ASTER GDEM data contain fewer errors. However, Hirt et al (2010, p20) found that in some cases errors present in the ASTER GDEM were significantly limiting (stripes (ibid.p13) and clouds (ibid. p11), for example).

Now that the data itself and associated issues have been reviewed, the process of generating the stream network models will be outlined below.

3.4.2 SRTM and ASTER stream network models

Because this research aimed to identify features of ancient water management, it was important to distinguish between natural and artificial channels and to understand the relationship of artificial features within their hydrological context. The most reliable way of doing this was to model the areas where flow is most likely to be concentrated using established algorithms; the ArcGIS Spatial Analyst toolset, which includes hydrology tools, was used so that this could be done simply and quickly.

This project found that the SRTM and ASTER stream networks identified natural channels effectively, an observation that could be confirmed by checking them against satellite images where the channels were visible.

In order to generate the stream networks a sequence of processing was undertaken for the data. The same method was used for both SRTM and ASTER. This sequence (represented in **Figure 3.15**) is a long-established and oft-tested one (e.g. see Jenson and Domingue, 1988 for an early example which outlines the basic processes). How this was employed in the context of the present research will now be outlined.

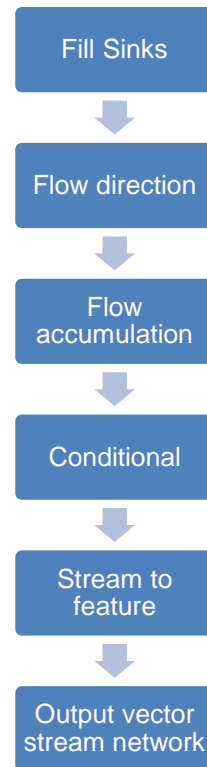


Figure 3.15: The process of creating a stream network using the ArcGIS hydrology tools is straightforward.

3.4.3 Fill sinks

Figure 3.16 shows a diagram of a typical sink. Both the SRTM and ASTER datasets contain these small errors of isolated pixels of lower elevations ('sinks') than surrounding pixels which the analysis would mistakenly identify as miniature drainage basins; such errors make the analysis impossible. However, these pixels can be 'filled'.

First, the sink tool can be run to identify their number and depth. The fill tool is then used to fill the sinks based on an inputted value. This value, the 'Z limit', represents the difference between a sink and its pour point, the pixel with the lowest elevation of the surrounding pixels which bound the sink. The tool will not fill any pixels identified as sinks if the difference is greater than the defined Z limit.

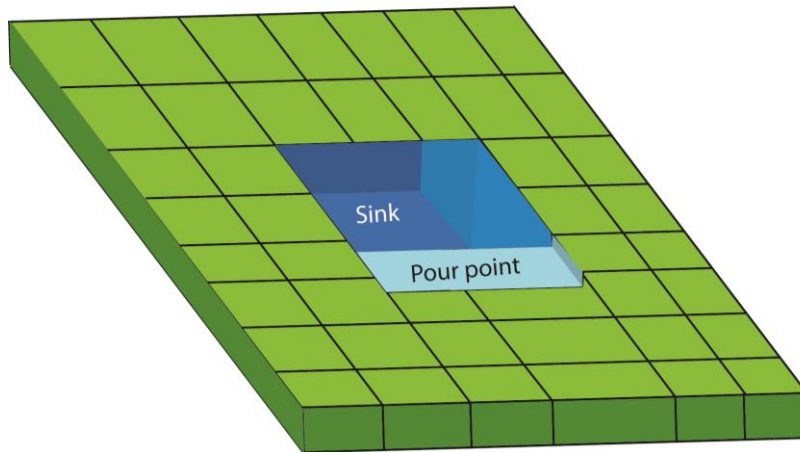


Figure 3.16: illustration showing how the difference between the lowest pixel and the lowest surrounding pixel forms the 'z limit'.

Sinks were found in both the SRTM and ASTER DEMs: for the SRTM, across an area of 8054 X 4801 cells, 116636 were identified as sinks (see **Figure 3.17**). The fill tool was used to remove these so that further processing could be undertaken.

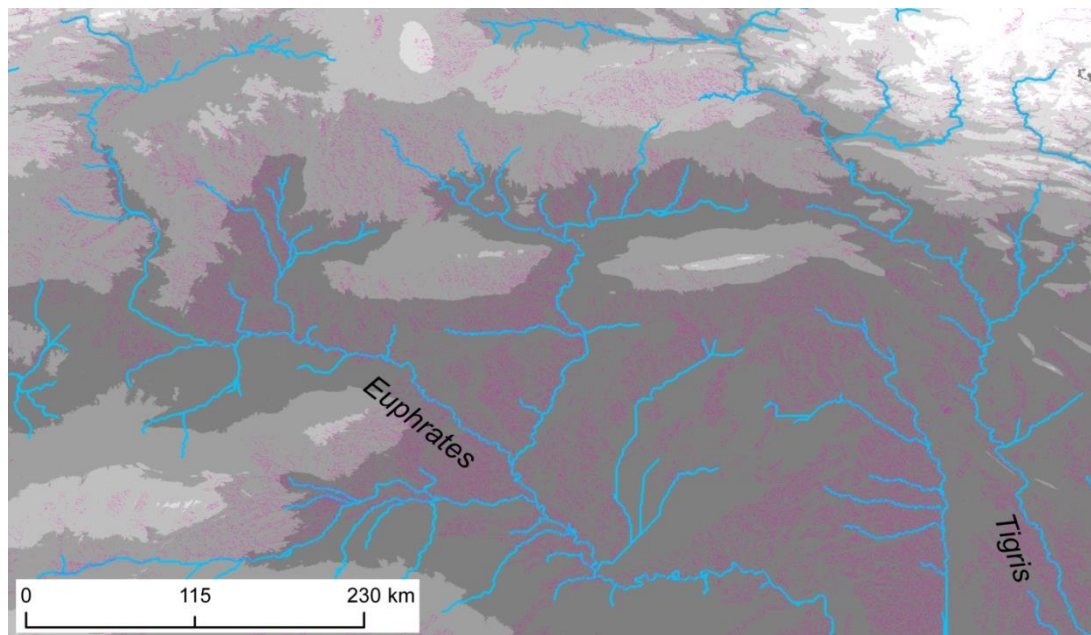


Figure 3.17: The pink dots represent sinks in the SRTM throughout the project area.

$$\text{Flow direction code} = \frac{a - b}{d}$$

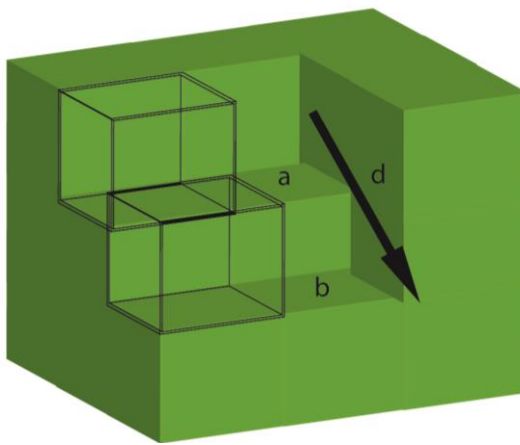


Figure 3.18: Flow direction coding.

3.4.4 Flow direction

Once sinks have been filled, it is necessary to find the direction of flow (see Verdin and Verdin, 1999, p5). This could go into any one of the 8 pixels which surround one pixel. The default algorithm offered by ArcGIS was used consistently. Future comparative exercises could make use of different DEMs and software to use alternative algorithms. The flow will follow the greatest descent; coded values are assigned for the output based on this.(e.g. see Jenson and Domingue, 1988, p1594). The output raster (**Figure 3.19**) shows the direction of flow for the SRTM DEM; however, further processing is needed in order to derive the stream network.

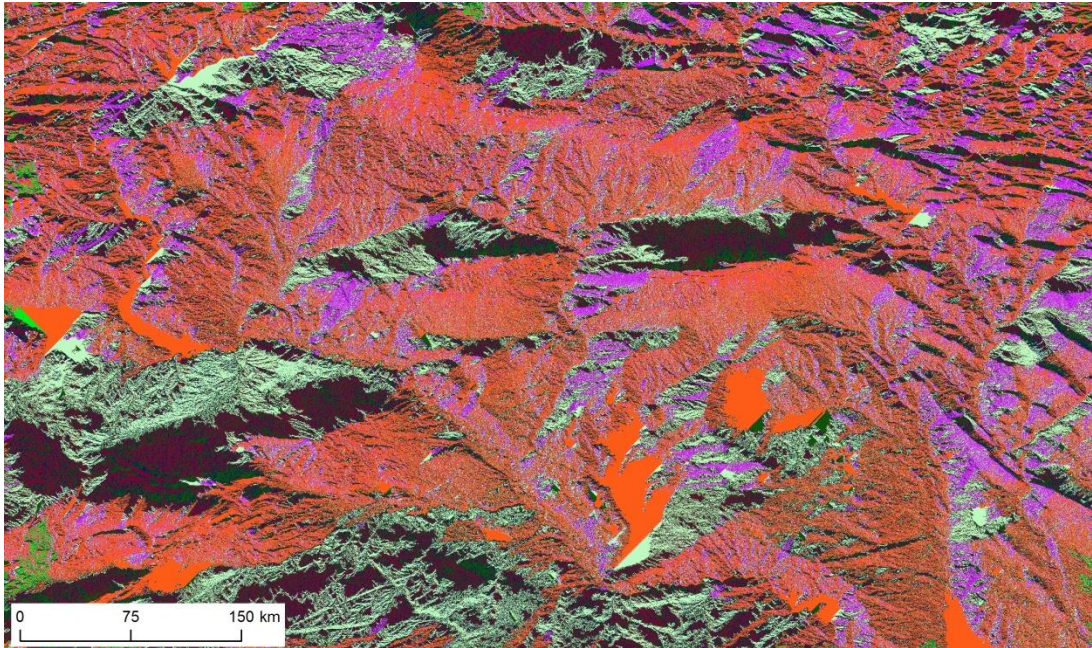


Figure 3.19: Flow direction can be modelled using an elevation model such as SRTM. The colours represent the coded values assigned by the flow direction algorithm.

3.4.5 Flow accumulation

Once the direction of flow is known, the accumulated flow into each pixel can be calculated because the pixels with the highest flow accumulation values are more likely to be streams. These values are the accumulated flow from all pixels in the flow direction raster that flow into each downslope pixel; the pixel values of the output represent the number of pixels that flowed into those pixels. The output of using this tool (**Figure 3.20**) is a representation of drainage patterns in Northern Mesopotamia.

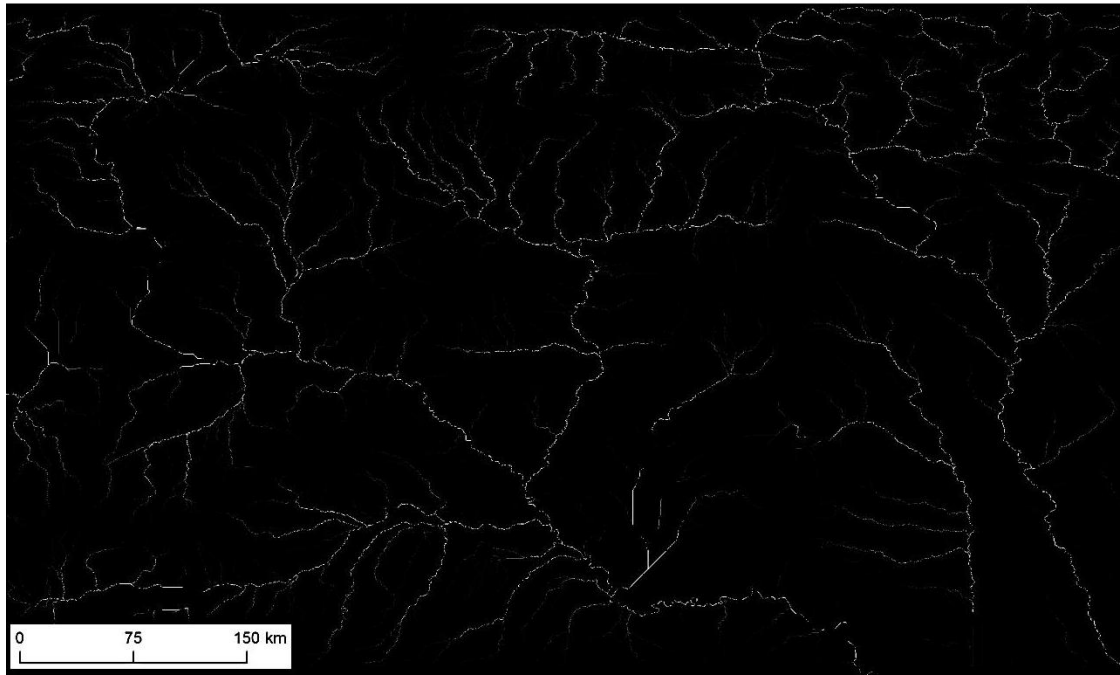


Figure 3.20: *The raster output of the Flow Accumulation tool identifies the locations where flow is most concentrated.*

3.4.6 Conditional evaluation

While the flow accumulation raster is informative, it is useful to generate a vector drainage network. The flow accumulation raster can therefore be thresholded to separate the pixels with the highest values (most likely to be streams) from those with lower flow accumulations (more ephemeral, seasonal streams or palaeo-drainages). Higher threshold values will delineate fewer streams, only selecting the more significant features. In this case, the Con [conditional] tool of the ArcGIS Spatial Analyst was used to undertake a conditional evaluation of the flow accumulation data to produce the output raster.

The channels which received the most flow were represented by larger cell values within the flow accumulation raster. For example, the Euphrates was in this category. Smaller wadis and seasonal streams had lower values. Choosing a higher threshold value will reveal less of the more ephemeral features but will make it more difficult to distinguish visually the significant channels; therefore, several different thresholds were used depending on the resolution required for specific tasks and maps; **Table 3.5** shows the values used to produce the stream

networks in **Figure 3.21**. For the SRTM flow accumulation raster a conditional value of > 100000 was used. This highlighted the most significant channels.

Table 3.5: *Conditional threshold applied to flow accumulation rasters; shown in Figure 3.21.*

	SRTM	ASTER
Conditional threshold cell value below which streams were discarded (see Figure 3.4.8)	100000	1500

3.4.7 Stream to feature

The conditional raster can be used to generate a vector stream network. Turning the raster into a vector makes it easier to manipulate and display. This works by using the flow direction raster and the conditional raster.

Again, the output of the conditional tool is thresholded; values above the inputted threshold will form vector features. Values below this will be discarded and will not form part of the output. In the example shown in **Figure 3.21**, as part of the conditional algorithm, all cell values in the SRTM flow accumulation above 100000 were retained and reclassified as 1, while values below this were classified as 0. Using the stream to feature tool, only the 1s will be converted into features.

The SRTM was used to identify the most prominent channels throughout the whole project area. Even if a lower threshold value had been selected for the conditional, the smaller wadis could not have been identified. The higher resolution of the ASTER DEM enabled a denser network of streams to be mapped, including narrow and ephemeral seasonal wadis. The flow models were later used to display the locations of natural channels and for comparison with the locations of artificial channels (see **Chapter 5** and **Chapter 6**). Many of the streams identified by the use of the hydro tools could be verified through comparison with satellite images whereas others were less clear and may be palaeochannels or seasonal streams.

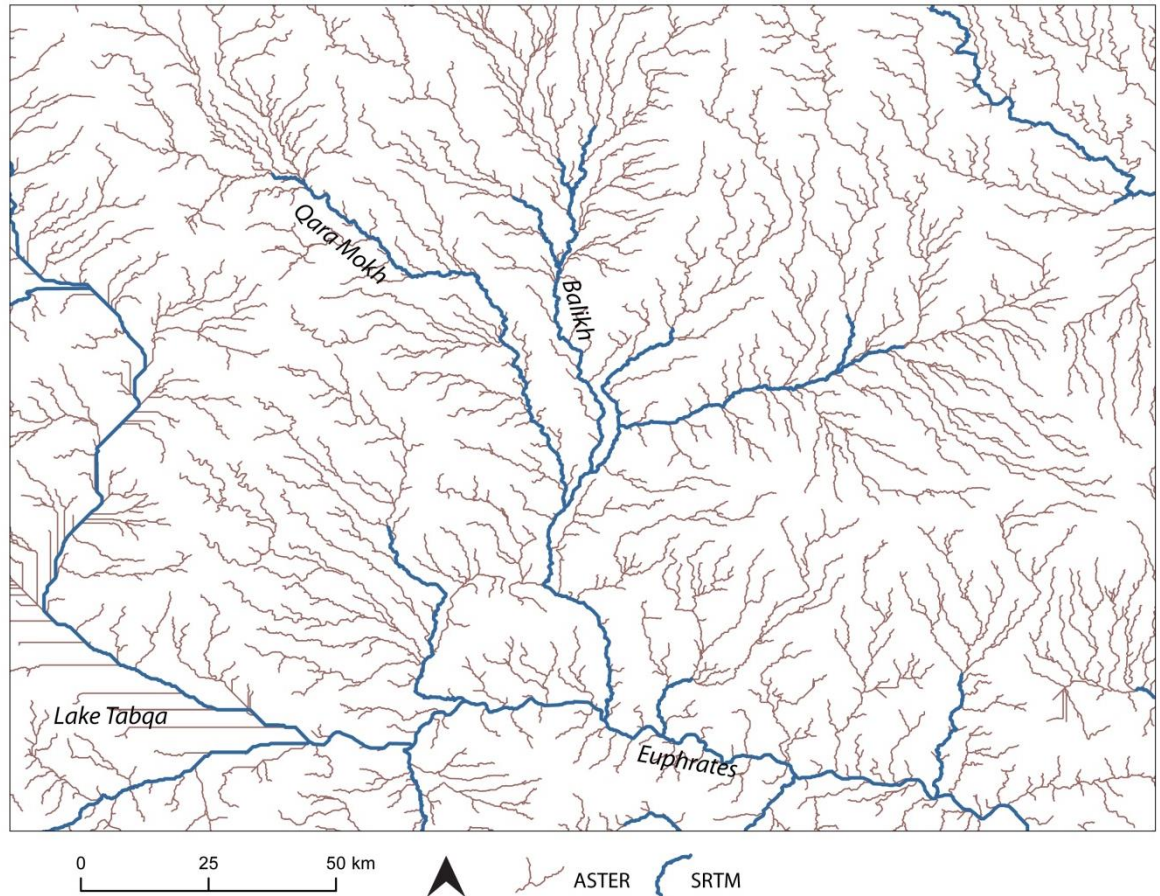


Figure 3.21: Drainage network as established using digital elevation models (SRTM and ASTER). Different resolutions can be obtained depending on the DEM used and on the threshold values selected.

3.4.8 Summary

The SRTM and ASTER DEMs were effective in determining the general gradient of the landscape and in delineating stream networks; that the two models corresponded to each other is an indicator of accuracy (also see Bolten and Bubenzer, 2006, p273). The stream network data can then be integrated with archaeological data to facilitate additional interpretations (see **Chapters 5 and 6**).

While the elevation and morphology of larger, occupation sites can be identified using these DEMs, relatively narrow, linear features such as the smaller canals cannot be picked up (see **Figure 3.4.1**). As **Figure 3.4.1** also shows, the time difference between the CORONA images used for mapping and the modern DEMs

used for gradient and hydrological analysis affects the data; for example, modern linear features are visible in the ASTER image. Therefore, a way of generating a DEM of a better resolution and representing better preservation of archaeological remains was researched; this will be described in the next section (**Chapter 3.5**).

3.5 CORONA Photogrammetry

3.5.1 Data

The use of CORONA can extend beyond image interpretation. CORONA involved several different satellite missions, which had varying image quality. The satellite KH-4B was equipped with two panoramic cameras, in forward and aft positions on the satellite (see **Figure 3.22**). A DEM of finer resolution than SRTM and ASTER could be generated using these 'stereopairs'. Fortunately, cloud-free stereoscopic imagery covering most of the Middle East are available and in this case mission 1105 of the KH-4B satellite was used. The parameters are detailed below; however each mission was different so these values are nominal. In this case, a stereo-pair dating to 4th November 1968 was used.

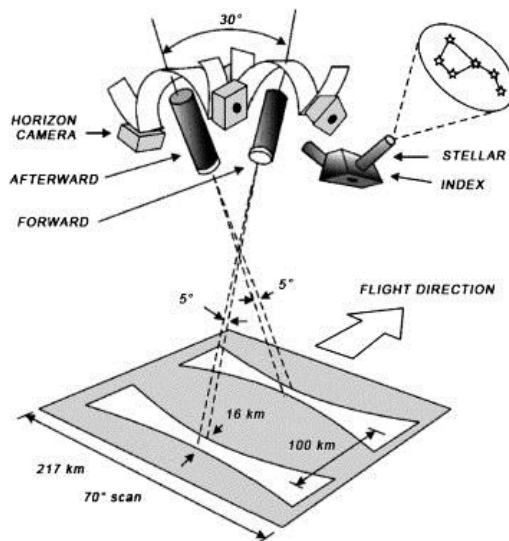


Figure 3.22: CORONA image capture, from Goossens et al, 2000, p749; after <http://www.nro.gov/history/csnr/corona/imagery.html>

Table 3.6: CORONA mission parameters, from <http://eros.usgs.gov/#/Guides/disp1>

Satellite	KH-4B
Successful missions	1101 through 1112, 1114 through 1117
Period of operations	September 1967-May 1972
Amount of film (ft.)	505,970
No. of primary camera frames	188,526

Satellite	KH-4B
Camera type	Panoramic
Film width	70 mm
Approx frame format (in.)	2.18 X 29.8
Focal length (in.)	24
Best approx film resolution (ln./mm)	160
Enlargement capability	16 times
Best approx ground resolution	6 ft
Nominal system altitude (nautical miles)	81
Nominal photo scale on film	1:247,500
Nominal ground coverage (miles)	8.6 X 117

3.5.2 The panoramic camera

KH-4B offers the best image quality and an overlap of 10% in the flight direction (Schmidt et al, 2001, p3123). The camera itself was panoramic, and was able to produce panchromatic images (Altmaier and Kany, 2002, p225). The camera worked by scanning across the direction of flight, using a Petzval lens and scan arm in a rotating drum; the film was parallel to the direction of scan (Galiatsatos, 2004, p19-27; NRO, <http://www.nro.gov/history/csnr/corona/sysinfo.html>), which enabled a large amount of spatial coverage as well as a high resolution (Sohn et al, 2004, p53).

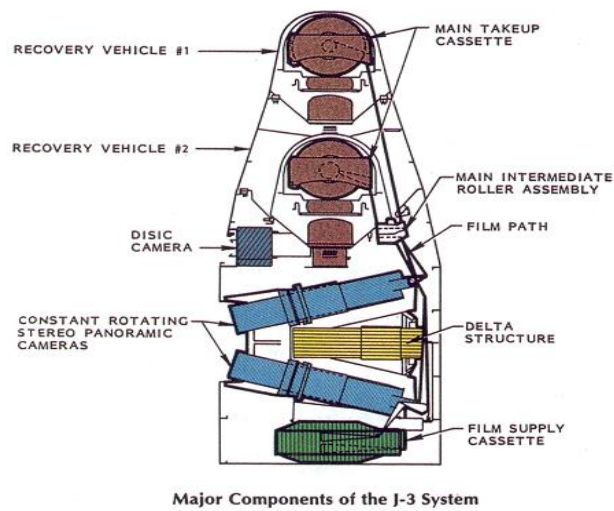


Figure 3.23: The J3 camera system used by CORONA mission KH4B, NRO, <http://www.nro.gov/history/csnr/corona/imagery.html>

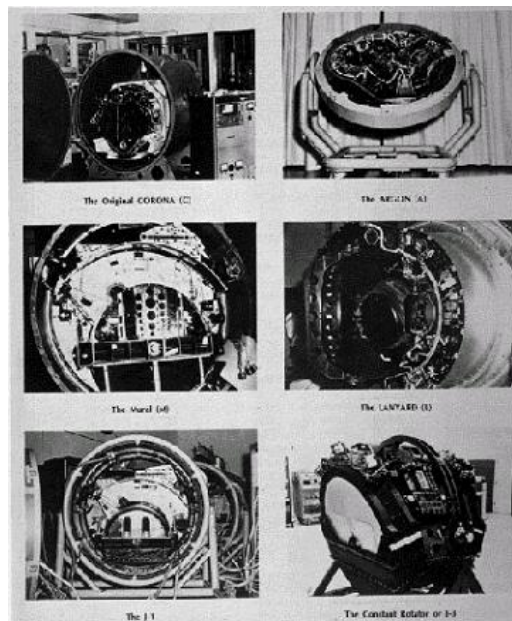


Figure3.24: CORONA camera systems <http://www.nro.gov/history/csnr/corona/imagery.html>

Distortions are inevitable when using panoramic cameras (ibid). Correcting for this is difficult and not necessarily robust, (Altmaier and Kany, 2002, p228).

Unfortunately, the study area of this project is at the edge of the available CORONA frames where distortion is highest.

Sohn et al (2004) attempted to develop algorithms to correct for the panoramic distortion that affects CORONA images. The collinearity equations (see below) were modified; other methods involve modelling the exterior orientation parameters as a function of time. Models like this are still unavailable for use in available software packages (Casana and Cothren, 2008, p4), so it was not possible to apply them within this project. As the following section will outline, however, it was possible to produce an output DEM using the available stereopairs with the ERDAS LPS software package.

3.5.3 Image parallax and relief displacement

The principles of image parallax and relief displacement explain how two images of the same scene, in this case CORONA, taken from a different angle, can be used to determine the height of features (e.g. see Lillesand et al, 2003, p123-188). When a tall object is viewed in an aerial image, the top of it appears to lean away from the principal point and the object's base. Relief displacement (see the building represented in **figure 3.525**) is the fundamental principle which allows the determination of height from aerial/satellite imagery (Wong, 1980, p48). When using a stereopair (two images), the images will have different vantage points; the relative positions of objects in relation to the principal point that are closer to the satellite/plane change more between the two images of a stereopair than the positions of objects that are further away (therefore lower); this is parallax. Using two images in this way is more accurate than only using the principle of relief displacement (Lillesand et al, 2003, p124-125). It is the ratio between the ground distance and between the photo centres at the times of exposure and the flying height of the satellite that determines the vertical exaggeration; the bigger that ratio, the bigger the exaggeration (Lillesand et al, 2003, p128). Relief displacement can be expressed as;

$$d = \frac{rh}{H}$$

Equation 3.5.1: Relief displacement (see Lillesand et al, 2003, p147).

Where;

d = Relief displacement of given object

r = Distance from photo principal point (image centres through which the flight axis/nadir line is located) to the top of the object

h = Height of the object

H = Flying height (with reference to the elevation of the base of the object, not to mean sea level)

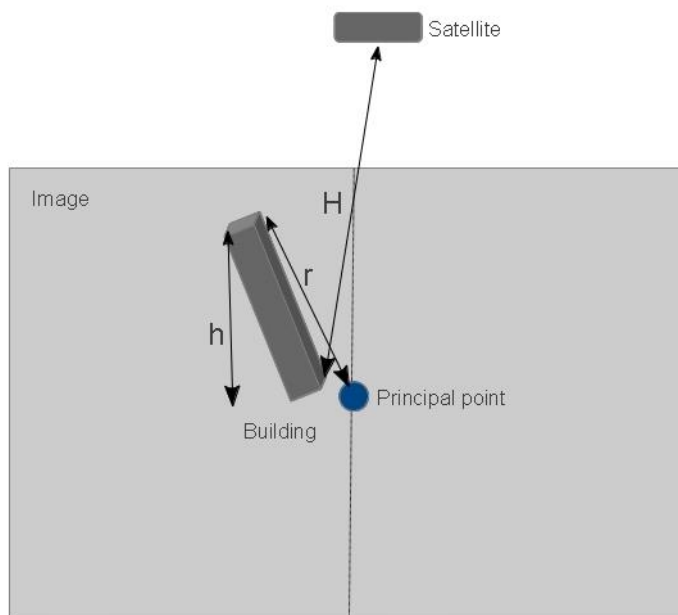


Figure3.25: Illustration of relief displacement (see **Equation 3.5.1** and Lillesand et al, 2003, p147).

When applying this principle to a stereopair in order to determine the location of points the relative orientation of the camera needs to be established from specific

parameters of camera rotation and base line direction (exterior orientation) (Mugnier et al, 2004, p245), as well as the ground coordinates of at least 3 points (Wong, 1980, p57). In the case of CORONA images some of these parameters have to be calculated by the software because they have not been released as part of the declassification process along with the images. The parameters include the angles omega, phi and kappa which describe the angular rotations of the image plane (e.g. see Lillesand et al, 2003, p176). This information is needed so that the collinearity equations can be applied (Mugnier et al, 2004, p292), which describe the relationship between the ground coordinates, image coordinates, and the exposure station position and angular orientation of a photograph, and enable the ground location to be calculated, (Lillesand et al, 2003, p176-179):

$$x_p = -f \left[\frac{m_{11}(X_p - X_L) + m_{12}(Y_p - Y_L) + m_{13}(Z_p - Z_L)}{m_{31}(X_p - X_L) + m_{32}(Y_p - Y_L) + m_{33}(Z_p - Z_L)} \right]$$

$$y_p = -f \left[\frac{m_{21}(X_p - X_L) + m_{22}(Y_p - Y_L) + m_{23}(Z_p - Z_L)}{m_{31}(X_p - X_L) + m_{32}(Y_p - Y_L) + m_{33}(Z_p - Z_L)} \right]$$

Equation 3.5.2: *The collinearity condition (Lillesand et al, 2003, p176-178).*

Where;

x_p, y_p = Image coordinates of any point P

f = focal length of the camera lens

X_p, Y_p, Z_p = ground coordinates of point P

X_L, Y_L, Z_L = ground coordinates (exterior orientation) of exposure station L

M_{11} etc = Coefficients of a 3x3 rotation matrix defined by angles omega, phi and kappa, which are needed to calculate a ground location.

The intersection of the epipolar plane that is formed by the projection centres and an image point gives the epipolar line where the predicted point is located (Mugnier et al, 2004, p260). There is a known relationship between the distance of any given point from this line, the flying height of the satellite and the elevation of the given point. Relief displacement increases both with the distance from the principal point and with the height of an object, (see equation 1 above and Lillesand et al, 2003, p150-151). It enables height to be measured;

$$h = \frac{dH}{r}$$

Equation 3.5.3: *A reorganisation of Equation 3.5.1 shows object height determination (Lillesand et al, 2003, p151).*

These equations were applied to the 1968 stereopair using ERDAS LPS software to generate a DEM. The necessary processes of gathering control points for triangulation and performing image matching using this software are outlined below.

3.5.4 Image preparation

Before assigning control points it was necessary to prepare the CORONA images. The area of interest is confined to the east of the frames (see **Figure 3.26**). It has been found that CORONA photogrammetry is more successful when applied to smaller images than to the whole 13.8 X 188.3 km frame (e.g. see Casana and Cothren, 2008, p4). This is probably because the detrimental effects of the distortion across a CORONA panoramic frame are reduced when using a smaller segment (ibid). For this study, the same method was applied to both smaller and larger areas, and it was confirmed that using smaller areas is more appropriate. Therefore, small subsets of the forward and aft frames were taken (see **Table 3.7** and **Figure 3.26**) of which the aft subset had to be rotated. A potential issue with both these processes is the inevitable resampling of a subsetting and rotated

image, which changes the pixel values. However this was found to be less problematic than using the whole, upside-down frame.

Table 3.7: CORONA frame subset sizes

Subset	Size (km)
Nahr al Abbara	2.6 X 4.5
Hammam et Turkman	1.4 X 0.8
Canal	0.9 X 1.0

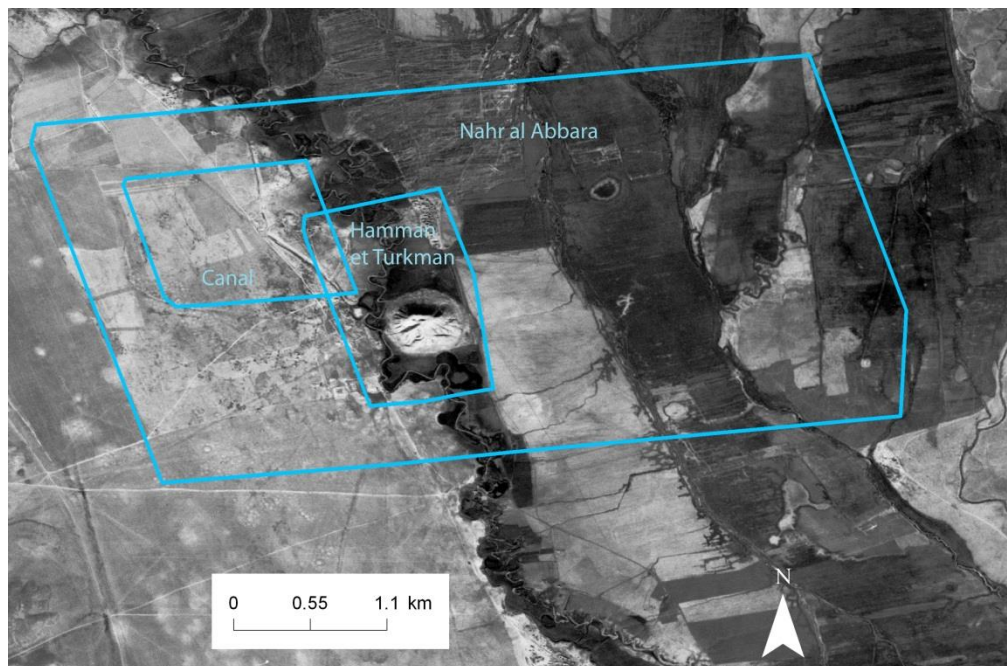


Figure 3.26: Areas of CORONA stereo-pair subsets. 4 November 1968.

3.5.5 Triangulation

3.5.5.1 Interior orientation

Triangulation is used to improve ground control and orientation of models (Forstner, 2004, p847). This works by estimating the optimal parameters by minimizing the adjustment residual's weighted sum-of-squares (Forstner et al, 2004, p854) to determine the coordinates of all the unknown points. As part of this process, the interior and exterior orientations of the images must be known. In order to define the interior orientation of the camera, the focal length, coordinates

of the principal point and the geometric distortion characteristics of the lens system are needed (Wong, 1980, p49). This information is generally added to the parameters of the blockfile when using ERDAS LPS. In the present case, the coordinates of the principal point were not known. In addition, as explained above, only a subset of the frame was used, which did not contain the principal point. The interior orientation of film cameras, such as CORONA, is generally not well defined (Mugnier et al, 2004, p231); the values provided may only be nominal for this kind of data (Forstner et al, 2004, p885). Furthermore the fiducial marks, which can be used to relate the image and the position of the camera, are not given for CORONA images. Given this lack of camera calibration the software had to determine some parameters and a general non-metric camera model was used. The parameters are outlined in **Table 3.8**.

Table 3.8: *Interior orientation and camera parameters.*

Camera model	Non-metric camera
Lens distortion	Unknown
Pixel size (μm) in x and y directions:	7
Camera focal length	609.6020
Principal point	Unknown

3.5.5.2 Exterior orientation

Similarly, most of the exterior orientation parameters were not available and had to be calculated by the software. This is done by space resection, a process which uses control point coordinates and the collinearity equations to perform a least squares solution (e.g. see Lillesand et al, 2003, p180). These parameters are listed in **Table 3.9**. They are the coordinates of the projection centre (principal point), and the rotation angles, and vary with the movement of the camera in space (Mugnier et al, 2004, p215). The calculated parameters are outlined in **Table 3.10**.

Table 3.9: *Exterior orientation parameters.*

Perspective centre	Unknown, determined by LPS, status initial
Rotation angles	Unknown, determined by LPS, status initial
Orientation	Down +X
Flying height	153900 m(approximate)

Table 3.10: *Estimated exterior orientation parameters calculated by LPS for a CORONA DEM of the Sahlan-Hammam canal.*

Image ID	Xs (m)	Ys	Zs	Omega (degrees)	Phi	Kappa
1	408756.400	3986418.167	154321.54	558.3963	-149.3468	467.4987
	2	3	79			
2	400353.798	4072751.942	154040.15	-12.8500	-33.5675	-82.0863
	0	0	83			

3.5.5.3 Ground Control Points (GCPs)

It is generally agreed that ground control is important to improve precision in photogrammetry (e.g. see Lillesand et al, 2003, p164). In order to perform triangulation successfully using the typical algorithms, control points need to be as accurate as possible (Jung et al, 2002, p126). However in this case it was not possible to obtain GPS points in the Balikh, because the political situation in Syria prevented a second season of fieldwork during which these would have been collected. As discussed in the literature review, most studies undertaking CORONA photogrammetry were able to collect GPS points, although changes to the landscape in recent years made this difficult (e.g. Altmaier and Kany, 2002, p227).

Good ground control points - GPS points - were not available for this project. Instead, x, y coordinates were collected from already-rectified CORONA (Fragile

Crescent Project) and z coordinates were obtained from SRTM. The benefits and limitations of this are discussed later.

Table 3.11: *Control points and automatically generated tie points.*

Blockfile	CPs
Nahr al Abbara	87, and 184 auto tie points generated
Hammam et Turkman	40 and 44 auto tie points generated
Canal	24 and 12 auto tie points generated

The identification of control points from GeoEye-1 images (see **Chapter 3.1**, **Table 3.1**) was attempted, however, the landscape had changed significantly between the 1960s and the 2000s, so this was not successful. Using the images rectified by the Fragile Crescent Project, however, it was possible to collect points. This was done using the point measurement tool in LPS. An even distribution was sought. However, for some areas of limited contrast very few points were identified. Clearly identifiable points were also sought, for example road intersections and the corners of buildings (see **Figure 3.27** for an example).

Sometimes there is no access to the original sensor model adjustable parameters, as in the case of CORONA. The best mitigation strategy is to use more, and accurate, control points (Forstner et al, 2004, p896). Therefore as many well distributed points as possible were sought when constructing this CORONA DEM, demonstrated by **Figures 3.28** and **3.29** (also see Appendix 1).



Figure 3.27: Features such as road intersections can make good control points. CORONA image 22 January 1967.

3.5.5.4 Auto-tie points

To improve triangulation it is also possible to generate tie points after the control points were inputted. These establish a relative orientation between the two images (Altmaier and Kany, 2002, p228). The software identifies similar points in the two images. Similarity between these points is then examined within a defined region (Jung et al, 2002, p127); the size of this region as well as the size of the correlation window are key parameters in determining the success of this method. As expected, in this case it was found that the number and accuracy of tie points corresponded to the number and accuracy of control points. Low contrast in the image also affected the ability of the software to match tie points.

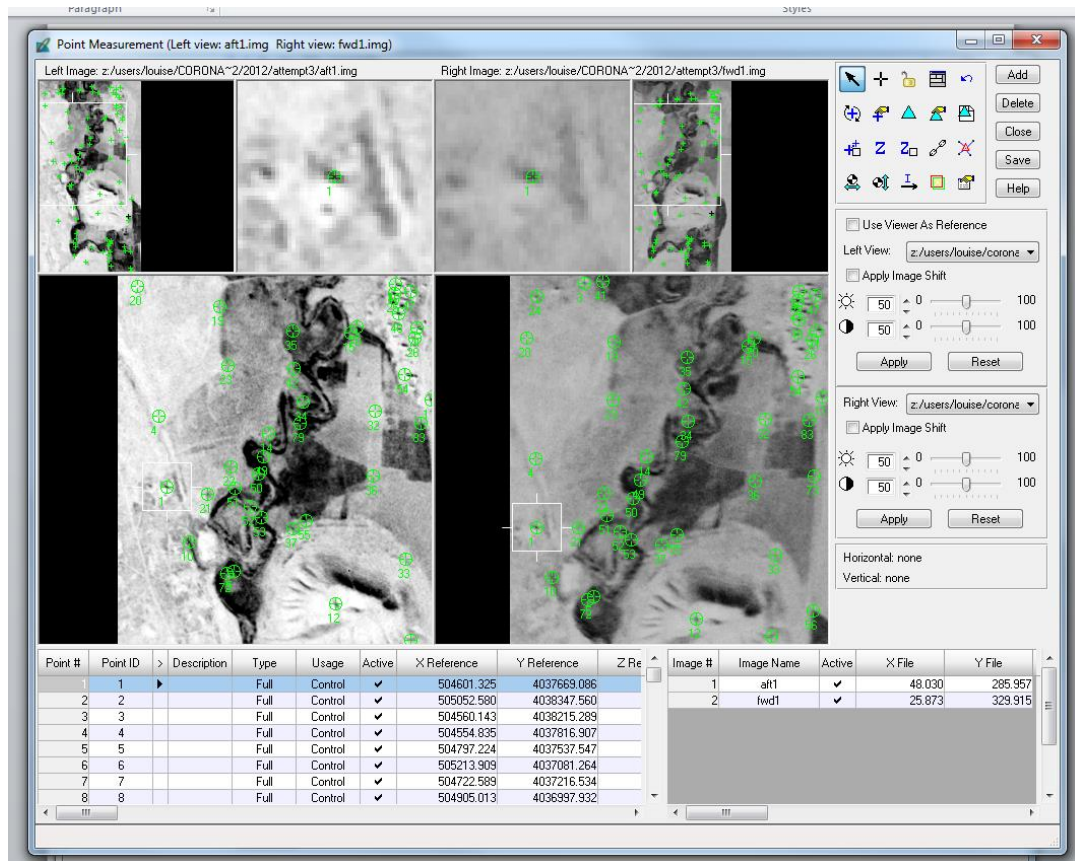


Figure 3.28: Tie-point generation using LPS. The green circles represent control points and tie points common to both the forward and aft images.

3.5.5.5 Triangulation report

Given the tie points and the interior and the exterior information, the collinearity equations can be applied (see **Equation 3.5.2** above) by the computer to perform triangulation using least squares adjustment. This process identifies points and orientation parameters (Wong, 1980, p88).

The initial computations are used to correct the exterior orientation parameters and the ground coordinates. Unknown values are then calculated. These new values are then used as new corrections and the procedure is repeated. This iteration procedure can be repeated a number of times until the corrections become small enough (Wong, 1980, p95-96). In this case, 10 iterations were undertaken.

The lens distortion model was used and a consideration of earth curvature was also made. A projected coordinate system (UTM) was used, for which Earth curvature is not eliminated (Mugnier et al, 2004, p302), therefore it was necessary to correct for this issue. If we assume for a single photograph covering a limited part of the Earth's surface that the reference surface is a sphere, the following equation can be applied;

$$r\Delta = \frac{r^3(H - h)}{2f^2R}$$

Equation 3.5.4: Correction for earth curvature (Mugnier et al, 2004, p302).

Where;

R = Earth radius (6,372,200 m)

H = Flying height above datum

h = Average terrain height

f = focal length

R = radial distance

r Δ = earth curvature

Table 3.12: Triangulation results.

Blockfile	RMSE (m)
Nahr al Abbara	2.6
Hammam et Turkman	1.3
Canal	1.15

The results of the triangulation of each point were examined in order to determine accuracy. For example, for the DEM of Hammam et Turkman a Root Mean Square Error (RMSE) of 1.3 was obtained. Initially however some erroneous control and tie points were identified through this process and removed, improving the rmse.

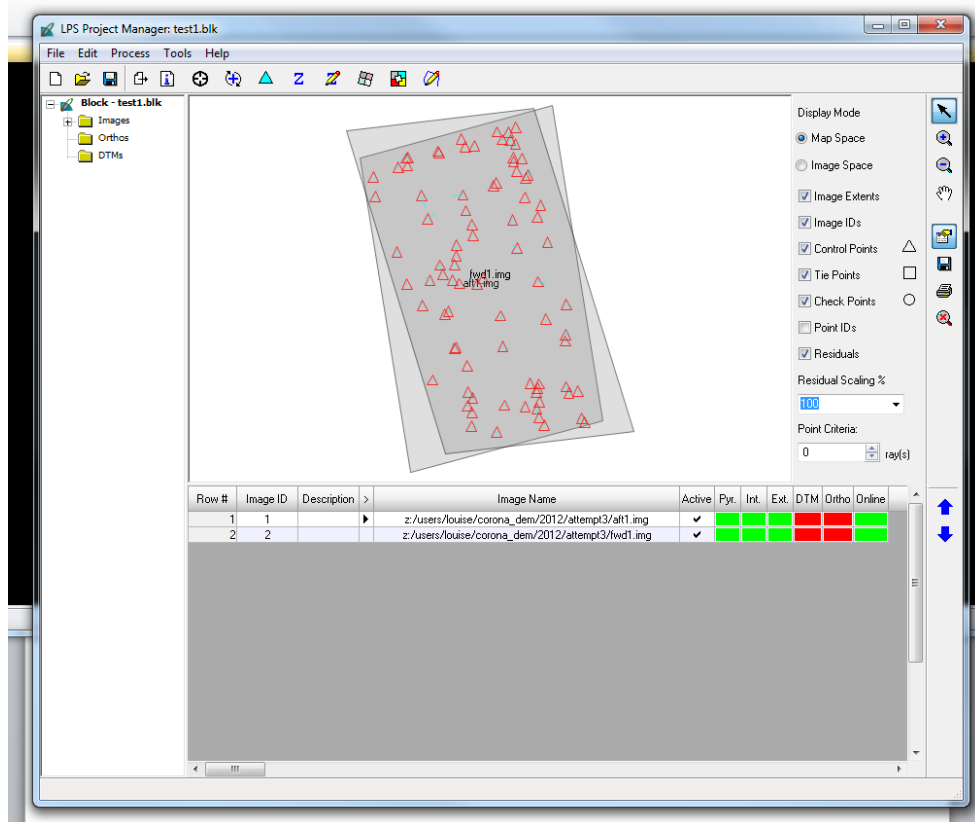


Figure 3.29: Blockfile setup using ERDAS LPS.

3.5.6 DEM extraction: Image matching strategy

DEM extraction was performed also using ERDAS LPS, using the eATE tool. This software uses a feature-based matching technique to generate points; features are extracted from both images and compared (Vosselman et al, 2004, p492). Points with the highest correlation are selected; the parameters which determine this correlation include the search and correlation window sizes and the correlation coefficient (Galiatsatos, 2004, p221-222). The parameters selected in this case are outlined in **Table 3.13** below (also see **Figure 3.30**).

Least squares estimation is used. Initially, a list of possible conjugate pairs is generated. When the cross correlation between a template and search window is greater than a certain threshold, the pair is listed as a possible conjugate point (Vosselman, 2004, p492). The result is two observation equations with 6 unknown parameters for each pair (ibid, p493). Approximate rotation and scale difference values are needed (Vosselman, 2004, p493). The template and search window

need to have an overlap to let the estimation converge to the correct solution (ibid).

The correct correlation algorithm for the data must be selected. In this case, the software offered two options: NCC (Normalised Cross Correlator) and SSD (Sum of Square Differences), although the associated software documentation does not describe these in any detail. The two correlators work differently in terms of how they account for differences in the matching windows (Hirschmuller and Scharstein, 2009, p1), which may be particularly significant for CORONA images, possibly due to the way the scale of the image varies across the long panoramic frame. It has been demonstrated that matching methods like SSD can be more accurate than ones like NCC (Wang et al, 2006, p1). Indeed in this case the NCC option failed to match the images, while the SSD algorithm was able to obtain some results. The SSD algorithm uses a template window (t) to examine every location in both the images (f), searching for correlation between the templates and the images. This can be most simply expressed as;

$$\sum_x (f(X + Y) - t(X))^2$$

Equation 3.5.5: *Sum of Squared Differences (SSD) (e.g. see Boyle and Thomas, 1988, p45).*

f = the image

t = the search template

The squared difference of intensity values is the matching cost; this is then summed over square windows to obtain aggregated values (Scharstein and Szeliski, 2002, p10). The size of both the template and search windows can be set. In this case quite large values were selected in order to maximise chances of matching (9x9 and 100 respectively). A larger template window is able to include enough intensity variation for reliable matching despite low contrast (Wang et al, 2006, p2), which was the case here. The size of the DEM pixel will be higher than

or equal to the template window size (in terms of number of pixels on a side (see Galiatsatos, 2004, p223).

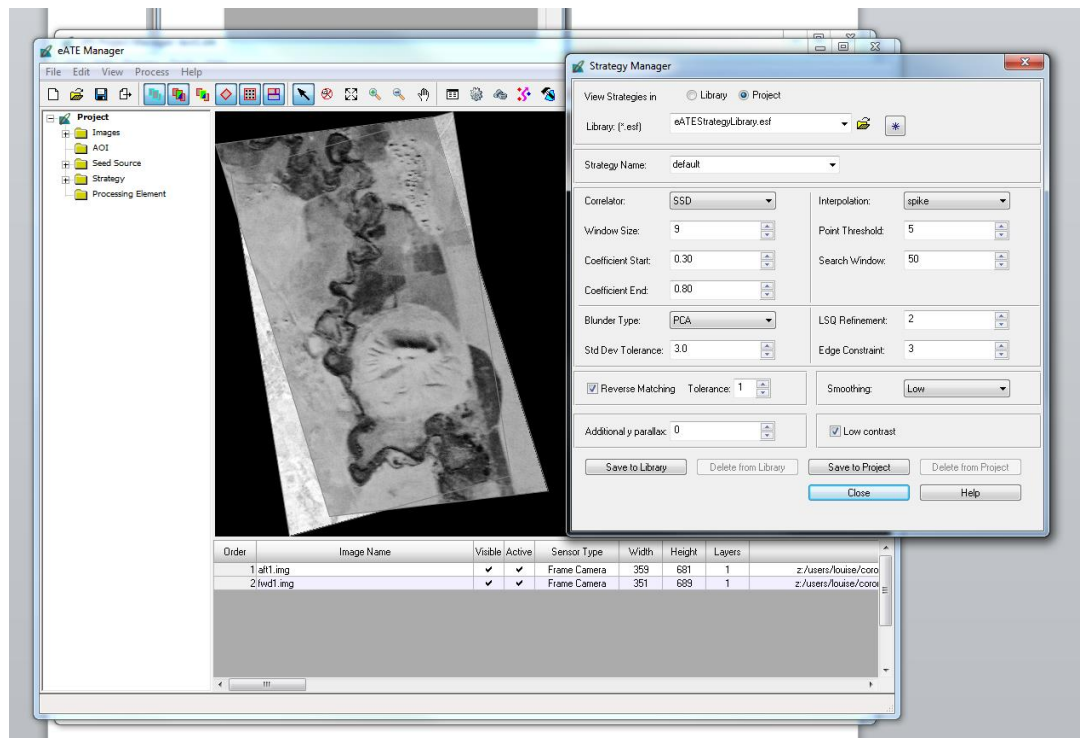


Figure 3.30: Image matching strategy selection using *lps eATE*.

Table 3.13: *Strategy parameters.*

Most nadir	yes
Gradient threshold	0
Use all spectral data	yes
Radiometric layer	no
Correlator	SSD
Window size	9
Coefficient	0.30-0.81
Blunder	PCA
Std Dev tolerance	3
Reverse matching	yes
RM tolerance	1
Additional y parallax	0
Interpolation	Spike
Point threshold	50
Search window	100
LSQ refinement	2
Edge constraint	3
Smoothing	Low
Low contrast	yes

3.5.7 Limitations and evaluation

There are some limitations and uncertainties which affect results when using CORONA stereopairs to extract DEMs, mostly relating to unknown information. It is possible that the use of the wrong camera model can lead to errors. This was an issue in this case because not all necessary parameters were known: the fiducial coordinates, lens distortion coefficients, principle point coordinates, position, velocity vectors and attitude angles are all unknown (Sohn et al, 2004, p52). Consequently, as many tie points as possible were created. In other studies, this has proved to be a way of improving the determination of the interior orientation (e.g. Altmaier and Kany, 2002, p230).

Another issue can arise from the subsetting of the image, which means that the principal point is shifted from its origin; the subset is treated as the whole image by the software. As Altmaier and Kany (2002, p228) suggest, however, the large flying height and the use of many GCPs can mitigate against this.

Furthermore, the control used to acquire GCPs in this case was not ideal. Due to political conditions, fieldwork to gather GPS points was not possible. Given the changes between CORONA images and modern imagery, a rectified CORONA image (Fragile Crescent Project) was used to find points. While this means that any error in this image will be multiplied into the DEM, it was impossible to find sufficient points using modern imagery such as GeoEye-1. Given this, the existing CORONA imagery was the best option.

Low contrast in some parts of the images also limited results. Smaller subsets were selected, avoiding areas of featureless desert. When an area has low contrast the software can fail to estimate parallaxes. Therefore, constraints can be assigned which regard the parallaxes as smooth, using surrounding areas to interpolate (Vosselman et al, 2004, p499). Distortions are also high in CORONA images, especially further away from the nadir at the image ends (Sohn et al, 2004, p52), which unfortunately was the location of the area of interest in this case. Overall, however, the most problematic issue is integral to the design of the software itself. Little scope for adapting parameters to specific imagery is allowed

for, because there is a lack of documentation to describe the algorithms that the software employs. Earlier versions of the software may have allowed for more flexibility, necessary given that spaceborne non-metric panoramic imagery is very uncommon.

The uncertainties inherent in the CORONA DEMs would limit its use in applications such as flood modelling. At present, however, it does enable a relatively high-resolution view of the landscape around Tell Hammam et Turkman. In the future, the DEM could be improved by advances in available software, more information about key parameters, and by the use of ground control.

3.5.8 Summary

This section has outlined the methods used to generate DEMs using subsets of panoramic black-and-white CORONA frames. Despite the limitations described in this section, which make DEM extraction difficult, by optimising the strategy chosen to undertake this it was possible to produce some results including DEMs with pixel sizes of about 10 m. These will be used to examine the morphology of individual channels (both natural and artificial) in **Chapter 6**.

3.6 Precipitation isohyets and inter-annual variability

3.6.1 Introduction

The study area of this project lies within a zone of low and highly variable precipitation. The quantity and reliability of rainfall were significant factors in determining whether cultivation relied on precipitation or whether irrigation was adopted; around 200-300 mm per year is the limit of rainfed agriculture (see **Figure 3. 32**). Problems of temporal variability (as **Figure 3.31** demonstrates) are also significant in the Near East. **Chapter 1** discusses the potential impact of these issues; in this section the methods used for recognising patterns of rainfall will be described.

It must first be understood that the data represented here are only for a recent 31 year period (1980-2010), which is not necessarily directly applicable to the past. Reconstructions of past climate in the Near East using proxies have been attempted (e.g. see Riehl et al, 2008; Wick et al, 2003; Bar-Matthews et al, 2003);.Recently, these data have even been compared statistically with modern rainfall averages (Kalayci, 2013). Black et al (2011) analysed rainfall statistics with an emphasis on Jordan. Kalayci's (2013) research involved incorporating comparisons with isotope data into his calculations in order to estimate rainfall trends for the Bronze Age. The modern rain gauge data is used by the present study to map trends such as the location of different rainfall zones and inter-annual variability.

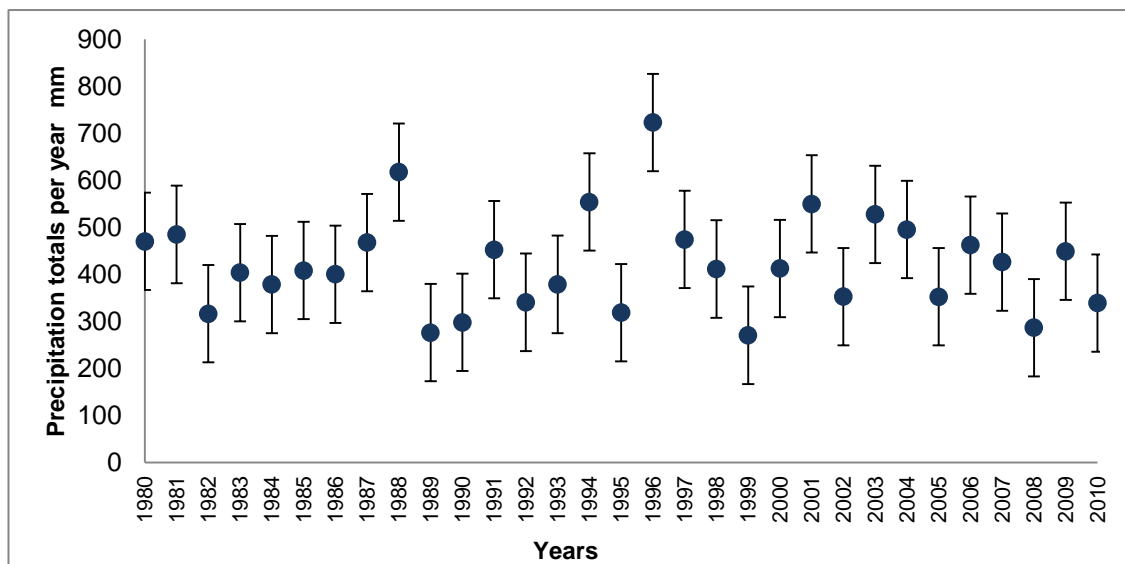


Figure 3.31: Rainfall at GPCC grid point 25 km from Carchemish.

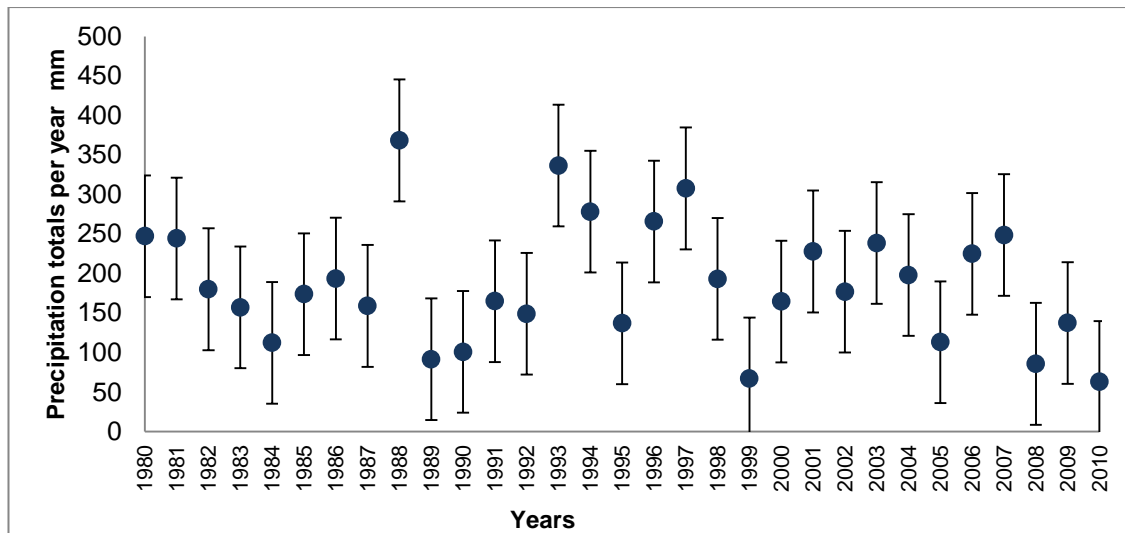


Figure 3.32: Rainfall at GPCC grid point 34 km south-west of Raqqa.

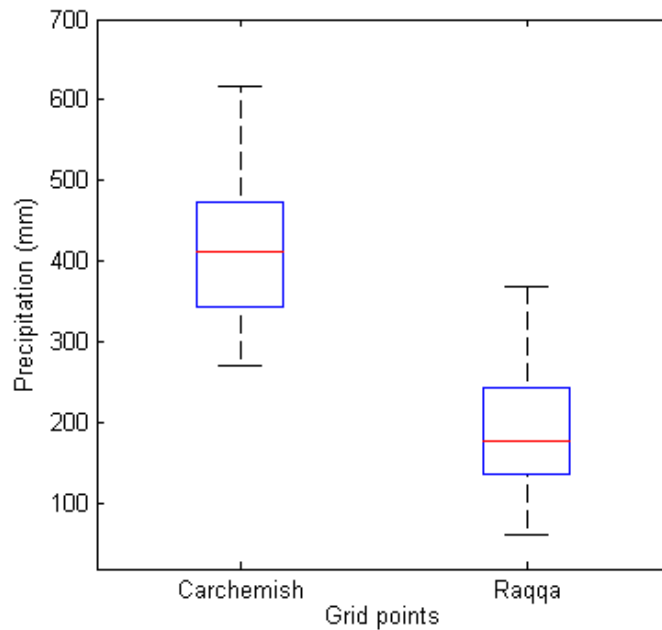


Figure 3.33: Boxplot showing statistics for grid points near Carchemish and Raqqa. Rainfall is higher in Carchemish, but similar amounts of variability are experienced in both locations.

3.6.2 Rain-gauge data processing

The Global Precipitation Climatology Centre (GPCC) was the source of rain gauge data for the present study (Deutscher Wetterdienst, 1996-2011). This is delivered

as grids of different resolutions, a 0.5° resolution grid being selected in this case. The specific precipitation values for each rain gauge itself are not provided (see Schneider et al, 2011, p1). The GPCC interpolated values from the gauges to the grid by using a method which took into account the distributions of gauges to the grid point and also the directional distribution of gauges in relation to the grid point (Schneider et al, 2011, p2).

The Full Data Reanalysis Product was used because this had a higher accuracy than the other products (Schneider et al, 2011, p3). Data was downloaded for the area with an upper left corner of 35.25° longitude and 38.75° latitude, and a lower right corner of 46.5° longitude and 30.73° latitude. Monthly precipitation data (mm) were selected for the years between 1980-2010; around 30 years is a typical range that is sufficient for analysing rainfall data.

Using Matlab software, the precipitation data were loaded into the dimensions of station (grid point), year and month. By adding the monthly values together for each station, the sum total of rainfall for each year, and for each point, was obtained. This was done because thresholds of water requirements are generally discussed in terms of averages that reflect yearly totals for any given point in the Near East, rather than in terms of averages based on monthly figures; e.g. 200 mm a year is regarded as the limit of rain-fed agriculture (see **Chapter 1.4**). An average value for the 30 year period was then calculated for each grid point and saved in an ascii file.

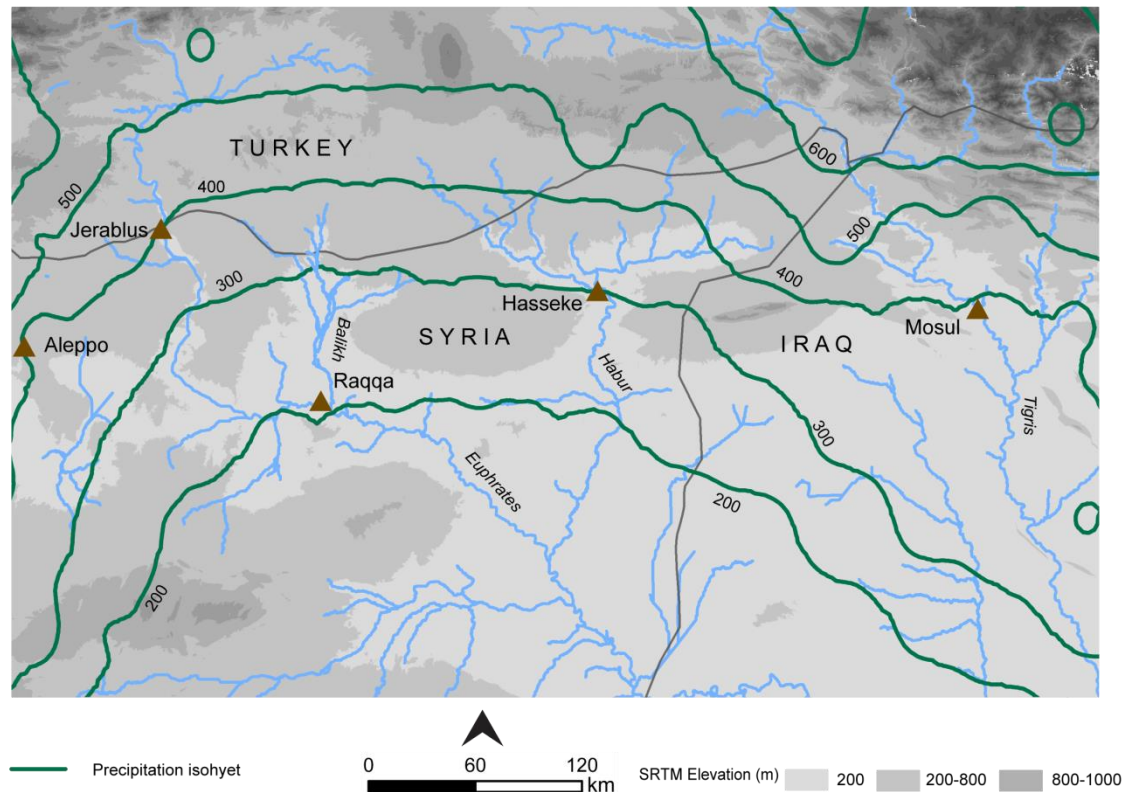


Figure 3.34: Isohyets (31 year average). Monthly values were downloaded from the GPCC visualiser and processed to create rainfall isohyets (see description of methods above).

Further analyses were done with these data; the average figure alone can hide problems such as the high variability of rainfall in the region and the proportions of wet and dry years (e.g. see Heathcote, 1983). Taking 200 mm as the boundary below which rain-fed cultivation is not usually possible, the yearly data were thresholded and the number of years which received rainfall above the threshold value of 200 mm were counted, again for each point.

Following Wallen's method (1967, p375), an interannual variability relative to the mean value was calculated for each point (see **Equation 3.6.1**). The differences between the total rainfall occurring in each year and its following year for each station were calculated ($[P_{i-1} - P_i]$). This involved using the Matlab functions *absolute value (abs)* and *rowwise difference (diff)*. *Absolute value* ensures that only the absolute value is returned i.e no negative values. *Rowwise difference* calculates the differences between each adjacent value along a row.

These were then summed (Σ) and divided by the mean rainfall (\bar{P}), (based on 31 years) which was multiplied by the number of years used in the calculation. A percentage was then calculated and the result saved in the form of ascii grid points.

$$IAV_{rel} = 100 \frac{\sum_{i=2}^n abs[P_{i-1} - P_i]}{\bar{P}(n-1)}$$

Equation 3.6.1 (Adapted from Wallen, 1967, p375).

$abs[P_{i-1} - P_i]$ = the absolute value of the difference in annual rainfall for the station in years $i - 1$ and i .

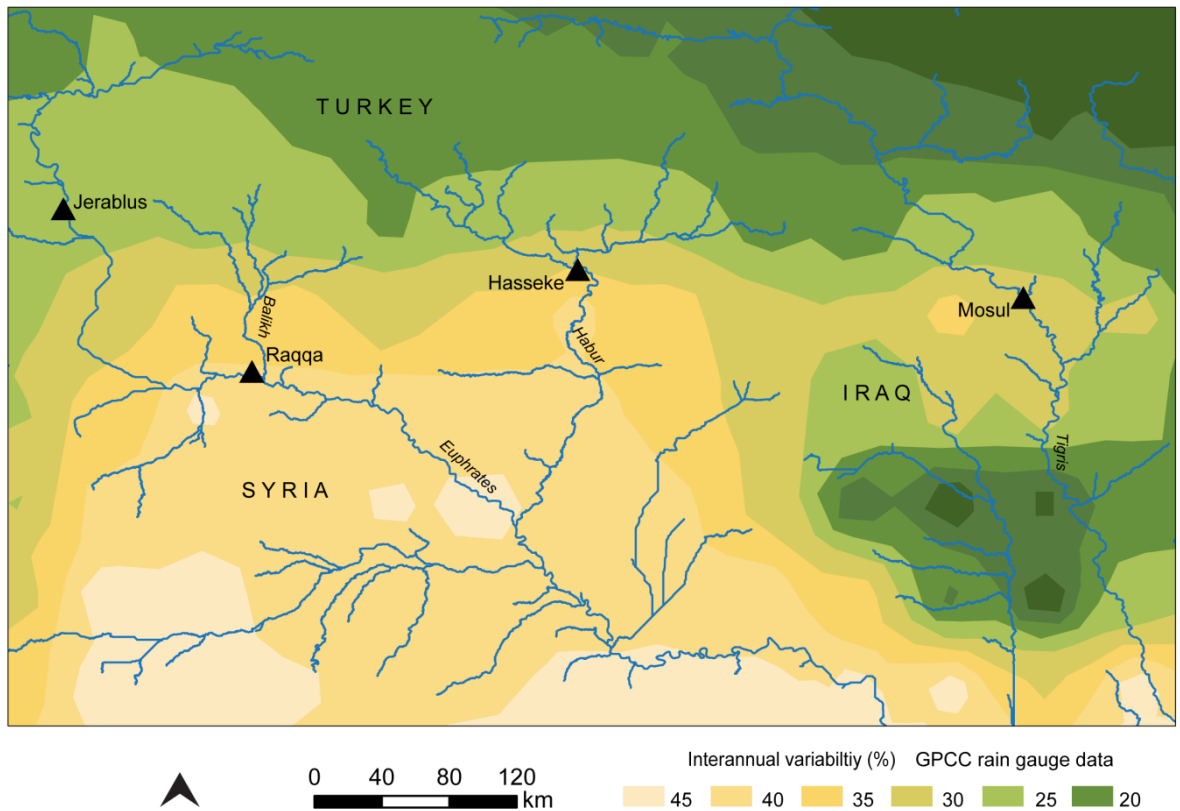


Figure 3.35: Interannual variability derived using Equation 3.6.1. Data were derived from the GPCP Full Data Reanalysis Product and processed using methods discussed above (e.g. see **Equations 3.6.1** and **3.6.2**). An area of low

interannual variability to the south of Mosul may be due to a small number of erroneous or anomalous points in the original grid.

3.6.3 Interpolation and contours.

Once the data were generated, the different analyses were imported into ArcGIS. At this stage, they were in the form of grids of points.

First, interpolation was used to generate rasters. Different interpolation techniques exist which can be used for rainfall mapping (see Tabios and Salas, 1985). However, in this case Inverse Distance Weighting (IDW) was found to give the smoothest interpolation visually, allowing for clearer isohyets to be generated. An IDW algorithm is provided as part of the Spatial Analyst toolbox in ArcGIS

$$P_j = \sum_{i=1}^n W_{ij} P_i$$

Equation 3.6.2 (After Ball and Luk, 1998).

P_j = Precipitation at point

P_i = Rainfall depth at gauge

W_{ij} = Interpolation weights

IDW generates a surface which depends on the distance between the input and the interpolated point; the nearest points will have the most influence (see Lu and Wong, 2008, p1044); IDW is particularly applicable in areas where local variability can be high (ibid, p1045). Compared to other algorithms provided in the GIS, the IDW produced a ‘smoother’ interpolation more suited to the generation of rainfall isohyets.

The default search radius of 12 points, using the variable option, was used in this case. A power of 2 was used. An IDW raster for the average rainfall over 31 years

was generated. An IDW was also generated for the inter-annual variability index (**Figure 3. 33**). These data indicate that much of the study area, including the Balikh Valley, is located in zones of between 30-40% variability.

Finally, the contour tool was run in order to generate the isohyets for the average rainfall data; this is a typical way of displaying hydrological spatial data (see Homberger and Wiberg, 2005, p13.1). The output consists of vector contour lines which divide the different parts of the IDW (at intervals of 100 mm of rainfall). **Figure 3.32** shows the result of this.

3.6.4 Evaluation

There is some degree of uncertainty inherent in using these data, as **Chapter 1** indicates. There are a number of factors which can affect the results generated. The GPCC used rain gauges to interpolate the grid used in this analysis. As part of this, they selected and rejected data according to particular parameters, for example the number of years of data available (Schneider et al, 2011, p8). The raw data used to make the grid was quality controlled, and errors identified corrected (Rudolf and Schneider, 2005, p8-9). Given this, it may be possible agree with their qualifier of the data as of 'higher accuracy' than their other products (see Schneider et al, 2011, p3).

It is important to recognise that the interpolation carried out by the present study is based on a relatively sparse grid (0.5 degrees) which itself is based on a relatively sparse distribution of rain gauges. Given this, it is important not to over-interpret the data at a local scale. As **Figure 3. 36** indicates, the GPCC data on rain gauge locations show relatively few rain gauges in the study area; this could hide aspects of rainfall trends, given that a high degree of local variation is common in the dryland zones (Heathcote, 1983, p26-7). The GPCC did not provide the locations of rain gauges in Iraq although they provided rainfall data for that region. Presumably the data exists; the GPCC Annual Report for 2007 indicates 56 stations in Iraq in 2007 (p4), for example, and Becker et al (2012) lists Iraq as a contributor. However, the station locations were not released.

Any local variability could be missed, and any errors present in the grid, as a result of errors in the original rain gauge, would be propagated by the interpolation. The GPCC recognise that the most significant potential sources of error arise from an insufficient network density, as well as from problems with measurement methods (Rudolf and Scheider, 2005, p1). Variability of precipitation can also affect the data (ibid, p11); **Figures 3.31-3.32** show that there are relatively high standard deviations for the 30 year period for each station.

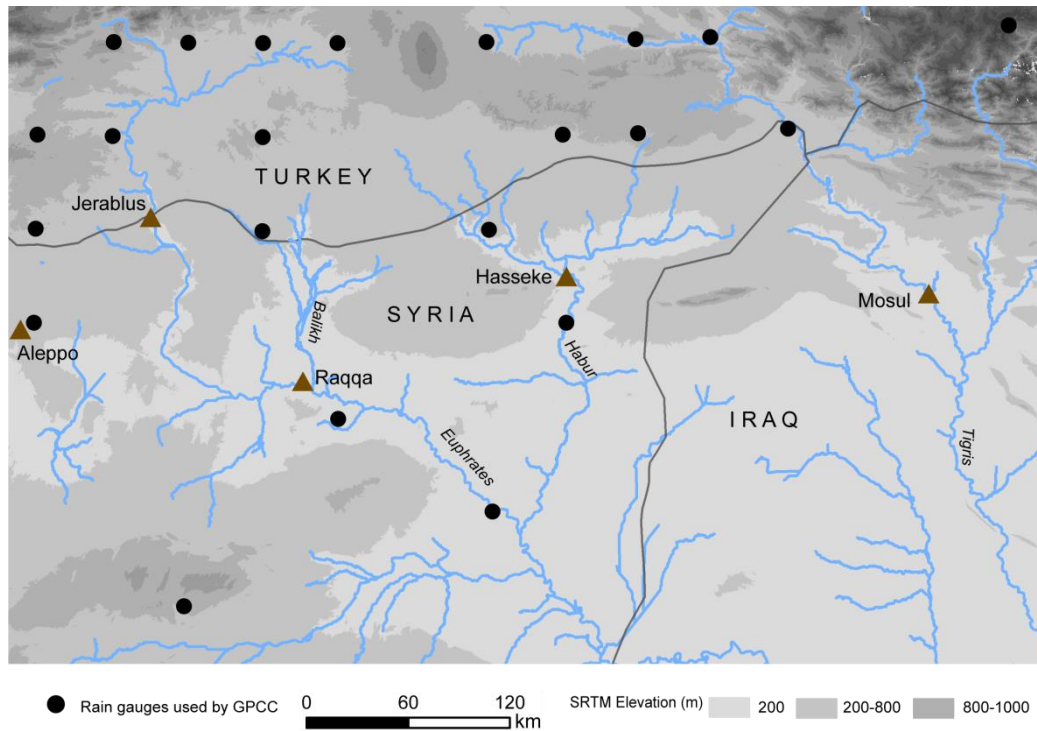


Figure 3.36: The distribution of rain gauges in Syria and Turkey is sparse (rain gauge location data for Syria and Turkey from GPCC). The locations provided by the GPCC may not represent all the rain gauges used in their grid creation method.

Secondly, the precipitation data are delivered in the form of interpolated grids by the GPCC. It is important to recognise that the points in the grid used to produce the IDW represent interpolated, rather than true, values. Various studies have compared different interpolation methods such as IDW and Kriging (e.g. see Groovaerts, 2000; Soenario and Sluiter, 2010). For example a study from West Africa found that different interpolation methods did not give the same results, with

IDW minimising rainfall amounts (Ruelland et al, 2008, p106); a similar problem was identified by Tabios and Salas (1985, p380).

The present study found that the two interpolations showed similar trends (see **Figure 3.37**). It was found that the difference between the two interpolations was less than 20 mm within the study area. Given that in this case rainfall in intervals of 100 mm was used for interpretations, the degree of difference is relatively small. The IDW interpolation was used by this study in most cases.

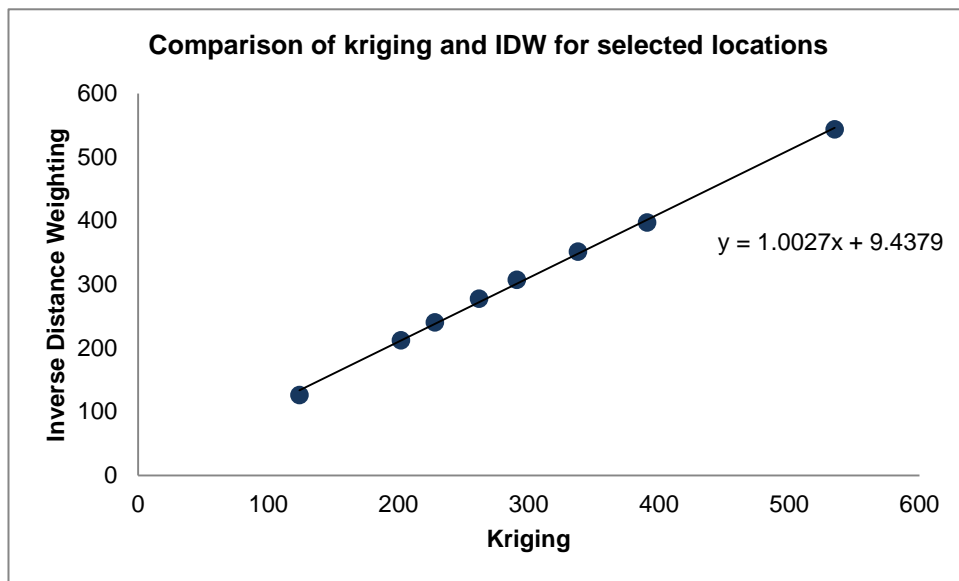


Figure 3.37: Comparison of interpolation methods showing a positive correlation. While the trend line does not fit the data perfectly, it is clear that as the values for the IDW increase, so do the values for the kriging.

An area of low interannual variability in Iraq, south of Mosul (see **Figure 3.35**), may represent errors in the original dataset which were further enhanced by interpolation. Five grid points in the GPCC data exhibited smaller differences from year to year than the other points, including those nearest to them. This meant that the absolute difference value for each of these points was low, affecting the outcome of the variability model and interpolation algorithms. Because the GPCC dataset is an interpolated grid, it is possible that a limited number of stations caused the error, which was propagated during interpolation. It is possible that some form of data infilling occurred to replace missing values in the GPCC grid or in a rain gauge record or that there was a problem with an individual rain gauge.

This resulted in higher values when variability was calculated, using the method described above (**Equation 3.6.1**). Inconsistencies in any such dataset are possible and can affect the outcome of a model (Bevan, 2011, p19-20). However, because it is impossible to know exactly why this problem arose in the original dataset, the points should not be removed entirely or edited; rather, an understanding of the limitations they represent should be recognised here.

Other issues of uncertainty could relate to a higher resolution variation over time than the monthly data show. The raw GPCC precipitation data are downloadable in the form of monthly totals. Many studies of precipitation patterns have analysed rainfall in much shorter time-steps (e.g. see Soenario and Sluiter, 2010). This might give a higher-resolution of some trends. Because archaeology generally uses yearly totals to describe rainfall, for this study, the monthly data were summed to create a yearly value for each station over a 30 year period. While data of a higher temporal resolution may have revealed some detailed trends in rainfall over the past 30 years, this may be less relevant for this project, which seeks instead to apply general rainfall patterns to ancient Northern Mesopotamia. It is also important to note here that the sources of evidence used represent the best data available, with the longest timescales of record, within the constraints of this research.

The problem of applying modern data to ancient climate has also been discussed above. In this case the only possible mitigation is to recognise what conditions might have prevailed in the past through the use of proxy data; this was described in **Chapter 1**. The proxy evidence does seem to suggest that conditions in the period of the later empires were similar to those of today, (e.g. Bar-Matthews et al, 1997, p166; Riehl et al, 2009, p112), making the modern data somewhat applicable to a study of ancient water management dated to the past 3000 years. The variability data are especially useful here, because the results of this method give an indication of the areas which would have benefited most from irrigation. Areas of unreliable rainfall, such as the southern Balikh Valley, could have produced higher yields with the application of careful water management, ensuring predictable tax yields for powerful states.

Uncertainty in the rain gauge dataset could potentially be reduced with a higher resolution gridded dataset, and with an accurate list of the locations of the rain gauges used to produce the GPCC product. It could also be more easily qualified if compared with different sources of data, for example TRMM. More detailed comparison of different interpolation methods could also be carried out. Problems inherent in applying the modern rainfall trends to antiquity could be further explored if proxy data were compared statistically with the modern data (e.g. see Kalayci, 2013). This work could form part of larger-scale research focused specifically and exclusively on precipitation trends.

3.7 Summary

This chapter has outlined a range of different methods used to record and validate features of ancient water management. Rather than focusing on only one approach, this thesis has used an interdisciplinary methodology in order to generate as detailed a database as possible. Image interpretation and fieldwork enabled the initial identification of canal systems; use of SRTM and ASTER DEMs allowed for gradient data to be collected and for remains to be distinguished from natural streams and other linear features; CORONA DEMs revealed the morphology of individual channels in more detail; and the precipitation analysis contextualised the need for irrigation in this zone of low and variable rainfall. The different types and scales of the recorded irrigation systems can now be discussed.

Chapter 4: Irrigation and drainage

4. 1 Introduction

Water management in Northern Mesopotamia comprises systems of different types, functioning at a range of scales, and distributed according to specific environmental niches. These systems and conditions need to be described in order to contextualise the detailed results of this thesis. An understanding of how irrigation systems function in general terms can provide insights into ancient examples. A discussion of location, the design of individual parts of systems and the success of different kinds of systems will be presented here, informed by modern guidelines (e.g. see Jensen, 1983; Zimmerman, 1966). In arid and semi-arid conditions, any source of water will be utilised under current economic conditions; around 90% of all global freshwater is now used for irrigation (Perez et al, 2011, p663). While rain-fed agriculture may have predominated in Northern Mesopotamia prior to the period of the later Empires, deliberate water management has since developed to the stage where only around 12% of arid lands now still rely on precipitation (Heathcote, 1983, p167).

Modern irrigation is meticulously controlled with an understanding of how water flows in any specific conditions. Even before more recent methods and technologies, however, managing water has always been a complex balance between providing enough water and preventing degradation. This notion can be described as the 'water balance':

$$\text{Precipitation} + \text{Irrigation water} = \text{Evaporation} + \text{Percolation}.$$

(After van den Berg et al, 1973, p23).

The processes and conditions which affect all of these variables may not have been as completely understood in the past as they are now. Some water management systems appear to have functioned efficiently in their specific landscapes (e.g. many qanats), therefore indicating that local conditions were often factored into the design of many systems.

4. 2 Local conditions and water resources

Water sources, soils, topography, drainage and climate will be unique to a specific location. These factors influence evaporation and percolation and control the design and efficiency of any water management network; a recognition of these needs to be made before more detailed explanations are given.

There are different natural water sources that can be utilised. Perennial rivers traditionally form the basis of most canal-based irrigation systems. While major water courses in this region like the Euphrates are fed by snow melt in Turkey, others, like the Balikh, have their origins in springs at the margins of uplands. Natural wadis that channel runoff often cycle between dryness and unpredictable peak discharges, with flash floods possible (Agnew and Anderson, 1992, p60-64). Some small-scale water management methods work by collecting and re-distributing runoff.

Groundwater can also be utilised. Modern use involves methods such as pumping to obtain water and sprinklers to distribute it, but ancient irrigation was also able to tap this resource more sustainably through using wells or qanats.

Where water is unevenly distributed temporally and spatially, water storage can be practised. Often, systems use a reservoir derived from a water course. This enables storage of water so that it can be used at times of low rainfall in crucial stages of crop growth. These can be high-capacity structures which can support a canal system, or smaller scale tanks and cisterns.

Other environmental and geomorphic conditions can also affect the type of water management strategy that can be adopted. The texture, depth, salinity and infiltration capabilities of soil affect irrigation strategies (Thompson et al, 1983, p48). For example, because some relatively impermeable soils can limit infiltration, an effective drainage strategy may be needed to prevent flood damage to irrigation systems. Other soil types, for example the alluvial soils of river valleys like the Balikh, have a higher capacity to hold moisture, making them conducive to cultivation. Soil conditions such as high salinity levels can limit yields (e.g. see Young, 1976, p209) and soil organic matter levels are also significant (ibid. p306).

The topography of the landscape must be considered. Canal-based irrigation systems need a continuous grade (Zimmerman, 1966, p222) that is neither too steep nor too shallow: the velocity at which the water in the channel travels must be balanced to avoid either erosion or siltation. Micro-topography in individual fields can also affect the flow of water.

A major consideration is climate, as discussed in **Chapter 1**. Amounts and timings of precipitation determine not only the kinds of methods used but also whether irrigation is used at all, especially in ancient contexts. When an area receives above 300 mm of rainfall of year, rain-fed cultivation is possible, although risky; estimates of necessary annual rainfall are around 200/250 mm (Wilkinson, 1994, p484; Bagg, 2000a, p309). Rainfall is often variable in arid areas and tends to be highly localised (Agnew and Anderson, 1992, p49-51). This is indeed an issue in the Middle East, where precipitation is highly variable and is mostly confined to the winter months (Fisher, 1978, p64). It may be that the annual average is not a useful value (see Heathcote, 1983, p27). Therefore it may be most informative to view it in terms of its variability. Yields that rely on this uncertain rainfall are often low and land can become rapidly degraded due to uncontrolled runoff (Oweis et al, 1999, p2). **Chapter 3.6** describes a method used in this project to model recent rainfall variability in Northern Mesopotamia; **Chapter 1** explains how this may be applicable to the ancient situation. The modelled rainfall variability index suggests that precipitation throughout the study

area tends to be variable, even where averages suggest that rainfall can in some years be sufficient. The lack of security caused by this variability may have been a significant factor behind the widespread distribution of water management features at this time. Therefore, the possibility of more secure crop yields encouraged the later empires to irrigate.

Timing of precipitation must also be considered. The summer in the Middle East is dry and hot, leading to high levels of evaporation. Water quantities must be sufficient to water the crop as well as meet its evapotranspiration needs. The choice of crop and scheduling of watering are significant because of the response of different crops to conditions at key growth stages. The impact of water availability on crops in the past has been inferred from studies of preserved plant material (e.g. Fiorentino et al, 2011). In terms of quantities, wheat needs most water during early growth stages (Shalhevet et al, 1981, p9), and a recent comparison of different barley strains has shown differing responses to drought (Thameur et al, 2012). A traveller's report from the Balikh suggests that barley, rice and opium were amongst the crops grown in the region in the early 20th century (Sykes, 1907, p240), taking advantage of these conducive soils and perennial water supply from the river.

4.3 Water management methods

4.3.1 Water harvesting

Small-scale methods of gathering water were used in antiquity as well as in some contemporary farming. These involve ways of diverting or collecting natural runoff and rainfall. These small scale techniques can be more sustainable than larger-scale systems. In some cases they can be as simple as an earth/stone diversion weir diverting flood water onto adjacent fields. **Figure 4.1** illustrates how water can be redirected to the fields straight from a natural channel, without the use of conveyance canals. Wilkinson recorded this kind of water harvesting in Yemen, where wadis were diverted using dams (Wilkinson, 1997, p387).

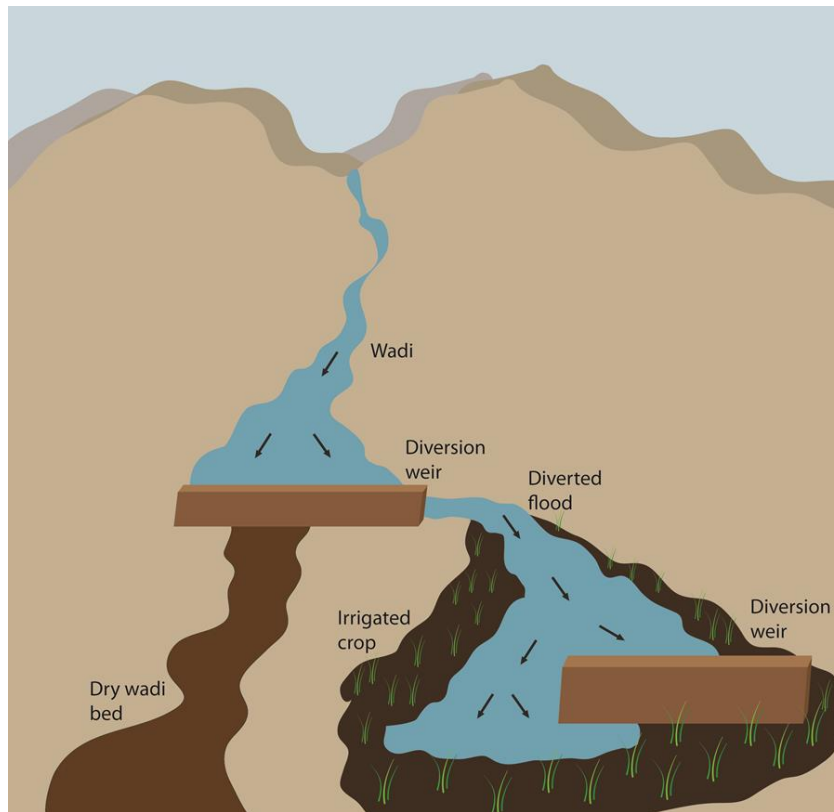


Figure 4.1: Water diversion from a wadi onto the fields using small weirs.

Water can be harvested from streams, wadis and by capturing runoff. Runoff harvesting makes use of surface water resources at times when they are abundant, with the amount of water which can be collected dependant on the size of the catchment area (Barrow, 1999, p54). The water running off hillsides and down wadis is collected behind some kind of interceptor. There are many kinds of earth and stone bunds which are used to trap and divert water (e.g. see Barrow, 1999, p62-63). An example of this kind of runoff collection has also been recorded in Yemen (Wilkinson, 1997, p387), where terraces were constructed to guide and hold moisture flowing downslope from more mountainous area.

Another example is the use of check dams, constructed in wadi beds, to retain flood water in small fields (Heathcote, 1983, p190). Often, a series of dikes and ditches is used to redirect and trap this water (Hart et al, 1983, p504). Water can then be passed through a series of basins (see Heathcote, 1983, p192). On examination of

CORONA images for Syria, examples of these kinds of field structures could be identified, especially in the steppe, although their dates and contexts remain unknown. Research undertaken in the American southwest recorded check dams measuring up to 15 m in length and as close together as 3 m (Doolittle, 1985, p284). Rather than creating terraces, the check dams may have functioned to protect fields (Doolittle, 1985, p289).

4.3.2 Conveyance systems

Many irrigation systems rely on the transport of irrigation water; these can be described as 'reticulation systems' (see Heathcote, 1983, p192). These are larger-scale, larger-capacity networks comprising extensive canal and channel systems, and often include storage, for example dams and reservoirs. As **Figure 4.2** demonstrates, they can involve both irrigation and drainage. Ancient examples are generally gravity-flow based systems which use the natural gradient of the landscape; unlike other linear features such as roads and tracks, they follow the contours. In some cases, canals were made to cut across gradients by the means of excavating a deep channel, or even by using water lifting devices such as shadufs.

Terminology used throughout this thesis must be defined here. 'Canal' refers to any artificial channel; sometimes it is possible to clarify this further to identify main conveyer canals and secondary irrigation canals (laterals). Where the secondary canals are being discussed in terms of what is visible in a satellite image, rather than in terms of their specific function, they are defined as 'offtakes'.

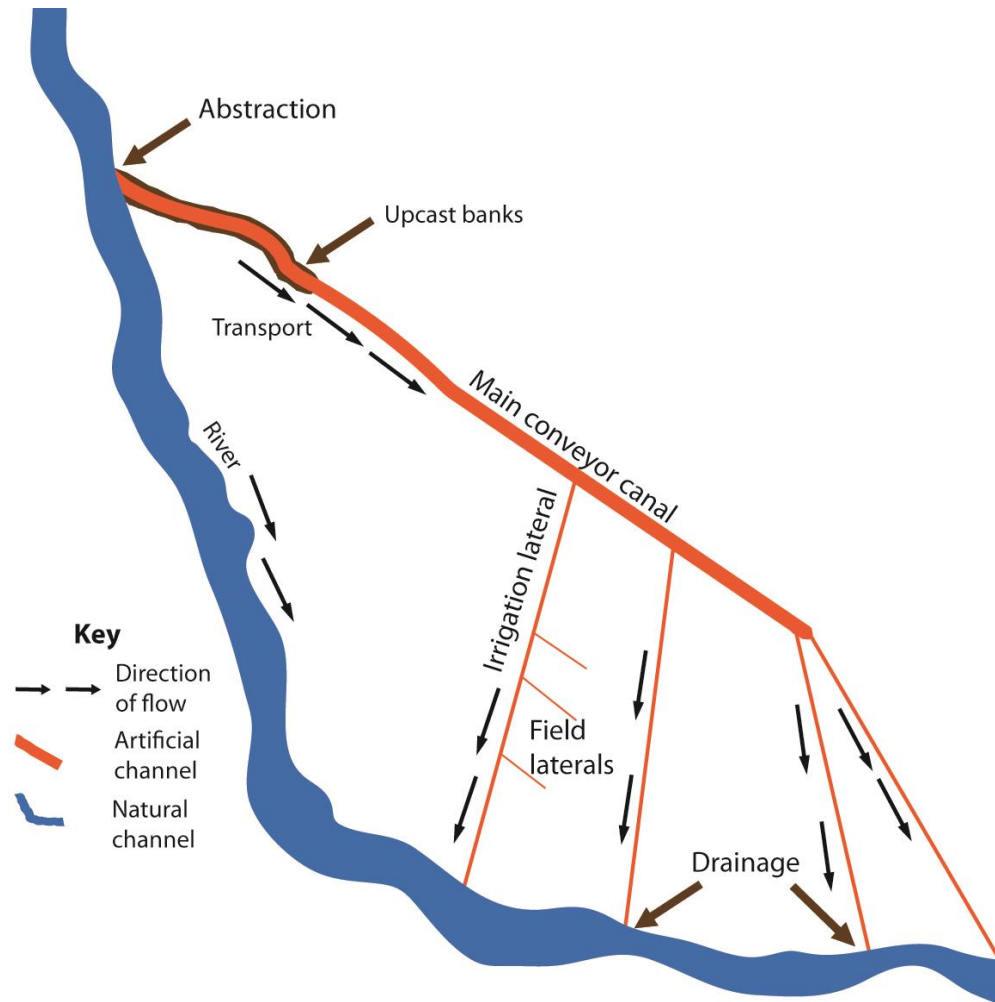


Figure 4.2: Conveyance systems comprise a series of canals enabling abstraction, transport of water, and drainage. Storage of water can also be incorporated into these systems.

4.4 Components of systems

While some systems are simple diversions of floods straight to the fields, and others involve complex irrigation and drainage networks, many will combine elements of both. For example, runoff might be gathered using check dams, and then diverted into a system of short canals and ditches. With this flexibility recognised, the different functions of parts of systems can now be discussed.

Firstly, an overview of the definitions of the sequence of channels must be given. **Figure 4.2** and **Figure 4.3** demonstrate this sequence. Water is abstracted either from a channel or reservoir by the main conveyor canal. This can branch into a number of submain conveyors which enable a larger area or areas of differing topography to be irrigated. The mains are the main transport canals and the largest channels in the system, and consequently the easiest to identify in satellite images. The irrigation lateral then takes water from the mains to the fields. Finally, the water is drawn from the irrigation lateral into the field lateral and delivered to the crops. Drainage channels can be incorporated at different points, but most successfully at the lowest point of each system.

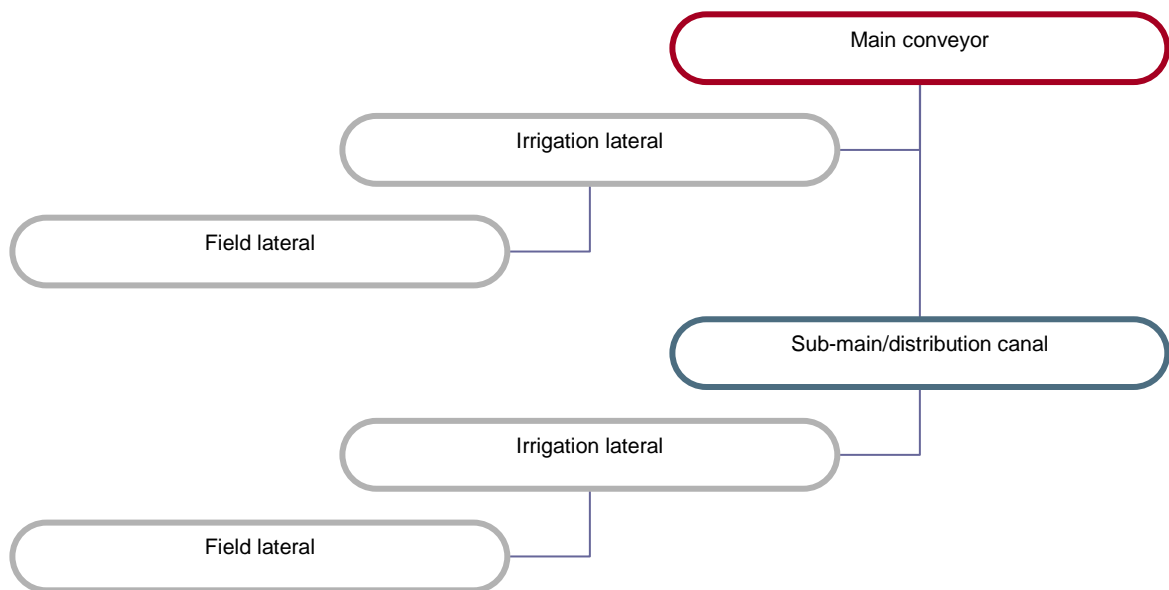


Figure 4.3: Sequence of irrigation channels.

4.4.1 Abstraction

Water can be obtained from a range of sources, including rivers, perennial wadis, springs and the groundwater itself. Currently wells are common throughout the Middle East (e.g. see Beaumont, 1996); water is extracted from the ground using diesel-powered pumps. However, abstraction can take the form of diversion structures in

wadis, designed to capture runoff and redirect it onto adjacent fields. In other cases, channels will be dug straight from the bank of a watercourse so that fields can be flooded, the water retained within earth dikes and basins. Some kind of sluice structure may be required here; in other situations the channels/walls are constantly reformed (this was observed near Tell Jerablus Tahtani in Syria in 2010). An example is the Nabataean systems in Jordan, which used wadi barriers to divert water (e.g. see Finlayson et al, 2011, p212; Oleson, 2007, p220).

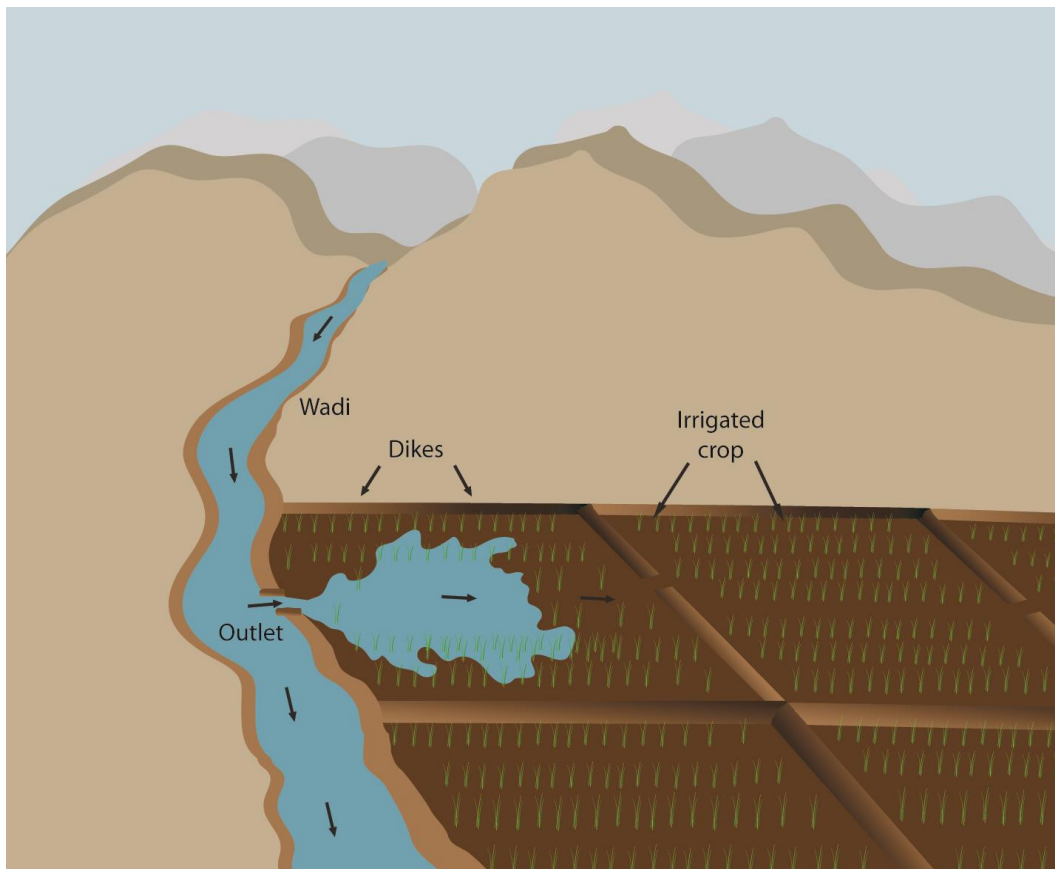


Figure 4.4: An outlet in a wadi floods a series of basins bounded by earth dikes.

Sometimes more complex structures will be used to provide water to a canal system. If there are times when natural water resources are low, reservoirs can be constructed. Found at the head of an irrigated area in order to serve it by gravity, these enable flow to be regulated and stored during times of low demand (Replogle et al, 1983, p332-334). Dams enable water to be impounded in a reservoir and

controlled outlets enable it to be released into the irrigation system (ibid, p336-337).

There are examples of even smaller-scale water storage in the form of cisterns and tanks. This technology has been used in northern Mesopotamia since at least the Iron Age, attested to by the Neo-Assyrian Harran census (see Fales and Postgate 1995), possibly referring to features in the Balikh Valley. Examples have been recorded in Jordan, where Nabataean rock-cut cisterns were constructed in a bottle shape to limit evaporation (Finlayson et al, 2011, p210; Oleson, 2007, p222).

4.4.2 Conveyance

As noted above, water can be conveyed to the fields in very simple ways that require relatively little maintenance. Usually, however, a main canal will be needed to transport water from the abstraction point across as large an area as possible. As **Figure 4.3** demonstrates, submains, irrigation laterals and finally the fields themselves will derive their water from this canal. In order to irrigate a substantial area, the gradient of the main canal should not be too steep; however, if it is too shallow, sediments will build up in the channel and limit its efficiency. The slopes of the water surface and channel bottom need to be equal, at a velocity that does not damage the channel (Kruse et al, 1983, p397). Recommended gradients from irrigation literature are listed in **Table 4.1**. For the main conveyor canal, a fairly shallow gradient of no less than 0.5% and up to 1% is proposed in order to irrigate the whole project area (Zimmerman, 1966, p218-221). This channel preferably follows the natural contours of the landscape (ibid, p217). The elevation of the conveyor canal needs to facilitate free flow at the diversion points (Kruse et al, 1983, p406). Prominent banks can be constructed from excavated spoil and further periodically enhanced with dredged material. Significantly, many of the ancient main canals recorded by this research flowed at lower gradients (as low as c.0.1%) than the modern recommended values.

Secondary conveyors (known as irrigation conveyors/irrigation laterals) take water

from the main and submain canals over a short distance to the fields. They generally need a gradient of between 0.1 and 0.4% (Kruse et al, 1983, p397) and up to 1.5-2% (Zimmerman, 1966, p221).

These irrigation laterals are usually the smallest parts of the system visible in CORONA images. Usually, they have a capacity of less than 0.3 m³/s; although for border or basin irrigation larger streams will be required (Kruse et al, 1983, p395-397). When the topography is flat, for example in the case of the Syrian Balikh, the channel may need to discharge water slightly above the field level (Kruse et al, 1983, p406) to allow adequate distribution to the fields.

Table 4.1: *Recommended gradients for parts of irrigations systems (After Zimmerman, 1966; Kruse et al, 1983)*

Feature	Recommended Gradient %
Main conveyor	0.5-2.5
Irrigation lateral	0.1-2
Field lateral/furrow (not usually visible in available imagery)	Depends on topography and soil type. 0.5-1.2

4.4.3 Field laterals

The field laterals (not to be confused with the irrigation laterals) deliver water from a canal, to the crop. These can be the use-point of both small-scale methods and larger, reticulated networks. While open turnouts (structures which divert part of the water from a canal to a lesser channel; see FAO 1985) exist (Agnew and Anderson,

1992, p149) a sluice gate or siphon can be used to control flow to the field laterals (see Kruse et al, 1983, p410-411). Some kind of managed outlet is often highly beneficial when using methods like furrow irrigation, enabling equal flows to all furrows (Hart et al, 1983, p550). Devices that can be made from brush and stakes located at the low points of fields slow down the flow and spread it, or earthen embankments and piles of rocks can divert flow (Doolittle, 1991, p143).

The field can simply be flooded straight from the irrigation conveyor/lateral/stream; a method known as 'wild flooding' (Hansen et al, 1980, p201). While this is the simplest method it can lead to waterlogging and salinization. Confining the water to basins isolated by dikes can be more efficient, especially when irrigating rice or orchards (Hansen et al, 1980, 204). **Figure 4.4** shows fields surrounded by earth bunds which are inundated with water until the soil is infiltrated. The flow can either reach each basin straight from a canal or stream, or, especially where land is sloping, it can pass through successive basins (Kay, 1986, p26-35).

Variations such as border irrigation exist, where narrower segments are separated by dikes, and contour levee irrigation, where levees are constructed along and perpendicular to contours to enclose basins which are inundated with water at the highest point and drained along the lowest levee (Hart et al, 1983, p512-p524).

Furrows are an efficient method of delivering water to the crop; they are easy to construct and can prevent excessively saline water directly touching plants (Hart et al, 1983, p532). Furrows will take different forms depending on the crop and soil type. **Figure 4.6** demonstrates a schematic series of ridges and small evenly spaced furrows, periodically flowing with water supplied from a channel, often using siphons; a drain at the end of the furrows should collect excess water (Kay, 1986, p57-58). In July 2010 furrows were observed in operation near Jerablus Tahtani (see **Figure 4.5**); in this area the water was pumped from the ground using a diesel pump and a small earth bank was breached by hand so that water could begin to infiltrate the furrows.



Figure 4.5: Furrow irrigation at Jerablus Tahtani, Syria, July 2010.

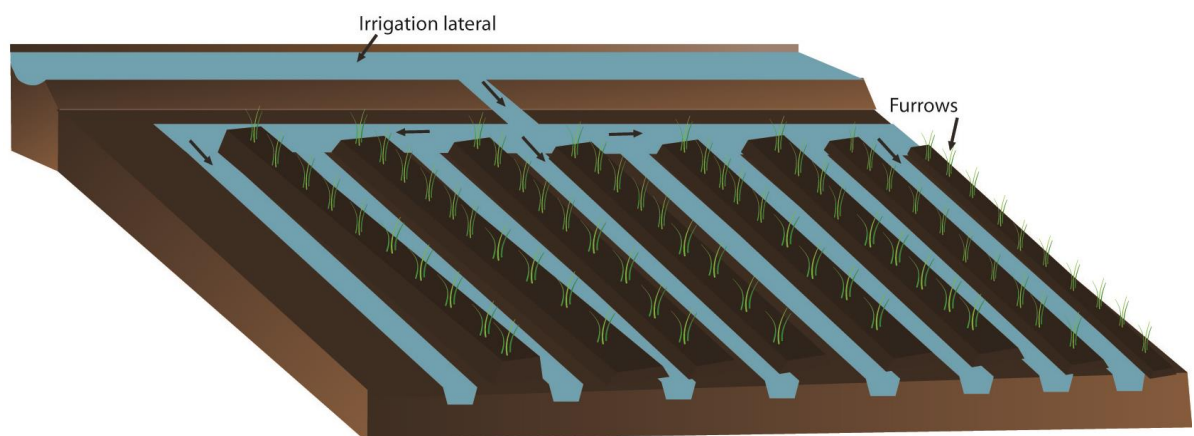


Figure 4.6: Illustration of furrow irrigation.

4.4.4 Drainage

Drainage is an essential aspect of water management that receives less attention than irrigation in studies of past Near-Eastern water management. In general, the history of drainage is less well known than the history of irrigation (Gulhati, 1973, p12), outside perhaps southern Iraq (e.g. Pournelle, 2003; Adams, 1981).

When the soil is saturated with water, it can pool on the soil's surface (FAO, 1985), potentially damaging crops and raising the water table (FAO, 1985). Unless the water table is deep, despite a dry climate, excess and poor quality (e.g. saline) water leading to salinization and/or erosion can be a significant problem where the natural drainage of soils is limited. Provision to collect and remove excess runoff and irrigation water is needed to prevent salt accumulation in the field, for both reticulated systems and water harvesting features.

Drainage canals can be used to remove this excess water. Flowing at elevations lower than the ground surface (Ochs et al, 1983, p236-248), and with relatively shallow gradients of between 0.05 – 0.15% (Hansen et al, 1980, p302), they can be located at the lower end of a series of basins or a reticulated canal system to prevent waterlogging. Field drains remove excess water from the crop, while interception drains run between a slope and the irrigated area, collecting runoff and seepage water that flows down the slope before it inundates the flatter irrigation area (e.g. see Donnan and Schwab, 1974). Some drains can be used specifically to lower a shallow water table. These need to be especially deep (ibid, p99).

When drainage is inadequate irrigation systems can fail, often due to increases in salinity. The ancient example of southern Iraq is well known (e.g. see Jacobsen, 1982). However, this can also be an issue in the northern zone; problems of salinity in the Harran Plain, Turkey, have been caused by mismanagement of water resources (Yesilnacer and Gulluoglu, 2008).

4.4.5 Maintenance

Maintenance of all the above channels will be necessary. Sediments and weeds can build up and need to be removed (Hansen et al, 1980, p250). The dredged material is often deposited on the channel banks, which, over the long-term, causes accumulations of upcast.

These tasks require some organisation, either at an individual, community, or state scale. The state can enforce periodic and regular maintenance tasks, or organisations of local stakeholders can enforce it. This can involve significant time and labour: for example, up to one and a half months is allocated to this task in the modern day Balikh (Alkhaier et al, 2012, p1835), where excessive siltation can be a problem, given very low gradients. Uncontrolled flood events can necessitate repairs. Scarborough suggests that repair costs after a channel is damaged can be so high that they affect the social groups involved (Scarborough, 2003, p93).

4.5 Qanats

While the reticulated systems summarised above are usually comprised of canals, a different kind of technology must also be described here. Many types of underground water-transport canals or galleries exist (e.g. Bagg, 2004); qanats are subterranean channels which tap groundwater and transport it downstream. Several known qanats throughout Syria were recorded by Lightfoot (1996). Increasingly, remote-sensing based research has revealed more examples in Syria and Iraq. The circular maintenance shafts of qanats are visible in aerial and satellite images throughout the Middle East (Wilkinson and Rayne, 2010).

As **Figure 4.7** shows, a qanat works by drawing water from a 'mother well', dug where the water table is high; a sloping subterranean channel then delivers this groundwater to irrigated areas (see Lightfoot, 1996, p321). Yazdi and Khaneiki (2010, p15-16, p46-50) provide summaries of the different use-points of such systems. For

domestic use, gallery-structures allow access both for public and private purposes. In terms of irrigation, open channels can originate straight from the point where the qanat tunnel meets the surface and irrigate land at a lower elevation from this outlet. In some cases irrigation water is stored in a pool which increases the head and the amount of water (ibid.)

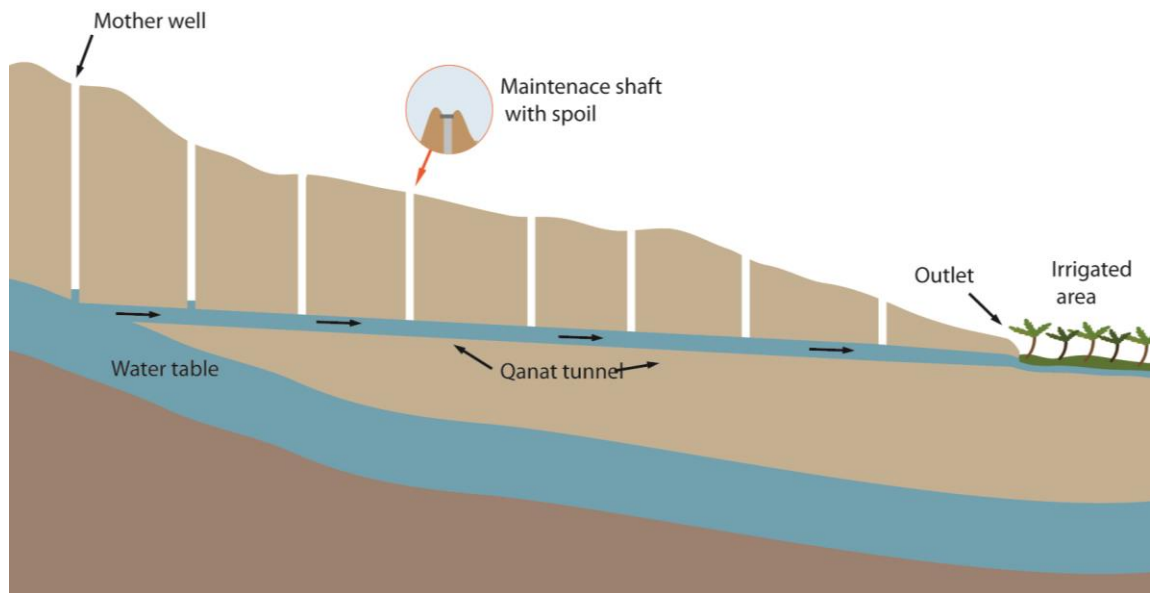


Figure 4.7: Subterranean qanat tunnels extract groundwater and transport it, by gravity flow, to the surface.

As long as the rate of groundwater extraction does not exceed the rate of recharge these structures can persist for many years, even centuries; unfortunately fossil-fuel powered pumping more recently has lowered the water table in many areas to the extent that qanats can no longer be used (e.g. see Yazdi and Khaneiki, 2010, p33-34).

4.6 Efficiency and environmental limitations

The efficiency of irrigation systems can be measured in terms of crop yields. Large scale gravity-based reticulated canal systems are expensive but can provide high returns. Pumping directly from the groundwater is a relatively cheap alternative and

can also enable large outputs. However, the effects of this highlight a need to recognise the other kind of 'efficiency'.

Many modern water management systems have proved to be unsustainable in the long term, suffering problems such as salinization and depletion. Such problems beset irrigators in antiquity (e.g. conflict over rights to abstract from the Balikh, see Wilkinson, 1998; Villard, 1987; Dossin, 1974). It can therefore be argued that some of the more 'traditional' methods are more efficient in the long term, able to deliver outputs without causing immediate problems. The longevity of systems such as qanats seems to confirm this (Agnew and Anderson, 1992, p140). The different impacts and efficiencies of archaeological systems will be discussed in subsequent chapters.

The limitations which nevertheless affect even the smaller scale techniques are now outlined here. For example, precipitation and subsequent runoff may not occur at the ideal times for plant growth (Hart et al, 1983, p551); if storage is not used, this water will therefore be wasted and can cause erosional damage to channels necessitating frequent maintenance for relatively low returns. Erosion can also be a major limiting factor at the field level when applying water using furrows (Hart et al, 1983, p532), as the photograph taken in Syria in 2010 shows (**Figure 4.5**).

Storage may then be the answer. However, substantial water losses affect many irrigation schemes through evaporation from reservoirs (Replogle, 1983, p338) and seepage from reservoirs and unlined canals where losses can be as great as 1/3 of the total water (Kruse et al, 1983, p395). In the case of seepage, the water enters the water table and causes further problems (Van Den Berg et al, 1973, p36), especially when, as is common, quantities in excess of crop-water requirements are applied (Agnew and Anderson, 1992, p148-149).

Where soils are not sufficiently permeable waterlogging can persist. Salts contained in the irrigation water will become concentrated on the soil surface when evaporation

occurs (Buol et al, 1980, p93). Irrigation can also lead to a rise in the water table; as **Figure 4.8** shows where evaporation dries the soil surface the shallow ground water will be drawn up to the surface by capillary movements and salts will accumulate in the root zone (e.g. Hoffman et al, 1980, p145). In high levels these salts can damage plants, reducing yields, and prevent further cultivation. Northern Mesopotamia is affected by this problem; recent remote sensing research has demonstrated that shallow groundwater with concomitant low drainage rates is common (e.g. Alkhaier et al, 2012, p1833).

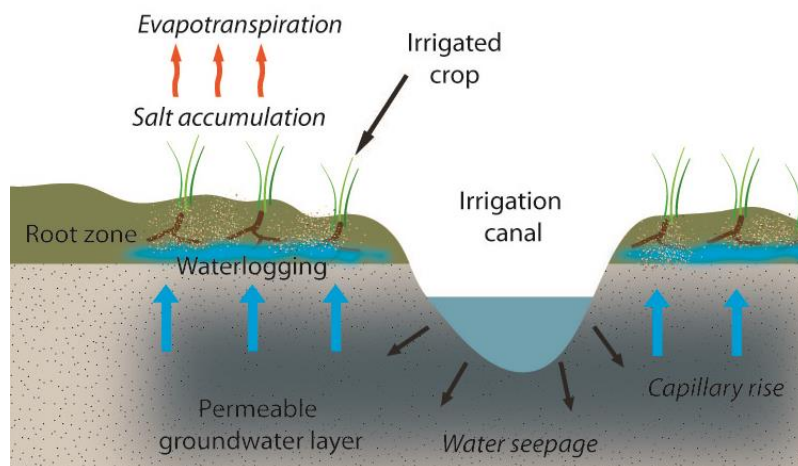


Figure 4.8: Waterlogging and canal seepage can lead to a rise in the water table, drawing salts into the root zone. Salts can also be left behind when surface water evaporates.

Mitigation strategies can be adopted to reclaim land and prevent further salinization. Drainage channels are often used to remove excess water from an irrigated area and lower the water table. Salts left on the soil surface can be removed by flooding the field (van den Berg et al, 1973, p19-36); they should then leach downwards. This can involve quickly flushing water across the field to remove surface salts. Clearly a balance of water that enables leaching but prevents waterlogging must be maintained (Jacobsen, 1982, p61).

Investigations in the Beni Amir district in Morocco, where rainfall conditions are similar to those of the Near East, show that drainage ditches were used to purge main canals

of excess water. In some cases this water was used for further irrigation (e.g. see Aragüés et al, 2011, p961). Slightly saline drainage water can be used for cultivation, especially when careful timing of applications is employed (e.g. see Sharma et al, 1994, p25). Water flowing through ancient irrigation systems may often have been somewhat saline; using more salt tolerant crops such as barley could have been a mitigation strategy (as Sykes, 1907, p240 suggests, this was one of the main crops grown in the Balikh in the early 20th century).

4.7 Case study: Hohokam water management

In order to better place these design factors in a real context which can inform understanding of the systems mapped by this thesis two case studies of well understood ancient water systems are presented here. Information which can help inform the current study includes details of system scales and layout, canal gradients, potential irrigated areas, and ways of administering water management.

The Hohokam systems of Arizona were selected because the climate and types of technology used are somewhat comparable to those of Syria. The complex and dynamic systems of the Phoenix basin in the USA form a useful example of reticulated water management. While it is not within the scope of this project to describe the results in detail of the many studies that have investigated it (e.g. Howard and Huckleberry, 1991; Breternitz, 1991) summaries of some key interpretations can be outlined here.

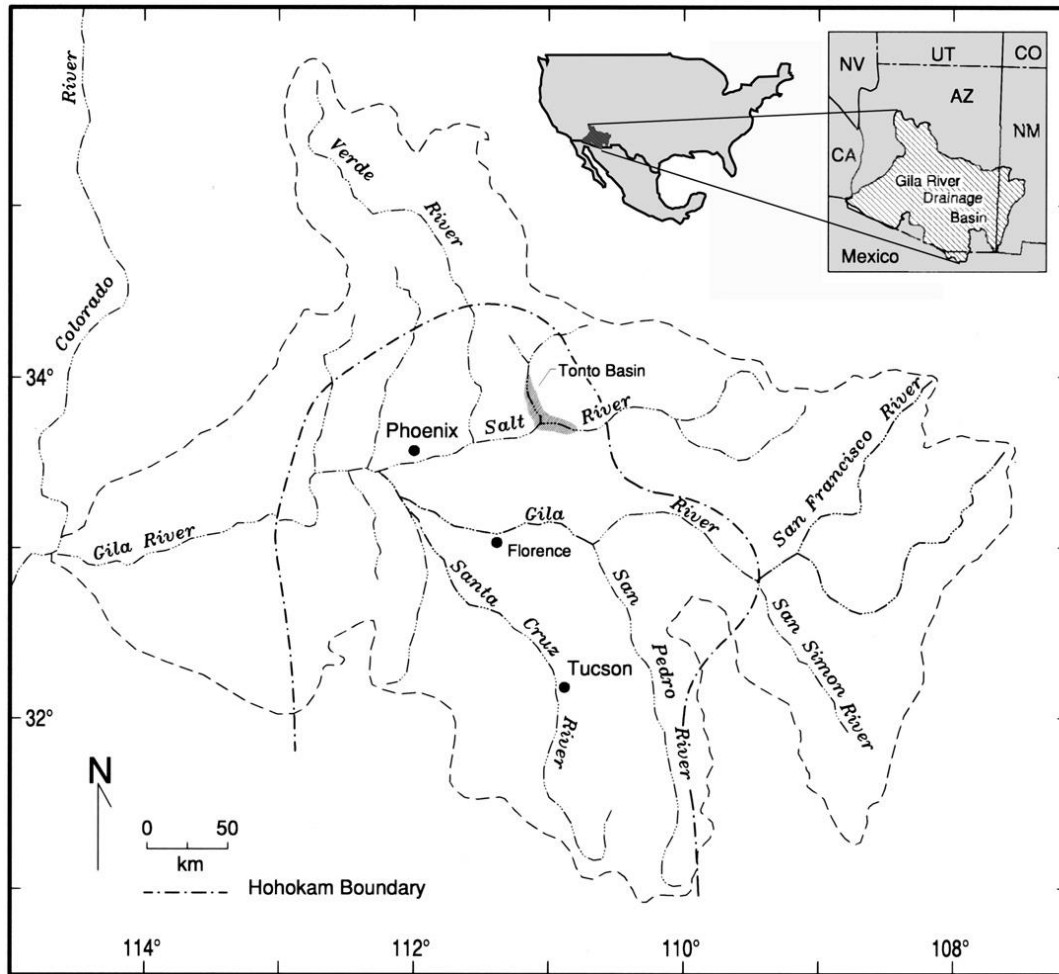


Figure 4.9: Drainage basins of Phoenix, Arizona (from Waters, 2008, p334).

Irrigation abstracting from the Salt and Gila rivers (see **Figure 4.9**) peaked between AD 300-AD 1400 (Waters, 2008, p339). Originally, small-scale methods including floodwater farming and small ditches were in use (Howard and Huckleberry, 1991, p167). Later, larger canals and associated systems, more comparable to many of the systems identified by the present study (see **Chapters 5** and **6**) were constructed. These were dynamic systems operating over a relatively long timescale: ceramic evidence in some cases suggests lifespans of at least 100 years (Woodbury, 1960, p270). The Hohokam canals underwent constant modification, change and replacement (Doolittle, 1991, p144-146). Understanding them as such dynamic entities may be a useful paradigm for many ancient systems.

The climate of the area ranges between arid and semi-arid, involving both water scarcity and occasionally catastrophic summer rainstorms (Hunt et al, 2005, p436-438). The upper part of the Phoenix basin receives between 220-300 mm of precipitation per annum while further downstream the Salt River it is generally limited to between 150-210 mm (Cable, 1991, p119). This pattern is not dissimilar to the conditions in the Balikh Valley and in the southern part of the study area dealt with by this project.

The naturally saline Salt River supported several irrigation systems. Some kind of water control structures may have been used to direct water from the Salt river into these main canals, possibly a series of dams (Hunt et al, 2005, p448). Elsewhere in the Phoenix basin, a reservoir was excavated on the Gila River. This dated to around 1150-1300 AD and served a main canal (Purdue et al, 2010, p132-140). Similarly, it has been suggested that throughout the Phoenix basin systems of weirs and gates were used to control abstraction (e.g. see Purdue et al, 2010, p131).

Several main canals have been recorded for 'Canal System 2' of the Salt river valley (Hunt et al, 2005, p442); estimates of the land irrigated by this system range from 6075-33916 ha (Howard and Huckleberry, 1991, p186) to 20000 ha (Hunt et al, 2005, p435) depending on evaporation and seepage losses and fallow rotation scheduling. While designations and definitions vary, eight of the channels have been classified as main conveyors, eight distribution (sub-main) channels were recorded, and four diversion points were located by archaeological research (Howard and Huckleberry, 1991, p19-20).

Excavated cross sections of the major canals revealed channels of up to 6-10 m wide and 3-4 m deep (Woodbury, 1960, p267). These main and sub-main canals flowed along the natural contours, having very shallow gradients (Murphy, 2009, p51); this is comparable to many of the canals recorded by this project throughout Northern Mesopotamia (see **Chapters 5 and 6**). Water was then diverted into irrigation

laterals/irrigation conveyors that flowed perpendicular to the main conveyors (see Murphy, 2009, p51), shown schematically by **Figure 4.10**. The laterals were secondary channels which terminated at the fields and tended to be less than 1m wide and around 50 cm deep (Doolittle, 1991, p141). They can be elevated above the field surface (Doolittle, 1991, p142). Analysis of aerial photographs indicates that they are spaced about 45-60 m apart. Masse suggests that this pattern is representative of the use of wild flooding (1981, p412).

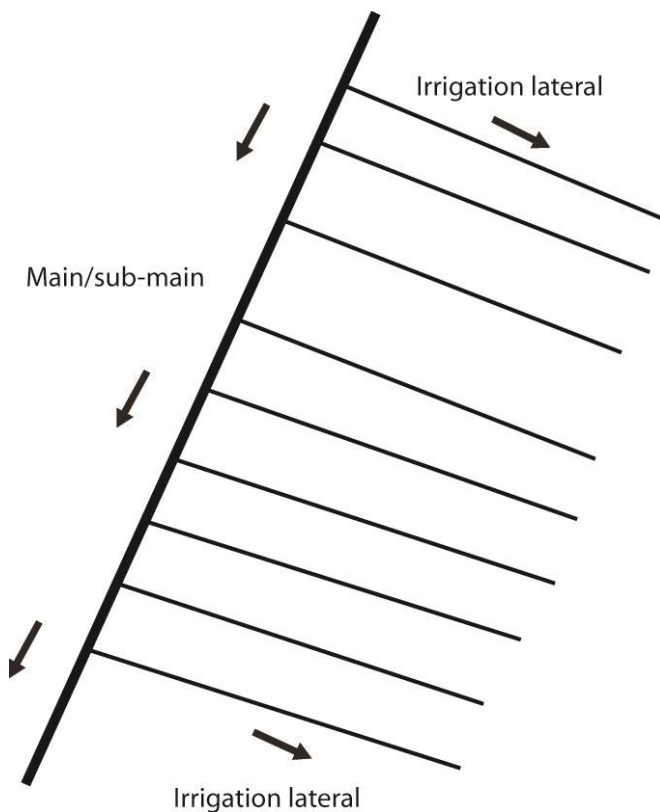


Figure 4.10: *Position of irrigation laterals relative to the main/sub-mains possibly indicative of wild flooding.*

Patterns of fields and field laterals have not always been clearly identified throughout the Hohokam region in the archaeological record, but inferences have been made based on analogies (e.g. see Hunt et al, 2005, p445; Doolittle, 1991, p140). Given a

lack of evidence of furrows, flood-based irrigation may have been used to deliver the water to the crop (Murphy, 2009, p52), which would be consistent with Masse's theory of flood-based irrigation (Masse, 1981, p412).

There is also evidence that indicates how the system was maintained. Many of the larger canals retain significant banks, initially formed from excavation spoil, and afterwards overlain with dredged silts (Woodbury, 1960, p269). Both dredging and the removal of excess vegetation may well have been necessary in order to keep channels clear. charcoal contained within some of these sediments suggests that the burning of vegetation was undertaken (Masse, 1981, p410). Given the low gradients of the canals recorded, which were as low as 0.6% for the northern canals of the Canal System 2 (Howard and Huckleberry, 1991, p154), it is not surprising that evidence for aggradation was noted (Howard and Huckleberry, 1991, p112) or that dredging was necessary. Some kind of drainage was presumably undertaken, with the distribution canals/irrigation laterals possibly serving a dual purpose of capturing and reusing outflow (Murphy, 2009, p53). A drainage function for a canal near the Salt River has been suggested based on its alignment (Masse, 1981, p409).

The effect that irrigation had on the environment has also been investigated. Howard and Hucklebury (1991, p115-121) argue against a predominantly shallow water table based on the relatively deep stratigraphy of metal oxides in the soil, with natural leaching possibly removing carbonates. However, given the salinity of the Salt River, the fine-textured soils of the region and high evapotranspiration rates, they concede that episodes of past salinization may have occurred (*ibid.*). Salinization has indeed been recorded historically for the region (Howard and Huckleberry, 1991, p115-121). Mitigation strategies to prevent excessive salt accumulation may therefore have been practised.

Analysis of the social impacts of the Hohokam systems has been made (e.g. Hunt et al, 2005). The stability of these systems was affected by flooding, possibly driving periods of reorganisation (Waters, 2008, p340). Organisation and reorganisation may

well have been overseen by some kind of administrative structure (e.g. see Masse, 1981, p414), although Hunt et al (2005, p434) suggest that there is no evidence for a powerful administrative entity. However, given the scale of many of the systems, specialist builders and a large labour force may well have been required (Doolittle, 1991, p149). This work-force and water management in general may eventually have been managed by the mounded villages interpreted as 'irrigation communities' (Waters and Raveslout, 2001, p291).

4.8 Case Study: Irrigation of the Wadi Zerqa, Jordan

Past irrigation systems in the Jordan Valley provide a case study geographically closer to the main study area in Northern Mesopotamia. The Jordan Valley is especially dry; comparably to the southernmost parts of the study area. Precipitation is less than 200 mm per annum (Black et al, 2011, p17), and winter rainfall may have declined between the early Holocene and the pre-industrial period (Brayshaw et al, 2011, p48) into which the ethnohistorical systems fall. Seasonal flash floods are frequent (Finlayson et al, 2011, p192), with the potential to cause catastrophic damage to canals.

Despite the extreme dryness of the area, it was selected as a case study because it represents similar kinds of irrigation systems to those found throughout the study area (especially the Nahr al Abbara in the Balikh—see **Chapter 6**). Key research into the systems in the area of the Wadi Zerqa was undertaken by Kaptijn (2009; 2010) and will be discussed here.

The Wadi Zerqa systems are known from traces of irrigation mapped from aerial photos (1920s-1960s) and ethnohistorical information (see Kaptijn, 2010, p148). In this period, the land was controlled by sheikhs and cultivated by villages working as sharecroppers (Kaptijn, 2009, p377), with the land redistributed every few years (ibid. p378). The ethnohistorical data were compared with archaeological remains to investigate the pre-1960s irrigation system. Kaptijn proposes earlier Bronze Age and

Iron Age irrigation (e.g. see Kaptijn, 2010, p155), based on site locations, but the origins of the pre-1960s canals may have been from the Mamluk (1250-1516 AD) and Early Ottoman (1517-1600) periods. It was suggested that the Mamluk system could have been the earliest phase of the ethnohistorical system (described below), with a focus on sharecropping of sugar production, controlled and taxed by the sultan (Kaptijn, 2010, p153).

The pre-1960s systems could be mapped fairly comprehensively by Kaptijn's study, including all parts of the systems (laterals etc). They derived from three main canals abstracting from the Zerqa river (Kaptijn, 2010, p147), and flow for around 6 km (the downstream canal), and up to 12 km (the two upstream canals) (see Kaptijn, 2010, fig.3). A dense network of irrigation laterals and submains branch out from these, with tertiary laterals as close together as 40m. Based on calculations using river discharge and crop water use, she suggested that around 1800-4500 ha could have been irrigated (Kaptijn, 2009, p352).

This pattern is comparable, although more extensive than, systems in the Balikh such as the Nahr Al Abbara, where the landscape was also divided up by irrigation laterals. Interestingly, Kaptijn found that the Wadi Zerqa canals were divided between different clans, with sheikhs controlling allocation in terms of volume (2010, p148), each farmer receiving enough water to irrigate about 10 ha (2010, p149). Based on ethnohistorical information, it was also suggested that land would be redistributed regularly, due to the varying quality of different plots (Kaptijn, 2010, p149), with maintenance organised communally (Kaptijn, 2010, p149). Information about crop choices and associated management strategies is also available for the Zerqa. A focus on sugar production, with several mills, is indicated (Kaptijn, 2009, p424).

4.9 Scales of control of water management strategies

The social aspects of water management, especially in terms of how they were organised and administered, need to be considered. Particular ways of managing

water can have certain effects on specific communities: while this comment seems ambiguous, patterns do exist. When a region shifts from rain-fed to irrigated agriculture changes will occur. While yields will be greater, many social structures could be affected.

When extraction exceeds recharge, conflict in some form is inevitable. Water allocation needs to be agreed on, but can frequently lead to disputes (see Scarborough, 2003, p92). This is often the stage where more powerful entities than individual communities or groups of farmers become or are already involved. It has been suggested that large systems and the changes to production that these bring necessitate the involvement of governments (e.g. see Wittfogel, 1957). In contrast there is a general belief that smaller systems tend to be community based and managed by the landholders themselves (Agnew and Anderson, 1992, p166). In reality, water management throughout an empire could have been a mixture of many different forms, with large-scale systems controlled directly by the state in some cases, and more locally in others. Similarly, smaller systems such as qanats and water tunnels could be part of an imperial landscape (for example at Raqqa), or controlled by local landowners and communities.

Sustainable methods like qanats and to some degree, water harvesting, tend not to cause problems of depletion. More 'reticulated' methods imposed by higher authorities may deliver more reliable crop yields but often at the expense of the original resource for many individuals and groups. Change from smaller-scale, sustainable methods to unregulated groundwater extraction, for example, can disrupt long-successful systems. Modern groundwater pumping across the Middle East has rendered many qanats unusable (e.g. see Lightfoot, 2009) by depleting resources faster than they can be recharged. Sheridan's analysis of the change from the traditional 'acequia' to diesel pumping in Cucurpe, Mexico, is also an illustration (1996). Management systems developed to regulate one kind of water strategy often cannot function after a shift to a different strategy; flexibility may be key to the long term success of any water management scheme.

4.10 Summary

It has been demonstrated in this chapter that water management is a more encompassing term than simply 'irrigation'. Many different ways of abstracting and delivering water are used, and drainage must also be incorporated into any model. This will include smaller-scale methods such as water-harvesting and also large scale systems consisting of complex layouts of main canals and irrigation laterals.

These systems must out of necessity conform themselves to certain aspects of their environment, including climate, precipitation and soil. Social and economic issues, less easily identifiable, also impact upon design choices. With these issues and conditions recognised, water management systems identified using CORONA throughout the project area can now be considered. The different types of water management, from small-scale water harvesting techniques to larger-scale reticulated systems, will be mapped, and the different parts of systems (e.g. laterals, mains) recorded where possible (see **Chapters 5 and 6**).

Chapter 5: Water management in northern Mesopotamia

5.1 Introduction

The literature review of **Chapter 2** has already presented the state of understanding of known water features in Northern Mesopotamia. The original contribution of the present study will now be addressed. This research has taken two forms: firstly, previously unknown water features were identified using CORONA imagery and digitised to create shapefiles. The channels were linked to features of known date where possible. Secondly, features known through archaeological survey, excavation and through interpretation of historical sources that had not previously been examined using CORONA were also recorded using this image dataset so that a GIS database could be generated. The entire area between the Euphrates at Jerablus in Syria and the Tigris in Iraq was scrutinised using CORONA at a nominal scale of 1:30,000 (see **Chapter 3.2**, image interpretation methods). DEMs (SRTM, ASTER and CORONA) were used to validate features where possible. Because it is recognised here that there are some uncertainties inherent in using these data (see **Chapter 3**), where possible, a range of potential values is given.

It is important to emphasise that this chapter does not represent the entire range of water features that are present. More detailed results for each specific area exist (see **Chapter 2**). For example, Geyer and Monchambert (2003) mapped many hydraulic features between Deir ez Zor and Mari. The intention here is to demonstrate the range and types of features that can be recognized on satellite images such as those of the CORONA programme.

Given the complexity of water management in the Balikh Valley when compared to other areas, this will be dealt with in a separate Chapter (**Chapter 6**). Results from the rest of the study area are presented here.

Geomorphological and landscape context

The different landscape zones referred to in this chapter should first be outlined. In these terms, the study area consists of several different landscapes. Most ancient and modern irrigation was focused in area where water was available, preferably year-round, and where soils are conducive to agriculture. This encompasses the river valleys of the Euphrates, Tigris and their tributaries, which have tended to be foci for cultivation, meaning that many older water management features in the river valleys have been erased by modern canals.

In between the perennial rivers there are also cultivable areas, which can be watered by a variety of means including rainfall, springs, pumped groundwater and by ephemeral seasonal wadis. They include areas such as the region immediately to the south of the Sinjar mountains in Iraq.

Much of the land, for example the zone between the Balikh and the Iraqi border, can be regarded as steppe. It is dominated by gypsiferous or stony soils, and has low precipitation and few permanent water sources (Hole and Zaitchik, 2006, p139-140). Therefore, it is less conducive to agriculture and large-scale irrigation

Geomorphological processes are directly linked to the preservation of water management systems. The main processes which affect the appearance and morphology of relict canals are erosion and infilling. Erosion both obscures and reveals archaeological remains. In some cases erosion exposed previously buried features; rock-cut conduits in the Wadi Amarna were revealed in this way (see section 5.2 below). Erosion also affects the shape of upcast banks of canals, which are reduced in height over time, as **Figure 5.1** shows.

Infilling gradually fills up the channel void with sediments, obscuring the original hydraulic cross-section of a canal. As **Figure 6.19** shows, the Sahlan-Hammam channel had become infilled by the 1990s. The post-Abbasid channel cutting through the site of Heraqlah had also been affected by these transformation processes. It's upcast banks (clear in the 1960s CORONA image—**Figure 6.62**) had been eroded away by the time it was visited in 2010, and the channel was infilled with sediment (see **Figure 6.60**). This means that the only way to record the original dimensions of a canal is to excavate it; the Nahr Maslama at Dibsi

Faraj (Harper and Wilkinson, 1975, p337) and Sahlan-Hammam canal in the Balikh (Wilkinson, 1998, p70) were excavated, allowing their dimensions to be determined, discharge to be calculated and dating information to be obtained.

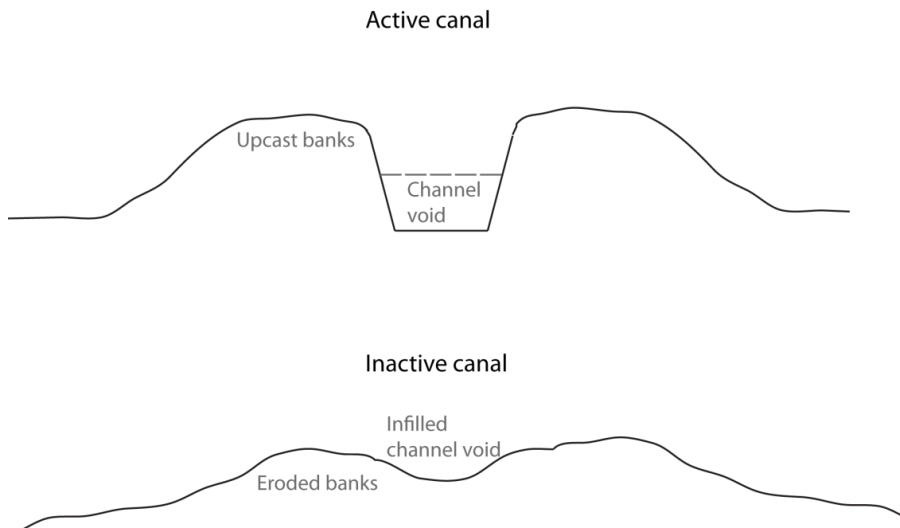


Figure 5.1: Schematic diagram showing the morphological difference between active and disused canals.

The dynamic nature of the rivers themselves has also removed archaeological evidence. However, these processes have been investigated within the study area (Demir et al, 2007). The floodplain of the Euphrates has been dated to a broad period of the Holocene; much of it, including the area close to Raqqa, must be post 14th century, based on the truncation of Early Islamic sites (Hritz, 2013a, p177; Challis et al, 2004, p144). For example, the first part of the canal between Tell Fray and Qa'lat Ja'bar has been removed by the Euphrates (see **Figure 5.19:**) therefore, the floodplain in these areas was not investigated as part of the image interpretation. It is worth noting here, however, that there is evidence for irrigation in the past by the use of water lifting devices (e.g. see Decker, 2009a, p199). It is possible that the floodplain was intensively cultivated during the time of the later Empires through the use of such techniques

Water management traces are known throughout all these different landscape contexts yet most of this area has not yet been thoroughly investigated or surveyed using CORONA images. This is surprising, given the high level of archaeological potential of the entire study area, and the possibility of locating

features using the CORONA imagery. This chapter will now summarise the results of the image interpretation for each region.

5.2 Jerablus

Relict water features around Jerablus were identified and visited during fieldwork in 2010, including the remains of two large canals. One still flows to the east of Carchemish (**A, Figure 5.4**), towards Tell Jerablus Tahtani (Wilkinson et al, forthcoming). In 2010, it was choked with vegetation (see **Figure 5.2**). It is possible that it dates to the 8th century BC (Wilkinson et al, forthcoming).

An infilled canal (**B, Figure 5.4**) flows south of the site of Tell Jerablus Tahtani and towards the village of Jemal. As Wilkinson et al (2007 p236) indicate, it was probably in use during the Byzantine-Early Islamic periods (dating information was based on association with sites). The SRTM and ASTER DEMs indicate that it flowed across a landscape with a gradient of about 0.12%- 0.16% respectively (this is dependent on the accuracy of the DEMs).

No use of canals was observed at Jerablus Tahtani in July 2010. Irrigation was conducted by extracting groundwater using diesel pumps; based on the depth of the pits in which the pumps were contained, the water table was over 1 m below the field level at Jerablus Tahtani.



Figure 5.2: Canal at Carchemish with vegetation.

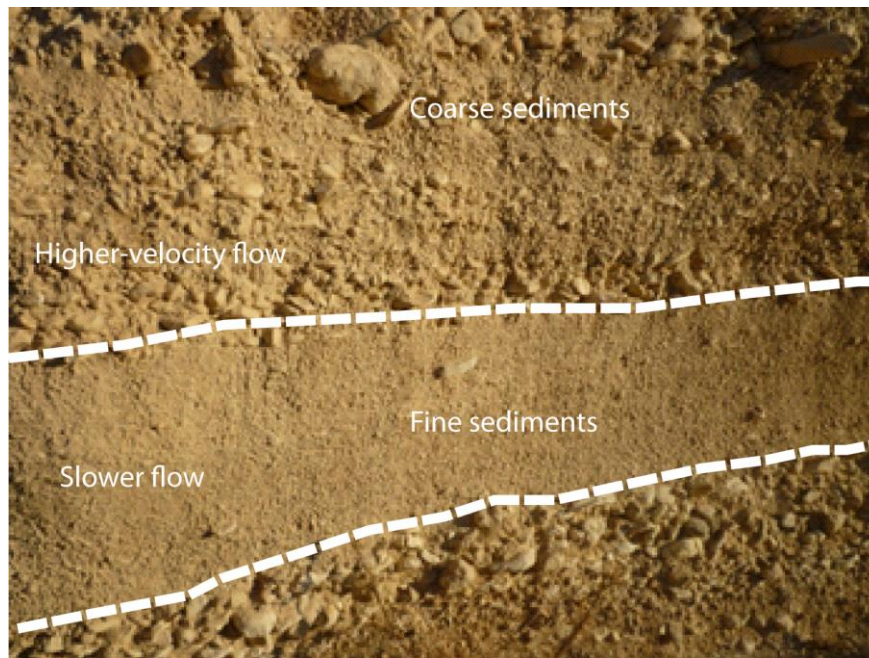


Figure 5.3: Exposed section in the Wadi Armana showing different layers of sediments.

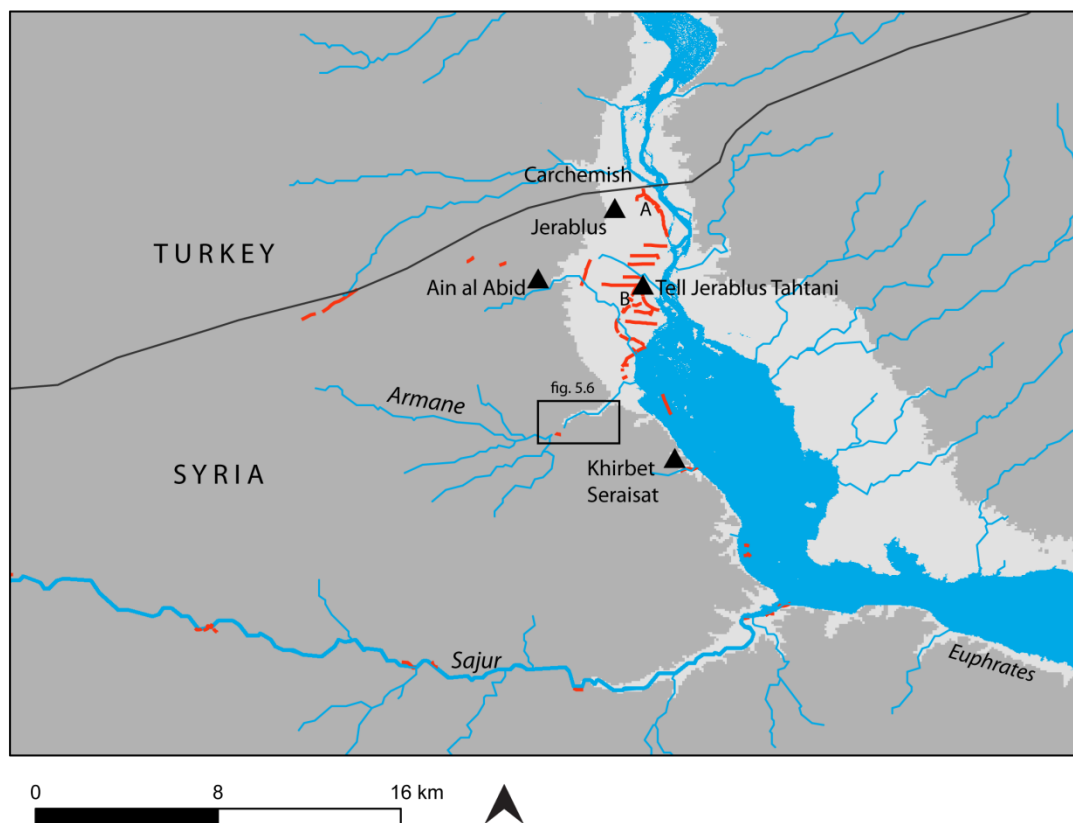


Figure 5.4: Channels in the Jerablus region.

Along the Wadi Amarna, traces of several rock-cut subterranean channels were recorded (see Wilkinson et al, 2007, p236-239). As **Figure 5.6** shows, these are not visible using CORONA, partly because of their position within the Wadi, and partly due to natural landscape conditions such as topography and soil type. It seems reasonable to suggest that these rather small channels were designed to conduct fairly regular flows of low volume (i.e base flows rather than high floods). Using a tributary like the Armana, despite lower base flows, might have been easier than irrigating from the Euphrates (see Van Liere, 1963, p115).

The deeply incised Wadi Amarna is now dry. An exposed section (**Figure 5.3**) shows that it had experienced episodic high-velocity flow (coarser sediments) as well as periods of slower flow. Past settlements appear to have taken advantage of this past flow, constructing several water management features along it. A wall of dressed stone blocks which may have been a dam, possibly Roman, was identified a short distance downstream of Tell Armana.

Figure 5.5 and Figure 5.6 show some examples of rock-cut conduits, several of which were constructed from stone blocks which were inscribed with claw chisel marks. A newly identified tunnel was recorded, consisting of a section of a stone-lined channel which had been exposed by recent erosion. The tunnel was associated with a large limestone block inscribed with a mason's mark (**Figure 5.7**). Although the large block may have been in situ, others appeared to have moved.

Three other tunnels which were identified during fieldwork were recorded by the land of Carchemish Project (e.g. see Wilkinson et al, 2007). As **Figure 5.5** illustrates, these were high up in the channel stratigraphy and flowed close to sites dating to the Hellenistic-Early Islamic periods (see Wilkinson et al, forthcoming).



Figure 5.5: Rock-cut tunnel in the Wadi Armana.

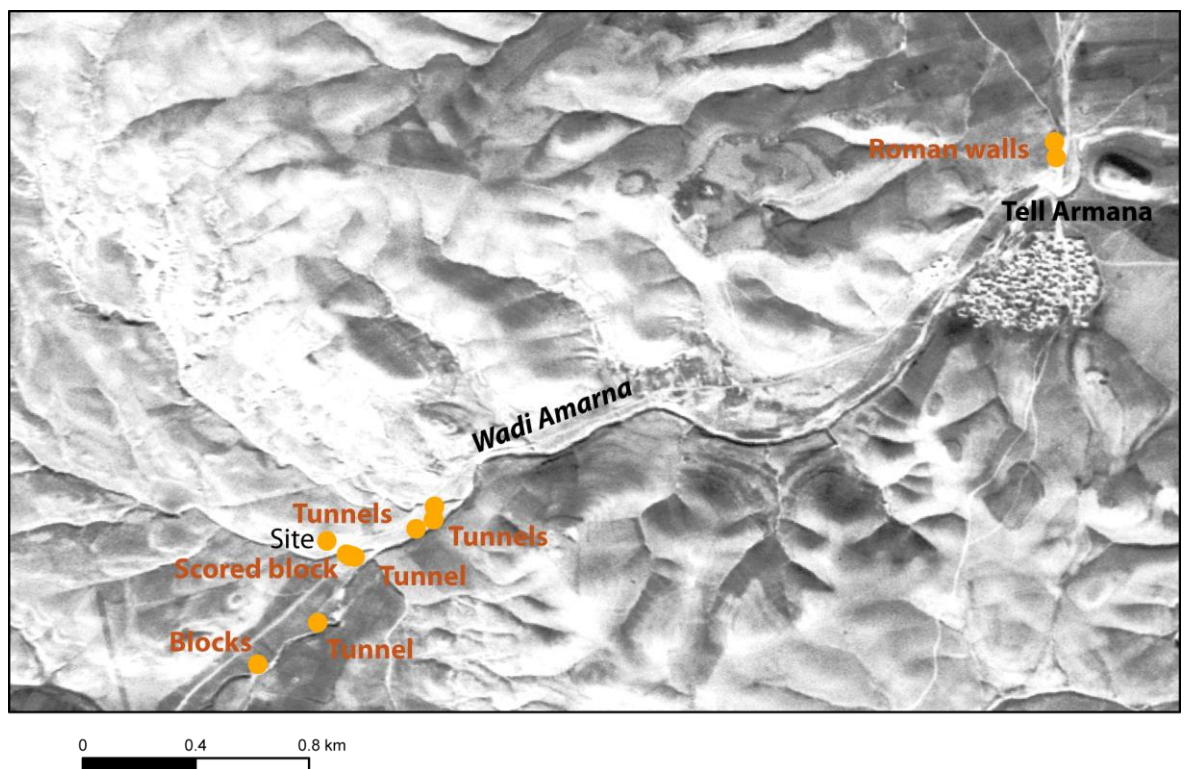


Figure 5.6: Map of locations of rock-cut channels and CORONA image. Image 22 January 1967.



Figure 5.7: *The block inscribed with a mason's mark was about 7.10 m below the field level, and was located 4.64m above the wadi bed, on layers of sediment and stones. Image July 2010.*

Other features within the LCP survey area were also visited in 2010. One of these was a subterranean conduit cut into a limestone hill c.5 km South-West of Carchemish, close to a site called Hajaliyyeh/Kaklice. The channel does not appear to be a qanat. Rather, it may have been conveying spring water. Local people informed us that it was ancient, and that the channel had been dry for 10 years, although some of them remembered it containing water in the winter.

Interestingly, most of the features identified by fieldwork in 2010 around Jerablus were not clearly visible in the CORONA images. Much of the floodplain had been scoured by the Euphrates (Wilkinson et al, forthcoming) and the undulating limestone areas were pale in the CORONA imagery (ibid), obscuring faint water features. This is an important point to consider, because it suggests that other features of a similar type and existing within similar landscape contexts (in terms of soil type, geomorphology etc) may also be invisible in the CORONA images. Only further fieldwork will identify them.

5.3 Euphrates - Balikh

Despite the difficulty of remotely identifying features in the Jerablus area, elsewhere, they could be clearly located using CORONA. Several relict water features were found in the less-heavily cultivated steppe area north-east of the Euphrates, between the river and the Balikh (see **Figure 5.8**). These consist of a few qanats of unknown date. Unfortunately the dates of the sites they are associated with have not been confirmed, although based on their morphology, tentative dates can be suggested.

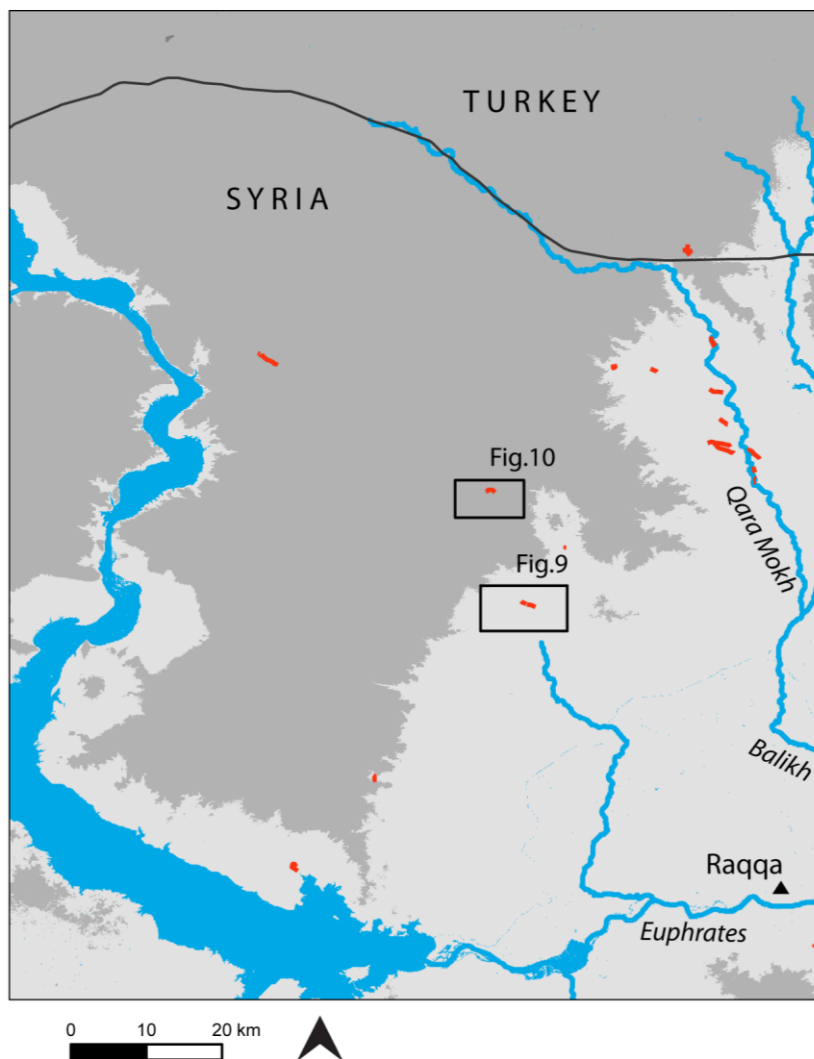


Figure 5.8: Water features in the steppe between the Euphrates and the Balikh.

The link between a particularly large site and a qanat trace should be noted: the CORONA image (**Figure 5.9**) shows a large, unwalled settlement of later antique date, possibly Early Islamic, close to the banks of a wadi, 28 km upstream of the West Balikh systems (see **Chapter 6**). Given the size of this site (about 840 x

1000m), it clearly once held some significance. The qanat trace also visible in the image probably supplied it with a reliable water supply. It should also be noted that the wadi which runs through the site may have been one of the sources for the relict canals in the west part of the Balikh horseshoe, which do have a link with some Early Islamic features. If water abstraction rights were already claimed by these systems, assuming the water resources were organised by some authority, then the upstream site may have needed to construct a separate water supply in the form of a qanat. This would also have ensured reliable flows at times of reduced flow in the natural stream.



Figure 5.9: See inset within **Figure 5.8**. Large site and trace of a qanat (marked by arrows) identified by present project and also recorded by Dan Lawrence and Niko Galiatsatos. CORONA image 22 January 1967.

There are also other short stretches of qanat in this extensive area of steppe, with relict, possible late antique-Islamic structures nearby (for example see the qanat and square site in **Figure 5.10**), again of later antique appearance.

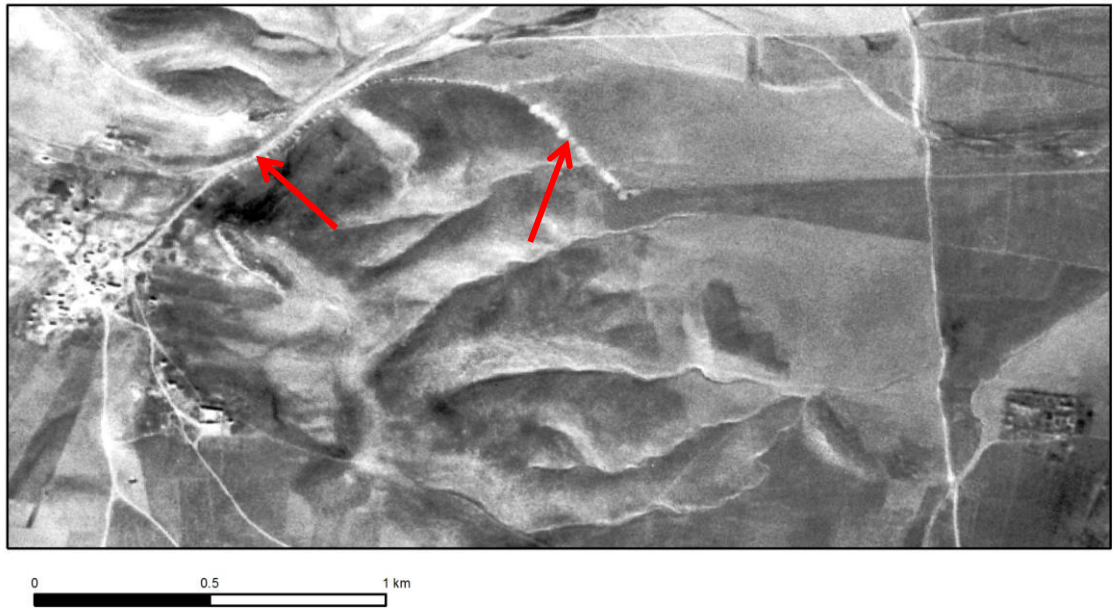


Figure 5.10: See inset within **Figure 5.8**. Features including a qanat in the steppe between the Euphrates and the Balikh. CORONA image 22 January 1967.

5.4 Membij-Dibsi Faraj

While water features in the steppe on the left bank of the Euphrates are relatively sparse, qanats have been mapped in the lands adjacent to the west and south banks of the Euphrates. Dan Lawrence and Niko Galiatsatos mapped numerous qanats and qanat segments (**Chapter 2**) around the town of Membij (ancient Hieropolis/Bambyce, possibly of Hellenistic/Roman date, and others between Tell Hadidi and Selenkahiye. The present study also recorded these features.

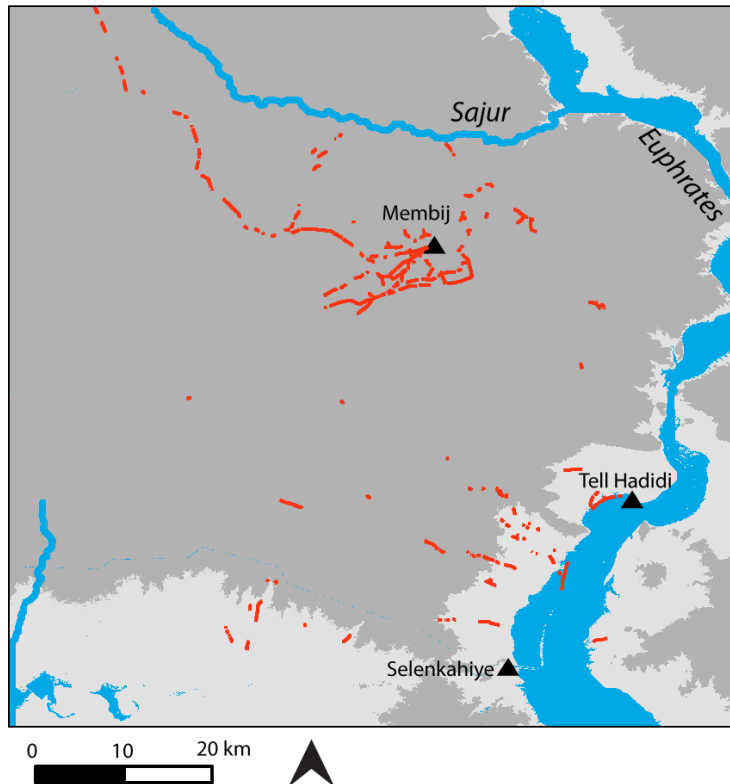


Figure 5.11: *Qanats between Membij and Dibsī Faraj. Mapped by Dan Lawrence, Niko Galiatsatos and present study.*

5.5 Dibsī Faraj

The large canal at Dibsī Faraj, the Nahr Maslama, is already well known through survey and excavation, and has been dated on the basis of Umayyad coins (Harper and Wilkinson, 1975, p337). Due to this excavation, the Nahr Maslama is one of the few dated ancient canals in Northern Mesopotamia. The present study (also see Wilkinson and Rayne, 2010, p127) found that it was also identifiable in CORONA images, taken shortly before the investigations in the 1970s were carried out. On the imagery, the canal is truncated by relict meanders of the Euphrates. This presumably represents post-medieval action, given the medieval date of the canal. Interestingly, fragments of a canal similar in appearance to the Dibsī Faraj one were found in the imagery further downstream (see **Figure 5.12**; also see **Figure 5.13** for location). Based on Harper and Wilkinson's (1975, p337) excavated section, the parameters of the canal can be outlined (**Table 5.1**) and the discharge of the canal suggested, giving a fairly small value in comparison to the Sahlan canal in the Balikh.

Table 5.1: *Parameters of the Nahr Maslama and discharge calculated using Manning's formula. The n value for a straight, earth channel was selected (see Philips and Tadayon, 2006). The gradient value is based on assuming a slightly shallower gradient than the Euphrates, which was measured using the SRTM DEM between the Tabqa Dam and Raqqa. This simply provides an estimated, rather than an absolute, idea of the potential values.*

Estimated gradient	Bottom width (m)	Depth (m)	Flow (m ³ /s)
0.0004-0.0003	2-3	1-2	2.7-15.5

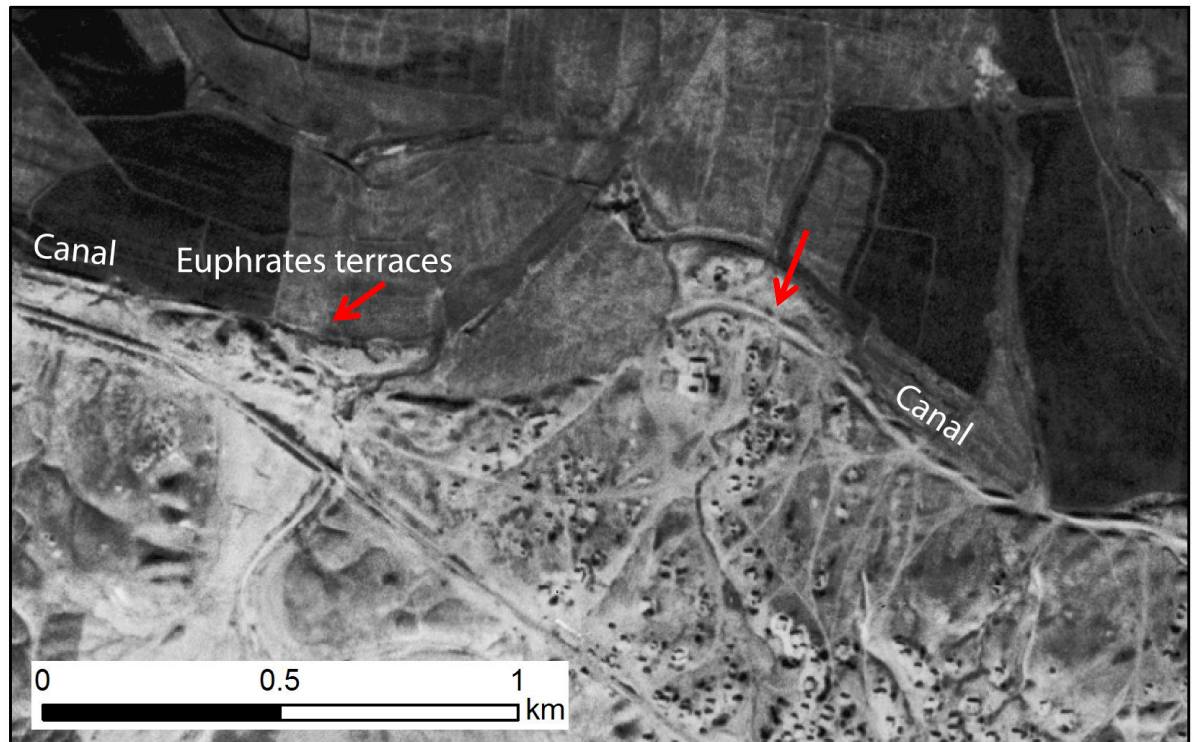


Figure 5.12: *A truncated canal on the edge of the Euphrates floodplain (not to be confused with the adjacent straighter, clearer-cut modern canal). CORONA image 22 January 1967.*

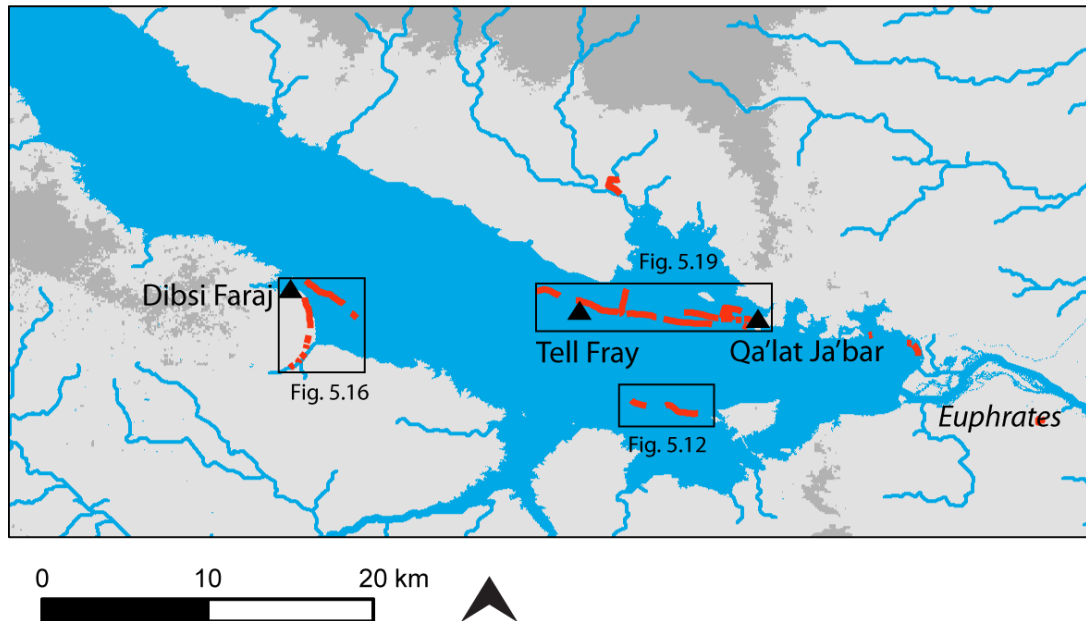


Figure 5.13: Features alongside the Euphrates between Dibsī Faraj and Qa'lat Ja'bar.

Figure 5.16 shows the water management features around the site. The Nahr Maslama was not the sole water supply of the Dibsī Faraj area. A qanat was identified by the present study (see **Figure 5.17**; also see Wilkinson and Rayne, 2010, p127). It stretched over 4 km from the limestone uplands above the site and faded out close to it. While the large-scale canal would have provided water for irrigation, the qanat may have supplied the site itself with water, and therefore presumably was used at some time within the Roman-Early Islamic period represented by the site.

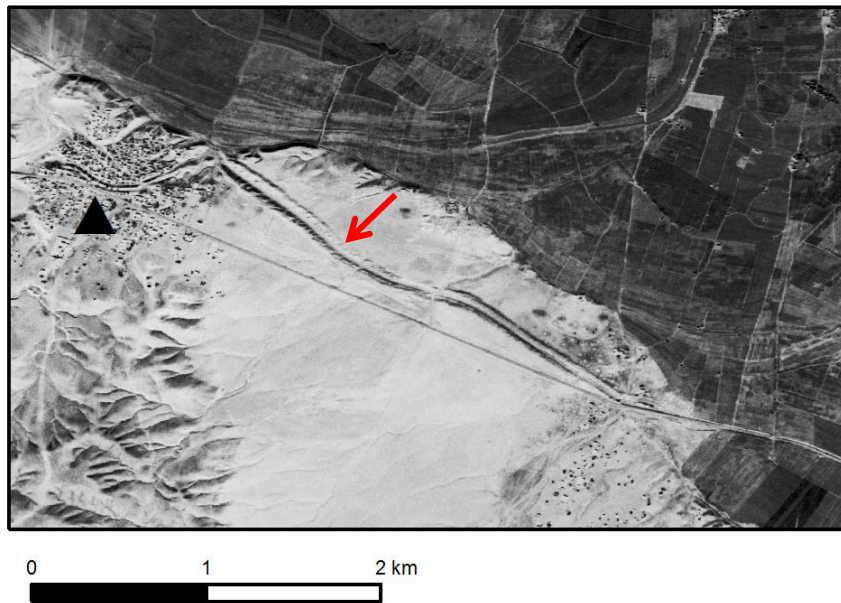


Figure 5.14: The Nahr Maslama and Dibsi Faraj. CORONA Image 22 January 1967.

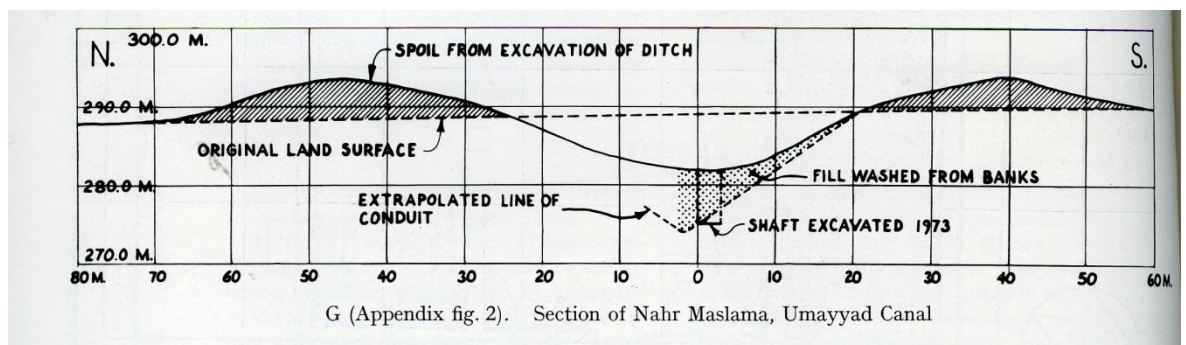


Figure 5.15: Section of the Nahr Maslama (from Harper and Wilkinson 1975, Fig.2).

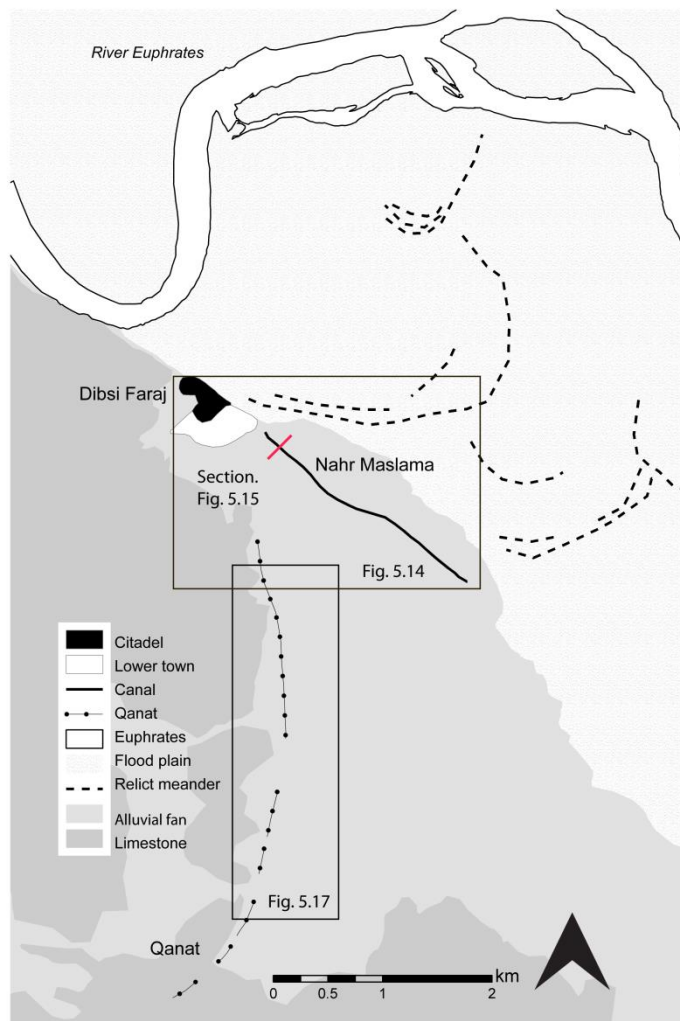


Figure 5.16: Water features at Dibsī Faraj (from Wilkinson and Rayne, 2010, p127) and location of section excavated by Harper and Wilkinson (1975).

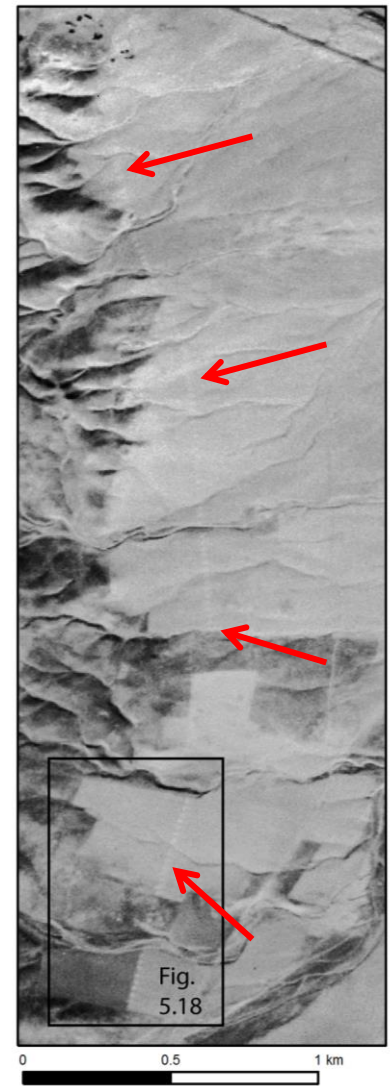


Figure 5.17: The qanat is visible as a line of white dots, representing upcast mounds. It is difficult to see at this scale of 1:24000. CORONA image 22 January 1967.

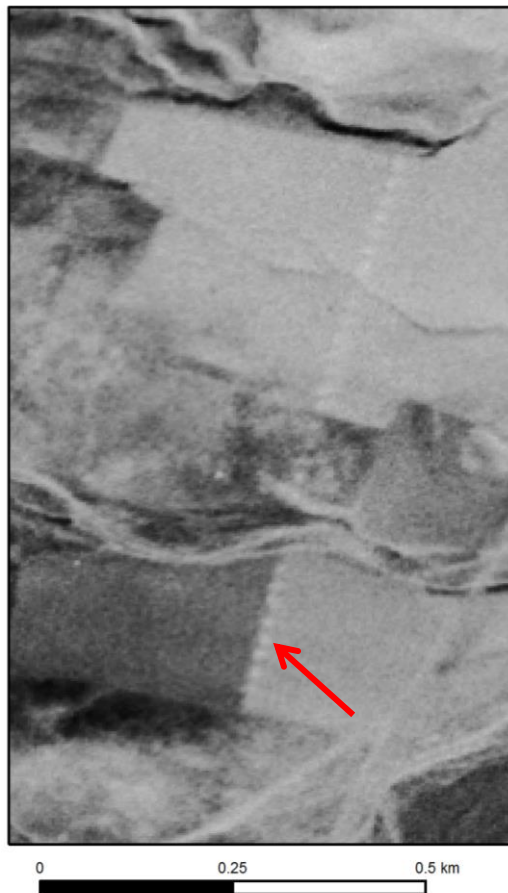


Figure 5.18: The scale at which the feature is clearly visible (1:10000) shows the care needed when undertaking an image interpretation study;.Features such as this qanat could be easily missed. CORONA image 22 January 1967.

5. 6 Tell Fray-Qa'lat Ja'bar canal

A segment of canal passing along one side of Tell Fray is already known (e.g. see Bounni, 1988. Also see **Figure 5.13** for a map). However, the present study, using CORONA images, found that it extended for some distance both up and downstream of Fray, over a distance of about 10 km. **Figure 5.13** shows its location and **Figure 5.19** shows the CORONA image. Unfortunately, given that the area is now under water, a DEM-derived gradient could not be assigned. The abstraction point of the canal could not be determined, because the canal is truncated by the Euphrates. The feature then seems to fade out at Qa'lat Ja'bar. Early Islamic features closer to Raqqa were also truncated by the Euphrates; the terraces around Tell Fray and Raqqa may therefore be of contemporaneous date.

An association with both/either Fray or Ja'bar for this canal seems possible. The evidence from Fray indicates a Bronze Age date (see Bounni, 1988, p363-69; also see **Chapter 2**). This could be a canal that either had a relatively early origin, perhaps in the Bronze Age, as suggested by the evidence from Fray, that continued to be maintained and used into the Early Islamic period, serving some purpose for Qa'lat Ja'bar. Alternatively it could have been a later (Early Islamic) feature.

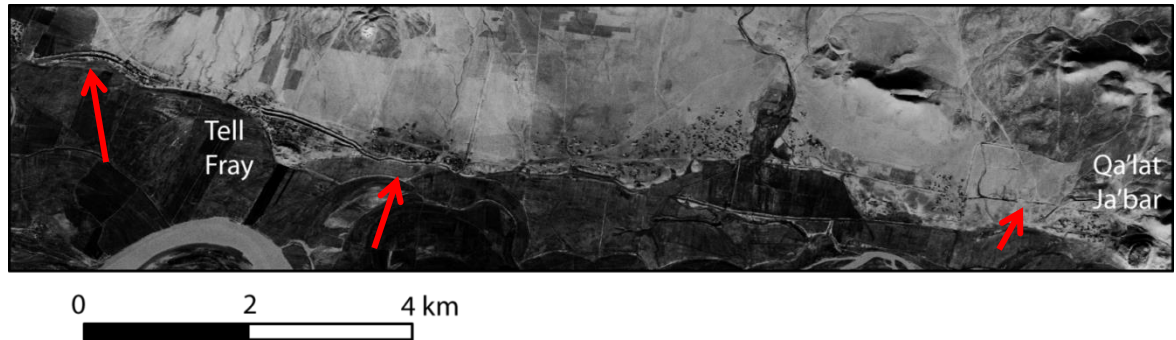


Figure 5.19: CORONA image of the Fray-Ja'bar canal. CORONA image 22 January 1967.

5.7 Resafa

Water features at Resafa, including a dam, canal and cisterns, have already been investigated in detail using archaeological excavation (e.g. see Beckers, 2007-9; Brinker, 1991) and hydrologically using DEMS (Berking et al, 2010). The present study was able to confirm the layout of the known features using CORONA, including a dam, canals and cisterns (shown in **Figure 5.21**). The CORONA images also highlighted ruined and relict structures around Resafa including possible water features in the basin of the Wadi es Sele (e.g. see **Figure 5.22**).

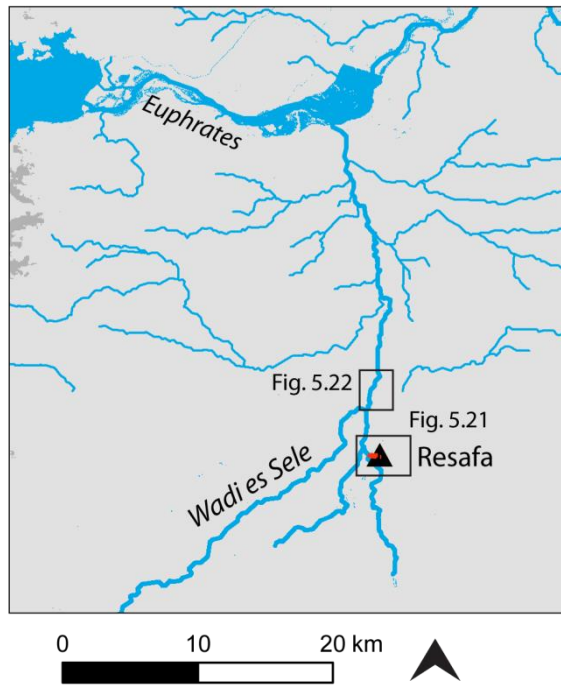


Figure 5.20: Location of Resafa.

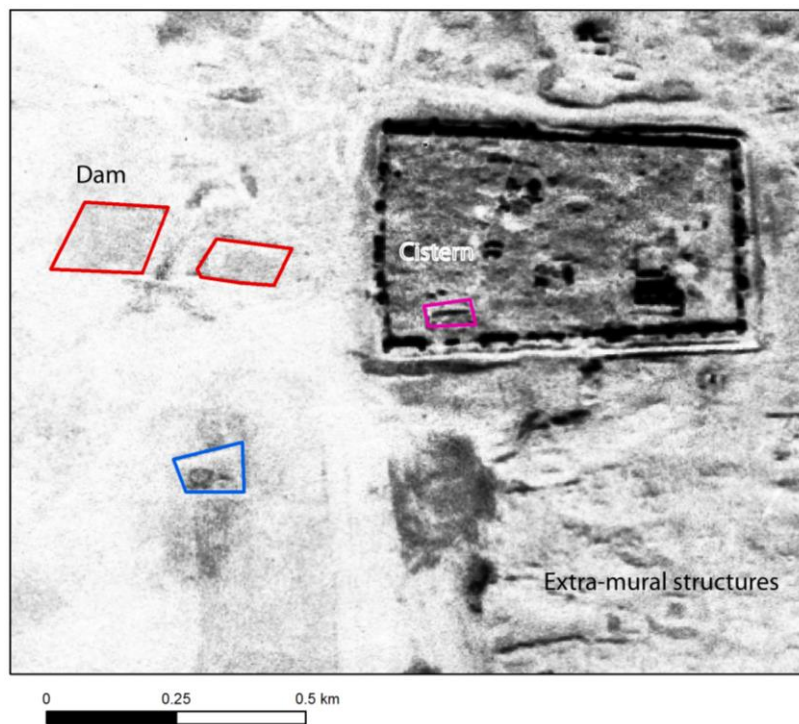


Figure 5.21: The CORONA image (22 January 1967) shows water features around Resafa (see Berking et al, 2010, p818).

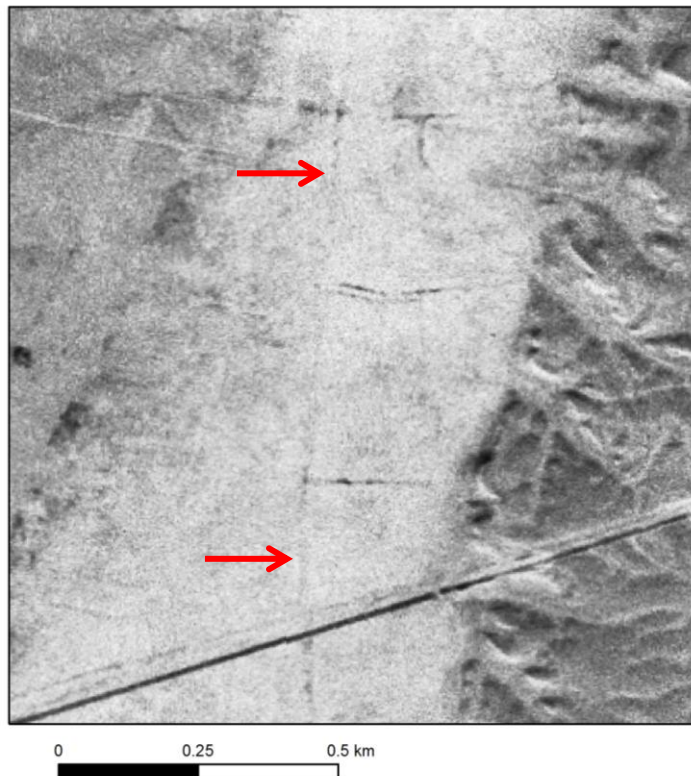


Figure 5.22: Canal traces in the basin of the Wadi es Sele, 3km north of Resafa. CORONA image 22 January 1967.

Because of the faintness of the qanat at Dibsi Faraj, image interpretation had to be undertaken carefully in order to locate the features which were visible using CORONA. A feature similar in appearance to the dam at Resafa is an example of this (see **Figure 5.23**). It was recorded in the steppe 28 km to the south west of Resafa, in an area which was generally devoid of identifiable water systems. Given that such ephemeral features are identifiable using CORONA, it is likely that this image interpretation study has located a good proportion of them.

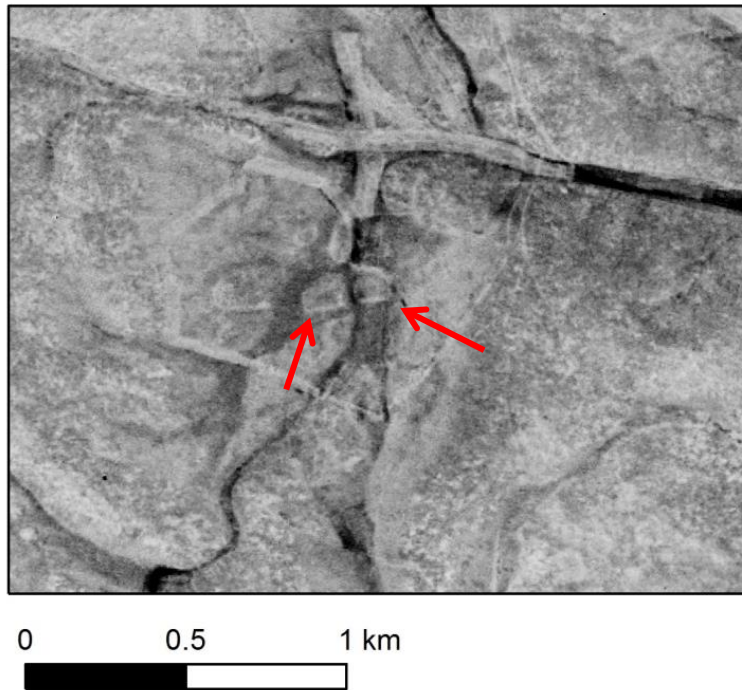


Figure 5.23: A similar feature to the dam at Resafa was identified 28 km to the south west. CORONA image 22 January 1967.

5.8 Balikh-Habur

Given the complexity of the Balikh, an entire chapter has been devoted to it (**Chapter 6**). Image analysis was also taken for the areas between the Balikh Valley and the Iraqi border. Very few relict water features could be identified in the steppe, however, several large-scale canal systems were located alongside the Euphrates and the Habur. The Euphrates terraces have been dated by archaeological remains and, conversely, their geomorphological context can be used to infer the age of some archaeological remains. The mapping undertaken by Besancon and Sanlaville (1981) and Demir et al (2007) indicates that the lowest terraces of the Euphrates, adjacent to the river, formed during the Holocene. This is shown by the location of the archaeological sites and relict canals. The canal at Tell Fray (at least Bronze Age in date, possibly Early Islamic) was truncated by former meanders of the river. Close to the Balikh, the floodplain cuts features of Early Islamic date and post-Abbasid date (for example the canal at Heraqlah, see **Chapter 6**), showing that it post-dates the early medieval period. Features of earlier date will have been removed.

Downstream, however, parts of the floodplain are older. The site of Mari and possibly associated canals are located within it. Geomorphological mapping identified the floodplain in this area as Bronze Age (Demir et al, 2007, p2851). It is possible, therefore, that other archaeological features on this terrace, including relict canals, could date to this period.

On the right bank of the Euphrates, especially between Sura and Deri ez Zor, the floodplain had clearly eroded right up to the plateau in some places. However, many canals have been identified between Deir ez Zor and Mari; Geyer and Monchambert (2003) recorded them using archaeological survey (also see **Chapter 2, Figure 2.12**). This study has been able to locate several segments of some of these relict canals between the Balikh and Mari using CORONA images.

As **Figure 5.24** shows, traces of a significant feature were located on the north bank of the Euphrates, but upstream of Deir ez Zor. The clearest segment visible in the CORONA imagery is short (1 km), but it can be seen that it has an infilled channel and eroded but visible embankments, and flows across a gradient of about 0.14-0.21% (depending on where the measurement is taken along the short segment of canal, using SRTM).

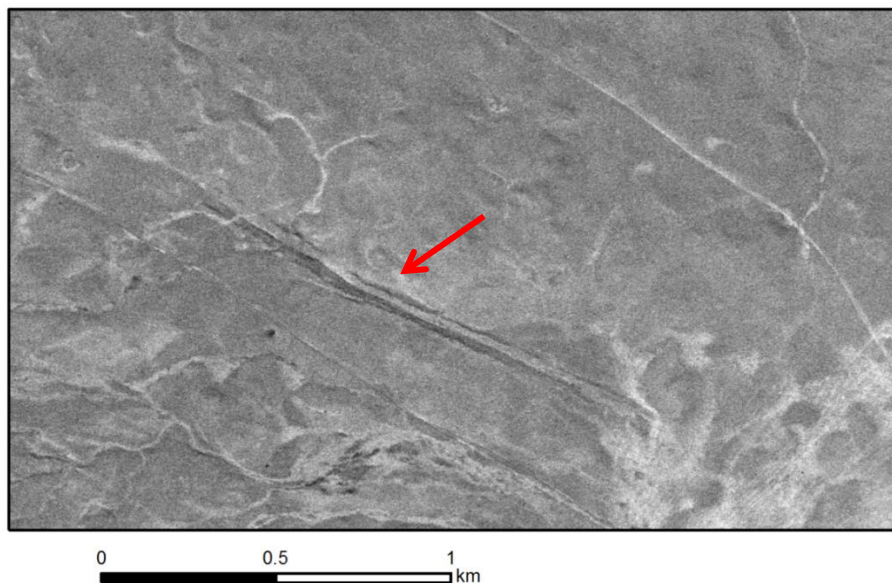


Figure 5.24: Canal on north bank of Euphrates. See **Figure 5.26** for location. CORONA Image 5 November 1968.

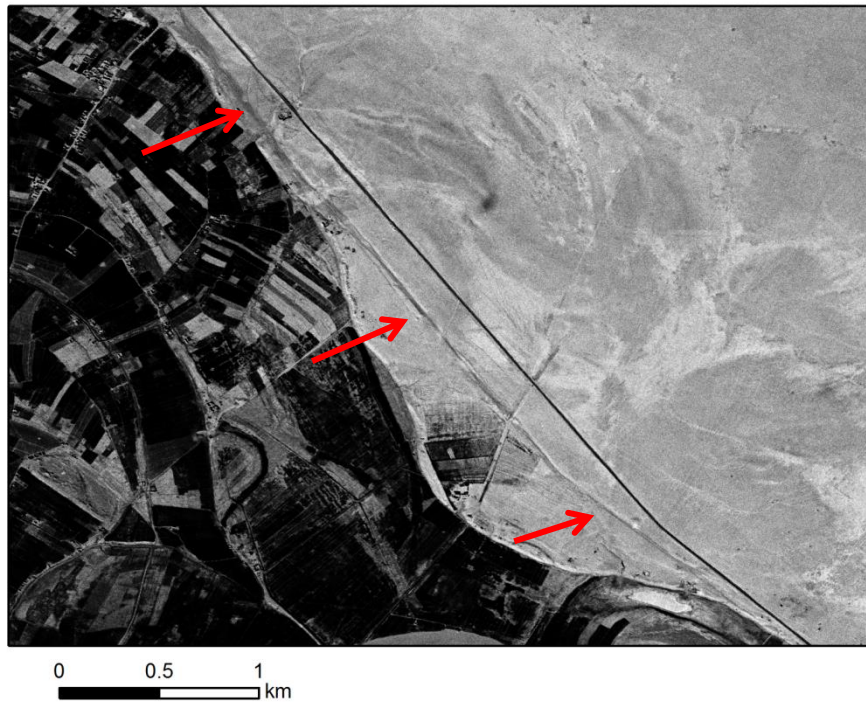


Figure 5.25: *Traces of the Nahr Semiramis are visible on the CORONA imagery. See **Figure 5.26** for location. CORONA image 5 November 1968.*

Further downstream, a feature also identifiable in the CORONA imagery has been recorded by Geyer and Monchambert (2003, p276) as the Nahr Semiramis and assigned a late antique date (ibid, p222). They also suggest that it might have its origins in a dam upstream near Zalabiya (ibid. p217-218). It may therefore be part of the same feature shown in **Figure 5.24**. Its' morphological similarity to the other large features alongside the Euphrates (for example the Nahr Maslama and Nahr Dawrin), should be noted. Flowing close to the floodplain, it is a wide, infilled channel with traces of embankments, and potentially was part of a large-scale irrigation system. Using CORONA, traces of channels which may also be part of the Nahr Semiramis can be traced up until the the Habur. Unfortunately, many of the channels recorded on the ground by Geyer and Monchambert (2003) were not visible on the CORONA imagery, especially those in the floodplain on the right bank of the Euphrates.

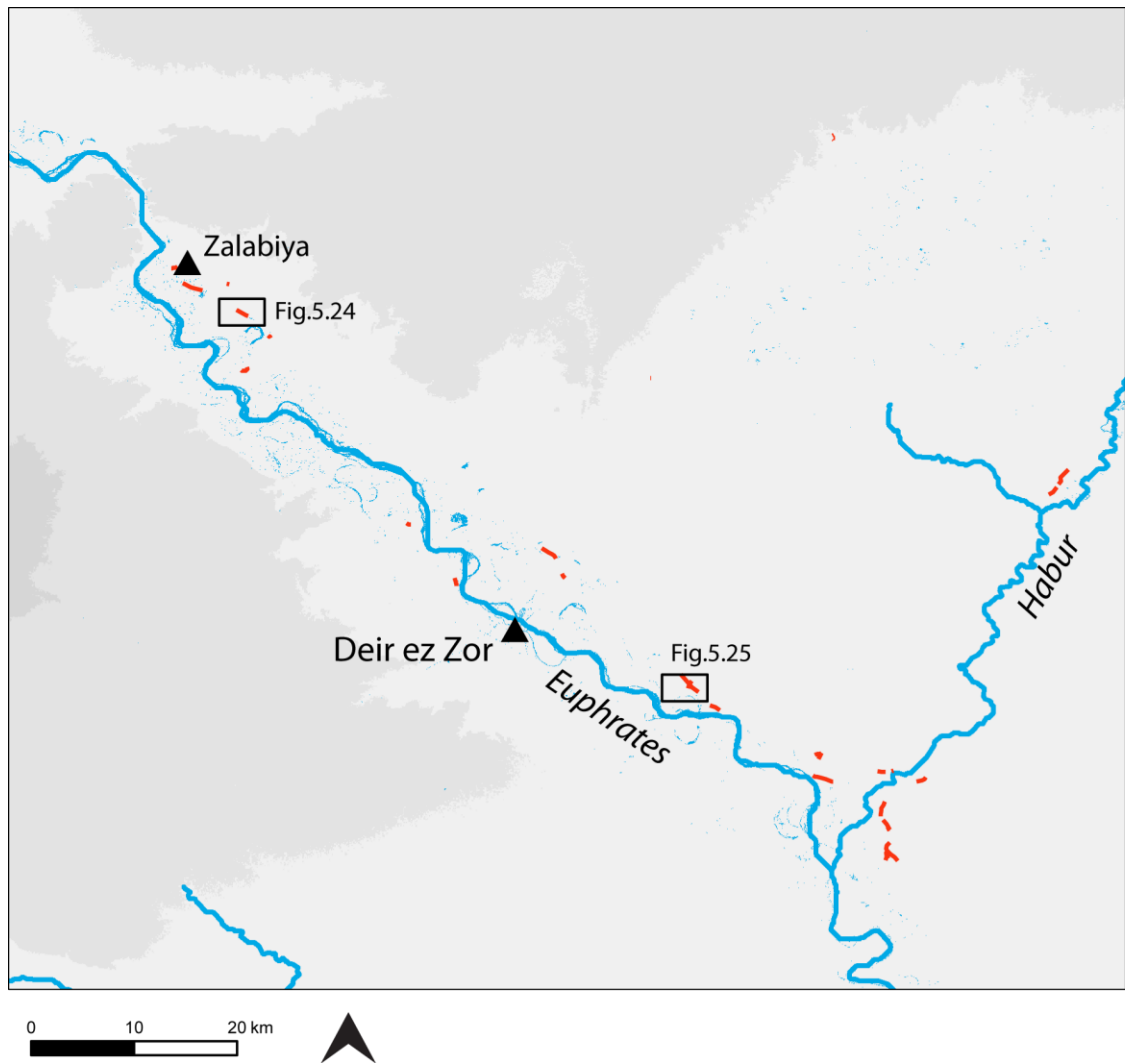


Figure 5.26: Relict water features alongside the Euphrates located using CORONA images. Geyer and Monchambert (2003) surveyed canals between Deir ez Zor and Mari in more detail.

5.9 The Habur

The results of image analysis for the Habur region are summarised here. Only limited evidence for irrigation in the Upper Habur was identified (e.g. see features around Hamoukar, Ur 2010). Careful image analysis undertaken by the present study in the same area corroborated this. However, significant canals alongside the Habur itself are of particular note (recorded by Van Liere and Lauffray, 1954-55; Ergenzinger et al, 1988; Ergenzinger and Kuhne, 1991). They may be two of the longest features in the entire study area. If they are in fact extant features, they join the Upper Habur area with the Euphrates, flowing over a distance of up to 190 km. The locations of the canals mapped by Ergenzinger et al (1988) have already been presented in **Chapter 2**. The parts of the features identifiable using CORONA are discussed and presented here (see **Figure 5.27**). The two Habur channels were originally researched before CORONA was available, but this project aimed to identify them using this remotely sensed dataset. Segments of these could be identified using the imagery. However, other parts were unclear, possibly because, like some channels in the Jerablus area, they were rendered obscure in the images by natural conditions, or because they had been removed by agricultural intensification and by infilling/erosion. The digitised segments are clear in the imagery (see figures below); **Figure 5.27** represents the results of image interpretation, rather than an exercise in interpolation.

Left bank canal

The canal on the left-hand bank of the Habur was easier to identify. being a prominent earthwork with upcast banks this could frequently be traced, although it had been removed by erosion and truncated by the floodplain in some areas. Neither the abstraction point nor the drainage point could be clearly identified using the CORONA images, but based on its position in the landscape, and on the SRTM DEM, gradients can be indicated. The natural gradient was found to be very shallow. Closer to Hasseke, one segment of the canal (see **Figure 5.27**, location 1) had a shallow gradient of 0.12-0.16%, based on the SRTM and ASTER data. It is important to note here that it is difficult to get an accurate measurement based on such a short segment, using the coarse-resolution elevation data. .

Further south (location 2; see **Figure 5.31**) a longer segment could be measured, making it more possible to obtain a more reliable, and very shallow, estimate of about 0.5-0.6% (SRTM and ASTER).

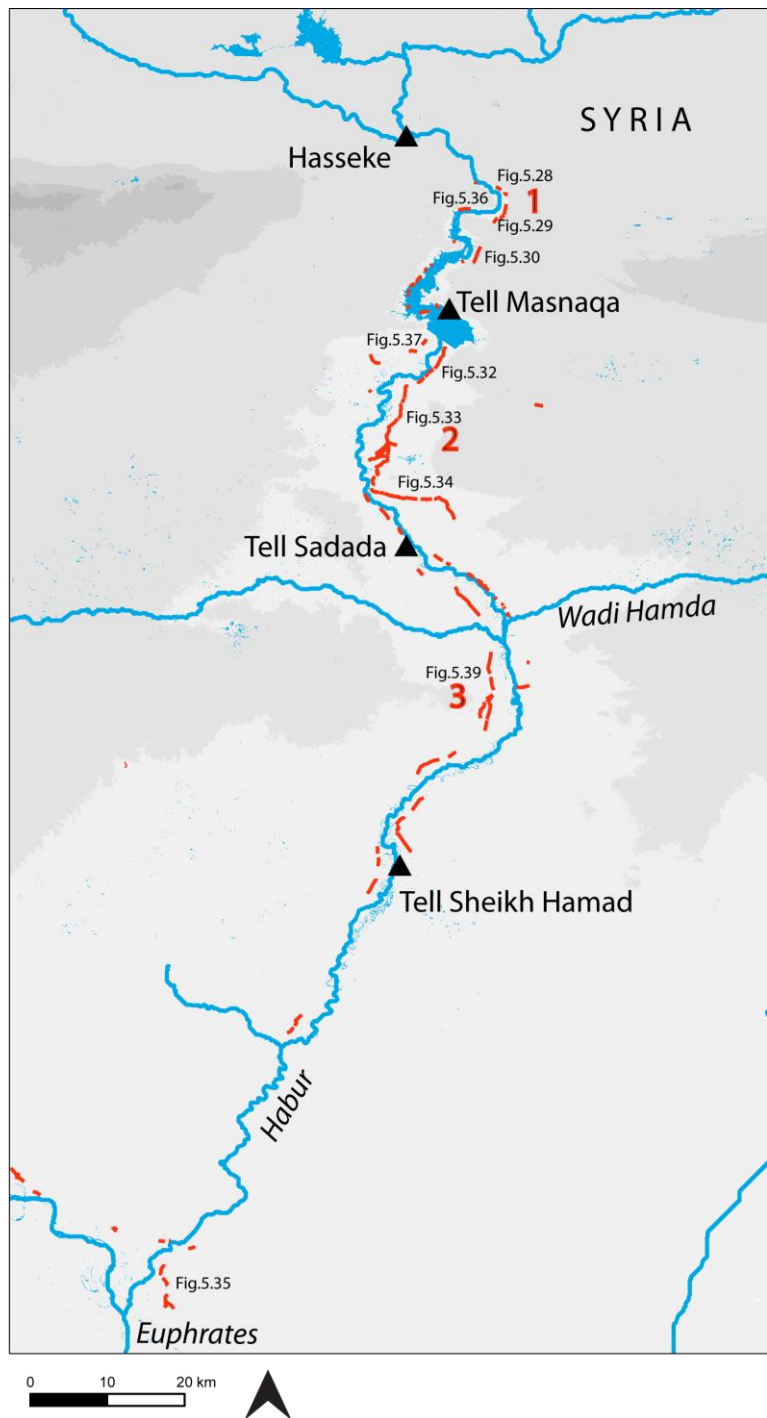


Figure 5.27: Segments of canals visible using CORONA and locations of profiles and CORONA screenshots.

The first clearly identifiable segment of it is shown in **Figure 5.28**. It is visible in the CORONA image as a darker line of soil and faint, very eroded banks. It appears to have flowed from an unknown point to the north.



Figure 5.28 CORONA image 11 December 1967.

Downstream, the canal is obscured again. Ergenzinger et al (1988, p115) mapped it as a long linear feature at this stage, although the same feature, when viewed in the CORONA image, is not entirely clear, and in places it is possible that it is simply a track. The linear feature is then obscured for about 500 m, but reappears on the other side of a wadi draining into the Habur. This time, it is a light coloured line between two darker lines, possibly ditches, stretching for about 1.4 km before meeting another wadi. It reappears on the other side of the stream as a much clearer feature, with a dark, possibly wetted channel flanked by embankments (see **Figure 5.29**). This stretch of the canal may have been re-used for irrigation in the 1960s. In some cases it crosses the natural drainages, possibly using structures such as aqueducts or inverted siphons (see **Figure 5.30**). Elsewhere, for example in the Wadi Zerqa in Jordan, dams were constructed to protect canals from wadis (e.g. see Kaptijn, 2009, p310).

For the next 5 km the Habur canal is difficult to identify, because there are several long linear features in the area on the same alignment, some of which are identifiable as recent canals and trackways.



Figure 5.29: CORONA image 11 December 1967.

10 km south of this, however, the feature is once more distinguishable (see **Figure 5.32**), now as a dark line of channel flanked by fairly prominent raised banks. Ergenzinger and Kuhne (1991, p171-172) recorded this part of the feature, between Tell Masnaqa and Tell Sadada, as being up to 12 m above the river level.

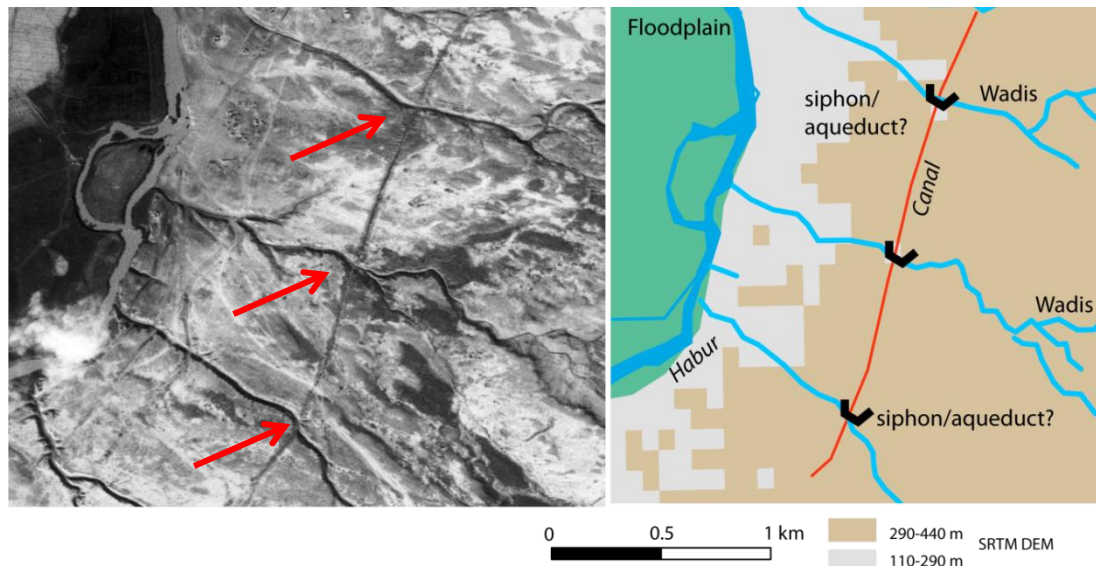


Figure 5.30: In some places segments of canals along the Habur cross wadis. It is possible that structures such as siphons or aqueducts were used to facilitate this. CORONA image 11 December 1967.

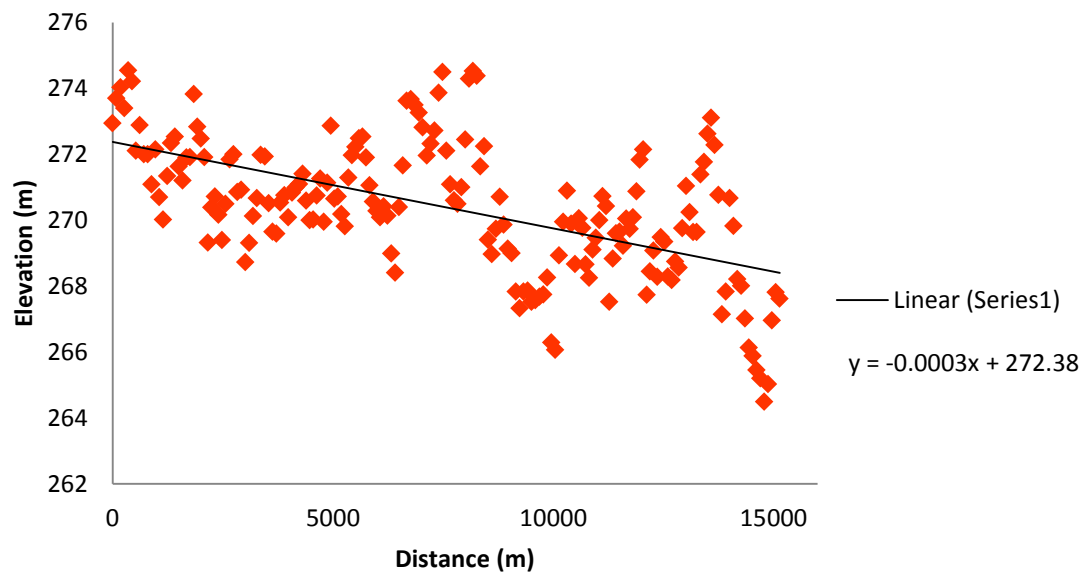


Figure 5.31: Longitudinal profile of a canal segment alongside the Habur, based on SRTM (Location 2, **Figure 5.27**). Gradient: c. 0.3-0.5%.



Figure 5.32: CORONA image 11 December 1967.

It takes this appearance for around 6 km, before fading out at an incised wadi; the canal reappears on the other side as a narrow feature, with less prominent embankments (**Figure 5.33**). Presumably this is part of the same canal system. Its different appearance may be due to the topographical and geomorphological conditions which affect it in this location. Given that this was one of the longest extant segments of canal along the Habur, the gradient was measured using SRTM (see **Figure 5.31**). At this stage, as **Figure 5.33** shows, some short offtakes draining towards the Habur can be seen. Whether these were contemporary with the original canal, or were later additions, is unclear.

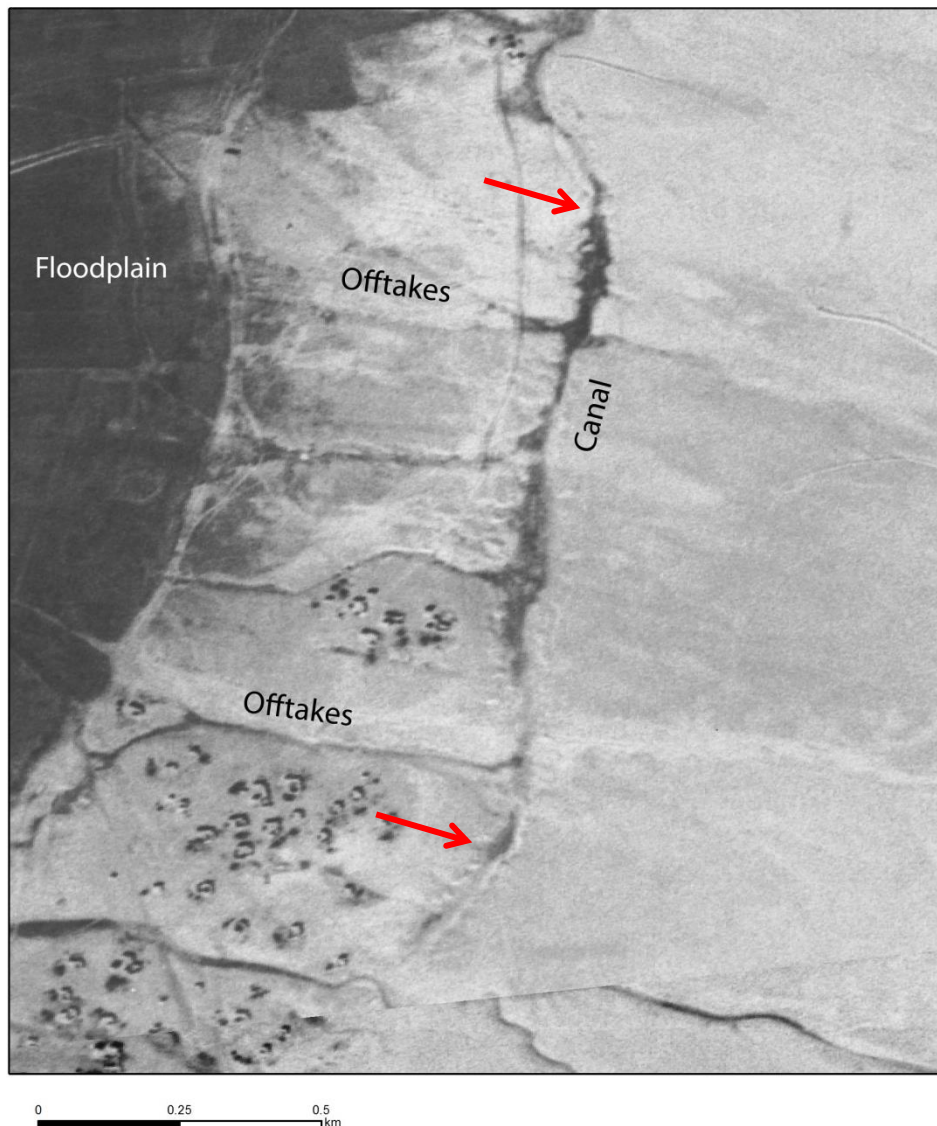


Figure 5.33: A canal and offtakes are visible in the CORONA image (11 December 1967).

The canal continues for around 8 km to the south, with embankments occasionally being visible, and some further offtakes, again of unknown date, until its position is again confused by multiple wadis, channels and tracks. Fragments of it cut and meander through the landscape. This pattern continues for 2 km, when the canal turns towards the east, following the Habur; at this stage it appears to have been part of a more recently active irrigation system, with faint offtakes visible (see **Figure 5.34**).

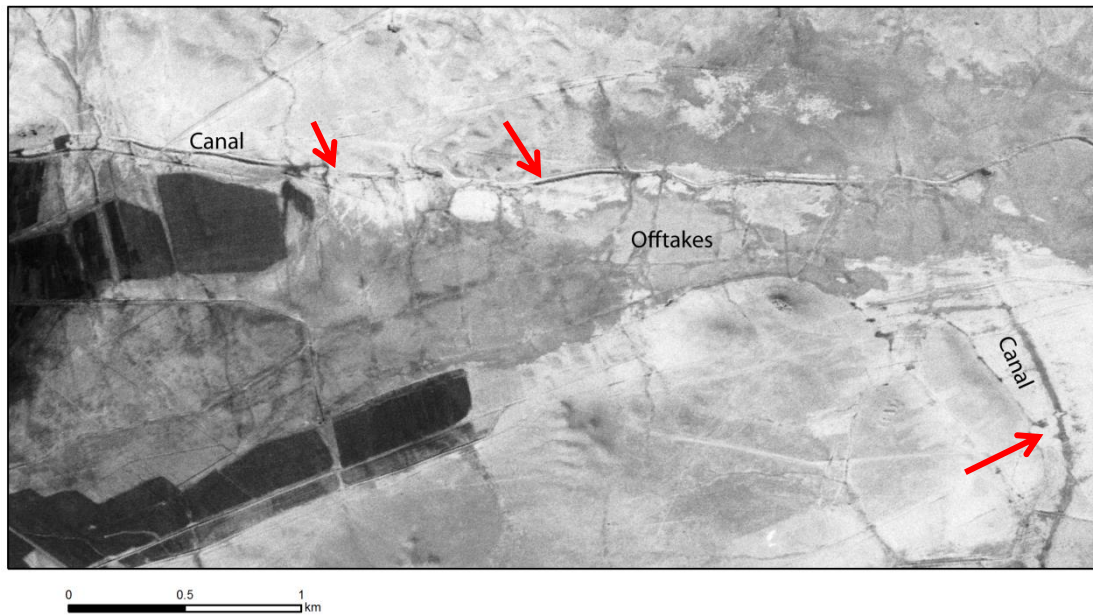


Figure 5.34: Canals and possible offtakes. CORONA image 11 December 1967.

About 6 km to the south the feature reappears as an embanked channel and flows for 11 km before fading out at a wadi. Interestingly, at one point there are two separate channels of similar appearance; unfortunately mostly truncated by the Habur floodplain. For the rest of its length, the canal becomes difficult to trace in the CORONA images, aside from a few, mostly faint, segments, and confusing trackways on the same alignment. Given its proximity to the floodplain, and the presence of more recent irrigation schemes, it is likely that by the 1960s much of the canal had been removed since the original investigations discussed in the literature review. Ergenzinger and Kuhne (1991, p172-173) noted offtakes in the vicinity of Tell Sheikh Hamad, although they could not be clearly distinguished from natural wadis in the CORONA images.

The termination point of the canal was not clear, but, **Figure 5.35** demonstrates that close to the Habur's confluence with the Euphrates, a segment of canal, possibly part of the same feature but in contemporary use, turns towards the East to follow the north bank of the Euphrates before again fading out.

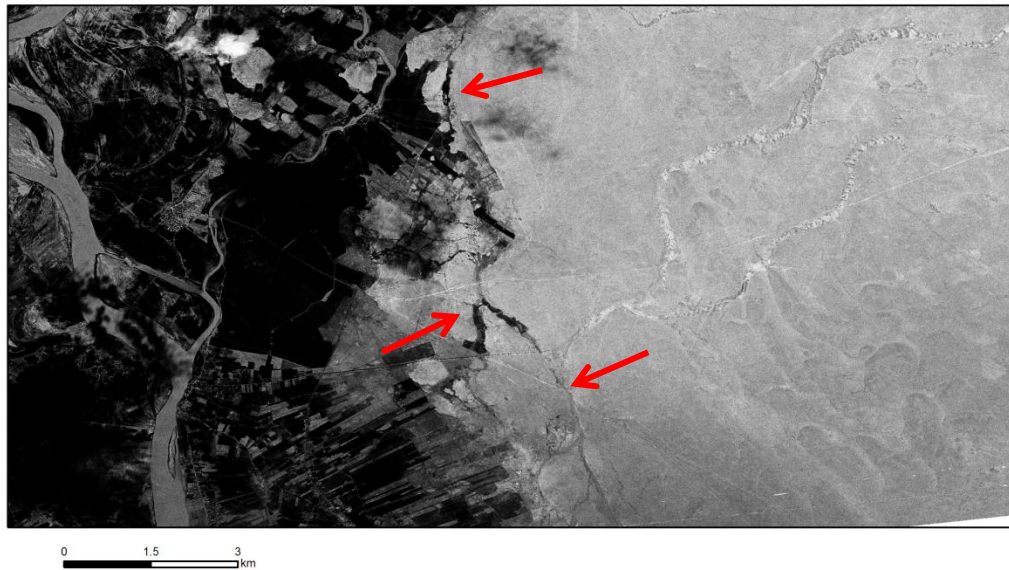


Figure 5.35: The canal is only identifiable in the CORONA images as short fragments after Tell Sheikh Hamad. A short stretch of canal is visible close to the Habur's confluence with the Euphrates. CORONA image 5 November 1968.

Right bank canal

The canal on the west side of the Habur can also be recognized. This channel was, in general, less clear in the CORONA images than the eastern canal, merging at some locations with more recent channels. Again, it was a fragmentary feature, making it difficult to obtain an overall gradient. However, based on the DEMs, one of the more extant segments (location 3, **Figure 5.27**) gave a gradient of c.0.1%-(SRTM and ASTER) (**Figure 5.38**).

Traces of a western canal are visible across the river from the eastern canal's first identifiable segments. However, again it is unclear which linear features are part of this canal, which are modern canals, and which are hollow ways or modern track ways, because they all follow the same alignment, parallel to the river along its natural gradient. **Figure 5.36** shows one of these faint, eroded segments.

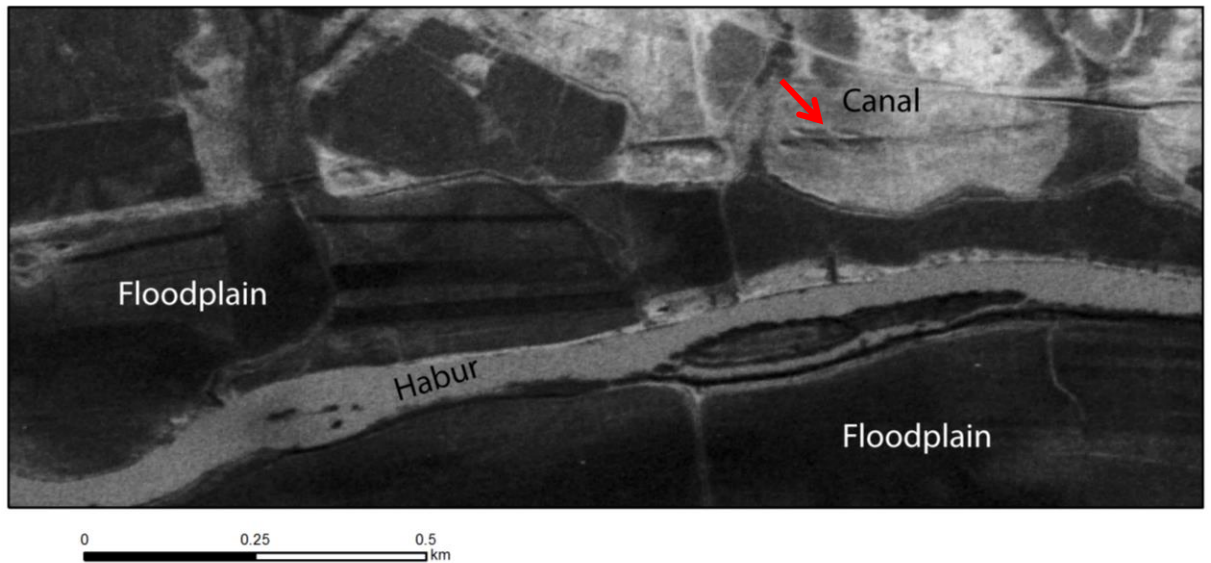


Figure 5.36: Traces of a canal are apparent on the right bank of the Habur. CORONA image 11 December 1967.

About 20 km downstream of the first identifiable fragments, a more substantial segment can be recorded; this flows as a faint, narrow and often sinuous feature alongside the Habur. Segments with larger upcast banks are then visible (for example see **Figure 5.37**), truncated by the floodplain and by modern irrigation.

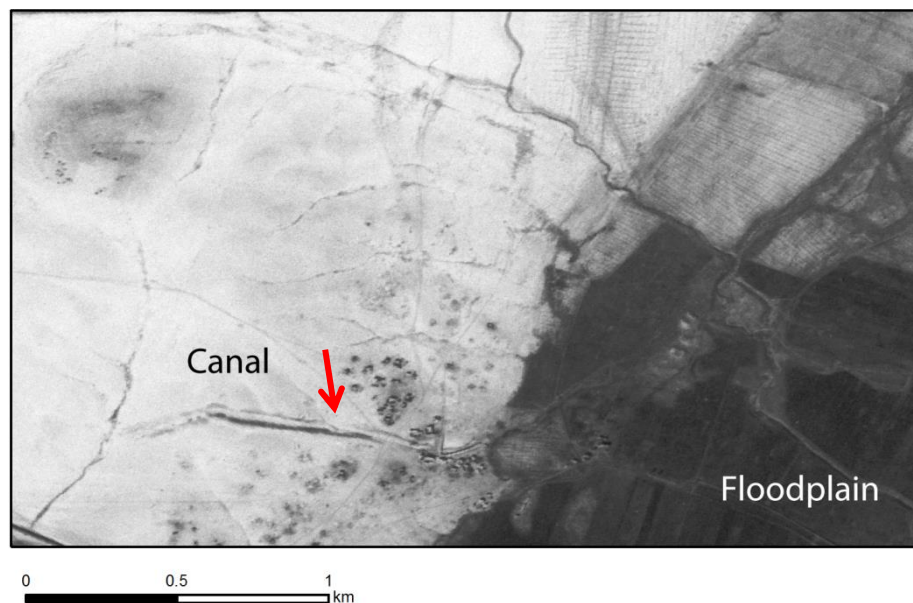


Figure 5.37: Segment of canal with upcast banks. CORONA image 11 December 1967.

This pattern continues for about 30 km to the south, until it is replaced by a flatter, wider channel that shows signs of more recent use, with associated offtakes in the form of submains and irrigation laterals (see **Figure 5.39**). If it is part of the same system, further to the north the channel may have been more elevated above the fields, generating the necessary height to allow it to flow over such a long distance. Gradient was measured for this segment, because it was the most extant part of the right bank canal; a figure of 0.1% was obtained (see **Figure 5.39**). As it gets closer to the Euphrates, it gets more difficult to identify and distinguish from contemporary 1960s irrigation. Relict channels in this area, however, which may be connected to it, could possibly also be linked to a very fragmentary channel flowing from upstream alongside the Euphrates (possibly the Nahr Semiramis).

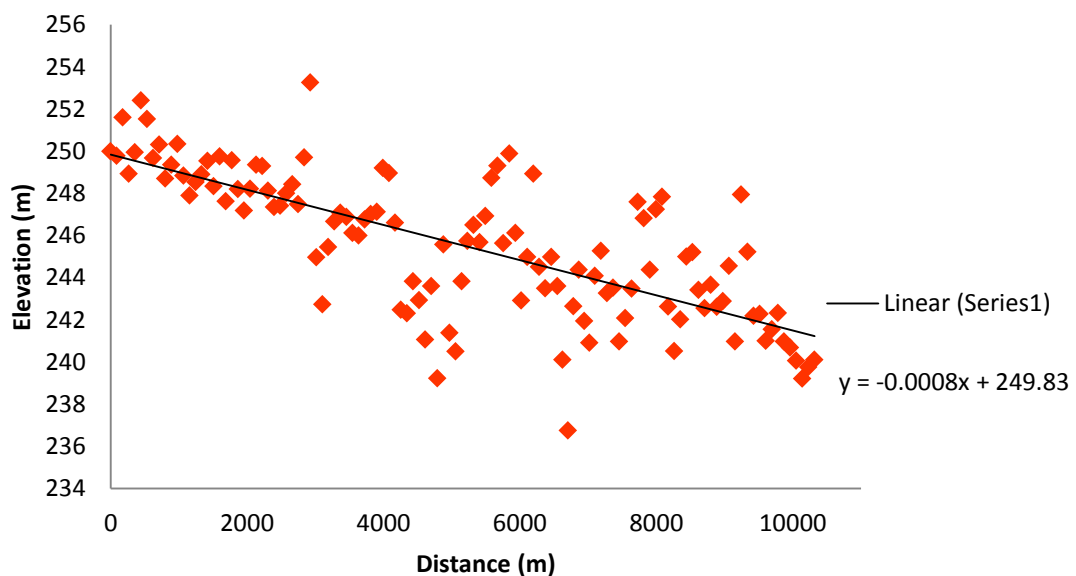


Figure 5.38: Longitudinal profile of a canal segment alongside the Habur, using SRTM (location 3 in **Figure 5.27**). Gradient: c.0.1%.

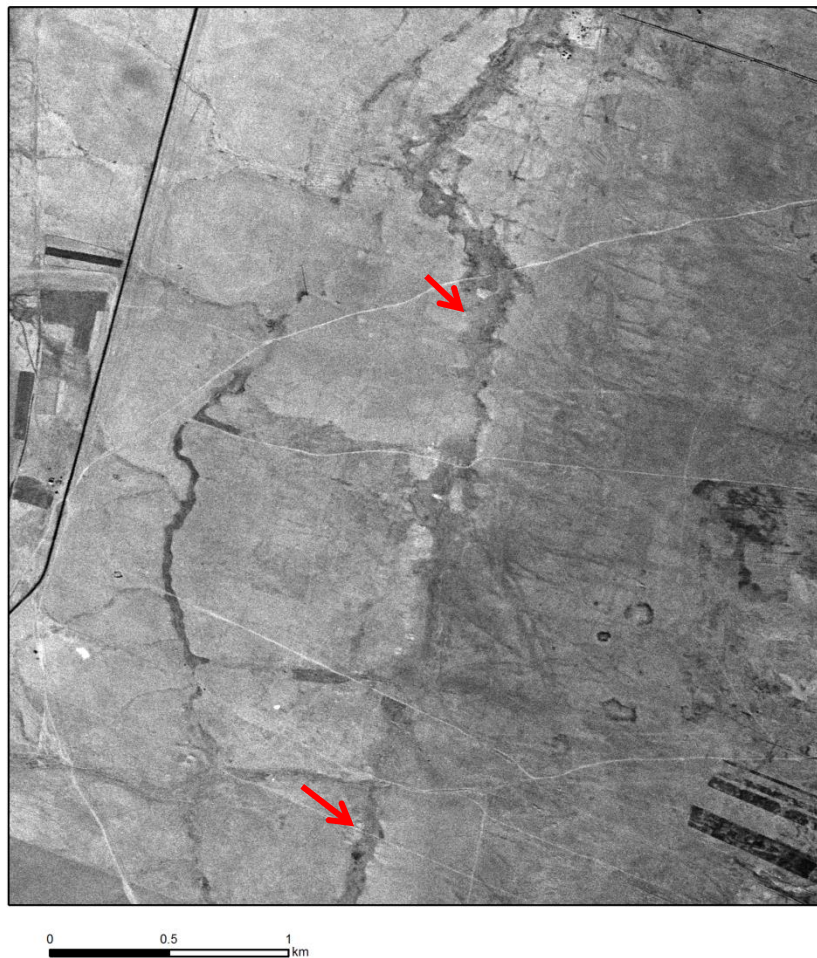


Figure 5.39: *Further downstream the canal is represented by a dark line lacking upcast banks, with associated offtakes. CORONA image 5 November 1968.*

5.10 Habur-Iraq border

Nahr Dawrin

While the steppe between the Habur and the Iraqi border proved to be devoid of water features visible on CORONA images, the land adjacent to the Euphrates floodplain was of more interest. The presence of a large canal, the Nahr Dawrin, is well-attested to in the literature (e.g. Geyer and Monchambert, 2003; Margueron 2004). Geyer and Monchambert (2003, p200) measured gradients ranging between 1:1000 – 3:1000 for this prominent canal, which flows over a distance of around 80 km. It has been proposed (e.g. Ergenzinger and Kuhne, 1991, p174) that it joined to the Habur systems. Kamash suggests that it may be Babylonian-Roman in date (Kamash, 2009, p76-77), although Bell's account (1924) would support a continuation into later periods. Kamash also suggested the presence of

Roman dams in the area, based on textual evidence (Kamash, 2009, p77). Early Islamic textual evidence gives an Islamic date for the Dawrin (e.g. see Kennedy, 2011, p194). While the canals around Mari are not clearly visible in the CORONA images, significant features between the Habur and the Iraqi border could be traced. A canal segment flowing from alongside the left bank of the Habur and then for a short distance along the Euphrates before fading out has already been described above (see **Figure 5.35**). It is not clear, from examination of the CORONA images, if this feature is joined to the Nahr Dawrin; there are areas for which data could not be obtained and there are issues with cloud and poor contrast. On the modern imagery (for example see Google Earth), the Euphrates has avulsed, potentially erasing features, and the area is obscured by modern irrigation and buildings. A join between the Habur canal and the Dawrin is therefore not discernable. However, the segments of the Dawrin which could be seen using the images (see **Figure 5.40**) will be described here.



Figure 5.40: Canal traces between the Habur and the Iraq.

The first part of the Dawrin that could be identified using CORONA consisted of two very large earthworks, representing channels flanked by embankments (see **Figure 5.41**). Geyer and Monchambert (2003, p202-204) suggest that they represent an earlier and a later channel, the first having been removed by the Euphrates.

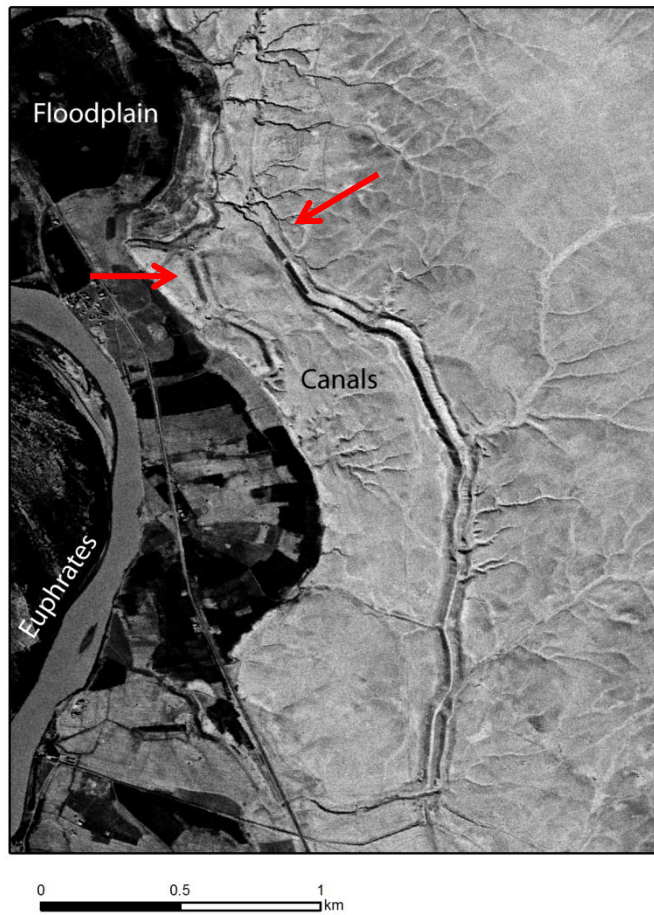


Figure 5.41: Two parallel segments of canal flow close to the floodplain (see Figure 5.40 for location). CORONA image 5 November 1968.

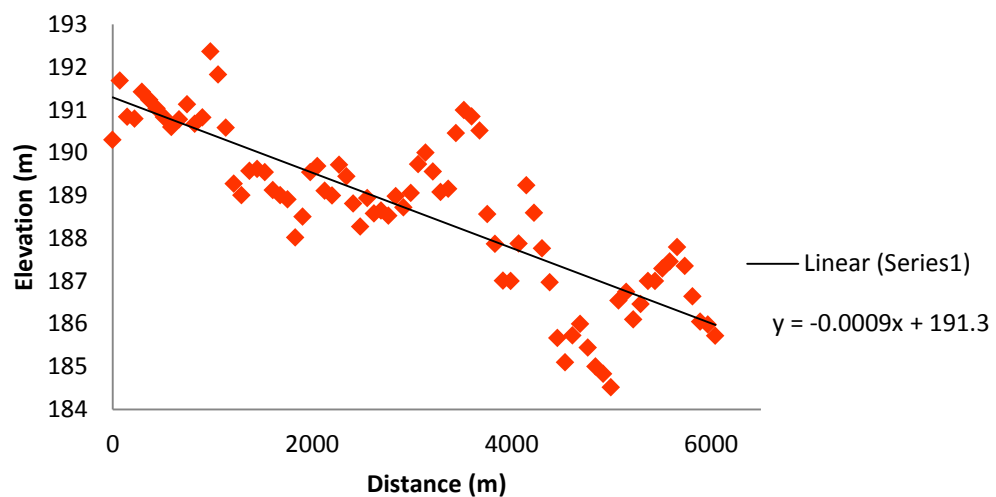


Figure 5.42: Longitudinal profile from SRTM of a segment of the Nahr Dawrin (see Figure 5.40, Location 1). Gradient: c.0.1%.

A narrower, less clear feature appears to stem from the upper of the two earthworks; it is unclear whether this is a trackway or a canal. This track/channel feature cuts across the natural contours, intercepting ephemeral runoff channels, for around 40 km, before it is lost under cloud. The gradient of the first 6 km of this segment could be measured using the ASTER and SRTM DEMs, giving a value of 0.05-0.1% (see **Figure 5.42**).

A clearer feature can then be identified, flowing about 1 km from the floodplain; this is more likely to be a canal, with flanking upcast banks (see **Figure 5.43**). The canal can be traced for about 5 km, before it disappears when reaching an incised wadi. After this, again, only faint lines can be located, which may or may not be part of the canal. Some very faint features, almost indistinguishable from natural streams, continue up to the Iraqi border.



Figure 5.43: A segment of the Nahr Dawrin is also visible closer to the Iraqi border. CORONA image 5 November 1968.

Mari

The two canals known from the opposite bank of the Euphrates, close to Mari, are not clear in the CORONA images (however see Geyer and Monchambert, 2003; Margueron, 2004). While faint linear features are visible, they are rendered obscure by cloud, poor contrast in the imagery, and also agriculture contemporary with the images.

Iraq

Parts of northern Iraq within the Jazira region were also examined using CORONA images. Existing research in this area has already used CORONA to map water features (Ur, 2005; Altaweel, 2008; Ur et al, 2013. See **Chapter 2.**). The present study simply affirms the CORONA image interpretation already undertaken in this region. One new feature close to the Lesser Zab was noted as part of the present study, as well as multiple qanats in the Sinjar plains.

5.11 Qanats on the Tell Afar/Sinjar Plain

The CORONA image analysis revealed a cluster of qanats below and south of the Jebel Sinjar range in the Tell Afar/Sinjar Plain, as well as archaeological sites and hollow ways. There are limited data in the available literature to contextualise these channels. One source briefly cites historical data attesting to pre-Ottoman qanats in this region (Fuccaro, 1991, p12).

One of the first uses of aerial imagery for recording archaeological features was undertaken by Poidebard (1934). This included the mapping of some qanats and associated canals at the Roman fortification of d'Al-Han, between the Habur and Sinjar (Poidebard, 1934, pl.CXLV). Cressey (1958, p41) lists several disused qanats in the area, suggesting that some stretched for considerable lengths. One channel in the Sinjar is mentioned briefly by Lightfoot (2009), who described reports of a very long conduit deriving its source from the Sinjar Mountains (Lightfoot, 2009, p20). Stein (1941) discussed Roman activity in relation to the site of Hatra (119 km to the south of Sinjar), and mentioned the presence of an important trading routeway going through the Sinjar plains (Stein, 1941, p303-304; Kennedy and Riley, 1990, p77). Lightfoot links this Roman activity to the presence of the Sinjar qanat (2009, p16). Interestingly, Lightfoot (1996) and also Kamash (2009, p84) emphasise that qanats are often found to be associated with Roman-Byzantine sites. Lloyd (1938), however, despite surveying and excavating in the area, did not mention the qanats, including one that crosses Tell Khoshi (see **Figure 5.51**) although he mentions that several of the existing villages had wells; an earlier traveller, Buckingham, also mentions them (1827, p254).

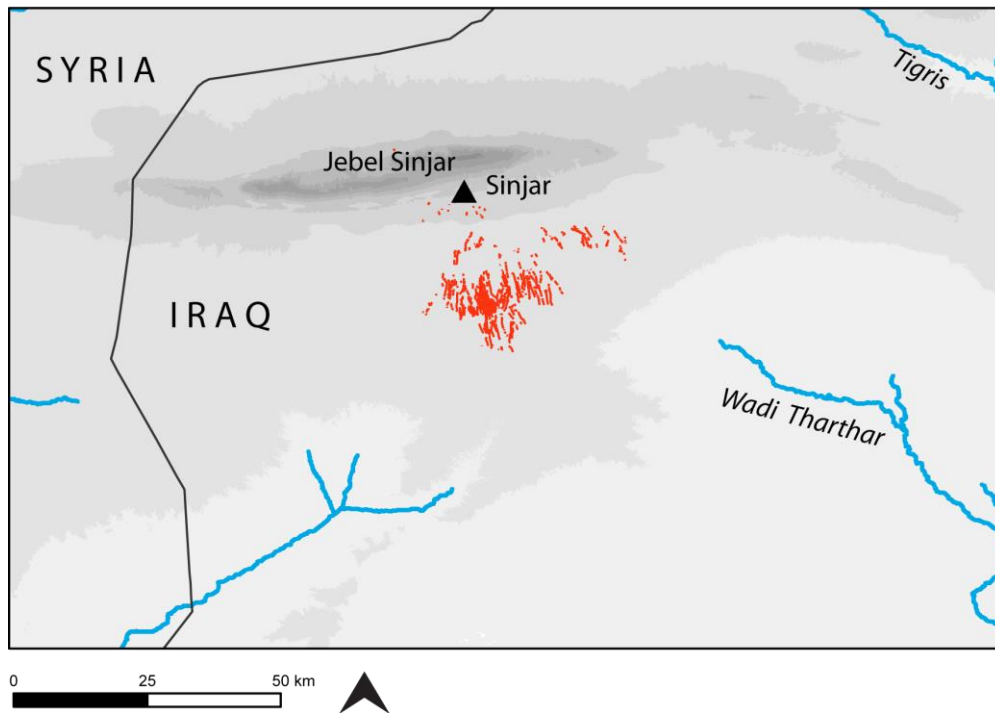


Figure 5.44: Qanats clustering south of Sinjar.

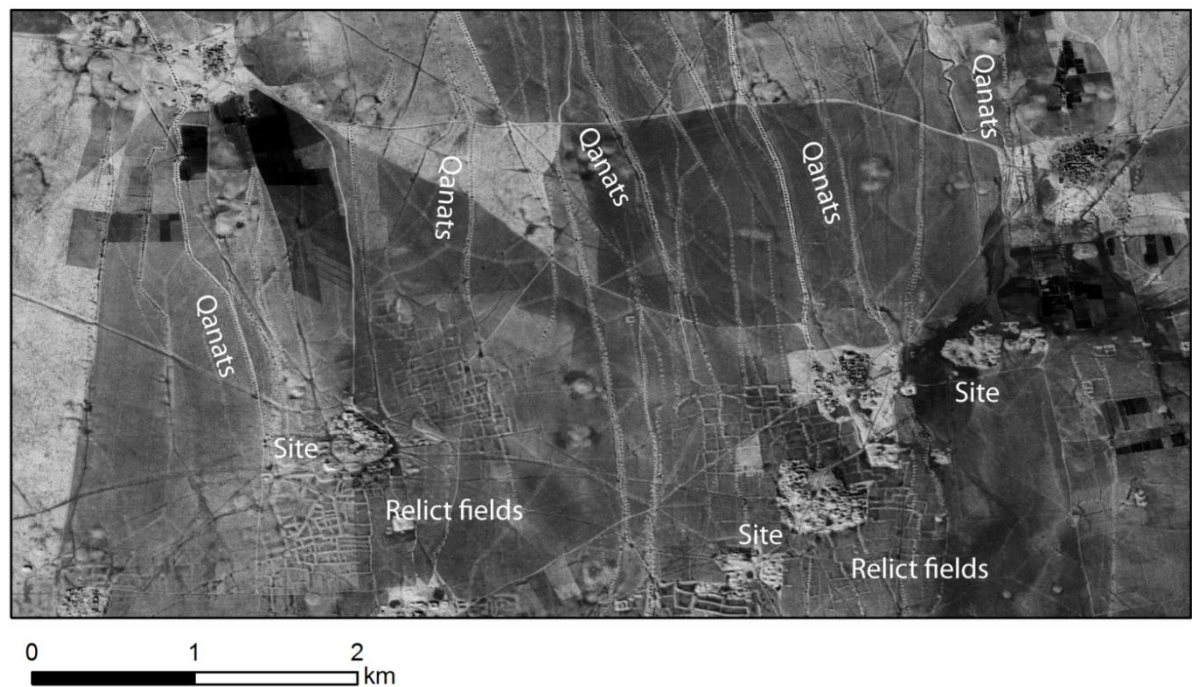


Figure 5.45: A dense cluster of qanats/tunnels as well as sites and follow ways south of Sinjar is identifiable using CORONA. Image 11 December 1967.

The CORONA images show a landscape full of qanats and tunnels (see **Figure 5.45**) unlike any other part of the study area. A dense cluster of qanats radiates

out from the town of Sinjar into the plain (see **Figure 5.44**), and is associated with sites, hollow ways and relict field systems.

Some of the qanats may be features contemporary with the 1960s imagery. There is evidence throughout Iraq of infiltration qanats, conduits and tunnels channelling spring water in use during the 20th century, although they had been declining (see Lightfoot, 2009). These are more clearly defined than the older channels, and tend to be of the ‘cut-and-cover’ type, which are constructed first as canals and then partially covered so that the maintenance gaps are left. As **Figure 5.46** shows, some of the conduits in the Sinjar area have a different appearance in the images to the traditional qanats. Shafts are represented by dark-coloured dots and are much closer together and arranged along a lighter strip.



Figure 5.46: ‘Cut and cover’ channel and resulting open channel south of Sinjar. CORONA image 11 December 1967.

The traditional-style qanats have more widely spaced shafts. Many of the shafts are faint and appear disused, as **Figure 5.47** shows, although some appear to have been modified in their lower reaches, possibly with excavation and covering, giving them a ‘cut-and-cover’ appearance. Some are associated with or close to settlements of apparent antiquity. These are shown in **Figures 5.47, 5.48, 5.49**. **Figure 5.47** shows the outlines of structures, while **Figure 5.48** shows a smaller site surrounded by walls.



Figure 5.47: More 'traditional' qanats; shafts are more widely separated. CORONA image 11 December 1967.

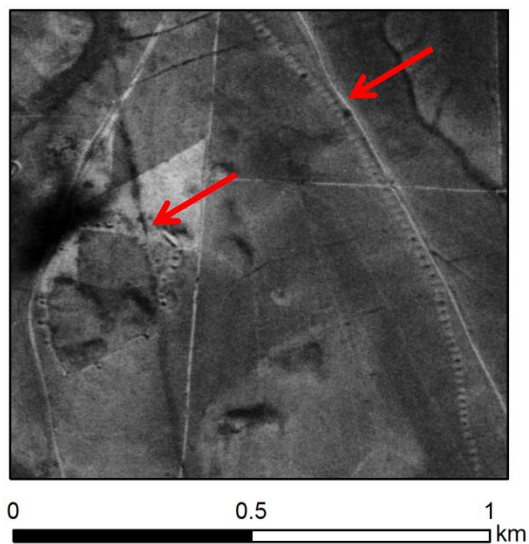


Figure 5.48: Qanats and sites. CORONA image 11 December 1967.

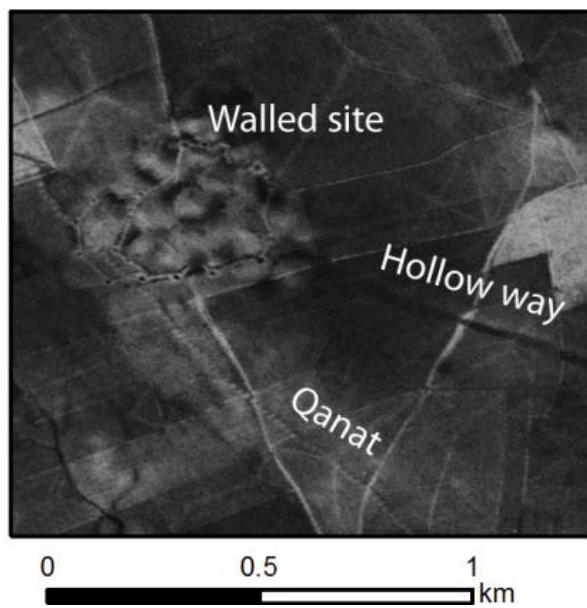


Figure 5.49: Walled site and qanat. CORONA image 11 December 1967.



Figure 5.50: Former settlement and qanat. CORONA image 11 December 1967.

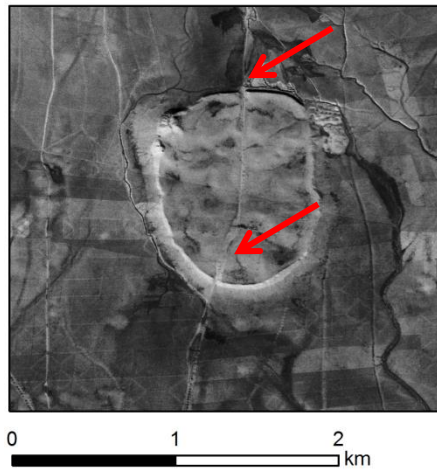


Figure 5.51: The major 3rd millennium BC site of Tell Khoshi cut by a qanat. This feature is presumably later than 1938, when Lloyd excavated, because he did not mention its presence. CORONA image 11 December 1967.

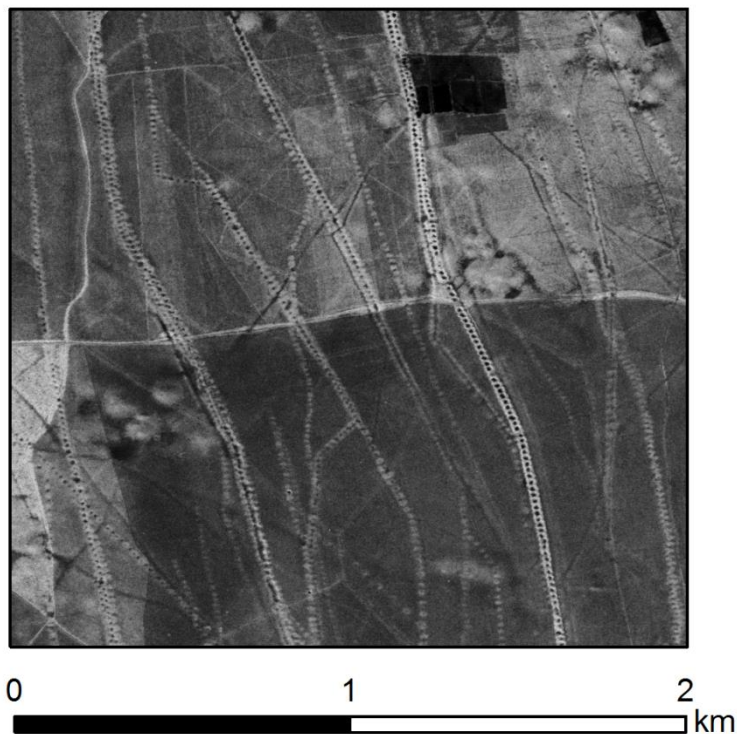


Figure 5.52: Complex qanat systems. CORONA image 11 December 1967.

The complexity of these qanat systems should also be noted. **Figure 5.52** shows a good example of this complexity: a mixture of new and older conduits is visible, with several of these overlying each other. Some of the channels seem to split into separate branches, and in other cases, short joining segments seem to link separate tunnels. There may be several reasons behind this pattern. Firstly,

sometimes it is necessary to dig new channels when older ones have become unusable, possibly due to factors such as a change in groundwater levels. In addition, the branching nature of the conduits may indicate attempts to irrigate larger areas through the modification and extension of existing tunnels.

Some of the features are also associated with open channels feeding irrigation systems. Despite the possible recent dates for these, it is worth considering them as comparable examples to the way in which ancient qanat systems may have functioned. Clusters of small, possibly ruined walled fields are sometimes located close to villages, presumably supplied by the qanats. The systems are also linked to patterns of hollow ways. **Figure 5.53** depicts a sample of these remains, showing Qanats terminating in open channels that feed into the areas of fields around the settlements. It is possible that the 'walls' evident in the images may only be earth bunds used for retaining water. While structures associated with the openings of qanats are known (see **Chapter 4**), in this example from the Sinjar Plain the water often passes straight out of the channels and into the field irrigation systems.



Figure 5.53: A small sample of the irrigation systems and qanats south of Sinjar. These were also associated with hollow ways and settlements.

Overall, these qanats form an interesting cluster, showing a density unknown throughout the rest of the study area. They presumably took advantage of high water tables around the Sinjar mountain and possibly also of springs in the same area. While their date is unknown, a link with the Roman *limes* (e.g. see Stein, 1941, p303-304; Lightfoot, 2009, p16) should not be entirely discounted, given the antique appearance of several of the systems. In terms of modern imagery, google earth (using spot images) was used. The more recent images showed that the infiltration qanats and cut-and-cover conduits were mostly not identifiable, although pumped wells and sprinkler systems are now present.

5.12 North Jazira

The corner of North-West Iraq above the Sinjar mountains was examined during this research. Archaeological survey has also been undertaken here in the past (e.g. see Wilkinson and Tucker, 1995). Interestingly, despite the availability of CORONA imagery and detailed contour maps (Fragile Crescent Project) no distinct water management features could be identified. Presumably rain-fed agriculture, wadis and springs formed the principal water resources for the settlements of all periods. This shows that an absence of features in the CORONA imagery in other areas could indeed in some cases indicate a general absence of water features, rather than a lack of visibility in the imagery. The north Jazira falls within an area where rainfed agriculture is possible, comparable to the northern Habur.

5.13 The Tigris and Northern Iraq

The upper reaches of the Tigris within northern Iraq form the eastern limit of this research. These were studied using CORONA images by Ur (2005), Altaweel (2008) and Ur et al (2013); the Assyrian canals in the region are well known and the research has been outlined in the spatial literature review (**Chapter 2**). This project also briefly examined the area of the Tigris using CORONA images, confirming the existing mapping and indicating that the hydraulic landscapes of the Syrian-Iraqi Jazira continued to the east of the Tigris. The boundary of the study area, however, had been drawn in this region. Extending mapping further to the east was beyond the scope of the present study.

A significant feature (see **Figure 5.54**) identified in the Tigris region by this project was a large canal along the south bank of the Lower Zab, where a channel similar in appearance is already known to exist on the opposite bank (e.g. see Altaweel, 2008, fig.33). This appears to abstract from the Lower Zab and flow for about 16 km. The upper part of it appears to be eroded and disused, while the lower part may be associated with some irrigation in the 1960s. There are further, probably recent, large scale earthworks in use nearby.

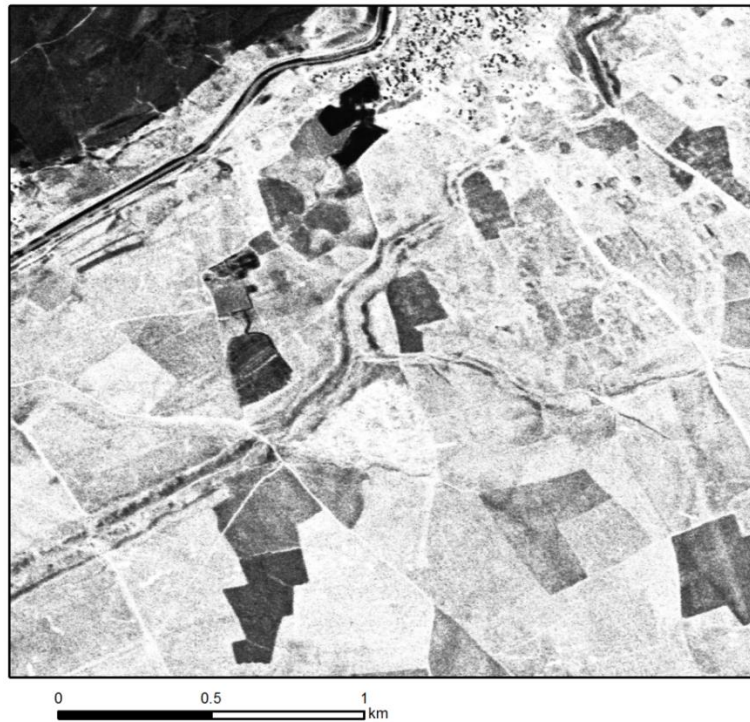


Figure 5.54: Canal on south bank of Lower Zab. CORONA image 9 August 1968.

5.14 Summary

The results presented in this chapter show that widespread evidence for ancient water management can be obtained from an image interpretation analysis of CORONA imagery. Digitisation revealed the location and layout of many large-scale systems throughout Northern Mesopotamia which have now been removed by agricultural intensification and urbanisation. Information provided by DEMs facilitated the recording of key hydraulic properties of the canals, such as gradients, width and depth (see **Table 5.2**). DEMs enable these data to be obtained quickly across a large study area; field-based survey cannot undertake this to a similar scale. A review of the literature reveals that relatively few analysis of ancient water management have explicitly provided gradient information for many channels. For example, it proved difficult to obtain this information from the published studies on the Habur canals.

The results of the present research show that many of the canals were located in areas of fairly flat terrain. For a longer system, this necessitated careful design. If the Habur canals are extant systems, this flatness would explain why the heads of

the canals are elevated with large upcast banks, while the southern ends appear to be flatter features without embankments.

Table 5.2: *Canal gradients in northern Mesopotamia.*

Canal	Gradient	Source
Jerablus canal	Tahtani-Jemal 0.12%- 0.16%	SRTM and ASTER
Dibsi Faraj	c. 0.03- 0.04%	Harper and Wilkinson 1975; SRTM (profile from near Raqqa)
Habur (segments of left canal)	0.12-0.6%	SRTM and ASTER
Habur (segment of right canal)	0.1%	SRTM and ASTER
Nahr Dawrin (segment)	0.05-0.1%	SRTM and ASTER
North Iraq canals	0.1-0.4%	Ur, 2005, p340 (using SRTM)

Chronological information in many cases could also be gained, listed in **Table 6.1 (Chapter 6)**.. Dating information was obtained from existing archaeological surveys and excavations and from historical accounts (e.g. see Le Strange, 1930). Relative dates could also be suggested based on associations between canals and qanats and features of known date. For example, the qanat at Dibsi Faraj appears to be directly linked to the site, and was therefore interpreted as contemporary with it.

The remote-sensing based results of this chapter show traces of relict water management across a large area. Given the multiple types of data available (imagery, DEMs, historical accounts, archaeological surveys) a more detailed analysis of a sub-region is possible. This was undertaken for the Balikh Valley. The Balikh represents an area of especially dense and complex former irrigation and also functioned as an important political and strategic location for different empires, making it an ideal case study.

Chapter 6: Water management in the Balikh Valley

6. 1 Geomorphology and land use

The physical environment of the Balikh Valley has provided a framework for the development of modern and ancient water management. In order to understand these locations, and to recognise to what degree archaeology is preserved, a discussion of the geomorphological context of the valley must be made. The river valley forms a narrow corridor of alluvial, cultivable soils (Wilkinson, 1998; Mulders, 1969) between the Turkish Harran Plain in the north and the Syrian part of the Euphrates in the south. As the topographic profiles show, the valley is bounded on either side by slightly more elevated lands of gypsum soils (see Mulders, 1969).

Figure 6.2 represents the stream network of the valley, as generated using ASTER DEM data (see **Chapter 3**). The long profile of the Balikh itself has a low gradient and drains into the Euphrates. The principal source of the Balikh is the karstic spring of 'Ain al Arous near the Turkish-Syrian border. As the cross section **(1)** (**Figure 6.3**) shows¹, at this point the corridor of the valley is narrow, being some 6 km in width. The stream of the Jullab, which originates in Turkey, joins the Balikh north of Tell Sahlan. Below this, and on the east side of the Balikh, the Wadi al Keder flows parallel, finally merging with the Balikh below Tell es Seman.

The differences between the spring-fed Balikh and the seasonal Wadi Al-Keder should be recognised here. The slower-flowing Balikh has meandered and avulsed, potentially removing channels and also affecting the positions of canals. It also flows all year round, functioning as a permanent water source, although over-abstraction in the 1990s caused it to dry up (Wilkinson pers. comm.). In contrast, the Wadi al Keder is seasonal (hence its name 'wadi') and does not serve as a permanent abstraction point for canals, and as such, is not used for irrigation. A straighter channel with a fairly deeply incised floodplain, it occasionally flows with higher-velocity run-off. This makes it more useful as a drain (e.g. see the Nahr al Abbara system) than as a water source. On the west side of the valley, the Qara

¹ The profiles in this chapter were generated using the SRTM DEM, unless otherwise specified. While SRTM is of a low resolution, it enables the general gradient of the landscape through which canals flow to be measured.

Mokh has its confluence with the Balikh. This stream has its origins close to the border. Runoff from other seasonal wadis draining off the steppe lands is also incorporated into these rivers and streams. Cloud burst rain storms in the winter occur in the Balikh and sometimes runoff rates are high (Mulders, 1969, p33-34).

In the south, relict terraces of the Euphrates show the river's movement across its floodplain. While some of these movements have erased ancient remains, the archaeology has also been used to constrain the date of the terraces, the most recent of which formed during the Holocene (Demir et al, 2007, p2848). Only remnants of earlier, Pleistocene, terraces still exist (Hritz, 2013a, p1978; Sanlaville and Besancon, 1981, p12).

Early Islamic remains on the Holocene terrace were truncated by the Euphrates near Raqqa, indicating that river movements occurred relatively recently, that is after 800-1400 AD (Hritz, 2013a, p1977; Challis et al, 2004, p144). Canals visible on the floodplain of the Euphrates post-date this era and it has been suggested that the flood-plain formed after the medieval period, when the Euphrates degraded to a lower level (Mulders, 1969, p44-45).

The Balikh has also followed a dynamic regime. On **Figure 6.2**, in the north near Tell Sahlan, a palaeochannel (evident on CORONA images) is indicated up to 2 km to the west of the present day course (as discussed below). The channel potentially erased earlier remains, but allowed later features to be assigned relative dates in association with it. Cross section 2 (**Figure 6.4**) crosses this feature. A flat, basin-like area that may be associated with the palaeochannel is apparent from the profile. It forms an area of natural drainage that may have been waterlogged and marshy in the past (Hritz, 2013b, p153; Akkermans, 1993, p170-80). On the other side of the Balikh, waterlogging can be inferred from the presence of subsidence hollows (also known as 'gilgai'—see **Figure 6.1**).

Gilgai are depressions and cracks that form in poorly drained vertisols (Young 1976, p186-187) through differential shrinking and cracking and subsequent expansion, when the soil dries out after irrigation (Mulders, 1969, p32). Vertisols are also often the most agriculturally fertile soils (Young, 1976, p180). Because gilgai features often form in formerly irrigated areas, it is significant that they are

present in this area of relict irrigation. They support the information from relict canals that this was a previously irrigated area.



Figure 6.1: *Gilgai are visible on this CORONA image. 22 January 1967.*

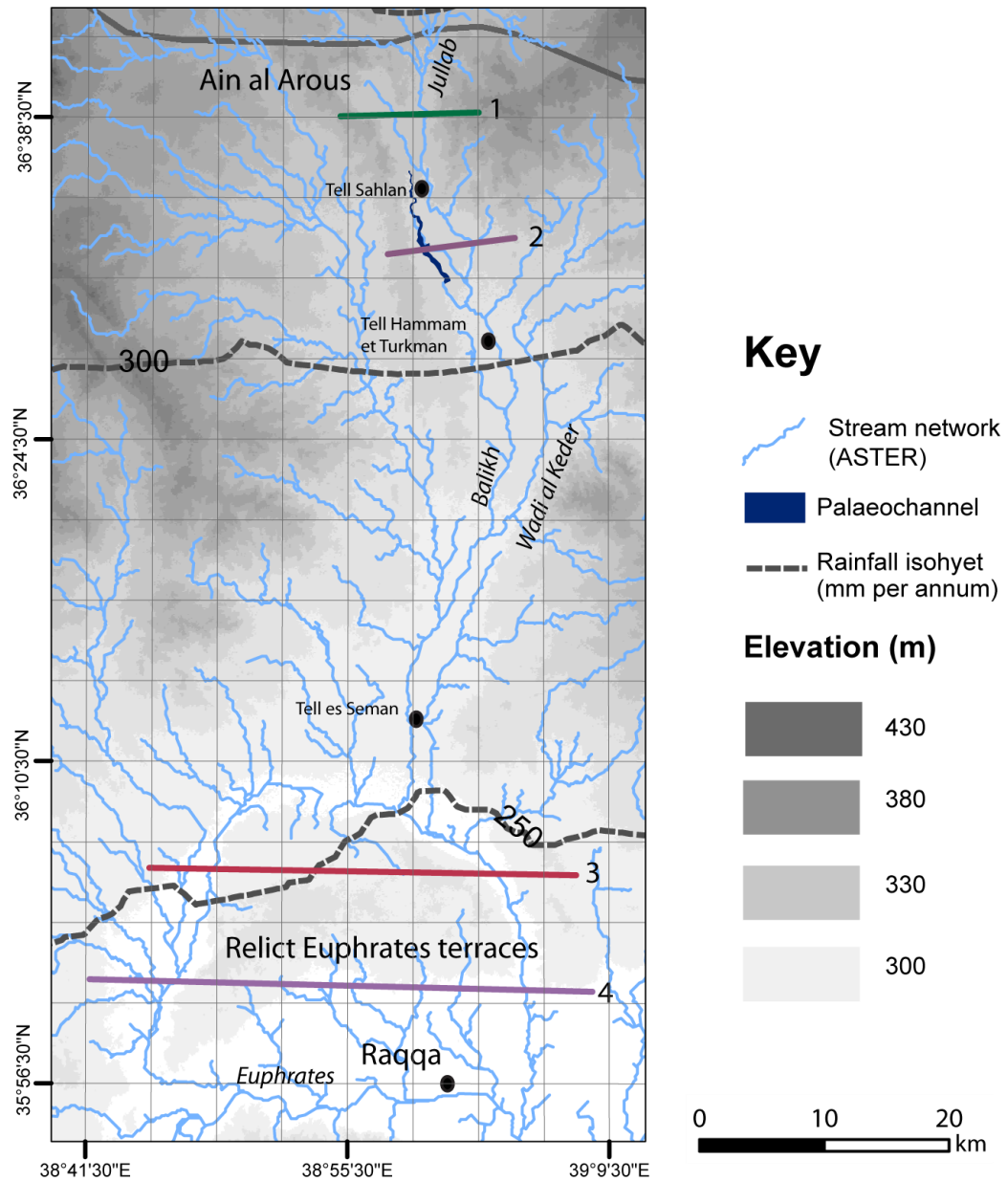


Figure 6.2: ASTER-generated stream network and palaeochannels, with locations of cross sections.

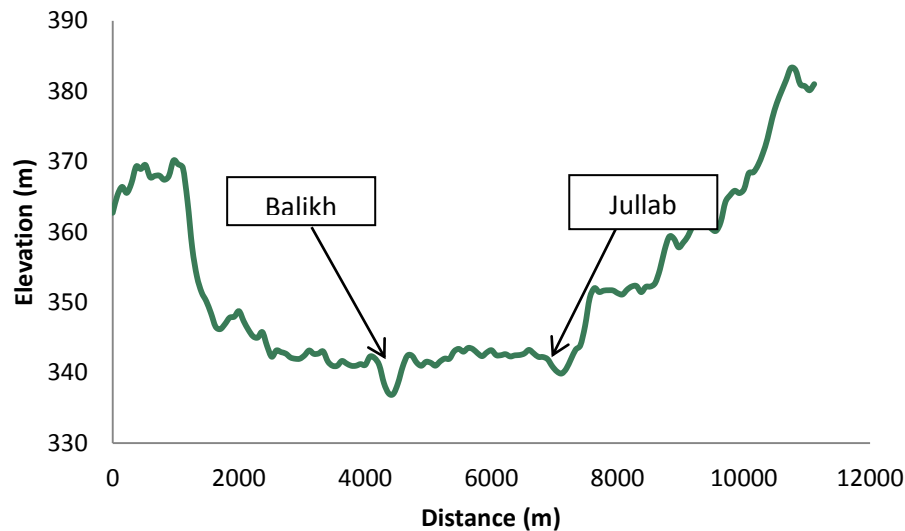


Figure 6.3: Cross section 1. For cross section locations see **Figure 6.2**.

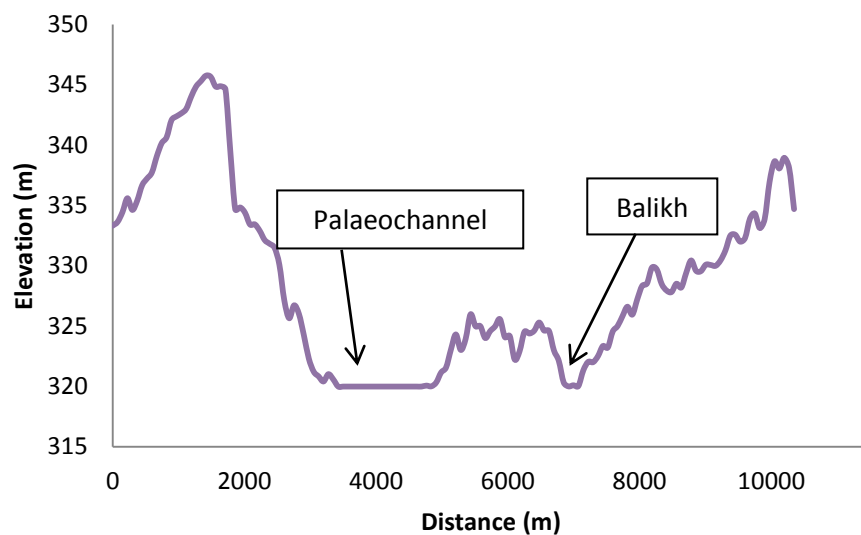


Figure 6.4: Cross section 2. For cross section locations see **Figure 6.2**.

Further south, another marshy area was present in the central part of the 'horseshoe'. This is a semi-circular, horseshoe-shaped band of cultivable land between the Balikh and the Euphrates. Marshy conditions in this area formed by pooling of the Balikh at times of Euphrates peak flow (Challis et al, 2004, p144). Modern intensive irrigation and poor drainage conditions have led to shallow water tables in in this region (Alkhaier et al, 2012, p1837), although it should also be noted, however, that water tables have been lowered throughout the study region by over-pumping from wells. In the Lower Balikh area in the 1960s, the water table

was at a depth of about 5-19 m (Mulders, 1969, p55). Recent research in the western part of the horseshoe indicated that the water table depth was between 1-8 m just after irrigation had stopped for the year (Alkhaier et al, 2012, p1836). This may also have been an issue in the past, leading to waterlogging and the development of gilgai. Overall, it appears that the over-pumping has led to the water tables being lowered, while in those areas where there has been copious irrigation, the water table has been raised, thereby making salinization more likely.

The 'horse shoe' shape of the lower valley contains relict terraces of the Euphrates. **Cross sections 3 and 4** show the morphology of this landform. The eastern part of the 'shoe' contains the modern course of the Balikh, whereas a parallel valley to the west forms the other side of the horseshoe. Recent research by Hritz suggests that this may have been formed by an earlier confluence of the Euphrates and Balikh before the Balikh moved to the east (Hritz, 2013a, p1978).

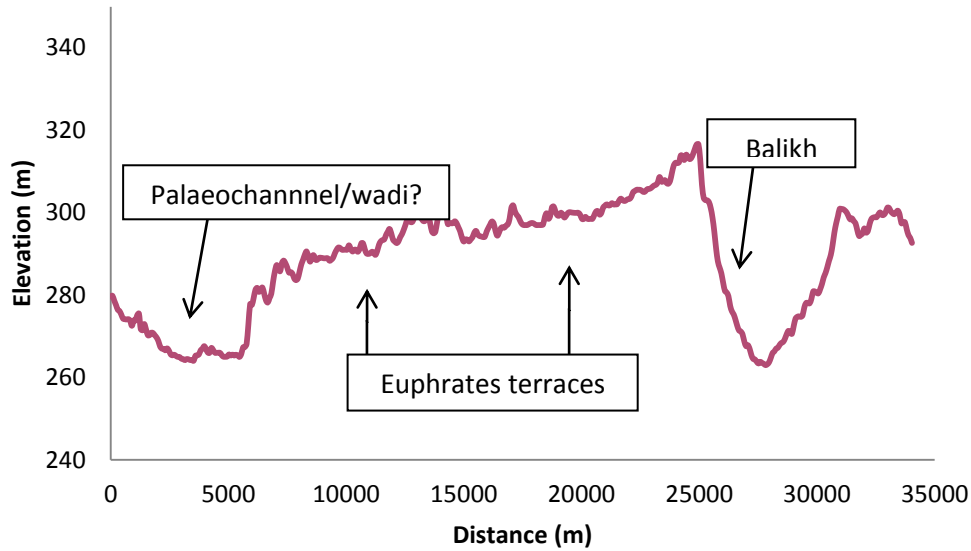


Figure 6.5: Cross section 3. For cross section locations see **Figure 6.2**.

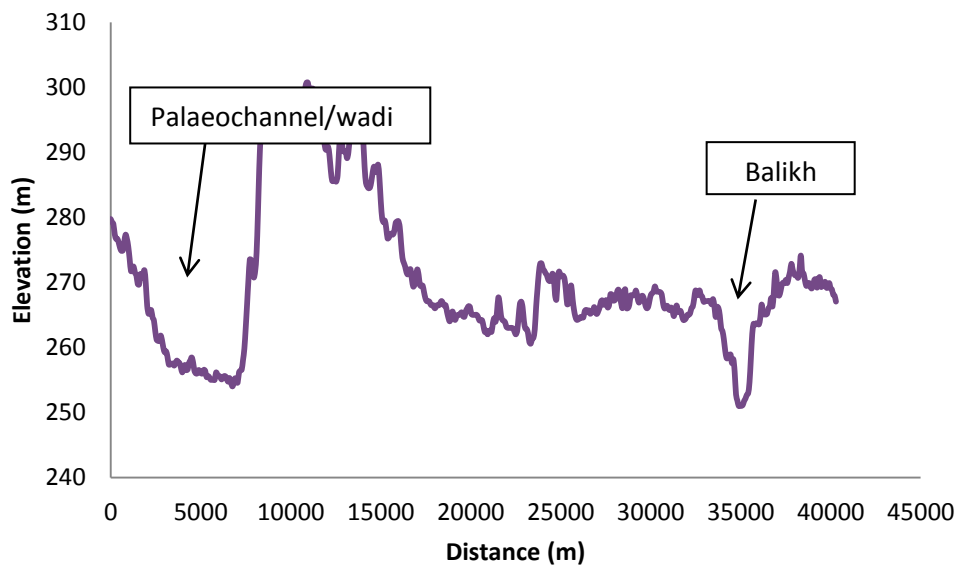


Figure 6.6: Cross section 4. For cross section profile locations see **Figure 6.2**.

The modern water management system has significantly altered the landscape of the Balikh since agricultural intensification occurred from the mid-20th century onwards, and this is particularly evident on Landsat images taken from 1984, 1990, and 2000 (see **Figure 6.7**). This landscape alteration makes it increasingly difficult to identify remains of ancient hydraulic structures in the field. Syrian abstraction as well as irrigation schemes in Turkey have both dramatically altered the river's discharge. When first recorded, the river had a flow of $6 \text{ m}^3/\text{s}$ (Mulders,

1969, p54). During the earlier 20th century, the valley seems to have relied on irrigating fields from the river, on small areas fed by groundwater, and on rainfall (Beaumont, 1996, p148-149). Away from the river itself, traditional rain-fed farming predominated prior to the 1980s (Hole and Zaitchik, 2006, p145; Beaumont, 1996, p137). By the 1970s, new large-scale irrigation projects had been initiated (Ababsa, 2011, p85; Rabo, 1989, p152-153).

It is clear from the pattern of fields (highlighted in the near infrared band of the landsat images) that in 1984 irrigation in the western part of the horseshoe was confined to the region north of the Euphrates, and that the upper valley was only locally irrigated, as the presence of some canals and offtakes shows.

In the 1990s, the flow of the Balikh was reduced to the point where the channel was sometimes dry (Wilkinson, 1998, p65); by 2010, it was flowing again, but mainly with irrigation outflow from Turkey; this outflow may add as much as 368 to 928 mm³ /yr to the Balikh, of dubious quality (Kolars and Mitchell, 1991, p111). As the Landsat images show, by 2000, the area of irrigated fields had substantially increased. Canals from the Tabqa dam on the Euphrates, 40 km to the south, now deliver useable water to much of the horseshoe zone, serving water management schemes which have yet to reach their full, planned, potential (Hole and Zaitchik, 2006, p150).

The shallow water tables measured by Alkhaier et al (2012) may result in problems of salinity in the present-day Balikh. Because for most of the year natural leaching does not occur, sodium and calcium minerals that are drawn to the surface are not removed (Mulders, 1969, p30-31). That the relatively salt-tolerant crop barley predominates in excavated remains in the Balikh (Hritz, 2013b, p117; Akkermans, 1993, p210-13) suggests that salinity may also have affected past cultivation.

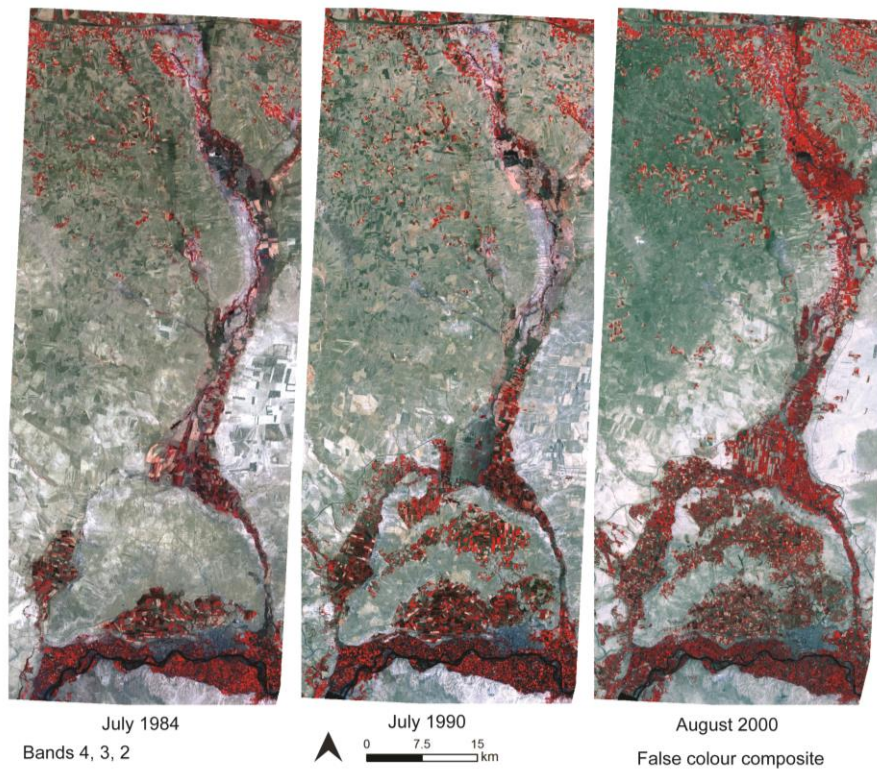


Figure 6.7: This sequence of Landsat images, all taken at a similar time of year, shows the expansion of modern irrigation in the Balikh. Images from NASA Landsat Program, 1984-2000.

In summary, much evidence of ancient cultivation has been obscured and erased by the modern irrigation systems of the Balikh valley. However, CORONA images preserve a view of the relict channels from the 1960s-70s, before significant landscape change occurred, enabling them to be recorded.

Water management systems

An analysis of rainfall trends was presented in **Chapter 1** and **Chapter 3**, which shows that the Balikh is within an area of temporally variable and generally low rainfall. In some years, rain-fed agriculture is possible and, in fact, was the predominant form of cultivation in the valley in the early 20th century (Beaumont, 1996, p137). However, relying on rainfall is risky and does not facilitate high crop yields. Research indicates that the climate of the region was also arid, although fluctuating, during the period of the later territorial empires (Mulders, 1969, p29; Bar-Matthews et al, 1997; Masi et al, 2013). Although at present it is not possible to directly compare the modern data with the past climate, arid/changing

conditions suggested by the proxy data would indicate that irrigation was therefore as much of a necessity in the past as it is today.

Prior to around 1200 BC, the majority of cultivation in the Bronze Age seems to have been reliant on rainfall. Survey data suggest that populations in the somewhat more reliably wet north were higher than those of the drier south (e.g. see Curvers, 1991).

By the time of the later empires (i.e. after 1200 BC), however, past irrigation can be identified, closely aligned to the stream network described above (**Figure 6.2**). This relationship will have resulted in the removal of some features from river movements and the covering of others with sediments. Despite this a complex pattern of intersecting, overlapping and fragmentary channels of potentially multiple phases is identifiable (**Figure 6.8**). Initially, this seems to be difficult to interpret. However, by undertaking an interdisciplinary, remote-sensing based study of the region and by drawing in evidence from existing survey² and excavation this study was able to reveal a sequence of identifiable layers of activity. These form a 'palimpsest' of water management in the Balikh.

² The database of sites was compiled from unpublished data (Wilkinson pers. comm) and from published surveys (Wilkinson, 1998; Curvers, 1991; Bartl, 1994).

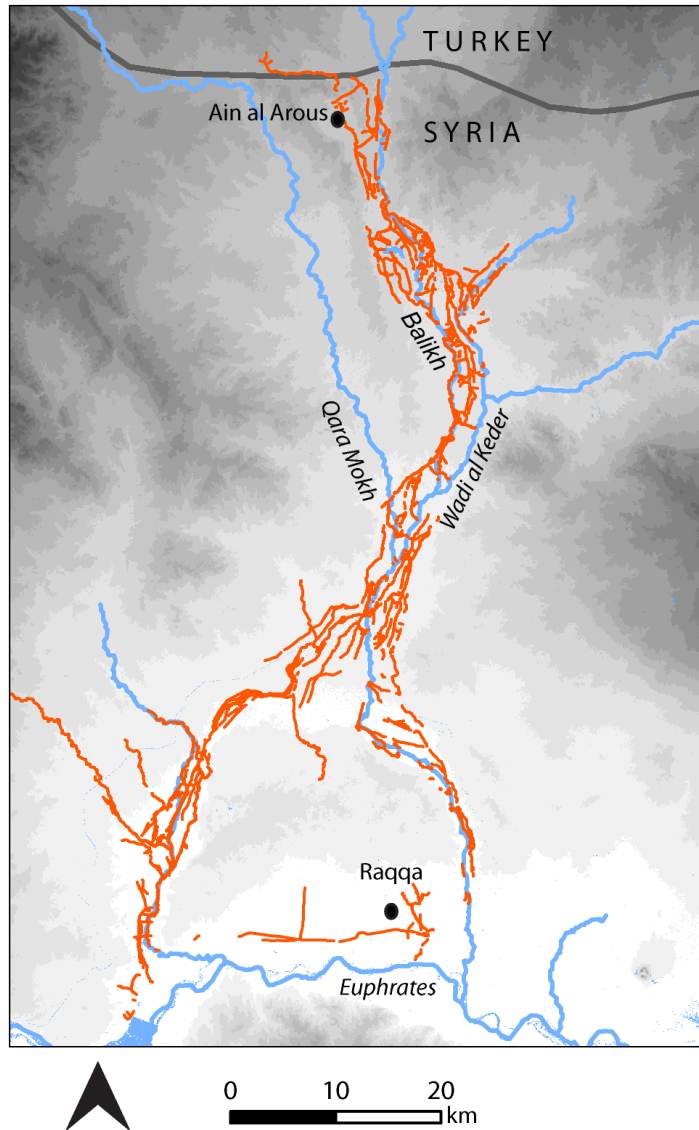


Figure 6.8: The Balikh Valley is crowded with artificial canals (mapped from the CORONA images). These represent a complex, tangled palimpsest of different cycles of use, reuse and modification.

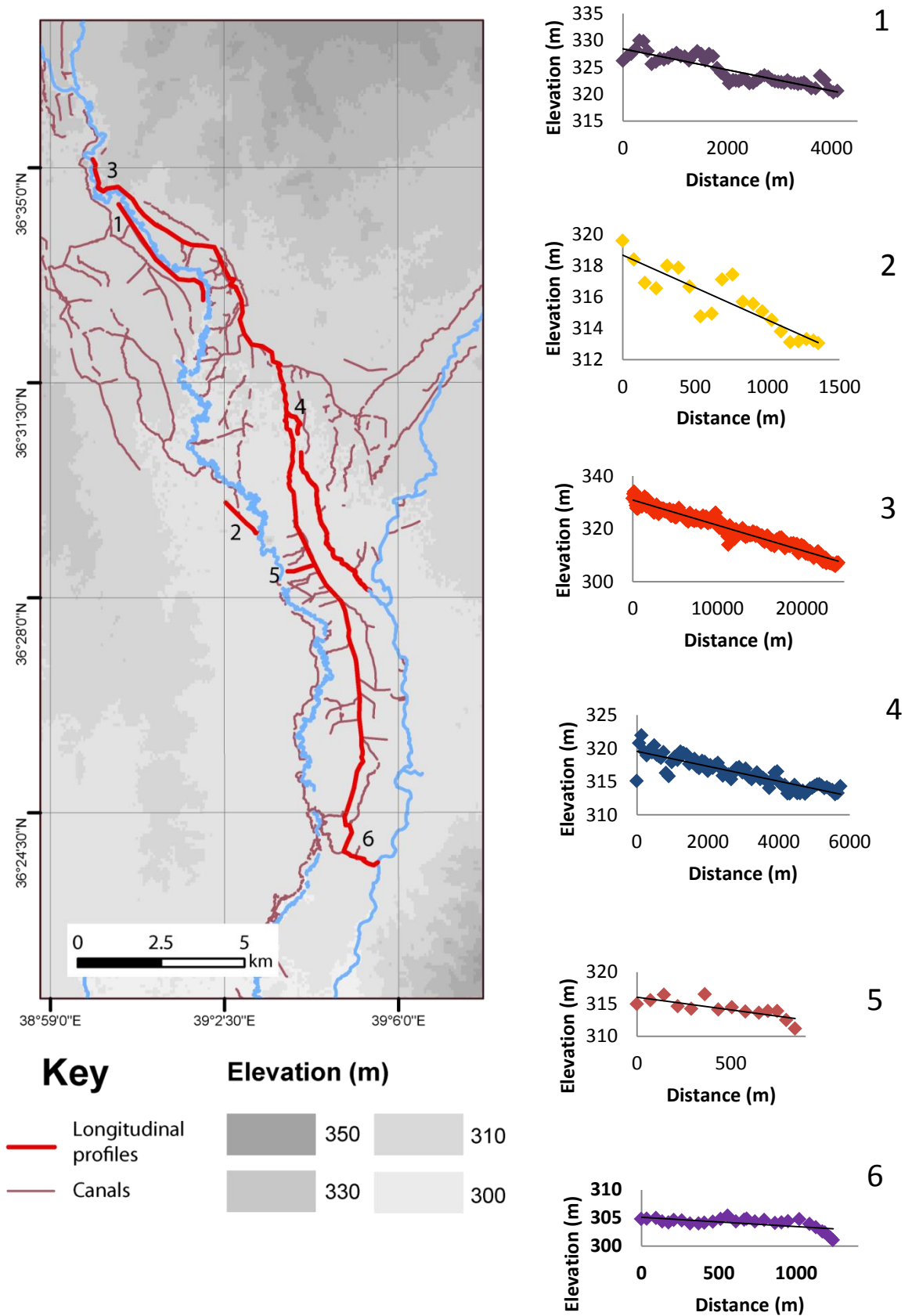


Figure 6.9: Locations of longitudinal canal profiles 1-6 shown in sections 6.2 and 6.3. A linear regression was applied to each profile.

6.2. Sahlan and Hammam canals

The earliest known well-dated canal in the Balikh valley is the Sahlan canal (see **Figure 6.11** for its route). Wilkinson's survey (1998) excavated a section in the Sahlan canal (**Figure 6.13**). The survey obtained a radiocarbon sample from the bed deposits of the later phases of the canal providing an uncalibrated date of 1380 ± 70 BP (Beta-78543) which is around 570 AD (Wilkinson, 1998, p71). This date is supported by the ceramics collected from the overlying deposits within the canal void. The dating information suggests that the feature was probably in use from the Hellenistic to the early Byzantine period (Wilkinson, 1998, p71).

As well as being the earliest well-dated feature in the Balikh, the channel is also one of the most prominent canals in the valley. Most of the later systems consist of narrower canals without significant upcast banks (visible on the CORONA image **Figure 6.10**). The Sahlan canal, in contrast, has clear banks and a wide bed.



Figure 6.10: The Sahlan canal is very apparent by the dark trace of the infilled channel and the pale-coloured upcast mounds on this CORONA image. Image 22 January 1967.

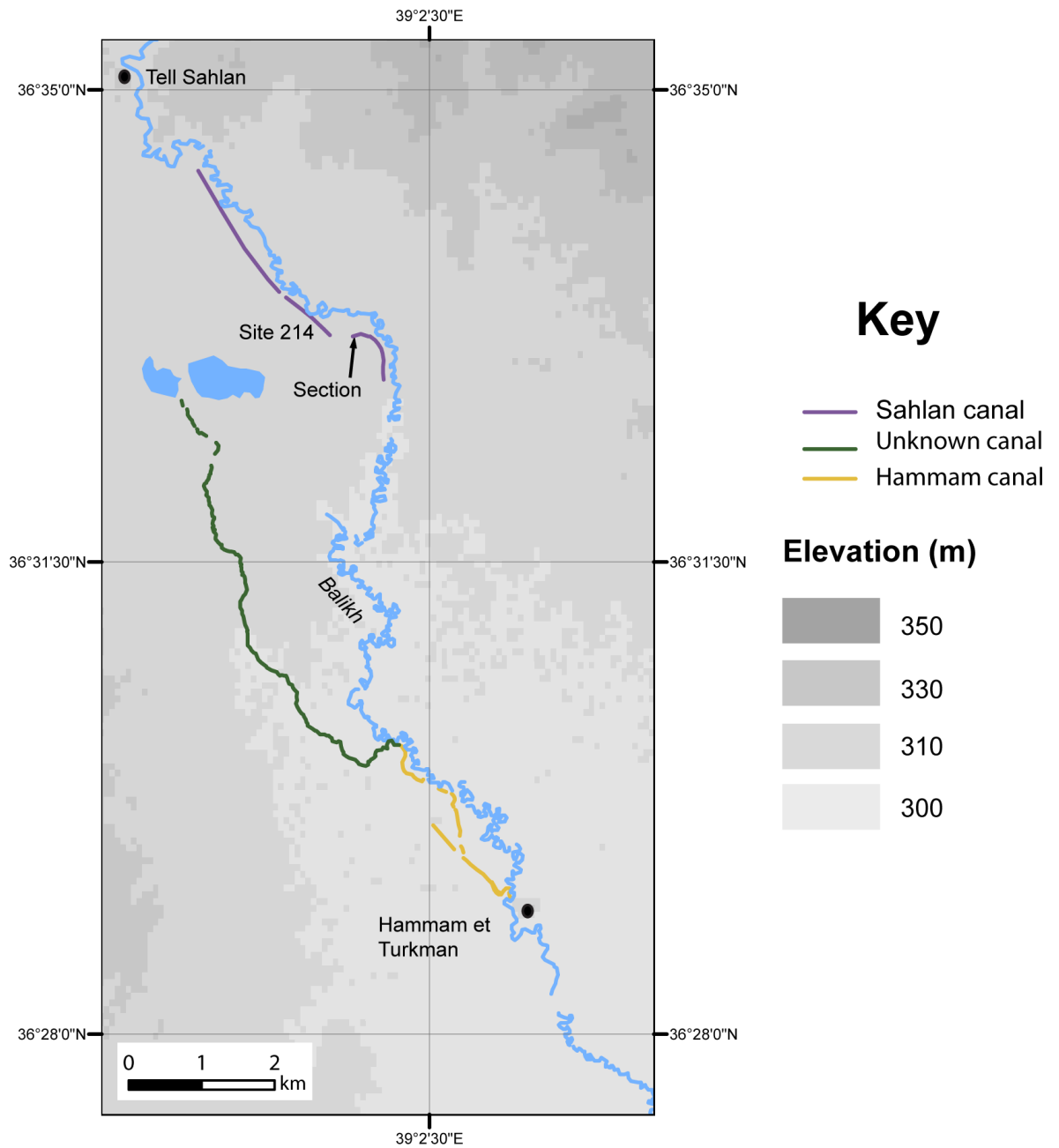


Figure 6.11: Sahlan-Hammam canals and a relict canal of unknown date.

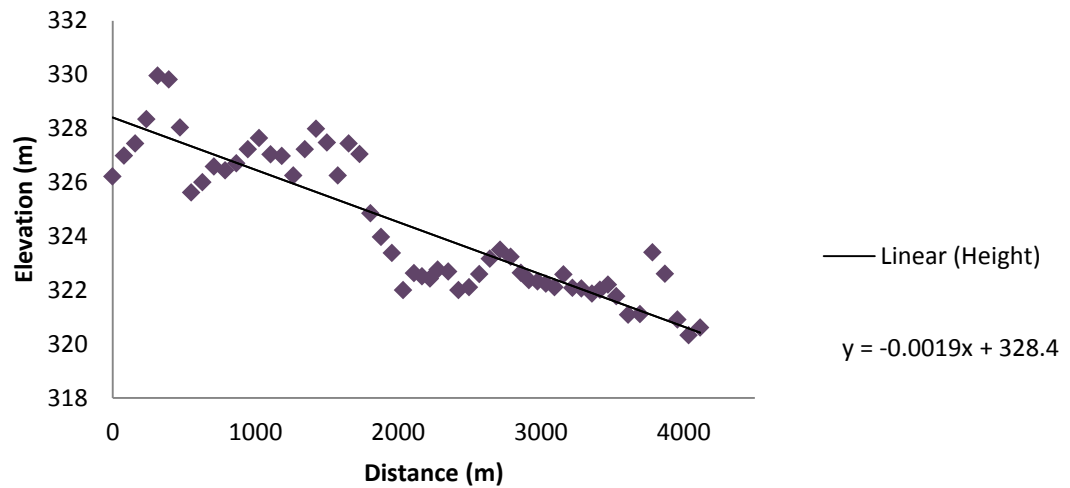


Figure 6.12: The gradient of the Sahlan channel estimated from SRTM. Canal profile 1 (see **Figure 6.9**). Gradient: 0.2%.

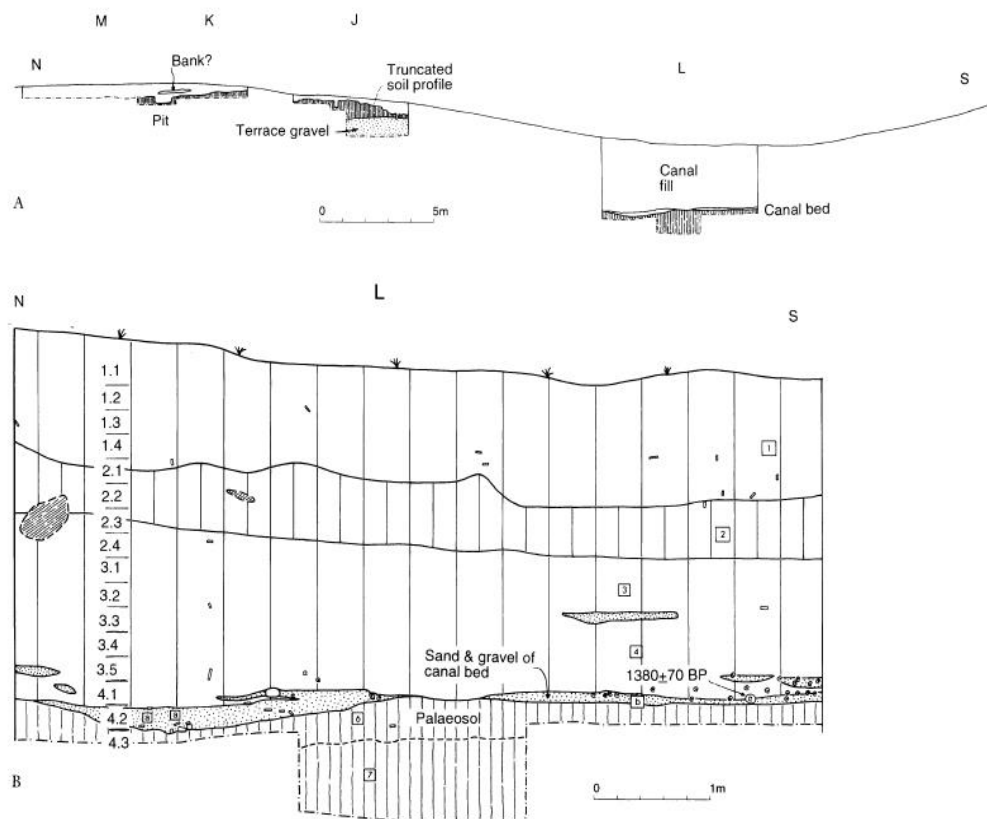


Figure 6.13: Section through Sahlan canal, from Wilkinson, 1998: fig. 5.

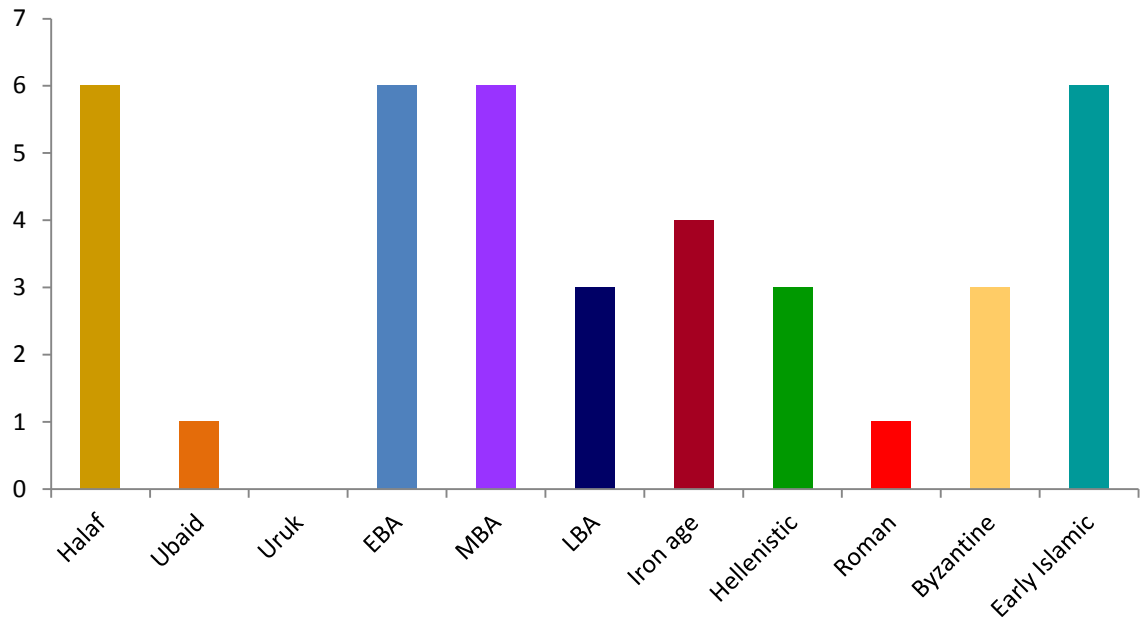


Figure 6.14: Sites occupied in each period period alongside the palaeochannel.

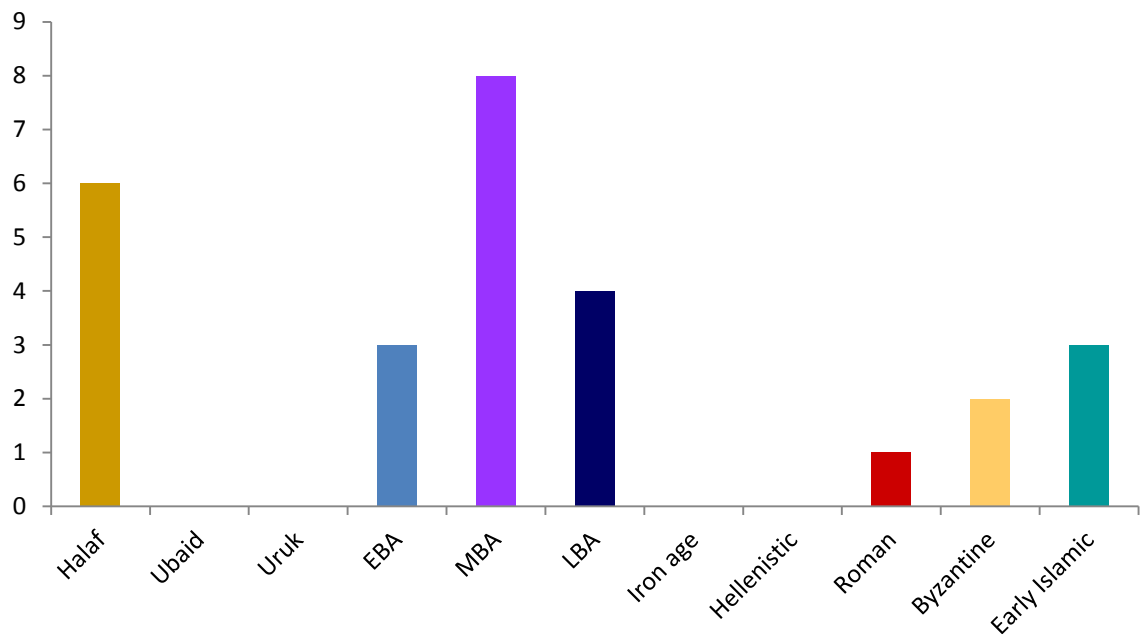


Figure 6.15: Numbers of sites occupied in each period period alongside the Sahlan canal.

The canal appears to abstract water from the west side of the Balikh at Tell Sahlan. As the CORONA image clearly shows, it is closely aligned to the current course of the Balikh, following it downstream, indicating that the canal was

constructed after the avulsion away from a palaeo-channel to the west. After running for c.4km, the canal trace seems to have been removed as a result of the erosional activity of the Balikh.

There appears to be a direct relationship between the palaeochannel and settlement locations in the area. Were these sites using the channel itself, or were they utilising the marshland or other resources in the immediate vicinity? The area was marshy at an unknown stage in the past (Hritz, 2013b, p153). Many smaller settlements lie close to the course of the palaeo-channel. The earlier sites may have been occupied while the channel still flowed and so had a functional relationship to the channel: the highest number of associated sites was in the Bronze Age (see **Figure 6.14**). Later on, the focus of settlements shifted closer to the current course of the Balikh, indicating that the avulsion creating the new channel probably occurred after the Bronze Age. There were several sites close to the palaeochannel that post-date the Bronze Age, however, presumably still exploiting the specific environmental niche which the palaeochannel and later marshes represented. Curvers (1991) interprets one site (322) as a seasonal camp —sites like this indicate temporary occupation in order to make use of the marshes.

The relationship between the canal itself and the archaeological sites is less clear, as **Figure 6.16** shows: there does not seem to be a clear relationship, and it is possible that most of these sites are only associated with it by chance. In other words, they were present in the area before the canal was dug, and because they do not appear to be in the area actually irrigated by the canal, which is not preserved. The irrigated area may have been somewhere to the west of the channel.

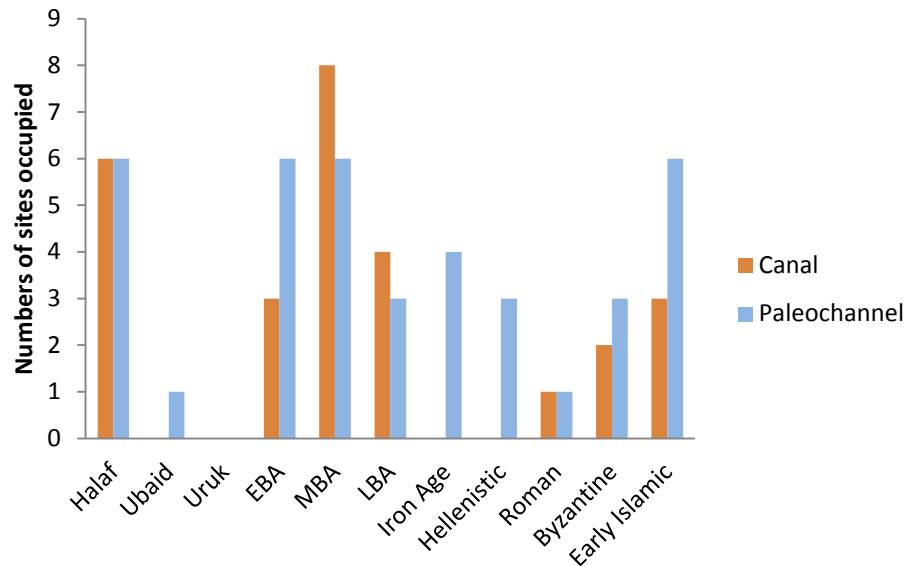


Figure 6.16: Archaeological sites alongside the Balikh palaeochannel and the Sahlan-Hammam canal.

An association between sites and canals can only be clearly defined where the sites fall within or close to the area irrigated by the canals; canals in the transport zone of the canal will only be associated with it by chance. This example highlights a more general point about ‘dating’ canals by their association with archaeological sites. They must have a functional relationship to those sites; many of the sites in the area may have existed prior to the construction of the canals, or after the water system was abandoned, and so could have had no relationship to those canals. It is only within those areas where there is a functional relationship with the canal water (i.e. where it is distributed via laterals to the fields) that it can be suggested that sites and canals are contemporary.

There are fewer sites in general along the canal. a comparison of **Figure 6.14-6.16** does not indicate any obvious trend. The canal itself can be seen to truncate some sites which can be assumed to be earlier in date than the canal. The lack of a pattern in site locations may be because there was in fact no pattern, as suggested above. it would appear this part of the channel functioned merely as transport, delivering water to an irrigation zone further downstream, the traces of which were lost even by the 1960s.

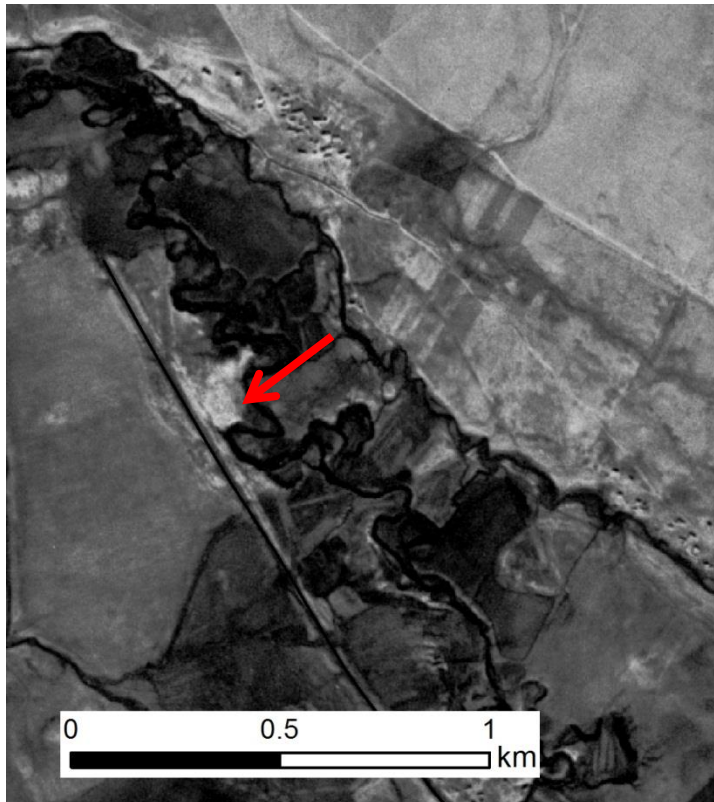


Figure 6.17: *The Sahlan canal truncates the Bronze Age site 242 (arrowed). Image 22 January 1967.*

Further downstream and close to Tell Hammam et Turkman, another prominent segment of canal was identified, which has a similar morphology and alignment to the dated Sahlan channel upstream. Like some other well-known ancient canals (e.g. the Neo Assyrian canals of northern Iraq) it is a large feature. Analysis of the SRTM data does not show the channel itself but when compared with the route of the infilled channel shows that it flowed at a shallow gradient of c.0.4% (see **Figure 6.20** and **Figure 6.9**). As discussed in **Chapter 5**, the values obtained from the coarse-resolution DEMs are guidelines only; higher resolution DEMs with ground validation could give a more accurate result. Overall, SRTM data for the Balikh seemed to be less ‘spikey’ than ASTER. There was some difference between the two datasets in some locations.



Figure 6.18: Lower end of Hammam channel, near Tell Hammam et Turkman. Image 22 January 1967.

The CORONA DEM, however, allows the morphology of the feature to be interpreted (see **Chapter 3** for an explanation of how the DEM was generated). The heights generated using the CORONA DEM were compared to the SRTM DEM, and it was found that 98% of the CORONA DEM pixel height values were within 7 m of the corresponding SRTM values. The resulting pixel size of the output DEM was 10 m (see **Chapter 3**). The original ancient elevation of the canal is unknown but it had been evident in the field in the 1990s from the prominent upcast banks that flanked the channel (Wilkinson pers.comm). Even in the 1960s, by which time erosion had presumably taken place, these stood at up to 6 m high. They may originally have consisted of spoil from the initial construction of the feature. Given the shallow gradient (see **Figure 6.20**) of the feature frequent dredging would have been necessary and the dredged material may then have been deposited on the banks. A photograph taken in the 1990s (**Figure 6.19**) shows that these banks had eroded further; by the fieldwork season of 2010, all traces of the canal were gone.



Figure 6.19: The upcast banks of the Hammam channel (foreground) were still visible in the 1990s (Photograph from Tony Wilkinson, who also provides scale).

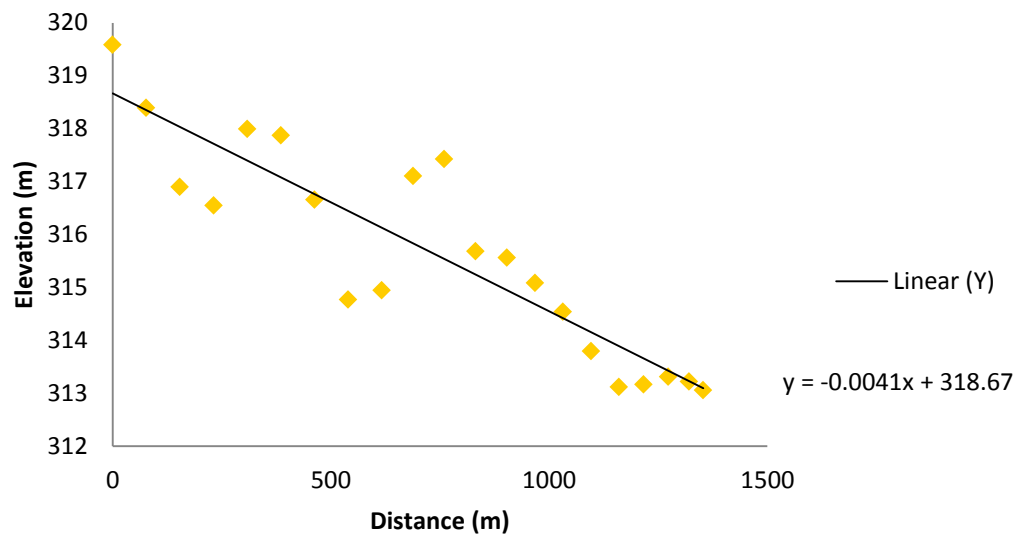


Figure 6.20: The lower part of the Hammam channel. Canal profile 2 (see **Figure 6.9**). Gradient: 0.4%

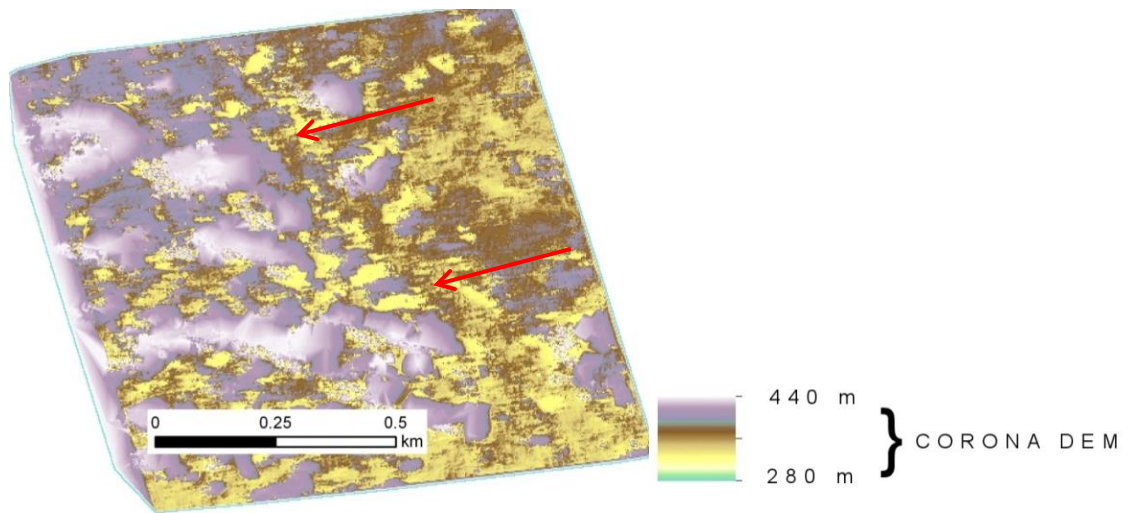


Figure 6.21: The canal is visible as a broad brown line in the CORONA DEM of c. 10 m resolution.

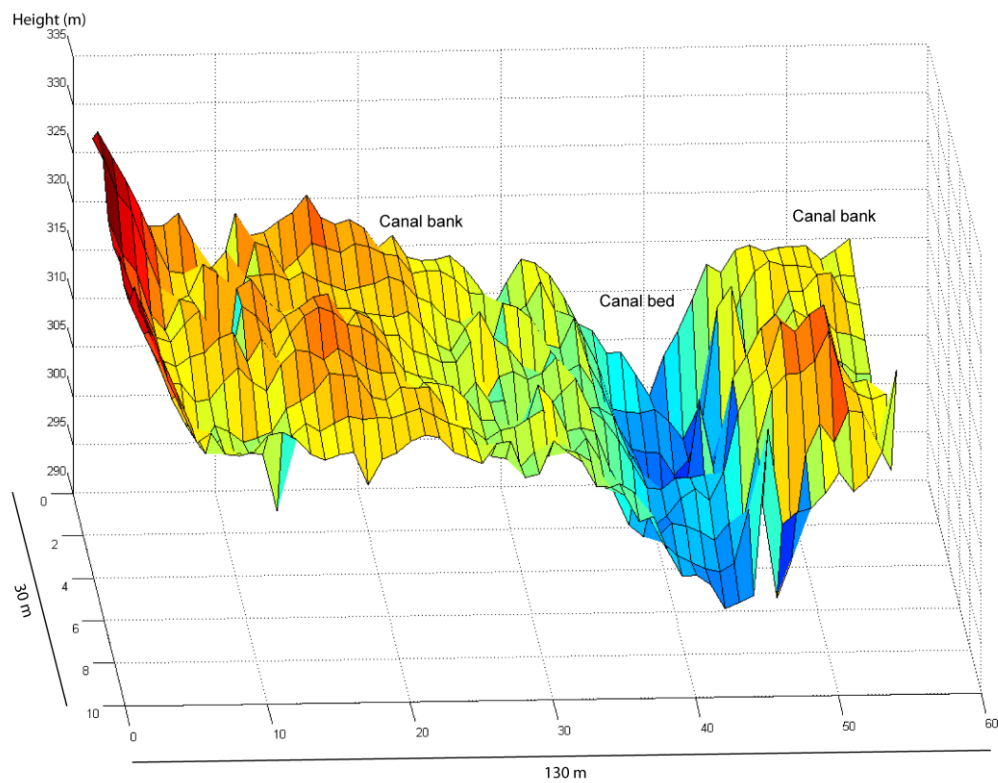


Figure 6.22: Filtered 3D surface of the Hammam canal created using the CORONA DEM. The surface was created by taking points at 3 m intervals along transects of 130 m in length.

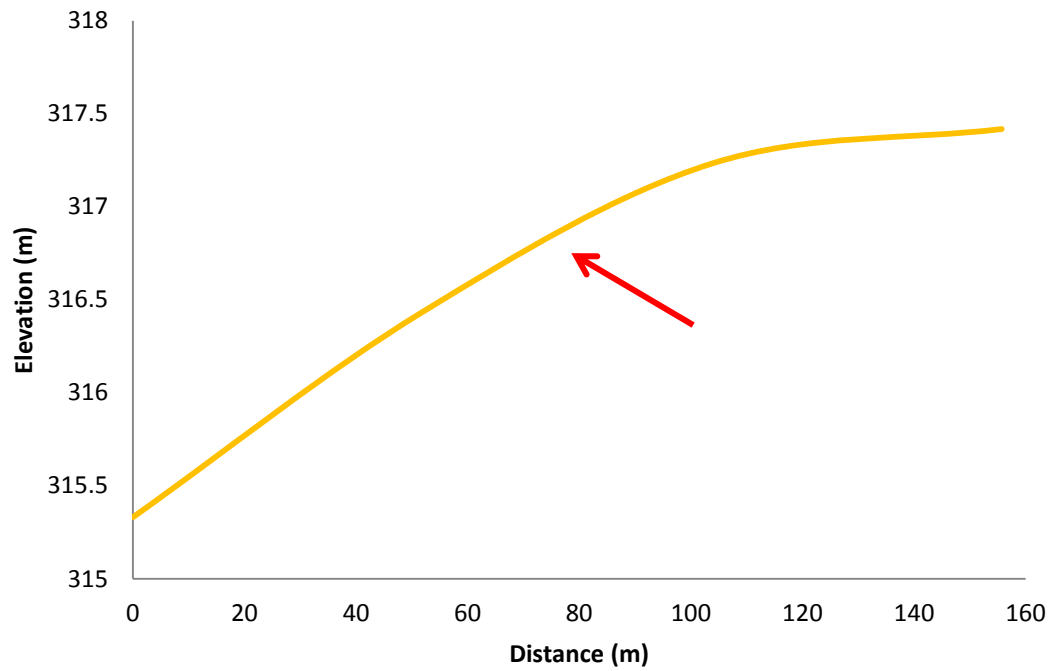


Figure 6.23: Cross section of the lower Hammam canal taken using SRTM. The arrow points to the location of the canal, which is not discernable using this coarse resolution DEM.

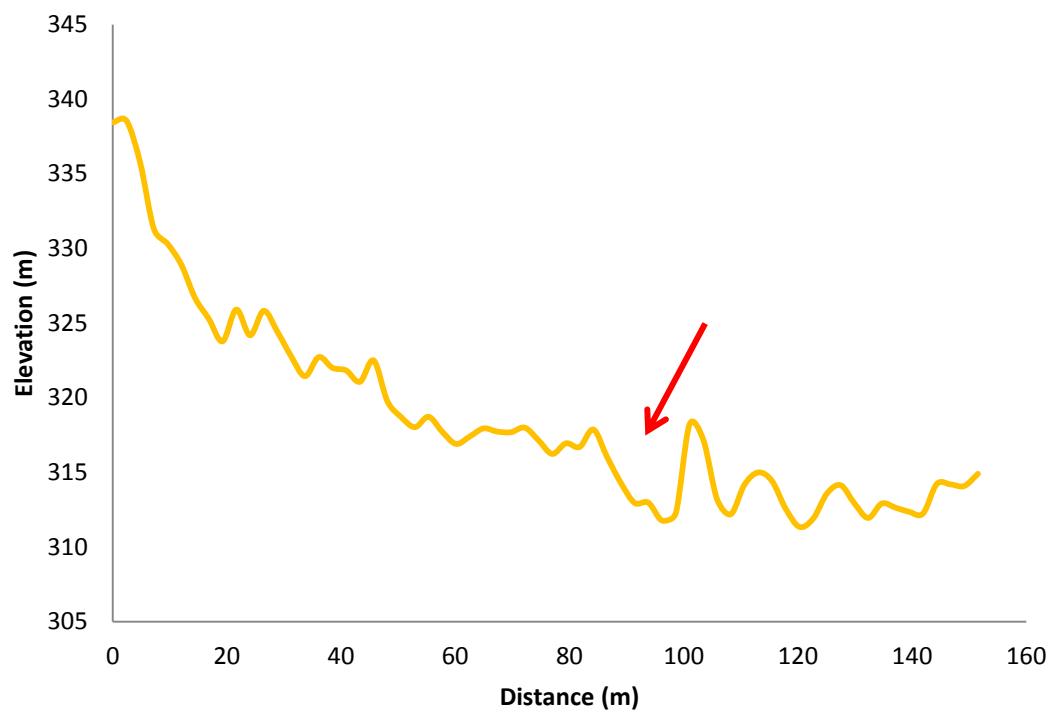


Figure 6.24: Cross section. The canal (see arrow) is discernible using the CORONA DEM.

The value of employing CORONA DEMs is evident when the cross sections obtained by using the two data sources are compared. The graphs (**Figures 6.23** and **6.24**) (taken from upstream of the area used for the surface (**Figure 6.22**) show that it is clear that the SRTM is too coarse to give fine detail, to the extent that it shows a different overall trend: the shape of the canal and its relationship with the surrounding topography can be discerned from the CORONA data, however. **Figure 6.24** shows the shape of the canal and its relationship with the surrounding topography. It separates an area of higher ground beyond its right bank, and lower-lying land that slopes towards the Balikh from the canal's left bank.

Given the similarities between the excavated Sahlan canal and the Tell Hammam et Turkman channel it can be suggested that they are part of the same system: the central part of the canal would have been removed by later lateral erosion of the Balikh. A pattern of gullying follows what would have formed the canal's path, possibly indicating its former presence. Another canal merges with the Hammam canal: this seems to be a later modification (this canal of unknown date is shown in **Figure 6.11**). Generally irrigation systems will comprise lateral canals that divert water from the main canals to the fields (see **Chapter 4**). However, in this case, only the main canals are apparent: one forming the transport end and the other the drainage end. The irrigated zone was probably within the basin to the west of the canals, an area which is obscured by later irrigation ('suggested use zone' on **Figure 6. 13**). This is supported by the presence of several sites of later date (Hellenistic to Early Islamic) in the area north of Hammam et Turkman; their distribution in relation to the canals is represented in **Figure 6.25**. Hammam et Turkman itself yielded some archaeological material dated to the Parthian-Late Antique periods (De Jong, 2011, p266).

If these sites were using and maintaining the Hammam-Sahlan canal, it could have enabled them to produce considerable agricultural yields. Other functions of the canal system such as transport or drainage should also be noted. For example, the canal could have served a purpose of protecting the area to its west (possible a cultivated/irrigated area) from being flooded by the Balikh.

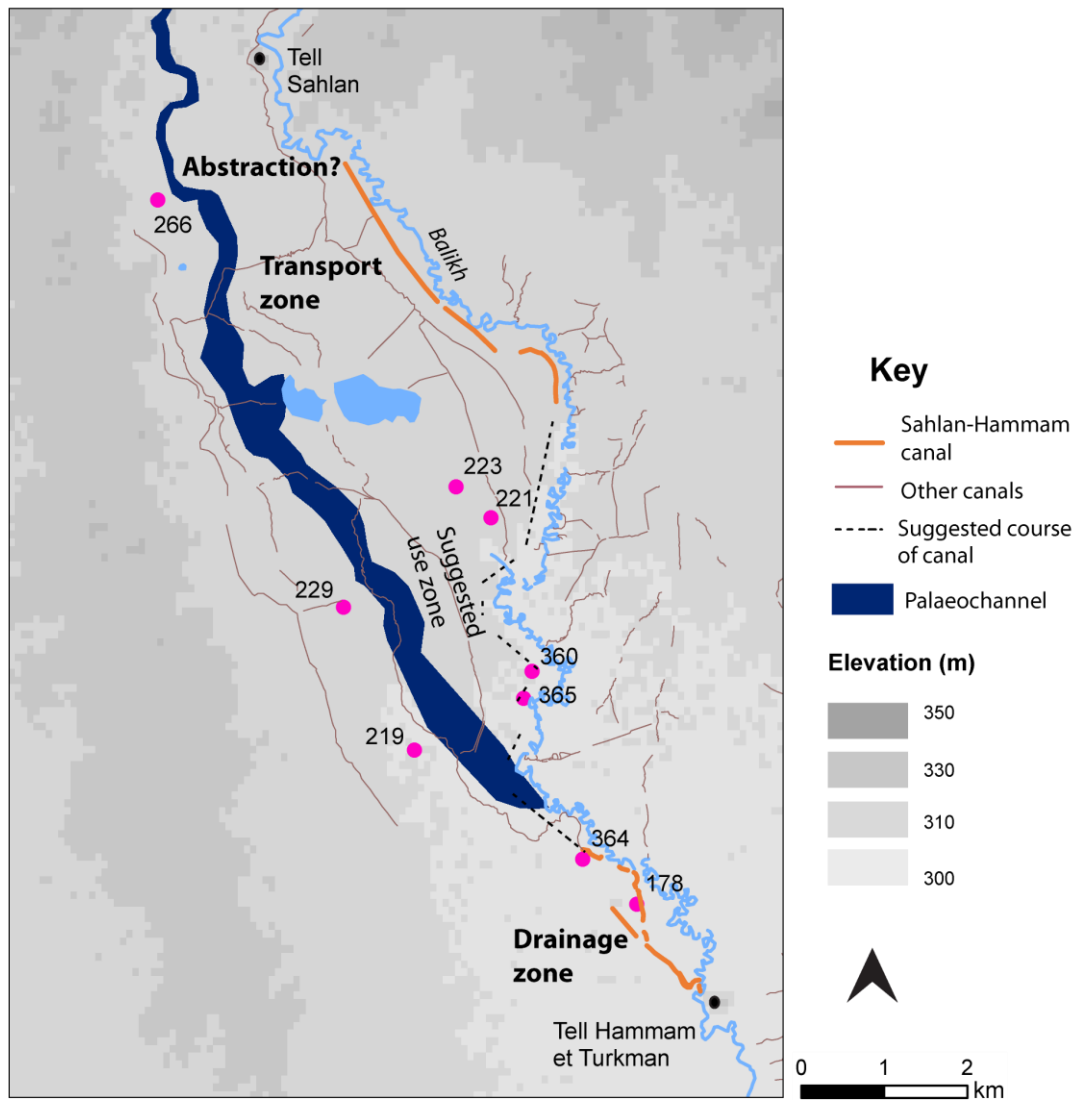


Figure 6.25: The locations of later sites in the vicinity of the Sahlan-Hammam canals (Hellenistic-Early Islamic) are indicated and the hypothetical route of the missing segment is suggested based on the location of gullying.

A greater understanding of the economic input of these canals can be gained if the discharge is estimated. Using Manning's formula, an estimate can be made for the discharge of both channels. Wilkinson's excavations of the Sahlan segment (1998, p80) enabled a value of $7.8 \text{ m}^3/\text{s}$ to be suggested (see **Figure 6.13**).

Applying Manning's formula to the Hammam segment of the canal, based on the CORONA DEM, gives a range as high as $5.6\text{--}73 \text{ m}^3/\text{s}$. Details including the width of the channel and its depth were used to calculate discharge:

$$Q = \frac{1.49}{n} A R^{2/3} S^{1/2}$$

Q is the discharge

N is the roughness coefficient

A is the cross sectional area

R is the hydraulic radius

S is the slope

Equation 6.1: *Manning equation (see Clifford Boyer, 1964, p15-32).*

However, excavations were not undertaken for the Hammam canal segment. While the CORONA DEM can be used to get an idea of the morphology of the canal at the time the stereopairs were collected, using the surface topography of the feature alone gives the impression that it is a very wide (between 5-10 m) feature of up to 0.5-8 m deep: as **Figure 6.26** shows, the 1960s surface does not give us the true (ancient) parameters of the canal. If it is part of the same system as the Sahlan canal, a similar discharge would be expected: therefore the true size of the actual channel would be similar. Conversely, the upcast banks do not need to be the same for both channels. The morphology of these will be more dependent on the natural topography and can change along the length of one canal depending on their initial form and on transformation processes.

Given the above problems, the Manning formula was applied using two different values, based on the CORONA DEM, one assuming a wider and deeper channel than the other. The 'n' value was given as 0.022 for a vegetated earth channel (e.g. see Philips and Tadayon, 2006). **Figure 6.27** and **Table 6.1** show the significant difference in flow between relatively similar width and depth values. The same gradient used by Wilkinson (0.002, see Wilkinson, 1998, p80) was applied.

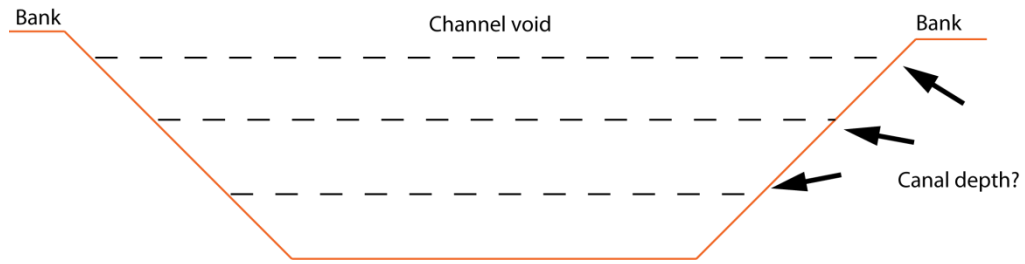


Figure 6.26: While a DEM can reveal the surface morphology of an ancient canal, excavation is needed to get a more accurate value for depth. From the surface alone it is difficult to identify the correct parameters.

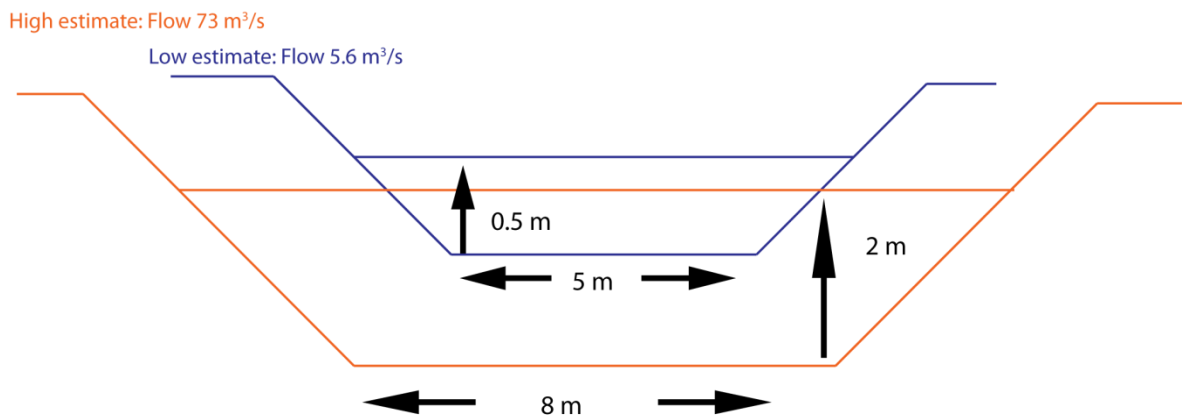


Figure 6.27: Sketch indicating the varying estimates of flow depending upon different parameters. Channel gradient was 0.002.

Table 6.1: *Discharge estimates. Small changes in the input parameters (based on the CORONA DEM), as these two examples show, have significant impact on the results (assuming a channel with an n value appropriate for an earthen construction, see Clifford-Boyer, 1964; Phillips and Tadayon, 2007). This table represents estimated rather than absolute values, given a lack of an excavated section in the Hammam canal, but they serve to illustrate the possibilities of using the dimensions of ancient canals.*

Value	Low estimate	High estimate
Gradient	0.002	0.002
Bottom width (m)	5	8
Depth (m)	0.5	2
Flow, (m^3/s)	5.6	73

Using this estimate for illustrative purposes shows the range of uncertainty present. The very different results obtained when slightly different parameters are input shows the hazards of estimating discharge where clear channel parameters are not available. Wilkinson (1998, p80) was able to suggest a more accurate value because his calculation was based on an excavated section; the CORONA DEM (which is accurate to about $\pm 7\text{m}$) only represents the surface of the channel in the 1960s, when it was already infilled and eroded. Further excavation in the future would enable the parameters for other sections of the canal to be obtained more accurately.

6.3 Nahr al Abbara

On the east side of the Balikh a more sophisticated canal system has been identified. Unlike the Sahlan-Hammam channels, other parts of the Nahr al Abbara (also known as the Nahr Turkman) network can be identified, including offtakes and drainage (see **Figure 6.28**). This enables a recognition of a more complete, large-scale irrigation system to be made. Parts of this system were investigated by Wilkinson in 1998: by association with adjacent sites and field scatters of pottery it was dated to the Byzantine-Early Islamic era (Wilkinson, 1998, p68). While the channel flowed in the early 20th century (Wilkinson, 1998, p67), by the time of the 1960s CORONA images, the channel appears to have become meandering and

silted for most of its length, suggesting that it was already out of use. By the 1990s, much of the Balikh valley consisted of fields watered by the river itself rather than from such large irrigation systems (Beaumont, 1996, p148). However, the Nahr al Abbara was dry by this time (Wilkinson, 1998, p67). During the 2010 field season the Nahr al Abbara system was no longer identifiable. Instead, well-like structures along its former course indicated some form of subsurface irrigation.

This system is not isolated: it functioned within a specific political and economic context in the Early Islamic period and may have been associated with nearby centres. The large Early Islamic site of Medinat al-Farr may have functioned as a way-station and garrison in the Abbasid period (de Jong, 2012, p520). As the CORONA image shows, (**Figure 6.29**), this was a prominent, walled site of around 124 ha (Bartl, 1994, p221). Streams associated with the site drain into the Nahr al Abbara system, into a north-eastern branch which was possibly part of the oldest visible channel. The site may also have had some role in managing the Nahr al Abbara, while using the Wadi Sluk for its own water supply. Some of the natural streams around Medinat al Farr show evidence of canalisation and the hydro (flow network) model shows which channels are likely to be natural (see **Figure 6.39**).

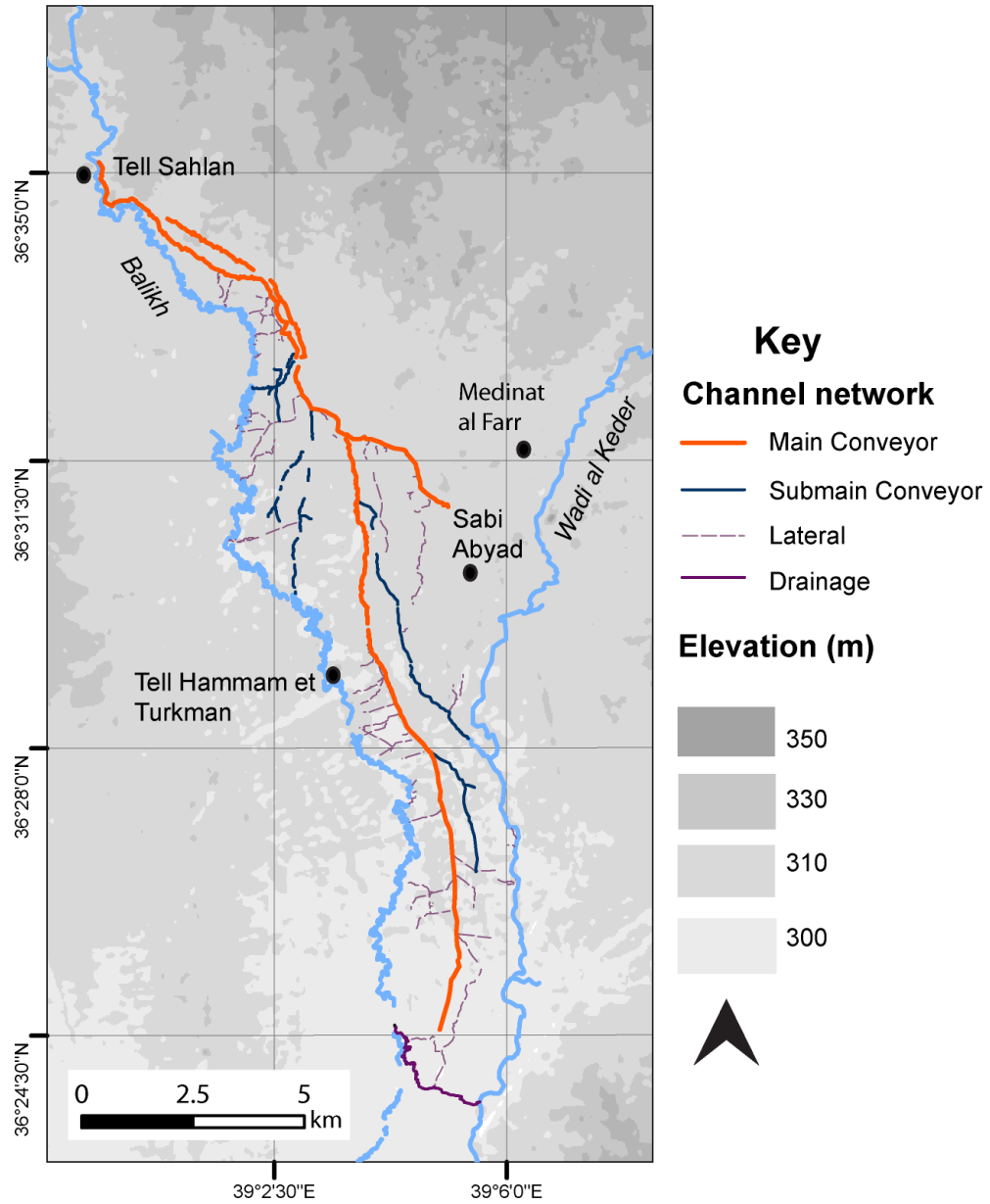


Figure 6.28: The Nahr al Abbara water management system.

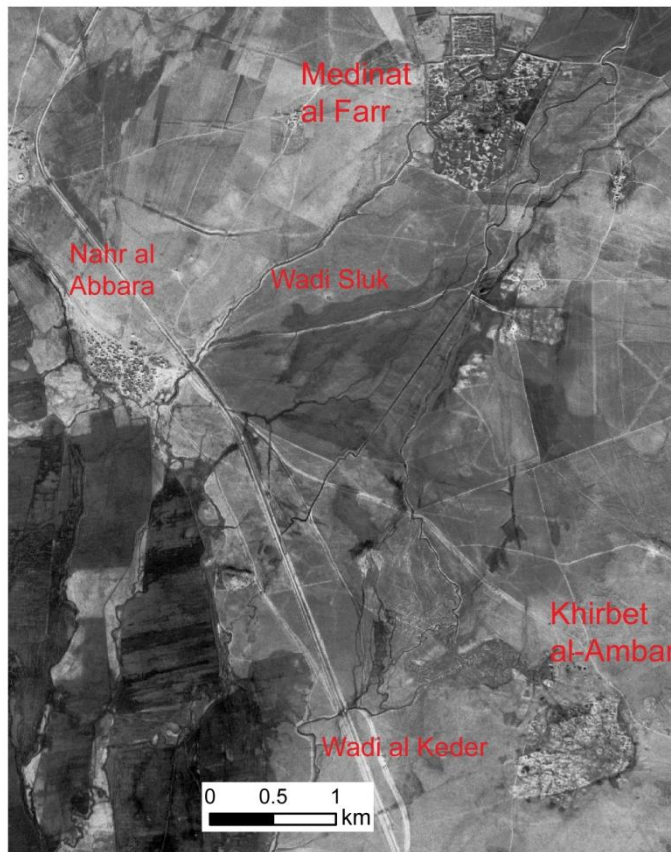


Figure 6.29: Early Islamic features are visible on the 1960s CORONA images. Image 22 January 1967.

At around 56 ha, the Early Islamic site of Khirbet al-Ambar is also one of the largest sites in the Syrian Balikh valley. This is a flat site (Bartl, 1994, p219), with a dense layout of structures visible in the 1960s CORONA images (see **Figure 6.29**). There are also at least 23 smaller Early Islamic sites within range of the Nahr al Abbara, ranging from less than 1 ha to 6 ha in size (**Figure 6.30**).

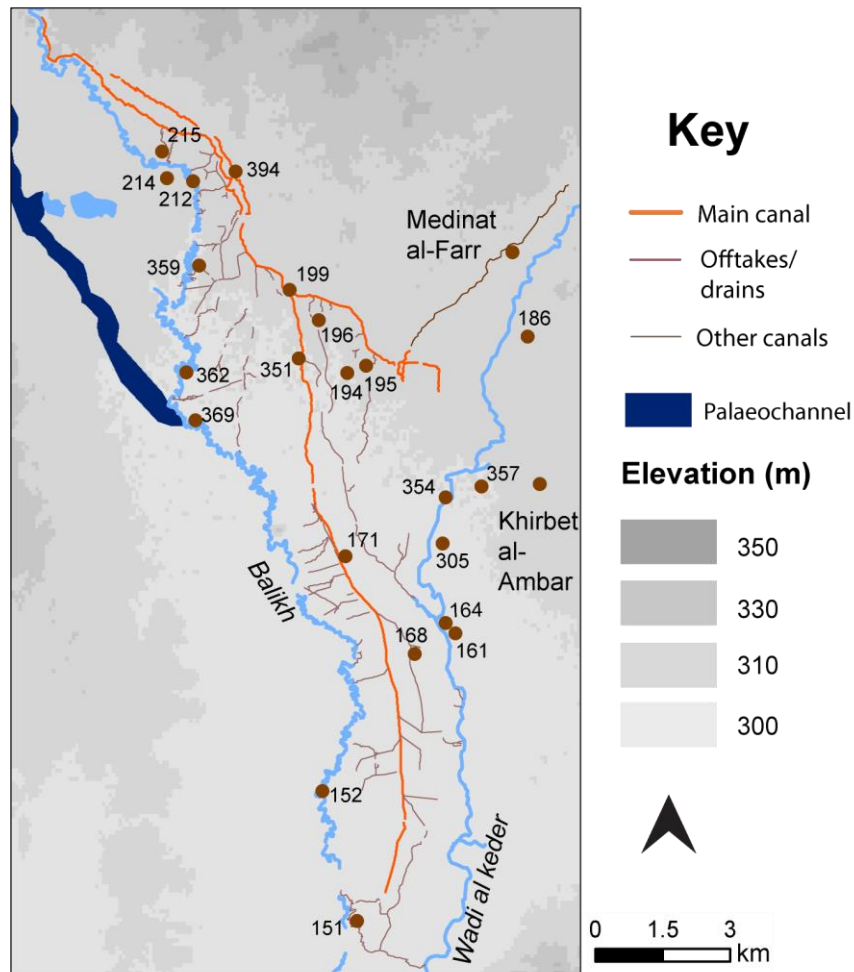


Figure 6.30: Early Islamic sites as recorded from survey in the vicinity of the Nahr al Abbara. See Wilkinson (1998) and Bartl (1994).

The system is more complete than other examples from the Balikh. While the ancient abstraction method used is not confirmed, Wilkinson noted that it used a refurbished dam near Tell Sahlan during the 20th century (Wilkinson, 1998, p687). Other ancient gravity-flow systems, such as the Hohokam canals, may have used reservoirs (Purdue et al, 2010, p132-140) and dams (Hunt et al, 2005, p448).

The main canals, laterals and drainage channels of the Nahr al Abbara are all identifiable from the analysis of the CORONA images. Like the other nearby systems, it is constrained by the flat topography of the Balikh, and it flows at a shallow gradient of about 0.1% (**Figure 6.31**).

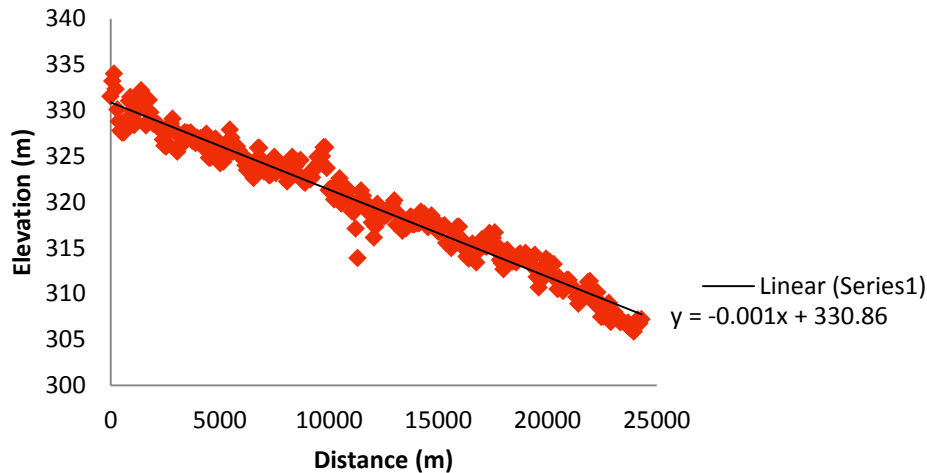


Figure 6.31: Canal profile 3. Nahr al Abbara main conveyor longitudinal profile, using SRTM (see **Figure 6.9**). Gradient: 0.1%. The ASTER DEM gave the same value.

At the same time, however, the designers of the canals made use of the natural topography to create a very functional system. **Figure 6.28** depicts the different parts of the mapped network. The main canal, which abstracts from the Balikh near Tell Sahlan, flows along a ridge of higher ground. An examination of the ASTER DEM (**Figure 6.32**) shows this almost imperceptible ridge. Although the elevations involved are small, making use of the ridge allowed the canal to supply a large area despite its shallow gradient of 0.1% (see **Figure 6.31**). Sub-mains flow diagonally down the ridge, also with low gradients (**Figure 6.33**) but enabling a larger area to be irrigated.

Unlike the more obscured Sahlan-Hammam channels, the lateral canals of the Nahr al Abbara are apparent in the CORONA image and their locations can also be identified, despite noise, in the CORONA DEM (**Figure 6.34**). The laterals flowed directly from the main canal perpendicularly down the ridge, giving them a steeper gradient of up to 0.5% (SRTM) – 1% (ASTER) (see **Figure 6.36**). The topography also constrains their length: they range in length between 400 to 1000 m. They are generally spaced at around 500 m apart. Limestone blocks along the main canal may have been part of former sluices (Wilkinson, 1998, p68), which directed water into the laterals. Presumably farms and small settlements would have been located so as to take advantage of the lateral canals from which water

could be delivered to the fields: there are in fact several sites close to these locations (see **Figure 6.30**).

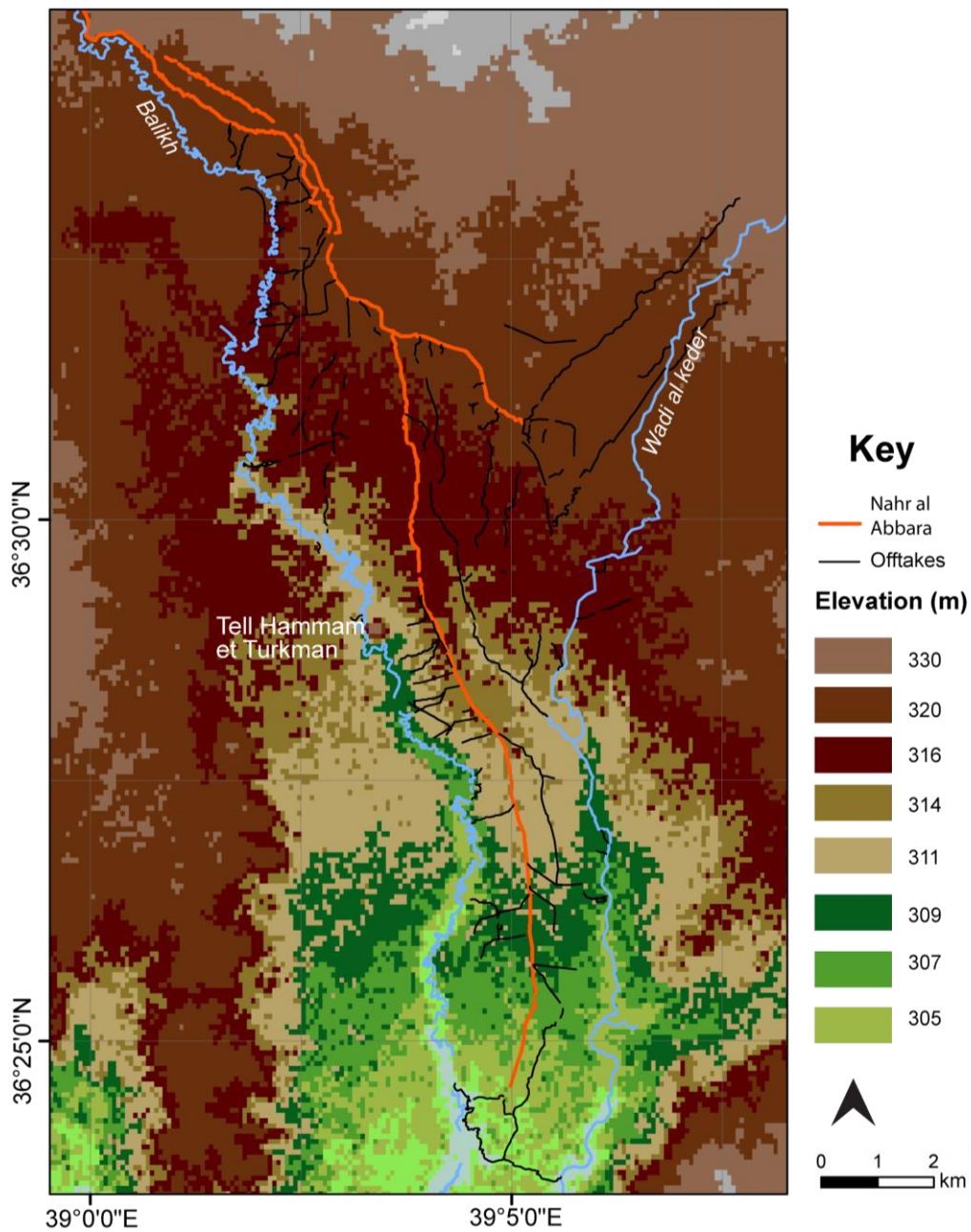


Figure 6.32: The ASTER DEM (spatial resolution 30 m) shows that the Nahr al Abbara main canal flows along a slight ridge, allowing the off-takes to flow at a steeper gradient in this very flat landscape.

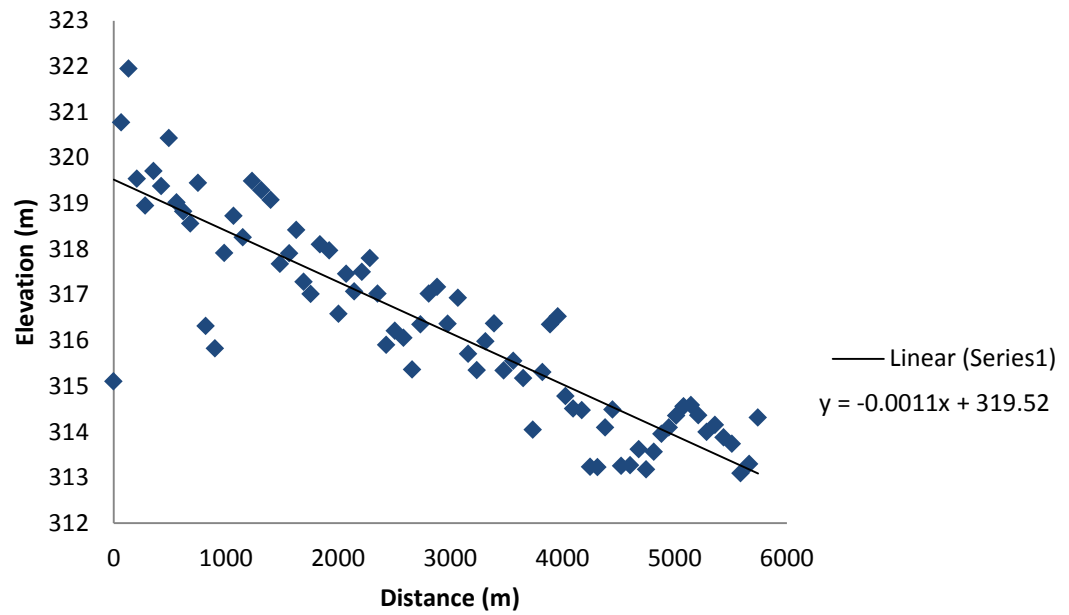


Figure 6.33: Canal profile 4, submain of the Nahr al Abbara. Gradient: 0.1%

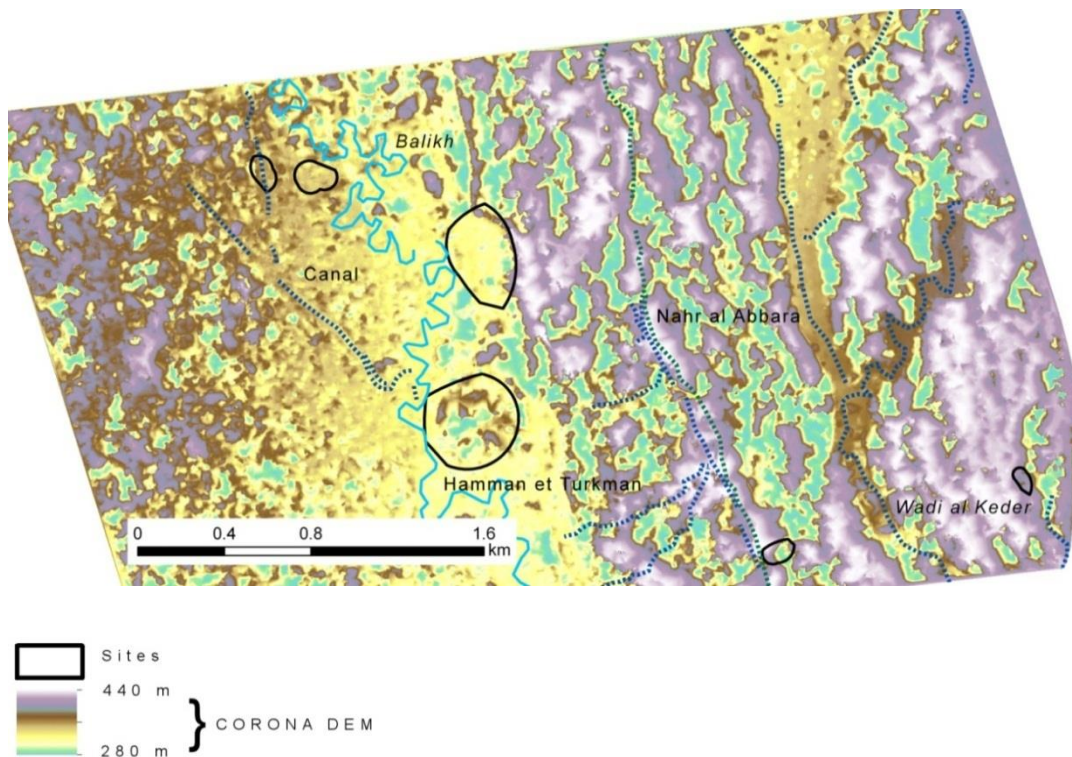


Figure 6.34: CORONA DEM showing the elevation of the distributary channels of the Nahr al Abbara.



Figure 6.35: Nahr al Abbara with laterals and location of Nahr al Abbara lateral longitudinal profile. Image 22 January 1967.

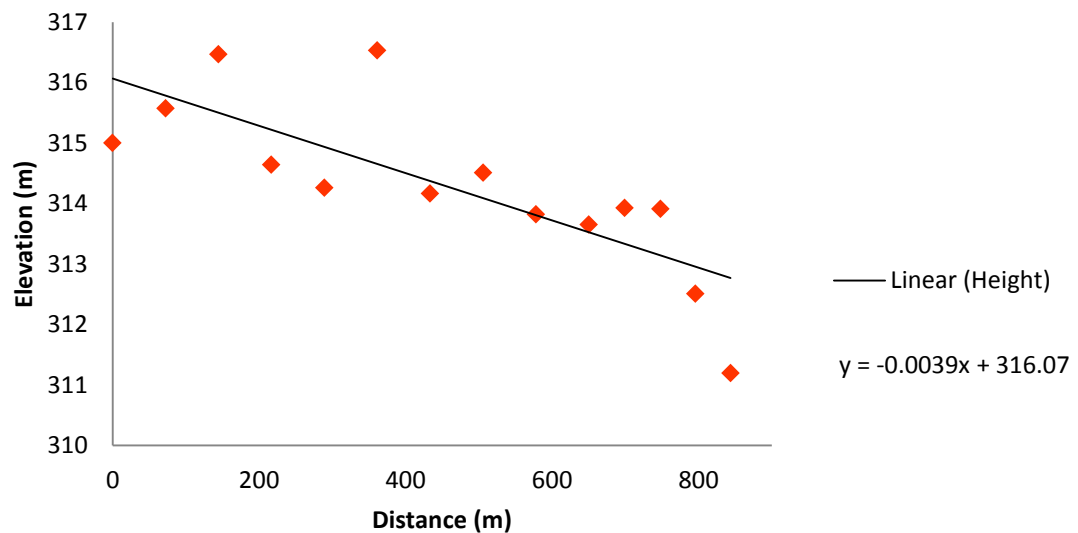


Figure 6.36: Canal profile 5. Nahr al Abbara lateral longitudinal profile (SRTM). Gradient: 0.5%. It is important to note that there are some outlying values which can affect the calculations of gradient. This is an issue when measuring shorter canals, because these represent relatively few points in the DEM. The ASTER DEM gave a value of 1% for this channel.

Table 6.2: Comparison between gradients of channels within Nahr al Abbara system (based on SRTM) and gradients suggested as ideal by the water management literature (in this example these are from Zimmerman, 1966).

Channel	SRTM gradient	Recommended gradient
Main conveyor	0.1%	0.1-2.5%
Submain	0.1%	
Lateral	0.5%	0.5-2%
Balikh drain	0.04%	
Keder drain	0.2%	

While this system was used in the Early Islamic period, it may have functioned over longer timescales. There are clearly two main canals of different phases of use running on contiguous alignments ca. 400 m apart at the north end of the system; eventually the channels merge, indicating two separate phases of use on the same alignment (see **Figure 6.38**). The main conveyor canal, visible on the CORONA images as a meandering channel, was still in use in the 20th century (for example, see **Figure 6.38** and also **Figure 6.34**) (Wilkinson, 1998). While one phase of use is Early Islamic, **Figure 6.37** shows a pattern of Bronze Age sites along the route of the main canal. Although these could be present as a result of coincidence, they could also represent the alignment of a former, earlier canal, on the same alignment as the Islamic one. Wiggermann (2000, p177) used Middle Assyrian texts from Sabi Abyad to suggest that some irrigation was taking place in the area in around 1200-1100 BC.

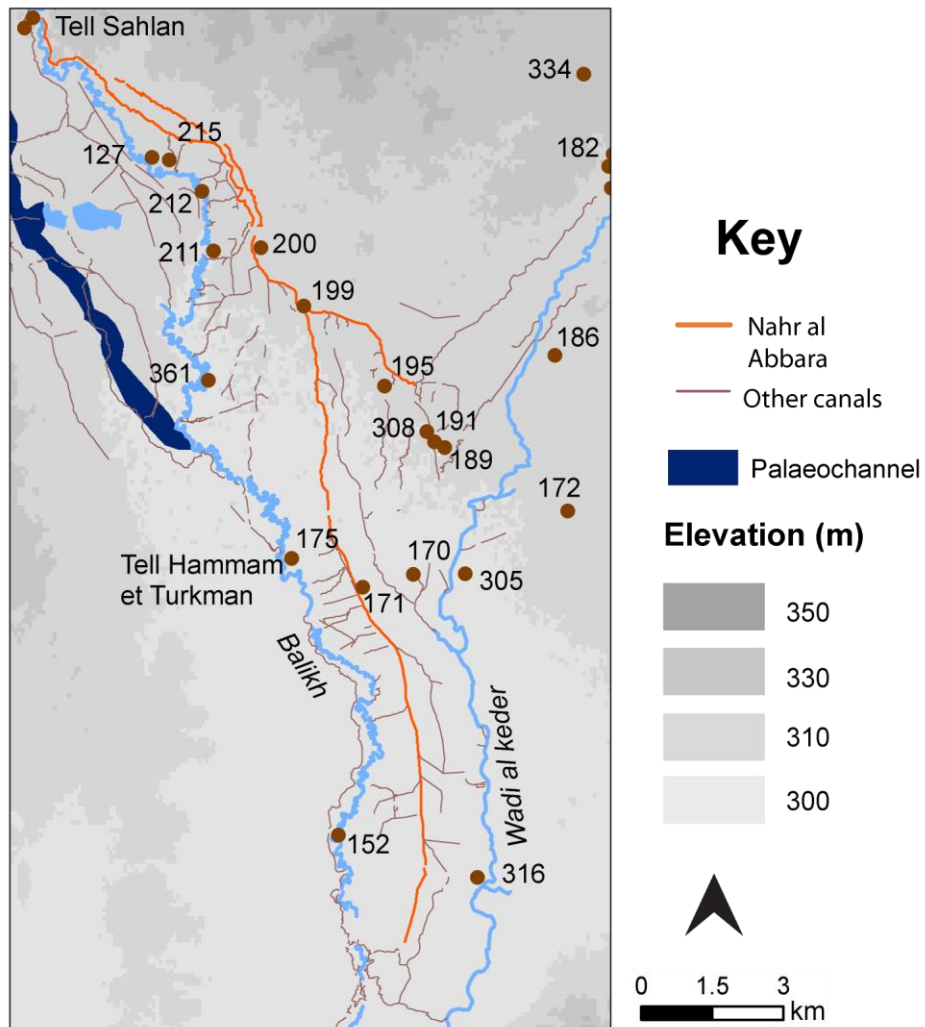


Figure 6.37: Bronze Age sites in relation to the Nahr al Abbara main conveyor³.

³ The database of sites was compiled from unpublished data (Wilkinson pers. comm) and from published surveys (Wilkinson, 1998; Curvers, 1991; Bartl, 1994).

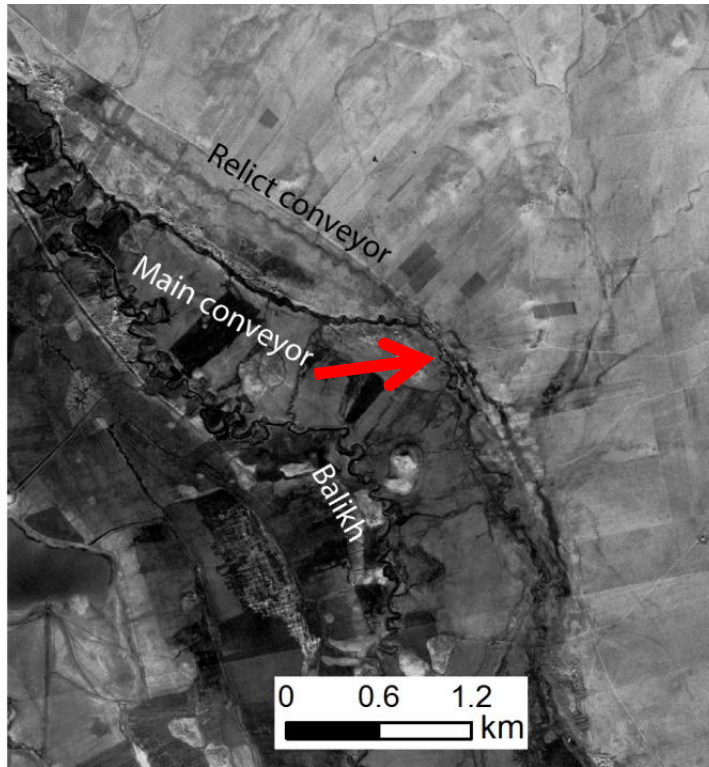


Figure 6.38: *Traces of two main canals along the route of the Nahr al Abbara can be seen in the CORONA image. Arrow points to the main conveyor canal. Image 22 January 1967.*

Drainage is an important factor in ancient water management in the Near East which is often overlooked. Despite the aridity of the climate, waterlogging due to over-irrigation can occur to the detriment of agricultural productivity. Occasional high episodic flows can damage canals and ditches. Salinity is also a problem where water tables are shallow and temperatures are high. Therefore there needs to be provision to remove excess water.

At the top end of the area irrigated by the Nahr al Abbara, gilgai formation may relate to previous waterlogging in the presence of expanding-lattice clays (see **Chapter 6.1**). Further south, however, it can be seen that the lateral canals mainly discharged into the Balikh after relatively short runs. The sub-main canals may also have a drainage function and they do not appear to have been associated with clear off-takes. The Wadi Al Keder isolates the system on the east side, preventing any uncontrolled runoff from the more elevated eastern steppe from being led straight into the fields. The ASTER-generated flow network (**Figure 6.39**) shows how the natural drainage system flows towards the Balikh, potentially into

and across the Nahr al Abbara. This would have been a significant problem at times of particularly high runoff.

However, the existing hydrological network could have been utilised to mitigate against this problem. The floodplain of the Wadi al Keder and wadis which drain into it from the north had large cross sectional areas (200-400 m in places) as the CORONA DEM (**Figure 6.34**) shows, suggesting that it sometimes carried relatively high flood discharges. Some lateral canals discharge into this natural channel. Finally, **Figure 6.40** shows how the system terminates in two channels allowing discharge into both the Balikh and the Wadi al Keder which also served to isolate the system from the area to the south. **Figure 6.29** shows the SRTM measurement of the gradient of one of these drains, which flows from the Nahr al Abbara towards the Wadi al Keder. **Figure 6.41** (*Canal profile 6*) shows that the gradient of this channel has a typical downward trend, but that it is affected by several unclear peaks and troughs, which may be partially due to modern features recorded by the DEM. Interestingly, the canal appears to drop quite sharply as it meets the natural stream channel.

While the Wadi al Keder may have been modified in the past, especially in the area between Medinat al Farr and Hammam et Turkman, the ASTER-derived flow network model indicates that it is a natural stream (**Figure 6.39**): the model only identifies the natural drainages and does not include canals.

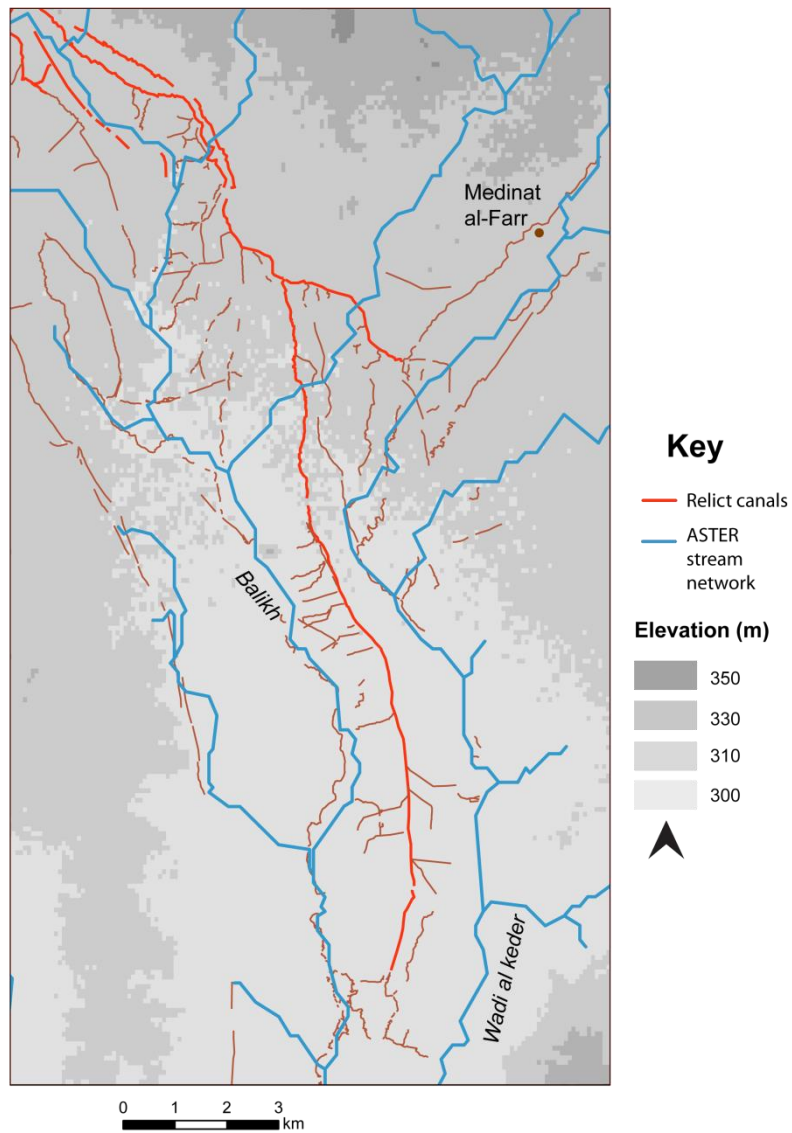


Figure 6.39: Flow network calculated using the ASTER DEM .The canal features were mapped from CORONA images.



Figure 6.40: Nahr al Abbara drainage zone. The wide Keder drain has a gradient of 0.2%; a clear trend in the gradient of the Balikh drain is not discernable using the available data. The CORONA image and DEM shows that these are very different channels in plan-form. Image 22 January 1967.

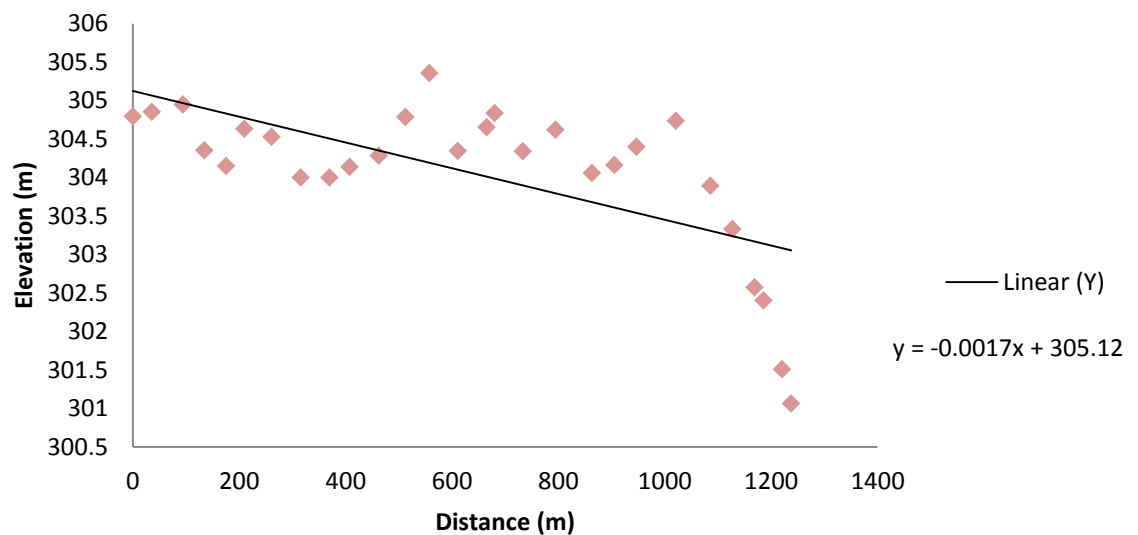


Figure 6.41: Canal profile 6. Longitudinal profile Wadi al Keder drain of Nahr al Abbara system using SRTM. Gradient: 0.2%

It is now appropriate to summarise how the Nahr al Abbara system was used. The general layout of the system and the gradient data are informative. As suggested above, the shallow gradient of the main canal (0.1%, **Figure 6.31**) allowed it to flow for a long distance (25 km), facilitating the irrigation of as large an area as possible. The problem of delivering water to the fields at a slighter steeper gradient was mitigated against by the layout of the lateral canals, which flowed perpendicularly off the ridge where the main canal is located: as a result, most of the laterals had gradients as high as 0.5%, consistent with values presented as ideal in modern irrigation literature (**Table 6.2**). At the lower end of the system, the split in the main channel allowed it to drain both into the Balikh and also into the Wadi al Keder (at a gradient of 0.2%).

Presumably, the irrigated zone, and individual farms, were located at the lower end of each of the irrigation lateral canals. Kaptijn's study (2009; 2010) of water management in the Wadi Zerqa can be compared to the Nahr al Abbara; in the Jordanian system, each farmer was assigned enough water to irrigate about 10 ha (Kaptijn, 2010, p149). If similar rules can be applied to the Nahr al Abbara, then each farm presumably irrigated using one or two of the lateral canals visible in the imagery. This would mean that there were at least 20 farms relying on the Nahr Al Abbara system, based on its pattern of lateral canals. The nearby Islamic sites of Medinat al Farr and Khirbat al-Ambar (possibly ancient Bajadda; see Heidemann, 2011, p46) could have administered the irrigation system.

There is a considerable difference in the scale, density and sophistication of the Early Islamic Nahr al Abbara when it is compared with the earlier Sahlan-Hammam system: links between this intensification and the imperial administration of the Balikh will be discussed in **Chapter 7**. Careful foresight and planning must have been employed in the construction of the Nahr al Abbara, enabling irrigators to make use of the natural topography of the landscape and of natural drainages. The survival of the system into the 1960s gives a rare insight into the different levels of water management within a network (the mains, laterals, drains etc).

6.4 Central Balikh

Another system which may have been used in the earlier imperial periods is located to the south within the central Balikh Valley. Wilkinson's 1998 survey identified part of this system and, by association with sites of Hellenistic date suggested a period of use between the 3rd and 1st centuries BC (p77; also see Wilkinson and Rayne, 2010). The CORONA images reveal that this system originated from a very long main canal, which abstracted from the Balikh about 1 km below the terminus of the Hammam canal and flowed with a very shallow gradient c.20 km south, finally draining into the stream of the Qara Mokh (**Figure 6.42**).

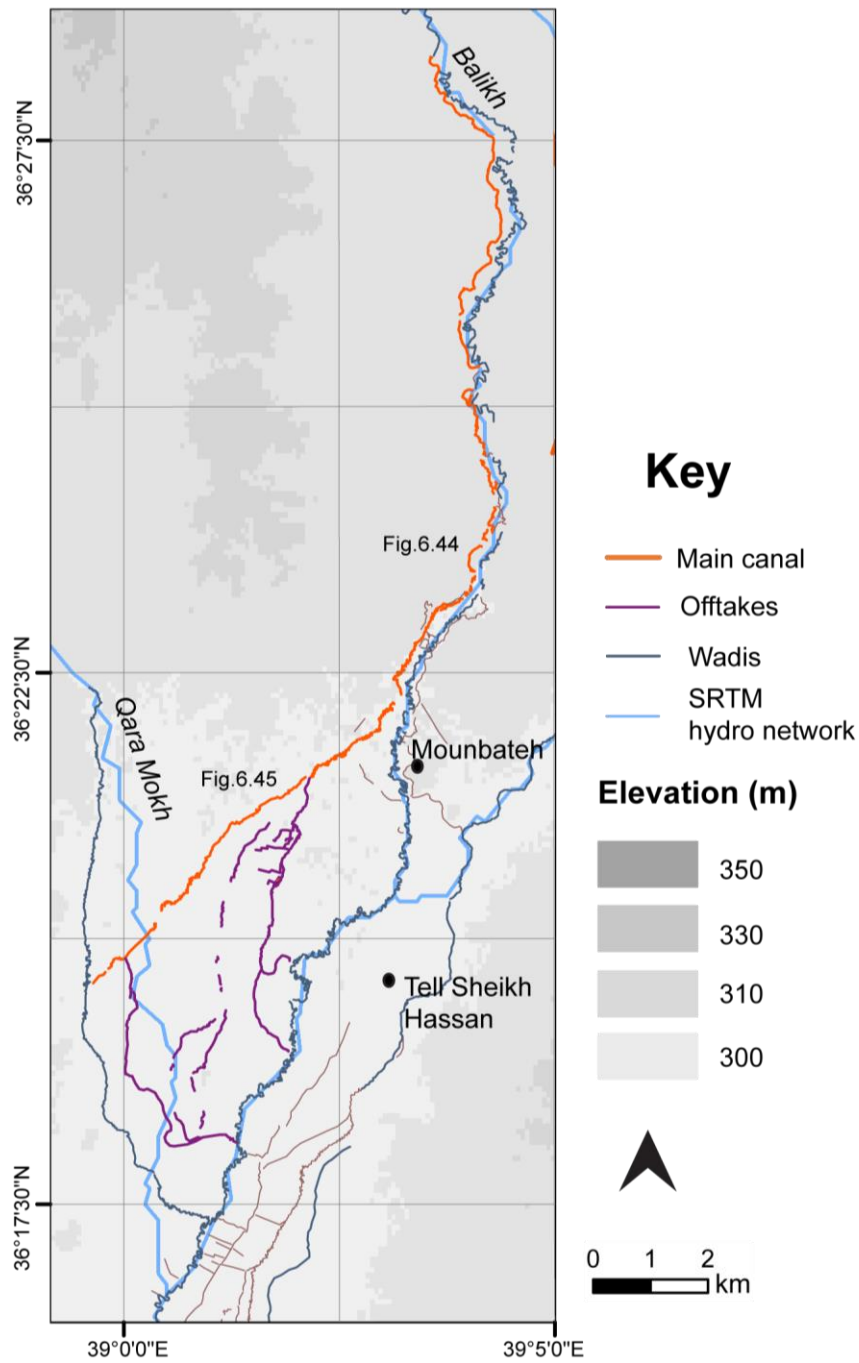


Figure 6.42: Canals in the central Balikh, near the Qara Mokh.

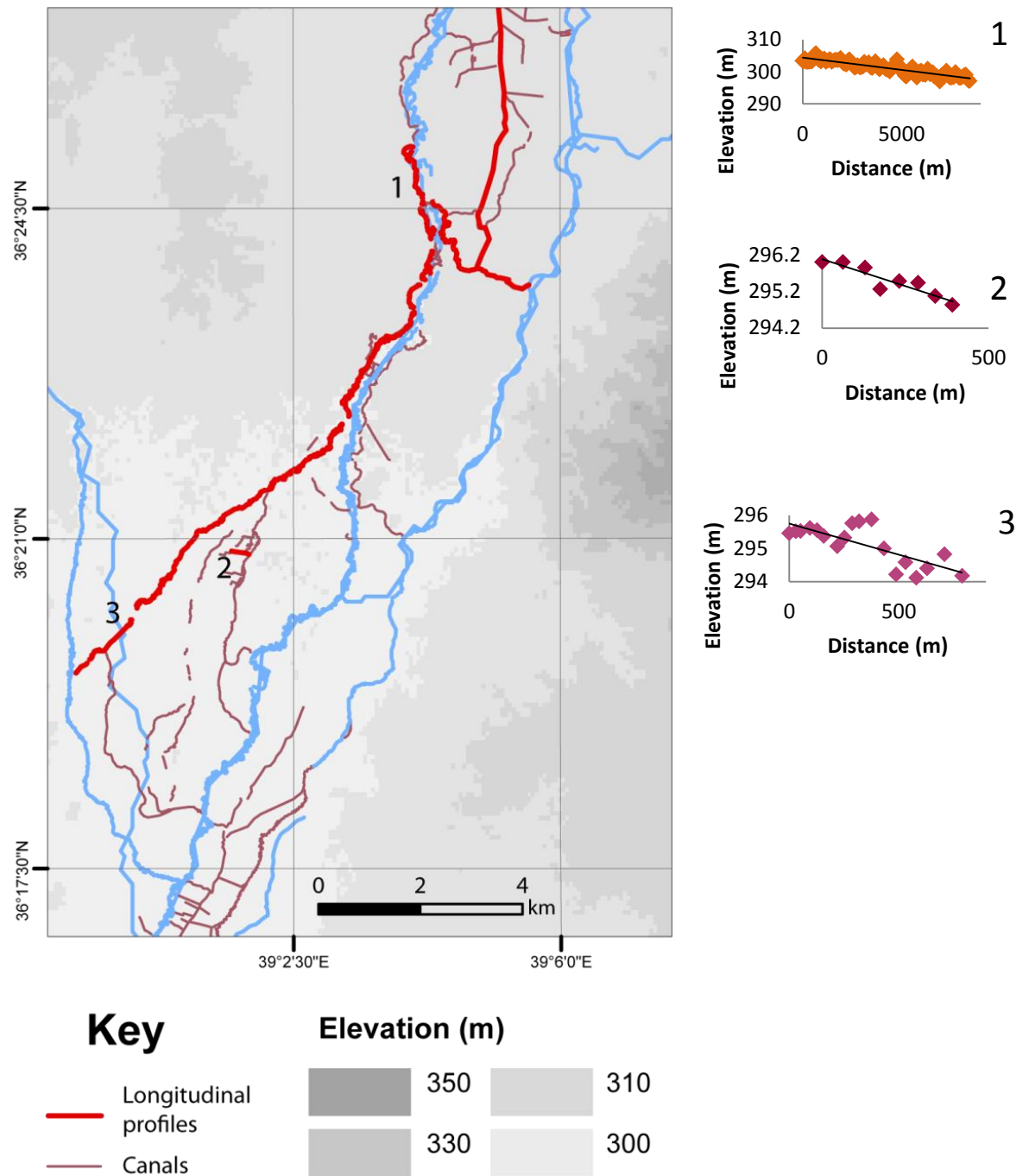


Figure 6.43: Locations of longitudinal profiles, based on the SRTM DEM.

Sub-mains and laterals branch from the main canal, and also drain into the Balikh. In the CORONA image, the Hellenistic main channel identified by Wilkinson (1998) appears to be linked to a much longer canal which abstracts from close to Hammam et Turkman. This flows for over 15 km and follows the alignment of the Balikh very closely (see **Figure 6.44**). The upper canal may represent the transport zone of the system, closely following the alignment of the Balikh.

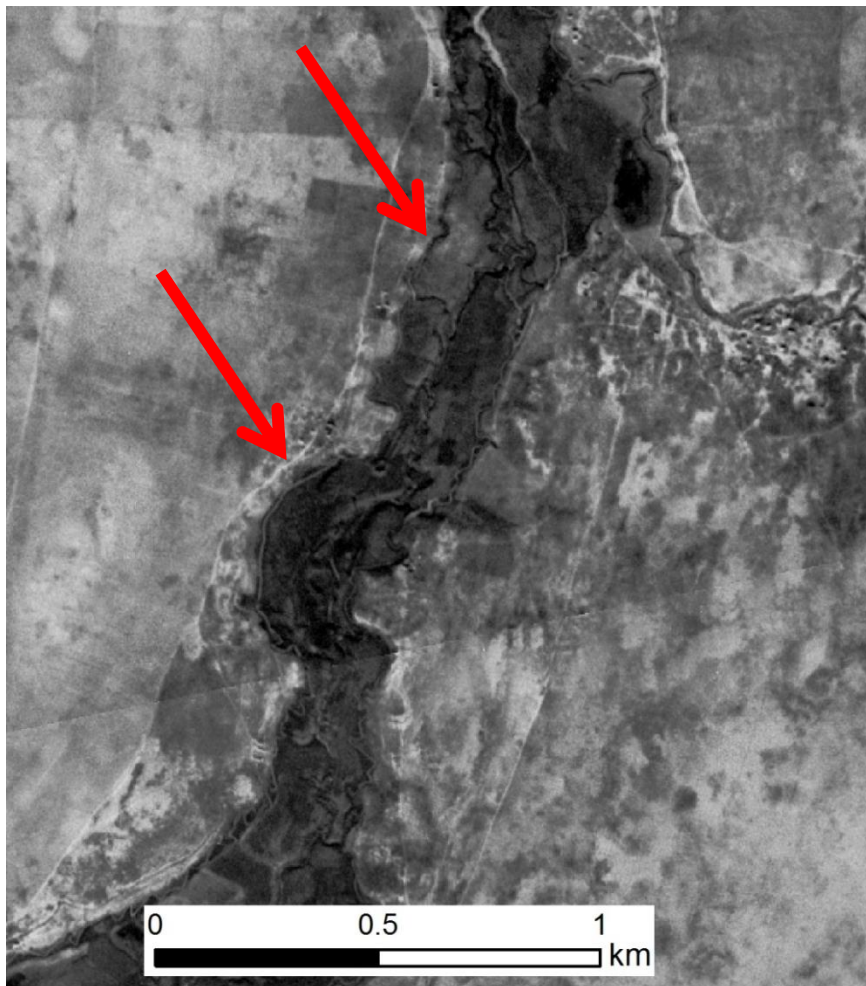


Figure 6.44: *The upper main canal within the central Balikh system.*

The other branch canals of this system (**Figure 6.45**) are situated at lower elevations relative to the main conveyor canal, but are still higher than the channel of the Balikh. Abstracting from higher up the Balikh enables the water to gain sufficient elevation for it to be distributed over slightly raised terrain to form a larger

irrigated zone. The creation of this zone enabled a larger area (of up to 1,300 ha) between the Balikh and Qara Mokh to be cultivated.

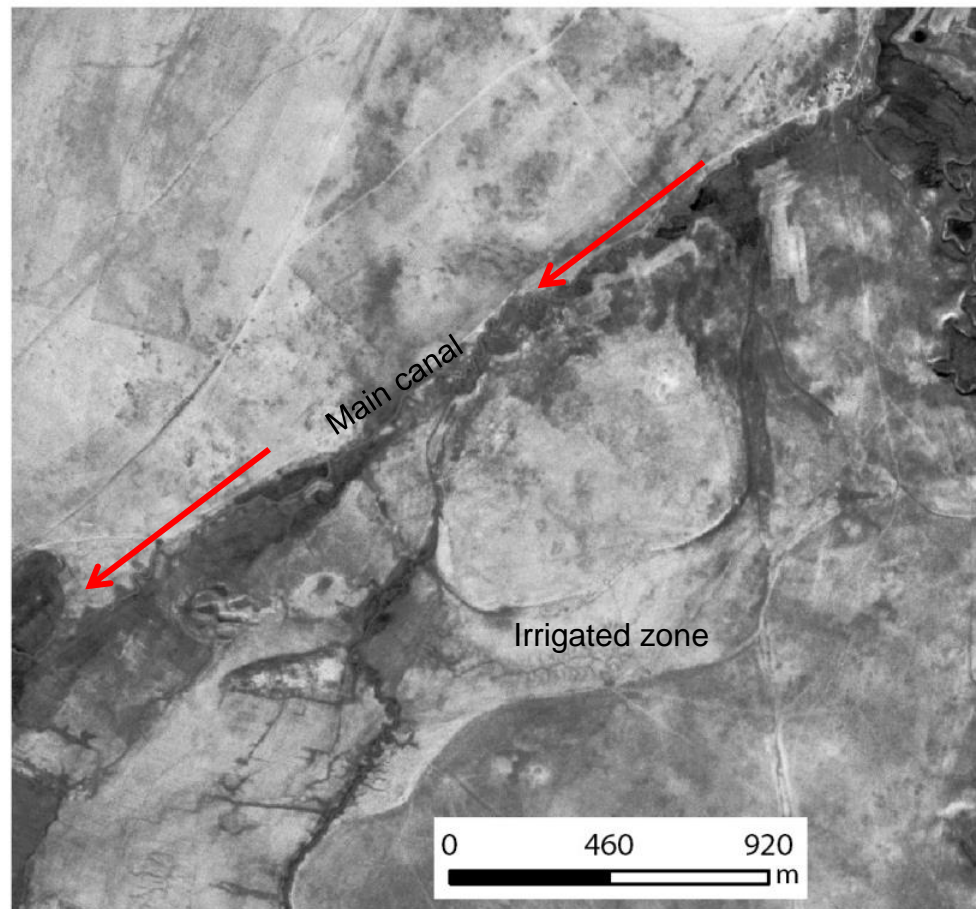


Figure 6.45: The irrigated zone of the Hellenistic system is south of the main canal. CORONA image 22 January 1967.

This system flows at a shallow gradient: just 0.07%-0.1% for the main conveyor, based on SRTM and ASTER (**Figure 6.46; Figure 6.43**). This presumably would have led to significant siltation, which necessitated frequent cleaning. Such siltation may also explain the meandering line of the main canals. The short laterals, however, were located at points where they could make use of the natural topography in order to flow at a steeper gradient of up to 0.4% (see **Figure 6.47, Profile 2** on **Figure 6.43**).

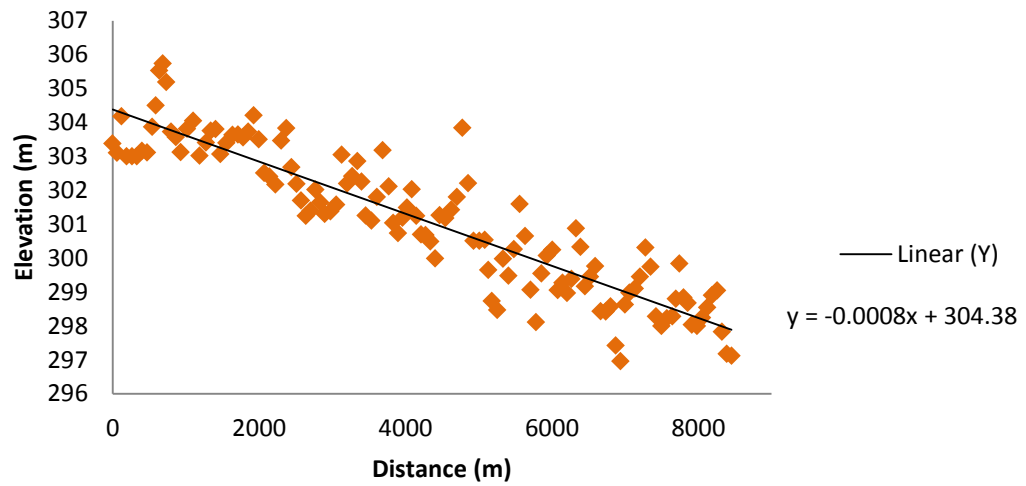


Figure 6.46: Canal long profile 1, main conveyor, measured using SRTM (see Figure 6.43). Gradient: 0.07%.

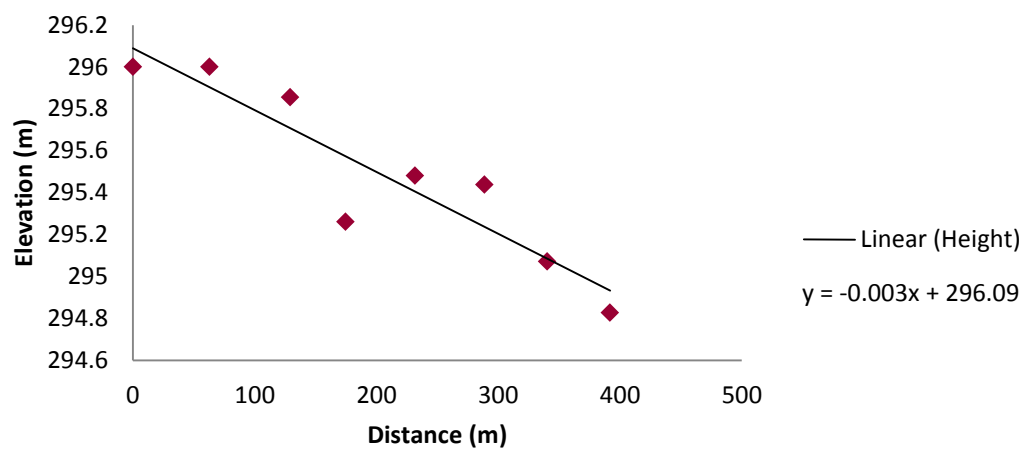


Figure 6.47: Canal long profile 2, lateral channel, measured using SRTM. Gradient: 0.4%.

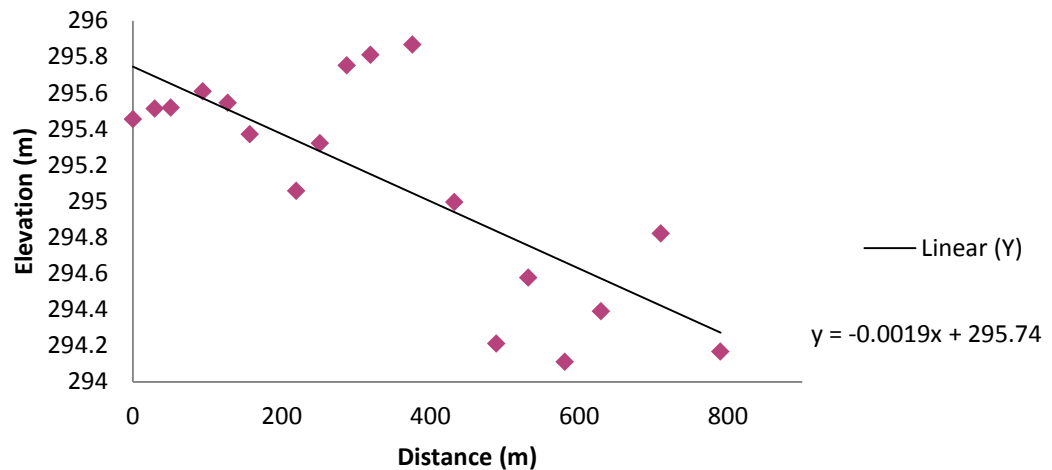


Figure 6.48: Canal profile 3, drain, measured using SRTM. Gradient: 0.2%. There is a high variance of scatter due to the short length of this canal and influence of modern features recorded by the DEM.

It is noteworthy that pre-Hellenistic sites in this central part of the Balikh are more linked to the natural watercourses than to the canals. However, **Figure 6.49** shows that during the Hellenistic period, a pattern of sites developed that is closely aligned to the canals.

Most of the sites cluster along the route of a submain canal and its associated laterals (see **Figure 6.42**). These sites are small, and could represent individual farming settlements which were making use of the irrigated lands. The biggest nearby Hellenistic settlement is Mounbateh (site BS 378), but it is on the other side of the Balikh. It is interesting that there is no major centre clearly associated with the canals in this area, rather they appear to have supplied irrigation water to a dispersed pattern of rural settlements.

It also worth noting that there are canals of a similar appearance and alignment on the opposite bank of the Balikh, above the large Islamic site of Sheikh Hassan (see Bartl, 1994 on this site). These canals also originate from a long canal that flows close to the river, and also have a meandered, partially aggraded appearance.

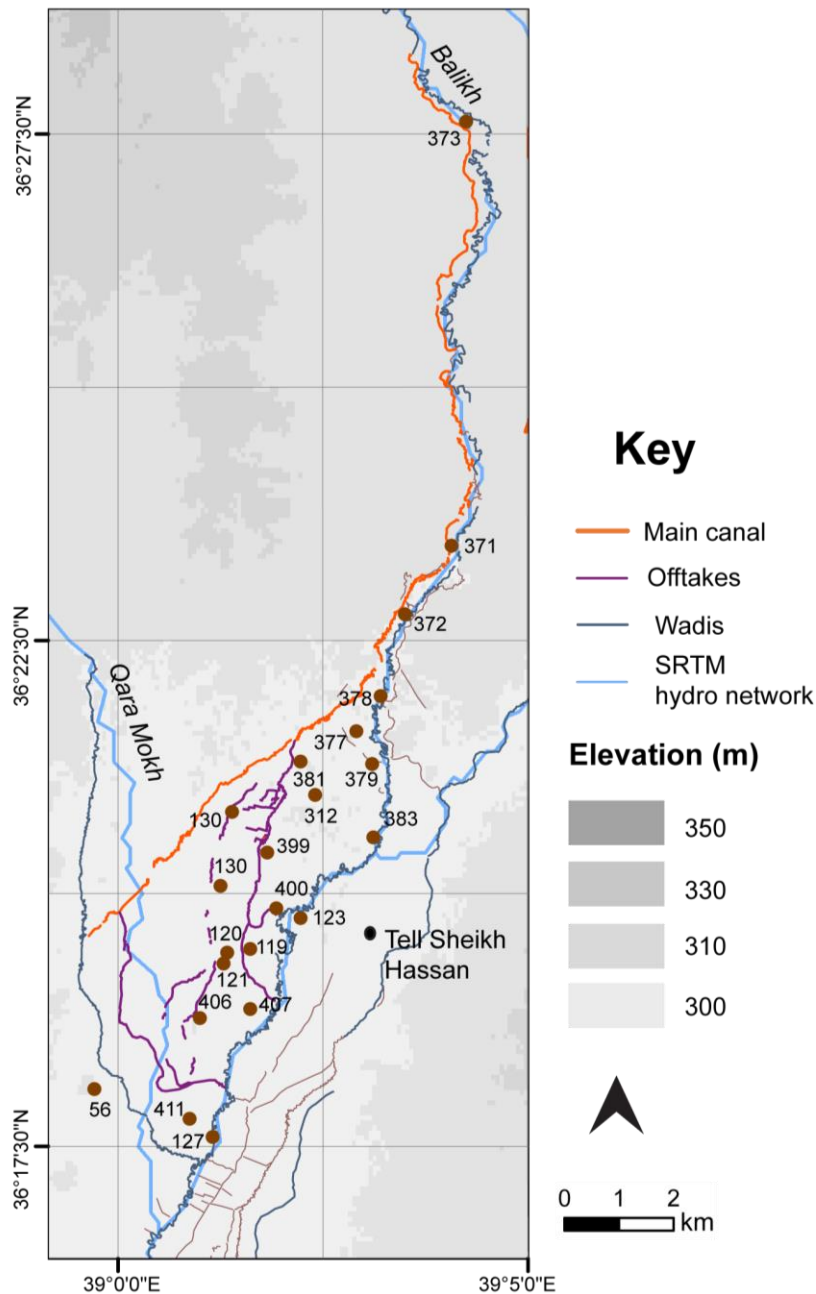


Figure 6.49: Settlement in the area achieved a peak during the Hellenistic period and sites of this date are closely aligned to the canal system.

After the Hellenistic peak, settlement alongside the canals in the central Balikh zone declined. A few Early Islamic sites were situated close to the south end of the system, near the drainage points. The evidence does therefore point towards a Hellenistic date for the main period of use of this canal at this location.

The drainage networks generated using SRTM and ASTER DEMs indicate where natural drainage basins—such as wadis—are located (see **Chapter 3**). However,

with the SRTM, noise can be a problem specifically in areas of low-relief (Sanders, 2007) such as the Balikh, and its resolution is relatively coarse at 90 m. ASTER also contains noise and errors (Slater et al, 2011). However, both datasets have been used for hydrological modelling with workable outcomes (e.g. see Sanyal et al, 2013 for the use of SRTM).

A comparison of the simple drainage network used in this case with a visual inspection of the satellite imagery reveals that the locations of natural drainages almost always correspond closely in both types of data, giving a good degree of confidence when using the DEMs.

In general, while the SRTM and ASTER-based drainage networks are successful at defining the natural streams and wadis, artificial channels are rarely identified as part of the natural drainage network, including some which were still visible at the time when the DEM data were collected. While the natural streams and seasonal channels are readily defined by the DEM networks, features recognised as canals, either in the field or on CORONA images, are evident as distinct anomalies.

There is a discrepancy between the current and mapped course of the Qara Mokh and the modelled one, as **Figures 6.42** and **6.49** show: if this is not due to errors in the SRTM and ASTER, it may suggest that the stream's course was diverted at some stage in the past, possibly due to human intervention. Because the Hellenistic system drains into the channel of the Qara Mokh that is visible on the imagery and not picked up by the hydro network, the diversion/avulsion presumably occurred no later than the Hellenistic period, if not before.

6.5 Qara Mokh: West system

This remote sensing analysis suggests that the Qara Mokh (a west-bank tributary of the Balikh) was used for irrigation as well as for drainage in the past. However, so far, the area to the south-west of the Qara-Mokh, including the western part of the horseshoe, has been neglected by research, representing an empty space on the map of the ancient Balikh. The CORONA evidence suggests that this landscape was heavily exploited even before the modern irrigation schemes

obscured it. Hritz interprets the region of the Wadi al Fayd as a previous course of the Balikh (Hritz, 2013a, p1978). She labels a channel visible in the historical imagery as the palaeochannel itself (ibid, p1981). While a previous course of the Balikh and its relationship with the Euphrates probably shaped this region, the visible channel bears more similarities to a canal than to a natural stream. The evidence for this will now be summarised.

Unlike the other irrigation systems discussed above, the West Balikh channels rely on the Qara Mokh rather than on the Balikh. There is also evidence of attempts to manage and incorporate seasonal runoff in the form of channel straightening and incorporation into canals. The ASTER -derived hydrological model (see **Figure 6.30**) made it possible to distinguish between natural wadis and anomalies in the form of artificial canals: these data were examined alongside information about the morphology of the channels from the CORONA images to identify which features may be man-made.

First, an explanation of dating evidence is needed. Unlike other relict irrigation systems in the Balikh, those of the Qara Mokh have not been excavated or surveyed. A few sites are visible close to the canals (see Hritz, 2013a, p1982), but their dates are not known. Several phases of use, reuse and modifications can be inferred from the complex layers of channels. As will be discussed below, at least one of these phases can be dated by a clear association with a subterranean tunnel. The tunnel diverts water from the Qara Mokh canals and terminates at the Early Islamic palaces north of Raqqa, visibly associated with these remains. This suggests an Early Islamic date for at least one phase of use of the Qara Mokh channels.

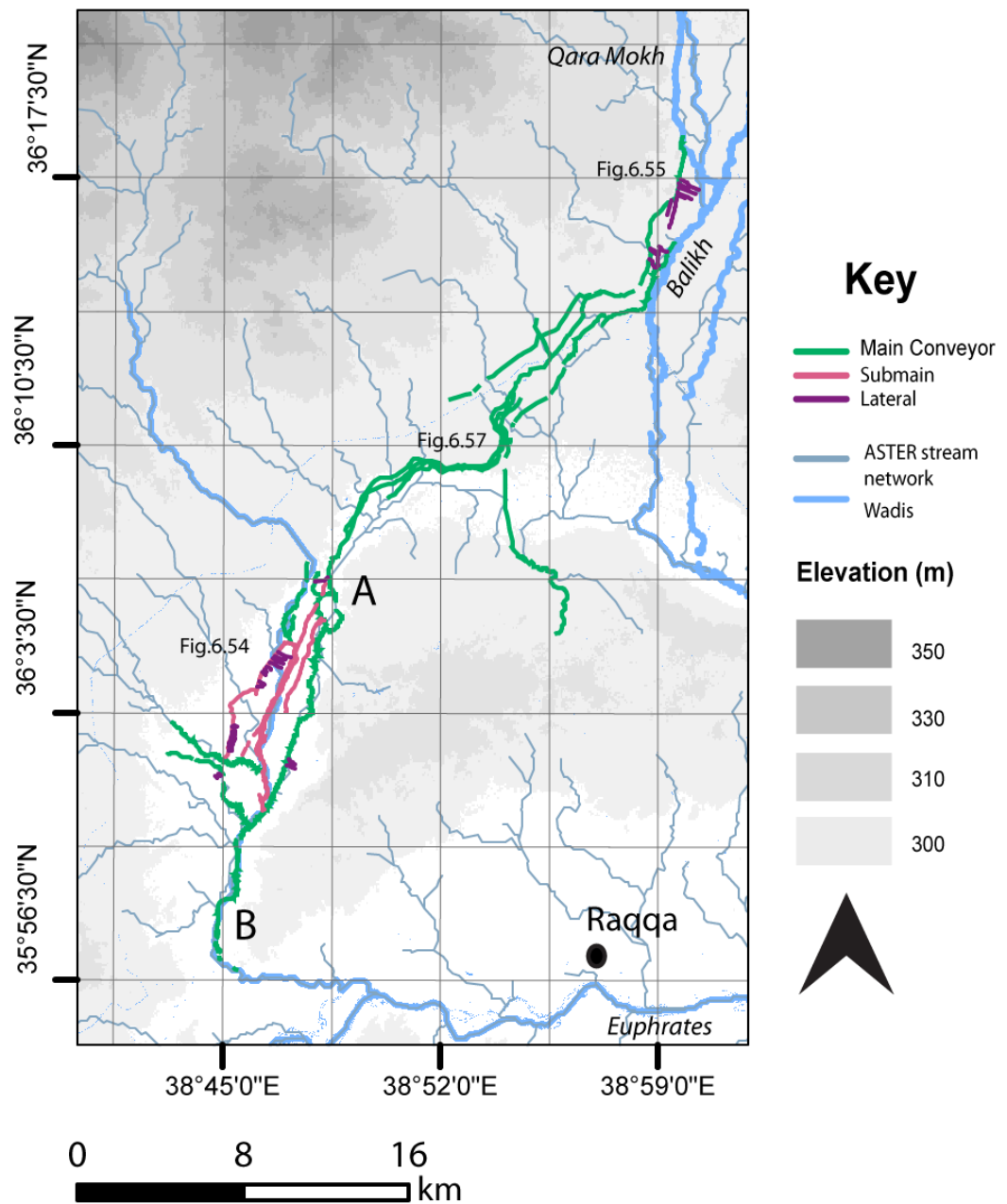


Figure 6.50: Flow network and wadis and canals digitised from CORONA imagery in the west Balikh horseshoe.

The analysis of a time series of images indicates that the West Balikh canals are not modern. The most recent images show that the modern systems have entirely obscured the earlier water management remains (**Figure 6.51**). Using a retrogressive analysis, a Landsat image (see **Figure 6.3**) of August 2000 shows that water management systems in the area are now intensive. An earlier Landsat image of 1990 shows less dense cultivation; and prior to this, the 1984 Landsat

image was clearly collected before the new irrigation scheme was completed. This programme of new water management schemes is well known and has attracted some research; irrigation as part of a major dam building scheme developed in the 1970s (Rabo, 1989, p152). Beaumont (1996) and Hole and Zaitchik (2006) mapped irrigations development in the area using Landsat imagery. Alkhaier et al (2012) studied its impact on groundwater levels and quality. Based on this evidence they suggested areas which might have undergone irrigation within a longer timeframe (ibid. p1837).

Significant use of the modern systems did not begin until the 1980s, however, and parts of this system can be observed under construction in the CORONA images (**Figures 6.52** and **6.54**). The 1972 image shows what appears to be a newly constructed grid of empty, dry canals being built throughout the western horseshoe zone. A regular pattern of large fields can be delineated (for example around 350 x 780m). At the time of the earlier 1967 image, only a few of the new main canals in the south of the zone, near the Euphrates, had already been built (**Figure 6.54**).



Figure 6.51: 2010 Google Earth image of the west Balikh area shows how modern irrigation schemes have transformed the landscape and removed and obscured the relict channels.

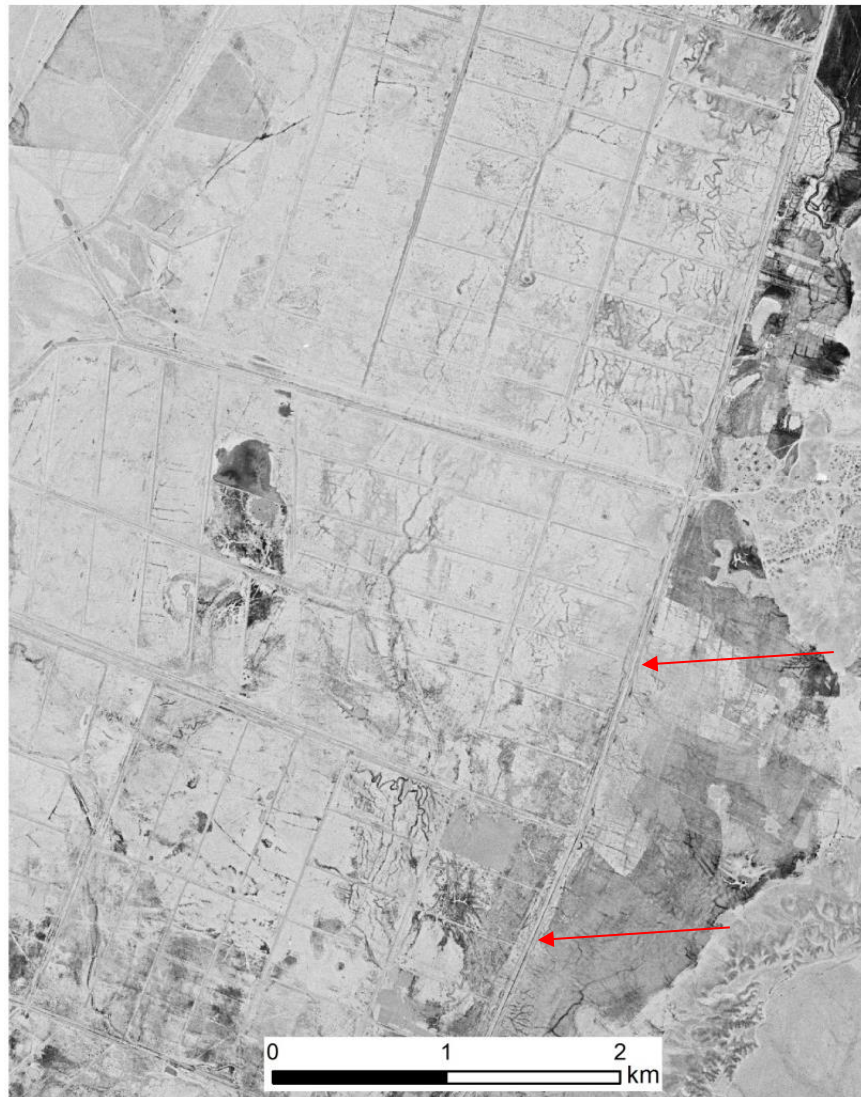


Figure 6.52: 16 May 1972 CORONA image. A newly constructed grid of canals is being built, overlaying the channel pattern visible in the earlier CORONA image. Arrows mark the main canal.



Figure 6.53: 16 May 1972 CORONA image. A newly constructed grid of (dry) canals is being built, overlaying the channel pattern visible in the earlier CORONA image. Arrows mark the main canal.



Figure 6.54: 22 January 1967 CORONA image showing the same area as **Figure 6.53** before the new irrigation scheme was constructed. Arrows mark the former main canal (of straight trace and meandering form) which was replaced by the system visible in the later images.

Based on this series of images it is clear that the current irrigation schemes in the West Balikh did not exist prior to the 1960s: their development from the late 1960s and into the 21st century can be mapped. Given this, what period of use can the many earlier, relict channels visible in the 1967 CORONA image be assigned to?

Aside from a few channels close to the abstraction point with the Qara Mokh, the canals in the West Balikh appear disused and poorly maintained in the 1967 image. No contemporary villages are apparent. As **Figure 6.54** shows, some of the canals are meandering, presumably due to siltation, and many are clearly dry and already eroded. Flooding appears to have damaged others, and un-managed waterlogging has led to the development of gilgai (see **Chapter 6.1**). The canals appear to have been abandoned for at least a few years prior to 1968.

It was only after the 1920s that agriculture began to intensify in the region (Wagstaff, 1985, p241), primarily after the Second World War (Lewis, 1955, p60). Although the introduction of canals after the 1940s would make their use very short-lived (possibly less than around 30 years), given that new systems were already replacing them in the 1960s, the period from around 1920-1960 is one contender for the West Balikh canals.

An earlier date is also possible. However, historical information suggests that this part of Syria was not intensively cultivated during the 18th, 19th and early 20th centuries. Permanent settlements were rare (Hole, 2006, p144). Insecurity in the provinces during the Late Ottoman period (Lewis, 1955, p48) might have been the reason behind this decline in cultivation.

During the 18th, 19th and early 20th centuries the area may well have been devoid of significant irrigation, although there has been little research into Ottoman water management in general. The West Balikh canals could have been used before this later Ottoman period. At intervals Raqqa had some importance as a regional centre, being at the frontier of the Ottoman empire (Winter, 2009), although a decline in cultivation may have occurred (Kanieski et al, 2013, p3865). Before this time, a surge in agricultural prosperity in Northern Syria is suggested for the Ayyubid-Mamluk periods by contemporary geographers (Kaniewski et al, 2012, p3864). New irrigation activity might have been concomitant with this. Canals of a similar appearance in the Wadi Zerqa mapped from 1940s images could be traced back using travellers' accounts at least to the 1840s (Kaptijn, 2009, p311): a similar trajectory for the Qara Mokh canals could be possible.

The association with the Raqqa tunnel may even indicate an Early Islamic phase of irrigation in the West Balikh area, a period when Raqqa and the Balikh were

even more politically important. It is possible, therefore, that water management in the West Balikh area began in the Early Islamic period, and continued into the Ottoman era. There might have also been a separate, short-lived phase of irrigation in the early 20th century.

Now that dating possibilities have been summarised, the different channels and their function within the network can be described. The CORONA images (see **Figure 6.55**) show that the first set of channels appear to have abstracted water from the Qara Mokh, and these are the only part of the system that appears to have been in use in the 1960s. Like the central canals, the main canal has a very shallow gradient of 0.07-0.1% (SRTM and ASTER data) (see **Figure 6.56**), but the laterals flow perpendicularly down the slope and attain somewhat higher gradients.

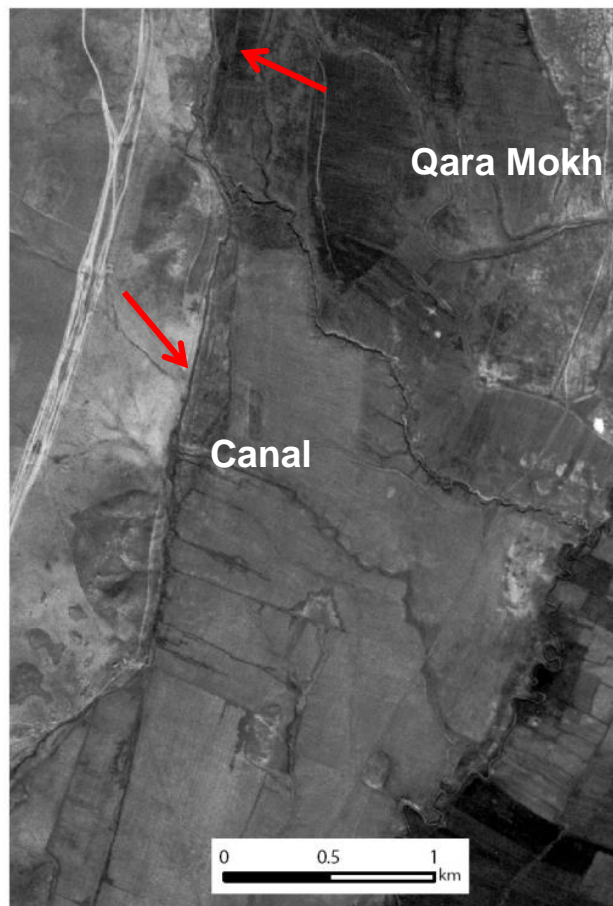


Figure 6.55: A main canal abstracting from the Qara Mokh is visible along with laterals draining eastwards towards the Balikh (Long profile 1). CORONA image 22 January 1967.

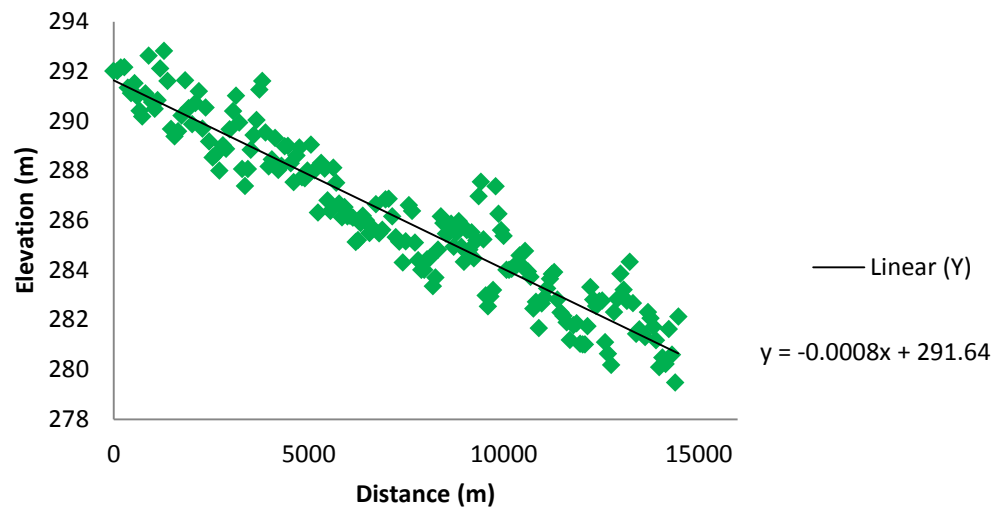


Figure 6.56: Longitudinal profile of the main canal of the Qara Mokh/West Balikh system, measured using SRTM (see **Figure 6.50**; profile taken along route of canals from point A to point B). Gradient c.0.07-0.08%.

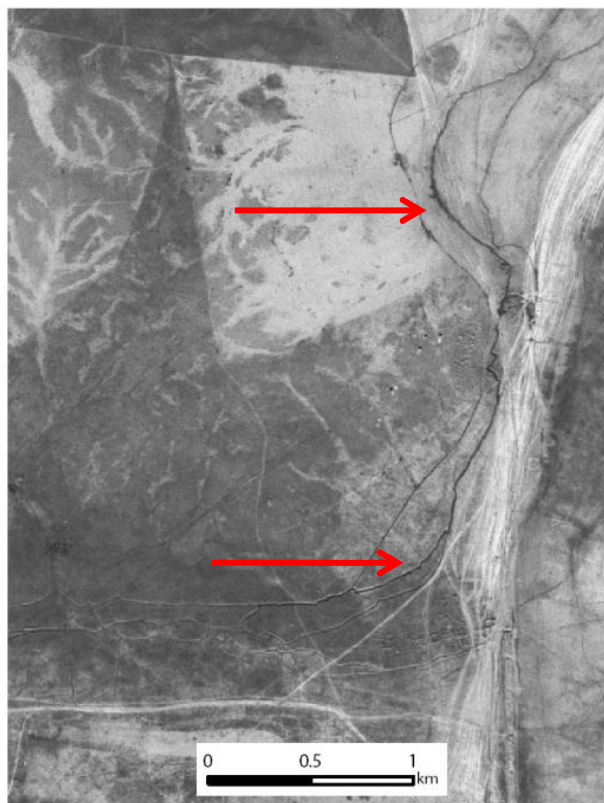


Figure 6.57: CORONA image showing multiple conveyors along a hillslope. Image 22 January 1967.

A parallel alignment of channels originating from the Qara Mokh canals is apparent and may be significant. As the CORONA image shows (**Figure 6.57**) these are fairly narrow features of straight appearance suggesting that they are unlikely to be paleo-channels of natural rivers (although they have been interpreted this way, see Hritz, 2013a). They appear to be associated with a loose pattern of remains forming an unstructured, possibly Early Islamic, settlement. The possible canals flow along a shallow hillside, following the contours (see **Figure 6.58**). This could constitute a specific form of irrigation that allowed the whole hillside to be watered. As such, they have shallow gradients.

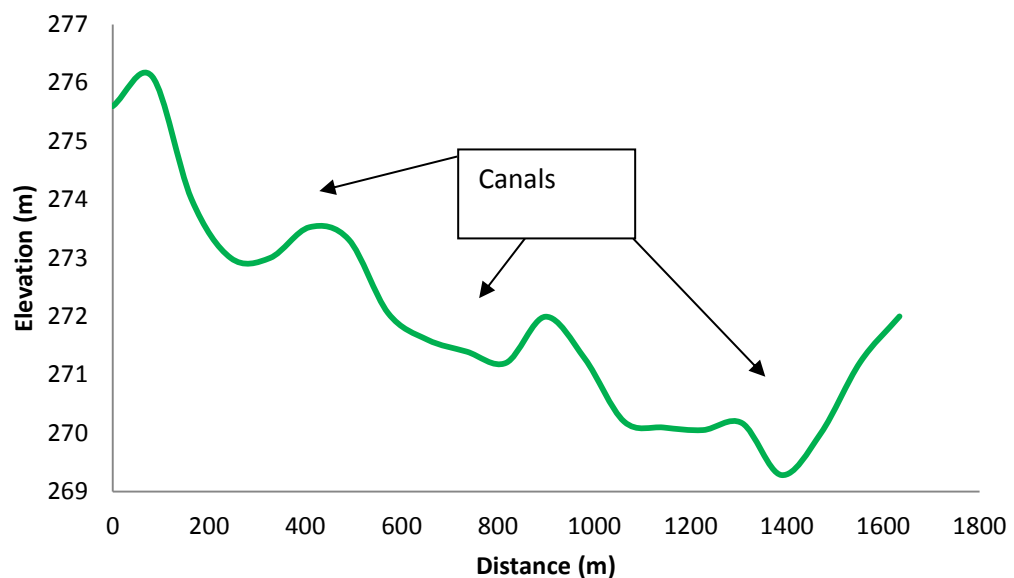


Figure 6.58: Cross section across multiple conveyors of Qara Mokh system (see **Figure 6.57**). These flow at different levels along the side of a slope and may have been intended to intercept runoff.

These canals are crossed by a wadi just after they begin to fade on the CORONA image. The channel of this wadi appears to be canalised. Another main channel of straight trace but meandering form originates here (e.g. see **Figure 6.50** and **Figure 6.54**). It may have been receiving water from both the Qara Mokh system and from runoff wadis. This channel has been interpreted by Hritz (2013a) as a paleochannel of the Balikh, and indeed the ASTER DEM does identify the downstream segments of this feature as a natural channel. Associated, flooded

laterals (again, see **Figure 6.54**) and the straight trace of the channel may be evidence of modification of this stream and are certainly evidence of its use for irrigation at some time in the past. The main channel flows for about 20 km before presumably draining into the Euphrates: its terminus was either obscured or erased by more recent cultivation or by movement of the river.

Some of the laterals are in the form of straight, short, narrow channels flowing perpendicular to a straight main or sub-main canal (see **Figure 6.54**), showing a similarly regular alignment to the examples of relict canals known from the Hohokam region (see **Chapter 4, Figure 4.9**). In the case of the Hohokam, it has been proposed that this alignment represents the technique of wild flooding (Masse, 1981, p412): it is possibly that a similar technique was used in the Balikh horseshoe.

Evidence of flooding surrounds the West Balikh canals (see **Figure 6.54**). Seasonal, excess water would have been relatively constrained between the two areas of higher ground on either side of the narrow valley, without recourse to the kind of drainage options which the Nahr al Abbara had. The ASTER hydro model and DEMs (**Figure 6.50**) show the large contributing area of this relatively small drainage basin.

In amongst faded traces of straight canals and laterals, there were many relict, sinuous streams within the west valley which may be a result of flooding and avulsion. The multiple canals constructed may in part have been an attempt to deal with this occasional but potentially catastrophic seasonal runoff. The runoff could have been a useful resource if collected and contained effectively. For the rest of the year, the system relied on the waters of the Qara Mokh. The maintenance and management associated with this problematic system would presumably have been complex and it may never have been as successful as the Nahr al Abbara.

6.6 Raqqa

Thus far this chapter has described the rural water management systems of the Balikh valley. In general, these seem to represent the later periods, primarily the Early Islamic period onwards. This was a time when the settlements of Raqqa and Al Rafika in the south of the Valley became especially prominent. Throughout the Imperial periods, Raqqa had been at the frontier of various empires, including the Seleucids and Byzantines (Challis et al, 2004). It then attained increased importance in the Early Islamic period, under the caliphs al-Mansur and Harun ar Rashid: For a brief time under Harun ar Rashid it was the centre of the Abbasid Empire.

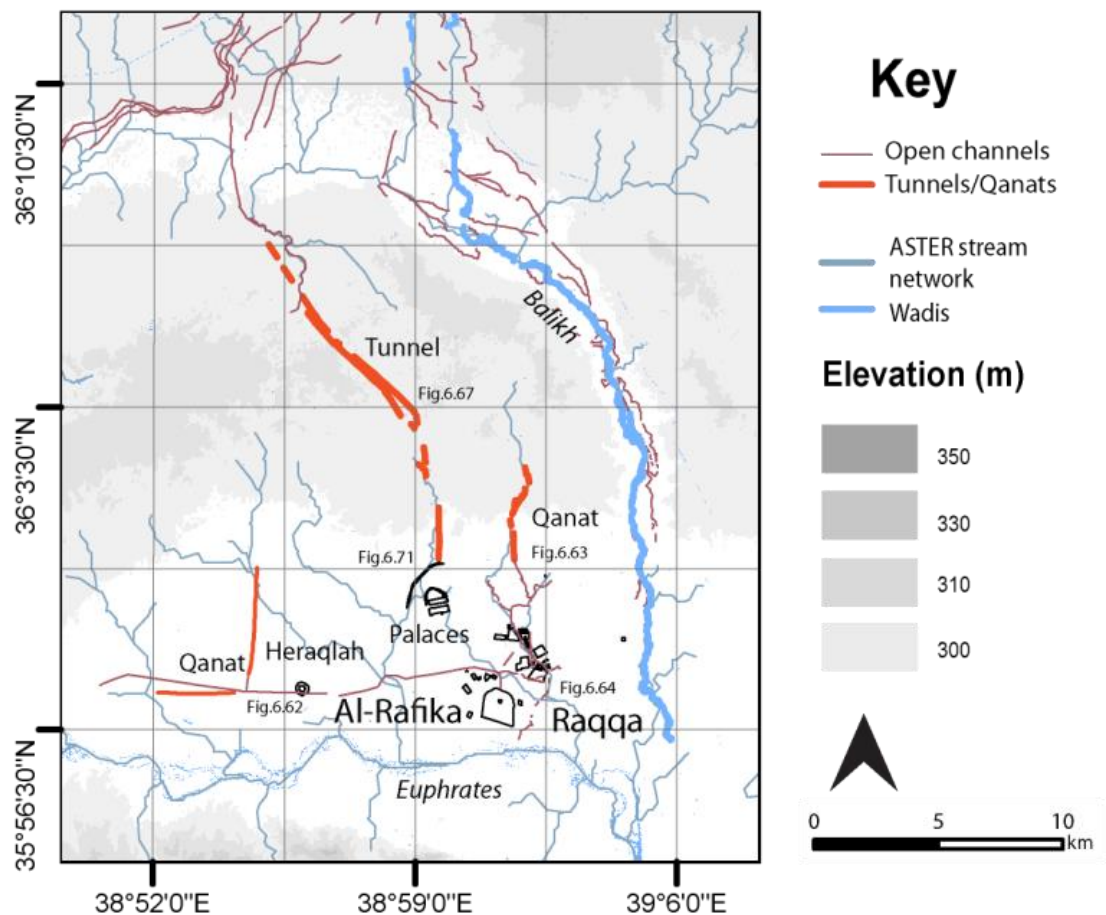


Figure 6.59: *Tunnels and qanats around Raqqa.*

The two settlements were originally separate entities (Raqqa and al-Rafika). Ancient Raqqa probably overlies the Hellenistic Nikephorion and Seleucid Kallinikos; Rafika (which is the centre of modern Raqqa) is the wall-enclosed town

to the west, built in the Early Islamic period (e.g. see Challis et al, 2004, p130). However, the whole area eventually came to be known as Raqqa.

The 1967 CORONA image enables the water supply which supported the power of this city to be identified. It reveals that Raqqa and the Abbasid palaces to the north-west of the city had separate water supplies. In addition, between Raqqa and Rafiq a several canals flow through an Early Islamic industrial area and are obscured by later activity. Although Heidemann interpreted these as Early Islamic features (Heidemann, 2006), this interpretation is incorrect for a long feature running west-east. On examining the large canal in the field in 2010, it was found that it clearly cut through the walls of the Abbasid site Heraqlah: it was also clear that the canal was long abandoned and in a dry and eroded state. The upcast banks were about 1.5-2 m high, with a channel void about 10-12 m wide.

This interpretation is re-enforced by the 1967 CORONA image which clearly shows this E-W canal cutting through the outer walls of Heraqlah (see **Figure 6.62**).



Figure 6.60: *eroded and overgrown post-Abbasid canal viewed from the north in 2010. The canal cuts through the site of Heraqlah (the canal is just behind the donkey).*

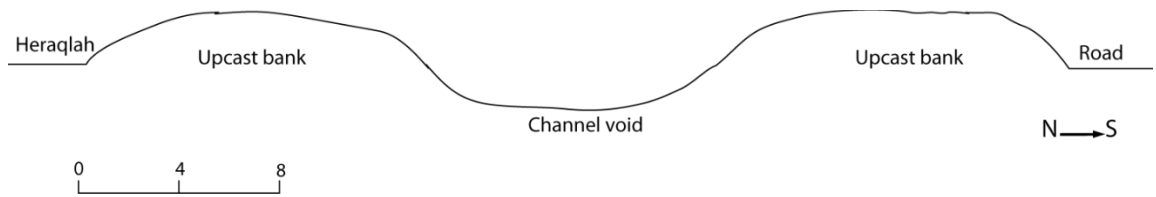


Figure 6.61: *Sketch profile of post-Abbasid canal.*

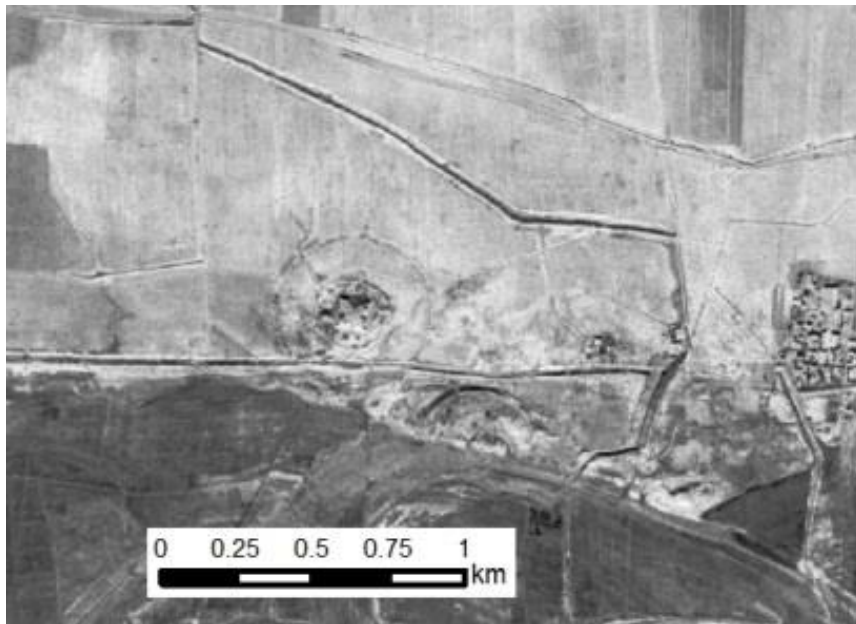


Figure 6.62: *The east-west canal which clearly truncated Heraqlah. 1967 CORONA image.*

There are also qanats flowing from the west and north of Heraqlah. It is unclear whether or not these are cut by the post-Abbasid canal. The qanats have been interpreted as Umayyad (Kamash, 2009, vol3, p4). The site itself contained two wells, on either side of the eastern iwan, c.10 m apart. A raised line of ground between them suggested that an underground tunnel connected the wells. The wells appear to be contemporary with the site, and when visited in 2010 were both choked with masonry. Significantly, this is similar to the construction at Dibsi Faraj (Harper and Wilkinson, 1975, fig. H). It is interesting that at both sites qanats were also present.

The Early Islamic canals which supply Raqqa from the north also seem to derive from a qanat, possibly the principal water source of the Early Islamic city. The qanat leads from the higher ground to the north down towards Raqqa, and then opens out into the surface canals (**Figure 6.63**).



Figure 6.63: A qanat north of Raqqa terminates in an open channel. CORONA image 22 January 1967.



Figure 6.64: General location of canals derived from a qanat which supplied Raqqa. CORONA image 22 January 1967.

As **Figures 6.64** and **6.65** show, three canals flowed into the area between Raqqa and Rafiqa. The large channel visible in **Figure 6.64** running west-east is the post-Abbasid canal discussed above. One of the other two canals clearly originates in a qanat. The longer canal either originates in the same set of qanats, or from another source that had disappeared by the time the CORONA images were taken. This was a much straighter channel and terminated in a depression which may represent the location of a former cistern (*birkeh*- cf. the cisterns at Resafa) amongst the Early Islamic palaces (**Figure 6.65**). The other channel is more meandering, and only flows for c.5 km before fading out in the vicinity of Tell Bi'a and presumably draining into the Euphrates. Interestingly, the two channels cross each other: it is possible to ask whether one post-dated the other, or if a device such as inverted siphon was used. A fragment of another qanat can be seen just 1 km from the walls of al-Rafika.

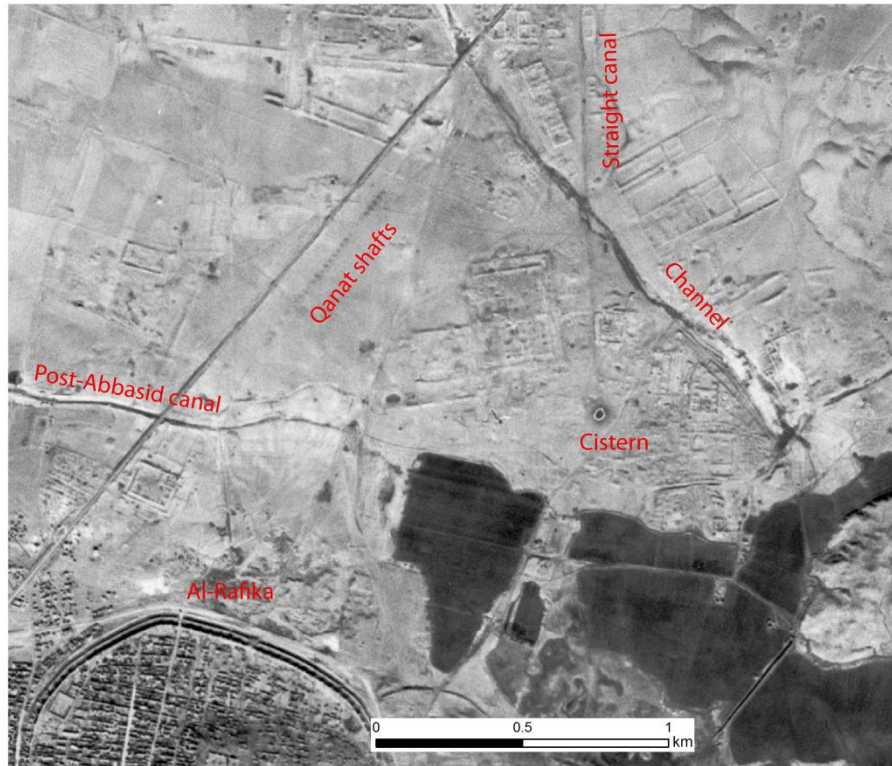


Figure 6.65: Canals, the depression of a former cistern, and part of a qanat identified on the 1967 CORONA image. The walled Islamic city is evident in the SW of the image.

Several palace complexes to the north of Raqqa have been identified on the CORONA images. A particularly large set of structures (**Figure 6.71**), also interpreted as an Abbasid palace (Challis et al, 2004, fig.2), is at the periphery of the Early Islamic palace complexes. The feature has similarities to other palaces of the same period, with components that may represent a race course and a hunting park (e.g. see Northedge's discussion of Samarra, 2005).

Significantly, however, this palace complex has its own water supply, separate from the qanat that feeds Raqqa and Rafika. It originates as an open channel (see **Figure 6.59** and Wilkinson and Rayne, 2010), connected to the west Balikh system of canals which abstract from the Qara Mokh. As the ASTER DEM shows (**Figure 6.66**), it then flows for about 25 km before reaching a major obstruction in the form of an elevated area of steppe.

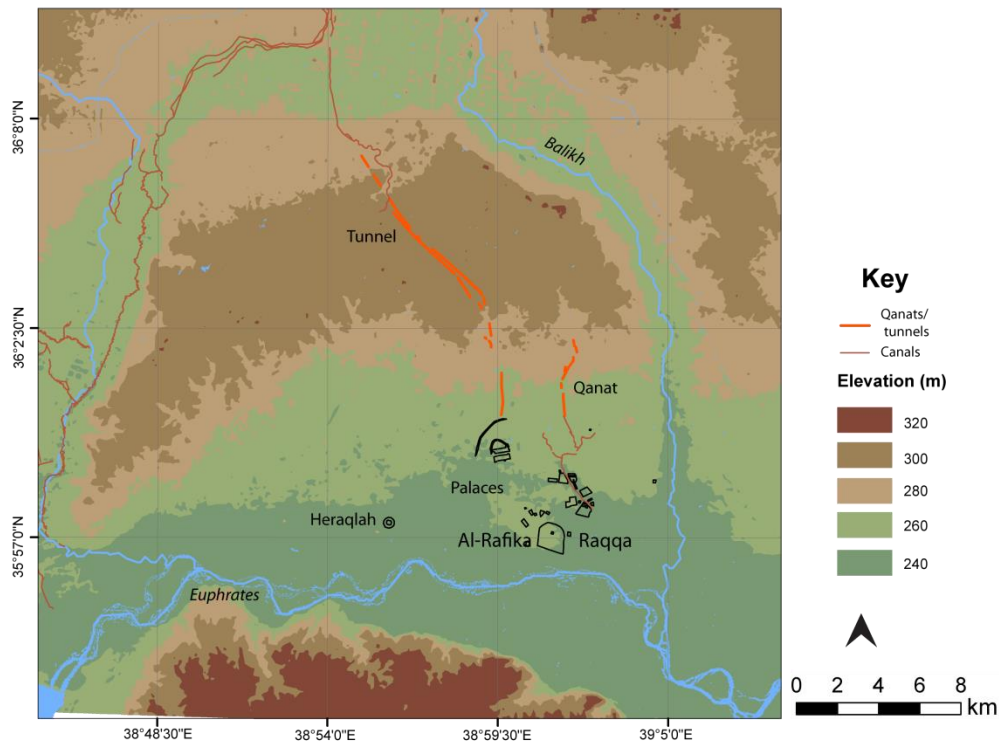


Figure 6.66: The ASTER DEM shows that a qanat originates in an area of elevated ground north of Raqqa. Another open channel becomes a tunnel in order to traverse this area.

In order to traverse this upland, the canal cuts straight through the higher ground, becoming a tunnel. Maintenance shafts at the surface give the feature a 'qanat-like' appearance (**Figure 6.67**). There are known, dated parallels for such tunnels in the Neo-Assyrian period in Iraq: for example the Negub tunnel which supplied 9th to 7th century BC Nimrud in Iraq (**Figure 6.68**). However, in this case the associated archaeological sites suggest that the tunnel is Early Islamic.

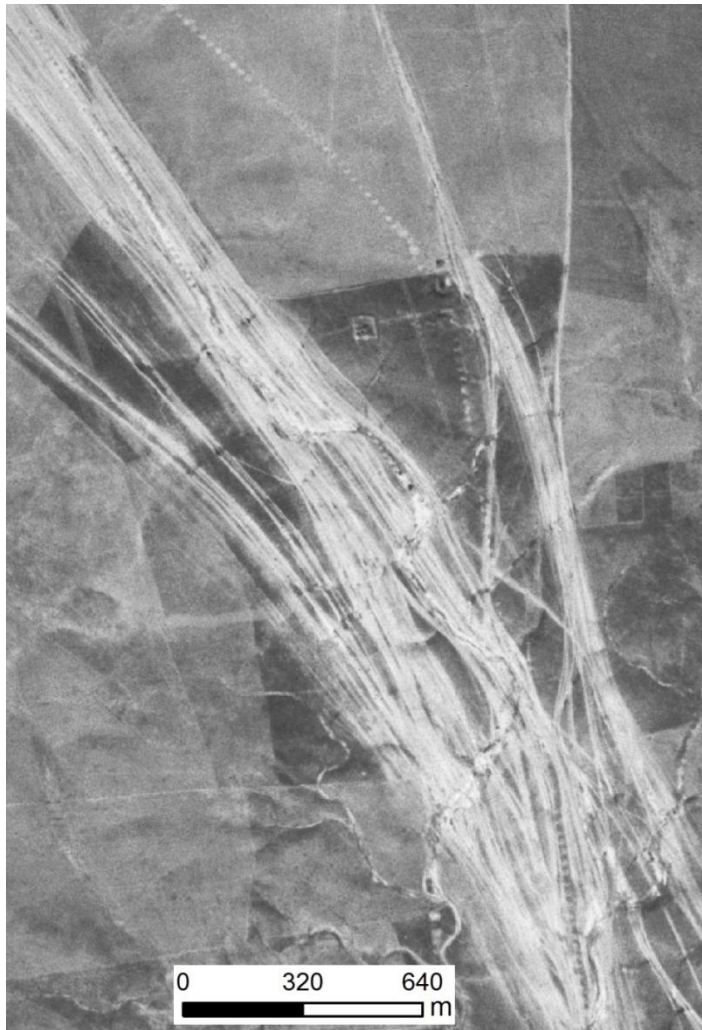


Figure 6.67: Tunnel shafts indicated by pale coloured upcast mounds. The large number of straight pale coloured features are modern dirt tracks leading north from Raqqa. CORONA image 22 January 1967.



Figure 6.68: This example of a Neo-Assyrian tunnel in Iraq can be used to gain an idea of what the Raqqa tunnel might have looked like (personal communication, Stephanie Dalley).

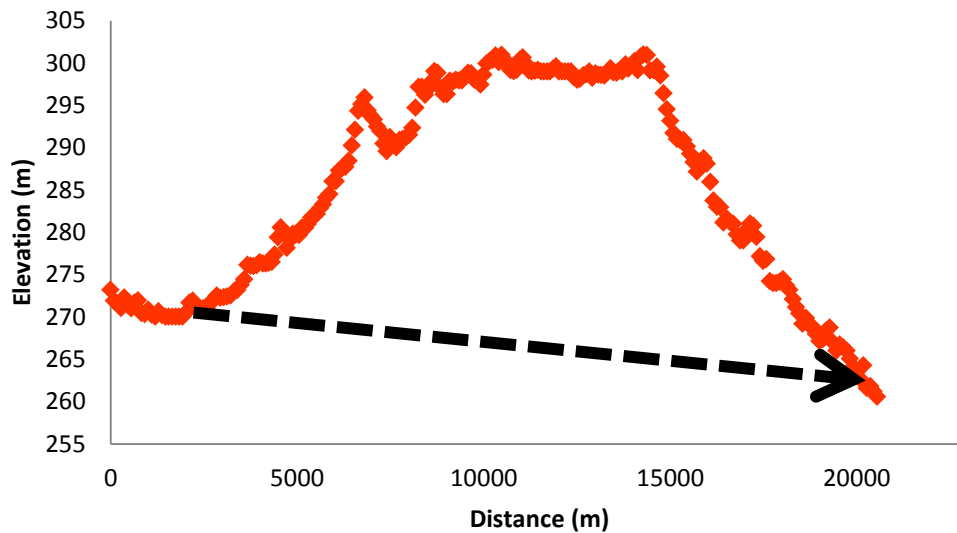


Figure 6.69: The surface of the Raqqa tunnel compared with its projected route.

Figure 6.69 shows the elevation of the ground surface above the tunnel from the point at which the channel meets the higher ground and becomes a tunnel. This indicates that the channel must have flowed as deep as 30m below the surface for about 10-15 km.

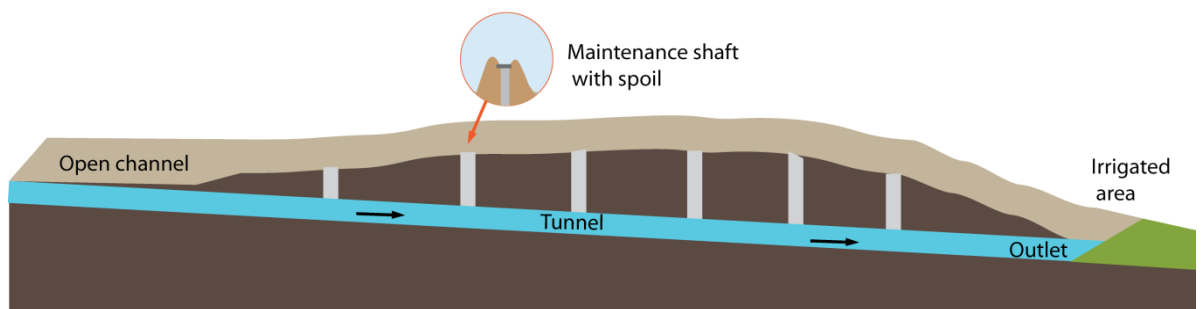


Figure 6.70: Schematic view of suggested tunnel

Figure 6.70 provides a schematic reconstruction of the feature. Once the higher ground is successfully traversed, it becomes an open channel again. Control structures in the form of cisterns are associated with it at this stage (see **Figure 6.71**). Finally, the channel fades out within the hunting park/race course area of the Abbasid palace. It is possible that it could have extended further south and supplied the other palaces, however this is not clear on the CORONA images.

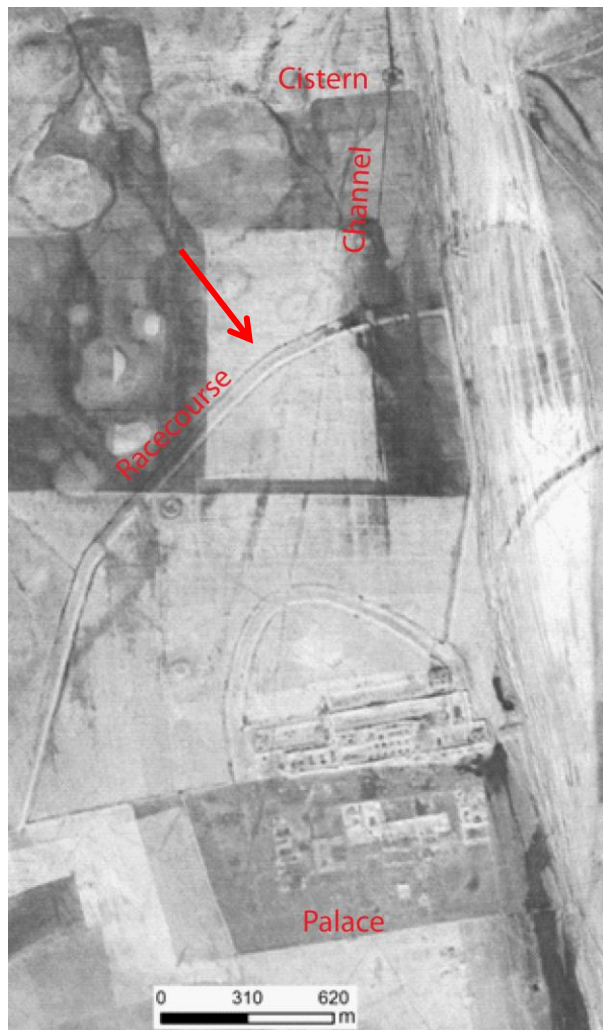


Figure 6.71: Abbasid palace with a possible race course (cf. Samarra) and an outlet channel with cisterns. CORONA image from 1967.

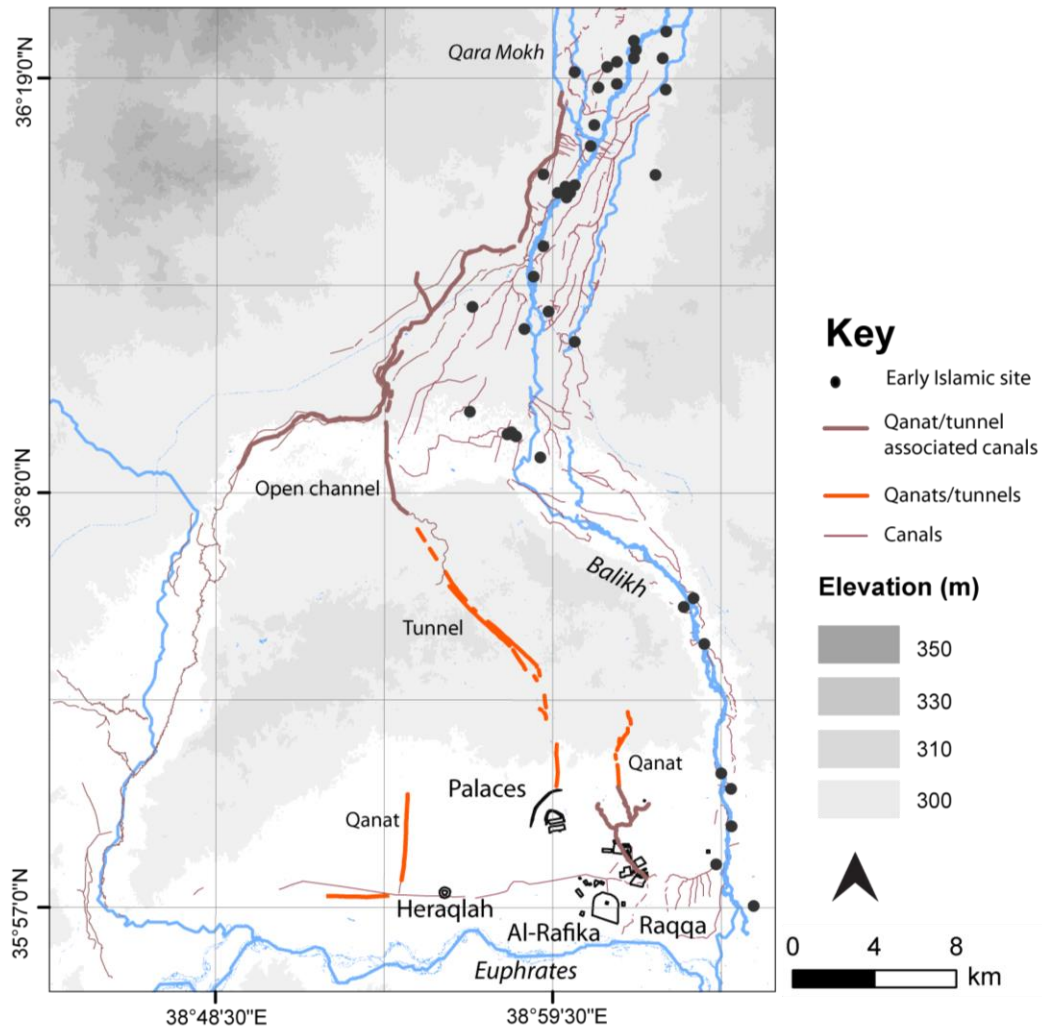


Figure 6.72: Early Islamic canals, sites and other water features around Raqqa and Heraqlah.

As **Figure 6.72** shows, Early Islamic settlement extended throughout the southern Balikh Valley. Many of these smaller settlements may have been relying on other canal systems such as the Nahr al Abbara in the north of the valley, but altogether this combined complex of canals, qanats and tunnels appears to have provided the support for the economic and political power of Raqqa. It is clear from the above evidence that the city itself utilised several separate sets of water management systems. In this semi-arid environment, the complexes of elite residences with associated parks and gardens and industrial activities must have required large volumes of water: the qanat could have supplied the settlements of Raqqa and Rafika, whereas the tunnel from the Qara Mokh area could have

supplied the palaces and parks. The qanats around Heraqlah could also have supplied Early Islamic sites and fields.

6.7 Summary

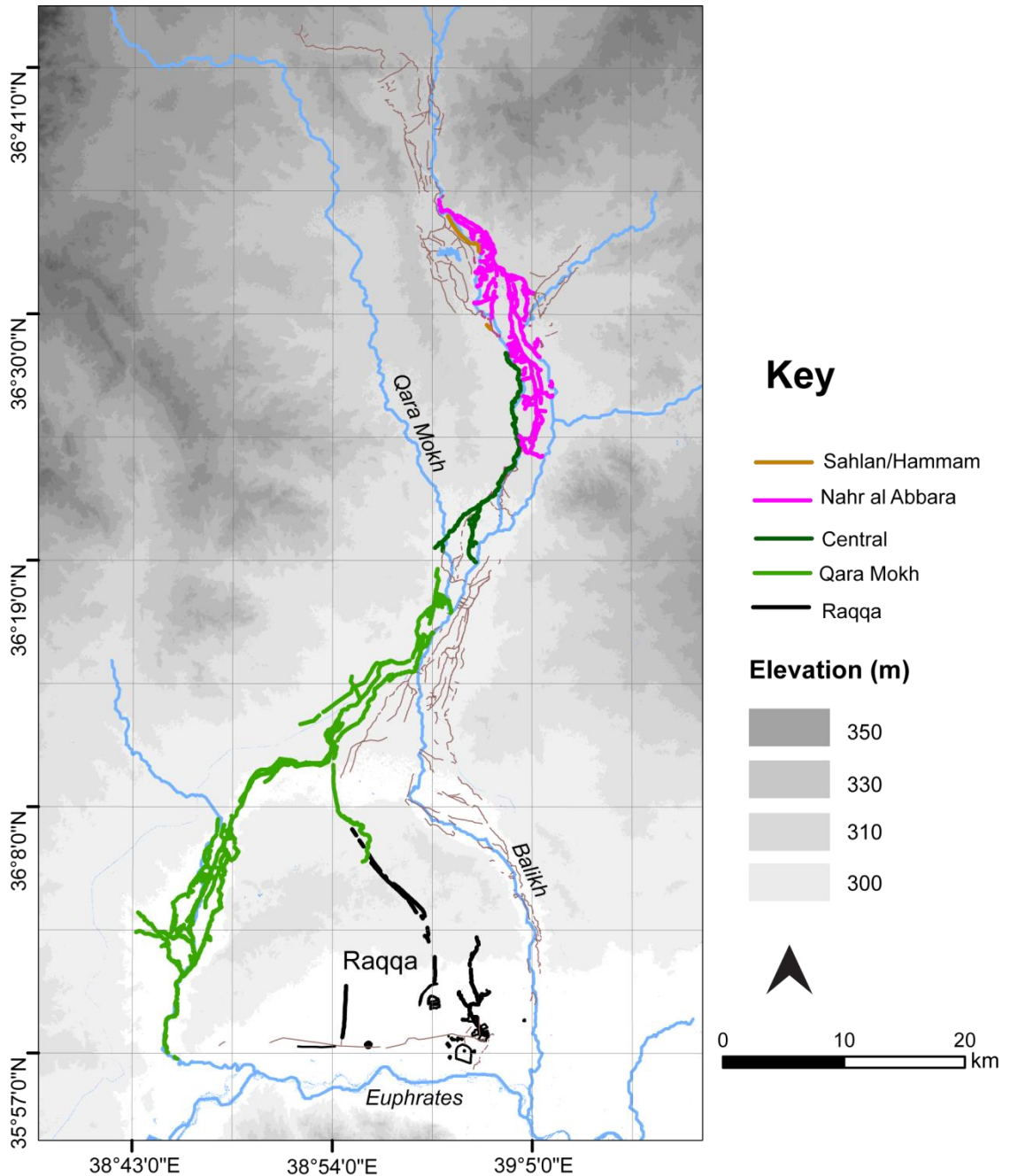


Figure 6.73: Several separate water management systems in the Balikh valley could be unpicked from the layers of channels and investigated using DEMs and archaeological data.

This chapter has described the relict water management features in the Balikh Valley for which a date can be suggested, either through excavation, survey, or by association with other dated archaeological sites. These are illustrated in **Figure 6.73**. Other potentially ancient channels in the valley exist, however, until such time as they can be investigated through fieldwork, these are not discussed here.

The results presented in this chapter can now be summarised. Despite the complex palimpsest of relict canals represented in **Figure 6.8**, by taking an interdisciplinary approach using remotely sensed and survey data specific water management systems could be identified. Several of these represent large-scale irrigation systems with the potential to abstract a significant proportion of the available water resources.

Table 6.3: *Summary of key results.*

Canal system	Gradient of a main canal, based on SRTM and ASTER	Dating information
Sahlan/Hammam	0.2-0.4%	Hellenistic-Byzantine
Nahr al Abbara	0.1%	Early Islamic
Central	0.07-0.1%	Hellenistic
Qara Mokh	0.07-1%	Early Islamic-later?
Raqqa	Qanats	Early Islamic

Table 6.3 lists the key results which enabled this identification. Image interpretation of the CORONA images showed five key groups of channels (see **Figure 6.73**; also **Table 6.3**). While some groups of channels were more fragmentary, it was possible to recognise the differences between individual systems, and also between main canals and offtakes. For example, the layout and hierarchy of the Nahr al Abbara system was very clear in the imagery. Topographic data derived from DEMs (SRTM, ASTER and CORONA) facilitated an analysis of gradient information. The data show that canals were flowing at very shallow gradients, generally lower than values recommended in the modern irrigation literature (see **Table 4.1**). All the canals were inevitably constrained by the shallow slope of the Balikh Valley, however, where possible, the lateral canals were generally located perpendicular to the main canals to allow more elevation to

be gained. The main conveyor canals of the Nahr al Abbara and the central Balikh area were aligned to the highest areas of ground in order to facilitate this.

By using information from survey and excavation reports it was possible to understand the phasing of each system. The Sahlan-Hammam canals and the canals in the central Balikh represent earlier phases of activity. The earliest system known archaeologically, the Sahlan-Hammam system, is fragmentary, short, and relatively simple when compared to the later systems, as **Figure 6.73** shows, despite its size and embankments. The irrigated fields that derived their water from the canal can no longer be traced, presumably because they have been erased by the more recent agricultural systems. The irrigated area of the canals in the central Balikh area could be ascertained, however, based on the presence of some offtakes and Hellenistic sites.

The Nahr al Abbara, the West Balikh/Qara Mokh canals and the channels around Raqqa are linked to the Early Islamic period. The Nahr al Abbara is a good example of how successful ancient engineering could be, by making use of natural topography to overcome the potential limitations of a landscape. **Figure 6.73** shows the significant extent of the West Balikh canals, parts of which appear to represent a reticulated system. Raqqa itself and the palaces around it had separate water supplies, suggesting the great demands placed on the available water resources by the presence of the imperial state.

The evidence from the Balikh shows a peak in irrigation development in the Early Islamic period. After this peak, settlement and cultivation in the Balikh seem to have declined so that by the early 19th century Raqqa and al-Rakifa were in ruins (see Bell, 1924, p55-56). The geographical and political scales of the Early Islamic peak in water management within a wider Near Eastern context will be investigated in the next chapter.

Chapter 7: Discussion

7. 1 Introduction

The results presented in **Chapters 5** and **6** have enabled the main aim of this research to be addressed; namely, to map ancient water management in northern Mesopotamia at the time of the later empires, taking an innovative and interdisciplinary approach which uses remote sensing, GIS and archaeological survey. The results facilitate a discussion of the implications of the scales of control over water exercised by the later territorial empires (Neo-Assyrian-Early Islamic), with interpretations of how empires might have imposed and incentivised the use of water management technology

First, existing concepts of ancient water management are discussed to emphasise how particular perceptions and methods have created a need for new evidence and a more multidisciplinary viewpoint, followed by a summary of the chronological trajectory of irrigation. The methodological advances that this research has applied to the field will then be assessed in terms of how this work has built upon a more traditional approach to understanding ancient water management, and the way in which this evidence can be evaluated. The distribution and scale of ancient canal systems across the northern Mesopotamia will then be discussed, followed by an analysis of how these results support a model of imperial control and enhancement of the landscape.

7. 2. Theoretical framework

In order to evaluate the contribution of the present study to the subject of ancient water management, the contribution of the existing literature to the project's theoretical framework will be assessed. It is important to understand how the different approaches used have shaped knowledge of ancient water management. As outlined in **Chapter 1**, ancient water management has traditionally been discussed in a framework of water and power. Wittfogel's hydraulic hypothesis (1957), which suggests that the management of water resources leads to state development in terms of despotic power, has underpinned much of the existing research.

Whether large scale systems always represent a complex level of administrative and possibly despotic power has been debated (e.g. see Adams, 1974; Mabry, 2000). Criticism of the hypothesis has suggested that it is possible for irrigation to function without the apparatus of a large state or empire, being instead organised by local groups (e.g. Hunt and Hunt, 1974, p153; Mabry, 1996). Sheridan (1996), analysing water management in Mexico, found that systems of canals were organised by local communities of farmers which organised the distribution of water and maintenance tasks such as canal cleaning. The canals formed mostly relatively simple systems consisting of narrow, unlined channels and diversion dams (Sheridan, 1996, p36-37). Although these were relatively small-scale regular and fairly complex organisation was needed to maintain them; yet this still did not require the kind of state that Wittfogel claimed is always necessary. Conversely, some scholars agree with Wittfogel in that they assert a need for a high level of control when irrigation is used (e.g. Steward and Murphy, 1977). Many large-scale contemporary systems, controlled by states, are an example.

Ultimately, the main problem with Wittfogel's hypothesis is that it is not fully grounded by evidence and this has restricted the productivity of the debate. The present study has approached water from a different perspective, aiming instead to generate a large database of empirical evidence for water management which can enable new conclusions to be drawn independently of the Wittfogel debate. These data suggest the inverse of Wittfogel, namely, that water management technologies were used by powerful later empires to enhance and underpin their economies (see sections 7.7 and 7.8 below). The extensive canal systems along the Euphrates (**Chapter 5**) are an example of this.

Since Wittfogel's 1957 publication, studies have gathered more detailed evidence, as **Chapter 2** outlines. The results of these have been included in the database collated by this research. However, the theoretical approaches of these studies should also be recognised. In general, the existing studies tend to be focused on specific features or sites in isolation, without an attempt to generate a more comprehensive dataset. In addition, these are taken from a range of perspectives which have focused on specific aspects of the evidence.

Not all of the existing research was undertaken from a 'landscape' perspective; disciplines such as ancient history, the history of technology and traditional archaeology were some of the first to contribute to knowledge of ancient water use. As the literature review (**Chapter 2**) indicates, the large-scale Assyrian systems in northern Iraq are associated with written inscriptions (e.g. Bagg, 2000b). This gives a useful indication of the purpose and ideological significance of irrigation under the Neo-Assyrian empire, but, aside from Ur's (2005) and Altaweel's (2008) studies there has been less interest in more geographical information such as the hydrological context of the canals and exactly how they were used. The availability of historical sources for the Neo-Assyrian canals has led to a focus on luxury and propaganda (e.g. see Bagg, 2000a, p303). Kamash's (2009; 2010) research compiled information about water management across a wider area, but also from a historical basis.

Geomorphological and modelling based studies of ancient water management in northern Mesopotamia, although rare, also exist. One example modelled runoff in the watershed in which Resafa is located in order to suggest the rate at which the Roman cisterns could have been filled (Berking et al, 2010). Geomorphological studies such as Demir et al (2007) and Hritz (2013a) recognised links between the locations of archaeological sites, many of which were associated with relict canals, and the dynamic activity of rivers over time.

In a few cases, excavation has been undertaken which allows for detailed information about the morphology of individual features to be gathered, as well as, crucially, providing dating evidence. Harper and Wilkinson's (1975) excavations and survey at the Nahr al Maslama at Dibsi Faraj recorded an Early Islamic date for the canal. The Sahlan part of the Sahlan-Hammam canal was also excavated, allowing for a date falling in the range of Hellenistic-Byzantine to be obtained (Wilkinson, 1998, p71).

A few of the studies reviewed in **Chapter 2** used aerial photographs, which enabled these projects to adopt a landscape perspective. For example, Ergenzinger and Kuhne (1988) used aerial images to record canals alongside the Hhabur, and Wilkinson (1998) used similar images for the Balikh. CORONA images, although gathered in the 1960s and 1970s, were not declassified until the

mid-1990s, and so are only recently beginning to be used for the purposes of identifying canals. Ur (2010) used them to record features in the Hamoukar area, and Ur (2005) and Altaweel (2008) also used them in northern Iraq (2005), digitising the Assyrian canals that had previously been researched primarily through textual and ground-based evidence. As **Chapter 3** described and as section 7.4 of this chapter will outline, this project also used CORONA imagery, as well as other remotely sensed data including modern satellite images and digital elevation models, taking advantage of the large spatial coverage supplied by satellite data to map water management at a region-wide scale.

The disparate nature of the existing research, and also the large range of theoretical perspectives which have informed the discipline of ancient water management, have influenced the way in which research has been conducted. This has potentially obscured significant patterns and trends. An awareness of what research biases might exist in the literature is necessary.

In general, particular areas and particular types of data have been interpreted in different ways: the Neo-Assyrian canals have been viewed in terms of power and propaganda, while the later features have been regarded as economic features. Features dating to the Roman period have been analysed in terms of historical sources rather than archaeology (e.g. Kamash, 2009). Overall, research has been more within the realms of ancient history/the history of technology (e.g. Wikander, 2000) than hydrology and geomorphology. The Early Islamic irrigation systems have also been examined in the light of the power of the empire, but with more focus on economics than on propaganda.

Current ideas about the chronology of irrigation should also be discussed. A detailed description of how water management technologies might have developed throughout the entire region of northern Mesopotamia had not yet been provided. A map of Early Islamic water management in particular was needed, given the density of remains dating to that period and a lack of a region-wide map of these. Given the detailed nature of the results of the present research, it was possible to undertake this. Thus far there has been relatively little discussion in the literature of the trajectory of irrigation development in northern Mesopotamia. Using the dataset developed by this project, it has been possible to investigate

when large-scale irrigation started to spread throughout the rain-fed zone and when it reached a peak in terms of density, scale and distribution (see sections **7.7** and **7.8**).

The problems with the existing theoretical framework have been recognised. This chapter now discusses how the multi-disciplinary approach used by the present study has enabled a more general and empirical dataset to be generated, and what this reveals about the scales across which the later territorial empires managed and controlled water resources.

7.3. Chronology

The overall chronology of water management in northern Mesopotamia deserves more attention than it has received. The review of known and newly identified features presented in this project (**Chapters 2, 5 and 6**) enables this research gap to be addressed; relict features of all periods were recorded, including some which cannot yet be dated. The features with dating evidence are outlined in **Table 7.1**.

The earliest known evidence for water management in the region is of Bronze Age date. The canal at the Hittite-Middle Assyrian site of Tell Fray (see **Table 7.1**) is known from Bronze Age texts discovered at the site and also from the investigations at the site itself (see Bounni, 1979, p7). The texts indicate that it was in use at the same time as the site (Bounni, 1988, p369). The present study located it using CORONA images, and found it extends for much further than had previously been recorded; traces of it are found upstream of Tell Fray, and also downstream of the site.

Two large canals near the site of Mari have been attributed the Old Babylonian period on the basis of Old Babylonian cuneiform texts (see Margueron, 2004; also **Table 7.1**), although dating evidence of the associated archaeological features is not secure. One linear feature which joins the Euphrates with the site may have functioned as a transport canal (ibid p69-70); and a long feature originating at the Wadi Es Souab may have been used for irrigation (Margeuron, 2004). A document found at Mari also refers to Bronze Age irrigation in the Balikh, possibly near Tell Hammam et-Turkman (Dossin, 1974; Villard, 1987; Wilkinson, 1998).

Table 7.1: *Chronology of features with dating evidence.*

Canals with dating information	Date	Evidence	Source
Canal at Tell Fray	Bronze Age	Historical document	Bounni, 1979, p7; Bounni, 1988, p369
Mari canals	Bronze Age?	Bronze Age texts & archaeology	Margueron, 2004
Balikh canal (location unknown)	Late Bronze Age	Historical Middle Assyrian texts	Wiggermann, 2000
Habur canals	Middle-Assyrian-Early Islamic	Association with sites, survey, excavation	Ergenzinger and Kuhne, 1991; Ergenzinger et al, 1988
Canals in northern Iraq	Neo-Assyrian-Early Islamic	Survey, remote sensing, inscriptions	e.g. see Bagg, 2000b; Ur, 2005, Jacobsen & Lloyd, 1935, Altaweel, 2008
Canals in central Balikh	Hellenistic	Survey, surface ceramic scatter	Wilkinson, 1998
Membij qanats	Hellenistic	Remote sensing, association with sites	Dan Lawrence and Niko Galiatsatos
Resafa channels and cisterns	Roman	Excavation and survey	e.g. see Brinker, 1991; Berking et al, 2010
Qanats and rock cut channels in the Jerablus region	Roman- Byzantine	Survey	Wilkinson et al, 2007
Rock-cut channels at Khirbet Serisat	Early Islamic	Survey	Wilkinson et al, 2007
Nahr Masalam and qanat at Dibsi Faraj	Early Islamic	Excavation, survey and remote sensing	Harper and Wilkinson, 1975; Wilkinson and Rayne, 2010; present study
Qanats at Heraqlah	Early Islamic?	?	Kamash, 2009
Raqqa qanats/tunnel	Early Islamic?	Survey, association with sites and remote sensing	Present study; Wilkinson and Rayne, 2010; Heidemann, 2006
Nahr al Abbara	Early Islamic	Survey and remote sensing	Wilkinson, 1998; present study

The Habur canals are of slightly later date than the two on the Mari side of the river. They have been interpreted, through survey, excavation and association with known sites, as originating in the Middle Assyrian period, with use and possible modification up until the Early Islamic era (Ergenzinger and Kuhne, 1991; Ergenzinger et al, 1988). The canal which has been interpreted as joining to the Nahr Dawrin, the left-bank canal, was linked to the Neo-Assyrian period (Ergenzinger and Kuhne, 1991, p163; p188).

Extensive Neo-Assyrian irrigation is well known to have existed in northern Iraq, where the systems functioned, in part, to supply the Assyrian capital cities and their agricultural hinterland. These systems consisted of several very large, prominent canals and traces of infrastructure such as aqueducts and tunnels. Much of the investment in irrigation seems to have originated under the auspices of the Neo-Assyrian king Sennacherib (8th century BC). Dating evidence in the form of inscriptions (e.g. see Bagg, 2000b) renders this one of the most securely dated regions of irrigation in northern Mesopotamia (see **Table 7.1**).

The next period attested to by the evidence is the Hellenistic period. Wilkinson (1998, p68) and Wilkinson and Rayne (2010, p132) suggest that canals in the central part of the Balikh may date to this time, based on a clear alignment of sites and on field scatters of pottery on the ground surface (see **Chapter 6**). Again, the long Habur canals may have continued to have been in use at this time (see **Table 7.1**). Further west, qanats around Membij (Hieropolis/Bambyce) may be associated with the Hellenistic settlement and temple (evidence gathered by Dan Lawrence and Niko Galiatsatos).

The Roman Empire is well known to have utilised large-scale water management systems. Kamash's publications (2009; 2010) provide an overview of Roman water features throughout the Near East, including parts of Northern Mesopotamia. The most researched known Roman water features in the present study area are the associated dam and channels at the fort of Resafa (e.g. see Brinker, 1991; Berking et al, 2010).

Features of later date are known throughout northern Mesopotamia; many of these seem to have originated in the Roman-Byzantine period and may have continued to be used for a long time. Fieldwork undertaken by this project and the Land of Carchemish Project (Wilkinson et al, forthcoming; Wilkinson et al, 2007) recorded many of these features in the Jerablus area. These include the canal at Jerablus Tahtani, dated to the Byzantine-Early Islamic periods (Wilkinson et al, 2007, p236) and rock cut channels in the Wadis Amarna, Sajur and al Gini'at which may also be Byzantine in date (see **Table 7.1**). During fieldwork in 2010, a new channel was recorded associated with a large limestone block inscribed with a mason's mark

(**Figure 7.1**) typical of the Byzantine period (Wilkinson et al, 2010, p16; Wilkinson and Rayne, 2010, p14).



Figure 7.1: *Limestone block with mason's mark, recorded in the Wadi Amarna during fieldwork in July 2010.*

A period of reduced cultivation and declining water management, possibly associated with plague (see Kennedy, 2007) has been suggested for the end of the Late Antique period, with activity resuming and intensifying in the Early Islamic period (Kennedy, 2011; Berthier and D'Hont, 2005 p265).

The results of this project certainly show that the Early Islamic era was associated with widespread management features. Some of them had an earlier origin: for example, the canal at Jerablus Tahtani may still have been in use into this period and rock-cut channels of a similar date were also recorded at Khirbet Seraisat, south of Jerablus (e.g. see Wilkinson et al, 2007). Following the Euphrates downstream, the Nahr al Maslama at Dibsi Faraj is a prominent canal securely dated to the Early Islamic period (Harper and Wilkinson, 1975). The present study used satellite images to show that this feature may have extended to the east (see **Chapter 5**). This study also discovered the faint trace of a qanat, stretching for about 4 km from the limestone uplands above Dibsi Faraj and fading out at the site itself. The canal and qanat may have been associated with wells excavated within the site (see Harper and Wilkinson, 1975, p337). Given the history of Dibsi Faraj, the qanat, which is clearly associated with it, was probably in use at some time during the Roman-Early Islamic periods.

On the opposite bank of the Euphrates the CORONA images show (**Chapter 5**) that the canal at Tell Fray is much longer than the known segment (see **Table 7.1** and Bounni, 1979) and in fact flows towards Qa'lat Ja'bar, seemingly terminating at the Early Islamic site. Given this, despite the Bronze Age date discussed above, Early Islamic use cannot be ruled out. In addition, several short stretches of qanat and canal in the steppe between the Euphrates and the Balikh were identified by the present study, associated with sites of Late Antique/Early Islamic appearance.

The Balikh stands out as a particularly complex area during the Early Islamic era, with investment in irrigation already attested in the Umayyad period (Heidemann, 2011, p47). In the Balikh 'horseshoe', Raqqa's temporary status as the centre of the Abbasid empire under the caliph Harun ar Rashid also gave it significance. While Heidemann (2006, p36) may be wrong about the canal that cuts through Heraqlah, which he associates with the Nahr al-Nil (Heidemann, 2011, p49), other features are probably Early Islamic, including short qanats and associated channels also noted by Heidemann and further elucidated by the present study (see Heidemann, 2006, p36; Wilkinson and Rayne, 2010, p135; also present study **Chapter 6**) and a tunnel connected to a canal which also appears to be linked to the Early Islamic remains. Further Early Islamic activity may have occurred at Heraqlah; Kamash suggests that there was an Umayyad qanat here (Kamash, 2009, vol3 p4). This may refer to either or both of the two qanats recorded by the present study (see **Chapter 6**). The site of Heraqlah itself has been excavated and interpreted as Abbasid in date (Toueir, 1983).

Canals in the western part of the Balikh horseshoe are linked to the tunnel system and therefore could also share a similar phase of use (see **Chapter 6**). Further north, on the basis of the associated sites, the extensive Nahr Al Abbara system has been interpreted as Early Islamic (Wilkinson and Rayne, 2010 p132; Wilkinson, 1998, p67-68). The present study demonstrated that this is a significant system, with mains and offtakes still visible in the 1960s imagery, allowing the layout of this large-scale system to be mapped.

Water features associated with the Early Islamic period were also located east of the Balikh, including the canals alongside the Habur (e.g. see Ergenzinger and Kuhne, 1991). Based on historical evidence, it is possible that at least some of the

qanats in the Sinjar Plain are Early Islamic (see Fuccaro, 1991, p12). One of the large canals in Northern Iraq, the Tarbisu canal, may post-date the Neo-Assyrian period (Ur, 2005, p333); again, an Early-Islamic date is possible given its similarities with other canals of that date. The results of this project indicate a great deal of activity in the Islamic period, both in terms of the re-use of older systems and construction of new systems, but Decker, (2009b), mainly using historical sources, emphasises a peak in cultivation and related activity in earlier periods, including the Sasanian (Decker, 2009b, p190) and Late Roman (Decker, 2009a). He suggests that the Islamic irrigation activity was just a 'restoration' and continuation of these (Decker, 2009b p190; p206), occurring along with some changes in settlement patterns (Decker, 2007 p249-250). Interestingly, in a later paper Decker (2011) presents a modified view, in which a peak in settlement and agriculture, with associated irrigation, was suggested for the Early Islamic period.

Less evidence of irrigation post-dating the Abbasid empire was found, aside from a few textual references and very brief remarks by travellers. However, as already stated elsewhere, water systems generally lack much dating evidence; it is likely that irrigation was also a feature of the Ottoman period. For example, the West Balikh canals may have had some Early Islamic associations, but there was also Ottoman activity in the area (Winter, 2009). Ottoman use and extension of Early Islamic canal systems is possible; that these are not modern (20th century) canals is also likely (see **Chapter 6**). Similarly, the Nahr Dawrin which flows alongside the Euphrates was mentioned by Bell (1924, p78), who notes that parts of it were indicated by a line of qanats, and that other segments were still used (p82).

This review of the chronology of water management in northern Mesopotamia enables further questions to be addressed; namely, what the link may have been between water management and specific empires, and how the remote sensing technologies used by this project might elucidate this.

7. 4. Advances in methods

By employing techniques of remote sensing and GIS (image interpretation, photogrammetry, hydrological interpretation), this project has analysed water systems at a regional scale in an innovative way. Currently fieldwork in the project

area is not possible, therefore remote sensing using satellite images and elevation models offers a way to identify and record archaeological features. Moreover, it makes it possible to view whole regions relatively quickly and cheaply (Donoghue et al, 2002). There have been many changes to the landscape in recent years, erasing and obscuring archaeological remains (see Cunliffe, 2013). Fortunately, the historical CORONA imagery offers a way to view the landscape before many of these changes occurred.

The bulk of the existing studies reviewed in **Chapter 2** were undertaken at a time when satellite images such as the valuable CORONA resource were not available, which limited the opportunity for those studies to record new features and locate the entire reach of canals. The scale and complexity of an irrigation system can only be understood if most of its extent (main channels, off-takes, and drainage points) can be identified. Research into ancient water management in general has consisted of several separate studies, often dealing with one sub-region or with a segment of a particular feature, or perhaps with a focus on features of a particular date (e.g. Kamash's thesis on Roman water management, 2009). Although the study of water management calls for an interdisciplinary approach, utilising multiple methods such as the analysis of historical documents, satellite images and archaeological survey, most of the research originates from specific perspectives.

While the many existing studies represent a large resource of information, the separate nature of the research makes drawing wider conclusions about imperial water management across such a large area difficult. This study used CORONA images to search the entire area of northern Mesopotamia, between the Euphrates and the Tigris, for all relict water management features (an area of about 100,000 km²). Because the nature of the evidence has proved to be mostly later in date, this research has concentrated on the systems of the later territorial empires (Neo-Assyrian-Early Islamic).

As described in **Chapter 3**, the use of remote sensing enabled this large area to be systematically examined from an interdisciplinary perspective, combining elements from the fields of archaeology (e.g. survey), remote sensing (image interpretation and photogrammetry) and physical geography (hydrological

interpretation). New features were recorded during fieldwork using GPS, and digitised from satellite imagery using GIS editing tools. Known features were also viewed and digitised using CORONA images and integrated into the GIS database; in many cases this enabled further extents and segments of the known features to be newly located.

7. 5 Data Validation

Because further fieldwork in Syria is currently limited it was not possible to confirm the function and dating of all newly identified features through excavation or survey. However, it is still possible to validate results, by for example cross referencing using a combination of different remotely sensed datasets.

First, as outlined in **Chapter 3.2**, it should be noted that there has been discussion in the literature about the differences between linear features such as canals and hollow ways (e.g. see Ur and Wilkinson, 2008). Given the complex patterns of such lines in many parts of the study area, this project used DEMs as a way to test features: if features rise up and over watersheds, they are unlikely to be a canal. Most ancient canals follow the hydraulic gradient of the land.

The features presented in the results are lines which passed this particular test (gradient graphs are shown in **Chapter 5** and **6**). For example, there are many layers of linear features present in the landscape around the Early Islamic site of Medinat al Farr in the Balikh. DEMs can show which ones cut across the natural contours, and which run parallel to them, enabling a distinction between hollow ways and canals to be made (**Figure 7.2** shows the linear features). For example, the hollow way to the west of the site rises up and drops down, disregarding the natural slope, whereas the canal flows consistently downslope at a gradient of 2:1000.

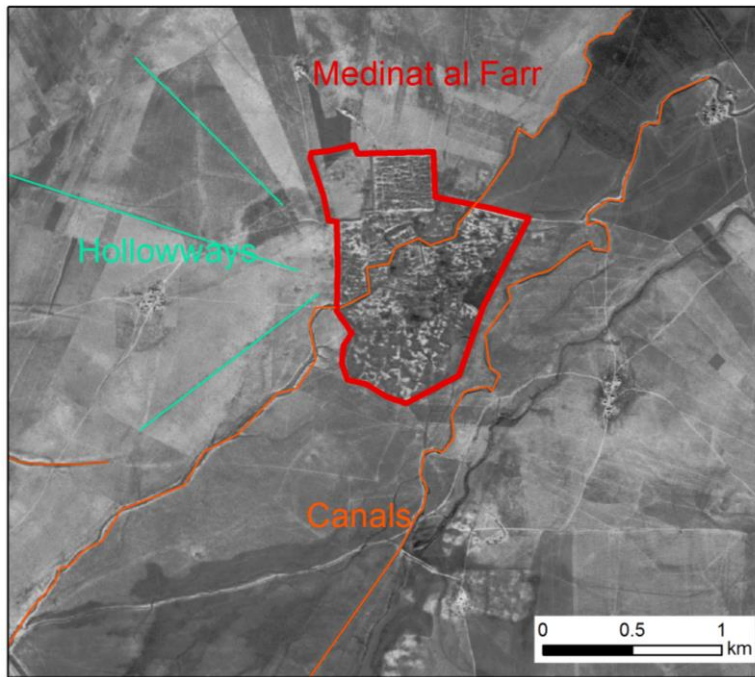


Figure 7.2: Linear features around Medinat Al Farr. CORONA image dating to 22 January 1967.

DEMs also provide information about the function and use of features, enabling a more detailed record of each to be generated. The landscape gradients through which each feature flowed were recorded, which is information which most of the existing studies do not provide in detail. It was then possible to compare this gradient data with guidelines listed in irrigation literature (see **Chapter 4**) which recommend, for example, that a main canal can attain an appropriate level of efficiency when flowing at gradients of 0.1-2.5% (Zimmerman 1966, p218-221).

Based on this, it was possible to identify which channels might have faced difficulties such as erosion or siltation, for example by flowing at too shallow a gradient. As **Chapter 6** shows, in general, higher gradients were identified for the shorter laterals in the Balikh, for example for the Nahr al Abbara, than were recorded for the longer mains. This is consistent with modern recommendations (see **Chapter 4**).

Even the relatively coarse SRTM DEM showed that the Nahr al Abbara in the Balikh was constructed to make efficient use of the natural topography. Despite the overall flatness of the landscape, by occupying a ridge of slightly higher ground between the Balikh and the Wadi Al Keder, the canal could flow for a long

distance, with the off-takes flowing perpendicular to it watering the fields by taking advantage of the slightly increased gradient (see **Chapter 6** for more details). It is possible that the Hellenistic systems in the central Balikh zone and the West Balikh/Qara Mokh systems were also using the topography in this way.

Gradient information derived from DEMs, alongside the visual inspection of the images, also allows the function of each different part of a system to be understood. **Chapter 4** reviews how main channels and irrigation and field laterals function in relation to topography. Being able to separate out each part of a system like this is useful, because it can facilitate an understanding of the system as a whole. Many past studies, most of which did not have access to remotely sensed data, only recorded segments of main channels and did not discuss how the water could be delivered from the main to the crop, if the irrigation systems were even considered in terms of economics at all. Some studies did note traces of offtakes: for example, Van Liere and Lauffray (1954-55, p146-7) and Ergenzinger et al (1988, p117). Using CORONA images as well as DEMs, the present study was able to identify multiple parts of some systems, the Nahr al Abbara and the West Balikh being good examples (**Chapter 6**). A more complete map such as these represent makes it possible to suggest the scale, size and shape of the irrigated area. For example up to 3600 ha of cultivated land can be proposed for the Nahr al Abbara, based on the layout of the irrigation system.

Of course, often the large main channel is the only part of the entire water supply system that survives, proving to sometimes be the case even when a range of sources are used. For example, the Nahr Maslama was excavated (Harper and Wilkinson, 1975) and also examined by this study using satellite images, yet no offtakes could be identified, presumably because they were eroded away by the action of the Euphrates. The same problem was encountered when the Sahlan Hammam canal was examined using CORONA images; the irrigation laterals may have been removed by subsequent agriculture, or by the Balikh.

Existing interpretations of some features were tested and updated using the remotely sensed data. In some cases, the image interpretation revealed that main canal features which had previously only been recorded as shorter segments by ground-based survey were in fact much longer canals. The canal flowing from

upstream of Tell Fray and terminating at Qa'lat Ja'bar is an example. Conversely, features shown to be relatively extant by the existing research were sometimes found to be less clear in the CORONA images. Thus only segments of the Habur canals mapped by Ergenzinger et al (1988) were identifiable. Similarly, a connection proposed between one of the Habur canals and the Nahr Dawrin (Ergenzinger and Kuhne, 1991, p163) was not evident using the CORONA images.

Subterranean features should also be mentioned in the context of DEMs. While the characteristic pattern of maintenance shafts often signifies a qanat, tunnels may take a similar appearance, yet function in a different way. A qanat-like feature in the Balikh, terminating near Raqqa, was examined in relation to the topography. In fact, rather than being an underground feature tapping water from an underground aquifer, it originated as an open channel that passed through a ridge of higher ground by means of a tunnel.

Secondly, as part of the validation process features need to be assigned dates. In many cases, especially in the Balikh valley, water features had a clear association with settlement sites that had already been excavated and surveyed. For example, the tunnel identified flowing towards Raqqa terminated amongst Early Islamic structures (e.g. see structures recorded by Henderson et al, 2005; Challis et al, 2004). This relationship could be clearly observed from a visual inspection of the CORONA images. Because the nearby structures had been dated, the tunnel can be proposed to be contemporary with them. Similarly, the West Balikh canal system to which the tunnel connects was also possibly used in the Early Islamic period, given its link to the tunnel and thereby to the palace features.

It is also important to note that these assessments are made cautiously; while the link between the palaces, the tunnel and the canals indicates that the canals may have been *used* at the same time as the tunnel, this link does not necessarily reveal when the canals were first built, or when they went out of use. It is possible that the canal system was constructed earlier than the tunnel system: it is equally possible that the canals were constructed later, as part of modifications to the existing tunnel-based system. Assigning dates to water features or lengths of canal is a particular problem which will be discussed later in this chapter.

Sometimes, however, clear sequences and 'layers' of features could be identified in the images, a simple method which at least enabled 'relative' dates to be assigned. **Figure 7.3** shows that there is a clear 'stratigraphy' of channels close to the Early Islamic site of Heraqlah, near the Balikh.

The oldest features (**Figure 7.3**, layer 3) may well be the two qanats, possibly associated with each other. One flows E-W, the other N-S. Kamash mentions that there is an Umayyad qanat in this area (2009, vol 3, p4), which may refer to one or both of these features. It is possible to recognise that these are the oldest channels because later features cut them. The first of these is a prominent earthwork (2) that also truncates the site of Heraqlah itself, demonstrating that it post-dates it. Heidemann (2006, p36), mapping the Raqqa end of the feature, suggests that the canal is Abbasid. However, based on its truncation of Heraqlah this seems to be incorrect and a post-Abbasid date can be assigned instead. Later, narrow channels (1) truncate the large canal: these are the 'youngest' features identifiable in the CORONA image. The value of the CORONA images in enabling this sequence to be untangled cannot be over-emphasised.

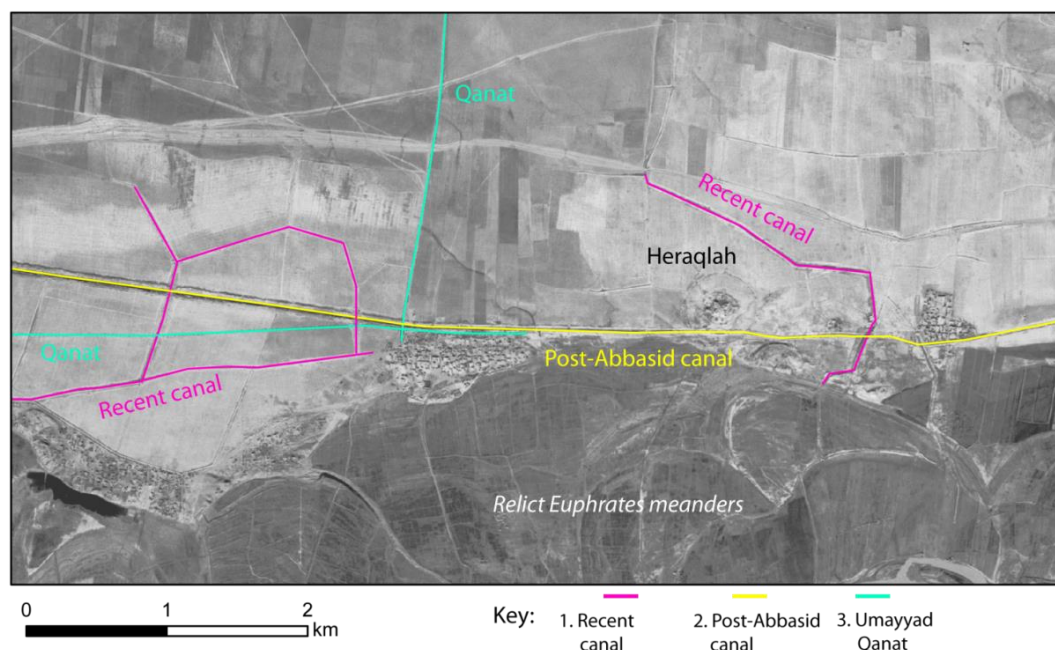


Figure 7.3: A sequence of channels around the Abbasid site of Heraqlah, regressing back from the most recent feature (1) to the oldest (3). The CORONA image dates to 22 January 1967.

While the above example only uses one satellite image to reconstruct a stratigraphic sequence of channels, using satellite images of more than one date can also help to place features in a sequence. Flooded/silted channels and gilgai in the West Balikh area (**Chapter 6**) may have been part of a former irrigation landscape, already in disuse by the time the CORONA images were produced. As the sequence of images presented in **Chapter 6** demonstrates, the 1967 image shows the relict, un-maintained channels clearly; the 1972 image shows that a new system was under construction, already erasing the former patterns and indicating that these systems were not part of modern water management. Google Earth and Landsat images show the new system in use.

The appearance of artificial channels can also provide information about their chronology, when compared with other data. It is worth describing the difference between an active and a disused canal here with reference to the results of this research. As **Chapter 3.2** shows, an active canal may well have water and/or vegetation in the channel (represented by a darker area); an example of this is the canal between Carchemish and Jerablus Tahtani, which contained water and vegetation when visited in 2010. Some of the canals in the Balikh, including parts of the Nahr al Abbara, contained water at the time of the CORONA images (**see Chapter 6**). These were therefore represented by dark lines.

Inactive canals that had been out of use for some time before the CORONA images were taken (most ancient canals) were dry and had less clearly defined morphologies (**see Chapter 3.2**). These were infilled, but still had upcast banks. This includes the canals along the Euphrates, such as the canal between Tell Fray and Qa'lat Ja'bar, the Nahr Maslama, and the Nahr Dawrin (**Chapter 5**) as well as the Sahlan-Hammam canal in the Balikh (**Chapter 6**) and segments of canals in the Habur (**Chapter 5**).

Others did not have clear upcast banks, either because they had never been prominent, or because they had been eroded/ploughed back into the canal, leaving a soil-mark. This includes canals in the Balikh such as some of the artificial channels in the West Balikh horseshoe.

It is worth considering the timescales involved in the 'decay' of such features. For example, the Sahlan Hammam canal was in use in the Hellenistic-Byzantine

periods, therefore by the time of the 1967 CORONA image it was both eroded and silted, although the upcast banks were still visible; by the 2010 field visit, it was gone. The Nahr Dawrin, which flowed alongside the Euphrates opposite Mari, is also a good example. Bell recorded some possible use of its lower reaches in the early 20th century (1924, p82). Bell visited at some time shortly before or during 1910. By the time of the 1968 CORONA image, around 50 years later, it was disused and severely eroded, with only short segments of it identifiable. At some point over the course of 50 years it went out of even the limited use that Bell identified and had almost vanished from the landscape. Given this, around 50 years therefore could be considered as a possible time frame for the last stages of use through to decay when a channel is simply abandoned. Canals of a similarly eroded/disused appearance elsewhere, for example, the West Balikh channels, could have gone out of use at a similar time, which would give them a *terminus ante quem* of around the end of the Ottoman period. Conversely, other canals have vanished much more quickly, due to deliberate human-induced changes. Wilkinson (1998) observed the Nahr Al Abbara in the Balikh in the 1990s. By 2010, the canal had been removed from the landscape and was replaced by wells

7.6 Types of channels: form and function

The types of water features identified by this study can now be outlined and the functions of each type considered, before patterns of scale and distribution are described. In **Chapter 4**, the parts of irrigation systems in general were considered: different types of system, such as small-scale water harvesting devices as well as large-scale canal-based systems and subterranean channels were reviewed. The results of this study can now be explained in the light of the earlier general review of irrigation. First, smaller-scale features present in the study area will be discussed, followed by a review of the large-scale systems.

Here, 'small-scale' describes methods which do not comprise long or multiple channels. Instead, it encompasses techniques of water harvesting and storage using cisterns. Overall, water harvesting methods could not easily be identified using remote sensing, because these are likely to be small and ephemeral structures such as check dams, cisterns and wells.

Some former wells and cisterns of unknown date were identifiable using the CORONA images, appearing more eroded than the modern examples, and being without associated fields. Around Raqqa, however, these were associated with relict channels and even sites (see **Chapter 6**). Cisterns as a means of storing water are attested in historical sources including the Neo-Assyrian Harran Census (e.g. see Fales and Postgate, 1995): therefore their presence in the Balikh as early as the Iron Age can be confirmed. Known cisterns of Roman date at Resafa have been recorded (Brinker, 1991) and of Early Islamic date in the Balikh (see de Jong, 2012, p519). Other rock-cut Hellenistic/Roman cisterns have also been identified archaeologically in the Carchemish survey area overlooking the Euphrates (Wilkinson et al forthcoming). Areas showing traces of past flooding may be indicative of former small-scale water-management such as floodwater harvesting or wadi diversion. The West Balikh systems appear to have incorporated seasonal wadis (see **Chapter 6**). Small fields, possibly bounded by check dams, are visible in the steppe between the Balikh and the Habur (for example see **Figure 7.4**). Runoff was collected and moisture and sediments trapped behind the dams, allowing for seasonal cultivation. It is possible that such structures may have been in recent use and of recent construction: for example, check dams in current use are known in India (e.g. see Balooni et al, 2008).

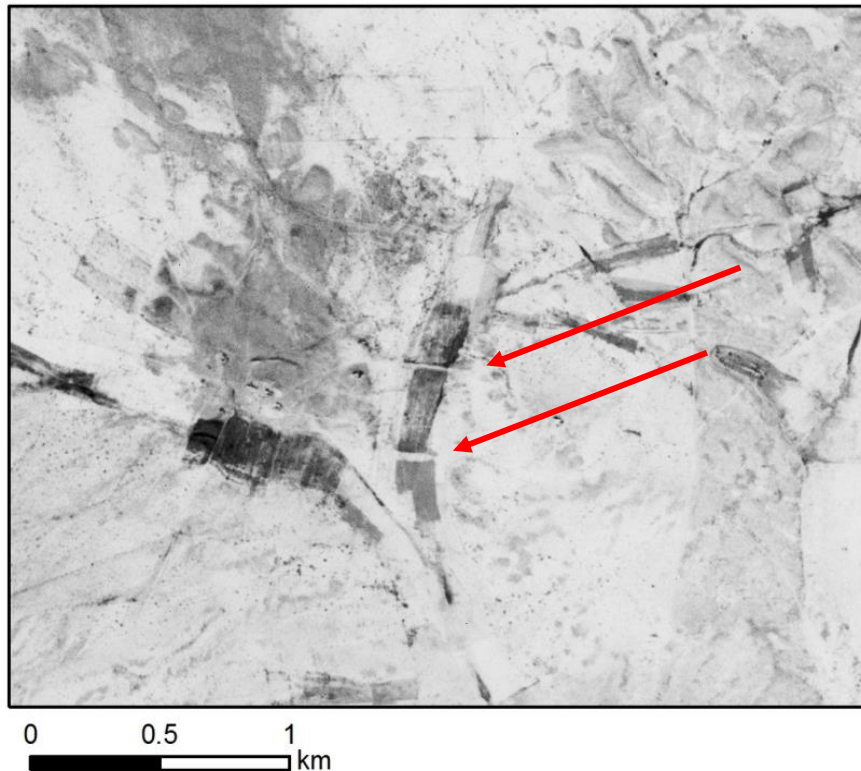


Figure 7.4: Possible check dams in the steppe, 68 km to the east of the Balikh. CORONA image dating to 22 January 1967. Arrows indicate the structures.

Runoff can also be captured in channels running parallel to a natural hillside, on the same alignment as the contours. Once it is captured, runoff is used to water crops in basins. Oweis et al (1999) have described mini-catchment runoff harvesting. Welderufael et al (2013, p219) also describe something along these lines, calling it infield rainwater harvesting. Interestingly, there is a pattern of narrow, parallel channels at the upper end of the western Balikh horseshoe (see **Figure 6.58**). While the slope they run across, given the overall flatness of the region, is relatively slight at 0.4%, it is possibly sufficient that these could have been constructed for some kind of runoff capture.

Water management involving excessive watering, including both large-scale canal systems and small-scale flood-water irrigation, may leave geomorphological indicators in the landscape. Gilgai are geomorphological features found in areas of vertisols (see **Chapter 1**). They are common throughout the Balikh, especially in areas associated with relict irrigation systems. It is possible that there is a direct link between the presence of gilgai and of areas of former irrigation and that these

formed as a result of repeated inundation and drying phases of particular irrigation schemes. Alkaier et al (2012, p1837) noted shallow water tables in the Balikh horseshoe which they attributed to poor drainage associated with modern irrigation; they also mention deeper water tables in the West Balikh area which they attribute to 'very old' cultivation (Alkaier et al, 2010, p1837). Several gilgai in this area can be identified in the CORONA images, and are possibly associated with relict irrigation channels. Similarly, gilgai can be seen around the upper reaches of the Nahr al Abbara; and significantly they are less prevalent in the region of the lower, better-drained part of the system. If this interpretation is correct, it might be interesting to use evidence of gilgai as an indicator of relict canal systems.

Larger-scale water management systems are prevalent throughout northern Mesopotamia. Large-scale in this case refers to systems consisting of a long main canal, rather than a short ditch or wadi diversion structure, capable of irrigating a large area and necessitating some investment in construction and maintenance. In some cases offtakes are preserved. These are generally easier to identify, especially when a main canal has prominent upcast banks. These banks may have been constructed as part of the original excavation of the canal, especially if there is a need to raise the head of the canal, or protect it from causing/being affected by flooding. Additionally, when modern canals are cleaned, material dredged from the bed of the canal can be deposited on the banks of the canal itself, causing the banks to increase in size. It should be recognised here that this kind of canal maintenance is today a regular occurrence: for example, a recent study from the Balikh indicated that it occurs every year in November (Alkaier et al, 2012, p1835). Given the low overall gradient of the Balikh region, the canals also flowed at very low gradients (see **Chapter 6**), barely the minimum required (of around 0.1-2.5 % for a main canal). Excessive siltation, necessitating frequent cleaning, would have been a significant problem and may have been the reason for the tightly sinuous morphology of the Nahr al Abbara. Potentially large amounts of labour, and some kind of regulation, might have been required to organise this.

There are numerous examples of these types of large embanked canals throughout the study area including the Nahr Maslama, the canal between Fray and Qa'lat Ja'bar, the Sahlan-Hammam canal, the Nahr Dawrin, and the Bandwai

canal (see **Chapters 5 and 6**). These are significant features: for example, the Sahlan-Hammam canal is about 6-7 m wide (Wilkinson, 1998, p71). Which part of each overall irrigation system they represent should be considered. The size of these large features suggests that they form the main canal. Interestingly, where the main canals survive, the rest of the irrigation system usually does not. In some cases the abstraction point can be inferred from field surveys or from the CORONA images. The Sahlan-Hammam canal appears to have abstracted from the Balikh close to Tell Sahlan. The reason for the lack of offtakes could simply be due to poor preservation of these smaller, secondary canals: the size of the large main canals may have aided their survival. The offtakes may have been more ephemeral to begin with, and also more likely to be removed by later cultivation and human activity.

Not all main canals are so prominent. Others are narrow, sinuous features, without upcast banks. These include the large canal between Carchemish and Jerablus Tahtani (see **Figure 7.5**) and the Nahr al Abbara in the Balikh. The former is still in use and of unknown date, and the latter had been in use during the 20th century, although it appears also to have functioned in the Early Islamic period.



Figure 7.5: *Canal between Carchemish and Jerablus Tahtani.*

The morphology of these canals is dictated by several factors. The general topography of the landscape must be considered; in a flat landscape there can be a need to raise the head of a canal sufficiently to allow it to irrigate a larger area, entailing a high embankment; this could explain the Sahlan-Hammam canal. A large embankment may also be maintained where there is risk of floodwater incursion damaging the canal. Meandering but straight canals like the Nahr Al Abbara can be a consequence of high siltation caused partly as a result of low gradient.

Main canals should technically not be viewed in isolation. In a few cases, offtakes survive. **Chapter 4** sets out the sequence of main, submain, irrigation lateral and field lateral. Again, the Balikh is an area with many clear examples of irrigation and field laterals. As already described in the results (**Chapter 6**), the Nahr al Abbara makes use of a slight ridge of land, so that the irrigation laterals (visible in the imagery and also indicated by sluice stones—see Wilkinson 1998 p67-68) can flow perpendicular to the main, gaining some elevation and taking advantage of the increased gradient. Similarly, a Hellenistic system further south in the valley uses these branching channels to irrigate a triangle of land between the Qara Mokh and the Balikh: the main canal runs along the upper edge of the flood plain, with the submains flowing downwards into the triangular cultivated area. Some of the other systems represented only by single, large canals may also have once been part of wider networks of laterals with associated control structures.

Very few examples of laterals can be identified in the study area outside the Balikh. Ergenzinger and Kuhne (1991, p172) mention some associated with the Habur canals, and Ur (2005) identified a few offtakes abstracting from the Neo-Assyrian systems (Ur, 2005, p337). Interestingly, some offtakes associated with Sennacherib's canals were found to have inscriptions at each branch point, indicating that their presence was part of the overall design of the systems (e.g. see Ur, 2005, p342). This supports the likelihood that the other large-scale, embanked canals originally could have been part of much more sophisticated systems.

The pattern of field laterals, which stem from the irrigation laterals to deliver water to the crop, cannot be identified easily. Generally these will have been so small

that they will not have survived. However, some examples of field laterals contemporary with the CORONA images are visible. For example, patterns of small bunds in the Balikh forming grids may represent basin-type irrigation, demonstrating the kind of units that can be watered in this landscape (see **Chapter 4**).

The associated infrastructure of irrigation such as dams, control structures and water-lifting devices can sometimes be inferred, but is generally not identifiable using satellite imagery. Travellers' accounts can give an impression of the use of these devices. For example, Bell (1924) mentioned that systems called 'jirds' lifted water over several levels, up from the Euphrates, to water the floodplain in the early 20th century (p80).

In general, the water management features identified by this project appear to have functioned by gravity-flow, although lifting cannot be ruled out. Dalley (1994, p53) discusses a device very similar to an Archimedes screw which may have watered Neo-Assyrian gardens, although this cannot be confirmed.

Several of the more complete irrigation systems, again well represented by the Balikh, are self-contained, enclosed entities. The Nahr al Abbara is bounded on both sides by natural drainages (the Nahr Balikh and the Wadi al Keder). The Hellenistic canals further south enclose a roughly triangular area between the Balikh and the Qara Mokh. The Sahlan-Hammam canal may have watered an area between the Balikh on its right bank and the slighter higher ground of the steppe to the west. Elsewhere in Northern Mesopotamia, the Nahr Maslama, the Fray-Ja'bar canal, the Mari irrigation canal and the Nahr Dawrin (discussed in **Chapter 5**) occupied boundary areas between the Euphrates flood-plain and the more elevated steppe. They were presumably designed to irrigate the lower terraces above the river level, increasing the irrigated area. Their position at the edge of the more elevated steppe may also have had an added benefit of capturing runoff, isolating the fields from potential damage.

The provision of drainage would further have improved the efficiency of the control and protection of past water management systems in Northern Mesopotamia. Given the aridity of the landscape, drainage is generally overlooked by the literature. As well as serving to remove excess runoff, drainage channels could

also remove the water used for irrigation, preventing waterlogging and subsequent salinization (see **Chapter 4** for an explanation of this problem). It seems unlikely that a main canal/system would be entirely emptied of water by the time it reached its termination, so some drainage point should be inevitable, generally downstream and discharging into the same water course which the main canal originally abstracted from.

There are several examples from the results of this study that illustrate this. The Nahr al Abbara was particularly sophisticated (see **Chapter 6**). It used both the Balikh and the Wadi al Keder to channel away drainage water. Offtakes on both sides of the main canal drained into these natural streams. The main canal itself isolates the system at the upper reaches. At its terminating point, the main canal appears to drain into a short channel which flows between the Balikh and Keder, effectively allowing drainage into both these streams and isolating the irrigation system.

Frustratingly, many of the canals identified and recorded by this research lack clear abstraction and termination points, although some conjectures have been made about their locations. This includes the canals alongside the Euphrates, which were eroded by the river. For example, part of the Nahr al Maslama was recorded at Dibsi Faraj, flowing downstream for 3 km (Harper and Wilkinson, 1975, p337); although its abstraction point is unknown, in order to abstract from the river it must have extended at least 8 km upstream (Harper and Wilkinson, 1975, p337). Interestingly, using the CORONA, short segments of a prominent, embanked canal can be traced between the Nahr Maslama at Dibsi Faraj and Sura (shown in **Chapter 5**). It is possible to conjecture that these were part of the same, long canal, but impossible to confirm this now that the area has been inundated by the Tabqa dam.

Another canal for which the abstraction point is not clear is the Nahr Dawrin, flowing alongside the Euphrates on the left bank opposite Mari. This has been interpreted as connecting to the eastern Habur canal (Ergenzinger and Kuhne, 1991, p188), although this link was not clear in the CORONA images. The drainage points of all these channels appear to have been removed by the Euphrates. Similarly, the abstraction point of the canal between Tell Fray and

Qa'lat Ja'bar is unclear. While the literature only dealt with the segment that passes directly below Tell Fray (e.g. see Bounni, 1970; 1988), using CORONA it can be traced as far as 2 km upstream of the site where a former meander of the Euphrates has truncated it.

The overall functions of the different types of systems are now reviewed. Irrigation is always the biggest consumer of water. The locations and layouts of the more extant systems, where patterns of laterals are preserved, show the potential for significant ancient water abstraction throughout northern Mesopotamia. It is likely that most of the other systems, considering the consumption required, would also have been used for irrigation. Other uses can also be considered here, however. The short canal between the Euphrates and Mari has been interpreted as a navigation canal (Margeuron, 2004), allowing vessels to reach the Old Babylonian port (Margeuron, 2004, p69-70), although this idea cannot be confirmed. The Nahr Dawrin has also received similar interpretations, indicating that it could have connected the Upper Habur with the Euphrates (Ergenzinger and Kuhne, 1991, p188; Margeuron, 2004, p72-73): again, this link could not be verified by the image interpretation study. However, a transport function could be possible in some cases.

Another use of water which has attracted attention specifically in terms of Sennacherib's canals is the idea of luxury parks and gardens (e.g. Reade, 1987). However, considering the scale of the canal systems, it seems surprising that these would have been their main use, although the gardens referred to by inscriptions and reliefs presumably would have required significant amounts of water. These water distribution systems may have been partly economic, growing more water- and labour -intensive crops such as fruit. For example, orchards are known historically from several areas where ancient irrigation has been recorded and in the Balikh, Neo-Assyrian orchards are referred to by the Harran Census (see Fales and Postgate, 1995). Le Strange cites historical sources which refer to 12th century AD date and orange orchards near Mosul (Le Strange, 1930, p88-90).

The possibility of parks and gardens as consumers of water elsewhere in northern Mesopotamia should not be discounted. Landscaped features such as hunting parks and racecourses are known from Abbasid Samarra (e.g. see Northedge,

2005; Northedge, 2011); a viewing platform comprising a pavilion within the racecourse was indicated, surrounded by a moat fed by qanats (Northedge, 2005, p156). Gardens have also been suggested for Samarra and other Abbasid sites (see Ruggles, 1990, p183) including the palaces of high-ranking early Islamic individuals (e.g. see Decker, 2011, p3).

Given this, it is possible that such viewing platforms were also a feature of the Raqqa palaces and could explain several circular structures in the vicinity of the palaces and racecourse. Supplying these areas may have been a function of the qanats and tunnels associated with Raqqa, which presumably also fulfilled the domestic needs of the palaces, city and industrial areas. Heidemann suggests that Harun ar Rashid brought water to Raqqa partly to supply the palace gardens (Heidemann, 2011, p49).

Historical sources indicate that other Early Islamic sites in the Balikh also had irrigated gardens. Le Strange cites these, indicating the presence of canal irrigation in the around Medinat al Farr (Le Strange, 1930, p105). Heidemann (2011, p51) also notes irrigated gardens in this area. The evidence for gardens does serve as a reminder of the relationship between water and power; gardens are certainly a luxury use of water in a semi-arid environment, and are generally associated by high-ranking individuals such as kings and caliphs.

7.7 Scale and distribution of water systems

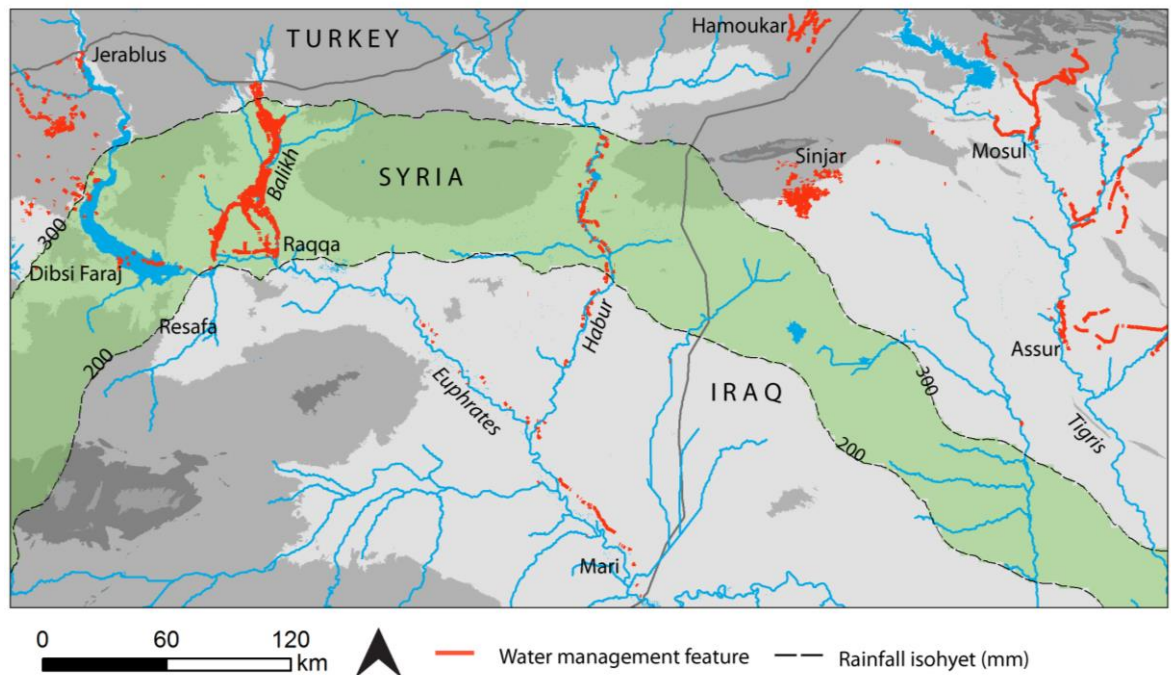


Figure 7.6: The results of the present research and other published CORONA studies (see **Chapter 2**) show ancient water management systems throughout northern Mesopotamia (see **Chapters 2, 5 and 6** for details of each feature). The green area marks the zone between the 200 mm and 300 mm average rainfall isohyets (data from GPCC).

Now that the function and form of the features recorded has been reviewed, the trends revealed by the research can be discussed. The results of this study have been combined into a GIS database, integrating information about newly identified water management features with information about known features.

Scale

The different scales of the types of water systems outlined above can now be discussed. The size, extent and gradient of a channel, as well as the available water resources, determine the amount of land which it could irrigate. For example, a narrow canal flowing at a steeper gradient would allow less land to be irrigated than a wider, deeper, less steep canal, which can flow across a longer distance. If the capability of a system can be recognised, an impression of its scale can also be suggested. Based on measurements made from satellite images,

DEMs, and field survey, scale can be determined for some of the systems examined by this research.

Calculation of canal discharge from the width, depth and gradient was possible for a few canals. The Manning formula can be applied (see **Chapter 6.2**). Eroded, infilled canals measured at ground surface level or through using photogrammetry do not clearly represent their original dimensions: however, in some cases excavation has revealed them. **Table 7.2** gives examples of channels for which dimensions have been recorded and **Table 7.3** suggests the potential areas which could have been irrigated, giving an impression of the scale of irrigation in these regions.

Wilkinson's (1998) excavation of the Sahlan part of the Sahlan-Hammam channel indicated a possible discharge of up to 7.8 m³/sec, which could have irrigated an area of about 1173-7800 ha (assuming that from 1-1.65 liters/second could water 1 ha; see **Table 7.3**; also see Wilkinson, 1998, p81). Other canals of similar dimensions (see **Table 7.2**), and flowing at similar gradients, include the Habur canals (see Ergenzinger et al, 1988, p117). With these sizes of irrigated areas possible for canals on either side of rivers such as the Balikh and Habur, and with the significant mapped extents of canals in northern Iraq and of canals alongside the Euphrates in Syria, it was possible that most of the cultivable parts of the river valleys were irrigated during the time of the later territorial empires.

Table 7.2: *Dimensions of selected ancient canals.*

Canal location and of measurement	Surface (m)	Width	Bed width (m)	Depth (m)	Gradient	Evidence
Sahlan-Hammam	c.10 bank tops	between	6.5	0.5-1	0.002	Wilkinson, 1998, CORONA DEM
Habur canals (near Tell Seh Hamad)	6 bank tops	between	?	1-2	0.001-0.002	Ergenzinger et al, 1988, p117; SRTM
Nahr Maslama (at Dibsi Faraj)	c.20 bank tops	between	c.2-3	c.1-2	Slightly less than gradient of Euphrates (about 0.0004 between Tabqa dam and Raqqa)	Harper and Wilkinson, 1975

Table 7.3: *Potential areas irrigated by selected ancient canals, assuming that about 1 litre/second irrigates 1 ha (see Wilkinson, 1998, p81).*

Canal	Length of main canal	Potential irrigable area (ha)	Source	Evidence
Hammam-Sahlan	c.14.3 km	1760-7800	Wilkinson 1998, p80-81; CORONA image	Flow calculation
Hammam-Mounbateh canal	c. 16 km?	1760-7800	Wilkinson 1998, p82; CORONA and SRTM	Flow calculation
Nahr al Abbara	c.24 km	3600-4600?	CORONA and SRTM	Layout of canals
Habur canals	c. 170 km?	1760-7800?	Ergenzinger et al 1988, SRTM	Flow calculation
Zerqa triangle canals, Jordan	c. 8-12 km?	c. 1800-4500	Kaptijn 2009 (p348-352).	Crop demand, water availability, size of irrigated area
Nahr Maslama	c. 8 km?	c.3340	Harper and Wilkinson, 1975; SRTM	Flow calculation

In some cases the irrigated area can be surmised from the outline of the system itself, based on mapping from satellite images, even where excavated channel sections are unavailable. The Nahr al Abbara, well preserved in the 1960s CORONA images, is the best example of this in Northern Mesopotamia. The main canals, offtakes and drainage canals, when examined in relation to their topography using the DEMs (see **Chapter 6**) enable a potential irrigated area of about 3600 ha to be mapped (see **Table 6.3**). This value falls into the range suggested by Wilkinson (1998) for the Sahlan-Hammam canal. If the base flow of the Balikh at Ain al-Arous was about 6 m³/s, which could water up to 6000 ha (see Wilkinson, 1998, p81), then the Nahr Al Abbara had the potential to abstract around half of the flow of the Balikh: this would be a significant proportion of the Balikh's discharge, and could have had the potential to severely diminish the flow of the river. It is likely that a proportion of the available land was under fallow, indicating that less than 3600 ha was actively under cultivation at any time, and

that different crops had different water requirements (see Kaptijn's 2009 study of the Zerqa Triangle discussed below). This allowed for a water surplus but still represented a large-scale system throughout which water allocation may have been organised to some degree.

The data from the Hohokam canal systems (see **Chapter 4**) also suggests large areas could be irrigated from similar gravity-flow based systems (e.g. see Howard and Huckleberry, 1991, p186). Kaptijn's (2009; 2010) example from Jordan may provide the best parallel for the Nahr al Abbara in terms of organisation (also see **Table 6.3**). It also had a similar layout to the Nahr Al Abbara, with several main canals, submains and laterals (see Kaptijn, 2010, Fig. 3). The Zerqa triangle covers about 4700 ha (Kaptijn, 2009, p352), and benefited from a water surplus, although water storage was not implemented (*ibid.* p349-350). Based on river discharge and crop water use, she suggested that between 1800-4500 ha could have been irrigated in the driest month (May) of sample years (*ibid.* p352), which is comparable to the area irrigated by the Nahr Al Abbara.

In the early 20th century Zerqa, water allocation was carefully distributed according to units of time and by controlled by the means of basic blockages in the canals (Kaptijn 2009 p306). It is possible that the Nahr al Abbara operated in a similar way. The fairly regular layout of offtakes in the Nahr al Abbara may suggest a similar cyclical redistribution, with at least 20 farms cultivating the land, and with organisation provided by nearby Early Islamic sites such as Medinet al Farr.

Geographical distribution

The distribution of these systems can first be discussed in terms of geographic spread. The above descriptions show that several distinct 'types' of irrigation system exist throughout northern Mesopotamia. Systems consisting of large canals, often with high upcast banks, but lacking offtakes, are found throughout most of the region. Other irrigation systems are represented by narrow main canals with clear associated offtakes. Finally, the prevalence of qanats/tunnels must also be noted.

First, the clearest pattern observable relates to the differences in types of landscape through Northern Mesopotamia. In broad terms, the landscape can be separated into the riverine valleys and floodplains, and the semi-arid/arid steppe lands. The majority of identifiable relict irrigation systems are situated within, or alongside, the river valleys and well-watered areas (as **Figure 7.5** shows), where a year-round supply of water for abstraction was available, along with cultivable soils (those with the correct nutrient content and structural and moisture retention properties—see Young, 1976). Cultivation outside of the river valleys is more restricted. In fact, large relict canals were not identified by image interpretation in the steppe, and modern attempts at irrigated agriculture in this area have proved to be unsustainable (Hole and Zaitchik, 2006).

These same landscape divisions have affected the degree of preservation of relict features: by the time the most recent (21st century) images (for this study GeoEye-1 and IKONOS were examined, as well as the images provided by Google Earth) had been taken, most of the features mapped by this study had been erased from the cultivable areas, being replaced by modern irrigation schemes or urbanisation. The same areas which proved conducive to agriculture in the past, naturally also prove conducive to agriculture in modern times. Therefore the 1960s-1970s CORONA images often constitute the final record of past irrigation systems.

Before the modern irrigation projects (later 20th-21st century) and landscape intensification occurred, some systems with early origins had persisted for many years. Some of these may have been used, albeit with modifications, from the Early Islamic period up until the 1960s. The Nahr al Abbara is an example (it still flowed in the 20th century) which also shows signs of more than one phase of ancient main canal on very similar alignments (see **Figure 7.7**). The original choice of location/design was successful enough that these systems outlasted their original builders and were adopted and maintained by subsequent empires/states.

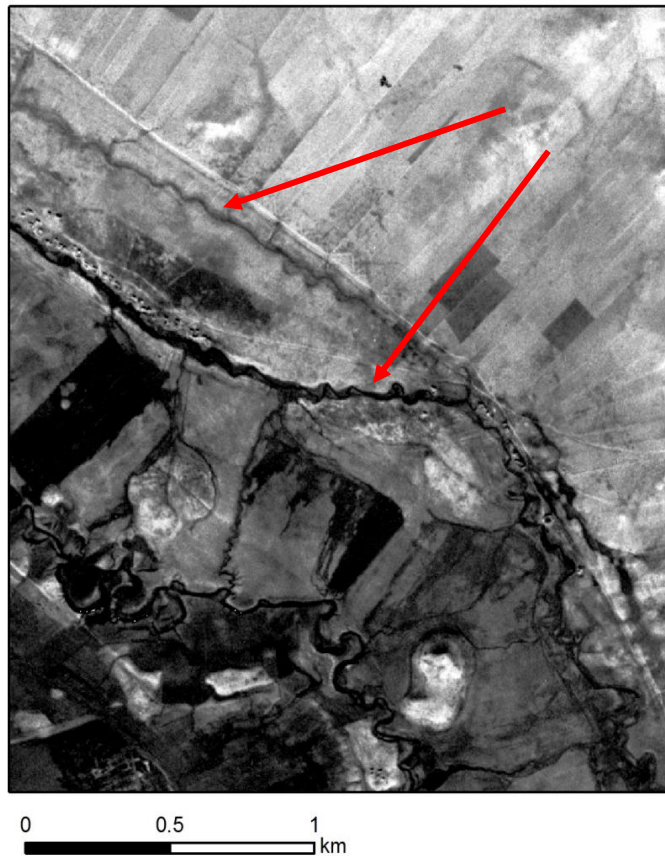


Figure 7.7: *Nahr al Abbara dual channels. CORONA image from 22 January 1967.*

The natural actions of the rivers themselves have often affected the preservation and survival of past water management. The river valleys have been transformed by their natural hydrological regimes; river avulsion, lateral erosion and flooding can all remove or obscure traces of canal systems. For example, the Euphrates floodplain evident in the CORONA images has been found to be relatively recent, post-dating some of the Early Islamic sites in the area, which have been truncated by the Euphrates (Demir et al, 2007, p2848; Hritz, 2013a, p1977; Challis et al, 2004, p144; Mulders, 1969, p44-45). The Balikh also avulsed, potentially erasing former, unknown remains near Tell Sahlan and Tell Hammam et Turkman. The Sahlan-Hammam canal, which has a fairly clear abstraction point, must have been constructed after this event.

A significant landscape zone in which ancient irrigation is found is the transition zone between the Euphrates valley and the steppe. Former large-scale canals flowed along the edge of the steppe, possibly for long distances: by the 1960s,

many of these large Euphrates canal systems were only preserved in segments, parts of them having been eroded by the river. More recently, the remaining traces of some canals (for example the Nahr Maslama and the Fray-Ja'bar canal) have been entirely obscured by the waters impounded by major dams.

Several of these major earthworks can be identified in the CORONA images. Most of these canals seem to be later in date (generally Early Islamic), which may represent an avoidance of using the less controllable flow of the Euphrates until a time when there was sufficient investment and availability of technology. For example, Van Liere (1963, p115) suggests that the tributaries were more easily used for irrigation than the Euphrates. How the steppe-edge canals might have functioned is now considered. The Nahr Dawrin's position would have meant that it was just outside the floodplain and therefore was protected from flood damage from the Euphrates. Partially eroded segments of this prominent and long canal could be digitised using the CORONA images. The point where it joins the Habur system (see Ergenzinger and Kuhne, 1991, p174), could not easily be identified, although somewhat ephemeral traces of the Habur canal were recorded upstream. An interesting construction of dual channels which seem to have some association with a former river meander may be close to a former abstraction point in the form of dams on the Euphrates (see **Chapter 5, Figures 5.40 and 5.41**).

Between the Balikh and the Habur, there are a few fragments of another large-scale earthwork that may be a canal and which is similar in appearance to the Nahr Dawrin (see **Figure 7.8**). **Figure 5.26** shows a map of the segments digitised from the CORONA images. If this is part the same feature located downstream by Geyer and Monchambert (2003, p276), it may be part of the Nahr Semiramis. A possible link with the Nahr Dawrin can be conjectured, if the canal could have crossed the Habur, perhaps by means of an aqueduct; similar situations have been proposed for the Neo-Assyrian canals of Northern Iraq (e.g. see Ur, 2005, p337). Another possibility is that it is part of the Nahr Sa'id, attested to in historical sources as an Early Islamic canal flowing on the left bank of the Euphrates past Circesium (see Le Strange, 1930, p105-106).

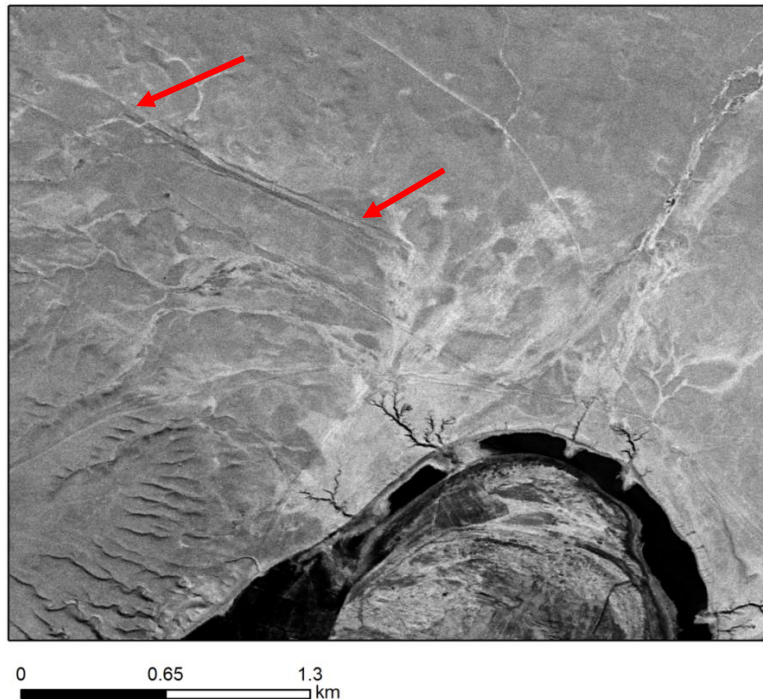


Figure 7.8: Earthwork of a possible canal segment between the Balikh and the Habur. CORONA image from 5 November 1968. Also see **Chapter 5, Figure 5.19**.

Upstream of this unknown canal and the Nahr Dawrin, the Nahr Maslama and the Fray-Ja'bar canal also flow along the boundary between the steppe and the Euphrates floodplain. Like the canals downstream, these are both wide features, with high upcast banks which were presumably a product of the need to raise the canal enough to carry water over a significant distance, of regular cleaning, and possibly also functioned as a way of protecting the canal/fields from flooding.

The CORONA images, unavailable at the times of the original investigations, revealed other segments of these canals. The early Islamic Nahr Maslama is less distinctive away from the Dibsi segment. However, traces of a very similar feature were found downstream (see **Figure 7.9**), also located at the boundary with the floodplain. This may also have been part of the Nahr Maslama. Given the size of the segments and the upcast banks, it is possible to conjecture that the canal would have been a significant feature when it was in use, possibly flowing for some distance.

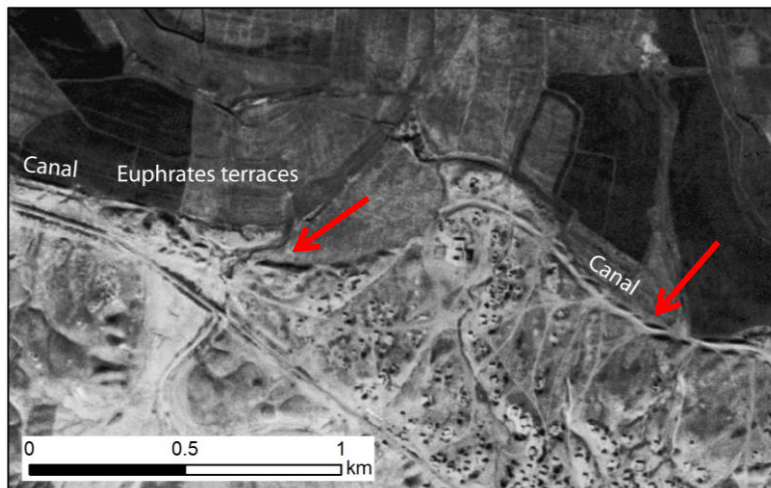


Figure 7.9: *Segments of an eroded canal on the edge of the Euphrates floodplain between Dibsī Faraj and Sura (not to be confused with the adjacent straighter, clearer-cut modern canal). CORONA image 22 January 1967.*

On the opposite bank of the Euphrates, the canal between Tell Fray and Qa'lat Ja'bar has a similar appearance. The known part of the canal at Tell Fray is only a small fragment of the overall channel (see **Chapter 2**) and is attributed to the Bronze Age (Bounni, 1988, p363) As **Chapter 5** demonstrates, it was, in the CORONA images, still extant over a length of up to 9 km. Its origin and destination are not entirely clear, although it may have associations with both Bronze Age Tell Fray and Islamic Qa'lat Ja'bar. The similarities between the Fray-Ja'bar, Nahr Maslama, Nahr Dawrin canals and the other Euphrates canals downstream of Raqqa as well as their presence on both sides of the river may suggest similar functions and designs. Their location may be related to the natural river level. Most of the known sites, and presumably their fields, are at the edge of the steppe, above the river. It might have been considered more practical to convey water in a canal from upstream, where the river level is higher, than to attempt to lift significant volumes of water. In general, their presence throughout the Euphrates valley shows the ability of the later empires, primarily the Early Islamic state, to impose and encourage water management.

Networks of water supply are also found in many of the Euphrates tributaries of northern Mesopotamia. Most of them consist of smaller channels (narrow with lower banks) than the Euphrates canals, and some of them are associated with offtakes, which give an indication of the size of the irrigated area. Their survival

may be partly due to later re-use and modification on the same alignments, as indicated above. The Balikh is the densest area of ancient irrigation, but tributaries such as the Habur, the Amarna, the Sajur and many smaller streams are also irrigated. The design of systems such as the Nahr al Abbara indicates that natural conditions were taken advantage of to maximise the irrigated area, making river valleys such as the Balikh economically significant. Cultural factors, such as the presence of a powerful state, may also have been a driver of water management in the Balikh. Interestingly, the Upper Habur shows relatively little indication of water management, aside from a few potential contenders identified by Ur near Hamoukar (2010, p88).

As well as canals, other features including tunnels and qanats are also found in the tributary river valleys. Traces of several rock-cut and masonry water conduits were recorded along the Wadis Amarna and Sajur, near Jerablus. Other subterranean water tunnels were identified using CORONA in the Balikh Valley, with multiple significant examples in the south around Raqqa, and several shorter qanats in the north near the Turkish border. These would have provided supplemental sources of water alongside smaller streams such as the Sajur.

Qanats and tunnels in Northern Mesopotamia can also be found in areas away from the natural streams, where permanent/easily used water sources were relatively distant. They tend to surround the hinterlands of the natural streams and rivers, around the edges of the canal-irrigated regions, rather than, with a few exceptions, watering the dry steppe lands. They include some rock-cut channels found in the Jerablus region, for example, the qanat near Hajaliyyeh (LCP 54; see **Table 2.1** and **Figure 2.2**). Similarly, the Membij canals radiate out from the Sajur area and the ephemeral water sources associated with it. The Balikh qanats and tunnel are another good example of this pattern. The qanats around Heraqlah were located in an area where the only other available watercourse was the Euphrates, which would have necessitated water lifting and flood mitigation. Using qanats may have been the most reliable way to ensure a regular water supply in the southern 'horseshoe' of the Balikh valley. The Raqqa tunnel could also have brought water into the dry horseshoe from the Qara Mokh/Balikh above, rather than lifting it from the Euphrates. Comparably, the Dibsi Faraj qanat seems to have supplied the site itself with water. These subterranean conduits, at the edges

of the natural permanent water sources, represent efforts to extend water into more marginal lands.

The larger groups of qanats tend to form distinct clusters. The qanats around Membij form a distinct group (see **Chapter 5**). The qanats south of south of the Sinjar mountains represent another cluster which seem to have tapped the enhanced groundwater at the foot of the Sinjar mountain, enabling cultivation to be extended further into the plain, carrying fresh water into a region where the available water is generally saline (UN-ESCWA and BGR, 2013, p586). The reason for the dense clustering of the Sinjar channels may be simply the presence of the appropriate hydrological and geological conditions. There may also be cultural factors, such as the presence of a state or community interested in investing in them.

The map of pre-modern water systems in northern Mesopotamia (**Figure 7.6**) shows that there are three main classes of water supply identifiable using CORONA images: large, longitudinal canals alongside the Euphrates; generally narrower canal features, with associated offtakes, in the valleys of the tributaries; and qanats and tunnels in the more marginal lands in the hinterlands of the river valleys (cf. Kamash, 2010, p45). It is worth noting that the tunnels and qanats are not always, as Kamash indicates, in zones entirely distinct from the valley canals; rather, they sometimes extend the irrigated area at the edges of more intensively cultivated valleys.

Outside of these areas of year-round water supply, hydraulic remains are far scarcer. The uncultivated steppe lands and plains of northern Syria and Iraq lack the large-scale, complex canal systems identified in the alluvial lands, although traces of small-scale water harvesting structures such as check dams are occasionally evident in the CORONA images. Several archaeological surveys, as well as the present study, have examined regions such as the North Jazira in Iraq (see Wilkinson and Tucker, 1995) and found no trace of ancient irrigation systems.

It is important to reiterate here that known features which could be located were mapped, and that features discovered through examination of the CORONA imagery were also recorded; any missing features will be those that are less visible when using remote sensing (this issue was confirmed during fieldwork (see

Chapter 3.2). Overall, a reasonably detailed picture of past water management in northern Mesopotamia was generated by this study.

The patterns identified by this thesis would suggest that water management was focused on areas where soils were the most conducive to agriculture, therefore, areas in which the investment of building canals was worthwhile. They were also located in areas where water sources were available, for example, the Neo-Assyrian canals of northern Iraq derive their water from perennial rivers. This may be why nearby areas, such as the North Jazira in Iraq (Wilkinson and Tucker, 1995), are devoid of canals, because they lack these year-round sources of water.

Political Distribution

The patterns mapped using satellite imagery and survey also relate to the territories of empires; specifically, the scale of water management systems can reflect the span of control of empires. Empires are only likely to invest in water management in areas in which they have some jurisdiction. This could include their heartlands, and also their frontiers: essentially, areas which already have some settlement and infrastructure. Where water management remains can be dated, and associated with sites linked to a particular state, the scale of the state's influence in the surrounding countryside can be 'mapped'. The Balikh is a good example. The reaches of the water management features supplying Raqqa and its environs stretch across most of the 'horseshoe', with possible activity as far west as Heraqlah (in the form of qanats). The Balikh horseshoe therefore must have been part of the Abbasid imperial landscape. In fact, their control of the countryside stretched beyond this: upstream in the north of the Balikh Valley, the Nahr al Abbara is a significant system, comprising main canals and offtakes and presumably requiring some careful planning and maintenance. Given the dating evidence (see Wilkinson, 1998, p67-68), and the proximity of the important Early Islamic sites of Medinat al Farr and Khirbet Ambar, this area presumably was also under the empire's influence. Similarly, long canals alongside the Euphrates of Early Islamic date, such as the Nahr Maslama, and possibly also the Nahr Dawrin, may indicate Early Islamic interest and investment throughout the Syrian Euphrates valley.

When choosing to construct a large scale system (i.e not water harvesting), there seem to be certain locational requirements:

1. Permanent water source (river or groundwater)
2. Soils conducive to agriculture
3. A sedentary population of sufficient size to supply labour.

Interestingly, within these cultivated and irrigated areas, there are several regions where the density of past water management features is particularly high. In terms of really long canals, the Habur and Euphrates regions stand out. In terms of overall density and quantity of features, the Balikh is the most complex irrigated area. Qanats are most dense around Membij (Hieropolis) and in the Sinjar region.

The features identified in the more marginal, less populated lands tend to be predominantly small-scale water-harvesting devices such as cisterns and check dams, and some qanats. Arguably these are irrigation methods which are more easily constructed at a community or even farm-based level.

In terms of population requirements, it is worth noting here that at the time when agriculture and presumably large-scale irrigation declined, during the Ottoman period, many communities were mobile rather than sedentary (Winter, 2009, p253).

7.8 Scales of Imperial control

This discussion of the scale and distribution of water management remains throughout northern Mesopotamia has demonstrated that many of them were constructed and/or used during the time of the later territorial empires. As the map (**Figure 7.6**) shows, canals were located throughout the region, with some systems flowing across large areas. Their presence and function can be discussed in terms of their historical context, facilitating a recognition of how they represent specific scales of imperial control from the time of the Neo-Assyrian empire onwards. This section will argue that strong states and empires used contemporary technologies effectively and employed multiple forms of control and administration of water management at empire-wide scales, supporting their

economies by constructing new systems and taking advantage of existing landscapes.

Technological development and reuse

The power to exercise control of water across such large geographical scales was exercised through an ability to invest in technology and to control abstraction. The technology required for the construction of canal systems and qanats was already in existence by the Neo-Assyrian period (Davey, 1985). Historical references to canal irrigation in northern Mesopotamia before the period of the later empires (for example attested in historical documents from Mari) have already been noted. Given this evidence, and also the studies of the well-known Bronze Age irrigation systems of southern Mesopotamia (Adams, 1974), it is clear that the later empires were able to draw on existing technology.

However, using the technology would still have necessitated knowledge, investment and organisation. Several of the systems of known date mapped by this research (see **Chapters 5 and 6**) show high levels of complexity and sophistication. They are represented by two kinds of scale, encompassing irrigated area and the size of the main canals themselves. This research identified examples of canals facilitating irrigation across larger landscape units, such as the Nahr al Abbara and possibly the West Balikh systems. It is also represented by long, wide features with significant upcast banks (primarily the Euphrates canals).

Wittfogel may have been working from a perspective that increased technological development in terms of water management was linked to the power of individual states (Foster, 2000, p245). Whether or not individual states constructed new systems, or took advantage of existing ones, is an important issue to consider here. It may be worth noting that water management systems, once they are established, become an integral part of the landscape. Maintaining and enhancing an existing landscape, assuming that it functions, is generally easier and more logical than replacing it.

There are several cases of technological re-use/borrowing. Sometimes, later irrigation systems appear to have followed the same alignments, or even reused

and modified the same canals as earlier systems. Again, the Nahr al Abbara can be noted here (see **Chapter 6**). Similarly, Ergenzinger et al (1988) indicate that the long canals alongside the Habur might have been in use from the Middle-Assyrian to the Early Islamic period, which could indicate use over a period of just over 1000 years, spanning the eras of several different states and showing that maintaining an existing landscape, despite political changes, was practised. By taking advantage of existing technological developments states could enhance their economic power at relatively low costs: certainly this would have been easier than designing new systems.

In the context of technological re-use the Sinjar qanats are also significant (see **Chapter 5**). Some of these appear to be relatively modern (early-mid 20th century) tunnels using an ancient technology; in this period, however, they stand out as an exceptionally dense area of irrigation in the midst of largely rain-fed plains; the CORONA images show that active irrigation in the 1960s was mostly confined to the river floodplains, or to the fields surrounding individual wells. If Lightfoot (2009 p20) and Fuccaro (1991) are correct that some of them may be ancient, this could be a case of much later states attempting to revitalise and apply ancient technology.

Decker emphasises ideas of technological re-use, suggesting that late antique water management often borrowed existing technology and further applied it (Decker, 2009a, p259). In addition, he indicates that Islamic agricultural systems were built upon Roman constructions (Decker, 2009b, p206): overall, he is reluctant to emphasise any large-scale intensification and innovation in the Early Islamic period, although he recognises these to some extent in a later paper (2011). Kennedy (2011) attributes more significance to Islamic irrigation, indicating that it supported the growth of large and powerful cities, specifically Baghdad (ibid.p195), intensifying agriculture and cultivating marginal lands, rather than only re-using the earlier systems. By using existing systems and by also expanding irrigation into more marginal lands empires were able to extend the scale of their economic control over the landscape.

The results of this research support Kennedy's ideas (2011) and Decker's (2011) modified theory, suggesting that the Early Islamic states may have introduced new

systems and modified old ones at a greater scale and density than Decker had originally indicated. The Nahr al Abbara may be a good example of this, representing an extensive and sophisticated system which seems to have been constructed in the Early Islamic period. If Kaptijn's Mamluk sharecropping example (Kaptijn 2010) is at all comparable to the Nahr Al Abbara, it might suggest a system which produced reliable yields and taxes which, overseen by the nearby site of Medinant al Farr, and possibly also by Khirbet al-Ambar, were directly managed by the Early Islamic elite. Medinat Al Farr may have been part of an estate owned by the Umayyad commander Maslama ibn Abd al-Malik, in the early 8th century AD (see Heidemann, 2011, p48). Heidemann interprets the site as a rural administrative centre, which became a small town in the Abbasid period (Heidemann, 2011, p48). Some of early Islamic evidence gathered by this research, therefore, may represent systems managed by elite individuals rather than directly by the state.

Scales of control and conflict

The expansion of imperial water organisation over large geographical scales may have led to conflict with existing populations. To what extent these states were powerful enough to control irrigation, and to what extent this was a source of conflict, can be reviewed here. It is possible that water abstraction which was outside of the control of the state may have been discouraged, or at least viewed in terms of competition. By managing water at empire-wide scales, the state could have limited this kind of threat.

As discussed in **Chapter 1**, some scholars have indicated that the potential economic power of even local communities organising irrigation could be regarded as a threat to the state (Hunt, 1988, p248; Davies, 2009, p29). However, this same organisation of water could in itself be a response to the power of the state: systems could have been planned, constructed and maintained by local groups, with a view to supporting or surviving the demands of the imperial economy.

There is historical evidence that water conflict existed in ancient northern Mesopotamia. A letter from Mari refers to a complaint between two sites in the

Balikh: the downstream settlement complained that the city upstream was abstracting too much water (Villard, 1987). This is an interesting example of a community attempting to deal with water threat received from another similar community by appealing to higher authorities. Large-scale irrigation systems like the Nahr al Abbara and the canals alongside the Habur could have abstracted considerable volumes of water. Whoever controlled these systems may have needed to also have some kind of general control over abstraction in the Balikh and Habur catchments. That a single system had the potential to abstract so much water certainly suggests that whoever administered it maintained the right to control abstraction.

That the later territorial empires imposed new irrigation systems on the landscape is clear from the results of this study. How well received these were by existing groups is not always so obvious: it is possible that the imposition of new landscape changes would be resisted by an established population. In general, whether at a local—or large-scale level, as Mabry suggests (2000, p291), farmers are likely to be more cooperative if they perceive themselves to be receiving direct benefits from an irrigation system.

Effectiveness of control

Whether or not a system was successful may be reflective of a state's ability to apply technology effectively, or to control abstraction and drainage throughout an irrigated area. How sustainable systems were has implications for how efficiently they might have functioned and how long they might have persisted. Failure would have been a waste of a state's resources. Complex systems of main canals and laterals like the Nahr al Abbara were probably constructed as part of a single project. The amount of water which could have been abstracted, and how it would have flowed throughout the system would need to have been understood. An understanding of drainage needs is also important to prevent waterlogging and salinization.

There are several instances of multiple parallel channels on the same alignments and it is possible that these may indicate repeated attempts to design an effective

channel with the right balance of flow. An example which may be part of the Nahr Dawrin (see **Figure 5.41**) and a similar system represented by the Nahr al Abbara (**Figure 7.7**) demonstrates this pattern. If the gradient of a system was too low, then excessive siltation would have required so much dredging that it could have become uneconomic, but if the gradient was too high, then excessive erosion could have damaged channels. In addition, other practices such as correctly assessing the necessary water availability and the management of drainage and mitigation of flooding would also have been needed.

Systems which show signs of failure include the West Balikh canals. In such cases, layers of eroded, silted channels meander across the landscape. Throughout the Balikh features such as gilgai indicate episodes of waterlogging and drying, and evidence of flooding is also apparent. The management of seasonally high runoff may have been significant in this particular case.

However, other systems show considerable success: the Nahr al Abbara made careful use of its topography, allowing a large area to be irrigated. That parts of the system were still in use during the 20th century (e.g. see Wilkinson, 1998, p68), but on ancient alignments, attests to its success and sustainability. This may well be a system which was initially designed as a comprehensive project, including offtakes at regular intervals and drainage channels. As proposed above, it may be comparable to the Zerqa example (Kaptijn, 2009; 2010), where irrigation was controlled as part of a hierarchical system, to produce an economic surplus for the sheikh or other elite individual (Kaptijn, 2009, p424).

There are certainly examples of qanat systems functioning effectively enough that they persisted for centuries. Whether or not these were controlled by a state or more independently would be interesting to investigate. Rock-cut channels around Jerablus appear to have functioned later than the Byzantine period (fieldwork 2010; see **Chapter 3.2**), which may also be true for many of the other qanats and tunnels identified in the project area. The implication is that these features were in use in the Islamic period, reinforcing the evidence for intensive water management at that time.

Certainly, where systems functioned efficiently, they would have supported agriculture in areas formerly dependant on unreliable and often low rainfall,

inevitably bolstering the economy of the communities that maintained and used them and the state which benefited from taxes levied on those communities.

Direct and indirect control

Control of water by the later territorial empires seems to have taken several different forms, often relating to the different scales of control empires were able to exercise over the different parts of their territories. In some cases these are identifiable. Examples of how states directly sponsored irrigation will now be discussed, as well as examples of more indirectly controlled/encouraged water management systems.

In some cases, the empire seems to have directly managed water resources. The results of this study (**Figure 7.6**) show particularly dense concentrations of artificial channels around centres such as Raqqa and Nineveh. The channels associated with important Early Islamic sites (for example, Baghdad, Samarra and Raqqa) are particularly indicative of imperial control, where the state was concerned with ensuring reliable supplies of water to the immediate hinterlands of their cities, presumably for irrigation as well as for domestic use. Contemporary sources support this (e.g. Toueir, 1990, who cites historical documents). Similarly, the Neo-Assyrian systems of northern Iraq have been attributed directly to investment by the king.

By organising water management directly, imperial states could ensure how and by whom agriculture was conducted. They might also have felt more secure in predicting yields, especially if the problem of over-abstraction by other groups could be eliminated. Constructing a long canal system could ensure that water was abstracted closer to the source, before other groups could divert it, and carried safely downstream to the use-point where it was managed by imperial authorities. However, Ertsen (2010) has also provided evidence of the opposite case, where the state constructed a main canal, and local users administered water abstraction further downstream.

Too much competition for water (and depletion of water in rivers) would have made it difficult to maintain sophisticated irrigation systems such as the Nahr al

Abbara, or the tunnels and qanats around Raqqa. These kinds of systems are generally carefully designed with specific water resources and requirements in mind: significant changes to both of these would be effected by uncontrolled abstraction upstream. The success of the larger-scale canal systems may, in part, have been due to careful control and exercise of power throughout whole catchments by imperial authorities or elite individuals.

This direct imposition of water management in general seems to have been related to the differential scales of control across an empire, because the best evidence for direct control comes from locations which formed centres of imperial control (Raqqa, Baghdad, Samarra). Spatially, the presence of complex irrigation systems in these areas directly reflects the strength of imperial control.

Less direct control involved encouraging and incentivising water management. It seems reasonable to suggest that many water management systems, across all geographical scales, were not directly administered by the imperial authorities, but rather functioned within an imperial administrative framework. For example, cisterns in the Harran/Balikh region were recorded by the Harran census (e.g. see Fales and Postgate, 1995), and were probably constructed and maintained by the individual farms listed, however, they were included in the census presumably because they were considered to be part of the farmsteads which the Imperial authorities regarded as Neo-Assyrian entities.

A situation combining different ways of managing water could easily have existed; with some irrigation systems being directly managed by the Imperial authorities, for example the water supplies of the imperial capitals and their hinterlands, but with others receiving less or no oversight. Groups at a local community or even individual farm scale could have taken advantage of the increased stability available during these times to construct and manage an irrigation system. Similarly, they could have been obliged to adopt these methods in the face of increasing taxation (e.g. see Wilkinson and Rayne, 2010, p138).

The way in which investment in irrigation was managed under the Early Islamic empires is an interesting example of how water management could be controlled. Aside from direct imperial sponsorship of canals, as historical sources suggest, wealthy individuals, often members of the royal family or other elites, were

encouraged to bring marginal lands under cultivation by tax breaks and land ownership laws (e.g. see Kennedy, 2011, p181-182). This is an example of the state (who made the laws) incentivising private individuals/groups to irrigate using their own financial resources. In fact, the Early Islamic laws in this case may be an explanation for the peak in irrigation at that time.

Irrigation in the Early Islamic period may have been sponsored by elite families (Decker, 2011, p5). This is an example of irrigation managed by groups that do not necessarily represent the state themselves, but who operated within and became powerful under an overall framework of empire. Kennedy (2011, p194) suggests, based on historical evidence, that the Nahr Dawrin may have been part of an irrigation scheme initiated by relatives of an Umayyad caliph. This would be an example of elites who were part of the state, but not necessarily themselves in control of it, taking advantage of the imperial power structures to invest in irrigation.

This form of water control seems to have occurred at empire-wide scales, and was not always necessarily confined to the centres of empires; as the Early Islamic sources suggest (Kennedy, 2011, p181-182) it also represent attempts to bring more marginal lands under cultivation. While the ability to promote this does to an extent indicate that imperial control extended beyond the main centres, it may also indicate that states were less interested in directly sponsoring and managing irrigation outside of these centres.

Centres and frontiers

The span of an empire's control over water management can also be discussed in terms of the scale of its political control. As discussed above, the clearest evidence of direct state involvement comes from the imperial centres (e.g. Raqqa, Nineveh and Assur): that is, direct state involvement in enhancing the agricultural production of their main power bases. The association between the water management features around Raqqa and the Abbasid capital and palaces also implies that they were part of the Early Islamic Imperial landscape.

Whether the same picture can be identified for the periphery of the later empires' territories should be assessed. The results of this study (**Figure 7.6**) show that irrigation was distributed throughout northern Mesopotamia and was not only confined to known centres such as Raqqa and Nineveh. Water management features dating to periods when specific areas were at the frontier of empires are known; the cisterns at Resafa, and their associated dam and channels, are a good example. In this case, the frontier status of the site may have been particularly significant; water management and defence were carefully integrated (Brinker, 1991) to ensure a reliable supply of water even during times of instability. Lightfoot (2009, p16) also raised the possibility that qanats at Sinjar may have been linked to the Roman *limes*. Fuccaro (1991, p12) suggests that these qanats are pre-Ottoman, giving an idea of a productive landscape of water mills and fields. These are specific examples of water management being tied directly to the presence of the frontier, to fortifications. Interestingly, at Dibsi Faraj and at Heraqlah water was also brought into the sites in a 'secure' way, using qanats and wells.

However, such a peripheral, unstable status may also have been detrimental to irrigated cultivation. Kennedy (2011, p196) suggests that when northern Mesopotamia was a frontier zone between the Roman and Sasanian empires, political conditions were too unstable for cultivation and associated irrigation. When more secure dating evidence can be obtained for more irrigation features, whether or not the frontier zone throughout the time of the Later Empires was a place where irrigated agriculture thrived can be further explored.

Chronological trajectory of water and power

The question of when the original landscape changes occurred which supported the succession of empires should be investigated. It may have been the Neo-Assyrian empire which initially imposed some reorganisation on the landscape (this reorganisation has been discussed in the literature, e.g. see Wilkinson and Barbanes, 2000). To some extent the patterns which the later empires took advantage of may have been established in the Iron Age, including investment in irrigation. Once the way in which water flows through a landscape has been

established, it is difficult and expensive to change it. If successful, irrigation systems will be reused, or new ones at least constructed on the same alignments.

The agricultural changes established by the Neo-Assyrians enhanced their economic power. The canals in the hinterland of Nineveh would have supported the agricultural demands of large Assyrian cities in Northern Iraq. Later on, these established systems may also have aided subsequent states, again supporting their agricultural economies.

That the later empires were capable of constructing new irrigation systems however, also seems to be clear. These hydraulic systems were evidently part of the visible, identifiable 'result' of their power. The Abbasid remains around Raqqa are a good example. Formerly Samarra had been the Early Islamic power-base, but once this shifted to the 'backwater' of the Balikh, the Abbasid state seems to have exercised its authority and economic strength to construct new water management features. The water management remains around Raqqa are a direct indicator of the state's power, and they reflect similar work undertaken at Samarra, where apparently at the time of Harun ar Rashid a canal was dug to water the city's hinterland (Northedge, 2011, p35).

It is possible to suggest that there was a gradual development of irrigation, with early patterns of use of the rain-fed zone initiated in the Assyrian period (for example large-scale irrigation in Northern Iraq). Subsequently, later states re-used some of these systems (e.g. the Habur canals), adding new features where necessary (such as the Hellenistic canals in the Balikh, and qanats at Membij). The Roman and Byzantine states intensified the use of irrigation, establishing the use of a range of water management systems including qanats (for example see the Jerablus region) and cisterns (Resafa). Cultivation may have affected by plagues in the 5th and 6th centuries AD (see Decker, 2009a, p260) and Morony (2007) compiled sources which recorded massive depopulation (ibid. p73), shortages of labour (ibid. p81) and neglected fields (ibid. p68). Similarly, Kennedy suggests that the outbreaks of plague could have been related to changes and decline in settlement patterns after the mid 6th century AD (Kennedy, 2007, p92-95).

However, even allowing for some decline in cultivation, by the time the Early Islamic empires were active in northern Mesopotamia, the landscape would have already contained water management features. These were often re-used by the Early Islamic states, who also constructed new systems (for example in the Balikh, at Dibsī Faraj and in northern Iraq). This appears to have been an Early Islamic peak in irrigation. It is possible that systems that had fallen into disuse in the 5th and 6th centuries were repaired at this time, alongside the construction of new systems. In the following period, the Ottoman era, irrigation to some extent may have declined, although some of the existing systems may have been re-used (for example the Nahr Dawrin).

Based on the results of this study, water management in northern Mesopotamia does appear to have intensified in the period of the later empires, developing from the landscape changes during the Assyrian period onwards. Whether most individual systems were directly governed by the imperial authorities or by local communities is unclear. However, it may be useful to recognise the systems as part of an imperial framework, in which powerful states were capable of constructing new systems, as well as repairing and maintaining existing systems. They were also interested in ensuring economic wealth and power through their manipulation of these resources, and through taxation of the communities which used/managed them. The differences in the scale, density and distribution of canals throughout each empire can also reflect the state's control over the landscape, with this more easily exercised in the centres, but also represented to a lesser extent by irrigation in the imperial peripheries.

Wittfogel recognised a link between water and power, but failed to explain it with clearly presented evidence (see Wittfogel, 1957). This research has discussed evidence for water management in northern Mesopotamia, showing that directly and indirectly, empires were controlling water, at varying scales of control across their territories. As **Table 6.3** shows, they were able to irrigate large areas of the river valleys, potentially dramatically depleting the available water resources. Having a strong administrative structure already in place, and the pressure of economic demands, encouraged and compelled the state to undertake and promote irrigation and landscape management. Water management seems to have been deliberately and directly controlled around the centres, and less

directly, but still significantly, encouraged throughout the rest of their lands, as the dense networks of canals mapped by this study show. It is less a case of needing or developing a certain level of bureaucratic structure, but more a case of using this structure effectively. The fact that irrigation is sometimes neglected when there is a conflict (cf. modern Syria; see **Chapter 8**) demonstrates the significance of the state in water management.

Water and power

This research has demonstrated that a detailed dataset of irrigation is needed in order to discuss the scale and distribution of water management at the time of the later territorial empires. Applying the Wittfogel debate is not productive for imperial northern Mesopotamia, given that his argument tends to refer to the drier southern Mesopotamia and that most problematically, Wittfogel does not provide the empirical evidence (such as data from surveys and excavations) needed to validate his theory.

Data about the form, distribution, scale and administration of water-management features makes it possible to address new and important questions about empires and water and to what degree empires were able to control their hydraulic landscape. The present study provides these data; an area of c.100,000 km, representing northern Mesopotamia, was examined for water-management features using multiple datasets including CORONA images, DEMs, and survey evidence. Traces of irrigation dating to the period of the later empires were identified throughout the region, including large-scale reticulated canal systems, qanats and tunnels.

The data gathered by the present study indicate a need for a discussion of how and why powerful empires used and developed water-management technologies to support their economies. By definition, an empire is a state which exercises control over its territories (e.g. Taagepera, 1978a, p113): this might take the form of deliberately influencing settlement patterns, for example the Assyrian practice of deportations, or by investing resources to construct new irrigation systems. Large-scale irrigation requires expensive investments in construction, maintenance,

administration and potentially in dealing with conflict. Having influence over agriculture, whether through imposition, incentives or pressure, would have been within the remit of the ancient territorial empires.

Chapter 1 identified a need to use new datasets to move away from Wittfogel and take an evidence-based approach to imperial water management. Satellite images allowed the large study area to be examined quickly and in detail; DEMs gave hydrological context; survey data provided dating information; and in some cases historical accounts revealed further information about how irrigation was imposed, incentivised and controlled. The results of this are presented in **Chapters 5** and **6**. **Chapter 1** also raises the question of how these data can be used to make interpretations of how empires could have imposed or encouraged the use of water management technologies.

Chapter 5 showed that irrigation features dating to the time of the later territorial empires are prevalent throughout northern Mesopotamia; from as early as the Assyrian period, these states were able to exert an organising influence on the landscape, represented by Assyrian canals in northern Iraq and the Habur. **Chapter 6** examined the complexity of irrigation the Balikh. Given that detailed survey and excavation data, as well as the remote sensing data, was available for the Balikh, it was possible to map intensive irrigation dating to the period of the later empires.

The present chapter has discussed the results of the interdisciplinary analysis. It was found that water-management features were distributed across the cultivable areas of northern Mesopotamia, reaching a peak during the Early Islamic era. The extensive distribution shows that the Early Islamic economy was capable of generating enough demand that even formerly marginal areas were brought into cultivation. Expanding cultivation would have been especially necessary in the context of the growth of large cities. Areas with permanent water sources, such as the Balikh, were irrigated using large-scale, reticulated canal systems. Even areas without perennial rivers were irrigated, using tunnels and qanats to tap groundwater.

This research has focused on the period of the later empires, which were the first states to exercise control over large areas of the landscape; their ability to apply

irrigation throughout their territories, despite transport costs and complex administrative structures, is symptomatic of this. The different degrees of control exercised in different parts of empires may be significant in the context of water and power. In many cases, the densest concentration of large-scale systems seems to have been close to imperial heartlands, for example the Neo-Assyrian canals in Northern Iraq, and the Islamic features around Raqqa in Syria. While these states may have had differing power structures overall, for both of these examples, historical evidence suggests that the state (e.g. Sennacherib and Harun ar Rashid) was involved in the sponsoring/construction of some of these large canals.

It is possible that canal systems outside the core areas may have been less tightly managed by individual states, but the need for irrigated cultivation in these areas was recognised by the Early Islamic empire and incentivised through systems such as tax breaks (e.g. Kennedy, 2011, p181-182). Large canal systems were recorded by the present study in areas away from the capital cities, for example, Neo-Assyrian canals in the Habur region, showing that the state was also willing to invest in irrigation, or apply demand, in more peripheral regions.

This widespread distribution of water management features throughout different zones of empires and different types of landscapes shows that empires were willing to invest in areas further from their heartlands, demonstrating their control over the landscape. States did not have to be directly involved in the management and maintenance of irrigation systems; often the influence of their resources, technological knowledge, organising abilities and economic demands was powerful enough to incentivise/impose irrigation which was then managed by local groups (see discussion in **Chapter 4**). Systems could have been deliberately controlled by the state, or administered by elite individuals. The Neo-Assyrian systems, some inscribed with Sennacherib's name, are an example of direct state involvement. The Wadi Zerqa example shows elite individuals managing a system of sharecropping (see Kaptijn, 2009; 2010). An example of local management is Glick's (1970) analysis of irrigation in medieval Valencia, where local groups managed irrigation communally.

Demands and incentives for enhanced agriculture led to the presence of the canal traces mapped by the present research, all the way down the Euphrates, from Carchemish to the Iraqi border. Early Islamic irrigation was not confined to Raqqa in the north, or Samarra and Baghdad in the south. Other areas of tight state control include frontiers and sites of strategic importance: examples such as Resafa and Dibsi Faraj show that states were also able to invest in water-management systems in frontier areas. Overall, empires were powerful enough to be able to invest in irrigation throughout their territories; this would have meant exercising control over local populations and over the resources required to apply irrigation technology.

A large body of research has discussed individual areas of irrigation in northern Mesopotamia (e.g. see Ur, 2005; Wilkinson, 1998; Geyer and Monchambert, 2003). The present study has linked these areas and revealed new irrigation systems, by using remote sensing to examine the whole region. The widespread distribution of water-management systems which this analysis identified, throughout different zones of an empire, and the apparent mixture between direct state control and incentives, show that the later territorial empires (Neo-Assyrian-Early Islamic) were able to exercise the power and command the resources necessary to invest in irrigation. Rain-fed cultivation is possible in these areas, although risky, as the rainfall analysis shows (**Chapter 3**). Large states, however, needed to ensure that their economic basis was more reliably supported with higher yields, making investment in irrigation a necessity.

7.9 Justification

This leads into an understanding of the present issues surrounding water in the Near East. As **Chapter 1** outlined, water management is currently a significant political issue that is likely to become even more contentious in the future. Syria and Iraq are dependent on Turkey's use of the Euphrates, a situation which has already led to conflict (Kliot, 1994).

The agricultural economic bases of many powerful states, including the later territorial empires, were dependant on irrigation to ensure reliable and significant

yields. While rain-fed cultivation had been practiced, and was indeed still practiced until very recently (Beaumont, 1996, p140), at times when powerful states are involved rainfall alone did not seem to be sufficient to secure high yields. Rain-fed agriculture often seems to predominate at times when there was something of a 'power vacuum', where there was less active organisation of the landscape, for example during the early 20th century.

The discussion has already dealt with the issues of water competition and how this might be a threat to states. Currently, impoundment and over-abstraction of water by the Euphrates riparian states can be viewed by downstream states as a threat to their own water security. As already mentioned, this was also an issue in the past. Many areas of the Middle East now rely on pumping from groundwater, often managed at the level of individual farms. Because pumping depletes the water table more quickly than it can be recharged, it renders traditional gravity-flow systems such as qanats unusable. Examples of the use of pumps were observed in the Jerablus region in Syria in 2010. Abstraction by individual farms even using ancient methods may have been viewed as a threat to the survival of more organised systems by past states.

When these data were analysed, it was generally not possible to view separate periods in isolation. Consequently, water management features with evidence for use from the Bronze Age and into the time of the later territorial empires were investigated as part of an interlinked trajectory. Many systems appear to have been reused, modified, abandoned and replaced with systems on the same alignment throughout this time. Irrigation may have declined after the Mongol conquests, but traces of check dams and wadi diversions may account for agriculture in this period, as well as a reliance on rainfall. A few larger-scale reticulated systems may have been used at this time, some with ancient origins, notably in the Balikh (e.g. see the West Balikh and the Nahr al Abbara). It was only in the mid 20th century onwards that attempts to change this pattern were made, with new irrigation schemes being constructed, many of which never reached their full potential (Hole and Zaitchik, 2006, p150).

The ability of a state to control water resources in terms of how they are organised and accessed is significant, demonstrating issues which seem to have applied to

northern Mesopotamia throughout history. In many ways, the current situation is a continuation of the same circumstances/developments that were involved in ancient water management.

7.10 Summary

This project aimed to generate a detailed map of ancient irrigation in northern Mesopotamia, using new and historic high resolution satellite images to record new features and digitise known ones. While fieldwork and availability of some data (e.g. detailed, accurate CORONA image parameters) was limited, the main aim was successfully achieved (see **Figure 7.6**).

This map has revealed important patterns, and made it possible to discuss issues such as the scale, distribution and chronology of water management in a region between the Euphrates and the Tigris. As section 6.7 shows, this included extensive systems which were capable of irrigating large areas. Technologies including gravity-flow canal systems, qanats and tunnels were applied according to natural climatic and hydrological conditions. These were concentrated in areas directly controlled by powerful empires, but also, in some cases, supported agriculture in more peripheral, but often strategic areas. The use of CORONA images and stereopairs in combination with other datasets such as DEMs and survey databases facilitated a more detailed and comprehensive reconstruction to be generated than had previously been possible, allowing for a discussion of the scale of ancient water management based on new and expanded empirical evidence.

The results of this research show the inverse of what Wittfogel (1957) proposed. The organising power of the later empires enabled them to impose and incentivise irrigation into the formerly marginal lands of the rain-fed zone. The map produced by this thesis shows evidence for water management in all the cultivable river valleys of northern Mesopotamia, giving an impression of an intensively cultivated and managed landscape.

Chapter 8: Conclusion

8. 1 Aims and results

The aim of this research was to map ancient water management systems in northern Mesopotamia at the time of the later territorial empires, taking a new and interdisciplinary approach that combines the use of remote sensing, GIS and archaeological survey.

Three principal research questions were addressed by the results of this study;

1. Is there archaeological evidence for extensive water management systems in Northern Mesopotamia, and if so, can this evidence be mapped from satellite imagery and validated using DEMs?
2. Can declassified 'historic' spy satellite data be used to interpret the function, historical context, scale and distribution of ancient water features?
3. How can we make interpretations from this data to investigate how the later territorial empires might have imposed, incentivised and encouraged the use of water management technology?

Chapters 5 and 6 show the extensive archaeological evidence for ancient water management compiled by this thesis across a 100,100 km² area. This involved mapping areas of water management that had previously not been known, and extending knowledge of known features.

By combining different remotely sensed and archaeological datasets, this research demonstrates a new approach to recording water management features, using the best available data. Image interpretation was undertaken using 1960s-1970s CORONA images. Newly identified irrigation systems and data collected by existing surveys and excavations were digitised and incorporated into a GIS database. This methodology enabled the construction of a detailed map of irrigation systems throughout northern Mesopotamia. **Figure 6.5** shows that extensive canal-based irrigation systems flowed alongside the Euphrates, and also

most of those tributaries of the Euphrates and Tigris which experienced year-round flow (this includes systems in the Balikh and Habur). Evidence for water management outside the main rivers was also found, for example, the qanats around Membij and Sinjar.

Hydrological information about how canals systems functioned and how much land they could have watered was derived from DEMs of resolutions between 10-90 m (SRTM, ASTER, and CORONA). The DEMs were used successfully in many cases to record the gradients of canals (see **Table 5.2**), which enabled canals to be distinguished from other linear features such as hollow ways, and for their efficiency to be estimated. Using DEMs to generate cross-sections was also informative. For example, the higher-resolution CORONA DEM cross-section (**Figure 6.24**) shows that the Hammam channel was protected by upcast banks and flowed along the bottom of the slope, on a similar alignment to the Balikh itself.

This project successfully used remote sensing to generate a map (**Figure 7.6**) of water management at the time of the later territorial empires, facilitating the interpretation proposed in the second and third research questions. This comprised a discussion of the scale and distribution of ancient water management. Based on this map, the chronological development of water management in northern Mesopotamia was discussed and the role of powerful states in establishing and encouraging it assessed.

The detailed map which was the result of this remote-sensing analysis allowed further interpretation. When the digitised data were examined alongside dating information from surveys and excavations (such as Wilkinson, 1998; Wilkinson and Harper, 1975) a peak in the Early Islamic period could be identified. Technological advancement, tax incentives and deliberate action by the state allowed water management systems to develop throughout all the irrigable areas in this period, intensifying agriculture beyond what was possible when relying on precipitation alone.

It was found that some canal systems had the potential to abstract a large proportion of the available flow (e.g. see **Chapter 6.5**), and that several were of dimensions which would have allowed for large areas to be irrigated (see **Table**

6.3), indicating that areas such as the Balikh and land alongside the Euphrates could have been heavily cultivated in the past. When this is compared with Le Strange's review of historical sources (1930), it generates a picture of an intensively cultivated and managed landscape in the medieval period.

8.2 Development of water management at the time of the later territorial empires

Based on the results of this research, the development over time of water management in northern Mesopotamia can be recognised. Although there is evidence for irrigation before the Iron Age, in northern Mesopotamia this seems to relate specifically to certain features, such as the canals at Mari, which may have Bronze Age dates (see Margeuron, 2004). The canals alongside the Habur may represent water management by the Middle Assyrian state, although they were reused by subsequent empires. Larger-scale changes in the landscape seem to have occurred during the Neo-Assyrian period (e.g. see Wilkinson and Barbanes, 2000) possibly representing deliberate policies. Given the evidence for Neo-Assyrian canal-based irrigation in northern Iraq (Oates, 1968; Reade, 1978; Ur, 2005; Altaweel, 2008) it can be suggested here that the Neo-Assyrian empire laid down the foundations for future imperial irrigation. The later states continued to reuse some of the older systems, also constructing new ones throughout the Near East (for example the Hellenistic-Byzantine Sahlan-Hammam canal). Qanats and rock-cut tunnels certainly seem to have spread throughout the study area from the Hellenistic-Byzantine period.

A new peak in this trajectory of development occurred in the Early Islamic period, which represents a time when significant large-scale systems were built. These included urban and royal supply (for example at Raqqa and Samarra) and large-scale irrigation canals throughout the countryside (for example along the Euphrates). Early Islamic Imperial authorities both deliberately imposed these systems on the landscape and encouraged and facilitated irrigation through financial incentives, producing complex systems of water management which were a reflection both of the power of the state but also of the power of private elite individuals operating within its supporting framework.

These changes over time appear to directly reflect the organising power of the state. Although some of the systems have been more locally/communally managed, most of the systems have associations with sites that are known to have been significant/powerful. For example the Nahr al Abbara must be linked to the Early Islamic sites of Medinat al Farr and Khirbet al-Ambar, and the canals in northern Iraq with key Assyrian cities such as Nineveh and Nimrud. While irrigation is the biggest consumer of water, the idea of water and luxury should not be discounted, with specific reference to the likely presence of gardens and parks at imperial sites such as Raqqa and Samarra. This link is a clear indicator of a state's power: if water in an environment where it was relatively scarce and expensive could be used for non-essential purposes it suggested that the user was able to exercise considerable control over this resource.

It is worth noting here that at times throughout the period studied when the landscape was less tightly or securely controlled, irrigation seems to have suffered. The late Ottoman period illustrates this. Travellers' reports indicate a less intensively managed countryside (e.g. see Bell, 1924). Others suggest that in the 18th-early 20th centuries cultivation, settlement and security declined (e.g. see Hole, 2006, p144; Lewis, 1955, p48; Kaniewski et al, 2013, p3865). There are also very recent parallels. Modern agriculture has been affected by the current instability in Syria, with damage to irrigation systems (FAO, 2013). Neglect in tasks such as dredging of canals and damage to canals was noted by a recent Syrian report (FAO, 2012, p2), including the Government-run irrigation schemes (FAO, 2012, p13). Associated social tensions and conflict have arisen over water allocation (FAO, 2012, p13).

Similar issues can be explored for earlier periods. Plagues at the end of the Byzantine period also seem to have occurred at the same time as the evidence for water management becomes less clear, in contrast to the medieval peak occurring at the time of the powerful Early Islamic empires. It is important to note here that during periods when states were less powerful or when conditions were more unstable/demand was lower, rain-fed agriculture was the norm. This seems to have been the case at least in the early-mid 20th century (Beaumont, 1996, p137), and also seems to have happened as a response to the recent crisis (FAO, Syria Crisis, 2013b). Rain-fed agriculture may also have predominated in northern

Mesopotamia during the Bronze Age, before the powerful territorial empires were established.

The security of the centre of empires certainly promoted irrigation. Again, Raqqa and Samarra must be cited here, as well as the Neo-Assyrian canals. Increasingly, especially from the Roman period onwards, water management strategies were also employed in the frontier lands, allowing for secure water supplies even in unstable conditions. The features associated with Roman sites throughout northern Mesopotamia, such as the canals and cisterns at Resafa, are examples of frontier water management. Some of the qanats/tunnels in the Sinjar plains (see Lightfoot, 2009, p16) may have links to this period. These patterns indicate that the presence of an empire imposed, necessitated and encouraged irrigation in previously unprecedented ways.

These results represent almost the inverse of Wittfogel's (1957) hypothesis: in this case, rather than water management leading to a rise in bureaucratic power itself, the later territorial empires of northern Mesopotamia were able to use their bureaucratic power to impose and encourage changes to the landscape, further enhancing their economic strength. When political conditions were unstable, irrigation systems were not maintained and fell into disrepair, a point illustrated by current events in Syria.

Despite the difficulty of dating ancient water management features, this project has demonstrated that they can be understood within their chronological contexts. Kaptijn's study of water management around the Wadi Zerqa in Jordan (2009; 2010) showed how relatively recent irrigation conducted in the 19th and early 20th centuries represented one phase of a series of longer term developments and changes. Irrigation systems should not be approached as single or even multi-period features, but as layers of developments. The complex palimpsests of water management in the Balikh are an example of this. Different states irrigated on the same alignments as their predecessors, choosing the same locations for canals based on the natural topography of the landscape, and also reusing existing systems.

It is interesting that this general pattern seemed to continue from the period of the later territorial empires into the middle of the 20th century, possibly with a decline

at the end of the Early Islamic empires. New irrigation systems have recently reshaped the landscape and removed traces of land-use which had developed over hundreds or even thousands of years. The modern systems have already encountered problems (Kliot, 1994; Hole and Zaitchik, 2006), facing huge and unsustainable demands, with large-scale dam building and water abstraction causing conflict and lowering water tables faster than they can recharge. Recently, the FAO indicated that demand in Syria was close to surpassing supply (Varela-Ortega and Sagardoy, 2003), and, based on Syrian statistics, indicated that areas such as the Balikh and Habur were already over-exploited (Varela-Ortega and Sagardoy, 2003). Given all this, it is uncertain whether the post-1950s irrigated landscape will have the longevity and sustainability of the systems established and developed by the later territorial empires.

8.3 Evaluation

The extent to which this project fulfilled the original aims should be recognised here. Two specific problems were potential limitations. First, the political situation in Syria prevented further fieldwork, making it impossible to confirm more than a sample of the remotely-sensed results in the field. While some channels had been visited and described in detail by other research (for example the Nahr Maslama; see Harper and Wilkinson, 1975), some had not, including the West Balikh systems, the Raqqa tunnel and the Sinjar qanats. Secondly, DEMs could not be used for all sites; in some cases (for example, at the now-inundated Dibsi Faraj) recent landscape changes rendered the modern DEMs unusable. Because the process of generating CORONA DEMs was time consuming, and required stereopairs sufficiently free of cloud and with sufficient contrast, these were only made for parts of the study area (comprising the area around Tell Hammam et Turkman in the Balikh). Acquiring control points for these areas in the field was not possible, and the available camera parameters were not clearly defined: for example, key information used in image matching such as the coordinates of the principle point and the lens distortion coefficients was unknown (Sohn et al, 2004, p52).

However, by employing a multidisciplinary approach and by combining different datasets it was possible to mitigate against these limitations to generate a

comprehensive map. Where one type of information was unavailable, there was often an alternative source. For example, the Sahlan Hammam canal could not be clearly located using the low-resolution SRTM and ASTER DEMs, but could be analysed using the higher resolution CORONA DEMs. Similarly, early 19th century/late 18th century travellers' reports (e.g. Bell, 1924; Sykes, 1907; Buckingham, 1827) contained descriptions for features which are now lost, and more recent archaeological surveys (for example Wilkinson, 1998; Bartl, 1994) provided dating information for sites which could not be visited in the field by the present study. As **Chapter 6** shows, a detailed picture of ancient water management was the result of this interdisciplinary investigation.

8.4 Future research

While the map generated by this thesis enables a detailed discussion of the scale and distribution of water management, the contribution to understanding of the subject that further research could make will be assessed here.

Although further fieldwork was not possible as part of this project, due to the ongoing political situation in Syria, if this were to change in the future specific work could be undertaken. For example, the collection of GPS points in the Balikh would provide better control for photogrammetric DEM creation. Total station or leveller surveys could produce cross-sectional profiles across the canals assessed using the DEMs: it would be beneficial to test the accuracy of the DEM-derived profiles in this way. The problem of obtaining dating evidence for all of the canals in the study area has been discussed above. Further fieldwork could mitigate against this by providing ceramic evidence and samples for scientific dating.

Further work using remote sensing is also possible. The CORONA-derived DEMs produced by this research were useful for gaining higher resolution information about irrigation in the Balikh than the coarser SRTM and ASTER could provide. With more time available for the complex processing required to build the DEMs, the same method could be performed for a wider area. For example, this might be especially applicable for areas where modern development has completely removed features, making DEMs derived from modern data unusable. Areas of former large-scale gravity flow irrigation alongside the Euphrates would be particularly appropriate for the creation of CORONA DEMs. Moreover, the

CORONA DEMs could be further improved if limitations in the algorithms currently on offer could be corrected, for example restrictions in the flying height settings offered by ERDAS LPS.

The new TanDEM-X dataset could also be used, using data acquired by the Fragile Crescent Project of Durham University. Although it would not reveal features of the landscape that are now removed or obscured, as CORONA can, it could provide a way of examining larger areas of archaeological landscapes relatively quickly and at a high resolution.

Additional research questions could be explored. For example, mapping could be expanded into southern Mesopotamia, an area with different climatic conditions and different developmental trajectories in terms of water management. This mapping might enable wider issues, such as the link between water and power, to be addressed in more detail. Comparing the rainfall variability analysis with proxy records (cf. Kalayci, 2013) might also reveal significant trends which could be discussed alongside the evidence for water management development.

Finally, the significance of a detailed understanding of ancient irrigation could be contextualised within possibilities for future water management. If the sustainability of more ancient systems can be assessed over long timescales, this might have implications for current water management practice.

Data references

CORONA

Data from the U.S. Geological Survey (available at <http://earthexplorer.usgs.gov/>)

1117: 16 May 1972

1105: 4 November 1968

Fragile Crescent Project (from USGS, <http://earthexplorer.usgs.gov/>)

1038: 22 January 1967

CORONA Atlas of the Near East, Center for Advanced Spatial Technologies, University of Arkansas/U.S. Geological Survey (available at <http://corona.cast.uark.edu>)

1102: 11 December 1967

1104: 9 August 1968

1105: 5 November 1968

1107: 1 August 1969

See also:

USGS Declassified imagery 1 https://lta.cr.usgs.gov/declass_1 USGS guide to declassified satellite imagery -1, <http://eros.usgs.gov/#/Guides/disp1>

National Reconnaissance Office (NRO)
<http://www.nro.gov/history/csnr/corona/imagery.html>

Landsat

*NASA Landsat Program, 2010 03 05, Landsat TM scene
LT51730351984211AAA04, Orthorectified, USGS, Sioux Falls, 29 July 1984*

*NASA Landsat Program , 2001-10-17 , Landsat TM scene
LT51730351990211XXX04, Orthorectified, USGS, Sioux Falls , 30 July 1990*

*NASA Landsat Program, 2008-02-22, Landsat ETM+, LE71730352000231SGS00,
USGS, Sioux Falls, 18 August 2000*

ASTER

The ASTER GLOBAL DEM data was obtained from the online Data Pool at the NASA Land Processes Distributed Active Archive Center (LP DAAC), USGS/Earth Resources Observation and Science (EROS) Center, Sioux Falls, South Dakota (https://lpdaac.usgs.gov/data_access)

ASTER GDEM is a product of METI and NASA. Obtainable from https://lpdaac.usgs.gov/products/aster_products_table/astgtm

SRTM (from FCP database)

USGS (2004), Shuttle Radar Topography Mission, 3 Arc Second scenes, Unfilled Unfinished 2.0, Global Land Cover Facility, University of Maryland, College Park, Maryland, February 2000

Rain gauge data

Deutscher Wetterdienst, 1996-2011, Global Precipitation Climatology Centre (GPCC) <http://kunden.dwd.de/GPCC/Visualizer>

Bibliography

- Ababsa, M. (2011). 'Agrarian Counter-Reform in Syria (2000-2010)', in Hinnebusch, R. El Hindi, A. Khaddam, M. and Ababsa, M. (eds). *Agriculture and reform in Syria*. Fife, University of St Andrews Centre for Syrian Studies, p83-109.
- Abrams, M., Bailey, B. Tsu, H. and Hato, M. (2010). 'The ASTER Global DEM', *Photogrammetric Engineering & Remote Sensing*, p344-348.
- Adams, R. M. (1974). 'Historic patterns of Mesopotamian irrigation agriculture', in Downing, T. E. and Gibson, McG. (eds). *Irrigation's impact on society*. Tucson, University of Arizona Press, p1-6.
- Adams, R. M. (1981). *Heartland of cities: Surveys of ancient settlement and land use on the central floodplain of the Euphrates*. Chicago, University of Chicago Press.
- Agnew, C. and Anderson, E. (1992). *Water resources in the arid realm*. London, Routledge.
- Akkermans, P. M. M. G. (1993). *Villages in the steppe: Later Neolithic settlement and subsistence in the Balikh Valley, Northern Syria*. Ann Arbor, Michigan, International Monographs in Prehistory.
- Akkermans, P. M. M. G. (1996). *Tell Sabi Abyad: The late Neolithic settlement*. Istanbul, Nederlands Historisch-Archaeologisch Instituut te Istanbul.
- Akkermans, P. M. M. G. (1989). 'The Neolithic of the Balikh Valley, Syria: A first assessment', *Paleorient*, 15(1):122-134
- Akkermans, P. M. M. G. and Schwartz, G. M. (2003). *The archaeology of Syria: From complex hunter-gatherers to early urban societies (ca.16000-300 BC)*. Cambridge, Cambridge University Press.

Alkhaier, F., Su, Z. and Flerchinger, G. N. (2012). 'Reconnoitering the effect of shallow groundwater on land surface temperature and surface energy balance using MODIS and SEBS', *Hydrology and Earth System Sciences*. 16:1833-1844.

Al-Khalaf, M. and Kohlmeyer, K. (1985). 'Untersuchungen zu ar-Raqqa-Nikephorion/Callinicum', *Damaszener Mitteilungen*, 2:133-162.

Al-Sawaf, D. S. F. (1977). *Hydrogeology of South Sinjar Plain Northwest Iraq*, PhD thesis, University of London.

Altaweel, M. (2008). *The imperial landscape of Ashur: settlement and land use in the Assyrian heartland*. Heidelberg, Heidelberg Orientverlag.

Altmaier, A. and Kany, C. (2002). 'Digital surface model generation from CORONA satellite images', *ISPRS Journal of Photogrammetry & Remote Sensing* 56:221-235

Anderson, E. W. (2000). *The Middle East: Geography and geopolitics*. London and New York, Routledge.

Aragüés, R. Urdanoz, V. Cetin, M. Kirda, C. Daghari, H. Ltifi, W. Lahlou, M. and Douaik, A. (2011). 'Soil salinity related to physical soil characteristics and irrigation management in four Mediterranean irrigation districts', *Agricultural Water Management*, 98:959-966

Bagg, A. M. (2004). 'Assyrian Hydraulic Engineering. Tunnelling in Assyria and Technological transfer'. in Bienert, H. D. and Haser, J. (eds). *Men of Dikes and Canals: The Archaeology of Water in the Middle East*. Verlag marie Leidorf GmbH, p355-264.

Bagg, A. (2000a). 'Irrigation in Northern Mesopotamia: Water for the Assyrian capitals, (12th-7th centuries BC)', *Irrigation and Drainage Systems* 14:301-324

Bagg, A. (2000b). *Assyrische Wasserbauten*. Mainz, Verlag Philipp von Zabern.

Ball, J. E. and Luk, K. C. (1998). 'Modelling spatial variability of rainfall over a catchment', *Journal of Hydrologic Engineering*, 3(2):122-130

Balooni, K. Kalro, A. H. Kamalamma, A. G. (2008). 'Community initiatives in building and managing temporary check-dams across seasonal streams for water harvesting in South India', *Agricultural Water Management*, 95:1314-1322

Bar-Matthews, M. Ayalon, A. and Kaufman, A. (1997). 'Late Quaternary Paleoclimate in the Eastern Mediterranean Region from Stable Isotope Analysis of Speleothems at Soreq Cave, Israel' *Quaternary Research*, 47:155-168

Bar-Matthews, M., A. Ayalon, M. Gilmour, A. Matthews, A. and Hawkesworth, C. J. (2003). 'Sea-land oxygen isotopic relationships from planktonic foraminifera and speleothems in the eastern Mediterranean region and their implication for paleorainfall during interglacial intervals', *Geochimica et Cosmochimica Acta* 67 (17): 3181–3199.

Barrow, C. J. (1999). *Alternative irrigation: The promise of runoff agriculture*. London, Earthscan.

Bartl, K. (1994). *Fruhlislamische Besiedlung im Balih-Tal/Nord Syrien*. Berlin, Dietrich Reimer.

Bassin, M. (1996). 'Nature, Geopolitics and Marxism: Ecological Contestations in Weimer Germany', *Transactions of the Institute of British Geographers, New Series*, 21(2):315-341.

Beaumont, P. (1989). 'The qanat: a means of water provision from groundwater sources'. In Beaumont, P. Bonine, M. and McLachlan, K. (eds). *Qanat, Kariz and Khattara. Traditional Water Systems in the Middle East and North Africa*. Wisbech, Cambridgeshire, MENAS Press. pp. 13-31.

Beaumont, P. (1996). 'Agricultural and environmental changes in the upper Euphrates catchment of Turkey and Syria and their political and economic implications', *Applied Geography* 16(1):137-157.

Beazley, G. A. (1919). 'Air photography in archaeology', *The Geographical Journal*, 53(5):303-335.

Beazley, G. A. (1920). 'Surveys in Mesopotamia during the war', *The Geographical Journal* 55(2):109-123.

Beck, A. Philip, G. Abdulkarim, M. and Donoghue, D. (2007). 'Evaluation of Corona and Ikonos high resolution satellite imagery for archaeological prospection in western Syria'. *Antiquity* 81:161-175.

Becker, A. Finger, P. Meyer-Christoffer, A. Rudolf, B. Schamm, K. Schneider, U. Ziese, M. (2012). 'A description of the global land surface precipitation data products of the Global Precipitation Climatology Centre with sample applications including centennial (trend) analysis from 1091-present'. *Earth System Science Data*, 5:71-99.

Beckers, B. (2007-09). 'Resafa – Rusafat Hisham, Syrien. Archaeologie und prospektion, physische geographie: Rekonstruktion der historischen wasserwirtschaft und der paläoumwelt' in Sack, D. (eds). *Resafa-Sergiupolois/Rusafat Hisham*. Berlin, Technische Universität Berlin, p28-30.

Beckers, B. Schutt, B. Tsukamoto, S. Frechen, M. (2013). 'Age determination of Petra's engineered landscape—optically stimulated luminescence (OSL) and radiocarbon ages of runoff terrace systems in the Eastern Highlands of Jordan', *Journal of Archaeological Science*. 40:333-348.

Bedford, P. (2009). 'The Neo-Assyrian Empire', in Morris, I. and Scheidel, W. (eds). *The Dynamics of Ancient Empires: State Power from Assyria to Byzantium*. Oxford Studies in Early Empires. Oxford, Oxford University Press USA, pp 30-66.

Bell, G. (1924). *Amurath to Amurath*. London, Macmillan and co Ltd.

Berking, J. Beckers, B. Schutt, B. (2010). 'Runoff in two semi-arid watersheds in a geoarchaeological context: A case study of Naga, Sudan, and Resafa, Syria'. *Geoarchaeology* 25(6):815-836.

Berthier, S. D'Hont, O. (2005). Ressources hydriques et peuplement sur le Moyen Euphrate, VI^e-XIX^e siècle, *Ruralia V*, p261-269.

Besançon, J. Sanlaville, P. (1981). Aperçu géomorphologique sur la vallée de l'Euphrate Syrien *Paléorient* 7(2):5-18.

Bescancon, J. Sanlaville, P. (1985). *Le milieu géographique*, in Sanlaville, P. (eds). Holocene Settlement in North Syria: Resultats de deux prospections archéologiques effectuées dans la région du nahr Sajour et sur le haut Euphrate syrien, BAR International Series 238 pp 7-40.

Beven, K. J. (2011). *Rainfall-Runoff Modelling*. Chichester, Wiley-Blackwell.

Bienert, H. D. and Haser. J. (eds). (2004). *Men of dikes and canals: The archaeology of water in the Middle East*. Rahden, Verlag Marie Leidorf GmbH.

Black, E. Hoskins, B. Slingo, J. Brayshaw, D. (2011). 'The present-day climate of the Middle East', in Mithen S, Black E, (eds). *Water, life and civilisation: climate, environment and society in the Jordan Valley*. Cambridge, Cambridge University Press, p13-25.

Bounni, A. (1979). 'Campaign and exhibition from the Euphrates in Syria', in Freedman, D. N, Lundquist, J. M. (eds). *Archaeological reports from the Tabqa Dam Project: Euphrates Valley, Syria*. The Annual of the American Schools of Oriental Research, 44:iii-182.

Bounni, A. (1988). Découvertes archéologiques récentes en Syrie, in *Comptes rendus des séances de l'Académie des Inscriptions et Belles-Lettres*, 132^e année, 2:361-380.

Boyle, R. D. and Thomas, R. C. (1988). *Computer vision: A first course*. Oxford, Blackwell Scientific Publications.

Brazier R E, Krueger T, Wainwright J, (2014). 'Uncertainty assessment', in Mueller E N (eds). *Patterns of land degradation in drylands: Understanding self-organised ecogeomorphic Systems*, Dordrecht, Springer.

Brayshaw, D. Black, E. Hoskins, B. Slingo, J. (2011). *Past climates of the Middle East*, in Mithen, S. Black, E. (eds). *Water, life and civilisation: climate, environment and society in the Jordan Valley*. Cambridge, Cambridge University Press, p25-51.

Breternitz, C. D. (1991). *Prehistoric Irrigation in Arizona symposium 1988*, Soil Systems Publications in archaeology 17, Phoenix, Soil Systems,.

Brinker, W. (1991). Zur wasserversorgung von Resafa-Sergiupolis. *Damaszener Mitteilungen* Band 5:119-146.

Buckingham, J. S. (1827). *Travels in Mesopotamia*. Cambridge, Cambridge University Press.

Bulatovic, V. Susic, Z. Ninkov, T. (2012). 'Estimate of the ASTER GDEM regional systematic errors and their removal', *International Journal of Remote Sensing*, 33(18):5915-5926.

Buol, S. W. Hole, F. D. and McCracken, R. J. (1980). *Soil genesis and classification*. Ames, Iowa University Press.

Burbank, J. and Cooper, F. (2010). *Empires in world history: Power and the politics of difference*, Princeton and Oxford, Princeton University Press.

Butzer, K. W. (1961). 'Climatic change in arid regions since the Pliocene', *Arid Zone Research (UNESCO)*, 17:31-56.

Butzer, K. W. (1996). 'Irrigation, raised fields and state management: Wittfogel redux?', *Antiquity*, 70:200-204.

Cable, J. S. (1991). 'The role of irrigation agriculture in the formation and socio-political development of early Hohokam villages in the lowlands of the Phoenix Basin, Arizona'. in Breternitz, C.D. (eds). *Prehistoric irrigation in Arizona symposium 1988*, Soil Systems Publications in archaeology 17, Soil Systems, Phoenix, p107-138.

Cantor, L. M. (196). *World geography of irrigation*. Edinburgh, Oliver and Boyd.

Casana, J. Cothren, J. (2008). 'Stereo analysis, DEM extraction and orthorectification of CORONA satellite imagery: archaeological applications from the Near East', *Antiquity*, 82(317):732-749.

Casana, J. Cothren, J. and Kalayci, T. (2012). Swords into Ploughshares: Archaeological Applications of CORONA Satellite Imagery in the Near East. *Internet Archaeology*, <http://intarch.ac.uk/journal/issue32/2/toc.html>

Chakravarty, K. K. Badam, G. L. and Paranjpye, V. (eds). (2006). *Traditional water management systems of India*. Bhopal, Indira Gandhi Rashtriya Manac Sangrahalaya.

Challis, K. Priestnall, G. Gardner, A. Henderson, J. and O'Hara, S. (2004). 'Corona remotely-sensed imagery in dryland archaeology: The islamic city of al-Raqqa', Syria. *Journal of Field Archaeology*, 29(1/2):139-153.

Charles, M. Pessin, H. Hald, M. M. (2010). 'Tolerating change at Late Chalcolithic Tell Brak: responses of an early urban society to an uncertain climate'. *Environmental Archaeology*, 15(2): 183-193.

Christensen, P. (1993). *The Decline of Iranshahr: Irrigation and Environments in the History of the Middle East, 500 BC to AD 1500*, Museum Tusculanum Press, Copenhagen.

Clifford Boyer, M. (1964). 'Streamflow Measurement', in Chow, V. T (eds). *Handbook of applied hydrology*, New York, McGraw-Hill, p15-3-15-41.

Copeland, L. Moore, A. (1985). 'Inventory and description of sites'. in Sanlaville P (eds). *Holocene Settlement in North Syria: resultats de deux prospections archaeologiques effectuees dans la region du nahr Sajour et sur le haut Euphrate syrien*, BAR International Series 238 pp 41-98.

Cressey, G. B. (1958). 'Qanats, Karez and Foggaras'. *Geographical Review*, 48(1):27-44.

Cullen, H. M. deMenocal, P. B. Hemming, S. Hemming, G. Brown, F. H. Guilderson, T. Sirocko, F. (2000). 'Climate change and the collapse of the Akkadian empire: Evidence from the deep sea'. *Geology* 28:379-382.

Cunliffe, E. (2013). *Satellites and Site Destruction: An analysis of modern impacts on the archaeological resource of the ancient Near East*. unpublished PhD thesis, Durham University.

Curvers, H. (1991). *Bronze Age society in the Balikh drainage (Syria)*. unpublished PhD thesis, University of Amsterdam.

Dalley, S. (1984). *Mari and Karana: Two Old Babylonian cities*. London, Longman.

Dalley, S. (1994). 'Nineveh, Babylon and the Hanging Gardens: Cuneiform and Classical Sources Reconciled', *Iraq* 56:45-58.

Davey, C. J. (1985). 'The Negub Tunnel', *Iraq* 47:49-55.

Davies, M. I. J. (2009). 'Wittfogel's dilemma: heterarchy and ethnographic approaches to irrigation management in Eastern Africa and Mesopotamia', *World Archaeology*, 41(1):16-35.

De Jong, L. (2011). 'Mallowan's Marshes. The archaeology of the Balikh Valley under Roman and Byzantine rule'. *Zeitschrift fur Orient-Archaeologie*, 4:262-282.

De Jong, L. (2012). '*Resettling the steppe: The archaeology of the Balikh Valley in the Early Islamic Period*', Proceedings of the 7th International Congress on the Archaeology of the ancient Near East 12th April-16th April 2010, p518-531.

De Jong, L. Kaneda, A. (2004-5). 'Uncovering Tell Sheikh Hasan, Balikh valley; architecture and pottery from the 2005 season'. *Annales archaeologiques Arabes Syriennes* 47-48:179-190.

De Vente, J., Poesen, J., Govers., G, Boix-Fayos, C., (2009). 'The implications of data selection for regional erosion and sediment yield modelling', *Earth surface processes and landforms*, 34:1994-2007.

Decker, M. (2007). 'Frontier settlement and economy in the Byzantine east'. *Dumbarton Oaks Papers*, 61:217-267.

Decker, M. (2009a). *Tilling the hateful earth: Agricultural production and trade in the Late Antique East*. Oxford, Oxford University Press.

Decker, M. (2009b). 'Plants and progress: Rethinking the Islamic agricultural revolution', *Journal of World History*, 20(2):187-206.

Decker, M. (2011). 'Settlement and Agriculture in the Levant, 6th-8th Centuries', in Borrut, A. and Debie, M. Papaconstantinou, A. Pieri, D. and Sodini, J. P. (eds). *Le Proche-Orient de Justinien aux Abbasides: Peuplement et dynamiques spatiales*. Turnhout, Brepols, p1-7.

Deckers, K. and Dreschsler, P. (2011). 'Spatial analysis of Early Bronze Age settlements and resource exploitation in the Upper Khabur Basin (NE Syria)', in Deckers, K. (eds). *Holocene landscapes through time in the Fertile Crescent*. Subartu XXVIII, Turnhout, Brepols, pp17-31.

Deckers, K. and Riehl, S. (2008). 'Resource exploitation of the Upper Khabur basin (NE Syria) during the 3rd millennium BC'. *Paleorient*, 34(2):173-189.

Demir, T. Westaway, R. Bridgland, D. R. and Seyrek, A. (2007). 'Terrace staircases of the River Euphrates in southeast Turkey, northern Syria and western Iraq: evidence for regional surface uplift'. *Quaternary Science Reviews*, 26:2844-2863.

Dennett, M. D. Keatinge, J. D. H. and Rodgers, J. A. (1984). 'A comparison of rainfall regimes at six sites in northern Syria'. *Agricultural and Forest Meteorology*, 31:319-328.

Dittman, R. (1995). 'Ruinenbeschreibungen der Machmur-Ebense aus dem Nachlass von Walter Bachman'. in Finkbeiner, U. (eds). *Beiträge zur Kulturgeschichte Vorderasiens*. Mainz, Festschrift für Rainer Michal Boehmer p87-102.

Donnan, W. W. and Schwab, G. O. (1974). 'Current Drainage methods in the USA', in van Schilfgaarde J, (eds). *Drainage for agriculture*. Madison, American Society of Agronomy.

Donoghue, D. N. M. Galiatsatos, N. Philip, G. and Beck, A. R. (2002). 'Satellite Imagery for Archaeological Applications: A case study from the Orontes Valley', in Bewley, R. H. Raczkowski, W. (eds). *Aerial Archaeology: Developing future practice*. Amsterdam, IOS Press, p211-224.

Doolittle, W. E. (1985). 'The use of check dams for protecting downstream agricultural lands in the Prehistoric Southwest: A contextual analysis'. *Journal of Anthropological Research*, 41(3):279-305.

Doolittle, W. E. (1991). 'A finger on the Hohokam pulse', in Breternitz C D (eds). *Prehistoric Irrigation in Arizona symposium 1988*, Phoenix, Soil Systems Publications in archaeology 17, Soil Systems, p139-155.

Dossin, G. (1974). 'Le site du Tuttal-sur-Balikh'. *Revue Assyriologique* 68:25-34

Eickhoff, T. (1985). *Kar-Tukulti-Ninurta, Eine mittelassyrische Kult- und Residenzstadt*. Berlin, Mann.

Eisenstadt, S. N. (1979). 'Observations and Queries about sociological aspects of imperials in the ancient world', in Larsen, M. T (eds). *Power and Propaganda: A symposium on ancient empires, Mesopotamia*. Copenhagen, Copenhagen studies in Assyriology, Volume 7, Akademisk Forlag.

Ergenzinger, P. J. Frey, W. Kuhne, H. and and Kurschner, H. (1988). 'The reconstruction of environment, irrigation and development of settlement on the Habur in North-East Syria'. Bintliff, J. L. Davidson, D. A. Grant, E. G. (eds). *Conceptual issues in Environmental Archaeology*, Edinburgh, Edinburgh University Press, pp108-128.

Ergenzinger, P. J. and Kuhne, H. (1991). 'Ein Regionales Bewässerungssystem am Habur', in Kuhne, H. (eds). *Die rezenten umwelt von Tall She Hamad und daten zur umweltrekonstruktion der Assyrischen stadt Dur-Katlimmu*. Berlin, Dietrich Reimer Verlag, pp163-190.

Ertsen, M. W. (2010). 'Structuring properties of irrigation systems: understanding relations between humans and hydraulics through modelling'. *Water History* 2:165-183.

Fales, F. M. Postgate, J.N. (1995). *Imperial administrative records*, Helsinki University press, Helsinki.

FAO, (1985). *Irrigation water management: Training manual No.1: Introduction to irrigation*, <http://www.fao.org/docrep/r4082e/r4082e00.htm#Contents> (Accessed: 10.11.2012).

FAO, (2003). *Syrian agriculture at the crossroads*, Agricultural policy and economic development Series No. 8.

FAO, (2013a). *Syrian agricultural production drops massively as conflict continues*, 23.01.2013, <http://www.fao.org/news/story/en/item/168676/icode/> (Accessed: 10.11.2012).

FAO, (2013b). *Syria Crisis, Executive Brief*, http://www.fao.org/fileadmin/user_upload/emergencies/docs/Syria%20Crisis%20Executive%20Brief%20-%204%2007%2013.pdf (Accessed: 10.11.2012).

FAO, UNESCO. (1962). *WMO Interagency Project on agroclimatology, draft general report on a study of agroclimatology in semi-arid and arid zones of the Near East*, Rome.

Farr, T. G. Rosen, P. A. Caro, E. Crippen, R. Duren, R. Hensley, S. Kobrick, M. Paller, M. Rodriguez, E. Roth, L. Seal, D. Schaffer, S. Shimada, J. Umland, J. Werner M, Oskin M, Durbank D, Alsdorf D. (2007). 'The Shuttle Radar Topography Mission', *Reviews of Geophysics* 45(2): 1-33.

Finlayson, B. Lovell, J. Smith, S. Mithen, S. (2011). 'The archaeology of water management in the Jordan Valley from the Epipalaeolithic to the Nabataean, 21,000 BP (19,000 BC) to AD 106', in Mithen, S. Black, E. (eds). *Water, life and civilisation: climate, environment and society in the Jordan Valley*, Cambridge, Cambridge University Press, p191-218.

Fiorentino, G. Caracuta, V. Casiello, G. Longobardi, F. Sacco, A. (2011). 'Studying ancient crop provenance: implications from $\delta^{13}\text{C}$ and $\delta^{15}\text{N}$ values of charred barley in a Middle Bronze Age silo at Ebla (NW Syria)'. *Rapid Communications in Mass Spectrometry* 26(3):327-335.

Fisher, W. B. (1978). *'The Middle East: A physical, social and regional geography'*. London, Methuen & Co Ltd.

Forstner, W. Wrobel, B. Paderes, F. Craig, R. Fraser, C. Dolloff, J. (2004). 'Analytical photogrammetric operations', in McGlone, J. C. (eds). *Manual of photogrammetry (5th ed)*. Bethesda, American Society of Photogrammetry and Remote Sensing p763-948.

Foster, J. B. (2000). *Marx's Ecology: Materialism and Nature*. New York, Monthly Review Press.

Freedman, D. N. and Lundquist, J. M. (1979). *Archaeological Reports from the Tabqa Dam Project: Euphrates Valley, Syria*. The Annual of the American Schools of Oriental Research, 44:iii-182

Fuccaro, N. (1994). *Aspects of the social and political history of the Yazidi enclave of Jabal Sinjar (Iraq) under the British mandate, 1919-1932*, unpublished PhD thesis, Durham University

Galiatsatos, N. (2004). *Assessment of the CORONA series of satellite imagery for landscape archaeology: a case study from the Orontes valley, Syria*, unpublished PhD thesis, Durham University

Galiatsatos, N. Wilkinson, T. J. Donoghue, D. N. M. and Philip, G. (2009). *The Fragile Crescent Project (FCP): Analysis of Settlement Landscapes using Satellite Imagery*. Computer Applications to Archaeology.

Geertz, C. (1980). *Negara: The threatre state in 19th Century Bali*. Princeton, Princeton University Press.

Gerritsen, F. A. (1996). *The Balikh Valley, Syria, in the Hellenistic and Roman-Parthian Age*. Unpublished MA Thesis, University of Amsterdam.

Geyer, B. and Monchambert, J. Y. (2003). *La Basse Vallee De L'Euphrate Syrien du Neolithique a l'avenement de l'Islam*, Mission Archaeologique de Mari, Beyrouth.

Ghanekar, P. K. (2006). 'Traditional water systems in the forts of Maharashtra', in Chakravarty, K. K. Badam, G. L. and Paranjpye, V. (eds). *Traditional water management systems of India*. Bhopal, Indira Gandhi Rashtriya Manac Sangrahalaya.

Gibson, McG. (1972). *The City and area of Kish*. Miami, Field Research Projects

Gibson, McG. Downing, T. E. (1974). *Irrigation's Impact on Society*. Tucson, University of Arizona Press .

Glick, T. F. (1970). *Irrigation and society in medieval Valencia*. Cambridge, The Belknap Press of Harvard University Press.

Goossens, R. De Wulf, A. Bourgeois, J. Gheyle, W. and Willems, T. (2006). 'Satellite imagery and archaeology: the example of CORONA in the Altai Mountains'. *Journal of Archaeological Science* 33: 745-55.

Global Precipitation Climatology Centre (GPCC). (2008). *GPCC Annual Report for year 2007: Development of the GPCC Data Base and Analysis Products*. Offenbach, Germany.

Goovaerts P, (2000). 'Geostatistical approaches for incorporating elevation into the spatial interpolation of rainfall', *Journal of hydrology*, 228:113-129.

Gulhati, N. D. (1973). 'Irrigation, drainage and reclamation', in Kovda V A, van den Berg C, Hagan R M (eds). *Irrigation, drainage and salinity: an international source book*. London ,FAO/UNESCO/Hutchinson.

Haase, C. P. (1996). 'Madinat al-Far: The regional late antique traditional of an early Islamic foundation', in Bartl K, Hasuer S R (eds). *Continuity and change in Northern Mesopotamia from the Hellenistic to the early Islamic period*. Berlin, Reimer, p7-20.

Hansen, V. E. Israelsen, O. W. Stringham, G. E. (1980). *Irrigation principles and practices*, 4th ed. New York, John Wiley & Sons.

Harper, R. P., and Wilkinson, T. J. (1975). *Excavations at Dibsi Faraj, Northern Syria, 1972-1974: A preliminary note on the site and its monuments*. Washington D C, The Dumbarton Oaks Center for Byzantine Studies.

Harrower, M. J. (2009). 'Is the hydraulic hypothesis dead yet? Irrigation and social change in ancient Yemen', *World Archaeology* 41:158-72.

Hart, W. E. Collins, H. G. Woodward, G. Humphreys, A. S. (1983). 'Design and operation of gravity or surface systems', in Jensen, M. E. (eds). *Design and Operation of Farm Irrigation Systems*. St Joseph, American Society of Agricultural Engineers.

Hayakawa, Y. S. Oguichi, T., and Lin, Z. (2008). 'Comparison of new and existing global digital elevation models: ASTER G-DEM and SRTM-3'. *Geophysical Research Letters* 35(17):1-5.

Heathcote, R. L. (1983). *The arid lands: their use and abuse*. London, Longman.

Heidemann, S. (2006). 'The history of the industrial and commercial area of Abbasid Al-Raqqā, called Al-Raqqā Al-Muhtariqa'. *Bulletin of SOAS* 69(1):33-52.

Heidemann, S. (2011). 'The agricultural hinterland of Baghdad, al-Raqqā and Samarra: Settlement patterns in the Diyar Mudar', in Borrut, A. Debie, M. Papaconstantinou, A. Pieri, D. and Sodini, J. P. (eds). *Le Proche-Orient de Justinien aux Abbasides: Peuplement et dynamiques spatiales*. Turnhout, Brepols.

Henderson, J. Challis, K. O'Hara, S. Mcloughlin, S. Gardner, A. and Priestnall, G. (2005). 'Experimentation and innovation: early Islamic industry at al-Raqqā', Syria. *Antiquity* 79:130-145.

Hillenbrand, R. (1985). 'Eastern Islamic influences in Syria: Raqqā and Qal'at Ja'bar in the later 20th century', in Raby, J. (eds). *The art of Syria and the Jazira 1100-1250*. Oxford, Oxford University Press, pp21-48.

Hirano, A. Welch, R. Lang, H. (2003). 'Mapping from ASTER stereo image data: DEM validation and accuracy assessment'. *ISPRS Journal of Photogrammetry & Remote Sensing* 57:356-370.

Hirschmüller, H. and Scharstein, D. (2009). 'Evaluation of stereo matching costs on images with radiometric differences'. *IEEE Transactions on Pattern Analysis and Machine Intelligence* 31(9):1582-1599.

Hirt, C. Filmer, M. S. and Featherstone, W. E. (2010). 'Comparison and validation of recent freely-available ASTER-GDEM ver1, SRTM ver4.1 and GEODATA DEM-9S ver3 digital elevation models over Australia', *Australian Journal of Earth Sciences* 57(3):337-347.

Hodge, A. T. (eds). (1991). *Future currents in aqueduct studies*. Leeds, Francis Cairns.

Hof, C. (2007-9). Resafa, Syrien. Die Stadtmauer, Bauforschung zur Klärung ihrer Entstehung und ihrer Veränderungen. Planmodifikation beim Wasserdurchlass, in Sack, D. (eds). Resafa-Sergiupolois/Rusafat Hisham. Berlin, Technische Universität, p32-33.

Hoffman, G. J. Ayers, R. S. Doering, E. J., and McNeal, B. L. (1980). 'Salinity in irrigation agriculture', in Jensen, M. E. (eds). *Design and operation of farm irrigation systems*. St Joseph, American Society of Agricultural Engineers, p145-188

Hole, F. (1974). 'Investigating the origins of Mesopotamian Civilisation', in Lamberg-Karlovsky, C. C., and Sabloff, J. A. (eds). *The Rise and Fall of Civilisations: Modern Archaeological Approaches to Ancient Cultures*. Menlo Park, Cummins Publishing Company

Hole, F. and Zaitchik, B. F. (2006). 'Policies, Plans, Practice, and Prospects: Irrigation in Northeastern Syria'. *Land Degradation and Development* 18: 133-152.

Homberger, G. and Wiberg, P. (eds). (2005). *Numerical Methods in the Hydrological Sciences*. Washington D C, American Geophysical Union.

Howard, J. B. and Huckleberry, G. (1991). *The operation and evolution of an irrigation system: the East Papago canal study*. Phoenix, Soil Systems Publications in Archaeology No.18.

Hritz, C. (2013a). 'A malarial-ridden swamp: using Google earth Pro and Corona to assess the southern Balikh valley', Syria. *Journal of Archaeological Science* 40:1975-1987.

Hritz, C. (2013b). 'Urbanocentric Models and 'Rural Messiness': A Case Study in the Balikh River Valley, Syria'. *American Journal of Archaeology* 117(2):141-161.

Hritz, C. Wilkinson, T. J. (2006). 'Using Shuttle Radar Topography to map ancient water channels in Mesopotamia'. *Antiquity*, 80(308):415-424.

Hunt, E. and Hunt, R. C. (1974). 'Irrigation, conflict, and politics: A Mexican case', in Downing, T. E. and Gibson, McG. (eds). *Irrigation's impact on Society*. Tucson, The University of Arizona Press, p129-157.

Hunt, R. C. (1994). 'Reply to Price'. *Journal of Anthropological Research* 50(2):205-211.

Hunt, R. C. Guillet, D. Abbott, D. R. Bayman, J. Fish, P. Fish, S. Kintigh, K. Neely, J. A. (2005). 'Plausible ethnographic analogies for the social organization of Hohokam canal irrigation'. *American Antiquity* 70(3):433-356.

Imber, C. (2002). *The Ottoman Empire, 1300-1650: The structure of power*. New York, Palgrave Macmillan.

Jacobsen, T. (1960). 'The waters of Ur'. *Iraq* 22:174-185.

Jacobsen, T. (1982). *Salinity and irrigation agriculture in antiquity*. Diyala Basin archaeological projects: report on essential results, 1957-58. Undena, Malibu.

Jacobsen, T. and Lloyd, S. (1955). *Sennacherib's Aqueduct at Jerwan*. Chicago, The University of Chicago Oriental Institute Publications.

Jas, R. M. (eds). (2000). *Rainfall and agriculture in Northern Mesopotamia*. Istanbul, Nederlands Historisch-Archaeologische Instituut te Istanbul.

Jean, C. F. (1952). *Six campagnes de fouilles à Mari, 1933-1939: Synthèse des resultats*. Tournai, Casterman.

Jenkins, E., Jamjoum, K., Al Nuimat, S., (2011). 'Irrigation and phytolith formation: an experimental study', in Mithen, S. J., Black, E. (eds). *Water, life and civilisation: climate, environment and society in the Jordan valley*, Cambridge University press, p347-372.

Jensen, M. E. (eds). (1983). *Design and Operation of Farm Irrigation Systems*. St Joseph, American Society of Agricultural Engineers.

Jenson, S. K. Domingue, J. O. (1988). 'Extracting Topographic Structure from Digital Elevation Data for Geographic Information System Analysis', *Photogrammetric Engineering and Remote Sensing* 54:1593-1600.

Jewitt, T. N. (1966). 'Soils of arid lands', in Hills, E. S. (eds). *Arid Lands: A geographical appraisal*. London, Methuen and Co Ltd, p103-126.

Johns, C. H. W. (1901). *An Assyrian doomsday book: or, Liber censualis of the district round Harran in the seventh century BC*. Leipzig, J C Hinrichs.

FAO (UN Food and Agriculture Organization).WFP (UN World Food Programme) and Syria's Ministry of Agriculture and Agrarian Reform. (2012) *Joint Rapid Food Security Needs Assessment (JRFSNA). Syrian Arab Republic: Report*. Available at: www.fao.org/gIEWS/english/otherpub/jrfsna_syrian2012.pdf

Jones, C. Sultan, M. Yan E, Milewski A, Hussein M, Al-Dousari A, Al-Kaisy S, Becker R. (2008). 'Hydrologic impacts of engineering projects on the Tigris-Euphrates system and its marshlands', *Journal of Hydrology* 353:59-75.

Jones, J. F. (1857). *Memoirs of Baghdad, Kurdistan and Turkish Arabia, 1857*: selections from the records of the Bombay Government, no.xliii, new series. Bombay, Bombay Government .

Jung, F. Fuchs, F. Boldo, D. (2002). 'Automization of aerotriangulation', in Kasser, M. and Egels, Y. (eds). *Digital Photogrammetry*. London, Taylor and Francis p124-145.

Kalayci, T. (2013). *Agricultural production and stability of settlement systems in Upper Mesopotamia during the Early Bronze Age (Third millennium BCE)*. unpublished PhD thesis, University of Arkansas.

Kamash, Z. (2009). *Water supply and management in the Near East 63 BC – AD 636*. unpublished PhD Thesis, University of Oxford

Kamash, Z. (2010). *Archaeologies of Water in the Roman Near East, 63 BC- AD 636*. Piscataway Gorgias Press.

Kaniewski, D. Van Campo, E. Weiss, H. (2012). 'Drought is a recurring challenge in the Middle East'. *Proceedings of the National Academy of Sciences*, 109(10):3862-3867.

Kaptijn, E. (2009). *Life on the Watershed*. Leiden, Sidestone Press.

Kaptijn, E. (2010). 'Communality and power: irrigation in the Zerqa Tirangle, Jordan'. *Water History* 2:145-163.

Karrou, M. Oweis, T. (2012). 'Water and land productivities of wheat and food legumes with deficit supplemental irrigation in a Mediterranean environment'. *Agricultural Water Management* 107:94-103.

Kay M. (1986). *Surface irrigation systems and practice*, Bedford, Cranfield Press.

Kennedy D, Riley D. (1990). *Rome's desert frontier from the air*. Austin, University of Texas Press.

Kennedy, H. N. (2007). 'Justinianic plague in Syria and the archaeological evidence', in Little, L. K. (ed). *Plague and the end of antiquity: The pandemic of 541-750*. Cambridge, Cambridge University Press p87-99.

Kennedy, H. N. (2011). 'The feeding of the five hundred thousand: cities and agriculture in early Islamic Mesopotamia'. *Iraq* 73: 177-199.

Kinsey-Henderson, A. E., Wilkinson, S. N., (2013). 'Evaluating shuttle radar and interpolated DEMS for slope gradient and soil erosion estimation in low relief terrain', *Environmental modelling and software*, 40:128-139.

Kirtane, S. Gandhi, K. (2006). 'Traditional water management systems in Bundelkhand', in Chakravarty K K, Badam G L, Paranjpye V, (eds). *Traditional water management systems of India*. Bhopal, Indira Gandhi Rashtriya Manac Sangrahalaya.

Kliot, N. (1994). *Water resources and conflict in the Middle East*. London, Routledge

Kolars, J. F. and Mitchell, W. A. (1991). *The Euphrates River and the southeast Anatolia development project*. Carbondale and Edwardsville, Southern Illinois University press.

Kovda, V. A, van den Berg, C. and Hagan, R. M. (eds). (1973). *Irrigation, drainage and salinity: an international source book*. London, FAO/UNESCO/Hutchinson.

Kruse, E. G. Humphreys, A. S. and Pope E. J. (1983). *Farm Water Distribution Systems*, in Jensen M E (eds). *Design and Operation of Farm Irrigation Systems*. St Joseph, American Society of Agricultural Engineers p395-446.

Kuhe, H. (1991). *Ein Bewässerungssystem des Ersten Jahrtausends v. Chr. Am Unteren Habur*, in Kuhne H (eds). *Die rezenten umwelt von Tall She Hamad und daten zur umweltrekonstruktion der Assyrischen stadt Dur-Katlimmu*. Berlin, Dietrich Reimer Verlag.

Lansing, J. S. (1987). 'Balinese 'Water Temples' and the management of irrigation', *American Anthropologist* 89:326-41.

Lansing, J. S. (1991). *Priests and Programmers: technologies of power in the engineered landscape of Bali*. Princeton, Princeton University Press.

Larsen, M. T. (1979). 'The tradition of empire in Mesopotamia', in Larsen, M. T (eds). *Power and propaganda: A symposium on ancient empires, Mesopotamia*. Copenhagen, Copenhagen studies in Assyriology, Volume 7, Akademisk Forlag, pp 75-106.

Lavee, H. Poesen, J. Yair, A. (1997). 'Evidence of high efficiency water-harvesting by ancient farmers in the Negev Desert, Israel'. *Journal of Arid Environments* 35:341-348.

Layard, A. H. (1853). *Discoveries in the ruins of Nineveh and Babylon*. London, John Murray.

Le Strange, G. (1930). *Lands of the Eastern Caliphate*. London, Frank Cass.

Lebeau, M. and Suleiman, A. (eds). (2011). *Tell Beydar: the 2004/2-2009 seasons of excavations, the 2004/2-2009 seasons of architectural restoration: a preliminary report*. Brepols, Subartu 29.

Lees, S. H. (1994). 'Irrigation and Society'. *Journal of Archaeological Research* 2(4):361-378.

Lewis, N. (1955). 'The frontier of settlement in Syria, 1800-1950'. *International Affairs (Royal Institute of International Affairs 1944-)* 3(1):48-60.

Lightfoot, D. R. (1996). 'Syrian qanat Romani: history, ecology, abandonment'. *Journal of Arid Environments* 33:321-336.

Lightfoot, D. (2009). *Survey of infiltration karez in Northern Iraq: History and current status of underground aqueducts*, UNESCO.

Lightfoot J L. (2003). *Lucian on the Syrian Goddess*, Oxford University Press, Oxford.

Lillesand, T M, Kiefer R W, Chipman J W. (2003). *Remote sensing and image interpretation* (6th ed). John Wiley and Sons.

Litt, T. Ohlwein, C. Neumann, F. H, Hense, A. Stein, M. (2012). 'Holocene climate variability in the Levant from the Dead Sea pollen record'. *Quaternary Science Reviews* 49:95-105.

Lloyd, S. (1938). 'Some ancient sites in the Sinjar district'. *Iraq* 5:123-142

Lu, G. Y. Wong, D. W. (2008). 'An adaptive inverse-distance weighting spatial interpolation technique'. *Computers & Geosciences* 34:1044-1055

Lyonnet, B. (eds). (2000). *Prospection archaéologique du haut-Khabur occidental (Syria du N E)*. Beriut, Institut français d'archaéologie du proche-Orient

Lyonnet, B. (1996). *Settlement pattern in the Upper Khabur (N E Syria) from the Achaemenids to the Abbasid period: Methods and preliminary results from a survey*, in Bartl, K. Hauser, S. R. (eds). *Continuity and change in Northern Mesopotamia from the Hellenistic to the Early Islamic period*. Berlin, Dietrich Reimer Verlag pp349-362

Mabry, J. B. (eds). (1996). *Canals and communities: Small-scale irrigation systems*. Tucson, University of Arizona Press.

Mabry, J. B. (2000). 'Wittfogel was half right: the ethnology of consensual and non-consensual hierarchies in irrigation management', in Diehl, M. W. (eds) *Hierarchies in Action: Cui bono? Centre for archaeological investigation*. Carbondale, Southern Illinois University, 284-295.

Mallowan, M. E. L. (1946). 'Excavations in the Balikh Valley' 193. *Iraq*, 8:111-159.

Margueron, J. C. (2004). *Mari: metropole de L'Euphrate*. Paris, Picard.

Masi, A. Sadori, L. Zanchetta, G. Baneschi, I. and Giardini, M. (2013). 'Climatic interpretation of carbon isotope content of mid-Holocene archaeological charcoals from eastern Anatolia', *Quaternary International*, 3030:64-72.

Masse, W. B. (1981). 'Prehistoric irrigation systems in the Salt river valley, Arizona'. *Science, New Series*, 214(4519):408-415.

Matschoss, P.R., Plattner, G.K., Yohe, G.W., and. Zwiers, F.W, (2010). *Guidance Note for Lead Authors of the IPCC Fifth Assessment Report on Consistent Treatment of Uncertainties*. Intergovernmental Panel on Climate Change (IPCC). Available at <<http://www.ipcc.ch>>.

Matthews, R. (2003a). Excavations at Tell Brak, Volume 4: Exploring an Upper Mesopotamian regional centre, 1994-1996, London, British School of Archaeology in Iraq.

Matthews, R. (2003b). The archaeology of Mesopotamia: Theories and approaches. London, Routledge.

McClellan, T. Grayson, R. and Gleby, C. O. (2000). 'Bronze age water harvesting in North Syria', in O.Rouault & M. Wäfler (eds.). *La Djéziré et l'E uphrate Syriens de la protohistoire à la fin du IIe Millénaire* . Turnhout, Brepols p137–55.

McQuilty, A. (2004). 'Harnessing the power of water: Watermills in Jordan', in Bienert, H. D. and Haser, J. (eds). *Men of Dikes and Canals: The Archaeology of Water in the Middle East*, Verlag marie Leidorf GmbH, p261-272.

Meijer, D. J. W. (1986). *A survey in Northeastern Syria*. Leiden, Nederlands Historisch-Archaeologisch Instituut Te Istanbul.

Menze, B. H. Ur, J. A. and Sherratt, A. G. (2006). 'Detection of ancient settlement mounds: Archaeological survey based on the SRTM terrain model'. *Photogrammetric Engineering & Remote Sensing* 72(3):321-327.

Mitchell, W. P. (1973). 'The hydraulic hypothesis: A reappraisal'. *Current Anthropology* 14(5):532-534.

Mithen, S. Black, E. (eds). (2011). *Water, life and civilisation: climate, environment and society in the Jordan Valley*. Cambridge, Cambridge University Press.

Morandi Bonacossi, D., (2000). 'The Syrian Jezireh in the Late Assyrian period: A view from the countryside', in Bunnens, G. (eds). *Essays on Syria in the Iron Age*. Louvain, Peeters Press pp.349-396.

Morell, F. J. Lampurlanes, J. Alvaro-Fuentes, J. Cantero-Martinez, C. (2011). 'Yield and water use efficiency of barley in a semiarid Mediterranean agroecosystem: Long-term effects of tillage and N fertilization', *Soil and Tillage Research* 117:76-84.

Morony, M. G. (2007). 'For who does the writer write?': The first bubonic plague pandemic according to Syriac sources, in Little, L. K (ed). *Plague and the end of antiquity: The pandemic of 541-750*. Cambridge, Cambridge University Press, p59-87.

Mugnier, C. J. Forstner, W. Wrobel, B. Paderes, F. and Munjy, R. (2004). 'The mathematics of photogrammetry', in McGlone J C, (eds) *Manual of photogrammetry (5th ed)*. Bethesda, American Society of Photogrammetry and remote sensing p181-316.

Mulders, M. A. (1969). *The arid soils of the Balikh Basin (Syria)*. Rotterdam, unpublished PhD thesis.

Murphy, J. T. (2009). *Exploring complexity in the past: the Hohokam water management simulation*, unpublished PhD thesis, The University of Arizona.

Northedge, A. (2005). *The historical topography of Samarra*. British School of Archaeology in Iraq, London.

Northedge, A. (2011). 'Sasanian and Abbasid Royal settlement at Samarra: Aspects of continuity and change', in Borrut, A. Debie, M. Papaconstantinou, A. Pieri, D. Sodini, J. P. (eds). *Le Proche-Orient de Justinien aux Abbasides: Peuplement et dynamiques spatiales*. Turnhout, Brepols p29-43.

NRO (no date). *CORONA system information*, <http://www.nro.gov/history/csnr/corona/sysinfo.html> (Accessed 11.12.2014).

Oates, D. (1968). *Studies in the ancient history of Northern Iraq*. London, Oxford University Press.

Oates, D. Oates, J. McDonald, H. (eds). (2001). *Excavations at Tell Brak*. Cambridge, McDonald Insitute for Archaeological Research.

Ochs, W. J. Willardson, L. S. Camp, C. R. Donnan, W. W. Winger. R. J. Johnson, W. R. and Johnson, W. R. (1983). 'Drainage requirements and systems', in Jensen, M. E. (eds). *Design and operation of farm irrigation systems*. St Joseph, American Society of Agricultural Engineers, p235-280.

Oleson, J. P. (2007). 'Nabataean water supply, irrigation and agriculture', in Politis, K. D. (eds). *The world of the Nabataeans*, Franz Steiner Verlag, p217-251.

Ortloff, C. R. (2009). *Water engineering in the ancient world: Archaeological and climate perspectives on societies of ancient South America, the Middle East, and South-East Asia*. Oxford, Oxford University Press.

Oweis, T. Hachum, A. and Kijne, J. (1999). *Water harvesting and supplemental irrigation for improved water use efficiency in dry areas*. Colombo, SWIM Paper 7, International Water Management Institute.

Parrot, A. (1956). *Mission archeologique de Mari*. Paris, Librairie Orientaliste Paul Geuthner.

Parsons, H. L. (1977). *Marx and Engels on Ecology*. Westport, Greenwood Press.

Peltenburg, E. Wilkinson, E. Wilkinson, T. Ricci, A. McCarthy, A. Lawrence, D. (2010). *The Land of Carchemish (Syria) Project 2009: Carchemish outer town survey*. Report submitted for Annales Archaeologiques Arabes Syriennes.

Perdue, L. Miles, W. Woodson, K. Darling, A. and Berger, J. F. (2010). 'Micromorphological study of irrigation canal sediments: Landscape evolution and hydraulic management in the middle Gila River valley (Phoenix Basin, Arizona) during the Hohokam occupation'. *Quaternary International* 216:129-144.

Perez, A. J. Abrahao, R, Causape, J. Cirpka, O. A. and Burger C. M. (2011). 'Simulating the transition of a semi-arid rainfed catchment towards irrigation agriculture'. *Journal of Hydrology*, 409:663-681.

Perry, P. J. (1988). 'Thirty Years on: or, Whatever happened to Wittfogel?', *Political Geography Quarterly* 7(1):75-83.

Poidebard, A. (1934). *La trace de Rome dans le desert de Syrie: le limes de Trajan à la conquete arabe: recherches aeriennes (1925-1932)*. Paris, Geuthner .

Pournelle, J. R. (2013). *Marshland of Cities: Deltaic Landscapes and the evolution of civilisation*, Available at: <http://www.yale.edu/agrarianstudies/colloqpapers/01pournelle-supp.pdf>

Pournelle, J. (2003). *Marshland of cities: Deltaic landscapes and the evolution of early Mesopotamian civilization*. Unpublished PhD thesis, University of California, San Diego.

Price, D. H. (1994). 'Wittfogel's neglected Hydraulic/Hydroagricultural distinction', *Journal of Anthropological Research* 50(2):187-204.

Pustovoytov, K. Schmidt, K. Taubald, H. (2007). 'Evidence for Holocene environmental changes in the northern Fertile Crescent provided by pedogenic carbonate coatings', *Quaternary research*, 67(3):315-327.

Rabo, A. (1989). 'Centre and periphery: The case of Raqqa province', *Bulletin d'études orientales*, T. 41/42, pp. 149-160.

Reade, J. (1978a). 'Studies in Assyrian Geography: part 1: Sennacherib and the waters of Nineveh'. *Revue d'Assyriologie et d'archéologie orientale* 72(1):47-72.

Reade, J. (1978b). 'Studies in Assyrian Geography: part 1: Sennacherib and the waters of Nineveh'. *Revue d'Assyriologie et d'archéologie orientale* 72(2):157-180.

Replogle, J. A. Marriam, J. L. Swarner, L. R. Phelan, J. T. (1983). 'Farm water delivery systems', in Jensen, M. E. (eds). *Design and operation of farm irrigation systems*. St Joseph, American Society of Agricultural Engineers p317-346.

Riehl, S. (2009). 'Archaeobotanical evidence for the interrelationship of agricultural decision-making and climate change in the ancient Near East', *Quaternary International* 197:93-114.

Riehl, S. (2012). 'Variability in ancient near Eastern environmental and agricultural development', *Journal of Arid Environments* 86:113-121.

Riehl, S. Bryson, R. Pustovoytov, K. (2008). 'Changing growing conditions for crops during the Near Eastern Bronze Age (3000-1200 BC): the stable carbon isotope evidence', *Journal of Archaeological Science* 35: 1011-1022.

Roberts, N. Eastwood, W. J. Kuzucuoglu, C. Fiorentino, G. Caracuta, V. (2011). 'Climatic, vegetation and cultural change in the eastern Mediterranean during the mid-Holocene environmental transition', *The Holocene* 21:147-162.

Rodriguez, E. Morris, C. S. Belz, J. E. (2006). 'A global assessment of the SRTM performance', *Photogrammetric Engineering & Remote Sensing* 72(3):249-260.

Rosen, A. M., Weiner, S. (1994). 'Identifying ancient irrigation: a new method using opaline phytoliths from emmer wheat', *Journal of Archaeological Science*, 21:125-132.

Rudolf, B., Schneider, U., (2005). *Calculation of gridded precipitation data for the global land – surface using in situ-gauge observations*, Proceedings of the 2nd Workshop of the International Precipitation Working Group IPWG, Monterey, October 2004, 231-247.

Ruelland, D. Ardoin-Bardin, S. Billen, G. Servat, E. (2008). 'Sensitivity of a lumped and semi-distributed hydrological model to several methods of rainfall interpolation on a large basin in West Africa', *Journal of Hydrology* 361:96-117.

Ruggles, D. F. (1990). 'The Mirador in Abbasid and Hispano-Umayyad garden typology', *Murqarnas* 7:73-82.

Ruggles, D. F. (2008). *Islamic gardens and landscapes*. Philadelphia, University of Pennsylvania Press.

Sack, D (eds). (2007-9). *Resafa-Sergiupolis/Rusafat Hisham: Pilgerstadt und Kalifenresidenz- intra und extra muros*. Berlin, Technische Universitat

Sanders, B. F. (2007). 'Evaluation of on-line DEMs for flood inundation modelling', *Advances in Water Resources* 30:1831-1843.

Sanlaville, P. Besancon, J. (1981). 'Aperçu géomorphologique sur la vallée de l'Euphrate syrien'. *Paléorient* 7(2):5-18.

Sanyal, J. Carbonneau, P. Densmore, A. L. (2013). 'Hydraulic routing of extreme floods in a large ungauged river and the estimation of associated uncertainties: a case study of the Damodar River, India', *Natural Hazards* 66:1153-1177.

Scarborough, V. L. (2003). '*The Flow of Power: Ancient water systems and landscapes*', Santa Fe, School of American Research.

Scharstein, D. and Szeliski, R. (2002). 'A taxonomy and evaluation of dense two-frame stereo correspondence algorithms', *International Journal of Computer Vision*, 47(1/2/3):7-42, April-June 2002.

Schmidt, M. Goossens, R. Menze, G. Altmaier, A. and Devriendt, D. (2001). '*The use of CORONA satellite images for generating a high resolution digital elevation model*', Geoscience and Remote Sensing Symposium, 2001, IGARSS 01. IEEE 2001 International.

Schneider, U. Becker, A. Meyer-Christoffer, M. and Ziese, B. (2011). *Global Precipitation Analysis Products of the GPCC*, Global Precipitation Climatology Centre (GPCC). Deutscher Wetterdienst, Offenbach, Germany.

Shalhevet, J. Mantell, A. Bielorai, H. Shimshi, D. (1981). *Irrigation of Field and Orchard crops under semi-arid conditions*. Bet Dagan, International Irrigation Information Centre.

Sharma, D. P. Rao, J. V. G. K. Singh, K. N. Kumbhare, E. S. Oosterbaan R. J. (1994). 'Conjunctive use of saline and non saline irrigation waters in semi-arid regions', *Irrigation Science* 15:25-33.

Sheridan, T. (1996). 'Le Gente Es Muy Perra: Conflict and cooperation over irrigation water in Curcurpe, Sonora, Mexico', in Mabry, J. B. (eds). *Canals and communities: Small-scale irrigation systems*. Tucson, University of Arizona Press.

Sinopoli, C. M. (1994). 'The Archaeology of Empires', *Annual Review of Anthropology* 23:159-180.

Slater, J. A. Heady, B. Kroenung, G. Curtis, W. Haase, J. Hoegemann, D. Shockley, C. Tracy, K. (2011). 'Global Assessment of the new ASTER Global Digital Elevation Model', *Photogrammetric Engineering and Remote Sensing* 77(4): 335-350.

Soenario, I. Sluiter, R. (2010). *Optimization of rainfall interpolation*. Koninklijk Nederlands Meteorologisch Instituut, Wilhelminalaan.

Sohn, H. G. Kim, G. H. Yom, J. H. (2004). 'Mathematical modelling of historical reconnaissance CORONA KH-4B imagery', *The Photogrammetric Record* 19(105):51-66.

Sommer, R. Piggin, C. Hadad, A. Hajdibo, A. Hayek, P. Khalil, Y. (2012). Simulating the effects of zero tillage and crop residue retention on water relations and yield of wheat under rainfed semiarid Mediterranean conditions. *Field Crops Research* 132:40-52.

Stark, F. (1966). *Rome on the Euphrates: the story of a frontier*. London, John Murray.

Staubwasser, M. Weiss, H. (2006). 'Holocene climate and cultural evolution in late prehistoric-early historic West Asia', *Quaternary Research* 66:372-387

Stein, A. (1941). 'The ancient trade route past Hatra and its Roman posts', *Journal of the Royal Asiatic Society of Great Britain and Ireland* 1994(4):299-316.

Stein G. (1994). 'Segmentary states and organizational variation in early complex societies: A rural perspective', in Schwartz, G. and Falconer, S. (eds). *Archaeological views from the countryside*. Washington, Smithsonian press p10-18.

Steward, J. C. Murphy, R. F. (1977). 'Wittfogel's irrigation hypothesis' in Steward, J. C. Murphy, R. F. (eds). *Evolution and ecology: Essays on Social transformation by Julian H Steward*. Urbana, University of Illinois Press, p 87-99'

Stride, S. Rondelli, B. Mantellini, S. (2009). 'Canals versus horses: political power in the oasis of Samarkand', *World Archaeology* 41(1): 73-87.

Strommenger, E. (1981). 'Die archaologischen Forschungen in Tall Bi'a a 1980', *Mitteilungen der Deutschen Orient-Gesellschaft zu Berlin* 113:23-34.

Sykes, M. (1907). 'Journeys in North Mesopotamia', *The Geographical Journal* 30(3):237-254.

Taagepera, R. (1978a). 'Size and duration of Empires: Systematics of size'. *Social Science Research* 7: 108-127.

Taagepera, R. (1978b). 'Size and duration of Empires: Growth-decline curves 3000 to 600 BC'. *Social Science Research* 7:180-196.

Taagepera, R. (1979). 'Size and duration of Empires: Growth-decline Curves, 600 BC to 600 AD'. *Social Science History* 3(3/4):115-138.

Tabios, G. O. Salas, J. D. (1985). 'A comparative analysis of techniques for spatial interpolation of precipitation'. *Water Resources Bulletin* 21(3):365-380.

Thameur, A. Lachiheb, B. Ferchichi, A. (2012). 'Drought effect on growth, gas exchange and yield, in two strains of local barley Ardhaoui, under water deficit conditions in southern Tunisia'. *Journal of Environmental Management* 113:495-500.

Thompson, G. T. Spiess, L. B. and Krider, J. N. (1983). 'Farm resources and system selection', in Jensen, M. E. (eds). *Design and operation of farm irrigation systems*. St Joseph, American Society of Agricultural Engineers p45-76.

Tonghini, C. (1998). *Qal'at Ja'bar pottery: A study of a Syrian fortified site of the late 11th-14th centuries* Oxford, Oxford University Press.

Toueir, K. (1983). 'Heraqlah: a unique victory monument of Harun ar-Rashid'. *World Archaeology* 14(3):296-304.

Toueir, K. (1990). 'Le Nahr El-Nil entre Raqqa et Heraqlah', in Geyer, B. (eds). *Techniques et pratiques hydro-agricoles traditionnelles en domaine irrigué: approche pluridisciplinaire des modes de culture avant motorisation en Syrie*. Paris, Geuthner p217-227.

Ulmen, G. L. (1978). *The Science of Society: Towards an understanding of the life and work of Karl August Wittfogel*. The Hague.

Ur, J. A. (2010b). 'Cycles of Civilisation in Northern Mesopotamia, 4400-2000 BC'. *Journal of Archaeological Research* 18:387-431.

Ur, J. (2005). 'Sennacherib's Northern Assyrian Canals: New Insights from Satellite Imagery and Aerial Photography'. *Iraq* 67(1): 317-345.

Ur, J. (2010a). *Tell Hamoukar Volume 1: Urbanism and cultural landscapes in northeastern Syria. The Tell Hamoukar Survey, 1999-2001*. Chicago, The Oriental Institute of the University of Chicago.

Ur, J. (2013). 'CORONA satellite imagery and ancient Near Eastern Landscapes', in Comer, D. C. and Harrower, M. J. (eds). (2013). *Mapping Archaeological Landscapes from space*. Springer Briefs in Archaeological Heritage Management.

Ur, J. de Jong, L. Giraud, J. Osborne, J. F. and MacGinnis, J. (2013). 'Ancient cities and landscapes in the Kurdistan region of Iraq: The Erbil Plain' *Archaeological Survey 2012 Season*. *Iraq* 75:89-118.

Ur, J. Wilkinson, T. J. (2008). *Settlement and economic landscapes of Tell Beydar and its hinterland*. Turnhout, Brepols.

USGS (2012). *Declassified Satellite Imagery -1*, https://lta.cr.usgs.gov/declass_1 (Accessed: 11.12.2014).

Van den Berg, C. Visser, W. C. and Kovda, V. A. (1973). Water and salt balances, in Kovda, V. A. van den Berg, C. and Hagan, R. M. (eds). *Irrigation, drainage and salinity: an international source book*. London, FAO/UNESCO/Hutchinson.

Van Liere, W. J. (1963). 'Capitals and citadels of Bronze-Iron Syria in their relationship to land and water'. *Les Annales Archaeologiques De Syrie*, vol XIII, p107-122.

Van Liere, W. J. and Lauffray, J. (1954-55). 'Nouvelle prospection archaéologique dans la haute Jazireh Syrienne'. *Les Annals Archaeologiques De Syrie*, IV et V, p129-148.

Van Liere, W. J. (1960-1961). *Observations on the Quaternary of Syria*, Berichten Rijksdienst voor Oudheidkunde en Bodemonderzoek 10/11: 7-69.

Van Loon, M. (1988). *Hammam et-Turkman I: Reports on the University of Amsterdam's 1981-84 Excavations in Syria*. Istanbul, Nederlands Historisch Archaeologisch Instituut te Istanbul.

Van Schilfgaarde, J. (eds). (1974). *Drainage for agriculture*. Madison, American Society of Agronomy.

Varela-Ortega, C. and Sagardoy J. A. (2003). 'Irrigation water policies in Syria: Current developments and future options', in FAO (eds). *Syrian agriculture at the crossroads, Agricultural Policy and economic development* Series No. 8.

Verdin, K. L. and Verdin, J. P. (1999). 'A topological system for delineation and codification of the Earth's river basins'. *Journal of Hydrology* 218:1-12.

Villard, P. (1987). 'Un conflit d'autorités à propos des eaux du Balih'. *Mari* 5:59-96.

Vosselman, G. Sester, M., and Mayer, H. (2004). 'Basic computer vision techniques', in McGlone J. C. (ed) *Manual of photogrammetry* (5th ed). Bethesda, American Society of Photogrammetry and Remote Sensing p455-505.

Wallen, C. C. (1967). 'Aridity definitions and their applicability'. *Geografiska Annaler* 49(2/4):367-384.

Wang, L. Gong, M. Gong, M. and Yang, R. (2006). *How far can we go with local optimization in real-time stereo matching*, Third International Symposium on 3D Data Processing, Visualization and Transmission (3DPVT). University of North Carolina, USA, 14-16 June 2006.

Waters, M. R. (2008). 'Alluvial chronologies and archaeology of the Gila River drainage basin, Arizona'. *Geomorphology* 101:332-341.

Waters, M. R. Ravesloot, J. C. (2001). 'Landscape change and the cultural evolution of the Hohokam along the middle Gila River and other river valleys in south-central Arizona'. *American Antiquity* 66(2):285-299.

Weiss, B. (1982). 'The decline of Late Bronze Age civilisation as a possible response to climatic change'. *Climate Change* 4:173-198.

Welderufael, W. A. Woyessa, Y. E. and Edossa, D. C. (2013). 'Impact of rainwater harvesting on water resources of the modder river basin, central region of South Africa'. *Agricultural Water Management* 116:218-227.

Whyte, R. O. (1966). 'The use of arid and semi-arid land', in Hills, (eds). *Arid lands: A geographical appraisal*, Methuen and Co Ltd, London, p301-363.

Wick, L. Lemcke, G. and Sturm, M. (2003). 'Evidence of Late glacial and Holocene climatic change and human impact in Eastern Anatolia: High resolution pollen, charcoal, Isotopic and Geochemical Records from the laminated sediments of lake Van, Turkey'. *The Holocene* 13(50):665-675.

Wiggermann, F. A. M. (2000). 'Agriculture in the Northern Balikh Valley', in Jas, R. M. (eds). *Rainfall and agriculture in Northern Mesopotamia*. Istanbul, Nederlnds Historisch-Archaeologische Instituut te Istanbul.

Wikander, O. (eds). (2000). *Handbook of ancient water technology*. Leiden, Brill.

Wilkinson, E. B. Wilkinson, T.J. and Peltenburg, E. (2011). Revisiting Carchemish: the land of Carchemish Project in Syria, 2009 and 2010. *Antiquity* 058(329) Available at: <http://www.antiquity.ac.uk/projgall/wilkinson329/>

Wilkinson, K. N. Beck, A. R. Philip, G. (2006). 'Satellite imagery as a resource in the prospection for archaeological sites in central Syria'. *Geoarchaeology*, 21(7):735-750.

Wilkinson, T. J. (1982). 'The definition of ancient manured zones by means of extensive sherd-sampling techniques'. *Journal of Field Archaeology* 9:323-333.

Wilkinson, T. J. (1994). 'The structure and dynamics of dry-farming states in Upper Mesopotamia'. *Current Anthropology*, 35(5):483-520.

Wilkinson, T. J. (1997). 'Holocene environments of the high plateau, Yemen. Recent geoarchaeological investigations'. *Geoarchaeology*, 12(8):833-864.

Wilkinson, T. J. (2000a). 'Settlement and land use in the zone of uncertainty in Upper Mesopotamia', in Jas, R. M. (eds). *Rainfall and agriculture in Northern Mesopotamia*. Istanbul, Nederlands Historisch-Archaeologisch Instituut Te Istanbul, p3-36.

Wilkinson, T. J. (2000b). 'Regional Approaches to Mesopotamian Archaeology: The Contribution of Archaeological Surveys'. *Journal of Archaeological Research*, 8(3):219-267

Wilkinson, T. J. (2003). *Archaeological landscapes of the Near East*. Tucson, The University of Arizona Press.

Wilkinson, T. J. (2010). 'Introduction'. *Water History* 2:85-90

Wilkinson, T. J. Barbanes, E. (2000). 'Settlement patterns in the Syrian Jazira during the Iron Age', in Bunnens, G. (eds). *Essays on Syria in the Iron Age*. Louvain, Peeters Press.

Wilkinson, T. J. and Peltenburg, E. (2010). 'Carchemish in context: Surveys in the hinterland of a major Iron Age city'. *Council for British Research in the Levant Bulletin* 5:11-20.

Wilkinson, T. J. (1998). 'Water and Human Settlement in the Balikh Valley, Syria: Investigations from 1992-1995'. *Journal of Field Archaeology* 25(1):63-87.

Wilkinson, T. J. and Tucker, D. J. (1995). *Settlement Development in the North Jazira, Iraq: A study of the archaeological landscape*. Warminster, Aris and Phillips.

Wilkinson, T. J. Peltenburg, E. McCarthy, A. Wilkinson, E. B. and Brown, M (2007). 'Archaeology in the Land of Carchemish: landscape surveys in the area of Jerablus Tahtani, 2006'. *Levant* (39):213-247.

Wilkinson, T. J. and Rayne, L. (2010). 'Hydraulic landscapes and imperial power in the Near East'. *Water History* 2(2):115-144.

Wilkinson, T.J., Rekavandi, H. O. Hopper, K. Priestman, S. Roustaei, K. and Galiatsatos, N. (2013). 'The Landscapes of the Gorgān Wall'. in Sauer, E. Rekavandi, H. O. Wilkinson, T.J. and Nokandeh J. (eds.) *Persia's Imperial Power In Late Antiquity: Sasanian Frontier Walls, Forts And Landscapes Of Northern Iran (The Joint Fieldwork Project On The Great Wall Of Gorgān, The Wall Of Tammīsheh And Other Sites In The Frontier Zone: 2005-2009)*. British Institute of Persian Studies Monograph: Oxford, Oxbow Books p 25-132.

Wilkinson, T.J., Peltenburg, E. and Wilkinson, E (eds.) forthcoming. *Carchemish in Context*. Oxford, Oxbow Books.

Willcocks, W. (1917). *Irrigation of Mesopotamia*, London, E & F N Spon.

Winter, S. H. (2009). 'The province of Raqqa under Ottoman rule, 1535-1800: A preliminary study'. *Journal of Near Eastern Studies* 68(4):253-268.

Wirth, E. (1971). *Syrien, eine geographische Landeskunde*, Wissenschaftliche Buchgesellschaft, Darmstadt.

Wittfogel, K. (1968). 'The theory of Oriental Society', in Fried, M. H. (eds). *Readings in Anthropology Volume II Cultural Anthropology second edition*. New York, Thomas Y Cromwell Company pp 179-198.

Wittfogel, K. (1957). *Oriental Despotism: A comparative study of total power*. New Haven and London, Yale University Press,.

Wong, K. W. (1980). 'Basic mathematics of photogrammetry', in Slama C C (ed). 1980, *Manual of photogrammetry* (4th ed). Falls Church, American Society of Photogrammetry p37-101.

Woodbury, R. B. (1960). 'The Hohokam Canals at Pueblo Grande, Arizona'. *American Antiquity* 26(2):267-270.

Woolley, C. L. (1921). *Carchemisch. Report on the excavations at Jerablus on behalf of the British Museum, part II: The Town Defences*. London, The Trustees of the British Museum.

Worster, D. (1993). *The Wealth of Nature: Environmental History and the Biological imagination*. Oxford, Oxford University Press.

Yazdi, A. A. S. and Khaneiki, M. L. (2010). *Veins of Desert: A review on the technique of Qanat/Falaj/Karez*. Iran Water Resources Management Organization.

Yesilnacer, M. I. and Gulluoglu, M. S. (2008). 'Hydrochemical characteristics and the effects of irrigation on groundwater quality in Harran Plain, GAP Project, Turkey'. *Environmental Geology* 54:183-196.

Yigezu, Y. A. Ahmed, M. A. Shideed, K, Aw-Hassan, A. El-Shater, T. and Al-Atwan, S. (2013). 'Implications of a shift in irrigation technology on resource use efficiency: A Syrian case'. *Agricultural Systems* 118:14-22.

Young, A. (1976). *Tropical soils and soil survey*. Cambridge, Cambridge University Press.

Zaqzuq, A. R. (1985). 'Fouilles de la citadelle de Ja'bar'. *Syria*, 62(1/2):140-141.

Zimmerman, J. D. (1966). *Irrigation*. New York, John Wiley& Sons.

Appendix: CORONA photogrammetry triangulation reports

Canal near Hammam et Turkman

The Triangulation Report With LPS

The output image x, y units: pixels
 The output angle unit: degrees
 The output ground X, Y, Z units: meters

The Input Image Coordinates image ID = 1

Point ID	x	y			
1	414.054	211.230	20	94.206	99.409
3	224.243	170.064	21	99.845	248.360
4	367.052	452.858	22	79.945	341.607
5	26.043	435.888	23	77.901	401.903
6	343.347	27.085	24	238.461	396.047
7	311.067	417.943	25	173.934	413.197
8	265.362	353.034	26	188.815	315.025
9	165.282	37.852	27	251.662	209.205
10	315.569	182.338	28	187.522	75.337
11	392.999	127.403	29	221.088	67.975
12	258.089	72.081	30	211.864	132.711
13	277.984	252.971	31	314.215	106.277
14	323.438	323.965	32	359.033	277.592
15	369.918	394.774	33	396.000	122.765
16	366.030	224.843	34	337.631	149.226
17	368.665	63.261	35	349.623	159.979
18	293.466	12.171	36	318.930	182.994
19	57.341	148.968	37	394.805	232.646

Affine coefficients from file (pixels) to film (millimeters)

A0	A1	A2	B0	B1	B2	
-1.5890	-0.000000	0.007000	-1.4840	0.007000	0.000000	

image ID = 2

Point ID	x	y			
1	426.881	282.205	20	100.136	106.975
3	236.148	208.000	21	120.199	264.108
4	409.827	525.925	22	114.174	356.960
5	74.801	449.891	23	120.809	420.419
6	336.245	77.210	24	279.304	445.209
7	352.183	479.155	25	217.915	449.686
8	299.985	405.277	26	219.453	349.365
9	161.263	56.164	27	265.139	253.879
10	327.599	234.313	28	188.093	99.588
11	396.150	191.394	29	218.997	97.112
12	254.016	107.975	30	221.720	169.793
13	297.630	299.283	31	312.994	158.037
14	351.559	382.716	32	380.940	341.890
15	406.440	467.118	33	398.736	186.919
16	382.282	286.995	34	344.898	204.068
17	364.245	120.295	35	373.308	227.289
18	283.804	53.941	36	330.736	235.060
19	69.267	153.068	37	409.997	302.076

Affine coefficients from file (pixels) to film (millimeters)

A0	A1	A2	B0	B1	B2
----	----	----	----	----	----

-1.8515 0.000000 0.007000 -1.6590 0.007000 0.000000

THE OUTPUT OF SELF-CALIBRATING BUNDLE BLOCK ADJUSTMENT

the no. of iteration =1 the standard error = 1.8861
the maximal correction of the object points = 0.00000

the no. of iteration =2 the standard error = 1.8861
the maximal correction of the object points = 0.00000

The exterior orientation parameters

image ID	Xs	Ys	Zs	OMEGA	PHI	KAPPA
1	397452.1731	4071491.4483	150784.0732	-372.5057	-394.6698	-442.1647
2	599534.3642	4089909.0019	-153841.3970	198.5702	-509.5860	-72.3136

The interior orientation parameters of photos

image ID	f(mm)	xo(mm)	yo(mm)
1	609.6020	0.0000	0.0000
2	609.6020	0.0000	0.0000

The residuals of the control points

Point ID	rX	rY	rZ
All residuals of fixed GCP are zero.			

The difference of intersected and measured control points

Point ID	rX	rY	rZ				
1	-3.1533	-5.4838	0.7860	20	-8.9578	-0.2793	10.4156
3	3.2235	4.9718	-9.6947	21	1.1453	0.2344	1.4776
4	-0.1518	0.1848	5.0720	22	-6.2930	-1.5689	4.5538
5	12.9581	-2.0258	-9.0979	23	-1.1280	-4.7917	0.3282
6	-0.7512	-2.0166	-0.0819	24	1.6509	2.7550	-4.6475
7	-1.9849	0.3937	2.9420	25	-0.0886	-2.3291	-0.2875
8	1.4933	5.0958	-4.6816	26	0.6935	2.8766	5.3408
9	-2.0992	-0.2702	3.0583	27	6.8975	-1.3628	-11.3525
10	-4.9653	-3.3135	4.0855	28	-3.7461	2.7869	3.1177
11	-1.3827	-3.9330	2.0009	29	-0.4827	1.4436	6.8583
12	-3.6289	-0.1197	3.0769	30	12.2168	1.8916	-19.6087
13	-10.1188	-0.1759	7.4889	31	9.8716	1.5551	-12.3730
14	-3.1035	2.0583	5.8925	32	-2.4705	0.4247	-2.2383
15	-4.7739	-0.1847	-1.9817	33	-1.4948	-0.4971	1.1080
16	-0.8648	-0.6031	5.2139	34	-1.2230	-0.2027	1.7742
17	3.9999	-2.9323	-1.5682	35	16.1600	7.2757	2.4685
18	-0.9565	-0.8072	-4.5649	36	-3.2768	-0.3132	5.2297
19	-3.5392	-0.2034	4.1278	37	0.2830	-0.5348	-4.1754

aX	aY	aZ
-0.0012	-0.0000	0.0018
mX	mY	mZ
5.5780	2.6244	6.2376
CE90	LE90	
8.9260	10.3969	

The image residuals of intersected GCP

Point	Image	Vx	Vy
1	1	-0.729	-0.087
1	2	0.737	-0.005

Point	Image	Vx	Vy
3	1	0.223	0.029
3	2	-0.226	-0.001

Point	Image	Vx	Vy
4	1	-1.049	-0.126
4	2	1.060	-0.006

Point	Image	Vx	Vy
5	1	0.529	0.072
5	2	-0.539	-0.006

Point	Image	Vx	Vy
6	1	0.395	0.049
6	2	-0.400	0.001

Point	Image	Vx	Vy
7	1	0.000	0.000
7	2	-0.000	0.000

Point	Image	Vx	Vy
8	1	0.509	0.064
8	2	-0.516	0.000

Point	Image	Vx	Vy
9	1	-0.039	-0.005
9	2	0.039	0.000

Point	Image	Vx	Vy
10	1	0.140	0.017
10	2	-0.142	0.000

Point	Image	Vx	Vy
11	1	-0.443	-0.054
11	2	0.448	-0.002

Point	Image	Vx	Vy
12	1	-1.436	-0.184
12	2	1.456	0.003

Point	Image	Vx	Vy
13	1	-0.672	-0.084
13	2	0.681	-0.000

Point	Image	Vx	Vy
14	1	-0.573	-0.070
14	2	0.579	-0.002

Point	Image	Vx	Vy
15	1	-0.545	-0.066
15	2	0.551	-0.003

Point	Image	Vx	Vy
16	1	-0.104	-0.013
16	2	0.106	-0.000

Point	Image	Vx	Vy
17	1	-0.363	-0.044
17	2	0.367	-0.001

Point	Image	Vx	Vy
18	1	-0.274	-0.035
18	2	0.277	0.000

Point	Image	Vx	Vy
19	1	0.076	0.010
19	2	-0.077	-0.001

Point	Image	Vx	Vy
20	1	0.481	0.065
20	2	-0.490	-0.005

Point	Image	Vx	Vy
21	1	-1.417	-0.191
21	2	1.441	0.012

Point	Image	Vx	Vy
22	1	-0.427	-0.058
22	2	0.434	0.004

Point	Image	Vx	Vy
23	1	0.173	0.023
23	2	-0.176	-0.001

Point	Image	Vx	Vy
24	1	0.769	0.097
24	2	-0.780	-0.001

Point	Image	Vx	Vy
25	1	0.809	0.105
25	2	-0.821	-0.003

Point	Image	Vx	Vy
26	1	0.335	0.043
26	2	-0.340	-0.001

Point	Image	Vx	Vy
27	1	-1.210	-0.154
27	2	1.227	0.002

Point	Image	Vx	Vy
28	1	0.127	0.017
28	2	-0.129	-0.001

Point	Image	Vx	Vy
29	1	-0.476	-0.062
29	2	0.483	0.002

Point	Image	Vx	Vy
30	1	1.414	0.183
30	2	-1.436	-0.005

Point	Image	Vx	Vy
31	1	-1.753	-0.219
31	2	1.776	-0.002

Point	Image	Vx	Vy
32	1	-0.599	-0.073
32	2	0.606	-0.003

Point	Image	Vx	Vy
33	1	-0.346	-0.042
33	2	0.350	-0.002

Point	Image	Vx	Vy
34	1	-0.049	-0.006
34	2	0.050	-0.000

Point	Image	Vx	Vy
36	1	0.009	0.001
36	2	-0.009	0.000

Point	Image	Vx	Vy
35	1	7.487	0.916
35	2	-7.574	0.026

Point	Image	Vx	Vy
37	1	-0.974	-0.117
37	2	0.985	-0.006

Mean error of 72 image points: ax=0.000, ay=-0.000
 RMSE of 72 image points: mx=1.443, my=0.125

The coordinates of object points

Point ID	X	Y	Z	Overlap
1	504559.9080	4038218.1330	314.0000	2
3	504049.0130	4038238.7580	317.0000	2
4	504600.3520	4037670.1510	312.0000	2
5	503716.7480	4037606.1200	317.0000	2
6	504252.2610	4038595.9630	317.0000	2
7	504436.5930	4037730.1590	316.0000	2
8	504278.7000	4037852.1190	316.0000	2
9	503802.9130	4038517.7900	319.0000	2
10	504291.1900	4038249.9370	313.0000	2
11	504448.8600	4038393.0380	311.0000	2
12	504061.6560	4038470.6640	317.0000	2
13	504241.4880	4038082.7990	317.0000	2
14	504402.6250	4037937.9850	314.0000	2
15	504577.3050	4037797.4380	314.0000	2
16	504442.8250	4038170.0240	314.0000	2
17	504338.0290	4038524.6110	314.0000	2
18	504116.5900	4038611.1200	317.0000	2
19	503606.0370	4038242.9530	318.0000	2
20	503669.3910	4038363.1050	316.0000	2
21	503775.0430	4038037.9060	318.0000	2
22	503795.2070	4037831.1270	319.0000	2
23	503829.8520	4037701.3260	320.0000	2
24	504239.3440	4037752.5990	317.0000	2
25	504083.1940	4037702.6120	320.0000	2
26	504050.7710	4037916.7650	316.0000	2
27	504140.0690	4038167.2670	316.0000	2
28	503888.4960	4038439.3330	317.0000	2
29	503962.7850	4038467.2630	315.0000	2
30	503993.1300	4038317.4600	317.0000	2
31	504226.7930	4038407.2940	314.0000	2
32	504464.6260	4038050.5620	317.0000	2
33	504453.1950	4038400.8030	312.6082	2
34	504321.9614	4038325.3614	313.2941	2
35	504383.5747	4038291.7099	282.8007	2
36	504296.8190	4038246.9363	313.7674	2
37	504524.0074	4038159.7274	315.2476	2

The total object points = 36

The residuals of image points

Point	Image	Vx	Vy
1	1	0.921	-2.447
1	2	2.078	-1.980

3	1	0.759	3.362
3	2	0.723	1.093

Point	Image	Vx	Vy
-------	-------	----	----

Point	Image	Vx	Vy
4	1	-2.241	-0.724

4	2	-0.189	0.469
Point	Image	Vx	Vy
5	1	-1.952	-0.254
5	2	-2.986	-3.135
Point	Image	Vx	Vy
6	1	0.939	-0.791
6	2	0.032	-0.803
Point	Image	Vx	Vy
7	1	-0.009	-0.123
7	2	-0.022	0.631
Point	Image	Vx	Vy
8	1	0.474	2.868
8	2	-0.203	1.715
Point	Image	Vx	Vy
9	1	0.049	-0.424
9	2	0.069	0.354
Point	Image	Vx	Vy
10	1	1.420	-1.736
10	2	0.907	-0.560
Point	Image	Vx	Vy
11	1	0.061	-1.986
11	2	0.708	-1.422
Point	Image	Vx	Vy
12	1	-0.793	-0.459
12	2	2.054	0.610
Point	Image	Vx	Vy
13	1	1.363	-0.646
13	2	2.620	1.695
Point	Image	Vx	Vy
14	1	-1.071	0.202
14	2	0.125	1.713
Point	Image	Vx	Vy
15	1	1.758	0.367
15	2	2.884	0.350
Point	Image	Vx	Vy
16	1	-0.970	-0.936
16	2	-0.860	0.219
Point	Image	Vx	Vy
17	1	-1.147	-1.339
17	2	-0.570	-1.889
Point	Image	Vx	Vy
18	1	1.291	0.271
18	2	1.859	-0.568
Point	Image	Vx	Vy
19	1	0.446	-0.450

19	2	0.218	0.635
Point	Image	Vx	Vy
20	1	1.396	-0.988
20	2	0.252	1.702
Point	Image	Vx	Vy
21	1	-2.236	-0.346
21	2	0.615	0.084
Point	Image	Vx	Vy
22	1	1.045	-1.042
22	2	1.748	0.410
Point	Image	Vx	Vy
23	1	1.089	-2.079
23	2	0.464	-1.944
Point	Image	Vx	Vy
24	1	0.943	1.857
24	2	-0.389	0.667
Point	Image	Vx	Vy
25	1	1.188	-0.879
25	2	-0.569	-1.036
Point	Image	Vx	Vy
26	1	-1.560	0.555
26	2	-2.147	1.569
Point	Image	Vx	Vy
27	1	-0.911	0.414
27	2	1.597	-2.258
Point	Image	Vx	Vy
28	1	0.462	1.027
28	2	0.321	1.902
Point	Image	Vx	Vy
29	1	-2.125	-0.319
29	2	-1.179	1.190
Point	Image	Vx	Vy
30	1	1.309	3.017
30	2	-1.170	-2.068
Point	Image	Vx	Vy
31	1	-2.673	1.612
31	2	1.092	-1.405
Point	Image	Vx	Vy
32	1	0.826	0.545
32	2	2.090	0.320
Point	Image	Vx	Vy
33	1	0.009	-0.332
33	2	0.667	0.040
Point	Image	Vx	Vy
34	1	0.007	-0.270

34	2	0.074	0.187	36	1	0.018	-0.670
				36	2	-0.081	0.639
Point	Image	Vx	Vy	Point	Image	Vx	Vy
35	1	-0.079	2.950	37	1	-0.005	0.195
35	2	-14.804	1.453	37	2	1.977	-0.580
Point	Image	Vx	Vy				
Total mean error of 72 image points: ax=0.000, ay=-0.000							
Total RMSE of 72 image points: mx=2.159, my=1.363							

The image residuals of the control points

The image ID = 1							
Point ID	Vx	Vy					
1	0.921	-2.447		20	1.396	-0.988	
3	0.759	3.362		21	-2.236	-0.346	
4	-2.241	-0.724		22	1.045	-1.042	
5	-1.952	-0.254		23	1.089	-2.079	
6	0.939	-0.791		24	0.943	1.857	
7	-0.009	-0.123		25	1.188	-0.879	
8	0.474	2.868		26	-1.560	0.555	
9	0.049	-0.424		27	-0.911	0.414	
10	1.420	-1.736		28	0.462	1.027	
11	0.061	-1.986		29	-2.125	-0.319	
12	-0.793	-0.459		30	1.309	3.017	
13	1.363	-0.646		31	-2.673	1.612	
14	-1.071	0.202		32	0.826	0.545	
15	1.758	0.367		33	0.009	-0.332	
16	-0.970	-0.936		34	0.007	-0.270	
17	-1.147	-1.339		35	-0.079	2.950	
18	1.291	0.271		36	0.018	-0.670	
19	0.446	-0.450		37	-0.005	0.195	
RMSE of 36 points: mx=1.217, my=1.408							

The image ID = 2							
Point ID	Vx	Vy					
1	2.078	-1.980		20	0.252	1.702	
3	0.723	1.093		21	0.615	0.084	
4	-0.189	0.469		22	1.748	0.410	
5	-2.986	-3.135		23	0.464	-1.944	
6	0.032	-0.803		24	-0.389	0.667	
7	-0.022	0.631		25	-0.569	-1.036	
8	-0.203	1.715		26	-2.147	1.569	
9	0.069	0.354		27	1.597	-2.258	
10	0.907	-0.560		28	0.321	1.902	
11	0.708	-1.422		29	-1.179	1.190	
12	2.054	0.610		30	-1.170	-2.068	
13	2.620	1.695		31	1.092	-1.405	
14	0.125	1.713		32	2.090	0.320	
15	2.884	0.350		33	0.667	0.040	
16	-0.860	0.219		34	0.074	0.187	
17	-0.570	-1.889		35	-14.804	1.453	
18	1.859	-0.568		36	-0.081	0.639	
19	0.218	0.635		37	1.977	-0.580	
RMSE of 36 points: mx=2.801, my=1.317							

Total number of all control image points = 72
Total rmsex = 2.159, rmsey = 1.363

Area around Hammam et Turkman

The Triangulation Report With LPS

The output image x, y units: pixels

The output angle unit: degrees

The output ground X, Y, Z units: meters

The Input Image Coordinates

image ID = 1

Point ID	x	y			
1	48.030	285.957	45	272.934	48.181
2	260.017	42.045	46	272.724	86.029
3	65.017	42.128	47	287.955	92.976
4	39.823	215.893	48	275.710	115.009
5	114.040	369.069	49	143.302	256.103
6	244.484	615.957	50	138.038	273.391
7	66.854	500.011	51	114.566	287.018
8	123.619	619.875	52	129.885	305.495
9	118.451	446.500	53	141.091	316.093
10	69.765	339.780	54	282.418	174.666
11	308.179	199.886	55	184.672	318.784
12	213.833	400.988	56	325.690	420.344
13	205.981	470.050	57	130.634	490.783
14	148.105	232.597	58	129.786	542.825
15	229.152	134.033	59	131.793	560.469
16	271.374	30.230	60	120.486	572.412
17	140.873	31.013	61	126.626	589.027
18	81.722	27.011	62	254.435	568.066
19	99.613	107.998	63	250.336	605.139
20	18.629	88.475	64	305.375	603.738
21	88.049	293.126	65	244.918	637.797
22	110.831	265.958	66	251.968	656.010
23	108.151	166.125	67	185.241	18.623
24	19.842	45.966	68	189.927	36.576
25	272.095	94.997	69	206.441	39.851
26	291.732	138.781	70	235.183	127.594
27	250.007	576.033	71	294.079	129.330
28	324.961	674.026	72	107.108	370.651
30	288.263	436.797	73	309.729	280.857
31	316.000	484.010	74	115.547	446.973
32	253.272	210.849	75	314.098	494.599
33	283.172	356.983	76	238.086	562.349
34	182.017	201.904	77	186.545	592.974
35	172.420	132.348	78	223.706	608.007
36	251.183	274.783	79	178.643	223.432
37	171.739	326.859	80	165.235	644.402
39	84.505	26.345	81	321.319	663.960
40	140.990	33.412	82	281.007	58.659
41	81.708	43.215	83	298.441	222.718
42	172.951	168.845	84	247.294	583.311
43	251.078	22.998	85	301.921	589.732
44	285.367	24.540	86	321.388	606.026

Affine coefficients from file (pixels) to film (millimeters)

A0	A1	A2	B0	B1	B2	
-2.3800	0.000000	0.007000	-1.2530	0.007000	0.000000	

image ID = 2					
Point ID	x	y			
1	25.873	329.915	45	289.504	60.157
2	277.104	56.025	46	284.251	96.939
3	72.826	89.055	47	299.714	101.184
4	24.529	261.669	48	283.833	124.799
5	82.000	397.866	49	128.334	283.169
6	188.946	615.733	50	121.067	301.017
7	19.765	533.967	51	94.517	318.308
8	62.798	639.294	52	108.354	333.627
9	78.208	474.505	53	118.501	341.949
10	41.407	379.468	54	283.248	181.362
11	307.008	200.867	55	163.654	337.192
12	182.909	419.908	56	297.586	411.762
13	166.080	482.941	57	86.611	512.960
14	134.426	260.157	58	80.761	569.213
15	234.202	150.952	59	79.252	580.617
16	290.137	43.010	60	66.292	593.925
17	153.741	64.896	61	70.177	609.065
18	92.817	70.730	62	205.744	567.060
19	102.343	146.927	63	196.658	603.934
20	16.307	142.719	64	254.138	592.931
21	66.711	329.934	65	187.091	636.153
22	92.075	295.983	66	192.202	652.785
23	101.027	203.518	67	201.510	45.087
24	25.821	101.922	68	204.370	61.787
25	283.196	105.980	69	221.105	62.190
26	297.041	144.963	70	240.243	143.086
27	197.889	576.020	71	301.127	135.501
28	265.753	658.547	72	76.345	401.161
30	256.749	437.091	73	298.534	279.159
31	279.845	475.047	74	75.489	474.553
32	251.034	222.811	75	277.248	486.489
33	261.448	356.520	76	189.763	563.986
34	174.727	225.113	77	131.877	602.472
35	174.040	161.694	78	168.398	611.395
36	241.002	283.703	79	169.270	245.247
37	148.503	346.910	80	103.217	656.262
39	95.711	69.605	81	263.011	649.057
40	153.797	66.727	82	296.504	69.094
41	90.823	86.835	83	294.171	224.318
42	170.512	193.459	84	196.147	582.788
43	269.591	39.034	85	252.347	579.766
44	305.270	34.815	86	270.560	592.240

Affine coefficients from file (pixels) to film (millimeters)

A0	A1	A2	B0	B1	B2
-2.4080	0.000000	0.007000	-1.2250	0.007000	0.000000

THE OUTPUT OF SELF-CALIBRATING BUNDLE BLOCK ADJUSTMENT

the no. of iteration =1 the standard error = 1.1530
the maximal correction of the object points = 0.00000

the no. of iteration =2 the standard error = 1.1530
the maximal correction of the object points = 0.00000

The exterior orientation parameters

image ID	Xs	Ys	Zs	OMEGA	PHI	KAPPA
1	408742.8180	3986422.9817	154316.5211	558.3953	-149.3423	467.4995
2	400367.1537	4072756.3707	154047.2375	-12.8510	-33.5628	-82.0861

The interior orientation parameters of photos

image ID	f(mm)	xo(mm)	yo(mm)
1	609.6020	0.0000	0.0000
2	609.6020	0.0000	0.0000

The residuals of the control points

Point ID	rX	rY	rZ
All residuals of fixed GCP are zero.			

The difference of intersected and measured control points

Point ID	rX	rY	rZ
----------	----	----	----

1	-1.1911	-0.1472	0.9960	45	-0.9925	0.3457	1.5532
2	2.2922	1.2160	-2.9622	46	-0.6616	0.2348	1.0585
3	-0.6217	-2.3927	-0.2114	47	-0.6672	0.2605	1.1745
4	1.9162	0.5260	-2.4775	48	-0.4381	0.1645	0.7436
5	-0.7428	-2.8913	0.7991	49	0.3532	-0.1480	-0.6690
6	-0.3669	5.0345	5.0917	50	0.3339	-0.1380	-0.6162
7	1.0755	0.0944	-0.5317	51	0.3227	-0.1139	-0.5052
8	4.8476	-2.1632	-0.9422	52	0.2687	-0.1061	-0.4734
9	-1.0322	-4.8172	8.2427	53	0.2520	-0.1058	-0.4784
10	-3.1943	-2.2674	3.0674	54	-0.0365	0.0372	0.1835
11	0.0544	-0.3683	-1.8784	55	0.3192	-0.1430	-0.6464
12	0.9797	5.5021	14.6123	56	1.2266	-0.3537	-1.4958
13	5.7990	1.2292	0.9915	57	-0.6200	0.2136	0.9319
14	-1.3482	5.6486	0.8672	58	-1.2416	0.4278	1.8894
15	-0.4469	-1.4183	2.4339	59	-1.1650	0.4054	1.7589
16	-1.7225	1.0940	7.1142	60	-1.3846	0.4930	2.1477
17	1.2705	-2.0146	-2.0506	61	-1.4759	0.5210	2.2560
18	0.8431	-1.6200	-1.6644	62	0.2700	-0.1193	-0.5318
19	3.4196	11.1686	-10.8796	63	0.0239	-0.0421	-0.1975
20	1.4120	-2.4580	0.6482	64	0.9077	-0.3039	-1.3062
21	-5.3473	-2.9701	-6.1039	65	-0.2259	0.0391	0.1491
22	1.0936	3.9081	-13.1910	66	-0.2317	0.0410	0.1563
23	8.0098	-4.8687	-11.2411	67	-0.5507	0.1224	0.5162
24	1.5290	1.7276	6.1236	68	-0.4788	0.1022	0.4288
25	-0.5446	-1.6586	-1.0070	69	-0.5989	0.1503	0.6480
26	4.3684	-8.5731	-1.0118	70	-0.2072	0.0457	0.1920
27	-5.2509	-0.6111	3.4986	71	-0.3864	0.1727	0.7941
28	-1.5303	-0.7535	1.2235	72	-0.0217	0.0225	0.1045
30	1.1938	2.5153	-10.0748	73	0.6125	-0.1486	-0.6168
31	1.2859	-3.9106	-13.7370	74	-0.4575	0.1730	0.7575
32	-3.4749	4.8576	12.4370	75	1.1789	-0.3617	-1.5730
33	6.5816	0.7969	-5.5177	76	0.0934	-0.0635	-0.2967
34	1.9156	0.0438	-0.7195	77	-0.7679	0.2320	0.9837
35	-9.1040	0.8567	11.2909	78	-0.3950	0.0954	0.3935
36	-4.4947	-1.8855	2.4307	79	0.2946	-0.1401	-0.6406
37	-2.8607	-0.3655	-4.1965	80	-1.5049	0.4984	2.1313
39	0.5618	-0.2199	-0.9912	81	0.9495	-0.3162	-1.3466
40	-0.0392	-0.0490	-0.2482	82	-0.9416	0.3403	1.5326
41	0.6369	-0.2390	-1.0649	83	0.2629	-0.0412	-0.1533
42	0.2098	-0.1169	-0.5388	84	0.1102	-0.0703	-0.3161
43	-1.0758	0.3442	1.5389	85	0.9027	-0.3023	-1.3022
44	-1.3175	0.4704	2.1269	86	1.1779	-0.3769	-1.6135

aX	aY	aZ
-0.0000	-0.0000	-0.0000
mX	mY	mZ
2.3103	2.3402	4.3616
CE90	LE90	
5.0199	7.2113	

The image residuals of intersected GCP

Point	Image	Vx	Vy
1	1	0.386	0.020
1	2	-0.381	-0.069
Point	Image	Vx	Vy
2	1	0.200	0.010
2	2	-0.198	-0.036
Point	Image	Vx	Vy
3	1	-0.115	-0.006
3	2	0.113	0.021
Point	Image	Vx	Vy
4	1	-0.450	-0.023
4	2	0.445	0.081
Point	Image	Vx	Vy
5	1	-0.954	-0.049
5	2	0.943	0.171
Point	Image	Vx	Vy
6	1	-0.127	-0.007
6	2	0.125	0.023
Point	Image	Vx	Vy
7	1	0.657	0.034
7	2	-0.649	-0.118
Point	Image	Vx	Vy
8	1	-0.096	-0.005
8	2	0.095	0.017
Point	Image	Vx	Vy
9	1	-0.177	-0.009
9	2	0.175	0.032
Point	Image	Vx	Vy
10	1	0.230	0.012
10	2	-0.227	-0.041
Point	Image	Vx	Vy
11	1	-0.197	-0.010
11	2	0.194	0.035
Point	Image	Vx	Vy
12	1	0.163	0.008
12	2	-0.161	-0.029
Point	Image	Vx	Vy
13	1	-0.350	-0.018

13	2	0.346	0.063
Point	Image	Vx	Vy
14	1	-0.887	-0.046
14	2	0.876	0.159
Point	Image	Vx	Vy
15	1	0.601	0.031
15	2	-0.593	-0.108
Point	Image	Vx	Vy
16	1	0.088	0.005
16	2	-0.087	-0.016
Point	Image	Vx	Vy
17	1	0.004	0.000
17	2	-0.004	-0.001
Point	Image	Vx	Vy
18	1	0.150	0.008
18	2	-0.148	-0.027
Point	Image	Vx	Vy
19	1	0.610	0.032
19	2	-0.602	-0.109
Point	Image	Vx	Vy
20	1	-1.219	-0.064
20	2	1.203	0.218
Point	Image	Vx	Vy
21	1	0.367	0.019
21	2	-0.362	-0.066
Point	Image	Vx	Vy
22	1	-0.823	-0.043
22	2	0.813	0.147
Point	Image	Vx	Vy
23	1	-0.749	-0.039
23	2	0.739	0.134
Point	Image	Vx	Vy
24	1	0.328	0.017
24	2	-0.324	-0.059
Point	Image	Vx	Vy
25	1	0.280	0.014
25	2	-0.276	-0.050

Point	Image	Vx	Vy
26	1	-0.336	-0.017
26	2	0.332	0.060

Point	Image	Vx	Vy
27	1	-1.000	-0.052
27	2	0.989	0.180

Point	Image	Vx	Vy
28	1	-0.004	-0.000
28	2	0.004	0.001

Point	Image	Vx	Vy
30	1	0.063	0.003
30	2	-0.062	-0.011

Point	Image	Vx	Vy
31	1	-0.189	-0.010
31	2	0.187	0.034

Point	Image	Vx	Vy
32	1	1.307	0.067
32	2	-1.290	-0.234

Point	Image	Vx	Vy
33	1	-0.253	-0.013
33	2	0.250	0.046

Point	Image	Vx	Vy
34	1	-0.292	-0.015
34	2	0.288	0.052

Point	Image	Vx	Vy
35	1	0.283	0.015
35	2	-0.279	-0.051

Point	Image	Vx	Vy
36	1	1.214	0.062
36	2	-1.199	-0.218

Point	Image	Vx	Vy
37	1	-0.420	-0.022
37	2	0.415	0.075

Point	Image	Vx	Vy
39	1	0.103	0.005
39	2	-0.102	-0.018

Point	Image	Vx	Vy
40	1	0.075	0.004
40	2	-0.074	-0.013

Point	Image	Vx	Vy
41	1	0.191	0.010
41	2	-0.189	-0.034

Point	Image	Vx	Vy
42	1	0.177	0.009
42	2	-0.175	-0.032

Point	Image	Vx	Vy
43	1	-0.066	-0.003
43	2	0.065	0.012

Point	Image	Vx	Vy
44	1	-0.033	-0.002
44	2	0.033	0.006

Point	Image	Vx	Vy
45	1	0.070	0.004
45	2	-0.070	-0.013

Point	Image	Vx	Vy
46	1	-0.092	-0.005
46	2	0.091	0.017

Point	Image	Vx	Vy
47	1	0.121	0.006
47	2	-0.120	-0.022

Point	Image	Vx	Vy
48	1	-0.040	-0.002
48	2	0.039	0.007

Point	Image	Vx	Vy
49	1	-0.046	-0.002
49	2	0.046	0.008

Point	Image	Vx	Vy
50	1	0.147	0.008
50	2	-0.145	-0.026

Point	Image	Vx	Vy
51	1	-0.036	-0.002
51	2	0.035	0.006

Point	Image	Vx	Vy
52	1	0.033	0.002
52	2	-0.032	-0.006

Point	Image	Vx	Vy
53	1	-0.085	-0.004
53	2	0.084	0.015

Point	Image	Vx	Vy
54	1	-0.145	-0.007
54	2	0.143	0.026

Point	Image	Vx	Vy
55	1	-0.066	-0.003
55	2	0.065	0.012

Point	Image	Vx	Vy
56	1	-0.321	-0.016
56	2	0.317	0.058

Point	Image	Vx	Vy
57	1	0.184	0.010
57	2	-0.182	-0.033

Point	Image	Vx	Vy
58	1	1.404	0.073
58	2	-1.389	-0.252
Point	Image	Vx	Vy
59	1	0.229	0.012
59	2	-0.226	-0.041
Point	Image	Vx	Vy
60	1	0.355	0.018
60	2	-0.351	-0.064
Point	Image	Vx	Vy
61	1	0.136	0.007
61	2	-0.135	-0.024
Point	Image	Vx	Vy
62	1	0.063	0.003
62	2	-0.063	-0.011
Point	Image	Vx	Vy
63	1	-0.020	-0.001
63	2	0.020	0.004
Point	Image	Vx	Vy
64	1	-0.059	-0.003
64	2	0.059	0.011
Point	Image	Vx	Vy
65	1	0.011	0.001
65	2	-0.011	-0.002
Point	Image	Vx	Vy
66	1	0.042	0.002
66	2	-0.041	-0.008
Point	Image	Vx	Vy
67	1	-0.069	-0.004
67	2	0.069	0.012
Point	Image	Vx	Vy
68	1	0.028	0.001
68	2	-0.028	-0.005
Point	Image	Vx	Vy
69	1	-0.022	-0.001
69	2	0.022	0.004
Point	Image	Vx	Vy
70	1	0.030	0.002
70	2	-0.029	-0.005
Point	Image	Vx	Vy
71	1	-0.100	-0.005
71	2	0.099	0.018
Point	Image	Vx	Vy
72	1	-0.034	-0.002

72	2	0.033	0.006
Point	Image	Vx	Vy
73	1	-0.206	-0.011
73	2	0.204	0.037
Point	Image	Vx	Vy
74	1	-0.079	-0.004
74	2	0.078	0.014
Point	Image	Vx	Vy
75	1	0.232	0.012
75	2	-0.230	-0.042
Point	Image	Vx	Vy
76	1	0.204	0.010
76	2	-0.202	-0.037
Point	Image	Vx	Vy
77	1	0.009	0.000
77	2	-0.009	-0.002
Point	Image	Vx	Vy
78	1	-0.089	-0.005
78	2	0.088	0.016
Point	Image	Vx	Vy
79	1	-0.054	-0.003
79	2	0.053	0.010
Point	Image	Vx	Vy
80	1	-0.014	-0.001
80	2	0.014	0.003
Point	Image	Vx	Vy
81	1	-0.135	-0.007
81	2	0.133	0.024
Point	Image	Vx	Vy
82	1	0.018	0.001
82	2	-0.018	-0.003
Point	Image	Vx	Vy
83	1	-0.146	-0.008
83	2	0.144	0.026
Point	Image	Vx	Vy
84	1	-0.091	-0.005
84	2	0.090	0.016
Point	Image	Vx	Vy
85	1	-0.043	-0.002
85	2	0.042	0.008
Point	Image	Vx	Vy
86	1	-0.064	-0.003
86	2	0.063	0.012

Mean error of 168 image points: ax=0.000, ay=-0.000

RMSE of 168 image points: $mx=0.407$, $my=0.054$

The coordinates of object points				
Point ID	X	Y	Z	Overlap
1	504601.3250	4037669.0860	306.0000	2
2	505052.5800	4038347.5600	303.0000	2
3	504560.1430	4038215.2890	302.0000	2
4	504554.8350	4037816.9070	303.0000	2
5	504797.2240	4037537.5470	300.0000	2
6	505213.9090	4037081.2640	298.0000	2
7	504722.5890	4037216.5340	307.0000	2
8	504905.0130	4036997.9320	303.0000	2
9	504831.8560	4037371.3390	302.0000	2
10	504674.1500	4037567.5760	308.0000	2
11	505232.3640	4038038.5190	300.0000	2
12	505042.7030	4037518.5000	317.0000	2
13	505053.7480	4037373.5860	310.0000	2
14	504835.6790	4037849.1950	301.0000	2
15	505009.4760	4038127.9510	299.0000	2
16	505080.0051	4038380.7582	294.4476	2
17	504748.2140	4038292.6020	301.0000	2
18	504598.4150	4038260.3100	300.0000	2
19	504669.5260	4038083.1060	311.0000	2
20	504451.9930	4038080.4800	305.0000	2
21	504709.7260	4037684.1300	312.0000	2
22	504757.7240	4037756.3810	304.0000	2
23	504699.2990	4037975.4160	318.0000	2
24	504442.4200	4038169.7400	302.0000	2
25	505103.5540	4038242.6550	303.0000	2
26	505162.8080	4038167.6160	302.0000	2
27	505216.9730	4037177.2680	299.0000	2
28	505439.4980	4037015.5730	302.0000	2
30	505256.2210	4037501.3480	321.0000	2
31	505350.2370	4037427.9810	312.0000	2
32	505099.1760	4037969.5730	294.0000	2
33	505219.5190	4037678.7680	300.0000	2
34	504908.1050	4037944.8880	304.0000	2
35	504865.6920	4038086.0060	302.0000	2
36	505120.7970	4037837.4620	298.0000	2
37	504933.0930	4037667.4600	303.0000	2
39	504605.4025	4038262.2718	299.2867	2
40	504752.0607	4038286.1871	297.2395	2
41	504603.5045	4038223.1687	300.7966	2
42	504879.2514	4038012.5907	299.3855	2
43	505025.7937	4038383.5631	298.7355	2
44	505113.5749	4038403.8646	298.1568	2
45	505089.5964	4038343.4715	299.8086	2
46	505101.6684	4038260.8131	300.1463	2
47	505143.2169	4038256.2719	300.1092	2
48	505118.8175	4038199.4984	301.2222	2
49	504833.8258	4037801.8444	299.9373	2
50	504826.5944	4037760.4199	300.6578	2
51	504771.1009	4037714.2482	301.2898	2
52	504816.6639	4037684.6455	301.0486	2
53	504848.6301	4037669.3086	300.7279	2
54	505156.7022	4038074.4295	300.7174	2
55	504960.1152	4037693.5902	300.4121	2
56	505352.3288	4037569.7610	299.6881	2
57	504884.7077	4037281.7180	299.6191	2
58	504890.1439	4037160.8493	321.6576	2

59	504911.5521	4037130.1840	300.5934	2
60	504887.9938	4037096.6496	299.7169	2
61	504908.5792	4037064.4077	300.0598	2
62	505224.0898	4037198.5350	300.6460	2
63	505225.7911	4037114.4425	301.7552	2
64	505365.0923	4037156.0039	300.7544	2
65	505224.4243	4037039.9356	300.4280	2
66	505248.2131	4037004.8579	301.2382	2
67	504858.6752	4038348.6288	297.0171	2
68	504876.9666	4038312.7757	297.1706	2
69	504919.9784	4038317.0213	296.8586	2
70	505022.2382	4038145.1364	298.9467	2
71	505170.5677	4038181.1192	300.5805	2
72	504780.4872	4037526.2284	302.9233	2
73	505264.1162	4037862.8067	298.6099	2
74	504826.6195	4037364.5908	305.8615	2
75	505348.1421	4037399.1621	303.2744	2
76	505181.8953	4037200.1896	299.3366	2
77	505061.6379	4037097.5084	299.4449	2
78	505158.9032	4037089.4838	302.2926	2
79	504912.6988	4037897.7812	298.5349	2
80	505024.9614	4036970.1090	300.5764	2
81	505424.8493	4037034.9706	303.1135	2
82	505113.2957	4038326.0415	300.2325	2
83	505216.4365	4037982.1552	296.9063	2
84	505211.5717	4037160.5858	299.6756	2
85	505351.9953	4037184.4129	299.9478	2
86	505406.8337	4037162.3599	300.0606	2

The total object points = 84

The residuals of image points

Point	Image	Vx	Vy
1	1	0.592	0.170
1	2	-0.141	-0.205
Point	Image	Vx	Vy
2	1	0.021	0.053
2	2	-0.524	0.771
Point	Image	Vx	Vy
3	1	0.321	-0.999
3	2	0.681	-0.965
Point	Image	Vx	Vy
4	1	-0.574	-0.201
4	2	0.226	0.544
Point	Image	Vx	Vy
5	1	-0.701	-1.177
5	2	1.381	-1.161
Point	Image	Vx	Vy
6	1	-1.603	2.614
6	2	-1.506	1.541
Point	Image	Vx	Vy
7	1	0.379	-0.090
7	2	-0.947	-0.060

Point	Image	Vx	Vy
8	1	-1.560	-1.601
8	2	-1.275	-1.049
Point	Image	Vx	Vy
9	1	-1.608	-1.420
9	2	-0.771	-3.139
Point	Image	Vx	Vy
10	1	0.793	-0.385
10	2	0.546	-1.280
Point	Image	Vx	Vy
11	1	0.288	-0.314
11	2	0.653	0.125
Point	Image	Vx	Vy
12	1	-4.297	3.358
12	2	-4.565	0.336
Point	Image	Vx	Vy
13	1	-2.876	-0.097
13	2	-2.229	0.161
Point	Image	Vx	Vy
14	1	-0.943	2.663

14	2	0.522	2.581
Point	Image	Vx	Vy
15	1	0.231	-0.362
15	2	-0.820	-1.031
Point	Image	Vx	Vy
16	1	-1.155	1.211
16	2	-1.214	-0.400
Point	Image	Vx	Vy
17	1	0.172	-1.188
17	2	0.226	-0.674
Point	Image	Vx	Vy
18	1	0.356	-0.927
18	2	0.108	-0.557
Point	Image	Vx	Vy
19	1	1.424	3.741
19	2	-0.701	6.060
Point	Image	Vx	Vy
20	1	-1.770	-1.268
20	2	0.805	-1.021
Point	Image	Vx	Vy
21	1	4.141	-1.089
21	2	3.434	-0.253
Point	Image	Vx	Vy
22	1	1.909	0.595
22	2	2.989	3.583
Point	Image	Vx	Vy
23	1	-0.603	-3.956
23	2	0.868	-0.903
Point	Image	Vx	Vy
24	1	-1.927	1.041
24	2	-2.527	-0.210
Point	Image	Vx	Vy
25	1	0.845	-0.722
25	2	0.360	-0.610
Point	Image	Vx	Vy
26	1	-1.207	-4.379
26	2	-0.080	-3.781
Point	Image	Vx	Vy
27	1	0.125	0.550
27	2	2.243	-0.290
Point	Image	Vx	Vy
28	1	0.305	-0.065
28	2	0.389	-0.415
Point	Image	Vx	Vy
30	1	2.050	0.249

30	2	1.523	2.391
Point	Image	Vx	Vy
31	1	3.095	-2.859
31	2	3.344	0.129
Point	Image	Vx	Vy
32	1	-0.869	3.516
32	2	-3.428	0.393
Point	Image	Vx	Vy
33	1	-1.372	-0.843
33	2	-1.061	0.794
Point	Image	Vx	Vy
34	1	-0.835	-0.277
34	2	-0.278	0.067
Point	Image	Vx	Vy
35	1	0.779	2.303
35	2	0.463	-0.713
Point	Image	Vx	Vy
36	1	2.404	-0.054
36	2	0.166	-1.131
Point	Image	Vx	Vy
37	1	1.763	-0.142
37	2	2.516	0.636
Point	Image	Vx	Vy
39	1	0.158	-0.231
39	2	-0.060	-0.011
Point	Image	Vx	Vy
40	1	0.156	-0.031
40	2	0.005	0.001
Point	Image	Vx	Vy
41	1	0.237	-0.249
41	2	-0.156	-0.030
Point	Image	Vx	Vy
42	1	0.243	-0.106
42	2	-0.116	-0.021
Point	Image	Vx	Vy
43	1	-0.075	0.389
43	2	0.075	0.013
Point	Image	Vx	Vy
44	1	-0.110	0.518
44	2	-0.017	-0.003
Point	Image	Vx	Vy
45	1	0.026	0.388
45	2	-0.094	-0.017
Point	Image	Vx	Vy
46	1	-0.129	0.255

46	2	0.069	0.012
Point	Image	Vx	Vy
47	1	0.056	0.286
47	2	-0.170	-0.030
Point	Image	Vx	Vy
48	1	-0.075	0.177
48	2	0.014	0.002
Point	Image	Vx	Vy
49	1	0.000	-0.158
49	2	0.084	0.015
Point	Image	Vx	Vy
50	1	0.187	-0.137
50	2	-0.113	-0.021
Point	Image	Vx	Vy
51	1	-0.021	-0.127
51	2	0.043	0.008
Point	Image	Vx	Vy
52	1	0.059	-0.111
52	2	-0.013	-0.002
Point	Image	Vx	Vy
53	1	-0.052	-0.115
53	2	0.112	0.021
Point	Image	Vx	Vy
54	1	-0.181	0.027
54	2	0.110	0.019
Point	Image	Vx	Vy
55	1	-0.012	-0.151
55	2	0.110	0.020
Point	Image	Vx	Vy
56	1	-0.379	-0.425
56	2	0.241	0.042
Point	Image	Vx	Vy
57	1	0.167	0.244
57	2	-0.187	-0.034
Point	Image	Vx	Vy
58	1	1.364	0.543
58	2	-1.405	-0.258
Point	Image	Vx	Vy
59	1	0.194	0.454
59	2	-0.238	-0.044
Point	Image	Vx	Vy
60	1	0.298	0.552
60	2	-0.379	-0.070
Point	Image	Vx	Vy
61	1	0.085	0.572

61	2	-0.157	-0.029
Point	Image	Vx	Vy
62	1	0.105	-0.119
62	2	-0.028	-0.005
Point	Image	Vx	Vy
63	1	0.024	-0.036
63	2	0.062	0.011
Point	Image	Vx	Vy
64	1	-0.048	-0.337
64	2	0.053	0.009
Point	Image	Vx	Vy
65	1	0.056	0.055
65	2	0.036	0.006
Point	Image	Vx	Vy
66	1	0.087	0.059
66	2	0.006	0.001
Point	Image	Vx	Vy
67	1	-0.001	0.154
67	2	0.144	0.026
Point	Image	Vx	Vy
68	1	0.093	0.135
68	2	0.043	0.008
Point	Image	Vx	Vy
69	1	0.029	0.184
69	2	0.082	0.015
Point	Image	Vx	Vy
70	1	0.056	0.060
70	2	-0.000	-0.000
Point	Image	Vx	Vy
71	1	-0.169	0.175
71	2	0.041	0.007
Point	Image	Vx	Vy
72	1	-0.053	0.018
72	2	0.015	0.003
Point	Image	Vx	Vy
73	1	-0.270	-0.193
73	2	0.132	0.023
Point	Image	Vx	Vy
74	1	-0.110	0.181
74	2	0.056	0.011
Point	Image	Vx	Vy
75	1	0.213	-0.399
75	2	-0.270	-0.047
Point	Image	Vx	Vy
76	1	0.249	-0.050

76	2	-0.161	-0.029
Point	Image	Vx	Vy
77	1	0.033	0.263
77	2	0.028	0.005
Point	Image	Vx	Vy
78	1	-0.046	0.112
78	2	0.136	0.024
Point	Image	Vx	Vy
79	1	0.008	-0.146
79	2	0.106	0.019
Point	Image	Vx	Vy
80	1	-0.022	0.548
80	2	0.034	0.006
Point	Image	Vx	Vy
81	1	-0.128	-0.353
81	2	0.123	0.021

Point	Image	Vx	Vy
82	1	-0.040	0.375
82	2	-0.056	-0.010
Point	Image	Vx	Vy
83	1	-0.204	-0.068
83	2	0.085	0.015
Point	Image	Vx	Vy
84	1	-0.047	-0.071
84	2	0.129	0.023
Point	Image	Vx	Vy
85	1	-0.031	-0.334
85	2	0.037	0.007
Point	Image	Vx	Vy
86	1	-0.071	-0.423
86	2	0.035	0.006

Total mean error of 168 image points: ax=0.000, ay=-0.000
 Total RMSE of 168 image points: mx=1.112, my=1.152

The image residuals of the control points

The image ID = 1			
Point ID	Vx	Vy	
1	0.592	0.170	
2	0.021	0.053	
3	0.321	-0.999	
4	-0.574	-0.201	
5	-0.701	-1.177	
6	-1.603	2.614	
7	0.379	-0.090	
8	-1.560	-1.601	
9	-1.608	-1.420	
10	0.793	-0.385	
11	0.288	-0.314	
12	-4.297	3.358	
13	-2.876	-0.097	
14	-0.943	2.663	
15	0.231	-0.362	
16	-1.155	1.211	
17	0.172	-1.188	
18	0.356	-0.927	
19	1.424	3.741	
20	-1.770	-1.268	
21	4.141	-1.089	
22	1.909	0.595	
23	-0.603	-3.956	
24	-1.927	1.041	
25	0.845	-0.722	
26	-1.207	-4.379	
27	0.125	0.550	
28	0.305	-0.065	
30	2.050	0.249	
31	3.095	-2.859	
32	-0.869	3.516	
33	-1.372	-0.843	
34	-0.835	-0.277	
35	0.779	2.303	
36	2.404	-0.054	
37	1.763	-0.142	
39	0.158	-0.231	
40	0.156	-0.031	
41	0.237	-0.249	
42	0.243	-0.106	
43	-0.075	0.389	
44	-0.110	0.518	
45	0.026	0.388	
46	-0.129	0.255	
47	0.056	0.286	
48	-0.075	0.177	
49	0.000	-0.158	
50	0.187	-0.137	
51	-0.021	-0.127	
52	0.059	-0.111	
53	-0.052	-0.115	
54	-0.181	0.027	
55	-0.012	-0.151	
56	-0.379	-0.425	
57	0.167	0.244	
58	1.364	0.543	
59	0.194	0.454	
60	0.298	0.552	

61	0.085	0.572
62	0.105	-0.119
63	0.024	-0.036
64	-0.048	-0.337
65	0.056	0.055
66	0.087	0.059
67	-0.001	0.154
68	0.093	0.135
69	0.029	0.184
70	0.056	0.060
71	-0.169	0.175
72	-0.053	0.018
73	-0.270	-0.193

74	-0.110	0.181
75	0.213	-0.399
76	0.249	-0.050
77	0.033	0.263
78	-0.046	0.112
79	0.008	-0.146
80	-0.022	0.548
81	-0.128	-0.353
82	-0.040	0.375
83	-0.204	-0.068
84	-0.047	-0.071
85	-0.031	-0.334
86	-0.071	-0.423

RMSE of 84 points: mx=1.094, my=1.199

The image ID = 2

Point ID	Vx	Vy
1	-0.141	-0.205
2	-0.524	0.771
3	0.681	-0.965
4	0.226	0.544
5	1.381	-1.161
6	-1.506	1.541
7	-0.947	-0.060
8	-1.275	-1.049
9	-0.771	-3.139
10	0.546	-1.280
11	0.653	0.125
12	-4.565	0.336
13	-2.229	0.161
14	0.522	2.581
15	-0.820	-1.031
16	-1.214	-0.400
17	0.226	-0.674
18	0.108	-0.557
19	-0.701	6.060
20	0.805	-1.021
21	3.434	-0.253
22	2.989	3.583
23	0.868	-0.903
24	-2.527	-0.210
25	0.360	-0.610
26	-0.080	-3.781
27	2.243	-0.290
28	0.389	-0.415
30	1.523	2.391
31	3.344	0.129
32	-3.428	0.393
33	-1.061	0.794
34	-0.278	0.067
35	0.463	-0.713
36	0.166	-1.131
37	2.516	0.636
39	-0.060	-0.011
40	0.005	0.001
41	-0.156	-0.030
42	-0.116	-0.021
43	0.075	0.013
44	-0.017	-0.003

45	-0.094	-0.017
46	0.069	0.012
47	-0.170	-0.030
48	0.014	0.002
49	0.084	0.015
50	-0.113	-0.021
51	0.043	0.008
52	-0.013	-0.002
53	0.112	0.021
54	0.110	0.019
55	0.110	0.020
56	0.241	0.042
57	-0.187	-0.034
58	-1.405	-0.258
59	-0.238	-0.044
60	-0.379	-0.070
61	-0.157	-0.029
62	-0.028	-0.005
63	0.062	0.011
64	0.053	0.009
65	0.036	0.006
66	0.006	0.001
67	0.144	0.026
68	0.043	0.008
69	0.082	0.015
70	-0.000	-0.000
71	0.041	0.007
72	0.015	0.003
73	0.132	0.023
74	0.056	0.011
75	-0.270	-0.047
76	-0.161	-0.029
77	0.028	0.005
78	0.136	0.024
79	0.106	0.019
80	0.034	0.006
81	0.123	0.021
82	-0.056	-0.010
83	0.085	0.015
84	0.129	0.023
85	0.037	0.007
86	0.035	0.006

RMSE of 84 points: mx=1.129, my=1.103

Total number of all control image points = 168
 Total rmsex = 1.112, rmsey = 1.152

Area of the Nahr al Abbara

The Triangulation Report With LPS

The output image x, y units: pixels
 The output angle unit: degrees
 The output ground X, Y, Z units: meters

The Input Image Coordinates image ID = 1

Point ID	x	y			
1	707.176	725.056	44	1110.061	891.057
2	727.881	728.089	45	1198.875	1101.337
3	665.938	803.136	46	756.255	1117.000
4	584.196	664.962	47	790.078	963.987
5	549.959	635.070	48	576.827	947.912
6	441.194	659.948	49	729.979	320.762
7	151.172	568.086	50	846.841	133.778
8	432.039	894.974	51	228.275	653.036
9	418.920	791.902	52	421.458	578.096
10	613.056	1036.847	53	1022.992	131.678
11	259.109	941.112	54	891.203	354.296
12	120.996	985.730	55	1709.913	696.754
13	163.179	798.921	56	1238.177	354.996
14	262.136	742.986	57	433.974	32.190
15	105.184	506.919	58	462.820	38.579
16	298.258	424.665	59	400.647	90.383
17	597.093	393.839	60	562.956	20.015
18	349.158	220.006	61	606.591	45.998
19	241.625	322.625	62	594.810	65.468
20	189.142	42.022	63	675.494	49.361
21	143.313	149.094	64	1373.655	52.525
22	425.035	72.937	65	1440.668	93.971
23	603.008	49.826	66	1429.183	105.064
24	492.289	153.998	67	1610.657	94.252
25	514.801	260.127	68	1566.474	114.181
26	499.002	364.007	69	479.364	160.325
27	646.066	511.094	70	583.593	141.475
28	830.974	505.126	71	616.663	194.594
29	801.024	360.853	72	713.733	130.973
30	1386.211	45.886	73	685.139	135.885
31	1455.894	1138.895	74	696.677	171.485
32	1402.230	768.073	75	661.154	215.165
33	1479.288	383.928	76	647.802	236.935
34	1792.127	420.903	77	714.421	236.120
35	1656.954	416.785	78	797.589	191.641
36	1592.853	305.927	79	1404.409	150.818
37	1610.064	125.070	80	1404.203	186.786
38	1648.720	983.954	81	1454.003	135.329
39	1143.189	30.874	82	1441.216	157.139
40	1171.983	205.950	83	1420.128	200.197
41	1078.262	387.245	84	1543.660	128.554
42	1056.296	614.075	85	1770.617	132.643
43	1095.759	730.018	86	1722.862	226.970

87	501.723	284.797	147	618.061	918.842
88	579.000	304.765	148	720.061	908.122
89	526.222	312.369	149	711.203	940.988
90	520.631	331.226	150	779.369	897.243
91	609.182	382.970	151	794.097	896.654
92	662.990	276.613	152	774.825	923.142
93	754.828	281.967	153	787.820	960.852
94	793.671	343.858	154	1377.210	968.007
95	813.215	365.226	155	1358.402	981.041
96	812.643	381.411	156	1368.729	983.078
97	1381.796	338.497	157	267.394	1025.878
98	1467.188	314.648	158	278.680	1147.042
99	1440.453	373.981	159	683.787	1056.213
100	494.028	391.669	160	770.820	1108.168
101	618.598	405.849	161	1358.041	1038.070
102	669.449	411.135	162	1403.288	1091.368
103	809.094	401.970	163	1423.666	1099.750
104	784.923	460.700	164	1455.299	1129.124
105	1402.431	404.908	165	540.670	42.168
106	1391.252	481.420	166	674.244	101.471
107	1420.343	423.161	167	1366.434	617.966
108	1631.722	490.627	168	1397.338	723.519
109	1664.463	430.398	169	513.847	55.946
110	533.904	636.329	170	648.552	114.186
111	631.627	637.707	171	1441.663	103.717
112	783.715	523.314	172	779.856	179.485
113	819.349	530.241	173	738.376	326.448
114	1379.205	521.484	174	710.838	377.354
115	1378.830	529.354	175	694.963	497.914
116	1390.735	534.408	176	807.926	486.960
117	1573.768	557.402	177	820.548	487.111
118	1588.747	563.350	178	1104.724	441.108
119	1569.587	590.972	179	1399.574	454.198
120	566.004	677.854	180	1438.970	419.453
121	600.626	706.254	181	1386.354	600.436
122	683.639	640.977	182	1603.936	582.142
123	822.298	716.467	183	1487.477	651.945
124	1369.943	667.647	184	671.737	802.389
125	1391.669	675.015	185	778.061	883.801
126	1365.132	690.455	186	1387.837	766.821
127	1377.844	693.007	187	1381.048	856.609
128	1477.268	729.148	188	1357.077	899.018
129	1466.274	756.947	189	1351.687	959.703
130	413.552	802.914	190	698.442	1055.882
131	615.518	773.092	191	731.866	1073.655
132	611.917	818.982	192	647.852	343.547
133	627.996	819.101	193	702.519	787.522
134	590.176	894.856	194	826.118	869.585
135	802.566	778.899	195	1378.269	489.666
136	800.407	792.373	196	630.117	839.487
137	787.629	819.315	197	1369.089	884.114
138	777.317	821.620	198	399.147	111.379
139	775.949	884.483	199	603.593	144.821
140	1386.210	780.472	200	657.083	108.332
141	1418.177	783.535	201	1433.960	175.151
142	1399.274	813.305	202	1418.396	182.068
143	1368.238	820.983	203	746.503	413.707
144	1409.252	783.848	204	763.701	448.364
145	218.639	972.940	205	755.211	456.765
146	428.472	912.366	206	622.986	752.703

207	672.565	641.715	240	1467.086	1152.426
208	772.021	697.697	241	640.538	425.386
209	754.481	718.625	242	1496.655	616.676
210	604.202	872.759	243	1452.002	735.486
211	720.529	885.216	244	267.264	1026.881
212	1117.073	871.653	245	1406.714	82.399
213	727.347	1113.165	246	795.848	182.806
214	1131.804	1130.615	247	1484.723	276.844
215	731.712	729.157	248	579.871	707.028
216	1401.856	776.081	249	1393.289	687.875
217	1458.864	745.882	250	629.623	1002.024
218	1446.297	119.921	251	787.352	954.291
219	745.603	1073.527	252	1364.634	928.359
220	1383.058	993.003	253	202.891	1071.604
221	1650.348	39.819	254	1447.136	1111.056
222	1398.199	203.339	255	1559.475	158.585
223	1460.446	313.476	256	1073.999	634.381
224	808.863	685.157	257	775.348	821.331
225	1391.234	718.337	258	212.581	1156.719
226	731.661	872.008	259	1364.396	584.473
227	1143.189	1115.917	260	827.364	763.990
228	819.073	1128.095	261	860.440	17.347
229	1173.361	216.400	262	1173.619	187.977
230	1604.199	310.285	263	1527.633	221.795
231	1605.387	119.786	264	802.363	270.918
232	550.260	182.648	265	226.437	1059.155
233	1413.653	418.757	266	725.963	364.302
234	727.901	633.569	267	1382.596	322.853
235	651.085	668.447	268	1069.567	617.426
236	770.097	717.963	269	714.286	869.566
237	1439.422	729.432	270	564.994	689.503
238	1379.205	746.737	271	750.607	1098.642
239	1439.094	737.836			

Affine coefficients from file (pixels) to film (millimeters)

A0	A1	A2	B0	B1	B2
-4.5045	0.000000	0.007000	-6.2825	0.007000	-0.000000

image ID = 2

Point ID	x	y			
1	907.037	788.952	21	172.185	211.919
2	929.085	790.959	22	428.024	136.010
3	891.242	873.969	23	597.167	113.959
4	767.913	735.901	24	520.064	219.083
5	723.028	703.990	25	574.963	326.001
6	624.054	729.326	26	591.050	429.979
7	306.043	635.035	27	781.107	579.145
8	686.103	967.996	28	964.932	574.037
9	642.588	863.237	29	889.841	427.056
10	909.342	1113.005	30	1370.899	110.835
11	525.854	1013.157	31	1781.314	1214.972
12	401.706	1059.117	32	1613.135	839.246
13	389.185	868.945	33	1572.795	457.100
14	471.205	811.997	34	1893.142	486.043
15	242.135	572.090	35	1757.262	485.818
16	400.013	475.162	36	1659.067	371.999
17	697.346	461.007	37	1620.910	191.930
18	397.033	284.824	38	1926.315	1058.353
19	322.458	394.808	39	1126.776	94.093
20	184.045	104.930	40	1211.138	270.963

41	1172.086	454.069	101	722.592	473.722
42	1221.046	683.823	102	774.812	478.888
43	1296.822	800.046	103	910.450	468.111
44	1362.062	966.208	104	904.909	528.404
45	1511.968	1177.565	105	1501.551	472.270
46	1077.729	1195.028	106	1514.169	549.679
47	1064.150	1038.844	107	1524.809	491.113
48	847.125	1022.794	108	1756.521	558.787
49	807.100	385.928	109	1770.497	497.720
50	865.997	200.053	110	708.957	706.026
51	408.953	722.107	111	806.646	708.357
52	579.024	646.910	112	921.675	592.006
53	1031.439	197.704	113	960.353	599.134
54	984.535	423.659	114	1514.338	590.414
55	1869.916	727.540	115	1516.568	598.117
56	1320.170	422.964	116	1529.932	603.460
57	424.803	95.907	117	1719.700	626.816
58	455.721	102.173	118	1736.531	632.723
59	409.457	154.231	119	1725.806	660.918
60	549.438	84.770	120	753.501	748.669
61	600.676	110.741	121	796.509	777.448
62	595.064	130.307	122	859.263	711.447
63	670.435	114.104	123	1020.586	787.697
64	1363.391	117.277	124	1550.878	738.434
65	1443.024	159.061	125	1574.708	745.020
66	1434.869	170.109	126	1553.453	762.206
67	1611.912	158.801	127	1566.518	763.922
68	1573.920	179.662	128	1676.490	800.644
69	509.188	225.161	129	1673.202	828.847
70	606.850	207.105	130	639.655	874.658
71	655.834	259.352	131	832.291	845.867
72	732.890	196.096	132	841.702	892.372
73	706.647	201.221	133	857.707	892.333
74	728.458	236.933	134	843.174	969.381
75	706.419	281.352	135	1020.138	850.392
76	700.368	303.409	136	1020.633	864.271
77	765.756	301.751	137	1016.958	891.427
78	834.516	255.501	138	1007.199	893.789
79	1424.295	216.343	139	1025.521	958.790
80	1435.177	252.560	140	1600.942	852.937
81	1468.992	200.643	141	1634.214	856.184
82	1462.926	222.551	142	1624.413	886.191
83	1455.426	265.901	143	1596.024	894.276
84	1556.034	193.417	144	1625.269	856.581
85	1782.700	197.371	145	496.091	1046.346
86	1764.506	292.520	146	686.872	987.114
87	569.275	351.164	147	878.638	993.310
88	652.527	371.557	148	977.158	982.691
89	602.370	378.996	149	978.379	1016.114
90	602.340	398.240	150	1032.913	971.635
91	706.212	450.349	151	1047.408	971.327
92	727.355	343.268	152	1036.177	997.872
93	819.358	347.817	153	1061.268	1036.112
94	877.708	409.739	154	1650.855	1043.714
95	903.365	430.957	155	1636.360	1057.067
96	907.582	447.235	156	1647.438	1059.224
97	1460.127	405.478	157	561.388	1100.460
98	1537.654	381.252	158	609.971	1223.846
99	1529.783	441.307	159	986.562	1133.577
100	593.980	457.642	160	1090.089	1186.586

161	1653.599	1115.247	217	1662.796	817.816
162	1715.485	1169.528	218	1456.495	185.068
163	1738.566	1177.852	219	1053.828	1151.279
164	1779.377	1207.706	220	1664.464	1069.271
165	534.006	106.872	221	1634.453	104.307
166	684.600	166.247	222	1434.350	269.902
167	1531.914	688.494	223	1530.524	380.342
168	1595.518	795.123	224	993.457	749.684
169	511.672	120.569	225	1587.818	790.103
170	663.393	179.489	226	976.993	945.794
171	1447.032	168.841	227	1462.798	1191.585
172	813.034	244.615	228	1143.554	1206.425
173	817.340	393.185	229	1214.321	279.632
174	805.167	444.338	230	1673.008	378.138
175	826.232	566.351	231	1614.591	184.862
176	935.541	554.192	232	586.358	248.180
177	948.236	554.161	233	1516.845	486.520
178	1215.777	508.075	234	900.998	703.695
179	1513.793	522.099	235	835.746	739.408
180	1541.553	487.238	236	968.083	782.102
181	1546.446	670.268	237	1639.170	801.395
182	1757.309	651.530	238	1583.900	819.086
183	1663.341	722.285	239	1640.918	809.943
184	896.077	873.654	240	1798.349	1231.266
185	1027.350	958.114	241	749.839	493.007
186	1598.420	839.126	242	1660.869	687.400
187	1619.967	930.423	243	1649.479	809.282
188	1609.315	973.435	244	561.580	1101.531
189	1622.923	1035.385	245	1405.815	147.682
190	1001.015	1133.035	246	830.028	246.551
191	1039.755	1151.268	247	1543.585	343.002
192	732.132	410.588	248	775.870	778.063
193	922.754	856.180	249	1574.068	762.791
194	1070.999	943.076	250	890.666	1070.243
195	1503.630	557.755	251	1058.569	1029.177
196	866.416	912.930	252	1625.875	1003.324
197	1616.417	958.303	253	510.223	1146.227
198	414.071	175.883	254	1765.760	1189.617
199	627.858	210.446	255	1580.628	223.618
200	670.470	173.718	256	1244.458	703.758
201	1461.404	240.608	257	1007.299	892.691
202	1448.042	247.755	258	546.113	1233.604
203	851.825	481.184	259	1519.130	653.927
204	879.678	515.845	260	1040.154	818.079
205	873.982	524.581	261	839.825	71.746
206	833.470	824.554	262	1208.173	260.986
207	848.295	712.533	263	1573.343	272.734
208	965.142	765.843	264	864.409	336.781
209	952.544	781.084	265	554.453	1141.120
210	850.475	946.576	266	816.795	431.386
211	970.664	959.562	267	1455.999	389.520
212	1360.512	944.304	268	1234.402	687.197
213	1047.777	1191.053	269	959.286	943.742
214	1455.989	1207.478	270	766.930	774.976
215	932.458	791.811	271	1066.405	1169.438
216	1615.556	848.674			

Affine coefficients from file (pixels) to film (millimeters)

A0	A1	A2	B0	B1	B2
-4.3715	0.000000	0.007000	-7.0525	0.007000	0.000000

THE OUTPUT OF SELF-CALIBRATING BUNDLE BLOCK ADJUSTMENT

the no. of iteration =1 the standard error = 2.6039
the maximal correction of the object points = 0.00000

the no. of iteration =2 the standard error = 2.6039
the maximal correction of the object points = 0.00000

The exterior orientation parameters

image ID	Xs	Ys	Zs	OMEGA	PHI	KAPPA
1	610890.8760	4002770.1317	153248.5928	12.8839	33.8929	-82.2626
2	408869.8469	3985914.9215	154321.9328	378.6637	-30.6871	277.5169

The interior orientation parameters of photos

image ID	f(mm)	xo(mm)	yo(mm)
1	609.6020	0.0000	0.0000
2	609.6020	0.0000	0.0000

The residuals of the control points

Point ID	rX	rY	rZ
----------	----	----	----

All residuals of fixed GCP are zero.

The difference of intersected and measured control points

Point ID	rX	rY	rZ
----------	----	----	----

1	22.5149	6.6374	-20.5718	33	10.2307	-1.9827	6.9246
2	26.2892	7.5607	-19.4998	34	-16.9006	0.7828	14.2445
3	9.1905	-2.0625	-7.1800	35	-22.5507	-2.7000	7.9457
4	1.4148	-5.2946	3.6203	36	-1.8180	7.2045	5.1552
5	2.5057	-1.6284	2.4747	37	-5.2284	-1.4087	2.2909
6	5.7139	-3.0673	4.7684	38	-16.8145	3.2596	21.0916
7	-2.9593	-2.7035	9.7339	39	4.4699	-1.5768	-7.3173
8	4.2497	-2.1002	0.8783	40	9.6151	-16.2112	-4.7127
9	3.7374	13.0874	5.9997	41	6.1459	1.3432	-6.0566
10	9.1323	-3.0738	-3.6078	42	-10.7442	-15.7645	-2.5328
11	6.0804	-4.2531	2.0669	43	-1.7274	-0.7936	-1.7367
12	2.8359	-7.8765	3.6183	44	-5.5540	1.2154	2.3519
13	3.5246	-3.7236	10.1006	45	-6.9747	1.8668	-0.6274
14	5.0043	-5.7020	9.4188	46	4.4795	17.9685	4.8129
15	-4.3186	-3.8829	13.6543	47	3.3700	-3.1015	1.5631
16	-1.6527	-9.5825	-5.7101	48	1.6473	-4.6656	4.2500
17	1.3935	-2.4625	3.0240	49	7.8558	2.1517	4.4303
18	6.2655	5.8017	4.9092	50	2.6368	-6.3406	-1.0516
19	0.3841	5.8049	9.5393	51	0.2622	-1.8631	9.0968
20	0.3663	5.7682	17.1765	52	3.1452	5.6152	3.0357
21	-21.6776	3.5304	19.3344	53	23.9634	0.8857	-22.2938
22	0.8448	8.7363	5.5600	54	-13.9490	-9.0609	11.5800
23	-21.7592	2.0951	7.0249	55	22.8921	9.1151	-28.3897
24	1.8724	1.2000	2.4009	56	-6.3976	-10.9834	-8.5935
25	3.8660	2.6967	4.2806	57	2.5572	-4.1417	2.2594
26	-1.4372	-2.2962	5.2940	58	1.8915	-3.6911	1.4118
27	19.2341	-13.9840	2.1363	59	3.3564	-4.3449	3.4470
28	2.4905	-5.3672	1.5390	60	-0.1659	-2.3315	-1.2886
29	6.0681	0.2033	-1.9138	61	-0.9159	-1.7101	-2.1969
30	19.8995	3.1890	-7.3397	62	-0.7019	-1.8251	-1.9000
31	-14.3761	9.1905	13.7724	63	-1.9646	-0.8683	-3.5000
32	-5.3051	1.4989	6.5648	64	-2.1000	4.2863	-1.5846

65	-0.9326	3.9570	0.1629	125	0.3025	-1.4093	-0.1113
66	-1.0665	3.8101	-0.1103	126	-0.0890	-1.3288	-0.6950
67	2.3289	4.0242	5.4833	127	0.1190	-1.4353	-0.4128
68	1.4779	3.7697	3.9782	128	2.0067	-2.5099	2.1841
69	1.5346	-2.9474	1.1832	129	1.8574	-2.6300	1.8931
70	-0.4657	-1.7840	-1.4962	130	2.1997	1.1732	3.9040
71	-0.9861	-1.3021	-2.0860	131	-1.1644	1.1706	-1.3574
72	-2.3705	-0.4214	-3.9327	132	-1.1727	1.4552	-1.2512
73	-2.0035	-0.7083	-3.4719	133	-1.3741	1.4476	-1.5752
74	-2.1203	-0.5620	-3.5880	134	-0.9998	1.9959	-0.7468
75	-1.6210	-0.8312	-2.9101	135	-2.8906	1.0431	-4.1702
76	-1.4213	-0.9107	-2.6257	136	-2.8819	1.0837	-4.1368
77	-2.2779	-0.3451	-3.7361	137	-2.8219	1.2074	-3.9916
78	-3.1572	0.3081	-4.8431	138	-2.7595	1.2398	-3.8781
79	-1.2473	3.2634	-0.6283	139	-2.7986	1.4889	-3.8097
80	-1.1023	2.8746	-0.5542	140	0.4489	-2.0742	-0.1429
81	-0.5303	3.4803	0.6184	141	1.0130	-2.3790	0.6413
82	-0.6467	3.2192	0.3245	142	0.7409	-2.3980	0.1948
83	-0.8017	2.7322	-0.1257	143	0.2318	-2.1572	-0.5191
84	1.0824	3.5780	3.2747	144	0.8539	-2.3006	0.4186
85	6.6066	3.1068	12.0768	145	6.4790	2.8523	11.2359
86	5.8025	1.7624	10.1910	146	1.6464	2.2594	3.5175
87	1.0524	-2.1088	0.7810	147	-1.3951	2.1196	-1.3251
88	-0.3515	-1.3109	-1.0960	148	-2.4211	1.7828	-3.0850
89	0.5747	-1.7447	0.1834	149	-2.3866	1.9892	-2.9377
90	0.6734	-1.7029	0.3541	150	-2.8294	1.5308	-3.8419
91	-0.8311	-0.7829	-1.6314	151	-2.9129	1.4725	-3.9935
92	-1.6116	-0.6960	-2.8324	152	-2.8244	1.6587	-3.7777
93	-2.6675	-0.0029	-4.2101	153	-2.9355	1.7719	-3.9019
94	-2.9511	0.2634	-4.5476	154	0.6248	-3.0326	-0.2156
95	-3.0778	0.3695	-4.7056	155	0.3240	-2.8767	-0.6280
96	-3.0597	0.3719	-4.6774	156	0.4996	-3.0056	-0.3961
97	-0.8603	1.3758	-0.7897	157	4.9797	3.6123	9.2344
98	0.4496	1.4420	1.3513	158	4.2521	5.2650	8.8139
99	0.2073	0.8982	0.7276	159	-2.3227	2.8149	-2.4523
100	1.1500	-1.6055	1.1513	160	-3.0356	2.6110	-3.6417
101	-0.9715	-0.6343	-1.7932	161	0.3857	-3.1220	-0.6023
102	-1.6562	-0.3093	-2.7400	162	1.2464	-3.9444	0.4725
103	-3.0174	0.3655	-4.6156	163	1.6454	-4.2649	0.9818
104	-2.8002	0.3270	-4.2947	164	2.3158	-4.8675	1.8317
105	-0.3135	0.7170	-0.1875	165	0.2680	-2.5813	-0.6959
106	-0.2426	0.0877	-0.3441	166	-1.8952	-0.8485	-3.3602
107	0.0393	0.4924	0.2823	167	-0.2449	-0.8435	-0.7448
108	4.6735	-1.3521	7.0111	168	0.5129	-1.7910	0.0763
109	5.2479	-0.8207	8.1790	169	0.8073	-2.9043	0.0215
110	0.2091	0.1466	0.3734	170	-1.5148	-1.1150	-2.8787
111	-1.2435	0.4383	-1.7885	171	-0.8738	3.8445	0.2109
112	-2.7659	0.4200	-4.2085	172	-3.0135	0.1780	-4.6941
113	-3.0008	0.5087	-4.5471	173	-2.4668	-0.0706	-3.9248
114	-0.3116	-0.1867	-0.5739	174	-2.1504	-0.1542	-3.4565
115	-0.2942	-0.2473	-0.5716	175	-1.9511	0.0739	-3.0537
116	-0.0920	-0.3444	-0.2875	176	-2.9514	0.4320	-4.4953
117	3.5465	-1.6916	5.0296	177	-3.0318	0.4664	-4.6095
118	3.9158	-1.8698	5.5540	178	-3.2916	0.9213	-4.8605
119	3.5683	-2.0144	4.9273	179	-0.1978	0.2887	-0.1849
120	-0.3538	0.5103	-0.3598	180	0.3386	0.4631	0.7535
121	-0.8887	0.7537	-1.1036	181	0.0238	-0.8334	-0.3091
122	-1.8621	0.5584	-2.7196	182	4.3444	-2.1969	6.1131
123	-2.9820	0.8412	-4.3914	183	1.9989	-1.9487	2.4084
124	-0.0671	-1.2090	-0.6154	184	-1.8502	1.3233	-2.4077

185	-2.8106	1.4776	-3.8335	229	-3.4820	2.2345	-4.5850
186	0.4473	-2.0024	-0.1144	230	3.2443	1.0653	5.7050
187	0.5110	-2.4835	-0.1994	231	2.3437	3.6669	5.3484
188	0.1859	-2.4705	-0.7101	232	0.1373	-2.0272	-0.6402
189	0.1862	-2.7056	-0.7848	233	-0.0869	0.5583	0.1073
190	-2.4483	2.7354	-2.6908	234	-2.3001	0.5951	-3.3996
191	-2.7356	2.6560	-3.1682	235	-1.5074	0.6270	-2.1269
192	-1.3867	-0.6410	-2.4513	236	-2.6557	0.9022	-3.9195
193	-2.1412	1.2296	-2.9423	237	1.2760	-2.1827	1.1478
194	-3.0463	1.2575	-4.3156	238	0.2599	-1.8032	-0.3291
195	-0.4209	0.0728	-0.6369	239	1.2894	-2.2433	1.1445
196	-1.4266	1.5737	-1.6057	240	2.5913	-5.1703	2.1646
197	0.3585	-2.5165	-0.4544	241	-1.2808	-0.4279	-2.1976
198	3.3890	-4.2442	3.5306	242	2.0757	-1.7050	2.6404
199	-0.7979	-1.5503	-1.9248	243	1.5164	-2.3483	1.4849
200	-1.6420	-1.0284	-3.0485	244	4.9794	3.6147	9.2492
201	-0.6881	3.0143	0.1735	245	-1.5025	4.0413	-0.7371
202	-0.9048	2.9334	-0.2125	246	-3.1523	0.3068	-4.8469
203	-2.4966	0.1004	-3.9039	247	0.6173	1.8265	1.7822
204	-2.6348	0.2308	-4.0708	248	-0.5944	0.7182	-0.6485
205	-2.5570	0.2114	-3.9562	249	0.3386	-1.5274	-0.0632
206	-1.2353	1.0513	-1.5273	250	-1.5515	2.5319	-1.5663
207	-1.7399	0.5403	-2.5309	251	-2.9286	1.7371	-3.9009
208	-2.6709	0.8321	-3.9241	252	0.3521	-2.6995	-0.5260
209	-2.5389	0.9168	-3.7457	253	6.5538	4.2489	11.9485
210	-1.1482	1.8195	-1.0626	254	2.1222	-4.6608	1.6067
211	-2.4002	1.6607	-3.1019	255	1.5461	3.1785	3.8543
212	-2.6312	-0.3077	-4.3462	256	-3.1144	0.3474	-4.8346
213	-2.7686	2.9312	-3.1001	257	-2.7506	1.2492	-3.8644
214	-2.4358	-0.6297	-4.0996	258	5.9372	5.5117	11.5582
215	-2.3569	0.9629	-3.4426	259	-0.0012	-0.0012	0.0009
216	0.7071	-2.1851	0.2316	260	0.0027	0.0067	-0.0081
217	1.6850	-2.4786	1.6820	261	-0.0044	-0.0030	0.0004
218	-0.7288	3.6619	0.3713	262	-0.0039	-0.0033	0.0012
219	-2.8305	2.5697	-3.3463	263	-0.0023	-0.0037	0.0025
220	0.7612	-3.2284	-0.0620	264	-0.0025	-0.0009	0.0002
221	2.9464	4.8390	6.8133	265	0.0049	0.0074	-0.0001
222	-1.1244	2.7046	-0.6740	266	-0.0017	0.0001	-0.0002
223	0.3240	1.4746	1.1579	267	-0.0023	-0.0032	0.0015
224	-2.9000	0.7801	-4.3409	268	0.0005	-0.0006	-0.0000
225	0.3978	-1.7096	-0.0714	269	0.0029	0.0021	-0.0014
226	-2.4750	1.5610	-3.2678	270	-0.0000	0.0000	0.0000
227	-2.3315	-0.7517	-4.0184	271	-0.0000	-0.0000	-0.0000
228	-3.2704	2.3474	-4.1238				

aX aY aZ
-0.0001 -0.0000 -0.0001
mX mY mZ
5.3141 3.5408 5.3759
CE90 LE90
9.5189 8.8516

The image residuals of intersected GCP

Point	Image	Vx	Vy
1	1	0.159	-3.893
1	2	-0.149	3.883
Point	Image	Vx	Vy
2	1	0.180	-4.408

2	2	-0.169	4.398
Point	Image	Vx	Vy
3	1	0.044	-1.069
3	2	-0.040	1.066

Point	Image	Vx	Vy
4	1	0.004	-0.103
4	2	-0.004	0.103

Point	Image	Vx	Vy
5	1	0.035	-0.865
5	2	-0.034	0.861

Point	Image	Vx	Vy
6	1	0.040	-0.985
6	2	-0.038	0.979

Point	Image	Vx	Vy
7	1	0.058	-1.463
7	2	-0.057	1.447

Point	Image	Vx	Vy
8	1	0.052	-1.228
8	2	-0.045	1.221

Point	Image	Vx	Vy
9	1	0.051	-1.229
9	2	-0.046	1.222

Point	Image	Vx	Vy
10	1	0.007	-0.156
10	2	-0.006	0.156

Point	Image	Vx	Vy
11	1	0.111	-2.605
11	2	-0.095	2.584

Point	Image	Vx	Vy
12	1	0.122	-2.846
12	2	-0.103	2.818

Point	Image	Vx	Vy
13	1	0.103	-2.474
13	2	-0.093	2.450

Point	Image	Vx	Vy
14	1	0.091	-2.214
14	2	-0.084	2.195

Point	Image	Vx	Vy
15	1	0.066	-1.663
15	2	-0.066	1.644

Point	Image	Vx	Vy
16	1	0.306	-7.914
16	2	-0.318	7.843

Point	Image	Vx	Vy
17	1	-0.011	0.285
17	2	0.012	-0.284

Point	Image	Vx	Vy
18	1	-0.045	1.207
18	2	0.050	-1.196

Point	Image	Vx	Vy
19	1	-0.149	3.894
19	2	0.159	-3.854

Point	Image	Vx	Vy
20	1	-0.100	2.769
20	2	0.119	-2.736

Point	Image	Vx	Vy
21	1	-0.055	1.486
21	2	0.063	-1.468

Point	Image	Vx	Vy
22	1	-0.063	1.726
22	2	0.074	-1.712

Point	Image	Vx	Vy
23	1	-0.069	1.917
23	2	0.083	-1.906

Point	Image	Vx	Vy
24	1	-0.062	1.679
24	2	0.071	-1.667

Point	Image	Vx	Vy
25	1	-0.037	0.973
25	2	0.040	-0.967

Point	Image	Vx	Vy
26	1	-0.002	0.052
26	2	0.002	-0.052

Point	Image	Vx	Vy
27	1	0.010	-0.262
27	2	-0.010	0.261

Point	Image	Vx	Vy
28	1	-0.005	0.137
28	2	0.005	-0.137

Point	Image	Vx	Vy
29	1	0.006	-0.160
29	2	-0.007	0.160

Point	Image	Vx	Vy
30	1	0.016	-0.436
30	2	-0.019	0.439

Point	Image	Vx	Vy
31	1	-0.113	2.576
31	2	0.093	-2.602

Point	Image	Vx	Vy
32	1	-0.018	0.435
32	2	0.017	-0.439

Point	Image	Vx	Vy
33	1	-0.085	2.219
33	2	0.092	-2.236

Point	Image	Vx	Vy
34	1	0.086	-2.253
34	2	-0.094	2.282

Point	Image	Vx	Vy
35	1	0.004	-0.114
35	2	-0.005	0.115

Point	Image	Vx	Vy
36	1	0.049	-1.314
36	2	-0.055	1.326

Point	Image	Vx	Vy
37	1	0.022	-0.615
37	2	-0.027	0.620

Point	Image	Vx	Vy
38	1	-0.100	2.348
38	2	0.088	-2.378

Point	Image	Vx	Vy
39	1	0.012	-0.332
39	2	-0.015	0.332

Point	Image	Vx	Vy
40	1	0.019	-0.523
40	2	-0.022	0.525

Point	Image	Vx	Vy
41	1	0.013	-0.342
41	2	-0.014	0.342

Point	Image	Vx	Vy
42	1	0.001	-0.033
42	2	-0.001	0.033

Point	Image	Vx	Vy
43	1	0.016	-0.399
43	2	-0.015	0.401

Point	Image	Vx	Vy
44	1	-0.064	1.528
44	2	0.057	-1.535

Point	Image	Vx	Vy
45	1	-0.077	1.761
45	2	0.064	-1.772

Point	Image	Vx	Vy
46	1	-0.036	0.822
46	2	0.029	-0.822

Point	Image	Vx	Vy
47	1	-0.010	0.223
47	2	0.008	-0.223

Point	Image	Vx	Vy
48	1	0.013	-0.310
48	2	-0.011	0.309

Point	Image	Vx	Vy
49	1	0.010	-0.275
49	2	-0.011	0.274

Point	Image	Vx	Vy
50	1	-0.054	1.468
50	2	0.063	-1.464

Point	Image	Vx	Vy
51	1	0.052	-1.280
51	2	-0.049	1.268

Point	Image	Vx	Vy
52	1	0.021	-0.518
52	2	-0.020	0.515

Point	Image	Vx	Vy
53	1	-0.037	1.020
53	2	0.044	-1.020

Point	Image	Vx	Vy
54	1	-0.046	1.196
54	2	0.049	-1.195

Point	Image	Vx	Vy
55	1	0.754	-18.851
55	2	-0.740	19.075

Point	Image	Vx	Vy
56	1	-0.007	0.174
56	2	0.007	-0.175

Point	Image	Vx	Vy
57	1	-0.088	2.453
57	2	0.106	-2.432

Point	Image	Vx	Vy
58	1	-0.080	2.216
58	2	0.096	-2.198

Point	Image	Vx	Vy
59	1	-0.073	1.992
59	2	0.085	-1.975

Point	Image	Vx	Vy
60	1	-0.095	2.635
60	2	0.114	-2.618

Point	Image	Vx	Vy
61	1	-0.080	2.222
61	2	0.096	-2.209

Point	Image	Vx	Vy
62	1	-0.077	2.120
62	2	0.091	-2.108

Point	Image	Vx	Vy
63	1	-0.070	1.946
63	2	0.084	-1.937

Point	Image	Vx	Vy
64	1	0.021	-0.578
64	2	-0.025	0.581

Point	Image	Vx	Vy
65	1	0.030	-0.819
65	2	-0.036	0.824

Point	Image	Vx	Vy
66	1	0.030	-0.837
66	2	-0.036	0.842

Point	Image	Vx	Vy
67	1	0.061	-1.699
67	2	-0.074	1.714

Point	Image	Vx	Vy
68	1	0.041	-1.120
68	2	-0.049	1.129

Point	Image	Vx	Vy
69	1	-0.056	1.523
69	2	0.064	-1.512

Point	Image	Vx	Vy
70	1	-0.067	1.830
70	2	0.078	-1.819

Point	Image	Vx	Vy
71	1	-0.030	0.819
71	2	0.035	-0.815

Point	Image	Vx	Vy
72	1	-0.048	1.305
72	2	0.056	-1.299

Point	Image	Vx	Vy
73	1	-0.053	1.437
73	2	0.061	-1.430

Point	Image	Vx	Vy
74	1	-0.043	1.164
74	2	0.049	-1.160

Point	Image	Vx	Vy
75	1	-0.046	1.244
75	2	0.052	-1.238

Point	Image	Vx	Vy
76	1	-0.046	1.215
76	2	0.051	-1.210

Point	Image	Vx	Vy
77	1	-0.025	0.671
77	2	0.028	-0.669

Point	Image	Vx	Vy
78	1	0.002	-0.043
78	2	-0.002	0.043

Point	Image	Vx	Vy
79	1	0.025	-0.678
79	2	-0.029	0.682

Point	Image	Vx	Vy
80	1	0.025	-0.681
80	2	-0.029	0.685

Point	Image	Vx	Vy
81	1	0.033	-0.892
81	2	-0.039	0.898

Point	Image	Vx	Vy
82	1	0.032	-0.873
82	2	-0.038	0.879

Point	Image	Vx	Vy
83	1	0.030	-0.813
83	2	-0.035	0.818

Point	Image	Vx	Vy
84	1	0.051	-1.395
84	2	-0.061	1.406

Point	Image	Vx	Vy
85	1	0.081	-2.241
85	2	-0.098	2.266

Point	Image	Vx	Vy
86	1	0.066	-1.788
86	2	-0.077	1.807

Point	Image	Vx	Vy
87	1	-0.038	1.009
87	2	0.042	-1.002

Point	Image	Vx	Vy
88	1	-0.034	0.901
88	2	0.037	-0.897

Point	Image	Vx	Vy
89	1	-0.032	0.831
89	2	0.034	-0.825

Point	Image	Vx	Vy
90	1	-0.033	0.859
90	2	0.035	-0.854

Point	Image	Vx	Vy
91	1	-0.018	0.469
91	2	0.019	-0.467

Point	Image	Vx	Vy
92	1	-0.035	0.938
92	2	0.039	-0.934

Point	Image	Vx	Vy
93	1	-0.013	0.343
93	2	0.014	-0.342

Point	Image	Vx	Vy
94	1	0.007	-0.194
94	2	-0.008	0.193

Point	Image	Vx	Vy
95	1	0.017	-0.444
95	2	-0.018	0.444

Point	Image	Vx	Vy
96	1	0.020	-0.510
96	2	-0.021	0.509

Point	Image	Vx	Vy
97	1	0.021	-0.546
97	2	-0.023	0.550

Point	Image	Vx	Vy
98	1	0.031	-0.825
98	2	-0.035	0.832

Point	Image	Vx	Vy
99	1	0.022	-0.586
99	2	-0.024	0.590

Point	Image	Vx	Vy
100	1	0.007	-0.191
100	2	-0.008	0.190

Point	Image	Vx	Vy
101	1	-0.020	0.510
101	2	0.021	-0.508

Point	Image	Vx	Vy
102	1	-0.014	0.361
102	2	0.015	-0.360

Point	Image	Vx	Vy
103	1	0.019	-0.497
103	2	-0.020	0.496

Point	Image	Vx	Vy
104	1	0.005	-0.127
104	2	-0.005	0.127

Point	Image	Vx	Vy
105	1	0.023	-0.601
105	2	-0.025	0.605

Point	Image	Vx	Vy
106	1	0.014	-0.361
106	2	-0.015	0.364

Point	Image	Vx	Vy
107	1	0.015	-0.377
107	2	-0.016	0.380

Point	Image	Vx	Vy
108	1	0.025	-0.630
108	2	-0.026	0.637

Point	Image	Vx	Vy
109	1	0.039	-1.023
109	2	-0.042	1.034

Point	Image	Vx	Vy
110	1	0.021	-0.530
110	2	-0.021	0.527

Point	Image	Vx	Vy
111	1	-0.000	0.012
111	2	0.000	-0.012

Point	Image	Vx	Vy
112	1	0.002	-0.051
112	2	-0.002	0.050

Point	Image	Vx	Vy
113	1	0.001	-0.024
113	2	-0.001	0.024

Point	Image	Vx	Vy
114	1	0.005	-0.125
114	2	-0.005	0.126

Point	Image	Vx	Vy
115	1	0.009	-0.233
115	2	-0.009	0.235

Point	Image	Vx	Vy
116	1	0.004	-0.107
116	2	-0.004	0.107

Point	Image	Vx	Vy
117	1	0.002	-0.051
117	2	-0.002	0.051

Point	Image	Vx	Vy
118	1	0.003	-0.085
118	2	-0.003	0.086

Point	Image	Vx	Vy
119	1	-0.007	0.176
119	2	0.007	-0.178

Point	Image	Vx	Vy
120	1	0.011	-0.283
120	2	-0.011	0.282

Point	Image	Vx	Vy
121	1	0.011	-0.275
121	2	-0.011	0.274

Point	Image	Vx	Vy
122	1	0.002	-0.060
122	2	-0.002	0.060

Point	Image	Vx	Vy
123	1	0.002	-0.057
123	2	-0.002	0.057

Point	Image	Vx	Vy
124	1	-0.017	0.412
124	2	0.016	-0.415

Point	Image	Vx	Vy
125	1	-0.001	0.019
125	2	0.001	-0.019

Point	Image	Vx	Vy
126	1	-0.034	0.830
126	2	0.033	-0.836

Point	Image	Vx	Vy
127	1	-0.017	0.423
127	2	0.017	-0.426

Point	Image	Vx	Vy
128	1	-0.030	0.730
128	2	0.029	-0.737

Point	Image	Vx	Vy
129	1	-0.037	0.897
129	2	0.035	-0.906

Point	Image	Vx	Vy
130	1	0.046	-1.116
130	2	-0.042	1.109

Point	Image	Vx	Vy
131	1	-0.001	0.017
131	2	0.001	-0.017

Point	Image	Vx	Vy
132	1	0.000	-0.004
132	2	-0.000	0.004

Point	Image	Vx	Vy
133	1	0.002	-0.049
133	2	-0.002	0.049

Point	Image	Vx	Vy
134	1	0.002	-0.045
134	2	-0.002	0.044

Point	Image	Vx	Vy
135	1	0.014	-0.339
135	2	-0.013	0.338

Point	Image	Vx	Vy
136	1	0.008	-0.194
136	2	-0.007	0.194

Point	Image	Vx	Vy
137	1	0.012	-0.291
137	2	-0.011	0.291

Point	Image	Vx	Vy
138	1	0.012	-0.293
138	2	-0.011	0.293

Point	Image	Vx	Vy
139	1	-0.016	0.380
139	2	0.014	-0.379

Point	Image	Vx	Vy
140	1	-0.043	1.037
140	2	0.040	-1.045

Point	Image	Vx	Vy
141	1	-0.048	1.156
141	2	0.045	-1.166

Point	Image	Vx	Vy
142	1	-0.050	1.198
142	2	0.046	-1.208

Point	Image	Vx	Vy
143	1	-0.055	1.334
143	2	0.051	-1.344

Point	Image	Vx	Vy
144	1	-0.049	1.189
144	2	0.046	-1.199

Point	Image	Vx	Vy
145	1	0.102	-2.383
145	2	-0.086	2.363

Point	Image	Vx	Vy
146	1	0.021	-0.505
146	2	-0.019	0.503

Point	Image	Vx	Vy
147	1	0.007	-0.176
147	2	-0.007	0.176

Point	Image	Vx	Vy
148	1	-0.009	0.220
148	2	0.008	-0.220

Point	Image	Vx	Vy
149	1	-0.011	0.266
149	2	0.010	-0.265

Point	Image	Vx	Vy
150	1	-0.015	0.352
150	2	0.013	-0.352

Point	Image	Vx	Vy
151	1	-0.023	0.533
151	2	0.020	-0.533

Point	Image	Vx	Vy
152	1	-0.015	0.358
152	2	0.013	-0.358

Point	Image	Vx	Vy
153	1	-0.018	0.429
153	2	0.016	-0.429

Point	Image	Vx	Vy
154	1	-0.098	2.291
154	2	0.085	-2.311

Point	Image	Vx	Vy
155	1	-0.101	2.375
155	2	0.088	-2.395

Point	Image	Vx	Vy
156	1	-0.105	2.458
156	2	0.091	-2.479

Point	Image	Vx	Vy
157	1	0.092	-2.134
157	2	-0.077	2.118

Point	Image	Vx	Vy
158	1	0.092	-2.083
158	2	-0.073	2.068

Point	Image	Vx	Vy
159	1	-0.025	0.567
159	2	0.020	-0.566

Point	Image	Vx	Vy
160	1	-0.049	1.114
160	2	0.040	-1.114

Point	Image	Vx	Vy
161	1	-0.123	2.862
161	2	0.105	-2.886

Point	Image	Vx	Vy
162	1	-0.149	3.433
162	2	0.125	-3.465

Point	Image	Vx	Vy
163	1	-0.151	3.466
163	2	0.126	-3.499

Point	Image	Vx	Vy
164	1	-0.166	3.799
164	2	0.138	-3.837

Point	Image	Vx	Vy
165	1	-0.089	2.468
165	2	0.107	-2.451

Point	Image	Vx	Vy
166	1	-0.055	1.509
166	2	0.065	-1.502

Point	Image	Vx	Vy
167	1	-0.016	0.408
167	2	0.016	-0.411

Point	Image	Vx	Vy
168	1	-0.029	0.714
168	2	0.028	-0.720

Point	Image	Vx	Vy
169	1	-0.086	2.377
169	2	0.102	-2.360

Point	Image	Vx	Vy
170	1	-0.063	1.726
170	2	0.074	-1.718

Point	Image	Vx	Vy
171	1	0.030	-0.840
171	2	-0.037	0.845

Point	Image	Vx	Vy
172	1	-0.027	0.734
172	2	0.031	-0.732

Point	Image	Vx	Vy
173	1	-0.017	0.449
173	2	0.019	-0.448

Point	Image	Vx	Vy
174	1	-0.008	0.216
174	2	0.009	-0.215

Point	Image	Vx	Vy
175	1	-0.001	0.014
175	2	0.001	-0.014

Point	Image	Vx	Vy
176	1	0.022	-0.552
176	2	-0.022	0.552

Point	Image	Vx	Vy
177	1	0.025	-0.651
177	2	-0.026	0.650

Point	Image	Vx	Vy
178	1	0.023	-0.590
178	2	-0.024	0.592

Point	Image	Vx	Vy
179	1	0.018	-0.467
179	2	-0.019	0.470

Point	Image	Vx	Vy
180	1	0.018	-0.460
180	2	-0.019	0.464

Point	Image	Vx	Vy
181	1	-0.004	0.105
181	2	0.004	-0.105

Point	Image	Vx	Vy
182	1	0.004	-0.098
182	2	-0.004	0.099

Point	Image	Vx	Vy
183	1	-0.011	0.268
183	2	0.011	-0.271

Point	Image	Vx	Vy
184	1	0.034	-0.824
184	2	-0.031	0.822

Point	Image	Vx	Vy
185	1	-0.017	0.392
185	2	0.015	-0.392

Point	Image	Vx	Vy
186	1	-0.040	0.985
186	2	0.038	-0.992

Point	Image	Vx	Vy
187	1	-0.065	1.546
187	2	0.059	-1.558

Point	Image	Vx	Vy
188	1	-0.072	1.718
188	2	0.065	-1.731

Point	Image	Vx	Vy
189	1	-0.095	2.224
189	2	0.083	-2.242

Point	Image	Vx	Vy
190	1	-0.023	0.519
190	2	0.019	-0.518

Point	Image	Vx	Vy
191	1	-0.033	0.769
191	2	0.028	-0.769

Point	Image	Vx	Vy
192	1	-0.023	0.600
192	2	0.025	-0.598

Point	Image	Vx	Vy
193	1	0.082	-1.976
193	2	-0.075	1.972

Point	Image	Vx	Vy
194	1	-0.007	0.177
194	2	0.007	-0.177

Point	Image	Vx	Vy
195	1	0.018	-0.456
195	2	-0.019	0.459

Point	Image	Vx	Vy
196	1	0.004	-0.094
196	2	-0.004	0.093

Point	Image	Vx	Vy
197	1	-0.070	1.662
197	2	0.063	-1.675

Point	Image	Vx	Vy
198	1	-0.077	2.101
198	2	0.089	-2.083

Point	Image	Vx	Vy
199	1	-0.064	1.739
199	2	0.074	-1.729

Point	Image	Vx	Vy
200	1	-0.065	1.787
200	2	0.077	-1.778

Point	Image	Vx	Vy
201	1	0.033	-0.892
201	2	-0.038	0.897

Point	Image	Vx	Vy
202	1	0.028	-0.753
202	2	-0.032	0.758

Point	Image	Vx	Vy
203	1	-0.006	0.143
203	2	0.006	-0.143

Point	Image	Vx	Vy
204	1	0.005	-0.128
204	2	-0.005	0.128

Point	Image	Vx	Vy
205	1	0.001	-0.022
205	2	-0.001	0.022

Point	Image	Vx	Vy
206	1	0.011	-0.279
206	2	-0.011	0.278

Point	Image	Vx	Vy
207	1	-0.004	0.103
207	2	0.004	-0.103

Point	Image	Vx	Vy
208	1	0.063	-1.542
208	2	-0.060	1.540

Point	Image	Vx	Vy
209	1	0.184	-4.511
209	2	-0.174	4.504

Point	Image	Vx	Vy
210	1	0.009	-0.202
210	2	-0.008	0.202

Point	Image	Vx	Vy
211	1	-0.011	0.255
211	2	0.010	-0.255

Point	Image	Vx	Vy
212	1	-0.017	0.414
212	2	0.016	-0.416

Point	Image	Vx	Vy
213	1	-0.029	0.653
213	2	0.023	-0.653

Point	Image	Vx	Vy
214	1	-0.075	1.710
214	2	0.061	-1.719

Point	Image	Vx	Vy
215	1	0.184	-4.502
215	2	-0.173	4.494

Point	Image	Vx	Vy
216	1	-0.046	1.122
216	2	0.043	-1.131

Point	Image	Vx	Vy
217	1	-0.037	0.916
217	2	0.036	-0.924

Point	Image	Vx	Vy
218	1	0.033	-0.896
218	2	-0.039	0.902

Point	Image	Vx	Vy
219	1	-0.038	0.885
219	2	0.032	-0.884

Point	Image	Vx	Vy
220	1	-0.109	2.550
220	2	0.095	-2.572

Point	Image	Vx	Vy
221	1	0.063	-1.759
221	2	-0.078	1.775

Point	Image	Vx	Vy
222	1	0.012	-0.329
222	2	-0.014	0.331

Point	Image	Vx	Vy
223	1	0.026	-0.676
223	2	-0.028	0.681

Point	Image	Vx	Vy
224	1	0.127	-3.142
224	2	-0.122	3.139

Point	Image	Vx	Vy
225	1	-0.033	0.800
225	2	0.031	-0.806

Point	Image	Vx	Vy
226	1	-0.004	0.101
226	2	0.004	-0.100

Point	Image	Vx	Vy
227	1	-0.052	1.199
227	2	0.043	-1.206

Point	Image	Vx	Vy
228	1	-0.052	1.178
228	2	0.042	-1.179

Point	Image	Vx	Vy
229	1	0.053	-1.439
229	2	-0.061	1.444

Point	Image	Vx	Vy
230	1	0.018	-0.484
230	2	-0.020	0.488

Point	Image	Vx	Vy
231	1	0.054	-1.476
231	2	-0.064	1.489

Point	Image	Vx	Vy
232	1	-0.055	1.474
232	2	0.062	-1.465

Point	Image	Vx	Vy
233	1	0.017	-0.452
233	2	-0.019	0.455

Point	Image	Vx	Vy
234	1	0.006	-0.145
234	2	-0.006	0.145

Point	Image	Vx	Vy
235	1	0.002	-0.057
235	2	-0.002	0.057

Point	Image	Vx	Vy
236	1	0.149	-3.652
236	2	-0.141	3.647

Point	Image	Vx	Vy
237	1	-0.038	0.922
237	2	0.036	-0.930

Point	Image	Vx	Vy
238	1	-0.042	1.032
238	2	0.040	-1.040

Point	Image	Vx	Vy
239	1	-0.040	0.990
239	2	0.039	-0.998

Point	Image	Vx	Vy
240	1	-0.174	3.962
240	2	0.143	-4.003

Point	Image	Vx	Vy
241	1	-0.008	0.214
241	2	0.009	-0.213

Point	Image	Vx	Vy
242	1	-0.021	0.534
242	2	0.021	-0.539

Point	Image	Vx	Vy
243	1	-0.078	1.918
243	2	0.075	-1.935

Point	Image	Vx	Vy
244	1	0.091	-2.111
244	2	-0.076	2.095

Point	Image	Vx	Vy
245	1	0.020	-0.561
245	2	-0.024	0.564

Point	Image	Vx	Vy
246	1	0.001	-0.027
246	2	-0.001	0.027

Point	Image	Vx	Vy
247	1	0.037	-0.987
247	2	-0.042	0.995

Point	Image	Vx	Vy
248	1	0.016	-0.383
248	2	-0.015	0.381

Point	Image	Vx	Vy
249	1	-0.104	2.564
249	2	0.101	-2.583

Point	Image	Vx	Vy
250	1	0.145	-3.380
250	2	-0.123	3.371

Point	Image	Vx	Vy
251	1	-0.012	0.283
251	2	0.010	-0.283

Point	Image	Vx	Vy
252	1	-0.083	1.957
252	2	0.074	-1.973

Point	Image	Vx	Vy
253	1	0.121	-2.787
253	2	-0.099	2.764

Point	Image	Vx	Vy
254	1	-0.164	3.766
254	2	0.137	-3.804

Point	Image	Vx	Vy
255	1	0.052	-1.431
255	2	-0.062	1.443

Point	Image	Vx	Vy
256	1	0.012	-0.298
256	2	-0.012	0.298

Point	Image	Vx	Vy
257	1	0.031	-0.740
257	2	-0.028	0.740

Point	Image	Vx	Vy
258	1	0.107	-2.425
258	2	-0.085	2.405

Point	Image	Vx	Vy
259	1	0.001	-0.033
259	2	-0.001	0.033

Point	Image	Vx	Vy
260	1	0.365	-8.894
260	2	-0.339	8.892

Point	Image	Vx	Vy
261	1	0.126	-3.520
261	2	-0.153	3.512

Point	Image	Vx	Vy
262	1	-0.131	3.536
262	2	0.151	-3.546

Point	Image	Vx	Vy
263	1	0.318	-8.634
263	2	-0.368	8.704

Point	Image	Vx	Vy
264	1	-0.012	0.319
264	2	0.013	-0.318

Point	Image	Vx	Vy
265	1	-0.028	0.653
265	2	0.023	-0.648

Point	Image	Vx	Vy
266	1	-0.013	0.338
266	2	0.014	-0.337

Point	Image	Vx	Vy
267	1	0.025	-0.652
267	2	-0.027	0.656

Point	Image	Vx	Vy
268	1	0.001	-0.015
268	2	-0.001	0.015

Point	Image	Vx	Vy
269	1	-0.011	0.263
269	2	0.010	-0.263

Point	Image	Vx	Vy
270	1	-0.275	6.729
270	2	0.260	-6.701

Point	Image	Vx	Vy
271	1	0.118	-2.709
271	2	-0.097	2.708

Mean error of 542 image points: ax=-0.000, ay=-0.000

RMSE of 542 image points: mx=0.083, my=2.104

The coordinates of object points

Point ID	X	Y	Z	Overlap	
1	505042.8910	4037516.5530	334.0000	2	
2	505094.4580	4037516.0800	334.0000	2	
3	505007.0820	4037333.8840	322.0000	2	
4	504713.0510	4037614.9930	313.0000	2	
5	504601.8990	4037669.2790	312.0000	2	
6	504340.9410	4037581.9580	315.0000	2	
7	503546.4500	4037696.7940	318.0000	2	
8	504478.7140	4037059.9280	316.0000	2	
9	504376.8300	4037267.7550	314.0000	2	
10	505031.1530	4036802.0190	316.0000	2	
11	504065.0060	4036910.2330	315.0000	2	
12	503746.9370	4036772.5050	317.0000	2	
13	503729.2680	4037192.5400	316.0000	2	
14	503942.2510	4037348.2760	315.0000	2	
15	503389.4730	4037819.3980	318.0000	2	
16	503808.0140	4038084.4600	316.0000	2	
17	504560.0830	4038214.9560	314.0000	2	
18	503804.0810	4038515.1330	319.0000	2	
19	503608.5600	4038248.3830	318.0000	2	
20	503281.3510	4038858.2580	316.0000	2	
21	503261.1760	4038610.6980	317.0000	2	
22	503902.7970	4038860.3510	318.0000	2	
23	504362.1760	4038971.5810	310.0000	2	
24	504129.2060	4038708.1280	319.0000	2	
25	504257.1420	4038479.5220	316.0000	2	
26	504293.1000	4038251.4910	315.0000	2	
27	504745.8870	4037983.4050	312.0000	2	
28	505231.9530	4038041.9560	314.0000	2	
29	505051.9480	4038347.4890	316.0000	2	
30	506309.0260	4039214.0090	316.0000	2	
31	507272.1840	4036813.5980	315.0000	2	
32	506873.0320	4037624.2000	316.0000	2	
33	506794.4240	4038491.2990	316.0000	2	
34	507639.9260	4038506.3540	319.0000	2	
35	507298.6220	4038476.2790	318.0000	2	
36	507038.2880	4038695.1040	317.0000	2	
37	506963.1070	4039105.8870	319.0000	2	
38	507661.3230	4037215.6830	316.0000	2	
39	505697.2910	4039181.2020	317.0000	2	
40	505887.7620	4038816.2940	319.0000	2	
41	505774.1650	4038371.0970	317.0000	2	
42	505891.5230	4037879.9820	316.0000	2	
43	506063.1880	4037621.5870	318.0000	2	
44	506215.7290	4037264.6540	317.0000	2	
45	506582.2600	4036829.4190	317.0000	2	
46	505456.8260	4036646.0290	309.0000	2	
47	505439.1030	4037015.5450	312.0000	2	
48	504887.1530	4036988.2390	311.0000	2	
49	504841.9650	4038413.2080	311.0000	2	
50	505017.5520	4038866.7640	315.0000	2	
51	503798.0520	4037531.3530	315.0000	2	
52	504236.9120	4037747.3880	317.0000	2	
53	505431.5500	4038920.9460	318.0000	2	
54	505307.0470	4038392.0040	315.0000	2	
55	507538.4570	4037915.1830	317.0000	2	
56	506170.9790	4038500.7010	319.0000	2	
57	503896.5982	4038964.7259	321.7708	2	
58	503975.4732	4038959.1282	322.2420	2	
59	503850.6524	4038826.6041	321.3275	2	

60	504219.9102	4039028.1599	321.6138	2
61	504349.4360	4038983.7908	321.1873	2
62	504332.6992	4038937.3326	321.3574	2
63	504528.6350	4038996.4607	321.4757	2
64	506307.4179	4039193.5892	315.8467	2
65	506505.7114	4039121.7306	316.3972	2
66	506483.9245	4039094.2069	316.2101	2
67	506935.6149	4039170.9978	315.7817	2
68	506837.2788	4039113.6835	315.4551	2
69	504100.9572	4038694.6551	320.6899	2
70	504355.4353	4038766.0624	320.1699	2
71	504476.1070	4038659.9088	319.7792	2
72	504681.4624	4038827.9786	319.9402	2
73	504612.5398	4038808.2822	321.2268	2
74	504665.6013	4038733.4878	319.9729	2
75	504604.3792	4038626.2275	319.4817	2
76	504585.8066	4038573.8820	320.4213	2
77	504754.8856	4038596.4529	319.4510	2
78	504936.6487	4038720.6982	319.3316	2
79	506452.1786	4038986.2734	316.4122	2
80	506476.0784	4038907.1442	316.6421	2
81	506567.4917	4039034.7741	316.5862	2
82	506549.8028	4038983.2104	316.6139	2
83	506525.8766	4038882.3604	317.3055	2
84	506789.7153	4039076.1077	316.4685	2
85	507365.1661	4039133.1058	315.7058	2
86	507308.8519	4038912.0484	317.0937	2
87	504243.2358	4038425.7213	319.1813	2
88	504455.5377	4038404.0923	319.6502	2
89	504325.3521	4038371.9055	319.5820	2
90	504323.6088	4038328.4414	318.9269	2
91	504585.9439	4038240.5173	318.7377	2
92	504651.4179	4038491.0217	319.7337	2
93	504888.6753	4038507.6036	318.1052	2
94	505031.1239	4038382.7315	319.5177	2
95	505095.1440	4038341.8573	318.9228	2
96	505104.4794	4038306.1063	318.5506	2
97	506522.9779	4038566.7777	318.5406	2
98	506722.9198	4038644.4245	318.4241	2
99	506696.1338	4038505.7433	319.6222	2
100	504295.9251	4038188.8026	318.0236	2
101	504625.7490	4038192.4754	318.5936	2
102	504759.5743	4038196.0742	318.7843	2
103	505109.5823	4038259.5196	318.6448	2
104	505088.7031	4038121.4838	319.1636	2
105	506620.9101	4038426.8018	319.9186	2
106	506644.8194	4038254.9595	320.6923	2
107	506678.4798	4038391.5498	319.6421	2
108	507259.3311	4038305.5606	322.2235	2
109	507301.0629	4038447.7564	321.7307	2
110	504566.3082	4037658.4403	317.1732	2
111	504817.7349	4037683.7095	317.5908	2
112	505126.7600	4037983.0417	316.5265	2
113	505223.9875	4037977.7811	318.7832	2
114	506641.3208	4038163.0532	320.4882	2
115	506645.9221	4038145.8147	320.9463	2
116	506679.4886	4038137.9756	320.9051	2
117	507158.7166	4038141.0541	323.0002	2
118	507200.6823	4038132.4673	323.3315	2
119	507170.8458	4038065.8791	323.0931	2

120	504676.9156	4037575.6531	316.7783	2
121	504784.8282	4037523.2997	316.5809	2
122	504952.8350	4037692.3603	317.6637	2
123	505358.9018	4037567.2729	318.7764	2
124	506718.2182	4037838.0753	322.8088	2
125	506778.0329	4037829.2483	323.0733	2
126	506722.0867	4037785.5714	323.4384	2
127	506755.3953	4037784.7947	323.0057	2
128	507031.3469	4037734.7091	323.7049	2
129	507021.2400	4037670.5824	322.0531	2
130	504370.9756	4037253.8647	314.2308	2
131	504869.4258	4037379.0524	317.1583	2
132	504890.1838	4037276.9226	314.8565	2
133	504931.3408	4037281.6993	314.9588	2
134	504886.2986	4037102.5153	314.0449	2
135	505351.1581	4037424.0188	318.7301	2
136	505352.8953	4037393.9679	315.7363	2
137	505339.7050	4037330.4479	317.1369	2
138	505314.6873	4037322.3008	316.6485	2
139	505354.8671	4037181.5031	317.0025	2
140	506834.9852	4037594.5942	321.9248	2
141	506918.6477	4037597.0236	323.1630	2
142	506890.8359	4037526.0696	322.9628	2
143	506817.7388	4037499.5166	322.9622	2
144	506896.0845	4037593.6549	322.7673	2
145	503984.5359	4036819.3483	308.1492	2
146	504482.9746	4037014.9861	311.0539	2
147	504974.4961	4037058.2002	314.9973	2
148	505228.3233	4037112.4304	316.4822	2
149	505228.1297	4037037.0300	316.2140	2
150	505372.4038	4037154.4149	317.1772	2
151	505409.6507	4037159.8573	317.2778	2
152	505378.2928	4037095.9118	316.7924	2
153	505438.0154	4037016.3082	318.0058	2
154	506941.3174	4037177.7846	325.2214	2
155	506902.8987	4037143.1990	325.5101	2
156	506930.6520	4037141.6539	325.9462	2
157	504147.1110	4036716.3116	309.2092	2
158	504259.7599	4036450.8079	308.7855	2
159	505237.1813	4036773.3686	315.7677	2
160	505496.2235	4036684.4155	318.4562	2
161	506940.8794	4037017.1356	325.9119	2
162	507092.1578	4036913.0438	327.6149	2
163	507149.6208	4036900.8480	328.3797	2
164	507249.8744	4036845.5900	329.5260	2
165	504177.7426	4038972.9432	321.4248	2
166	504560.2097	4038881.6506	320.1821	2
167	506675.3761	4037946.1294	322.0513	2
168	506825.7927	4037723.0123	323.6744	2
169	504118.4226	4038934.7831	321.6330	2
170	504503.7185	4038845.4042	320.9124	2
171	506514.8619	4039100.6220	316.4975	2
172	504883.0470	4038740.9082	318.8539	2
173	504877.9728	4038403.7512	319.1910	2
174	504841.7382	4038283.6076	318.2352	2
175	504883.3798	4038012.4251	317.4795	2
176	505164.8787	4038071.2606	318.7569	2
177	505197.3145	4038074.8356	319.0234	2
178	505888.8443	4038260.5024	317.9071	2
179	506647.0337	4038317.5030	320.0318	2

180	506722.2472	4038405.5797	318.4344	2
181	506713.9813	4037991.0940	322.3658	2
182	507251.5753	4038095.8927	323.3740	2
183	507005.3250	4037907.6339	324.1234	2
184	505031.4957	4037333.7021	315.7032	2
185	505359.7088	4037183.6582	316.8954	2
186	506829.9074	4037625.0925	321.9588	2
187	506874.6845	4037424.7647	323.7426	2
188	506843.0641	4037324.1109	324.1128	2
189	506871.1415	4037188.2908	324.9464	2
190	505274.3166	4036778.7971	315.9183	2
191	505371.8747	4036749.4915	316.2406	2
192	504657.4408	4038339.2209	318.1147	2
193	505100.4935	4037378.1420	317.7202	2
194	505472.7734	4037230.1616	317.8392	2
195	506617.2902	4038233.3222	320.4353	2
196	504951.1759	4037237.1950	315.5940	2
197	506862.9723	4037360.6643	323.6032	2
198	503860.8047	4038779.3336	320.4215	2
199	504409.1302	4038764.5420	320.3323	2
200	504522.1161	4038860.5375	321.6612	2
201	506543.8277	4038941.5340	317.0356	2
202	506509.0996	4038921.6156	317.0205	2
203	504957.8476	4038213.7505	318.2419	2
204	505025.5857	4038142.6537	318.4943	2
205	505009.8870	4038121.2496	318.7210	2
206	504874.4895	4037427.0805	317.4459	2
207	504924.8265	4037687.1246	317.1757	2
208	505217.7916	4037596.5148	319.7951	2
209	505184.3825	4037551.9278	317.9485	2
210	504907.1640	4037156.0131	314.5782	2
211	505213.9548	4037163.0691	316.6467	2
212	506213.7207	4037314.4302	319.2143	2
213	505387.8563	4036660.9771	316.9735	2
214	506429.2889	4036746.8597	322.5429	2
215	505132.5354	4037522.0212	316.4715	2
216	506872.1405	4037608.5750	322.7423	2
217	506995.5123	4037692.3913	322.6109	2
218	506537.3995	4039066.4971	316.3429	2
219	505407.4560	4036753.6409	317.2156	2
220	506973.2590	4037124.2545	325.5907	2
221	506998.8885	4039301.7123	314.8994	2
222	506472.2521	4038868.2714	316.6954	2
223	506705.0160	4038644.7631	318.2278	2
224	505296.8150	4037640.7256	312.0804	2
225	506806.8139	4037732.3789	323.4858	2
226	505232.3744	4037196.3036	315.5008	2
227	506448.0185	4036783.7484	322.8420	2
228	505631.9313	4036655.8037	317.7692	2
229	505909.3802	4038777.7243	316.6031	2
230	507067.1020	4038692.4944	319.1178	2
231	506939.7060	4039112.9998	316.0274	2
232	504298.0696	4038665.7222	320.0908	2
233	506658.5930	4038399.4026	319.7183	2
234	505060.8605	4037722.2691	317.9347	2
235	504888.9683	4037621.5436	318.2078	2
236	505224.3186	4037556.2163	318.0633	2
237	506936.2520	4037722.2397	323.8432	2
238	506794.7865	4037666.3193	322.1908	2
239	506940.4572	4037703.8159	322.8869	2

240	507295.5484	4036797.9456	330.0114	2
241	504694.4794	4038156.5293	317.5652	2
242	507003.7137	4037987.4024	322.2611	2
243	506967.0282	4037712.4768	315.5857	2
244	504147.4926	4036713.9980	309.2076	2
245	506412.0166	4039136.9817	316.5655	2
246	504926.1011	4038739.7409	319.2828	2
247	506741.8090	4038732.7239	318.4673	2
248	504731.8896	4037515.6173	316.0402	2
249	506783.3060	4037798.9575	309.9281	2
250	505026.5589	4036895.6174	267.9588	2
251	505432.0077	4037031.0512	317.6451	2
252	506882.1718	4037261.6148	324.3609	2
253	504011.2885	4036596.2671	306.3991	2
254	507217.1078	4036882.6080	329.3633	2
255	506849.5447	4039014.9190	315.9370	2
256	505942.1834	4037825.1008	317.8201	2
257	505312.2208	4037322.3373	321.0007	2
258	504095.1286	4036409.5062	305.9175	2
259	506646.4053	4038019.5715	320.2800	2
260	505398.7748	4037483.5694	318.1728	2
261	504968.3628	4039134.9284	308.5868	2
262	505891.6732	4038831.2768	314.2652	2
263	506817.5122	4038882.5068	332.2422	2
264	505001.1387	4038545.7233	315.6698	2
265	504103.1865	4036617.6229	363.5526	2
266	504870.0135	4038316.3410	315.7135	2
267	506513.3137	4038603.1763	317.4795	2
268	505915.7034	4037861.1149	311.9026	2
269	505184.4898	4037197.4582	312.8917	2
270	504698.4655	4037530.4738	334.2671	2
271	505433.3822	4036710.1410	315.2334	2

The total object points = 271

The residuals of image points

Point	Image	Vx	Vy
1	1	-13.964	-4.934
1	2	-3.959	3.272

Point	Image	Vx	Vy
2	1	-15.229	-5.096
2	2	-5.701	4.128

Point	Image	Vx	Vy
3	1	-4.875	-3.415
3	2	-1.972	-1.154

Point	Image	Vx	Vy
4	1	0.943	-1.997
4	2	-1.520	-1.897

Point	Image	Vx	Vy
5	1	-0.137	-1.369
5	2	-1.643	0.298

Point	Image	Vx	Vy
6	1	-0.628	-1.972
6	2	-3.489	-0.121

Point	Image	Vx	Vy
7	1	3.784	-1.173
7	2	-1.248	1.543

Point	Image	Vx	Vy
8	1	-1.095	-2.249
8	2	-1.971	0.172

Point	Image	Vx	Vy
9	1	-1.478	5.094
9	2	-2.737	7.546

Point	Image	Vx	Vy
10	1	-3.934	-2.465
10	2	-2.791	-2.088

Point	Image	Vx	Vy
11	1	-1.186	-4.500
11	2	-3.069	0.619

Point	Image	Vx	Vy
12	1	0.840	-5.944

12	2	-2.224	-0.420
Point	Image	Vx	Vy
13	1	1.606	-2.922
13	2	-3.964	1.788
Point	Image	Vx	Vy
14	1	1.105	-3.689
14	2	-4.412	0.500
Point	Image	Vx	Vy
15	1	5.364	-1.284
15	2	-1.667	1.752
Point	Image	Vx	Vy
16	1	0.704	-12.773
16	2	1.538	2.999
Point	Image	Vx	Vy
17	1	0.463	-0.447
17	2	-1.303	-1.091
Point	Image	Vx	Vy
18	1	-1.920	4.085
18	2	-3.502	1.629
Point	Image	Vx	Vy
19	1	1.276	7.694
19	2	-2.169	-0.165
Point	Image	Vx	Vy
20	1	3.135	7.605
20	2	-4.013	1.861
Point	Image	Vx	Vy
21	1	12.199	6.735
21	2	4.129	3.561
Point	Image	Vx	Vy
22	1	-0.096	6.241
22	2	-1.439	2.777
Point	Image	Vx	Vy
23	1	9.524	4.871
23	2	7.022	1.018
Point	Image	Vx	Vy
24	1	-0.342	2.436
24	2	-1.221	-0.949
Point	Image	Vx	Vy
25	1	-0.801	2.537
25	2	-2.462	0.532
Point	Image	Vx	Vy
26	1	2.053	-0.154
26	2	-0.734	-0.369
Point	Image	Vx	Vy
27	1	-5.107	-7.052

27	2	-8.341	-6.686
Point	Image	Vx	Vy
28	1	0.042	-2.125
28	2	-1.436	-2.461
Point	Image	Vx	Vy
29	1	-2.760	-0.640
29	2	-1.930	-0.294
Point	Image	Vx	Vy
30	1	-9.642	-1.047
30	2	-5.958	-0.084
Point	Image	Vx	Vy
31	1	7.529	9.239
31	2	2.519	3.749
Point	Image	Vx	Vy
32	1	3.364	2.260
32	2	0.524	1.253
Point	Image	Vx	Vy
33	1	-2.149	1.778
33	2	-5.600	-2.830
Point	Image	Vx	Vy
34	1	9.784	0.910
34	2	3.022	5.165
Point	Image	Vx	Vy
35	1	10.802	0.942
35	2	6.782	1.027
Point	Image	Vx	Vy
36	1	1.099	2.648
36	2	-0.462	5.194
Point	Image	Vx	Vy
37	1	2.717	-0.653
37	2	1.427	0.547
Point	Image	Vx	Vy
38	1	10.881	7.521
38	2	1.556	2.323
Point	Image	Vx	Vy
39	1	-3.206	-2.252
39	2	-0.036	-1.470
Point	Image	Vx	Vy
40	1	-2.836	-8.738
40	2	-2.938	-7.685
Point	Image	Vx	Vy
41	1	-3.892	-0.894
41	2	-0.941	-0.097
Point	Image	Vx	Vy
42	1	5.338	-6.726

42	2	4.536	-6.677
Point	Image	Vx	Vy
43	1	0.360	-0.893
43	2	1.065	-0.063
Point	Image	Vx	Vy
44	1	2.458	2.669
44	2	1.685	-0.443
Point	Image	Vx	Vy
45	1	2.218	2.868
45	2	2.975	-0.667
Point	Image	Vx	Vy
46	1	-2.713	9.102
46	2	-2.574	7.485
Point	Image	Vx	Vy
47	1	-0.555	-1.102
47	2	-1.747	-1.590
Point	Image	Vx	Vy
48	1	0.940	-1.866
48	2	-1.762	-1.356
Point	Image	Vx	Vy
49	1	-2.168	0.872
49	2	-4.127	1.337
Point	Image	Vx	Vy
50	1	-0.554	-1.572
50	2	-0.831	-4.530
Point	Image	Vx	Vy
51	1	2.320	-0.878
51	2	-2.356	1.491
Point	Image	Vx	Vy
52	1	-1.106	2.178
52	2	-1.894	3.201
Point	Image	Vx	Vy
53	1	-14.426	-2.856
53	2	-3.989	-4.542
Point	Image	Vx	Vy
54	1	9.007	-0.472
54	2	2.590	-3.106
Point	Image	Vx	Vy
55	1	-15.690	-19.894
55	2	-2.575	18.627
Point	Image	Vx	Vy
56	1	1.709	-5.485
56	2	4.379	-5.694
Point	Image	Vx	Vy
57	1	-0.033	0.838

57	2	-1.512	-4.132
Point	Image	Vx	Vy
58	1	-0.027	0.713
58	2	-1.050	-3.765
Point	Image	Vx	Vy
59	1	-0.013	0.411
59	2	-2.136	-3.667
Point	Image	Vx	Vy
60	1	-0.062	1.453
60	2	0.448	-3.795
Point	Image	Vx	Vy
61	1	-0.051	1.222
61	2	0.953	-3.179
Point	Image	Vx	Vy
62	1	-0.045	1.101
62	2	0.791	-3.104
Point	Image	Vx	Vy
63	1	-0.049	1.184
63	2	1.679	-2.633
Point	Image	Vx	Vy
64	1	-0.049	1.182
64	2	1.252	2.389
Point	Image	Vx	Vy
65	1	-0.040	0.981
65	2	0.360	2.633
Point	Image	Vx	Vy
66	1	-0.034	0.868
66	2	0.475	2.561
Point	Image	Vx	Vy
67	1	-0.027	0.706
67	2	-2.229	4.007
Point	Image	Vx	Vy
68	1	-0.041	1.007
68	2	-1.515	3.178
Point	Image	Vx	Vy
69	1	-0.010	0.327
69	2	-0.874	-2.758
Point	Image	Vx	Vy
70	1	-0.034	0.872
70	2	0.589	-2.762
Point	Image	Vx	Vy
71	1	0.004	0.016
71	2	0.900	-1.587
Point	Image	Vx	Vy
72	1	-0.026	0.700

72	2	1.922	-1.828
Point	Image	Vx	Vy
73	1	-0.028	0.752
73	2	1.668	-2.050
Point	Image	Vx	Vy
74	1	-0.019	0.534
74	2	1.733	-1.722
Point	Image	Vx	Vy
75	1	-0.021	0.565
75	2	1.373	-1.866
Point	Image	Vx	Vy
76	1	-0.019	0.531
76	2	1.223	-1.849
Point	Image	Vx	Vy
77	1	-0.001	0.124
77	2	1.813	-1.144
Point	Image	Vx	Vy
78	1	0.024	-0.415
78	2	2.404	-0.228
Point	Image	Vx	Vy
79	1	-0.028	0.726
79	2	0.667	2.109
Point	Image	Vx	Vy
80	1	-0.020	0.557
80	2	0.586	1.942
Point	Image	Vx	Vy
81	1	-0.028	0.743
81	2	0.082	2.530
Point	Image	Vx	Vy
82	1	-0.022	0.613
82	2	0.194	2.367
Point	Image	Vx	Vy
83	1	-0.013	0.406
83	2	0.357	2.048
Point	Image	Vx	Vy
84	1	-0.021	0.570
84	2	-1.206	3.309
Point	Image	Vx	Vy
85	1	-0.016	0.461
85	2	-5.522	4.707
Point	Image	Vx	Vy
86	1	-0.000	0.098
86	2	-4.760	3.476
Point	Image	Vx	Vy
87	1	-0.004	0.145

87	2	-0.596	-1.900
Point	Image	Vx	Vy
88	1	-0.006	0.199
88	2	0.416	-1.588
Point	Image	Vx	Vy
89	1	-0.000	0.067
89	2	-0.266	-1.607
Point	Image	Vx	Vy
90	1	-0.004	0.132
90	2	-0.344	-1.602
Point	Image	Vx	Vy
91	1	0.004	-0.053
91	2	0.724	-0.962
Point	Image	Vx	Vy
92	1	-0.011	0.329
92	2	1.340	-1.493
Point	Image	Vx	Vy
93	1	0.008	-0.100
93	2	2.072	-0.700
Point	Image	Vx	Vy
94	1	0.026	-0.551
94	2	2.247	-0.072
Point	Image	Vx	Vy
95	1	0.035	-0.770
95	2	2.326	0.214
Point	Image	Vx	Vy
96	1	0.037	-0.831
96	2	2.310	0.283
Point	Image	Vx	Vy
97	1	0.004	-0.008
97	2	0.528	1.108
Point	Image	Vx	Vy
98	1	0.005	-0.031
98	2	-0.510	1.602
Point	Image	Vx	Vy
99	1	0.007	-0.103
99	2	-0.264	1.061
Point	Image	Vx	Vy
100	1	0.033	-0.791
100	2	-0.764	-0.447
Point	Image	Vx	Vy
101	1	-0.000	0.039
101	2	0.822	-0.950
Point	Image	Vx	Vy
102	1	0.004	-0.063

102	2	1.318	-0.733
Point	Image	Vx	Vy
103	1	0.036	-0.814
103	2	2.279	0.272
Point	Image	Vx	Vy
104	1	0.018	-0.426
104	2	2.132	-0.087
Point	Image	Vx	Vy
105	1	0.015	-0.296
105	2	0.156	0.915
Point	Image	Vx	Vy
106	1	0.016	-0.357
106	2	0.165	0.375
Point	Image	Vx	Vy
107	1	0.008	-0.124
107	2	-0.090	0.628
Point	Image	Vx	Vy
108	1	0.022	-0.504
108	2	-3.563	0.618
Point	Image	Vx	Vy
109	1	0.024	-0.531
109	2	-4.075	1.357
Point	Image	Vx	Vy
110	1	0.013	-0.426
110	2	-0.190	0.625
Point	Image	Vx	Vy
111	1	-0.003	0.025
111	2	0.927	0.038
Point	Image	Vx	Vy
112	1	0.012	-0.298
112	2	2.102	-0.113
Point	Image	Vx	Vy
113	1	0.011	-0.266
113	2	2.279	-0.128
Point	Image	Vx	Vy
114	1	0.012	-0.270
114	2	0.252	-0.007
Point	Image	Vx	Vy
115	1	0.017	-0.405
115	2	0.239	0.075
Point	Image	Vx	Vy
116	1	0.013	-0.292
116	2	0.095	-0.073
Point	Image	Vx	Vy
117	1	0.012	-0.290

117	2	-2.629	-0.291
Point	Image	Vx	Vy
118	1	0.015	-0.350
118	2	-2.904	-0.293
Point	Image	Vx	Vy
119	1	0.009	-0.221
119	2	-2.610	-0.676
Point	Image	Vx	Vy
120	1	0.000	-0.090
120	2	0.224	0.484
Point	Image	Vx	Vy
121	1	-0.001	-0.049
121	2	0.617	0.526
Point	Image	Vx	Vy
122	1	0.002	-0.089
122	2	1.393	0.086
Point	Image	Vx	Vy
123	1	0.003	-0.128
123	2	2.240	0.072
Point	Image	Vx	Vy
124	1	0.007	-0.199
124	2	0.169	-1.016
Point	Image	Vx	Vy
125	1	0.023	-0.631
125	2	-0.116	-0.669
Point	Image	Vx	Vy
126	1	-0.006	0.157
126	2	0.211	-1.498
Point	Image	Vx	Vy
127	1	0.009	-0.270
127	2	0.044	-1.113
Point	Image	Vx	Vy
128	1	0.006	-0.181
128	2	-1.327	-1.693
Point	Image	Vx	Vy
129	1	0.002	-0.098
129	2	-1.195	-1.941
Point	Image	Vx	Vy
130	1	0.001	-0.193
130	2	-1.826	1.972
Point	Image	Vx	Vy
131	1	-0.018	0.406
131	2	0.805	0.405
Point	Image	Vx	Vy
132	1	-0.022	0.525

132	2	0.787	0.565
Point	Image	Vx	Vy
133	1	-0.019	0.443
133	2	0.943	0.579
Point	Image	Vx	Vy
134	1	-0.031	0.780
134	2	0.606	0.895
Point	Image	Vx	Vy
135	1	0.007	-0.295
135	2	2.144	0.465
Point	Image	Vx	Vy
136	1	0.001	-0.128
136	2	2.139	0.342
Point	Image	Vx	Vy
137	1	0.002	-0.154
137	2	2.079	0.508
Point	Image	Vx	Vy
138	1	0.001	-0.130
138	2	2.028	0.534
Point	Image	Vx	Vy
139	1	-0.026	0.665
139	2	2.057	-0.017
Point	Image	Vx	Vy
140	1	-0.004	0.083
140	2	-0.138	-2.000
Point	Image	Vx	Vy
141	1	-0.006	0.145
141	2	-0.549	-2.193
Point	Image	Vx	Vy
142	1	-0.006	0.132
142	2	-0.334	-2.282
Point	Image	Vx	Vy
143	1	-0.012	0.304
143	2	0.047	-2.369
Point	Image	Vx	Vy
144	1	-0.008	0.190
144	2	-0.430	-2.209
Point	Image	Vx	Vy
145	1	-0.010	0.024
145	2	-5.293	4.605
Point	Image	Vx	Vy
146	1	-0.035	0.867
146	2	-1.473	1.831
Point	Image	Vx	Vy
147	1	-0.026	0.646

147	2	0.898	1.035
Point	Image	Vx	Vy
148	1	-0.028	0.712
148	2	1.733	0.338
Point	Image	Vx	Vy
149	1	-0.033	0.867
149	2	1.690	0.400
Point	Image	Vx	Vy
150	1	-0.025	0.653
150	2	2.076	0.027
Point	Image	Vx	Vy
151	1	-0.030	0.793
151	2	2.151	-0.193
Point	Image	Vx	Vy
152	1	-0.028	0.724
152	2	2.061	0.085
Point	Image	Vx	Vy
153	1	-0.031	0.836
153	2	2.140	0.056
Point	Image	Vx	Vy
154	1	-0.031	0.896
154	2	-0.162	-3.707
Point	Image	Vx	Vy
155	1	-0.034	1.008
155	2	0.061	-3.754
Point	Image	Vx	Vy
156	1	-0.036	1.056
156	2	-0.063	-3.877
Point	Image	Vx	Vy
157	1	-0.022	0.414
157	2	-4.198	4.542
Point	Image	Vx	Vy
158	1	-0.043	1.165
158	2	-3.779	5.214
Point	Image	Vx	Vy
159	1	-0.053	1.594
159	2	1.574	0.520
Point	Image	Vx	Vy
160	1	-0.061	1.932
160	2	2.156	-0.220
Point	Image	Vx	Vy
161	1	-0.045	1.387
161	2	0.043	-4.354
Point	Image	Vx	Vy
162	1	-0.053	1.694

162	2	-0.548	-5.217
Point	Image	Vx	Vy
163	1	-0.051	1.632
163	2	-0.832	-5.354
Point	Image	Vx	Vy
164	1	-0.054	1.777
164	2	-1.299	-5.895
Point	Image	Vx	Vy
165	1	-0.051	1.237
165	2	0.123	-3.691
Point	Image	Vx	Vy
166	1	-0.029	0.772
166	2	1.600	-2.176
Point	Image	Vx	Vy
167	1	0.002	-0.051
167	2	0.276	-0.857
Point	Image	Vx	Vy
168	1	0.003	-0.089
168	2	-0.223	-1.527
Point	Image	Vx	Vy
169	1	-0.045	1.078
169	2	-0.270	-3.686
Point	Image	Vx	Vy
170	1	-0.037	0.922
170	2	1.340	-2.473
Point	Image	Vx	Vy
171	1	-0.037	0.915
171	2	0.323	2.607
Point	Image	Vx	Vy
172	1	-0.010	0.319
172	2	2.343	-1.051
Point	Image	Vx	Vy
173	1	0.002	0.007
173	2	1.928	-0.813
Point	Image	Vx	Vy
174	1	0.011	-0.214
174	2	1.680	-0.578
Point	Image	Vx	Vy
175	1	0.011	-0.270
175	2	1.502	-0.238
Point	Image	Vx	Vy
176	1	0.033	-0.825
176	2	2.224	0.369
Point	Image	Vx	Vy
177	1	0.037	-0.920

177	2	2.279	0.473
Point	Image	Vx	Vy
178	1	0.030	-0.683
178	2	2.450	0.600
Point	Image	Vx	Vy
179	1	0.017	-0.355
179	2	0.108	0.586
Point	Image	Vx	Vy
180	1	0.010	-0.171
180	2	-0.324	0.739
Point	Image	Vx	Vy
181	1	0.012	-0.304
181	2	0.054	-0.510
Point	Image	Vx	Vy
182	1	0.019	-0.454
182	2	-3.213	-0.381
Point	Image	Vx	Vy
183	1	0.014	-0.363
183	2	-1.386	-0.953
Point	Image	Vx	Vy
184	1	0.012	-0.473
184	2	1.298	1.224
Point	Image	Vx	Vy
185	1	-0.026	0.670
185	2	2.067	-0.037
Point	Image	Vx	Vy
186	1	-0.003	0.066
186	2	-0.145	-1.912
Point	Image	Vx	Vy
187	1	-0.015	0.400
187	2	-0.138	-2.704
Point	Image	Vx	Vy
188	1	-0.019	0.526
188	2	0.119	-2.914
Point	Image	Vx	Vy
189	1	-0.031	0.918
189	2	0.151	-3.537
Point	Image	Vx	Vy
190	1	-0.050	1.485
190	2	1.677	0.511
Point	Image	Vx	Vy
191	1	-0.055	1.653
191	2	1.913	0.185
Point	Image	Vx	Vy
192	1	-0.000	0.056

192	2	1.147	-1.098
Point	Image	Vx	Vy
193	1	0.056	-1.724
193	2	1.496	2.285
Point	Image	Vx	Vy
194	1	-0.014	0.306
194	2	2.264	0.036
Point	Image	Vx	Vy
195	1	0.021	-0.490
195	2	0.301	0.439
Point	Image	Vx	Vy
196	1	-0.020	0.452
196	2	0.971	0.679
Point	Image	Vx	Vy
197	1	-0.018	0.475
197	2	-0.013	-2.857
Point	Image	Vx	Vy
198	1	-0.022	0.573
198	2	-2.163	-3.723
Point	Image	Vx	Vy
199	1	-0.034	0.840
199	2	0.822	-2.602
Point	Image	Vx	Vy
200	1	-0.041	1.003
200	2	1.434	-2.509
Point	Image	Vx	Vy
201	1	-0.017	0.486
201	2	0.242	2.280
Point	Image	Vx	Vy
202	1	-0.020	0.547
202	2	0.425	2.071
Point	Image	Vx	Vy
203	1	0.010	-0.218
203	2	1.925	-0.428
Point	Image	Vx	Vy
204	1	0.019	-0.448
204	2	2.011	-0.111
Point	Image	Vx	Vy
205	1	0.014	-0.338
205	2	1.957	-0.216
Point	Image	Vx	Vy
206	1	-0.005	0.038
206	2	0.861	0.630
Point	Image	Vx	Vy
207	1	-0.005	0.086

207	2	1.305	-0.069
Point	Image	Vx	Vy
208	1	0.055	-1.571
208	2	1.948	1.589
Point	Image	Vx	Vy
209	1	0.157	-4.485
209	2	1.741	4.605
Point	Image	Vx	Vy
210	1	-0.022	0.510
210	2	0.731	0.945
Point	Image	Vx	Vy
211	1	-0.027	0.690
211	2	1.728	0.246
Point	Image	Vx	Vy
212	1	0.003	-0.170
212	2	2.088	-0.920
Point	Image	Vx	Vy
213	1	-0.054	1.670
213	2	1.910	0.433
Point	Image	Vx	Vy
214	1	-0.033	1.013
214	2	1.994	-2.345
Point	Image	Vx	Vy
215	1	0.154	-4.424
215	2	1.598	4.641
Point	Image	Vx	Vy
216	1	-0.006	0.157
216	2	-0.328	-2.105
Point	Image	Vx	Vy
217	1	0.001	-0.033
217	2	-1.073	-1.909
Point	Image	Vx	Vy
218	1	-0.031	0.794
218	2	0.222	2.595
Point	Image	Vx	Vy
219	1	-0.055	1.712
219	2	1.996	0.015
Point	Image	Vx	Vy
220	1	-0.036	1.081
220	2	-0.246	-4.044
Point	Image	Vx	Vy
221	1	-0.050	1.158
221	2	-2.778	4.551
Point	Image	Vx	Vy
222	1	-0.032	0.819

222	2	0.636	1.500
Point	Image	Vx	Vy
223	1	-0.001	0.112
223	2	-0.407	1.450
Point	Image	Vx	Vy
224	1	0.115	-3.239
224	2	2.074	3.128
Point	Image	Vx	Vy
225	1	-0.001	0.019
225	2	-0.138	-1.589
Point	Image	Vx	Vy
226	1	-0.019	0.473
226	2	1.790	0.340
Point	Image	Vx	Vy
227	1	-0.017	0.454
227	2	1.913	-1.881
Point	Image	Vx	Vy
228	1	-0.056	1.829
228	2	2.362	-0.445
Point	Image	Vx	Vy
229	1	0.045	-0.918
229	2	2.443	2.070
Point	Image	Vx	Vy
230	1	-0.023	0.603
230	2	-2.640	1.457
Point	Image	Vx	Vy
231	1	-0.030	0.752
231	2	-2.199	3.609
Point	Image	Vx	Vy
232	1	-0.019	0.498
232	2	0.127	-2.446
Point	Image	Vx	Vy
233	1	0.010	-0.188
233	2	-0.001	0.718
Point	Image	Vx	Vy
234	1	0.007	-0.227
234	2	1.725	0.130
Point	Image	Vx	Vy
235	1	-0.002	0.007
235	2	1.112	0.164
Point	Image	Vx	Vy
236	1	0.128	-3.650
236	2	1.861	3.727
Point	Image	Vx	Vy
237	1	-0.002	0.053

237	2	-0.779	-1.825
Point	Image	Vx	Vy
238	1	-0.007	0.182
238	2	-0.015	-1.888
Point	Image	Vx	Vy
239	1	-0.004	0.092
239	2	-0.782	-1.921
Point	Image	Vx	Vy
240	1	-0.054	1.836
240	2	-1.487	-6.171
Point	Image	Vx	Vy
241	1	0.009	-0.207
241	2	1.032	-0.594
Point	Image	Vx	Vy
242	1	-0.001	0.038
242	2	-1.457	-1.090
Point	Image	Vx	Vy
243	1	-0.037	1.009
243	2	-0.918	-2.876
Point	Image	Vx	Vy
244	1	-0.020	0.440
244	2	-4.200	4.521
Point	Image	Vx	Vy
245	1	-0.051	1.180
245	2	0.812	2.334
Point	Image	Vx	Vy
246	1	0.021	-0.400
246	2	2.404	-0.246
Point	Image	Vx	Vy
247	1	0.002	0.027
247	2	-0.679	1.976
Point	Image	Vx	Vy
248	1	0.003	-0.126
248	2	0.387	0.655
Point	Image	Vx	Vy
249	1	-0.069	1.867
249	2	-0.044	-3.282
Point	Image	Vx	Vy
250	1	0.066	-2.400
250	2	0.908	4.394
Point	Image	Vx	Vy
251	1	-0.023	0.673
251	2	2.131	0.187
Point	Image	Vx	Vy
252	1	-0.023	0.681

252 2 0.014 -3.244

Point Image Vx Vy
253 1 -0.014 0.315
253 2 -5.484 5.704

Point Image Vx Vy
254 1 -0.055 1.816
254 2 -1.166 -5.786

Point Image Vx Vy
255 1 -0.015 0.416
255 2 -1.535 3.214

Point Image Vx Vy
256 1 0.024 -0.641
256 2 2.378 0.049

Point Image Vx Vy
257 1 0.018 -0.571
257 2 2.004 0.986

Point Image Vx Vy
258 1 -0.038 1.205
258 2 -5.112 5.893

Point Image Vx Vy
259 1 0.002 -0.033
259 2 -0.001 0.032

Point Image Vx Vy
260 1 0.361 -8.893
260 2 -0.338 8.894

Point Image Vx Vy
261 1 0.128 -3.521
261 2 -0.152 3.511

Point Image Vx Vy

Total mean error of 542 image points: ax=-0.000, ay=-0.000

Total RMSE of 542 image points: mx=2.415, my=2.753

262 1 -0.129 3.535
262 2 0.152 -3.547

Point Image Vx Vy
263 1 0.320 -8.635
263 2 -0.368 8.703

Point Image Vx Vy
264 1 -0.011 0.319
264 2 0.014 -0.319

Point Image Vx Vy
265 1 -0.031 0.656
265 2 0.021 -0.645

Point Image Vx Vy
266 1 -0.012 0.338
266 2 0.015 -0.337

Point Image Vx Vy
267 1 0.026 -0.653
267 2 -0.027 0.655

Point Image Vx Vy
268 1 0.000 -0.016
268 2 -0.001 0.015

Point Image Vx Vy
269 1 -0.013 0.264
269 2 0.009 -0.262

Point Image Vx Vy
270 1 -0.275 6.729
270 2 0.260 -6.701

Point Image Vx Vy
271 1 0.118 -2.709
271 2 -0.097 2.708

The image residuals of the control points

The image ID = 1
Point ID Vx Vy

1 -13.964 -4.934
2 -15.229 -5.096
3 -4.875 -3.415
4 0.943 -1.997
5 -0.137 -1.369
6 -0.628 -1.972
7 3.784 -1.173
8 -1.095 -2.249
9 -1.478 5.094
10 -3.934 -2.465
11 -1.186 -4.500

12 0.840 -5.944
13 1.606 -2.922
14 1.105 -3.689
15 5.364 -1.284
16 0.704 -12.773
17 0.463 -0.447
18 -1.920 4.085
19 1.276 7.694
20 3.135 7.605
21 12.199 6.735
22 -0.096 6.241

23	9.524	4.871	83	-0.013	0.406
24	-0.342	2.436	84	-0.021	0.570
25	-0.801	2.537	85	-0.016	0.461
26	2.053	-0.154	86	-0.000	0.098
27	-5.107	-7.052	87	-0.004	0.145
28	0.042	-2.125	88	-0.006	0.199
29	-2.760	-0.640	89	-0.000	0.067
30	-9.642	-1.047	90	-0.004	0.132
31	7.529	9.239	91	0.004	-0.053
32	3.364	2.260	92	-0.011	0.329
33	-2.149	1.778	93	0.008	-0.100
34	9.784	0.910	94	0.026	-0.551
35	10.802	0.942	95	0.035	-0.770
36	1.099	2.648	96	0.037	-0.831
37	2.717	-0.653	97	0.004	-0.008
38	10.881	7.521	98	0.005	-0.031
39	-3.206	-2.252	99	0.007	-0.103
40	-2.836	-8.738	100	0.033	-0.791
41	-3.892	-0.894	101	-0.000	0.039
42	5.338	-6.726	102	0.004	-0.063
43	0.360	-0.893	103	0.036	-0.814
44	2.458	2.669	104	0.018	-0.426
45	2.218	2.868	105	0.015	-0.296
46	-2.713	9.102	106	0.016	-0.357
47	-0.555	-1.102	107	0.008	-0.124
48	0.940	-1.866	108	0.022	-0.504
49	-2.168	0.872	109	0.024	-0.531
50	-0.554	-1.572	110	0.013	-0.426
51	2.320	-0.878	111	-0.003	0.025
52	-1.106	2.178	112	0.012	-0.298
53	-14.426	-2.856	113	0.011	-0.266
54	9.007	-0.472	114	0.012	-0.270
55	-15.690	-19.894	115	0.017	-0.405
56	1.709	-5.485	116	0.013	-0.292
57	-0.033	0.838	117	0.012	-0.290
58	-0.027	0.713	118	0.015	-0.350
59	-0.013	0.411	119	0.009	-0.221
60	-0.062	1.453	120	0.000	-0.090
61	-0.051	1.222	121	-0.001	-0.049
62	-0.045	1.101	122	0.002	-0.089
63	-0.049	1.184	123	0.003	-0.128
64	-0.049	1.182	124	0.007	-0.199
65	-0.040	0.981	125	0.023	-0.631
66	-0.034	0.868	126	-0.006	0.157
67	-0.027	0.706	127	0.009	-0.270
68	-0.041	1.007	128	0.006	-0.181
69	-0.010	0.327	129	0.002	-0.098
70	-0.034	0.872	130	0.001	-0.193
71	0.004	0.016	131	-0.018	0.406
72	-0.026	0.700	132	-0.022	0.525
73	-0.028	0.752	133	-0.019	0.443
74	-0.019	0.534	134	-0.031	0.780
75	-0.021	0.565	135	0.007	-0.295
76	-0.019	0.531	136	0.001	-0.128
77	-0.001	0.124	137	0.002	-0.154
78	0.024	-0.415	138	0.001	-0.130
79	-0.028	0.726	139	-0.026	0.665
80	-0.020	0.557	140	-0.004	0.083
81	-0.028	0.743	141	-0.006	0.145
82	-0.022	0.613	142	-0.006	0.132

143	-0.012	0.304	203	0.010	-0.218
144	-0.008	0.190	204	0.019	-0.448
145	-0.010	0.024	205	0.014	-0.338
146	-0.035	0.867	206	-0.005	0.038
147	-0.026	0.646	207	-0.005	0.086
148	-0.028	0.712	208	0.055	-1.571
149	-0.033	0.867	209	0.157	-4.485
150	-0.025	0.653	210	-0.022	0.510
151	-0.030	0.793	211	-0.027	0.690
152	-0.028	0.724	212	0.003	-0.170
153	-0.031	0.836	213	-0.054	1.670
154	-0.031	0.896	214	-0.033	1.013
155	-0.034	1.008	215	0.154	-4.424
156	-0.036	1.056	216	-0.006	0.157
157	-0.022	0.414	217	0.001	-0.033
158	-0.043	1.165	218	-0.031	0.794
159	-0.053	1.594	219	-0.055	1.712
160	-0.061	1.932	220	-0.036	1.081
161	-0.045	1.387	221	-0.050	1.158
162	-0.053	1.694	222	-0.032	0.819
163	-0.051	1.632	223	-0.001	0.112
164	-0.054	1.777	224	0.115	-3.239
165	-0.051	1.237	225	-0.001	0.019
166	-0.029	0.772	226	-0.019	0.473
167	0.002	-0.051	227	-0.017	0.454
168	0.003	-0.089	228	-0.056	1.829
169	-0.045	1.078	229	0.045	-0.918
170	-0.037	0.922	230	-0.023	0.603
171	-0.037	0.915	231	-0.030	0.752
172	-0.010	0.319	232	-0.019	0.498
173	0.002	0.007	233	0.010	-0.188
174	0.011	-0.214	234	0.007	-0.227
175	0.011	-0.270	235	-0.002	0.007
176	0.033	-0.825	236	0.128	-3.650
177	0.037	-0.920	237	-0.002	0.053
178	0.030	-0.683	238	-0.007	0.182
179	0.017	-0.355	239	-0.004	0.092
180	0.010	-0.171	240	-0.054	1.836
181	0.012	-0.304	241	0.009	-0.207
182	0.019	-0.454	242	-0.001	0.038
183	0.014	-0.363	243	-0.037	1.009
184	0.012	-0.473	244	-0.020	0.440
185	-0.026	0.670	245	-0.051	1.180
186	-0.003	0.066	246	0.021	-0.400
187	-0.015	0.400	247	0.002	0.027
188	-0.019	0.526	248	0.003	-0.126
189	-0.031	0.918	249	-0.069	1.867
190	-0.050	1.485	250	0.066	-2.400
191	-0.055	1.653	251	-0.023	0.673
192	-0.000	0.056	252	-0.023	0.681
193	0.056	-1.724	253	-0.014	0.315
194	-0.014	0.306	254	-0.055	1.816
195	0.021	-0.490	255	-0.015	0.416
196	-0.020	0.452	256	0.024	-0.641
197	-0.018	0.475	257	0.018	-0.571
198	-0.022	0.573	258	-0.038	1.205
199	-0.034	0.840	259	0.002	-0.033
200	-0.041	1.003	260	0.361	-8.893
201	-0.017	0.486	261	0.128	-3.521
202	-0.020	0.547	262	-0.129	3.535

263	0.320	-8.635
264	-0.011	0.319
265	-0.031	0.656
266	-0.012	0.338
267	0.026	-0.653

268	0.000	-0.016
269	-0.013	0.264
270	-0.275	6.729
271	0.118	-2.709

RMSE of 271 points: mx=2.683, my=2.653

The image ID = 2

Point ID	Vx	Vy
1	-3.959	3.272
2	-5.701	4.128
3	-1.972	-1.154
4	-1.520	-1.897
5	-1.643	0.298
6	-3.489	-0.121
7	-1.248	1.543
8	-1.971	0.172
9	-2.737	7.546
10	-2.791	-2.088
11	-3.069	0.619
12	-2.224	-0.420
13	-3.964	1.788
14	-4.412	0.500
15	-1.667	1.752
16	1.538	2.999
17	-1.303	-1.091
18	-3.502	1.629
19	-2.169	-0.165
20	-4.013	1.861
21	4.129	3.561
22	-1.439	2.777
23	7.022	1.018
24	-1.221	-0.949
25	-2.462	0.532
26	-0.734	-0.369
27	-8.341	-6.686
28	-1.436	-2.461
29	-1.930	-0.294
30	-5.958	-0.084
31	2.519	3.749
32	0.524	1.253
33	-5.600	-2.830
34	3.022	5.165
35	6.782	1.027
36	-0.462	5.194
37	1.427	0.547
38	1.556	2.323
39	-0.036	-1.470
40	-2.938	-7.685
41	-0.941	-0.097
42	4.536	-6.677
43	1.065	-0.063
44	1.685	-0.443
45	2.975	-0.667
46	-2.574	7.485
47	-1.747	-1.590
48	-1.762	-1.356
49	-4.127	1.337
50	-0.831	-4.530
51	-2.356	1.491

52	-1.894	3.201
53	-3.989	-4.542
54	2.590	-3.106
55	-2.575	18.627
56	4.379	-5.694
57	-1.512	-4.132
58	-1.050	-3.765
59	-2.136	-3.667
60	0.448	-3.795
61	0.953	-3.179
62	0.791	-3.104
63	1.679	-2.633
64	1.252	2.389
65	0.360	2.633
66	0.475	2.561
67	-2.229	4.007
68	-1.515	3.178
69	-0.874	-2.758
70	0.589	-2.762
71	0.900	-1.587
72	1.922	-1.828
73	1.668	-2.050
74	1.733	-1.722
75	1.373	-1.866
76	1.223	-1.849
77	1.813	-1.144
78	2.404	-0.228
79	0.667	2.109
80	0.586	1.942
81	0.082	2.530
82	0.194	2.367
83	0.357	2.048
84	-1.206	3.309
85	-5.522	4.707
86	-4.760	3.476
87	-0.596	-1.900
88	0.416	-1.588
89	-0.266	-1.607
90	-0.344	-1.602
91	0.724	-0.962
92	1.340	-1.493
93	2.072	-0.700
94	2.247	-0.072
95	2.326	0.214
96	2.310	0.283
97	0.528	1.108
98	-0.510	1.602
99	-0.264	1.061
100	-0.764	-0.447
101	0.822	-0.950
102	1.318	-0.733

103	2.279	0.272	163	-0.832	-5.354
104	2.132	-0.087	164	-1.299	-5.895
105	0.156	0.915	165	0.123	-3.691
106	0.165	0.375	166	1.600	-2.176
107	-0.090	0.628	167	0.276	-0.857
108	-3.563	0.618	168	-0.223	-1.527
109	-4.075	1.357	169	-0.270	-3.686
110	-0.190	0.625	170	1.340	-2.473
111	0.927	0.038	171	0.323	2.607
112	2.102	-0.113	172	2.343	-1.051
113	2.279	-0.128	173	1.928	-0.813
114	0.252	-0.007	174	1.680	-0.578
115	0.239	0.075	175	1.502	-0.238
116	0.095	-0.073	176	2.224	0.369
117	-2.629	-0.291	177	2.279	0.473
118	-2.904	-0.293	178	2.450	0.600
119	-2.610	-0.676	179	0.108	0.586
120	0.224	0.484	180	-0.324	0.739
121	0.617	0.526	181	0.054	-0.510
122	1.393	0.086	182	-3.213	-0.381
123	2.240	0.072	183	-1.386	-0.953
124	0.169	-1.016	184	1.298	1.224
125	-0.116	-0.669	185	2.067	-0.037
126	0.211	-1.498	186	-0.145	-1.912
127	0.044	-1.113	187	-0.138	-2.704
128	-1.327	-1.693	188	0.119	-2.914
129	-1.195	-1.941	189	0.151	-3.537
130	-1.826	1.972	190	1.677	0.511
131	0.805	0.405	191	1.913	0.185
132	0.787	0.565	192	1.147	-1.098
133	0.943	0.579	193	1.496	2.285
134	0.606	0.895	194	2.264	0.036
135	2.144	0.465	195	0.301	0.439
136	2.139	0.342	196	0.971	0.679
137	2.079	0.508	197	-0.013	-2.857
138	2.028	0.534	198	-2.163	-3.723
139	2.057	-0.017	199	0.822	-2.602
140	-0.138	-2.000	200	1.434	-2.509
141	-0.549	-2.193	201	0.242	2.280
142	-0.334	-2.282	202	0.425	2.071
143	0.047	-2.369	203	1.925	-0.428
144	-0.430	-2.209	204	2.011	-0.111
145	-5.293	4.605	205	1.957	-0.216
146	-1.473	1.831	206	0.861	0.630
147	0.898	1.035	207	1.305	-0.069
148	1.733	0.338	208	1.948	1.589
149	1.690	0.400	209	1.741	4.605
150	2.076	0.027	210	0.731	0.945
151	2.151	-0.193	211	1.728	0.246
152	2.061	0.085	212	2.088	-0.920
153	2.140	0.056	213	1.910	0.433
154	-0.162	-3.707	214	1.994	-2.345
155	0.061	-3.754	215	1.598	4.641
156	-0.063	-3.877	216	-0.328	-2.105
157	-4.198	4.542	217	-1.073	-1.909
158	-3.779	5.214	218	0.222	2.595
159	1.574	0.520	219	1.996	0.015
160	2.156	-0.220	220	-0.246	-4.044
161	0.043	-4.354	221	-2.778	4.551
162	-0.548	-5.217	222	0.636	1.500

223	-0.407	1.450	248	0.387	0.655
224	2.074	3.128	249	-0.044	-3.282
225	-0.138	-1.589	250	0.908	4.394
226	1.790	0.340	251	2.131	0.187
227	1.913	-1.881	252	0.014	-3.244
228	2.362	-0.445	253	-5.484	5.704
229	2.443	2.070	254	-1.166	-5.786
230	-2.640	1.457	255	-1.535	3.214
231	-2.199	3.609	256	2.378	0.049
232	0.127	-2.446	257	2.004	0.986
233	-0.001	0.718	258	-5.112	5.893
234	1.725	0.130	259	-0.001	0.032
235	1.112	0.164	260	-0.338	8.894
236	1.861	3.727	261	-0.152	3.511
237	-0.779	-1.825	262	0.152	-3.547
238	-0.015	-1.888	263	-0.368	8.703
239	-0.782	-1.921	264	0.014	-0.319
240	-1.487	-6.171	265	0.021	-0.645
241	1.032	-0.594	266	0.015	-0.337
242	-1.457	-1.090	267	-0.027	0.655
243	-0.918	-2.876	268	-0.001	0.015
244	-4.200	4.521	269	0.009	-0.262
245	0.812	2.334	270	0.260	-6.701
246	2.404	-0.246	271	-0.097	2.708
247	-0.679	1.976			

RMSE of 271 points: mx=2.113, my=2.850

Total number of all control image points = 542

Total rmsex = 2.415, rmsey = 2.753